Repurposing as a Strategy for the Discovery of a New Antileishmanial

CHARLTON, REBECCA,LOUISE

Repurposing as a Strategy for the Discovery of a New Antileishmanial

A thesis submitted in partial fulfilment of the requirements for the degree of Doctor of Philosophy from Durham University by

Rebecca Louise Charlton

September 2019

Department of Chemistry

Repurposing as a Strategy for the Discovery of a New Antileishmanial

A thesis submitted in partial fulfilment of the requirements for the degree of Doctor of Philosophy from Universidade Federal do Rio de Janeiro by

Rebecca Louise Charlton

September 2019

Instituto de Biofísica Carlos Chagas Filho

REBECCA LOUISE CHARLTON

Repurposing as a Strategy for the Discovery of a New Antileishmanial

A thesis in international joint supervision submitted in partial fulfilment of the requirements for the degree of Doctor of Philosophy in Chemical Biology (Durham University, United Kingdom) and Doctor of Philosophy in Biological Sciences (Federal University of Rio de Janeiro, Brazil).

Supervisor in United Kingdom: Prof. Patrick G. Steel

Dr. Paul W. Denny

Supervisor in Brazil: Prof. Bartira Rossi Bergmann

ABSTRACT

CHARLTON, Rebecca Louise. **Repurposing as a strategy for the discovery of a new antileishmanial.** Thesis (PhD in Chemical Biology), Chemistry Department, Durham University, UK; (PhD in Biological Sciences), Instituto de Biofísica Carlos Chagas Filho, Universidade Federal do Rio de Janeiro, Brazil.

Leishmaniasis is a vector-borne Neglected Tropical Disease, caused by protozoan parasites of the genus *Leishmania* for which there is a shortage of effective and viable non-toxic drugs. There are approximately 1.3 million new cases of leishmaniasis each year with the greatest impact in the poorest communities. Therefore, repurposing is an important strategy as established medicines have cheaper and faster development times.

Leishmania major inositol phosphorylceramide synthase (*Lmj*IPCS) is involved in the biosynthesis of sphingolipids and has been identified as a potential drug target by our group. A set of screens against *Lmj*IPCS and the parasite were performed on a library of 1040 bioactive compounds. The over-the-counter antihistamine clemastine was selected as the most promising compound to develop further. Clemastine has now shown submicromolar activity against species that cause cutaneous (*L. major* and *L. amazonensis*) and visceral leishmaniasis (*L. donovani* and *L. infantum*) as well as being effective against *L. amazonensis* intramacrophage amastigotes (EC_{50} = 0.4 μM, SI = 50). Progression of clemastine into a mouse model of *L. amazonensis* infection showed significant reduction in parasite burden when given *via* the intralesional (IL) or intraperitoneal (IP) route. In order to optimise the antileishmanial activity, two series of clemastine analogues were synthesised. The first series, named nor-clemastine analogues, lack the clemastine quarternary methyl group. An enantioselective route was developed to show the role stereochemistry plays on antileishmanial activity with greatest activity residing in the (*R*, *R*)-configuration of nor-clemastine. The second series, named N-linked analogues, identified a more synthetically accessible and selective analogue against *L. amazonensis* intramacrophage amastigotes (EC_{50} value = 0.5 μM, SI = 146). This compound was progressed into a mouse model infected with *L. amazonensis* and significantly reduced the parasite burden when given *via* the IL route. Overall, this thesis demonstrates the potential of drug repurposing as well as the development of new analogues in the search of a new antileishmanial therapy.

Keywords: leishmaniasis, repurposing, clemastine, drug target, antileishmanial, therapy, synthesis.

RESUMO

CHARLTON, Rebecca Louise. **Reposicionamento como estratégia para o descobrimento de um novo antileishmanial.** Tese (PhD em Química Biológica), Departamento de Química, Durham Universidade, Reino Unido; (PhD em Ciências Biológicas) Instituto de Biofísica Carlos Chagas Filho, Universidade Federal do Rio de Janeiro, Brasil.

As leishmanioses são doenças negligenciadas transmitidas por inseto vetor e causadas por protozoários do gênero *Leishmania,* para os quais existe uma carência de medicamentos eficazes e seguros. Aproximadamente 1.3 milhões de novos casos de leishmaniose são registrados por ano, com grande impacto nas populações mais pobres. Portanto, o reposicionamento de fármacos torna-se uma estratégia importante, uma vez que medicamentos já comercializados possuem tempo de desenvolvimento mais rápido e barato. A enzima inositol fosforilceramida sintase de *Leishmania major* (LmjIPCS) envolvida na biossíntese de esfingolipídeos e já foi identificada como um potencial alvo de drogas pelo nosso grupo. Neste estudo, uma biblioteca de 1040 compostos bioativos foi avaliada quanto à atividade cruzada entre a LmjIPCS e toxicidade contra o parasito. Dentre os compostos, o anti-histamínico clemastina foi selecionado como o mais promissor por seu alto efeito inibitório contra a enzima, e contra promastigotas de espécies causadoras das formas cutânea (*L. major* e *L. amazonensis*) e visceral (*L. donovani* e *L. infantum*) da leishmaniose, e amastigotas intracelulares de *L. amazonensis* (EC_{50} = 0.4 μM, SI = 50). *In vivo*, a clemastina reduziu significativamente a carga parasitária de camundongos infectados com *L. amazonensis* quando administrada por via inralesional (IL) ou intraperitoneal (IP). Buscando sua otimização, foram sintetizadas duas séries de análogos da clemastina. Na primeira série de compostos denominados nor-clemastina, os análogos eram desprovidos do grupamento metila quaternário. Uma rota enantiosseletiva evidenciou nos compostos nor-clemastina o papel da estereoquímica na atividade antileishmanial, sendo as moléculas na configuração (R, R) as mais ativas. Na segunda série de compostos denominados N-linked, foi identificado um análogo ainda mais seletivo contra amastigotas intracelulares de *L. amazonensis* (EC_{50} value = 0.5 μM, SI = 146). Quando testado pela via IL em camundongos infectados com *L. amazonensis*, este análogo N-linked também reduziu significativamente a carga parasitária. Em conclusão, esta tese demonstrou o potencial do reposicionamento de fármacos bem como o desenvolvimento de novos análogos na busca por uma nova terapia contra a leishmaniose.

Palavras-chave: Leishmaniose, reposicionamento, clemastina, alvo terapêutico, antileishmanial, terapia, síntese química.

Acknowledgments

Firstly, I would like to thank my supervisors Prof. Patrick Steel, Dr. Paul Denny and Prof. Bartira Rossi-Bergmann and the funding body, the Royal Society, for the opportunity to work on this interesting and exciting project.

Patrick, thank you for being such a great source of knowledge, many ideas stemmed from your 'brain dumping' sessions. Paul, thank you for your guidance throughout. Bartira, thank you for the opportunity to work in your lab in Rio! You helped me to settle in to both the lab and life in Rio. Everyone in your lab was kind and made me feel welcome. You introduced me to my hosts, Fernando and Sarah. They ensured I had a fantastic experience and, because of them, I met my friend, Mari, who I hope to stay close to, despite the distance.

I'd like to acknowledge the staff at Durham University, especially everyone in the NMR, mass spectrometry and chromatography service for their assistance.

Thanks to everyone in CG001, past and present. It has been very enjoyable working in the lab with you and I will miss our trips to the Court Inn for lasagne and gin & tonics. A special thank you goes to Douglas as my PhD would have been significantly harder without his advice and training in both Durham and Rio. Jay and Courtney, I am lucky to have worked with you both. Talking about chemistry with you has been helpful and motivational but, equally, thank you for the general life chats as I think they're the ones that have kept me sane! Vanessa, thank you for all your help and being as equally crazy as me - it has made finishing my PhD so much more fun. Tim, I still appreciate your help as much as I did 8 years ago on our first day of undergraduate labs... when you taught me how to use a padlock!

Thank you Ryan for your encouragement, patience and holidays throughout my PhD. Seeing you at the weekend always lifted my spirits. Finally, my deepest gratitude to my parents for their endless love and support throughout my time at Durham University, this journey would not have been possible without you.

'You can do anything you set your mind to' is the life lesson my dad taught me when I was 13… it turns out he was right.

Declaration

The work presented in this thesis was carried out in the Department of Chemistry at Durham University, UK and in the Instituto de Biofísica Carlos Chagas Filho at Universidade Federal do Rio de Janeiro, Brazil between October 2015 and May 2019. All work is the author's own, except for collaborative, which is acknowledged where appropriate. No part of this work has been submitted for any other degree at this or any other University.

Statement of Copyright

Contents

Abbreviations

A. annua: *Artemisia annua*

AmpB: amphotericin B

aq.: aqueous

Ar: aryl

ATP: adenosine triphosphate

A.U.: arbitrary units

BMDM: bone-marrow-derived macrophages

Cbz: carboxybenzyl

CC_{50}: 50% cytotoxic concentration

CL: cutaneous leishmaniasis

COSY: correlation spectroscopy

DAG: diacylglycerol

DCE: 1,2-dichloroethane

DCM: dichloromethane

de: diastereomeric excess

DMF: dimethylformamide

DNA: deoxyribonucleic acid

EC_{50}: median effective concentration

eq.: equivalent(s)

ER: endoplasmic reticulum

ES-MS: electrospray mass spectrometry

GFP: green fluorescent protein

G1 phase: gap 1 phase

G2 phase: gap 2 phase

GC-MS: gas chromatography-mass spectroscopy

h: hour(s)

HDAC: histone deacetylases

HIV: human immunodeficiency viruses

HMBC: heteronuclear multiple bond correlation

HMGR: 3-hydroxy-3-methylglutaryl coenzyme A reductase

HPLC: high performance liquid chromatography

HPTLC: high performance thin-layer chromatography

HSQC: heteronuclear single quantum coherence

IC_{50}: half maximal inhibitory concentration

IgG: immunoglobulin

IPC: inositol phosphorylceramide

IPCS: inositol phosphorylceramide synthase

IR: infrared

IV: intravenous

IL: intralesional

IP: intraperitoneal

KDAC: lysine deacetylases

L-AmpB: liposomal amphotericin B

LC-MS: liquid chromatography-mass spectrometry

LDA: limiting dilution assay

lit.: literature value

Lmj: Leishmania major

min: minute(s)

ML: mucocutaneous leishmaniasis

M.p.: melting point

MMV: Medicines for Malaria Venture

mTor: mammalian target of rapamycin

NBD: nitrobenzoxadiazole

NCE: new chemical entity

NINDS: National Institute of Neurological Disorders and Stroke

NMR: nuclear magnetic resonance

NOESY: nuclear Overhauser effect spectroscopy

PI: phosphatidylinositol

PI3K: phosphoinositide 3-kinases

ppm: parts per million

p-TSA: *para*-toluenesulfonic acid

RCM: ring-closing metathesis

rt: room temperature

SAR: structure-activity relationship

S. cerevisiae: Saccharomyces cerevisiae

SI: selectivity index

SLS: sphingolipid synthase

SMS: sphingomyelin synthase

S_N: nucleophilic substitution

S phase: synthesis phase

SPT: serine palmitoyl transferase

$t_{1/2}$ = terminal elimination half-life

T. brucei: *Trypanosoma brucei*

T. cruzi: *Trypanosoma cruzi*

THF: tetrahydrofuran

TLC: thin-layer chromatography

TMS: trimethylsilyl

TOR: target of rapamycin

VL: visceral leishmaniasis

WHO: World Health Organisation

WT: wild type

X: a fixed proportion

1. Introduction

1.1. Overview

The work in this thesis is aimed at utilising the antileishmanial drug target inositol phosporylceraminde synthase (IPCS), an essential enzyme involved in sphingolipid biosynthesis. Previous work identified clemastine **1**, an over-the-counter antihistamine, as an inhibitor of *Leishmania major* IPCS (*Lmj*IPCS) and therefore later chapters will investigate repurposing clemastine **1** as a potential therapy for the neglected tropical disease leishmaniasis.

This thesis is made up of 8 chapters. Chapter 2 will provide details on the drug target IPCS and describe previous work carried out by the group including the identification of the drug candidate clemastine **1**. Chapter 3 will discuss the activity of clemastine **1** *in vitro* and its efficacy in a mouse model. Chapter 4 and 5 will present the work undertaken to develop synthetic routes to clemastine analogues and obtain structure-activity relationship (SAR) data to probe *Lmj*IPCS and identify a more potent and selective drug candidate. Chapter 6 will discuss any additional work including the synthesis of fluorescent analogues and imaging *in vitro*. Finally, Chapter 7 and 8 will detail the chemical and biological experimental procedures developed in this project.

The remaining section of this chapter reviews previous drug repurposing strategies in the search for new treatments for leishmaniasis.[1]

1.2. Drug repositioning

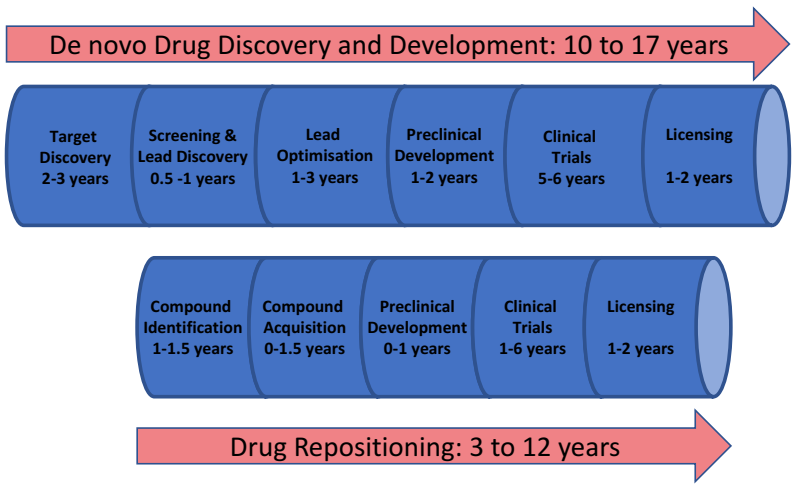

Figure 1: Drug discovery and repositioning pathways[2]

The introduction of a new drug from initial concept to public release is a slow expensive process. Developing a new chemical entity (NCE) drug and delivering it to market, d*e novo* drug discovery (Figure 1), is estimated to take 10-17 years and cost ~$1.8 billion.[3] Moreover, the probability of success is lower than 10% and the costs of late stage failures in this process are significant and are accounted for in the high cost of patented drugs. Consequently, the discovery of new drugs for leishmaniasis, and other neglected tropical diseases, for which the average patient suffering from visceral leishmaniasis (VL) exists on an income of less than $2 per day, is simply not a commercially viable operation for pharmaceutical companies without significant cross-subsidy.

Alternative strategies are therefore needed and the process of drug repositioning or repurposing, where new applications for existing drugs or drug candidates are discovered and refined, has become increasingly common.[4,5,6,7,8,9,10] When using a drug repositioning strategy several development phases necessary to develop NCE drugs can be bypassed or considerably shortened (Figure 1) because candidates will have passed various checkpoints and information is available about their pharmacokinetic and safety profiles. Reflecting this, the process of finding new uses for drugs outside their original indication is becoming increasingly successful as more companies are screening their libraries for repositioning candidates. Figure 2 illustrates two examples of approved drugs possessing optimum properties for their new indication. However, it should be noted that these cases are relatively rare and some development work is still commonly required. Moreover, whilst serendipity (phenotypic screening) can play a sizeable role in identifying repurposed drugs, it is important to establish the molecular connection between old drugs and new targets as this information aids the development of the new therapeutics. Despite these caveats drug repositioning can reduce time, cost and risk, and is a particularly attractive approach for neglected tropical diseases where new medications are needed urgently to treat the poorest of people. This review, will focus on the neglected tropical disease, leishmaniasis, and how repositioning strategies have shown potential to enable the discovery of new medicines for this disease.

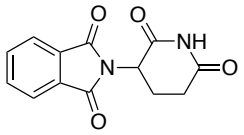

Thalidomide first marketed as a mild sleeping pill caused birth defects around the world. It is now used to treat certain cancers and leprosy.

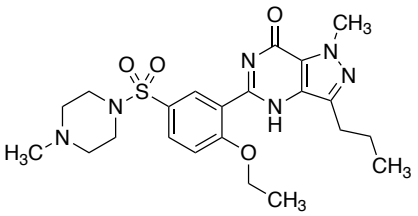

Sildenafil (Viagra) origionally discovered as a treatment for cardiovascular disorders. It is now used as a treatment for erectile dysfunction and pulmonary arterial hypertension.

Figure 2: Examples of old drugs directly repositioned as treatments for new diseases and dysfunctions

1.3. Leishmaniasis

Leishmaniasis is an important vector borne ´Neglected Tropical Disease' caused by protozoan parasites of the genus *Leishmania*.[11] *Leishmania* spp. (causative agent of Leishmaniasis), *Trypanosoma brucei* (causative agent of Human African Trypanosomiasis, HAT), and *Trypanosoma cruzi* (causative agent of Chagas disease) belong to the Trypanosomatidae family. *Trypanosomatids* are a subgroup of *Kinetoplastids* and distinguished by having only a single flagellum (Figure 3).

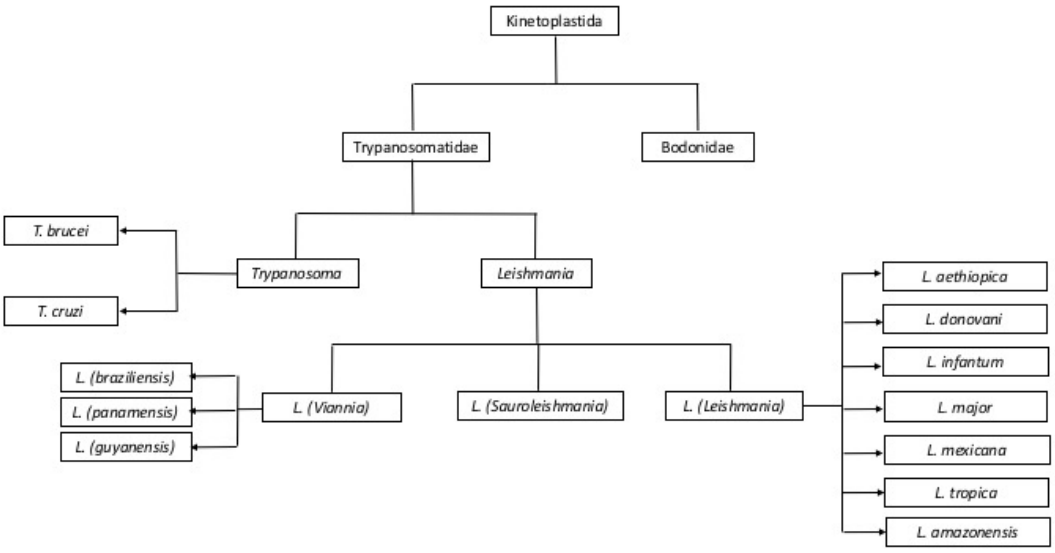

Figure 3: Taxonomy of Kinetoplastida (the *Leishmania* species shown are those of major medical importance to humans)

Over 350 million people world wide are considered at risk of leishmaniasis, 12 million people currently infected[12] and one million new cases reported annually. This has resulted in more than 30,000 deaths each year[13] and an economic cost that can be best estimated in terms of 2.4 million disability adjusted life years, the health challenge is only surpassed amongst parasitic diseases by malaria, schistosomiasis and lymphatic filariasis.[14,15] Consequently, leishmaniasis has been classified by the World Health Organisation (WHO)

as Category I: emerging or uncontrolled diseases. In particular, the spread and severity of infection is exacerbated by its status as an important co-infection of AIDS patients and the overlap in prevalence of HIV and *Leishmania* spp.[16] The disease is endemic in 98 countries across 5 continents and has strong links with poverty, principally affecting low income regions of Africa, Asia and Latin America.[17] However, the impact of the disease is spreading and, reflecting population movements and climate change, leishmaniasis has also been recorded with growing frequency in Southern Europe.[18]

Leishmaniasis is transmitted through the bite of infected female phlebotomine sandflies. Subsequently, in the mammalian host, flagellated promastigote *Leishmania* spp. are taken up by macrophages where they transform into the non-flagellated amastigote form, proliferate and cause disease. Infected macrophages can then be taken up by the insect vector during a second blood meal, the parasite then transforms back to the promastigote form and the cycle is perpetuated (Figure 4). Importantly, many *Leishmania* spp. can infect multiple mammalian species leading to animal reservoirs for human infection, most notably in canines.[19]

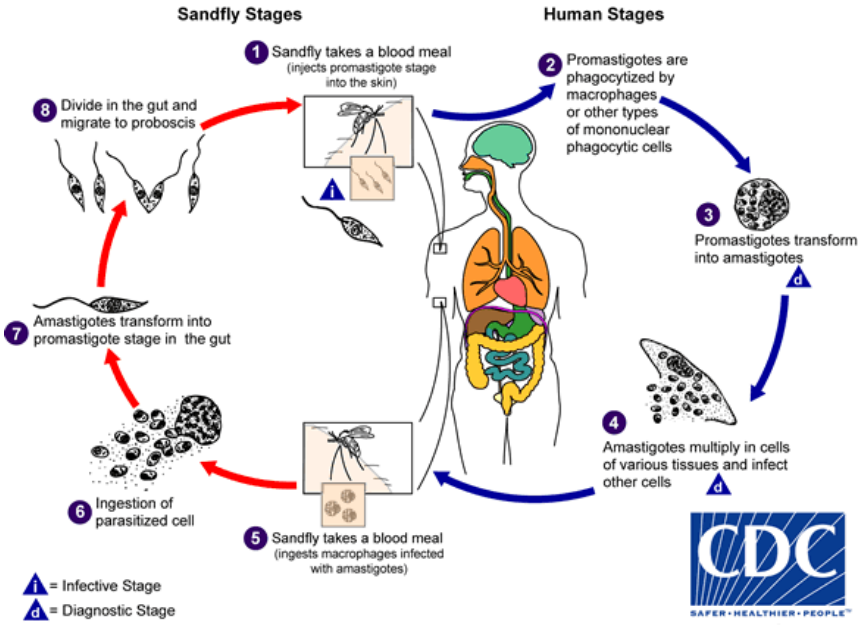

Figure 4: Life cycle of *Leishmania* spp. (reproduced from CDC[19] with permission)

Human disease is caused by 20 of the 31 parasite species that infect mammals with the different species leading to different clinical manifestations.[20] Depending on parasite tropism for skin or visceral macrophages, and host immune status, clinical forms range from localised cutaneous leishmaniasis (CL), diffuse CL, disseminated CL, mucosal leishmaniasis (ML), to visceral leishmaniasis (VL) (Table 1). The most common form of the

disease is CL which, although not fatal, leads to slow growing skin lesions which leave permanent scars and in some cases cause serious disability. ML is the most disfiguring form and causes destruction of soft tissue in the nose, mouth and throat. In contrast, VL is the most severe form of the disease as it affects the vital organs of the body and is fatal if left untreated.[21]

Treatment of leishmaniasis is challenging and there are currently no vaccines or prophylactic drugs to prevent human infection. For over 70 years, the mainstay of antileishmanial therapy has been pentavalent antimonials (Pentostam **2** and Glucantime **3**) which are administered by slow intravenous or intramuscular injections.[22] The mode of action is not fully understood but one possibility involves the biological reduction of Sb(V) to Sb(III) by the parasite or by infected host cells to create antileishmanial activity.[23,24] Unfortunately, antimonials are also toxic[25] and reports of resistance are becoming increasingly common. For example, a study of the efficacy of Pentostam **2**, in North Bihar, India, revealed that only 36% of patients could be cured when treated with a dose of 20 mg kg^{-1} for 30 days.[26]

For the past seven decades, amphotericin B **4** (AmpB) and pentamidine **5** have been used in case of antimonial failure.[22] Pentamidine **5** is an antimicrobial medication that was commonly used as a second line, parenteral, treatment for leishmaniasis in the case of antimonial failure. The primary mode of action of pentamidine **5** in kinetoplastids is not well understood but there is some evidence that it inhibits the active transport system and disrupts the mitochondrial membrane potential. However, pentamidine **5** has lower efficacy than AmpB **4**[27] and this, coupled with severe toxicity, have resulted in a gradual decline in its use.[28]

The antifungal drug AmpB **4**, first isolated in 1955, was reported to have antileishmanial activity in the early 1960s. AmpB **4** binds to ergosterol, forming pores in the membrane which leads to the death of the parasite.[29] Whilst severe side effects limited its use, liposomal formulations that circumvent these problems have been developed. However, a course of L-AmpB **4** still requires parenteral administration and, without extensive subsidy is expensive (up to $3,000 per course). This makes L-AmpB **4** inaccessible to most patients who live in the poorest, least developed regions. In comparison, an equivalent course of

pentavalent antimonials costs between $150 and $198.[30] Despite this, L-AmpB **4** is now often preferred over Pentostam **2** for VL because it is less toxic and there are fewer reports of parasitic resistance.[26,31]

Along with L-AmpB **4**, paromomycin **6** and miltefosine **7** are now approved drugs for VL.[32] Paromomycin **6** is an antibiotic and a relatively new therapy for the parenteral treatment of VL in India. It has been shown to be effective and relatively cheap first-line treatment with low toxicity, requiring a course of 15 mg/kg for 21 days.[28,33] The mechanism of action is not fully understood but it is thought to inhibit protein synthesis.[34] As with the other treatments there are drawbacks, the drug is administered by injection[35] and shows poor efficacy in some regions in Africa.[36]

As discussed above, these current medications all involve prolonged parenteral administration which leads to many complications, including poor patient compliance, blood-borne disease from unsanitary conditions and the need for medical facilities. Therefore, in the past two decades there has been a focus on developing new oral therapies. In 2002 miltefosine **7**, originally developed as an anticancer agent, was introduced as the first oral antileishmanial agent.[37] The primary mechanism of action is poorly understood, although the drug is thought to involve disruption of ether-phospholipid metabolism, glycosylphosphatidylinositol anchor biosynthesis and signal transduction within the parasite.[28] Miltefosine **7** efficacy against both VL and CL has been reported and, in 2014, the US Food and Drug Administration approved the drug for all forms of leishmaniasis.[38] However, this oral therapy does have limitations, including high costs and teratogenic effects. Moreover, the long-term effectiveness of miltefosine **7** is questionable, with reports of VL relapses in Nepalese patients treated with this drug. In addition, miltefosine **7** resistance is readily induced in *L. donovani in vitro*.[39]

In conclusion, all current treatments (Figure 5) have serious limitations such as high cost, route of administration, severe toxic side effects and increasing drug resistance. Currently, there are some new therapies under clinical investigation as monotherapies or in combination with existing antileishmanials.[40,40,41,42,43,44] These include paromomycin **6** topical cream, currently in phase 3 trials as a treatment for CL, and sitamaquine **8** in phase 2 to treat VL.

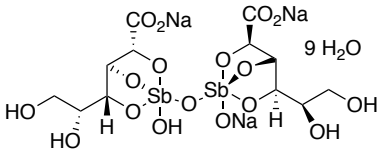

Pentostam **2**

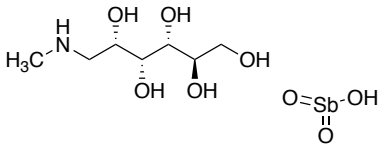

Glucantime **3**

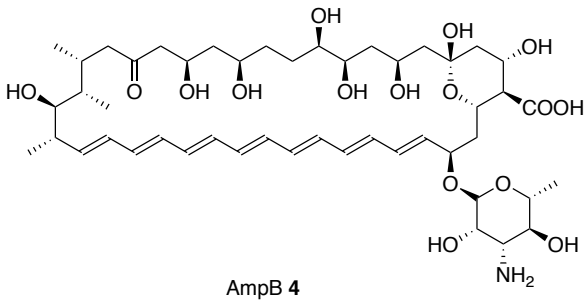

AmpB **4**

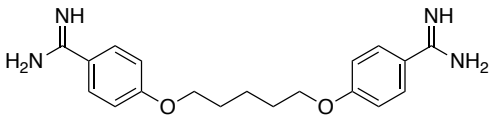

Pentamidine **5**

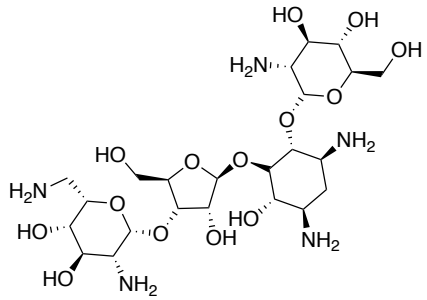

Paromomycin **6**

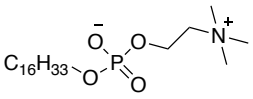

Miltefosine **7**

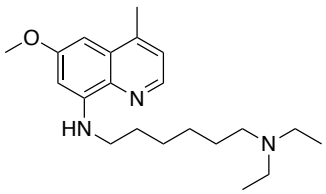

Sitamaquine **8**

Figure 5: Current antileishmanials

1.4. Repositioning of drugs targeting leishmaniasis

Significantly, as noted above in the Introduction, many of the existing therapies for leishmaniasis are licensed or were initially intended for other illnesses. For example, AmpB **4** is an antifungal drug, paromomycin **6** is an aminoglycoside antibiotic used to treat intestinal infections, and miltefosine **7** was originally developed as an anticancer agent. This section will review drugs for different disease states; cancer, microbial infection, depression, allergies and others; that have shown potential to be repurposed as new antileishmanial therapies, and discuss their putative parasitic drug targets.

It should be noted that many natural products often used in traditional medicines have antileishmanial activity, including vast numbers of different alkaloids,[45,46] flavonoids,[47,48] chalcones[49,50,51,52] and terpenoids.[53,54,55,56] These compounds have been discussed extensively in previous literature[57,45,46,58] however, they are structurally complex

molecules, often affecting multiple targets and possess properties that make them unlikely to be orally active drugs. As such the greatest potential of natural products is for the identification of novel targets required to underpin target-based drug discovery and not as starting points for a repositioning strategy and therefore they will not be discussed further in this review.

1.4.1. Anticancer drugs

Both cancerous cells and *Leishmania* spp. have the ability to proliferate in a host organism for prolonged periods of time and some enzymes targeted by anticancer therapies can also be used in the development of antileishmanials (Figure 6, Appendix A).[59,60]

Kinases have long been recognised as a major target in oncology and this has spawned a number of efforts to repurpose a range of kinase inhibitors for leishmaniasis. For example, miltefosine **7** is the first, and still the only, oral drug in the treatment of VL but was originally developed as a treatment for breast cancer. Like many anticancer drugs, miltefosine **7** induces apoptosis through kinase inhibition. In this case the PI3K/Akt/PkB pathway is targeted and it has been reported that inhibition of this pathway may influence the susceptibility of host cell to *Leishmania* infection.[38]

The genomes of trypanosomatids encode at least 12 proteins belonging to the PI3K protein superfamily, many of which are unique to the parasites. The Target of Rapamycin (TOR) kinase is a member of the PI3K-related kinase (PKK) subfamily and has a central role in fundamental processes such as growth, cell shape and autophagy. Trypanosomatids possess four distinct genes belonging to the TOR family whereas mammals only possess one mTOR protein. On this basis, a targeted set of eight known mTOR inhibitors with varied potencies and selectivity for mTOR/PI3K were screened against *T. brucei*, *T. cruzi*, cutaneous *L. major* and visceral *L. donovani.* From these data, the mTor/PI3K inhibitor, Dactolisib **9**, was identified as being the most active against all the species tested and therefore was tested in animal models of *T. brucei rhodesiense*, *T. cruzi* and *L. major*. Unfortunately, no efficacy was observed against either *T. cruzi* or *L. major*; this may reflect the need for the drug to cross into the phagolysosomal compartment where the parasite resides. In contrast, and consistent with this hypothesis, Dactolisib **9** significantly reduced the parasite burden and extended the survival of mice infected with *T. brucei rhodesiense,*[61]

a blood stream parasite. Although the exact mechanism of action has yet to be identified this investigation has demonstrated a potential target in the search for antitrypanosomal therapies.

Similar small scale focused screens against specific kinase targets have been conducted. For example, through exploring Aurora kinases, hesperidin **10** has been identified as a putative antileishmanial lead but host cell toxicity was observed when the compound was screened against the hepatic cancer cell line.[62] Although, further structure-activity relationship (SAR) studies demonstrated that these inhibitors are not general toxins but can be modified to improve selectivity, useful antileishmanial selectivity was not obtained. More significantly, and consistent with other reports,[63] there was no correlation between activity against promastigotes and axenic amastigotes with the latter being the less sensitive form.

Although target-based screening is an attractive strategy, the need for a specific orthologous target protein may not be essential as many kinase inhibitors affect multiple proteins and simply the proven cellular accessibility of these compounds is a sufficient starting point. For example, tyrosine kinases are not expressed in trypanosomatids, but protein phosphorylation occurs in parasites and therefore kinase inhibitors may interact with other enzymes.[64,65] Reflecting this, in a screen of eleven tyrosine kinase inhibitors, sunitib **11**, sorafenib **12** and lapatinib **13** showed antileishmanial activity against intracellular *L. donovani* amastigotes.[66] Control experiments confirmed that the leishmanial targets were unlikely to be the same as those found in mammalian cells and these kinase inhibitors showed a degree of selectivity against amastigotes compared with mammalian cells. In addition, an oral dose of sunitib **11**, sorafenib **12** and lapatinib **13** reduced liver parasite burden in mice infected with *L. donovani*. Whilst these screens identify new leads, the challenge for such studies is in the identification of the actual target to guide further optimisation.

Kinases also proved to be the most common predicted target from a set of 192 antileishmanial compounds identified from a high throughput phenotypic screen of 1.8 million compounds against representative kinetoplastid species, including *L. donovani*.[65] However, since most of these compounds have no literature precedent this was not strictly

a repurposing study, and further discussion is outside the scope of this review. Finally, an interesting, and somewhat different, study involving the repurposing of kinase inhibitors, was the use of imatinib **14** (Gleevec, another tyrosine kinase inhibitor used in the treatment of multiple cancers) to target the host macrophage AbI and Arg kinases believed to be involved in parasite entry to the cell. Mice infected with *L. amazonensis* were treated with oral imatinib **14** which resulted in smaller lesions that developed later and a reduction in parasite burden relative to controls.[67] Imatinib **14** is a clinically approved drug with relatively benign side effects when compared to antileishmanials on the market. It would be of great benefit to further understand the cell entry pathway to provide new lines of therapy for leishmaniasis.

The approach of starting with inhibitors with known modes of action, for example against mammalian kinases, and screening for new antileishmanial activities for which orthologous protozoal targets can then be identified is an attractive concept. However, good levels of host parasite selectivity are required before any hits can be repurposed as antiparasitic therapeutics. This was nicely illustrated in a study exploring Lysine Deacetylases (KDAC) as putative antileishmanial drug targets. KDACs are one of the most studied epigenetic drug targets of humans[68] and inhibition of their activity is a validated strategy for cancer treatment.[69] As with the kinases discussed above, *Leishmania* spp. have multiple genes encoding different KDACs isoenzymes some of which are essential to parasite survival.[69] Whilst, the homology between kinetoplastid and mammalian KDACs is low (~40%) much higher levels of similarity are found in active site residues.[68] Reflecting this only one compound, Hydroxamate **15**, showed significant selectivity (~10 fold) between host cell and parasite and high (nanomolar) activity against axenic *L. donovani* amastigotes.[68]

Paclitaxel **16** is sold under the brand name Taxol and is used to treat a number of cancers. Drugs that target microtubule assembly may be a class of potential antileishmanials since tubulin is one of the most abundant leishmanial proteins.[70] Unlike many drugs that target tubulin, paclitaxel **16** does not inhibit microtubules but stabilises their assembly, which in turn blocks mitosis. Taxol at nanomolar concentrations inhibits the growth of both *L. donovani* promastigotes and intracellular amastigotes and was selective for the parasite over the mammalian macrophage.[71,70]

In the cell cycle, the interphase is before the mitotic (M) phase and is an important period for antileishmanials to target. The interphase can be broken down into three steps: The G1 phase responsible for cell growth and increasing number of proteins and organelles; the S phase involving DNA duplication and histone production and finally the G2 phase which is the last chance the cell has to prepare for mitosis and involves further duplication of DNA, organelle replication and protein synthesis.[72]

Hydroxyurea **17** is used to treat myelogenous leukemia and cervical cancer as well as sickle-cell disease. More recently, hydroxyurea **17** has been shown to possess *in vitro* activity against *L. mexicana* causing cell cycle arrest at the G1/S transition in promastigotes. As such, hydroxyurea **17** is a potential drug candidate to treat leishmaniasis with the added advantage of conventionally being administered orally.[73]

Cisplatin **18** is another anticancer drug, which has been shown to cause cell cycle arrest in *Leishmania*, but this time at the S and G2 phases in promastigotes and axenic amastigotes. This platinum-containing drug is used to treat various cancers and has shown *in vitro* and *in vivo* activity against VL.[74,75] However, cisplatin **18** does not completely eliminate the parasite at the low dosages of 0.5 and 1 mg kg^{-1} and higher doses (≥ 1 mg kg^{-1}) can cause nephrotoxicity. Therefore, a more recent study has used 5 and 2.5 mg kg^{-1} of cisplatin **18** in combination with different antioxidants (e.g. vitamin C, vitamin E and silibinin) to successfully reduce nephrotoxicity and parasite burden making the combination a potential antileishmanial therapy.[76] In addition, nanocarriers (e.g. single- and multi-walled carbon nanotubes) improve the intracellular uptake of the drug in infected cells, and effectively reduce the dosage. For example, a recent study showed that cisplatin **18** bound to multi-walled carbon nanotubes had greater activity and selectivity against *L. major* amastigotes compared to free cisplatin **18**; however, the efficacy of this therapy still needs to be evaluated in an animal model.[77]

Doxorubicin **19** is used to treat a range of cancers through inhibition of topoisomerase II and shows *in vitro* activity against VL. Like cisplatin **18**, nanocapsules bearing doxorubicin **NCs-19** have been prepared and show greater activity than free doxorubicin **19** both *in vitro* and *in vivo*.[78]

A final class of anticancer agents that may have potential as antileishmanials are the selective estrogen-receptor modulators, tamoxifen **20** and raloxifene **21**. Tamoxifen **20** is used to prevent and treat breast cancer and whilst raloxifene **21** can reduce the risk of breast cancer in those at high risk, it is mostly used to prevent and treat osteoporosis in post-menopausal women. Both have been identified as potential candidates for leishmaniasis treatment with micro-molar potency against intracellular *L. amazonensis* amastigotes.[79,80,81] The exact mechanism of action of tamoxifen **20** and raloxifene **21** is still unclear as estrogen responses have not been described in *Leishmania* spp.[82,83] However, a recent study showed one of the most likely targets of tamoxifen **20** is inositol phosphorylceramide synthase (IPCS). As it will be discussed in chapter 2, this enzyme is involved in the biosyntheisis of sphingolipids, which are essential components of the cell membrane in *Leishmania*. Sphingolipids are important in a range of biological processes such as cell signalling, growth, differentiation and apoptosis. In addition, inositol phosphorylceramide (IPC) is the most abundant sphingolipid in *Leishmania* and is absent in mammalian cells.[84] Therefore, IPCS, which is the enzyme responsible for IPC, has the potential to be a valuable target for new antileishmanials and will be discussed in more detail in later chapters of this thesis.

In contrast, raloxifene **21** is thought to damage the cell membrane and the mitochondrion of the parasite.[79] Whilst the antileishmanial activity of these compounds has not necessarily been optimised, the proven safety profile of these repurposed drugs allows them to be considered as synergists in combination therapies to help combat growing concerns about the emergence of parasitic resistance. For instance, combination of tamoxifen **20** and miltefosine **7** *in vitro* and *in vivo* revealed no interaction between the two drugs and suggested that tamoxifen **20** could slow the emergence of miltefosine **7** resistance.[80]

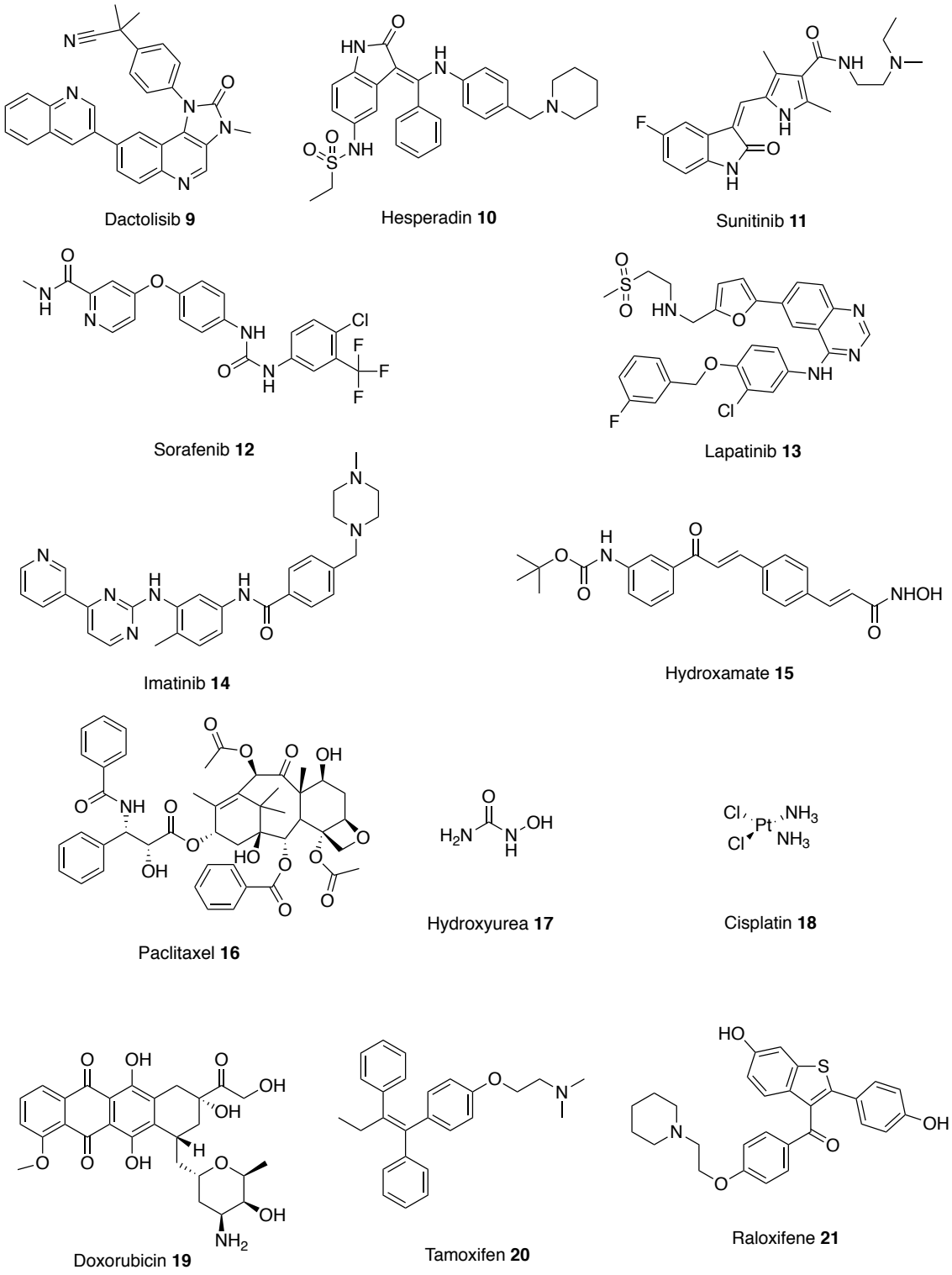

Figure 6: Treatments for cancer that could be repurposed as antileishmanials

1.4.2. Antimicrobial drugs

An antimicrobial is any compound that kills or inhibits the growth of a microorganism; this can include bacteria, fungi, viruses and protozoa. Antimicrobial drugs that were originally licensed for other indications have already been repurposed as antileishmanial therapies. For example, AmpB **4** and pentamidine **5** are antifungal medications and paromomycin **6** is

used to treat the parasitic diseases, cryptosporidiosis and amoebiasis. These examples of successfully repurposed antimicrobials as treatments for leishmaniasis have encouraged further investigation into the leishmanicidal activity of other antimicrobial drugs (Figures 7-10, Appendix A).

1.4.3. Antifungals

As discussed above, the main use of AmpB **4** is in the treatment of a wide range of fungal infections but is now also used to treat VL. Liposomal AmpB **4** is the treatment of choice for immunocompetent patients in the Mediterranean region and the preferred drug for HIV/VL co-infection.[85] AmpB **4** functions by binding to ergosterol disrupting the plasma membrane. This is the major sterol of the fungal plasma membranes and there are other antifungal azoles, which inhibit C14α-demethylase, an essential enzyme in the biosynthesis of ergosterol. As the sterol biosynthesis pathway is conserved in *Leishmania* spp. parasites and is important for their survival,[86] these antifungal azoles have the potential to be repurposed as antileishmanials.

Fluconazole **22** and terbinafine **23**, two antifungal azoles which have similar modes of actions, can be administered orally and possess low levels of toxicity; therefore, the use of these drugs as putative antileishmanials in clinical trials can be approached with some confidence. Oral fluconazole **22** was shown to be a safe and useful drug for the treatment of CL caused by *L. major* [41] and was reported to be more efficacious in higher doses after a phase 2 clinical study.[87] However, a recent phase 3 clinical trial of the use of high dose fluconazole **22** in the treatment CL caused by *L. braziliensis* and *L. guyanensis* was terminated due to a low cure rate, suggesting species dependent activity.[88] The potential for terbinafine **23** as a new treatment for CL was first described in 1997. Significantly, at the dosage used, no patients reported any side effects. However, the efficacy appears lower than other azole antifungals notably, ketoconazole **24** and itraconazole **25**, and further investigation is required to optimise the efficacy of the drug before it can be considered as an effective solution.[40] One method being investigated is using terbinafine **23** in combination therapies. For example, oral terbinafine **23** and cryotherapy has completed phase 1 of clinical trials for treatment of CL and results show a similar level of efficacy to glucantime **3**.[89] In addition, the antileishmanial effect of terbinafine **23** has led to the discovery of butenafine **26** which is another allylamine antifungal drug able to eliminate promastigotes and amastigotes of *L. amazonensis* and *L. braziliensis*.[90]

Positive results, coupled with attractive pharmacokinetic and safety profiles, with these antifungal azoles have encouraged the investigation of similar compounds. For example, itraconazole **25** and posaconazole **27** exhibit *in vitro* and *in vivo* activity against *L. amazonensis*, *L. donovani* and *L. infantum*.

In addition, in a separate study, econazole **28**, bifonazole **29** and chlotrimazole **30** showed activity against *L. infantum chagasi* promastigotes and econazole **28** showed similar intramacrophage effectiveness to miltefosine **7**. Unfortunately, bifonazole **29** and chlotrimazole **30** showed no activity against intracellular amastigotes.[91] However, chlotrimazole **30** complexed to ruthenium shows activity against *L. major* intracellular amastigotes and a reduction in parasite burden in an animal model of CL.[92, 93]

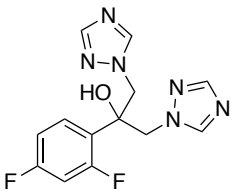

Fluconazole **22**

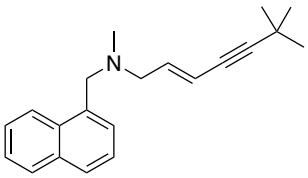

Terbinafine **23**

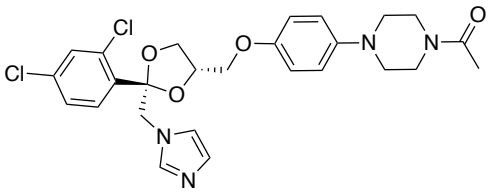

Ketoconazole **24**

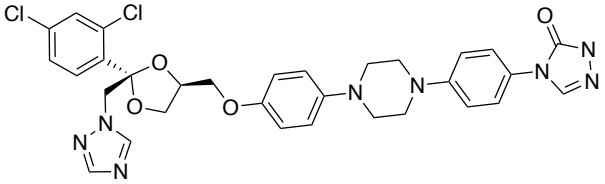

Itraconazole **25**

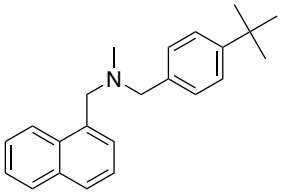

Butenafine **26**

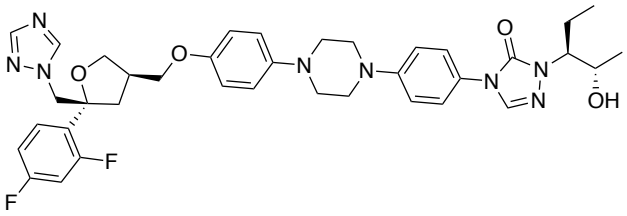

Posaconazole **27**

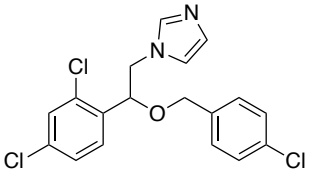

Econazole **28**

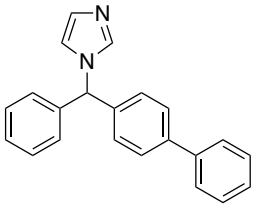

Bifonazole **29**

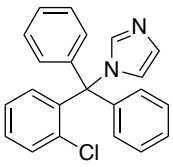

Clotrimazole **30**

Figure 7: Antifungal drugs that could be repurposed as antileishmanials

1.4.4. Antiparasitics

A second source of antimicrobial compounds that have been exploited as antileishmanials are, not surprisingly, other antiparasitics. In one approach, a collection of 400 compounds obtained from Medicines for Malaria Venture (MMV) was screened for antileishmanial activity. Significantly, in contrast to many other such approaches which use promastigote or axenic amastigotes, this study developed an assay using intracellular amastigotes, thus enabling screening against the most clinically relevant form of the parasite.[94] The results identified 14 antimalarial drugs that have antileishmanial activity. The compound of most

interest was the anticancer drug, MMV666080 **31**, which, with an IC_{50} of 15 nM, is more potent and also less toxic than AmpB **4**. In addition, a series of substituted aminobenzimidazoles (**32-34)** were identified from this screen as active antileishmanials with IC_{50} values ranging from 61 nM to 134 nM. A current focus for these compounds is to validate the results using *in vivo* models.[95]

A second set of studies has focused on the use of nitazoxanide **35**, an oral drug used in the treatment of infectious diarrhea caused by the protozoan parasites, *Cryptosporidium parvum* and *Giardia lamblia.* The lethal action of nitazoxanide **35** against *L. infantum* involves upregulation of reactive oxygen species resulting in oxidative stress and parasite death.[96] Nitazoxanide **35** *also displays activity against L. donovani* and *L. amazonensis,*[97,98] with spleen and liver parasite load being reduced by 86% in *L. donovani*-infected mice.[97] In addition, nitazoxanide **35** demonstrates low cytotoxicity against mammalian VERO cell line and exhibits activity against *Giardia intestinalis* and *Trichomonas vaginalis*; therefore derivatives of nitazoxanide **35** would generally be attractive starting points for new antiparasitic drugs [98].

Due to the closer taxonomy lineage, it would be expected that anti-trypanosomal drugs would be more likely repurposed to leishmaniasis than other antiparasitics. However, apart from pentamidine **5** used to treat African trypanosomiasis caused by *Trypanosoma gambiense*, no other anti-trypanosomal drugs including those used to treat Chagas disease are presently used against leishmaniasis.

Whilst nitroaromatics, such as nitazoxanide **35**, are generally avoided in the pharmaceutical industry due to the known potential mutagenicity and carcinogenicity of the nitro group, recent research has revealed the potential of nitroaromatics to treat neglected parasitic diseases.[99] Reflecting this, another antiparasitic nitroaromatic compound, fexinidazole **36**, is being explored as a potential treatment for leishmaniasis. Fexinidazole **36** is in clinical trials for treating African trypanosomiasis (*T. brucei*) and Chagas disease (*T. cruzi*) where the mechanism of action is proposed to involve reductive activation of the nitro group by NADH-dependent bacterial-like nitroreductase. A study involving the overexpression of the leishmanial orthologue of the nitroreductase demonstrated that a similar mechanism occurs in *Leishmania spp*. Building on this fexinidazole **36** and its two predominant *in vivo*

metabolites (fexinidazole sulfoxide and sulfone) displayed excellent activity against *L. donovani* promastigotes and axenic amastigotes. However, fexinidazole **36** was inactive against intracellular amastigotes whereas fexinidazole sulfoxide and sulfone remained potent against intracellular amastigotes (both EC_{50} values equal to 5.3 μM). When progressed into a murine model infected with *L. donovani* a 98% suppression of infection was observed with a single daily dose of fexinidazole **36** for 5 days.[100] With this positive data, fexinidazole **36** was progressed into clinical trials as a treatment for VL. In 2013, a phase two study tested fexinidazole **36** on 14 patients suffering with VL and all patients showed clinical improvement during treatment. Unfortunately, treatment relapses were observed and thus the study was terminated in 2014 due to lack of efficacy.[101] However, fexinidazole **36** is now being investigated as a combination therapy with miltefosine **7** in Eastern Africa.[102]

Artemisinin **37** was first isolated in 1971 from the plant, *Artemisia annua*, and today artemisinin **37** and its derivatives are well established anitimalarials.[103] This sesquiterene lactone contains an unusual endoperoxide bridge, which is essential for antimalarial activity. One of the proposed mechanisms of actions is the cleavage of this bond to generate free radicals that could act as alkylating agents and chemical modify a variety of parasite molecules.[104] In 1993 artemisinin **37** was shown to have efficacy *in vitro* and *in vivo* against CL but it was unknown whether the endoperoxide bridge was essential for activity.[105] More recently, gelatin capsules containing dried *Artemisia annua* (*A. annua*) leaf powder have been developed as an oral therapy for parasitic diseases. These capsules proved to be an effective treatment in a hamster model infected with *L. (V) panamensis* and 2 patients with CL were cured with 30 g of *A. annua* capsules, without any adverse reactions.[106] A separate study investigating the effects of artemisinin **37** against VL revealed that artemisinin **37** is 7 times more active against *L. donovani* amastigotes than promastigotes.[107] Although IC_{50} values are in the micromolar range, whereas only nanomolar concentrations are required for antimalarial activity, artemisinin **37** has a good selectivity index and should be progressed into an *L donovani*-infected animal model where micromolar concentrations can be achieved using oral, parenteral and rectal dosages.[107]

Mefloquine **38**, chloroquine **39** and hydroxychloroquine **40** are antimalarials which have been investigated for *in vitro* and *in vivo* activity against *L. amazonensis*. Their activity

against the promastigote form was first evaluated and mefloquine **38** was the only compound to show any significant activity. However, all three of these compounds showed activity against intracellular amastigotes. It has been suggested that the drug action is based on impairment of macromolecule absorption rather than an enhancement of the immune response.[108] Mefloquine **38** and chloroquine **39** were tested in a mouse model and results showed that treatment with chloroquine **39** by the oral route reduced lesion size and parasite burden. In contrast, mefloquine **38** administered by oral and topical routes reduced the lesion size but not the parasite burden. Further work is needed to understand the mechanism of action of chloroquine **39** but these results reveal that this antimalarial drug is also a potential drug candidate to treat CL.[108]

Levamisole **41** is a heterocyclic compound that is immunoregulatory and an effective antihelminthic agent.[109] Since the 1970s it has been studied as a therapy for CL[110] and a more recent study compared the effects of levamisole **41** and imidocarb **42**, a veterinary medicine used to treat parasite infection, in murine models infected with *L. amazonensis*. The results from a number of parameters (IgG levels, vacuolar area, megakaryocyte count in spleen and parasite burden) demonstrate that imidocarb **42** has the most potential as a therapy for CL.[111]

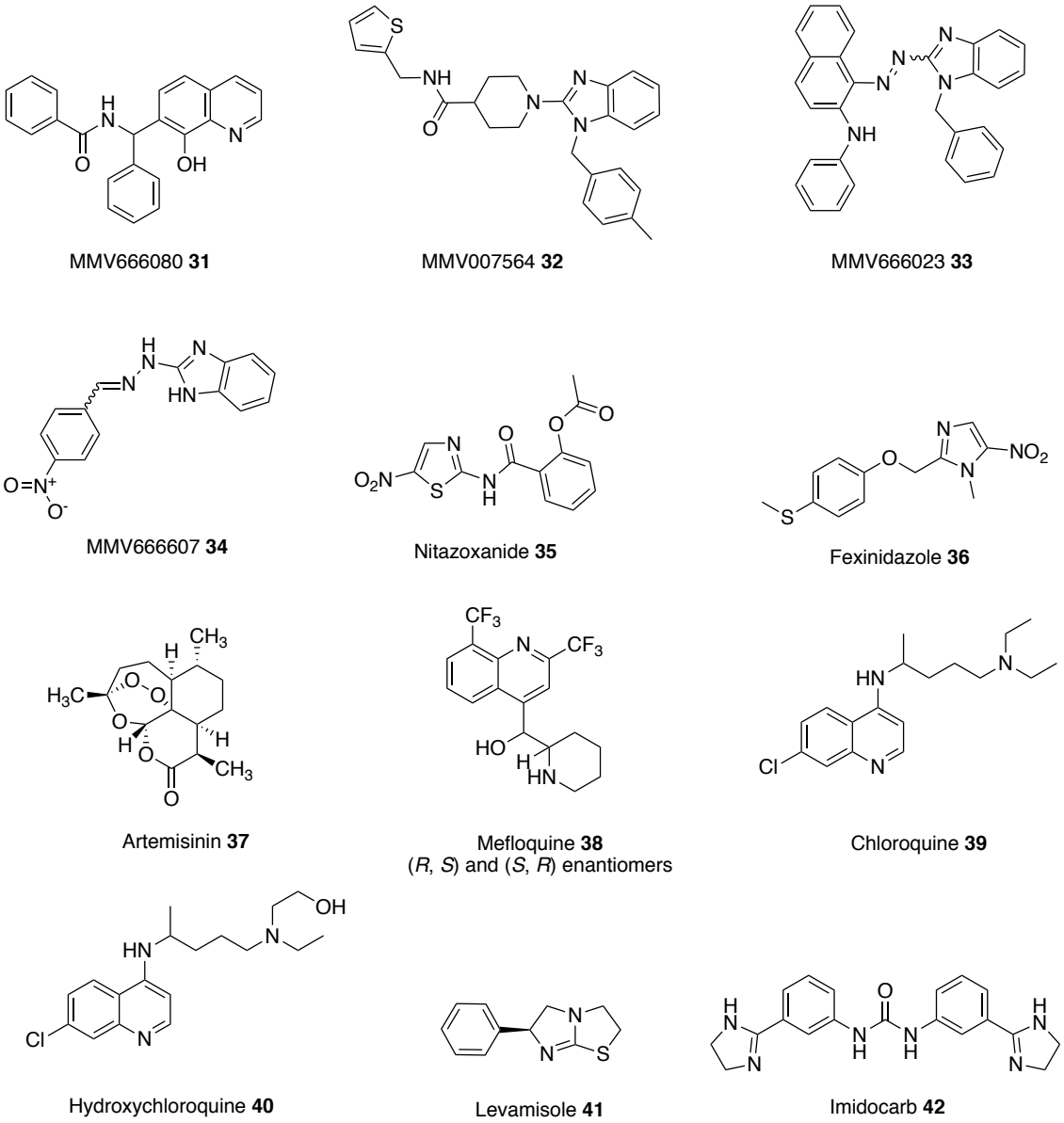

Figure 8: Antiparasitic drugs that could be repurposed as antileishmanials

1.4.5. Antibacterials

Metronidazole **43** is an antibiotic and antiprotozoal medication. It is not sold as an antileishmanial but has been employed to treat leishmaniasis for a number of years.[112,113] For instance, in 1976 21 of 30 patients with South American leishmaniasis were reported as cured when treated with metronidazole **43**.[114] However, the inefficacy of metronidazole **43** in animal models infected with *L. donovani* and *L. mexicana* has been reported.[115] In addition, two separate studies testing on patients suffering from cutaneous and mucocutaneous in Iran and Ethopia showed that intralesional metronidazole **43** injections were painful and had little effect on the treatment of leishmaniasis.[116,117] Therefore, further study into the route of administration and efficacy of metronidazole **43** as a treatment for leishmaniasis is required.

Azithromycin **44** is an antibiotic used to treat several bacterial infections and can also be used in combination with other medications to treat malaria. This azalide, a type of macrolide antibiotic, concentrates in the tissue and especially the macrophages. *Leishmania* resides in these cells and therefore it is an attractive drug candidate for *in vitro* and *in vivo* studies. One study showed promising activity against *L. major* promastigotes and intramacrophage amastigotes as well as *in vivo* efficacy against *L. major* infected mice.[118] This treatment was given *via* subcutaneous injection and more recent investigations have shown the superior activity of oral azithromycin **44** over oral miltefosine **7** in the treatment of *L. major* infected mice. However, a combination therapy of miltefosine **7** and azithromycin **44** showed signs of relapse after the end of treatment.[119] The effect of azithromycin **44** on other species of *Leishmania* was evaluated and revealed *in vitro* activity against *L. amazonensis*, *L. braziliensis* and *L. chagasi*.[120] An *in vivo* study showed activity against *L. braziliensis* and oral azithromycin has been used to treat patients with CL caused by this species.[121] However, it should be noted that this *in vivo* study was unsuccessful against *L. amazonensis*. Hence, azithromycin **44** could be used as a potential therapy for CL but there should be studies into its limitations in certain *Leishmania* species and in combination with other medications.

Clofazimine **45** is used in combination with rifampicin **46** and dapsone to treat leprosy. Clofazimine **45** has *in vitro* activity against *L. amazonensis*, *L. donovani* and *L. major* as well as being effective both orally and topically in an animal model of CL.[122] In addition, it is a highly lipophilic drug and therefore also concentrates in the macrophages where *Leishmania* resides. Unfortunately, clofazimine **45** was ineffective when used to treat cutaneous *L. major* infection in humans. Higher doses of the drug could be effective but clofazimine **45** has shown undesirable dose-related side effects. Therefore, further clinical trials of this drug for CL have been discouraged.[123] In contrast, positive results have been shown when rifampicin **46** is given as an oral therapy to treat humans with CL. In comparison to other antileishmanials available, rifampicin **46** is simple to administer, cheap and well tolerated by patients.[121] However, one study highlighted the failures of rifampicin **46** to cure patients with CL from Israel.[124] Therefore, efficacy against CL is uncertain and investigations are also focused on combination therapies.[125,126]

The activity and safety profile of fexinidazole **36** sparked the search for other nitroimidazoles which may have potential as oral treatments for VL. This identified the antituberculosis drugs PA-824 **47** and delamanid **48**, which can also undergo bioactivation by a nitroreductase, as potential leads.[127,128,129,130] As with fexinidazole **36** the presence of the nitro group has been shown to be essential for antileishmanial activity.[129,127] However, the nitroreductase found in *Mycobacterium tuberculosis* [deazaflavin (F420)-dependent nitroreductase (Ddn)],[131] is absent in *Leishmania* and over-expression of the leishmanial nitroreductase did not provide enhanced sensitivity to the drugs, suggesting a different mode of action. This suggests the potential for future combination therapies involving fexinidazole **36** and these antituberculosis drugs. These differences are reinforced by the observation that whilst the *(S)*-enantiomer of PA-824 **(*S*)-47** is currently in phase two clinical trials for tuberculosis it is the *(R)*-enantiomer of PA-824 **(*R*)-47** which shows superior activity against *L. donovani* parasites, both *in vitro* and *in vivo,* with a twice daily dose of PA-824 **(*R*)-47** at 100 mg kg^{-1} effectively curing a murine model of infection, suppressing infection by 99.9%.[129] More recently, the structurally similar compound delamanid **48**, (*R*)-enantiomer, has demonstrated high activity *in vitro* against intracellular *L. donovani* amastigotes. In addition, a twice-daily oral dose of this nitroimidazole at 30 mg kg^{-1} for 5 days cured the mice infected with *L. donovani.*[127] Whilst these compounds appear to show considerable potential, a cautionary note arises from the history of the chimeric nitroimidazole, DNDI-VL-2098. This compound, following promising early results, was at the final stages of preclinical development for the treatment of VL. However, results from animal models showed a link between dose, length of treatment and testicular toxicity leading to a decision to halt progression.[132] Whether this is a compound specific effect or a class problem remains to be established.

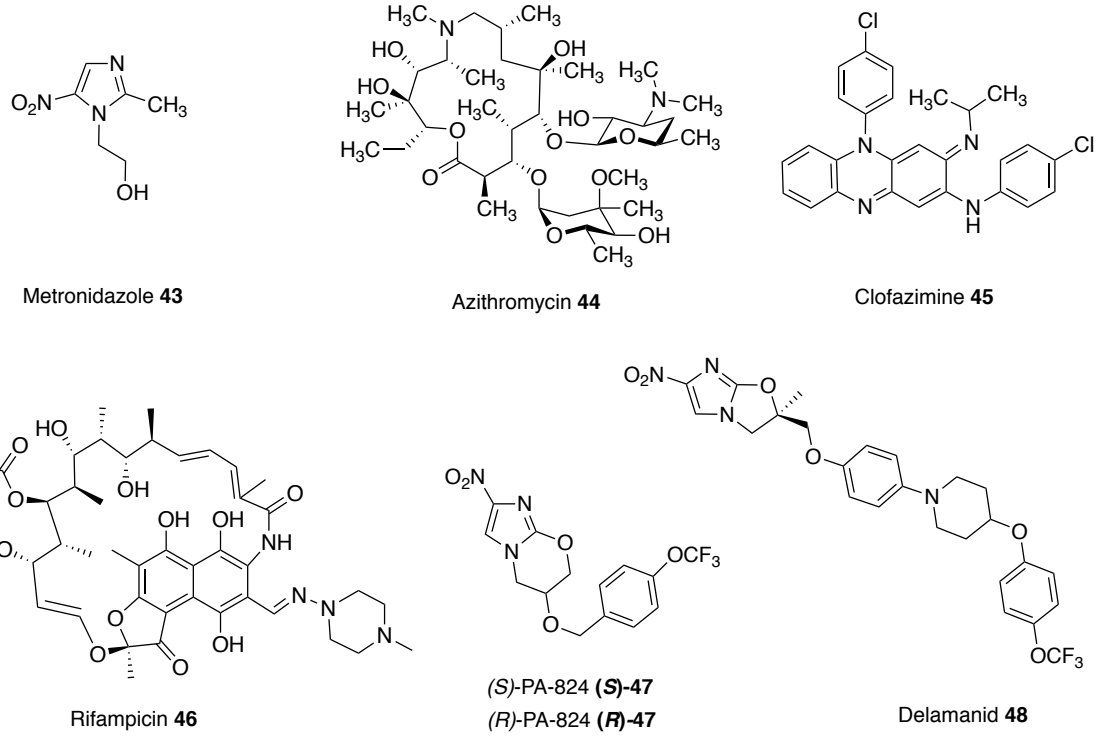

Figure 9: Antibacterial drugs that could be repurposed as antileishmanials

1.4.6. Antivirals

Tucaresol **49** is an investigational drug that has completed phase 2 clinical trials as a treatment for HIV[133,134] and, similar to the antiparasitic drug Levamisole **40**, is an immunomodulator that demonstrates antileishmanial activity *in vivo*. This novel immunomodulator was inactive in *L. donovani* intracellular amastigote assays but showed a reduction in parasite burden in mice infected with *L. donovani*. Tucaresol **49** could be delivered orally at an optimum dose of 5 mg kg^{-1} to produce a 44 to 62% suppression of liver amastigotes.[135]

Another drug with immunomodulatory effects being studied as a therapy for leishmaniasis is imiquimod **50**. This immune-response modifier is a treatment for genital warts caused by human papillomaviruses and works through activation of immune cells, including macrophages. Macrophages are the host cells of *Leishmania* and therefore in 1999 a study was conducted to determine if imiquimod **50** could be used as potential therapy for leishmaniasis. *In vitro* results determined that imiquimod **50** could induce leishmanicidal properties in infected macrophages and a possible mode of action is through stimulated signal transduction increasing the synthesis of nitric oxide which is toxic to the intracellular parasites. Progression of 5% imiquimod **50** cream into a *in vivo* study showed a significant reduction in the severity of the lesions but was ineffective at treating CL in human

trials.[136,137] In 2005, a study focused on new approaches such as combination therapies and conducted a clinical trial of parental antimony plus topical imiquimod **50** to treat patients with CL. Results from this study showed that 72% of patients treated with imiquimod **50** achieved a cure at 3 months *vs* 35% treated with the vehicle cream. In addition, accelerated healing and less prominent scarring was observed in the group treated with antimony and imiquimod **50** compared to therapy with antimony alone demonstrating that the next clinically available treatment for leishmaniasis might not rely on one but a combination of drugs.[138]

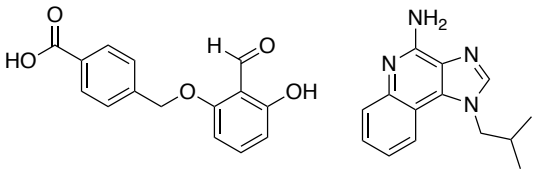

Tucaresol **49** Imiquimod **50**

Figure 10: Antiviral drugs that could be repurposed as antileishmanials

1.4.7. Antihistamines

Anti-allergic compounds, such as quercetin found in *Kalanchoe* plant extracts, display potent antileishmanial effects. This reflects a capacity to restore the Th1/Th2 T-cell balance and also to inhibit mast cell histamine release.[139,140,141,142,143] Consistent with these observations, a set of seven H1-antagonists were reported to display activity against *L. infantum* promastigotes with IC_{50} values in the range of 13 – 84 μM.[144] The activity recorded for cinnarizine **51** (Figure 11, Appendix A) was particularly noteworthy as, unlike the other six H1-antagonists tested, it also demonstrated potency against intracellular amastigotes (EC_{50} = 21 μM and NCTC cells EC_{50} = 87 μM). Whilst, initial *in vivo* experiments using hamsters infected with *L. infantum* revealed a lack of efficacy, a liposomal formulation circumvented this problem and enabled effective treatment of infection in the liver but not the spleen, which could be ascribed to the higher parasite burden (amastigotes/gram of organ) in this latter organ. Cinnarizine **51** has also been described as a calcium channel blocker which is significant because Reimão *et al*. (2010) demonstrated the activity of eight calcium channel blockers against intracellular *L. infantum* amastigotes (EC_{50} = 5 – 176 μM).[145] Further development of cinnarizine **51** will require the synthesis of more active analogues, an approach challenged by the fact that no target has yet been identified.[144]

This thesis will explore a separate study which has successfully used an enzyme assay to explore the potential of IPCS as a new antileishmanial drug target.[146,147] This assay was employed to screen a set of 1040 pharmacologically active compounds selected from the National Institute of Neurological Disorders and Stroke (NINDS). Many of the most active and selective hits have reported antihistamine activity. As these maintained activity in infected cell models they have considerable potential for repurposing as target specific antileishmanials. A compound of particular interest from this screen and one, which will be discussed in depth in this thesis, is the orally available antihistamine, clemastine **1** (Figure 11). This compound showed good *in vitro* activity against a range of promastigote species and maintained activity against intracellular amastigotes. In addition, clemastine **1** has shown activity against *T. cruzi*[148] and Ebola virus[149] as such this compound could be considered a broad spectrum antimicrobial. It should be noted that an *in vivo* study on mice with *T. cruzi* infection showed clemastine **1** was ineffective as a monotherapy but in combination with posaconazole **27** could suppress parasitemia.[148]

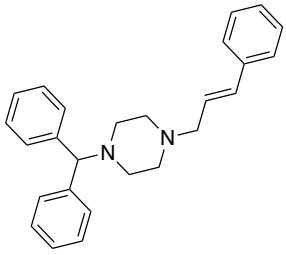

Cinnarizine **51**

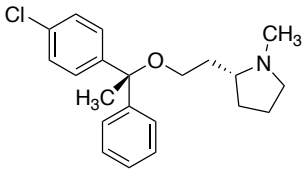

Clemastine **1**

Figure 11: An antihistamine that could be repurposed as an antileishmanial

1.4.8. Central nervous system (CNS) active drugs

Tricyclic heterocycles are part of numerous therapeutic agents and therefore important structures in medicinal chemistry.[150] Chlorpromazine **52** is perhaps the best known of the phenothiazine drugs (tricyclic heterocycles) for treatment of neurological disorders. In 1984 this compound was identified as having activity against *L. donovani in vitro* and *in vivo*[151] and in a separate study also showed it could kill *L. mexicana*, *L. aethiopica* and *L. major* promastigotes at a concentration of 7.5 μg mL^{-1}.[152] The same study determined the *in vivo* effect for chlorpromazine **52** in a murine model infected with *L. major* and *L. mexicana* and demonstrated leishmanicidal effect in the spleen but not in the skin lesion.[152] Therefore, like pentamidine **5**, this compound has shown to be effective against VL but with only partial effect against the cutaneous form. Chlorpromazine **52** will probably not be useful in the treatment of VL due to toxicity concerns but analogues of chlorpromazine

52 have been developed to explore SAR. For instance, analogues like compound **53** with a quaternary nitrogen atom have demonstrated antileishmanial, antitrypanosomal and antimalarial activity.[153,154] These analogues are trypanothione reductase inhibitors which are likely to affect the redox defence of the parasite and hence increase the parasites sensitivity to redox-damaged-based drugs. In addition, the enzyme, trypanothione reductase, is present in *Leishmanias* and *Trypanosomes* but not the mammalian hosts providing the opportunity to design a selective inhibitor.[153,154]

It should be noted that other tricyclic heterocycles are being studied[155] including cyclobenzaprine **54** which like chlorpromazine **52** analogues inhibits trypanothione reductase. Oral cyclobenzaprine **54** has recently been tested *in vivo* on *L. infantum*-infected BALB/c mice and the results showed significant reduction in parasite load in both the spleen and liver. In addition, cyclobenzaprine **54** induces oxidative stress in the parasite, which is consistent with trypanothione reductase inhibition, and also modulates the immune response of the host contributing to the *in vivo* efficacy. However, cyclobenzaprine **54** is thought to have off-targets effects and these should be further investigated when exploring the potential of this drug against VL.[156]

Imipramine **55** is an example of another tricyclic antidepressant that has antileishmanial activity. One study showed that this drug administered orally can effectively treat mice and hamsters infected with antimony sensitive and antimony resistant *L. donovani*.[157] A more recent study showed the *in vitro* activity of imipramine **55** against *L. amazonensis* and an effect on the biosynthesis of sterols. In addition, they concluded that it would be beneficial to study imipramine **55** in combination with azoles, which inhibit other steps of the sterol biosynthesis pathway, to treat leishmaniasis.[158]

The opioid receptor antagonist naloxonazine **56** was identified in a high-throughput screen against *L. donovani* intramacrophage amastigotes. This was the only compound from the screen to affect intracellular but not axenic parasites. Curiously, the structurally related opioid naloxone (Narcan®) was completely inactive against both parasitic forms. Since homologs of opioid receptors have not been identified in the *Leishmania* genome it is possible that opioids are involved in modulation of host resistance to parasite infection. In support of this, Loperamide **57**, a μ-opioid receptor agonist, was also identified in this study

as inhibiting parasite growth with greater activity against the intracellular stage of the parasite.[63]

Antileishmanial activity was observed when the broad spectrum antidepressants, ketanserin **58** and mianserin **59**, were screened against *L. donovani* promastigotes and intramacrophage amastigotes. Amongst other enzymes these compounds are known to target 3-hydroxy-3-methylglutaryl coenzyme A reductase (HMGR). This is the rate-limiting enzyme of the sterol biosynthesis which is also the putative pathway targeted by AmpB **4**. In support of this proposal both compounds inhibited recombinant *L. donovani* HMGR, although given the diverse reported activities, other modes of action cannot be discounted.[159,160]

Finally, another antidepressant under investigation for its antileishmanial activity is sertraline **60**. This oral antidepressant has shown activity against *L. infantum* and *L. donovani* promastigotes and intracellular amastigotes and tested successfully in animal models of VL.[161,162] Unlike the previous antidepressants mentioned, sertraline **60** has a tetrahydronaphthalene core and is a selective inhibitor of serotonin reuptake. Unfortunately, there has been no reported *Leishmania* orthologue to the serotonin reuptake transporter and the target cannot be solely based on its inhibition of one efflux pump because of its broad spectrum antimicrobial activity.[149] Instead sertraline **60** targets different essential metabolic pathways of *Leishmania* and kills the parasite through a multi-target mechanism of action. Therefore, sertraline **60** could be a valuable drug candidate to be repurposed for VL.[162]

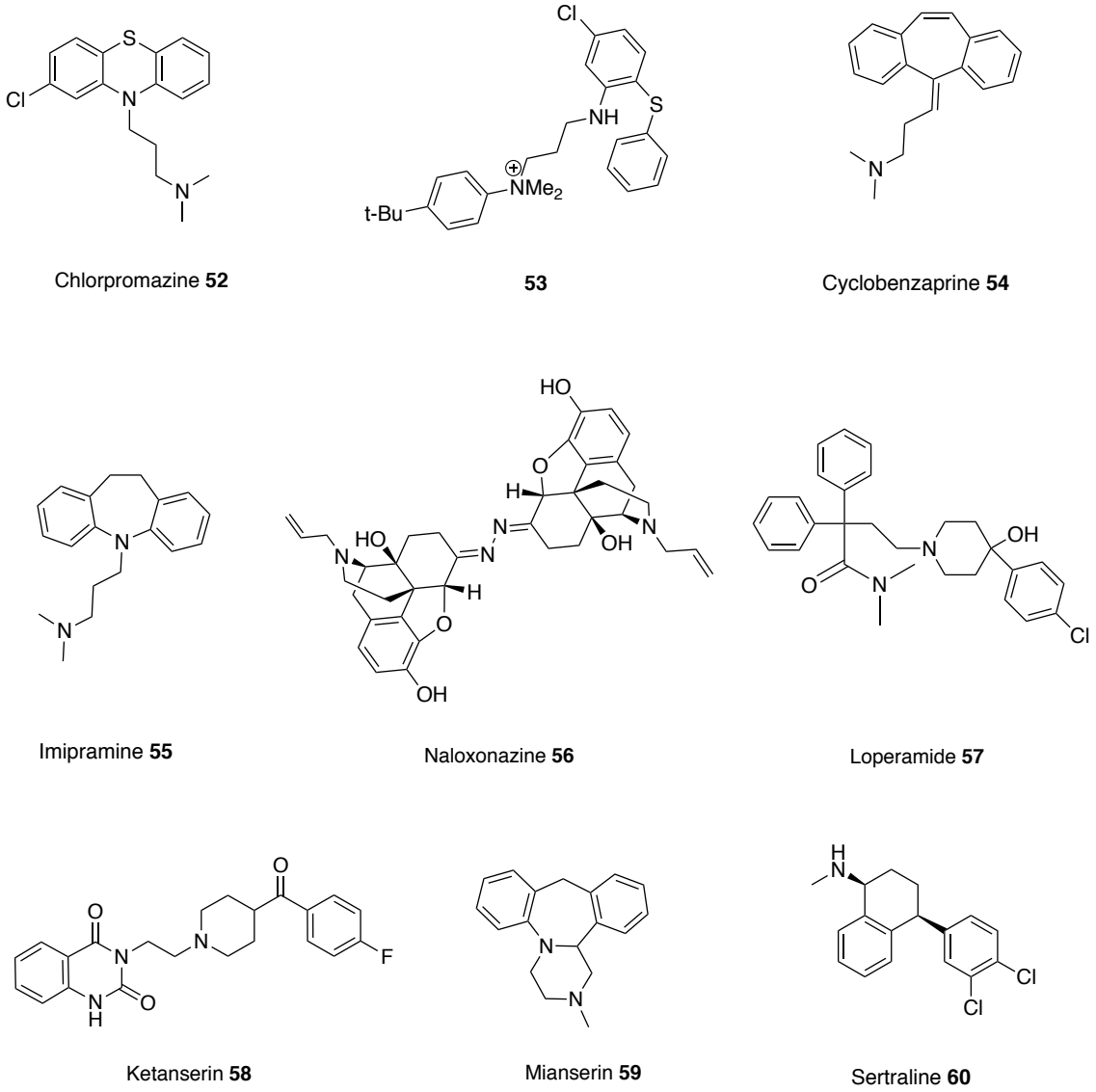

Figure 12: CNS drugs that could be repurposed as antileishmanials

1.4.9. Cardiac medication

Similar to ketanserin **58** and mianserin **59** discussed above, statins target HMGR. Statins are currently on the market to reduce cardiovascular disease by lowering the level of low-density lipoprotein cholesterol ('bad cholesterol') in the blood. Studies have shown that statins also have the potential to be repurposed as antileishmanials.[163,164] For example, mevastatin **61** also inhibits recombinant *L. donovani* HMGR enzyme with an IC_{50} value of 42 ± 3 μM. It also shows correspondingly good activity against both *L. donovani* promastigotes and intracellular amastigotes with no toxicity exhibited towards the host cell line.[165]

Amiodarone **62** and dronedarone **63**, (Figure 13) used to treat cardiac arrhythmias, have antileishmanial activity against *L. mexicana* promastigotes and intramacrophage

amastigotes, and inhibit oxidosqualene cyclase, another enzyme essential for ergosterol biosynthesis. However, as with the antihistamines discussed above, these drugs are also known to disrupt Ca^{2+} homeostasis in *Saccharomyces cerevisiae* and *Trypanosoma cruzi,* so may have multiple modes of action.[166] A murine model infected with *L. mexicana* was treated with oral amiodarone **62** and although it prevented the development of lesions during the course of treatment, reoccurrences of the infection were observed once treatment had ended. Amiodarone **62** was then tested in combination with miltefosine **7** and showed permanent control of lesion size. Hence, using this drug in combination with currently available antiparasitics could lower the dosage and reduce the known side effects of amiodarone **62** (e.g. cardiotoxicity, thyroid dysfunction and pulmonary fibrosis).[167] Alternatively, dronedarone **63** appears to have great potential to be repurposed as it has greater antiparasitic activity coupled with lower mammalian toxicity than amiodarone **62**.[168]

Like the antihistamine cinnarizine **51** discussed above, bepridil **64** is a calcium channel blocker and was originally developed as a treatment for angina. Bepridil **64** was shown to be active against a range of promastigote species and *L. chagasi* intracellular amastigotes but showed a lack of activity at 12 mg kg^{-1} in a hamster model infected with *L. chagasi*.[169] The mechanism of action for *in vitro* activity is unknown but the chemical structure of bepridil **64** shares similarities to clemastine **1** and tamoxifen **20** which are known inhibitors of IPC synthase.

Two other calcium channel blockers that have been studied for their antileishmanial effects are amlodipine **65** and lacidipine **66** which are used to treat cardiovascular disease and high blood pressure. They showed good *in vitro* activity and, unlike bepridil **64**, amlodipine **65** and lacidipine **66** showed *in vivo* antileishmanial efficacy in *L. donovani*-infected BALB/c mice.[170] This demonstrates that structural modification to drugs belonging to the same pharmacological class can strongly affect antileishmanial activity.[169]

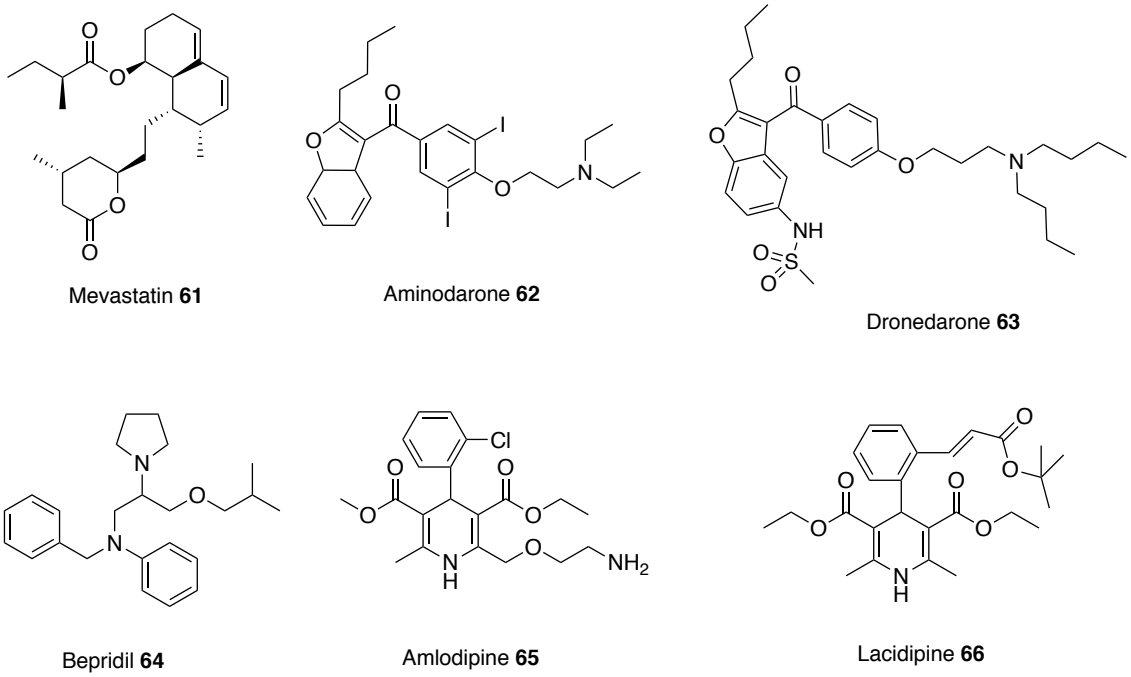

Figure 13: Cardiac medication that could be repurposed as antileishmanials

1.4.10 Other drugs

Calpains are a family of neutral calcium-dependent cysteine peptidases which when inhibited could treat a variety of diseases such as muscular dystrophy, neurological disorders, and cataracts. *Leishmania* cells express calpain-related proteins and the calpain inhibitor, MDL28170 **67**, showed activity against 6 different species of *Leishmania* in both the promastigote and amastigote forms. In addition, MDL28170 **67** was selective for *Leishmania* amastigotes over mammalian macrophages.[171] The next stage for this compound is to investigate if the lack of intrinsic variation in species sensitivity to MDL28170 **67** is reflected *in vivo*. Little intrinsic variation in drug sensitivity could lead to the development of a single drug for all species of *Leishmania*.[171] However, it should be noted that MDL28170 **67** and other calpain inhibitors need micro-molar concentrations for activity which could reflect low affinity for the calpain target or potential off-target effects.[172]

This review has focused on repurposing synthetic small molecules, though there are studies that have investigated polymers and natural products. For instance, a recent study confirmed that polyhexanide **68**, a wound antiseptic and disinfectant, has antileishmanial activity with IC_{50} values of 0.41 μM against *L. major* promastigotes, 69-fold more potent than miltefosine **7**, and 4 μM against intracellular *L. major* amastigotes. Polyhexanide **68** is

thought to kill the parasite by disruption to membrane structure and selective chromosome condensation and damage. Interestingly, it was also discovered that this cationic polymer can be used as a vehicle to transport cargoes to the macrophage and thus has the ability to deliver immunomodulatory agents[173].

Whilst the focus of this review has been on repurposing human therapeutics, there is the potential for investigating other groups of bioactive chemicals, including both agrochemicals and veterinary medicines for human use as treatments for neglected diseases. For example, more than 600 commercial agrochemicals were screened against parasitic protozoans and zoxamide **69** was found to be the most effective against *L. donovani* promastigotes. Zoxamide **69** is an oomyceticidal compound used in fruit and vegetables, and acts through the inhibition of microtubule formation. Zoxamide **69** killed the promastigotes with an IC_{50} value of 250 nM.[174] Although explored in other contexts,[7] there has been little reported effort to repurpose veterinary medicines for leishmanaisis, possibly due to the potential human toxicity issues which could arise and negate the benefits of the repurposing approach.

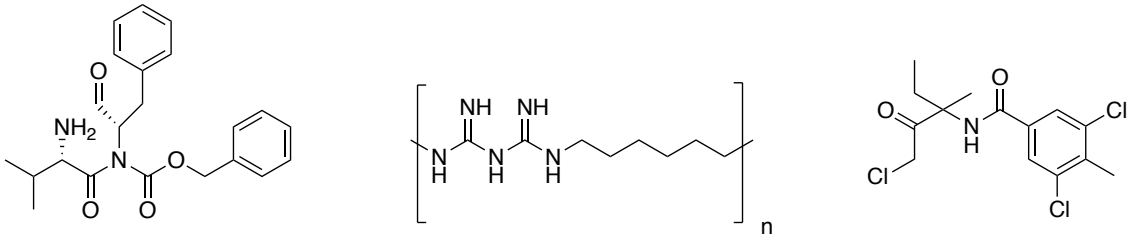

Figure 14: Other drugs that could be repurposed as antileishmanials

1.5. Concluding remarks

The repositioning of old drugs for new uses is not a new concept and is a particularly attractive approach for neglected tropical diseases. Here the use of approved drugs is particularly beneficial as clinical trials have already successfully been conducted and often their patents have expired leading to shorter, cheaper discovery pipelines. As discussed in the various sections above, a wide range of structures have been explored for antileishmanial activity. Significantly, most of the medicines used to treat leishmaniasis, either on the market or under development in the drug discovery process, were initially intended for other indications. Furthermore, more novel approaches show drug repositioning is extending beyond the scope of human medication as investigation into the human use of agrochemicals and veterinary therapeutics is underway. However, drug

repurposing is limited by the number of approved drugs and compounds with established pharmacokinetic data, in addition the repositioning discovery process tends to mean that there is less chance of finding treatments that act through a new mechanism of action. Overall, whilst not the sole solution, drug repositioning represents a valuable, relatively fast and cost-effective, strategy for developing essential new therapies, particularly for neglected tropical diseases such as leishmaniasis.

Table 1: Clinical manifestations and the related species and geographical location[175]

Clinical manifestation	Leishmania species	Geographical area
Cutaneous Leishmaniasis	*L (L.) tropica*	Eastern hemisphere
	L (L.) major	Eastern hemisphere
	L (L.) aethiopica	Eastern hemisphere
	L (L.) amazonensis	Western hemisphere
	L (V.) braziliensis	Western hemisphere
	L. (L.) mexicana	Western hemisphere
	L (V.) panamensis	Western hemisphere
Mucosal Leishmaniasis	*L (V.) braziliensis*	Western hemisphere
	L (V.) panamensis	Western hemisphere
	L (V.) guyanensis	Western hemisphere
	L (L.) amazonensis	Western hemisphere
	L (L.) major	Eastern hemisphere
Visceral Leishmaniasis	*L (L.) donovani*	Eastern hemisphere, except Europe
	L. (L.) infantum	Europe, Africa and South America

2. Project Background

As discussed in Chapter 1, previous work in the group had identified *Leishmania major* inositol phosphorylceramide synthase (*Lmj*IPCS) as an attractive drug target. IPCS is an essential enzyme in the biosynthesis of sphingolipids and this chapter will provide a background to this topic.

2.1. Sphingolipids

Sphingolipids, discovered more than a hundred years ago, are an essential structural component of eukaryotic cells and play crucial roles in a range of biological processes such as signal transduction, cell growth, differentiation and apoptosis.[146] They are amphipathic lipids characterised by their backbone called long-chain or sphingoid bases. Underivatised free sphingoid bases consist of hydroxyl groups (at C1 and C3) and an amino group (at C2).[176] However, most simple sphingolipids are amide-linked with a long-chain fatty acid to form ceramides that can be further derivatised by the addition of a head group (at C1) (Figure 15).[177]

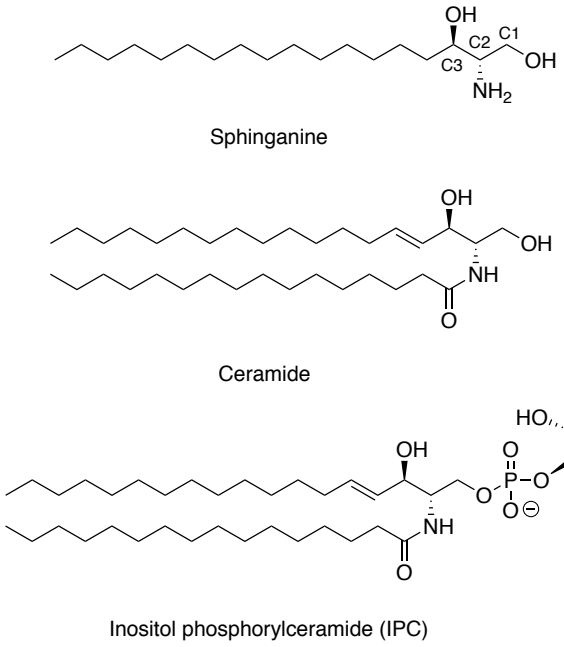

Figure 15: Structures of sphingolipids

2.2. *De novo* biosynthesis

The *de novo* biosynthesis of sphingolipids takes place in the endoplasmic reticulum (ER) and Golgi apparatus and begins with the condensation of palmitoyl-CoA **70** with L-serine **71** (Scheme 1). This reaction is catalysed by serine palmitoyltransferase, a membrane

bound enzyme, producing 3-ketosphinganine **72** which is then reduced by an NADPH-dependent reductase to form sphinganine **73**.[176,147]

At this point there is an evolutionary divergence in the pathway. In animals and trypanosomatids, sphinganine **73** is acylated to form dihydroceramide **74,** which is then desaturated to produce ceramide **75**. In contrast, in fungi and plants sphinganine **73** is first hydroxylated to phytosphingosine **76** and then acylated to form phytoceramide **77**.[147]

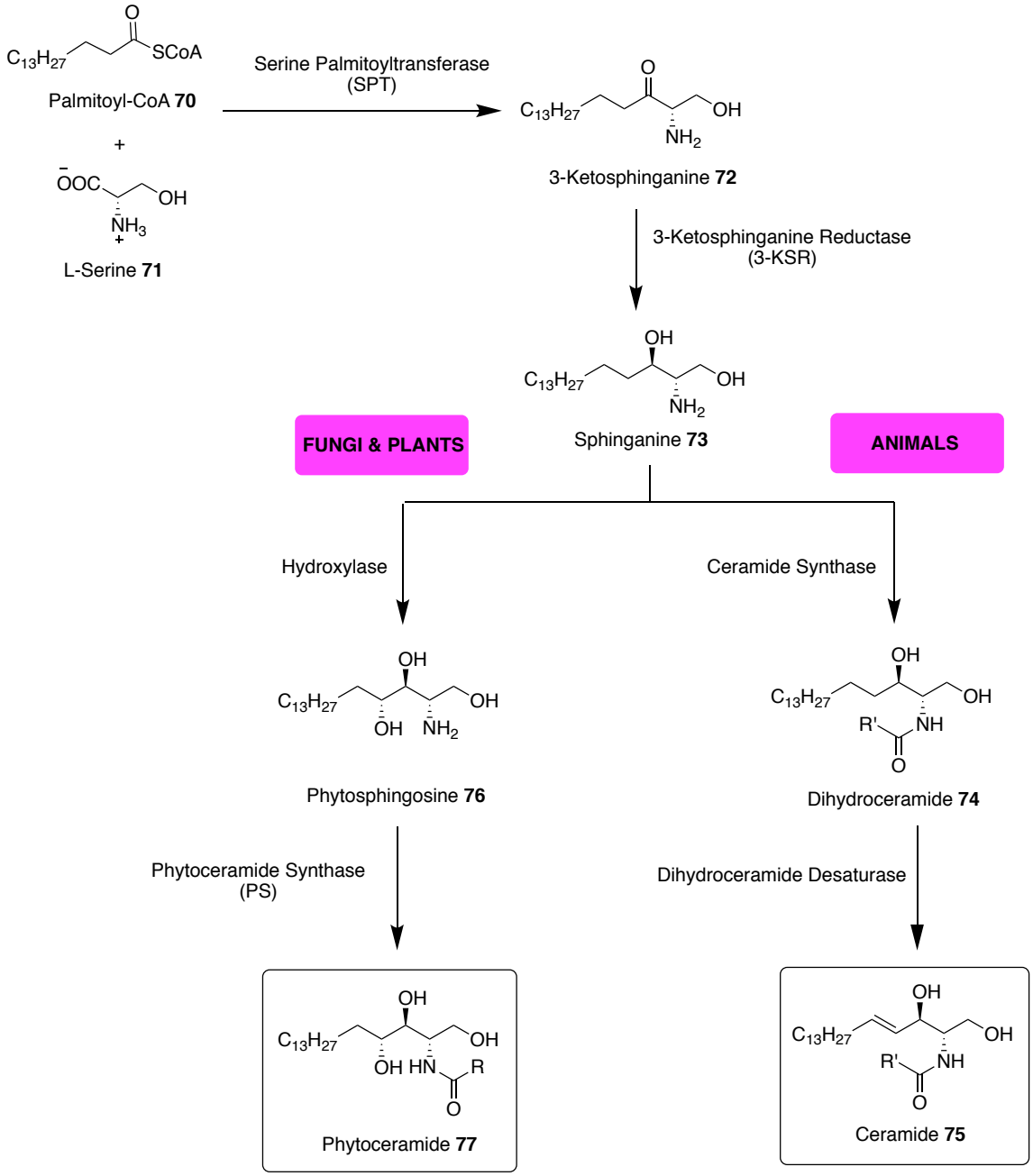

Scheme 1: Divergence in pathway for ceramide 75 biosynthesis

There is further variance in the biosynthetic pathway for animals and kinetoplastids (including *Leishmania* spp.). In animal cells, ceramide **75** is transformed into sphingomyelin **78** which is catalysed by sphingomyelin synthase (SMS). In contrast, trypanosomatids use

ceramide **75** to produce inositol phosphorylceramide **79** (IPC) catalysed by IPCS (Scheme 2). In fungi and plants a similar reaction occurs where phytoceramide is transformed to IPC.[147]

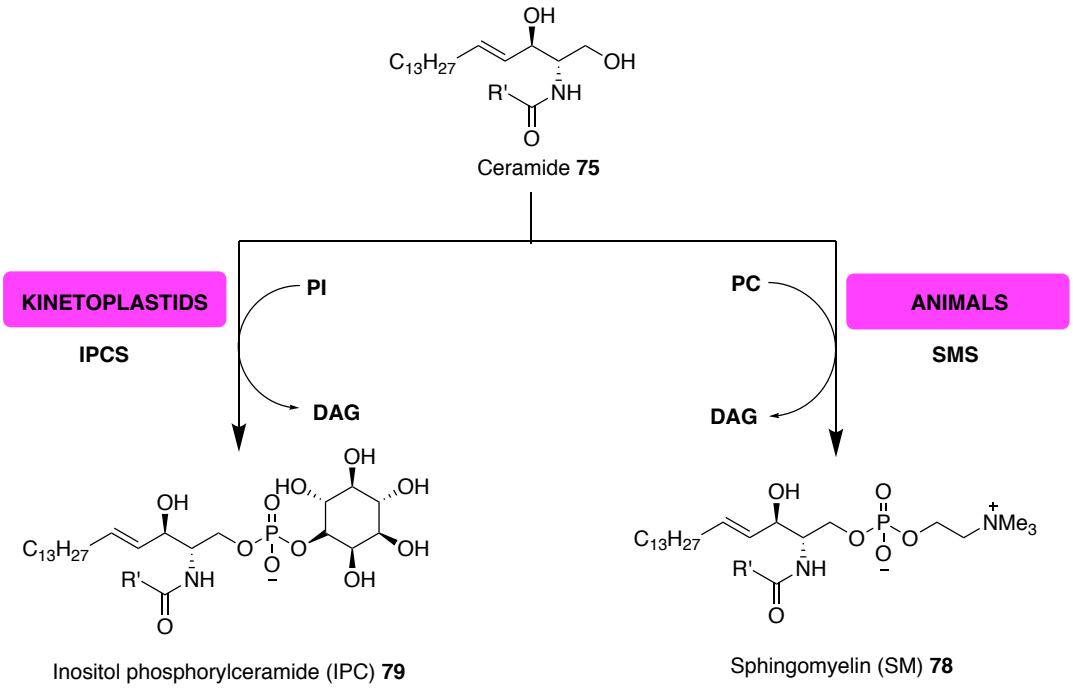

Scheme 2: Divergence in pathway from ceramide 75

2.3. Serine palmitoyl transferase (SPT)

Serine palmitoyltransferase (SPT) catalyses the first and rate limiting step of the biosynthetic pathway as shown in Scheme 1. Denny and Beverley have independently deleted one SPT subunit, *Lm*LCB2, to generate SPT knock-out mutant *L. major* promastigotes (*Δ* LCB2). As a result, these parasites can no longer synthesise ceramide **75** and *de novo* sphingolipids.[178,179,180] The *Δ* LCB2 promastigotes were viable in the procyclic stage, but unable to generate metacyclic parasites, which are in the infective stage of their life cycle. However, *L. major Δ* LCB2 amastigotes were fully virulent to macrophages and mice. These studies suggest that in the promastigote stage, *de novo* sphingolipids play an essential role in metacyclogenesis whereas *Δ* LCB2 amastigotes can salvage host sphingolipids to maintain their virulence.[180]

2.4. IPCS

IPCS is another key *de novo* biosynthetic enzyme in kinetoplastids and fungi. This enzyme is responsible for producing the major phosphosphingolipid, IPC **79**, by catalysing the transfer of the phosphorylinositol group from phosphatidylinositol (PI) to ceramide **75**. This

reaction controls the balance between pro-apoptotic ceramide **75** and mitogenic diacylglycerol (DAG) (Scheme 2). If the activity of this enzyme was inhibited it could cause destruction to the cell structure and function and is therefore an attractive drug target.[147] In addition, the mammalian orthologue of IPCS (SMS) has a different function which can be utilised to develop selective antifungal and antiprotozoal therapies.[146]

2.4.1. Discovery of *L. major* IPCS

In support of this hypothesis, IPCS, encoded by the AUR1 gene, has been validated as an antifungal drug target. It is located within the Golgi apparatus of *Saccharomyces cerevisiae*[181] and a mutant defective in IPCS will accumulate ceramide **75**, leading to cell death. In addition, mutations in AUR1 have shown to give resistance to the antifungal drug aureobasidin A enabling this depsipeptide to be identified as a potential inhibitor of IPCS in fungi.[182] However, it should be noted that although aureobasidin A is active across a range of *Leishmania species*[183] it does not act as an IPCS inhibitor in kinetoplastids but functions through a different and as yet unknown mechanism. This highlights the difference between IPCS in yeast (AUR1p) and in *Leishmania* (*Lmj*IPCS).

Denny *et al.* identified and characterised the single gene from *L. major, Lmj*IPCS (GeneDB, *Lmj*F35.4990), which is the functional *AUR1* orthologue through bioinformatics and functional genetic approaches.[184] The gene codes for a membrane-bound protein consisting of 338 amino acids with a mass of approximately 38 kDa.

The macromolecular structures of fungal AUR1p and *Lmj*IPCS are similar but only share a limited amino acid sequence identity. A greater similarity is observed with orthologues in the related kinetoplastids *L. major*, *L. don*ovani, *T. cruzi* and *T. brucei*. In fact, the sequence identity of protozoan enzymes is more closely related with the animal SMS even though the fungal AUR1p performs an equivalent function (Table 2). This is demonstrated by the 100% sequence identity in domain D1 for kinetoplastids and mammals (Figure 16). Both *Leishmania* and mammals utilise the substrate ceramide **75** therefore the conserved D1 domain may play an important role in the binding of this substrate.[184]

*Lmj*IPCS is predicted to contain six transmembrane helices (Figure 17a) and two regions located in the luminal domains of D3 and D4 are conserved relative to animal SMSs and are also similar to fungal AUR1p.[147] These regions possess active histidine and aspartate

residues that form the catalytic triad which participates in nucleophilic attack on lipid phosphate ester bonds.[147] Sigal *et al*. have proposed a general mechanism for phosphoryl transferases, which was adapted by Mina *et al.* for *Lmj*IPCS (Figure 17b). Sigal demonstrated that one arginine residue close to the nucleophilic histidine of the active site is conserved across different families of enzymes and organisms. Investigations of the *Lmj*IPCS sequence identified Arg262 as a conserved residue and potentially involved in the stabilisation of the transition state during the phosphate group transfer (Figure 17b). [147,185]

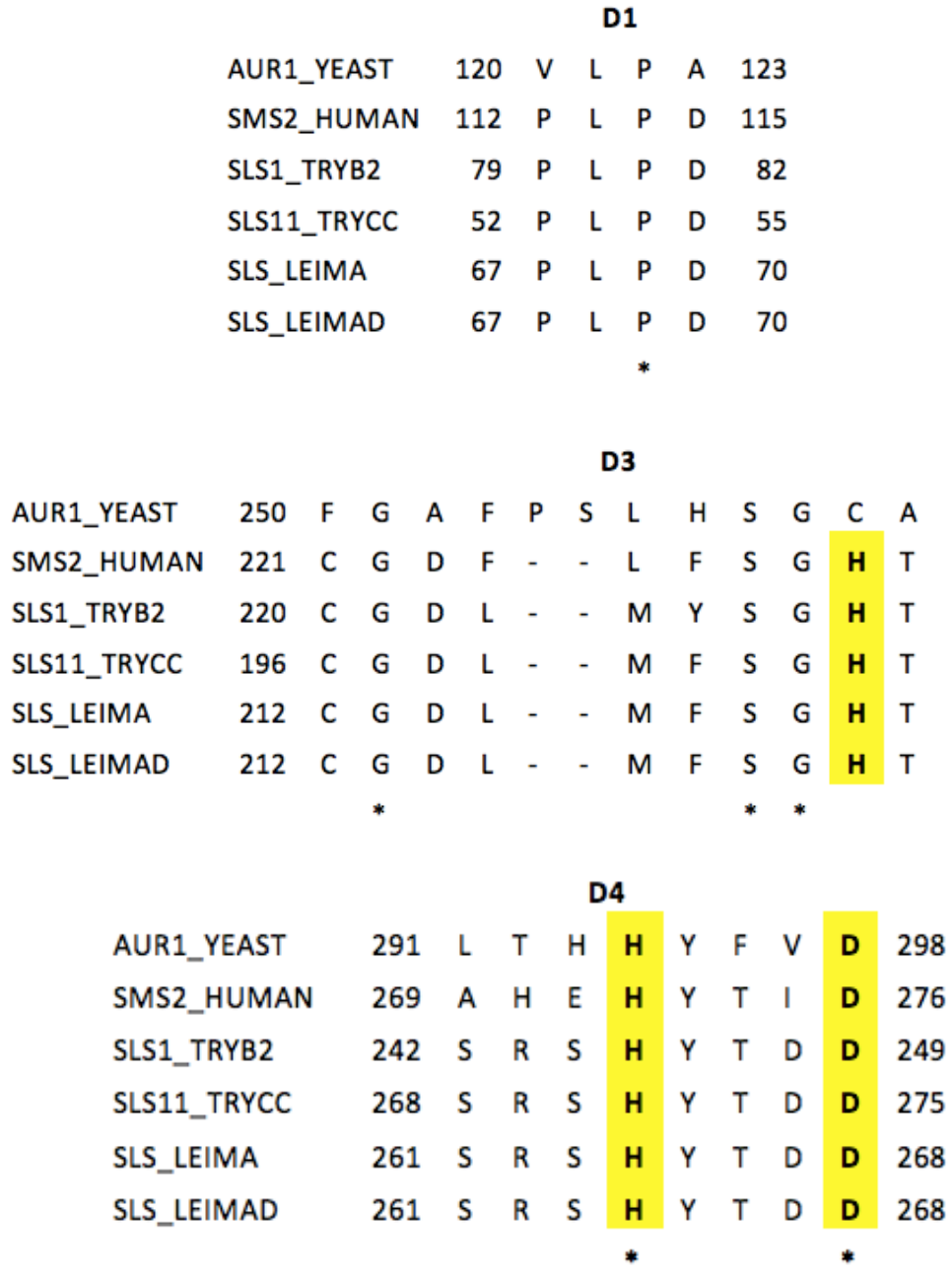

Figure 16: The sequence alignment of highly conserved regions from fungus AUR1 protein, human SMS, *T. brucei brucei* (TRYB2) SLS, T. cruzi (TRYCC) SLS, *L. major* (LEIMA) IPCS and *L. donovani* (LEIMAD) IPCS. * Indicates highly conserved residues and the residues in the catalytic triad are highlighted in yellow.[186]

Table 2: Percentage sequence identity of orthologous sphingolipid synthases from yeast, human, *T. brucei brucei* (TRYB2), *T. cruzi* (TRYCC), *L. major* (LEIMA) *and L. donovani* (LEIMAD).[186]

Protein	AUR1 YEAST	SMS2 HUMAN	SLS1 TRYB2	SLS11 TRYCC	SLS LEIMA	SLS LEIMAD
AUR1 YEAST	100	19	17	16	16	17
SMS2 HUMAN	19	100	24	24	24	24
SLS1 TRYB2	17	24	100	47	41	39
SLS11 TRYCC	16	24	47	100	49	46
SLS LEIMA	16	24	41	49	100	93
SLS LEIMAD	17	24	39	46	93	100

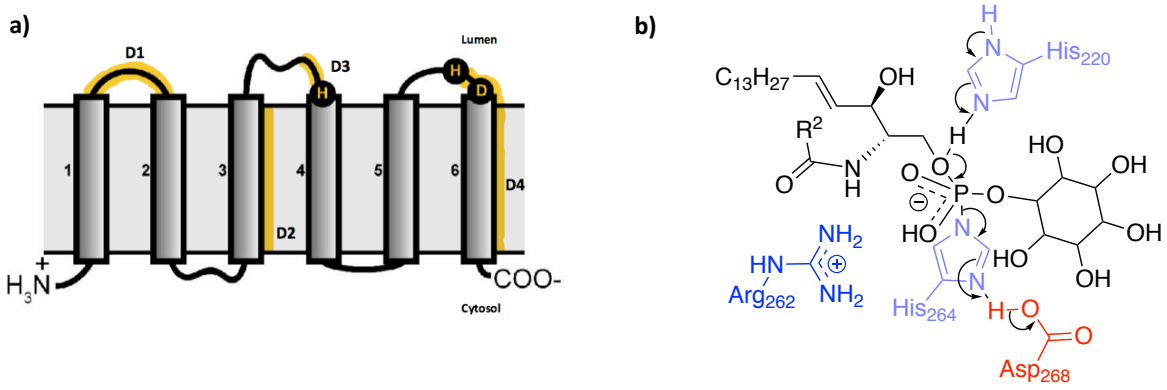

Figure 17: a) Predicted topology model of IPCS from kinetoplastids (adapted from Goren *et al.* with permission).[187] **Four domains are highlighted in yellow. b) *Lmj*IPCS catalytic triad showing phosphorylation of ceramide 75 (adapted from Mina *et al.* with permission).**[147]

2.4.2. Characterisation of IPCS in *Leishmania*

Unfortunately, the function and structure of *Leishmania* IPCS cannot be analysed by conventional methods[188,189] as this enzyme is membrane-bound with multiple transmembrane domains making protein purification and crystallisation challenging.[190] To circumvent this problem, Denny *et al.* developed an enzyme assay using *S. cerevisiae* as a vehicle. The AUR1 gene in *S. cerevisiae* was deleted to generate a yeast knock-out mutant. This was transformed with the exogenous *Lmj*IPCS gene to generate a mutant yeast strain which has only *Lmj*IPCS as its functional sphingolipid synthase (SLS).[191]

These cells were propagated and then used to isolate microsomal membranes enriched in IPCS. The enzyme assay, which can be formatted into a 96-well plate format, uses these microsomes to convert fluorescent NBD-C_6-ceramide **80** into NBD-C_6-IPC **81** (Scheme 3).

The substrate and product are then separated using anion exchange chromatography and the fluorescence is measured to quantify NBD-IPC **81**.[146]

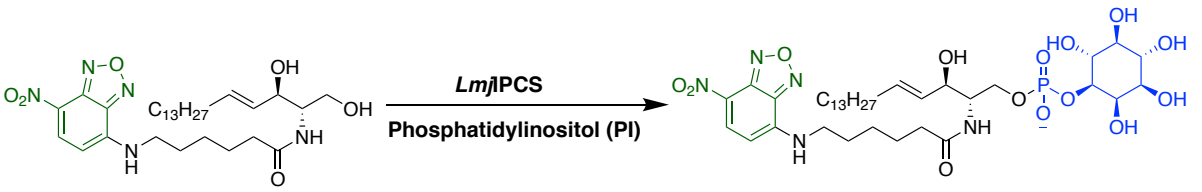

NBD-C_6-Ceramide 80 **NBD-C_6-Inositol Phosphorylceramide 81 (IPC)**

Scheme 3: *Lmj*IPCS biochemical assay

The biochemical assay outlined above was used to characterise *Lmj*IPCS and demonstrated that this enzyme proceeds *via* a double-displacement mechanism (Scheme 4). Out of the two substrates, ceramide **75** has a higher affinity for the enzyme compared to the more abundant substrate, PI. This suggests that ceramide **75** is the rate-limiting substrate in the reaction[146] and therefore, analogues of ceramide **75** were synthesised to probe the active site. The biochemical assay described above was used to identify a number of structure-activity relationships (SARs) (Figure 18a). Interestingly, it was found that the free amino analogue **82** (Figure 18b) could function as an IPCS inhibitor rather than as an alternative substrate. Analogue **82** was shown to be active against *L. major* promastigotes but on-target effects required validation.

Knock-out *L. major* promastigotes which lack IPCS could not be generated and Denny *et al* proposed that this may be due to the build-up of toxic metabolites (data unpublished).[191] Fortunately, mutant *L. major Δ* LCB2 can test the activity of potential *Lmj*IPCS inhibitors as this enzyme is redundant in these parasites. These mutants are 3-4 fold less sensitive to analogue **82** than wild type *L. major* promastigotes. This suggests mostly on-target effects and demonstrates the potential of IPCS as a viable target for the development of new antileishmanials.[147]

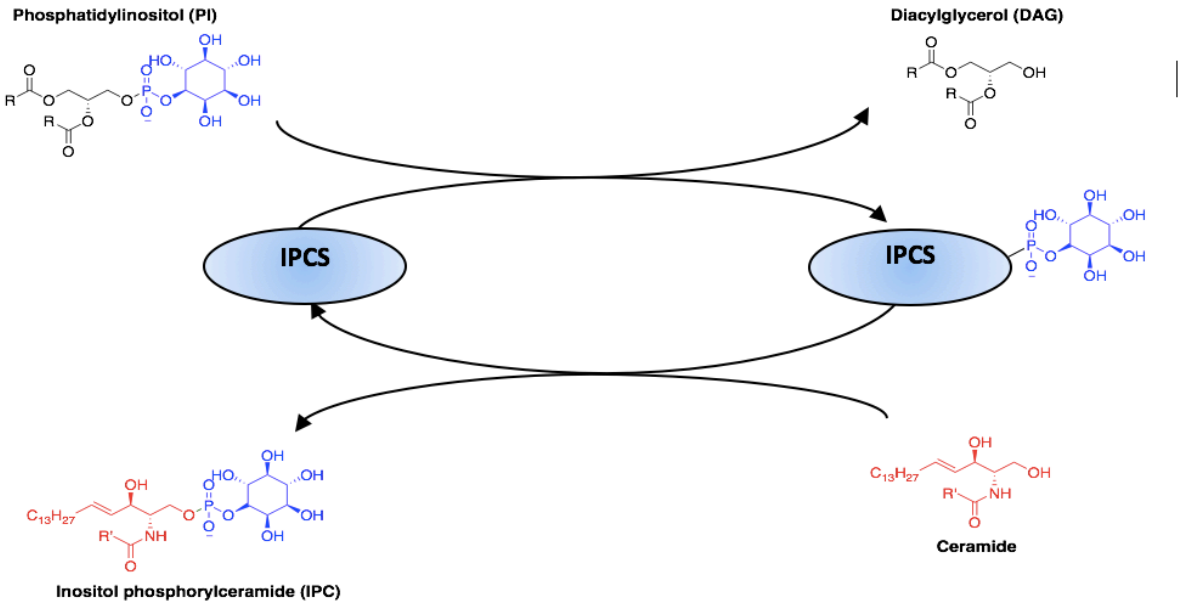

Scheme 4: Double-displacement mechanism of *Lmj*IPCS

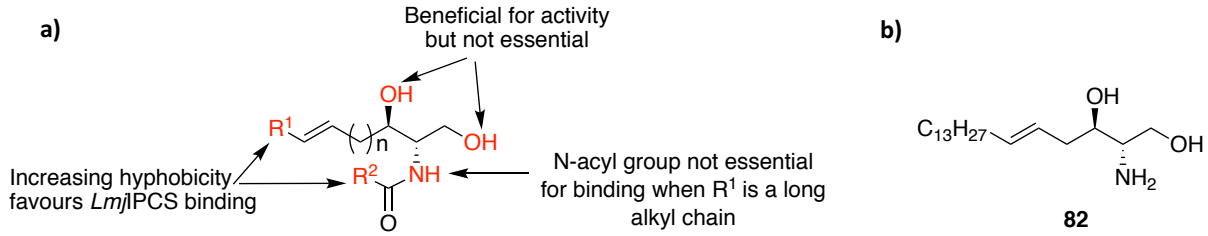

Figure 18: a) SAR data for ceramide analogues b) Free amino ceramide analogue with inhibitory effects

2.5. National Institute of Neurological Disorders and Stroke (NINDS) compound screen

Utilitising the biochemical assay[12] described above (Scheme 3) a screen was performed on 1040 pharmacologically active compounds from the National Institute of Neurological Disorders and Stroke (NINDS) (data unpublished). 57 compounds, at a concentration of 20 μM, showed greater than 70% inhibition of IPCS and these were tested at 10 μM for activity against the parasite. The anti-promastigote assay was carried out with *L. major* promastigotes using a resazurin-based cell-viability assay and the results are shown in Figure 19.[192] The known cytotoxic compounds used as controls were removed and 16 potential lead compounds were identified (Figure 20).

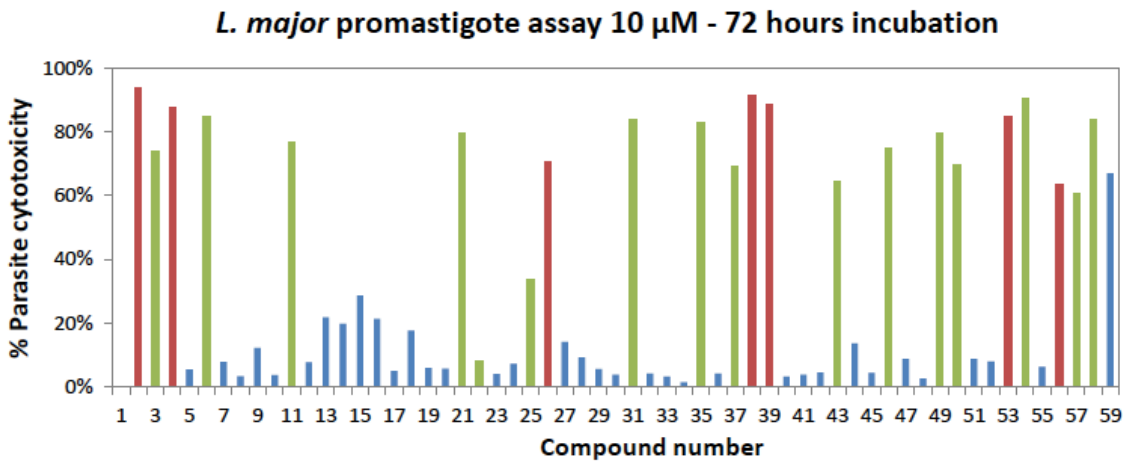

Figure 19: Cytotoxicity of NINDS library against *L. major* promastigotes. Green bars are potential lead compounds; blue bars are compounds with poor activity; red bars are known cytotoxic and non-selective compounds; lane 1 is no inhibitor; lane 59 is amphotericin B control (from Brown with permission).[192]

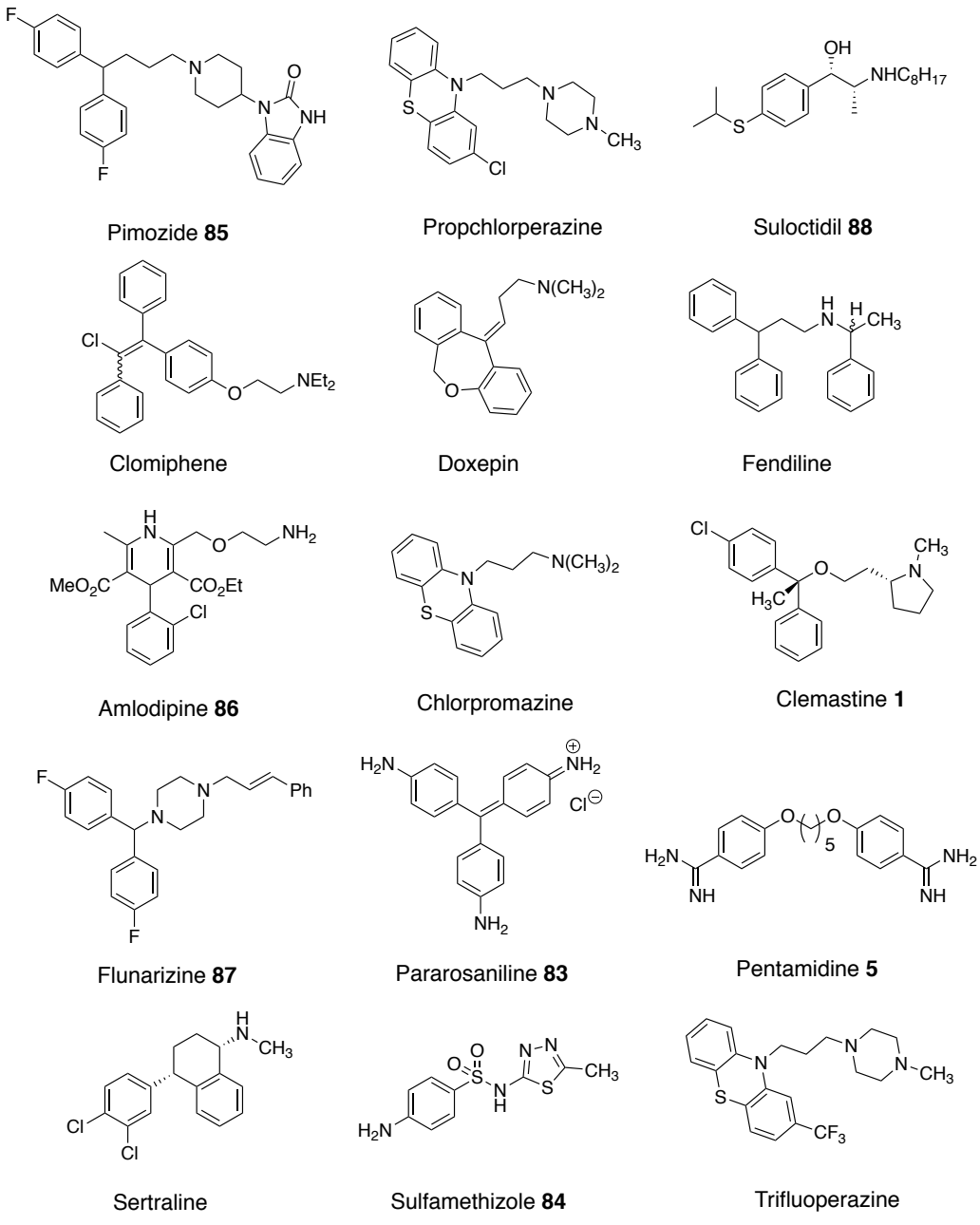

Figure 10: Hit compounds identified from enzyme and parasite screen[191]

2.5.1. Confirmation of hit compound activity

Pure material of the 16 chosen inhibitors was purchased from commercial sources and a dose-response study was performed to confirm activity (Figure 21).

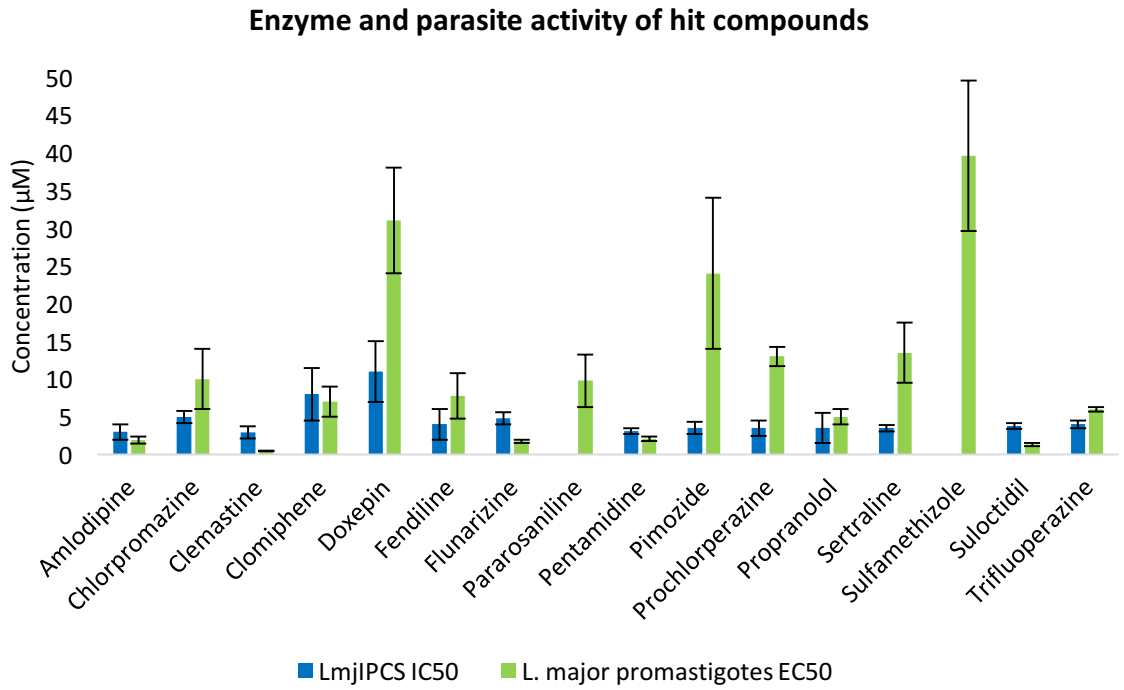

Figure 21: Activity of hit compounds against *Lmj*IPCS and promastigotes (adapted from Brown with permission)[191]

The dose-response studies highlight compounds that disagree with the initial enzyme and parasite screens. For example, IC_{50} values against *Lmj*IPCS could not be obtained for pararosaniline **83** or sulfamethizole **84** and both drugs displayed poor antileishmanial activity (EC_{50} = 9.78 μM and 39.63 μM respectively). In addition, doxepin and pimozide **85** exhibit EC_{50} values greater than 10 μM against *L. major* promastigotes (30.03 μM and 22.93 μM respectively). Subsequently, these compounds were not investigated further.

The known antileishmanial pentamidine **5** was confirmed as a *Lmj*IPCS inhibitor with an IC_{50} value of 3.10 μM and an EC_{50} against the parasite of 2.05 μM. Four compounds exhibited antileishmanial activity greater than pentamidine **5**. These compounds were amlodipine **86** (EC_{50} = 1.91 μM), clemastine **1** (EC_{50} = 0.47 μM), flunarizine **87** (EC_{50} = 1.73 μM) and suloctidil **88** (EC_{50} = 1.33 μM). Interestingly, all these compounds showed higher activity against the parasite than the enzyme. The cause of this difference in activity is unknown but may be due to the drugs having multiple targets, undergoing metabolism to more active compounds or the microsomes possessing higher concentrations of the enzyme relative to the cell.

2.5.2. Intramacrophage *L. major* anti-amastigote assay

Amlodipine **86**, clemastine **1**, flunarizine **87** and suloctidil **88** were then tested against murine peritoneal macrophages infected with *L. major* amastigotes. Flunarizine **87** showed poor antileishmanial activity against the clinically relevant amastigotes (EC_{50} > 30 μM) but amlodipine **86**, clemastine **1** and suloctidil **88** displayed single digit micromolar potency (EC_{50} = 3.65 μM, 3.06 μM and 4.28 μM respectively). The cytotoxicity against uninfected macrophages of amlodipine and suloctidil **88** was greater than 10 μM whereas for clemastine **1** it was greater than 20 μM. Hence, clemastine **1** was identified as the most selective compound for *Leishmania* and was progressed as the lead compound.

Clemastine **1** is an orally available antihistamine sold under the brand name Tavegil® and acts as an antagonist for the histamine H1-receptor.[193] Also, clemastine **1** is currently in phase 2 clinical trials as remyelinating therapy for treatment of multiple sclerosis.[194] This over-the-counter drug has a well-established safety profile[195,196] with the major side effects being sedation, dizziness, disturbed coordination, epigastric distress and dry mouth.[197] In addition, clemastine has good pharmacokinetic properties such as a high volume distribution of 9.5 ± 3.8 L kg^{-1} which contributes to a terminal elimination half-life ($t_{1/2}$) of 21.3 ± 11.6 h.[198] This positive drug profile highlights clemastine as an appealing drug candidate for repurposing as an oral antileishmanial and this will be explored in Chapter 3.

2.5.3. On-target validation

Work performed in collaboration with Mike Barrett (University of Glasgow) measured the effect of clemastine **1** on the metabolome of *L. major* promastigotes. The promastigotes were incubated with clemastine **1** for 42 h before the metabolites were extracted and analysed by LC-MS. Results found that parasites treated with clemastine **1** showed an increase in the substrate ceramide **75** (Figure 22), which is expected of an IPCS inhibitor.

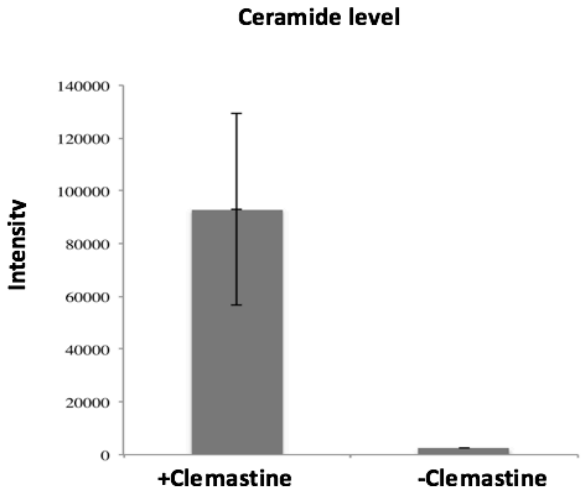

Figure 22: Metabolomic analysis of *L. major* promastigotes which had been treated with clemastine 1 for 42 h (data unpublished)

Lipidomic analysis performed in collaboration with Terry Smith (University of St Andrews) supports the findings from the metabolomic study. *L. major* promastigotes were again incubated with clemastine **1** for 42 h before the lipids were extracted and analysed by ES-MS and GC-MS. Focus was on the inositol lipids and the ratio of IPC **79** relative to PI was quantified (Figure 23). The results showed that promastigotes treated with clemastine **1** demonstrate a reduction in the ratio of IPC **79** relative to PI. This is consistent with clemastine **1** acting as an IPCS inhibitor.

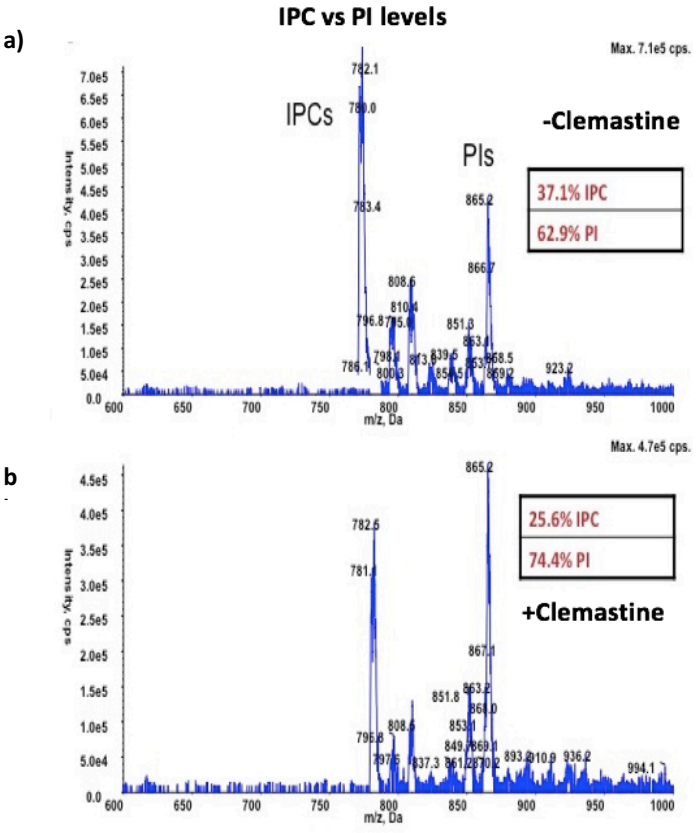

Figure 23: Lipidomic analysis of *L. major* promastigotes with a) DMSO b) 5 µM clemastine 1 for 42 h (data unpublished)

2.6. Synthesis of clemastine

In 1976 the synthesis of all four possible stereoisomers of clemastine **1** was reported by Ebnöther and Weber. Clemastine **1** is sold as the most active diastereomer, (*R, R*)-isomer **1**, with the stereochemistry of the quaternary benzhydryl carbon determining activity to a greater extent than the stereocentre in the pyrrolidine ring.[199] All published routes to clemastine **1** employ the disconnection at the ether bond to give tertiary alcohol **89** (tail group) and chloroethylpyrrolidine **90** (head group) shown in Scheme 5.[199,200,197,201] It should be noted that until recently resolution was employed to separate the diastereomers but in 2010 Clayden *et al.*[202] and in 2015 Lee *et al.*[200] developed asymmetric synthetic routes to clemastine, discussed further in 2.6.1. and 2.6.2.

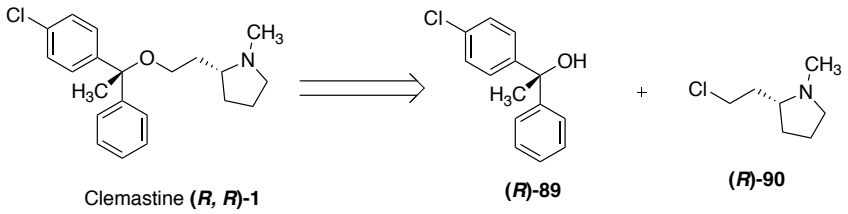

Scheme 5: Disconnection of clemastine 1

2.6.1. Tertiary alcohol (tail group)

A patent published in 2009 uses a simple Grignard reaction to form the tail group **89** but as a racemic mixture in a low yield of 25% (Scheme 6a).[197] Both Lee and Clayden developed enantioselective reactions to afford the tail group as one enantiomer. In Lee's synthetic route (Scheme 6b), the chiral benzyl group, alcohol **91**, acts as a chiral auxiliary as well as a protecting group. The key reaction is the chelation-controlled asymmetric nucleophilic addition of 4-chlorophenylmagnesium bromide to phenyl ketone **92**, pre-complexed with $MgBr_2$.OEt in DCM (Scheme 6b), to afford compound **93** with good diastereoselectivity, 97% diastereomeric excess (de).[200] Overall the route consists of 6 steps with variable yields in comparison with Clayden's route which is only 4 steps and benefits from an overall higher yield. In Clayden's procedure (Scheme 6c) the (*S*)-tertiary alcohol **(*S*)-89** is made from *p*-chloroacetophenone **94** that is reduced to alcohol **(*S*)-95** *via* a Noyori asymmetric hydrogenation. Alcohol **(*S*)-95** is converted into carbamate **(*S*)-96** which is treated with LDA to form a lithiated carbamate that undergoes aryl migration to compound **(*S*)-97** with a moderate enantiomeric excess of 68%. Finally, tertiary alcohol **(*S*)-89** was formed by refluxing compound **(*S*)-97** with NaOEt in ethanol.[202]

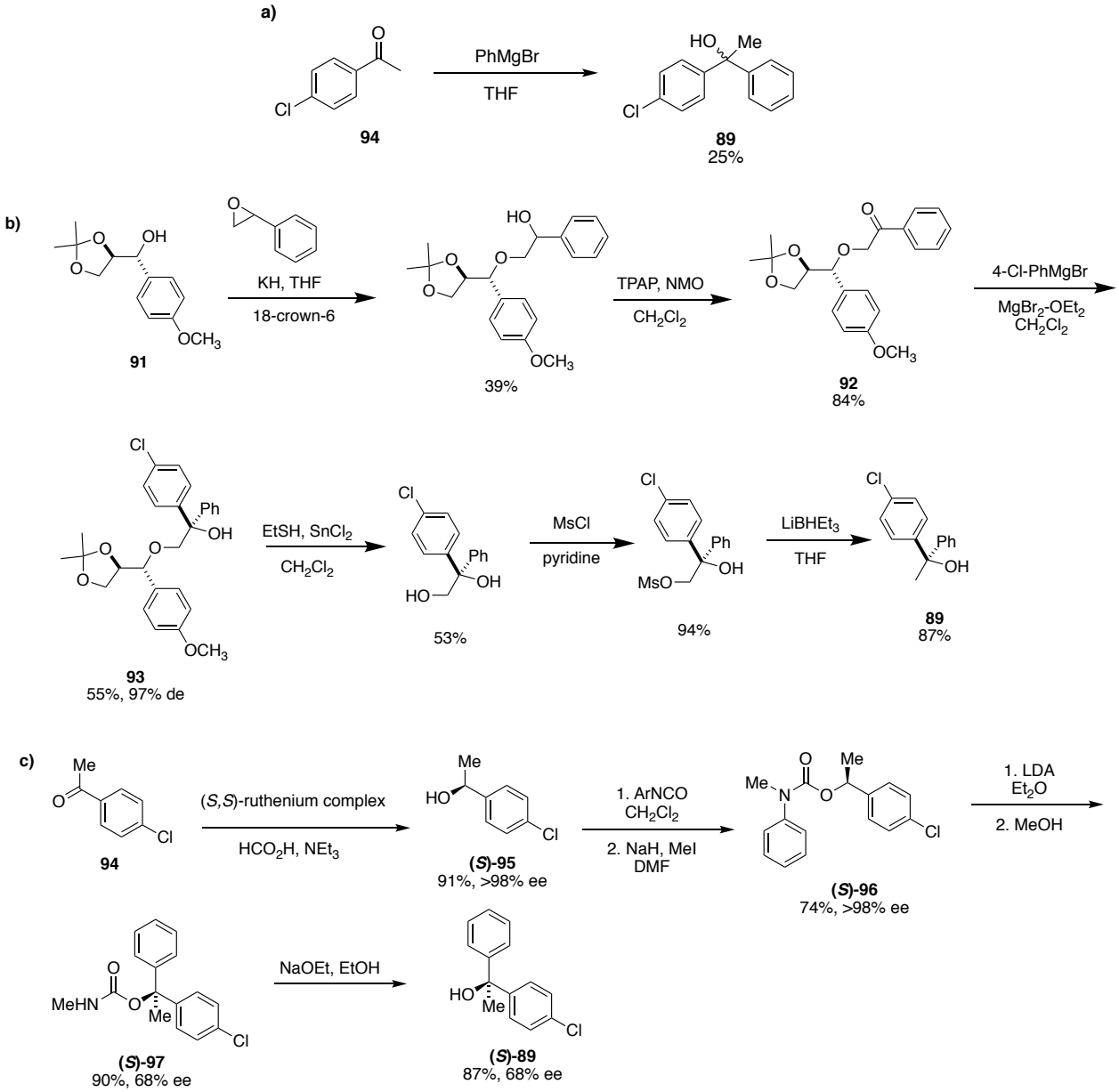

Scheme 6: Synthesis of tail group 89 reported a) in US patent;[196] asymmetric synthesis of tail group 89 b) by Lee et al.[199] and c) Clayden et al.[201]

2.6.2. Chloroethylpyrrolidine (head group)

The patent involves the straightforward homologation of proline **(*R*)-98** *via* nitrile **(*R*)-99** to form the head group **(*R*)-90** and although the yields are good for each individual step it is a long synthesis (seven steps) (Scheme 7).[197]

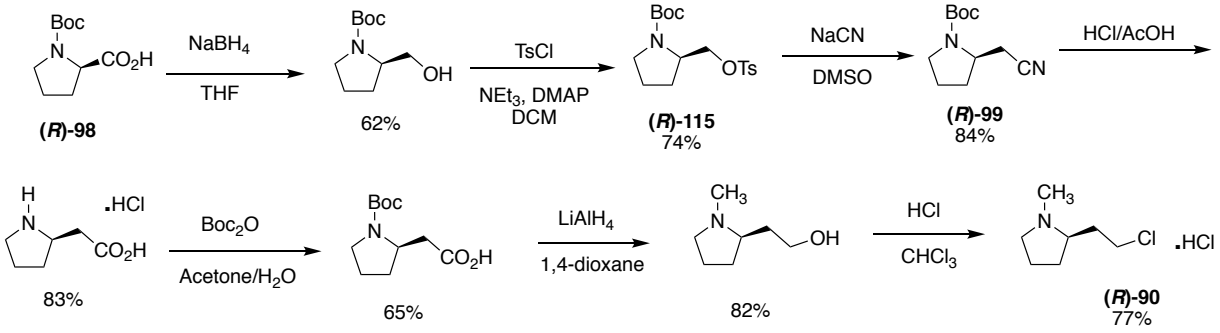

Scheme 7: Formation of (*R*)-head group 90 via straightforward homologation of (*R*)-proline 98[196]

The route described by Nikiforov (Scheme 8) in 1990 comprises of six steps but yields from the steps are not reported. It starts from 1-methyl-2-thiopyrrolininone **100** which is S-alkylated and then directly subjected to a sulfide contraction to form compound **101**. The crucial step was to resolve benzyl ester **102** to yield the (*R*)- enantiomer. This was achieved using the *R*-isomer of di-*p*-toluoyl-tartaric acid and **(*R*)-102** was subsequently reduced and chlorinated to form head group **90**.[203]

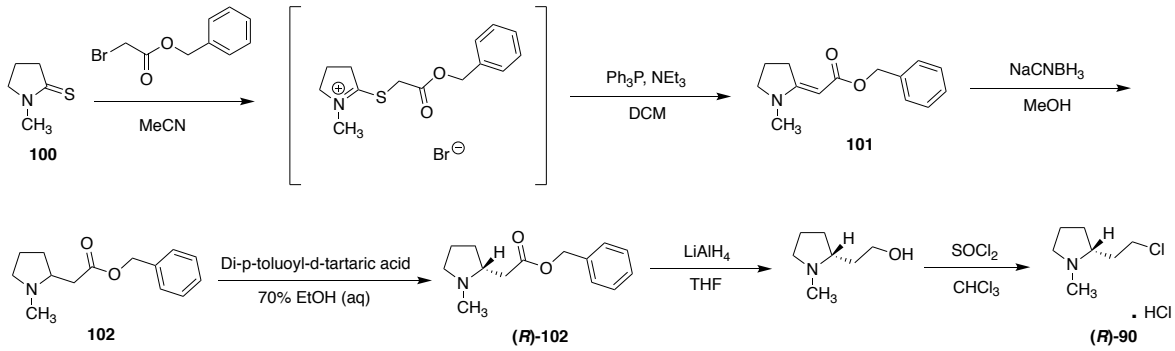

Scheme 8: (*R*)-head group 90 formation involving the resolution of benzyl ester 102[202]

Lee *et al*. starts from *L*-homoserine lactone **(*S*)-103** (Scheme 9). Following racemisation-minimized N-allylation three further steps afford the acyclic diene **(*S*)-104** ready for ring-closing metathesis (RCM)[204]. After this RCM step, chloroethylpyrrolidine **(*R*)-90** was accessed by a two-step reduction and chlorination.[200]

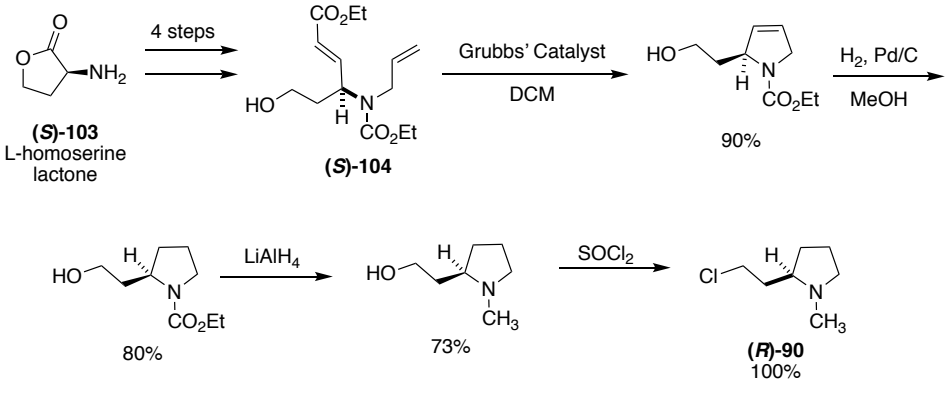

Scheme 9: Synthesis of (*R*)-head group 90 *via* ring-closing metathesis[199]

Clayden's synthesis of (*S, S*)- clemastine **(*S, S*)-1** (Scheme 10), forms the head group **(*S*)-90** from *N*-Cbz-proline **(*S*)-105** using an Arndt-Eistert reaction. The first step involves conversion of *N*-Cbz-proline **(*S*)-105** into diazoketone **(*S*)-106** and then a Wolff-rearrangement to form the chain-extended methyl ester **(*S*)-107** with retention of stereochemistry. Both the ester and carbamate protecting group were reduced to afford homoprolinol **(*S*)-108**, which again was treated with thionyl chloride to form the head group **(*S*)-90**. This procedure benefits from only being 4 steps and a moderate overall yield of 38%.[202]

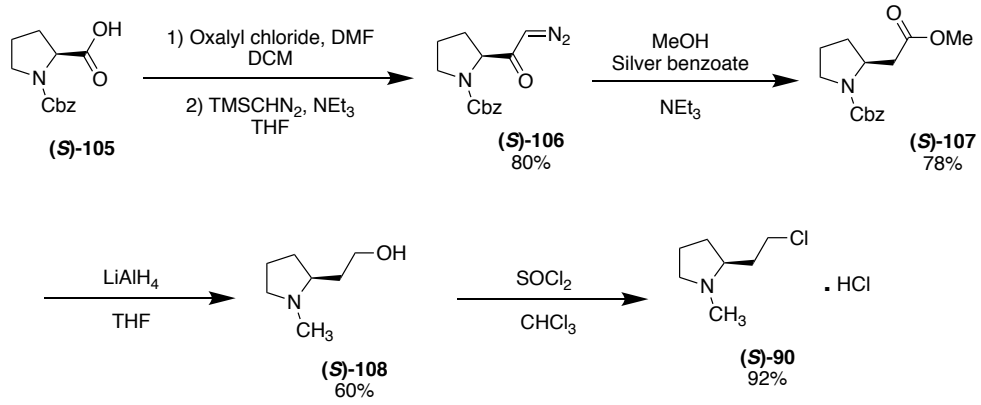

Scheme 10: Synthesis of (*S*)-head group 90 *via* an Arndt-Eistert reaction[201]

2.6.3. Etherification to form clemastine

The formation of the hindered ether is challenging and both reported procedures involve free-basing the head group and deprotonating the tertiary alcohol with either $NaNH_2$ or NaH. This is followed by heating alkoxide **89** with alkyl chloride **90** under reflux for 16h to afford clemastine **1** in moderate to low yields and azepane **109** as a by-product (Scheme 11).[197,202] Clayden assumed that the formation of isomer **109** arises through intramolecular alkylation to form the reactive bicyclic cation **110** (Scheme 12) which can then undergo expansion with alkoxide **89**. Consistent with this, amine protection as a carbamate on the head group showed no coupling and therefore participation of the amine N is involved in the pathway of both products.[202]

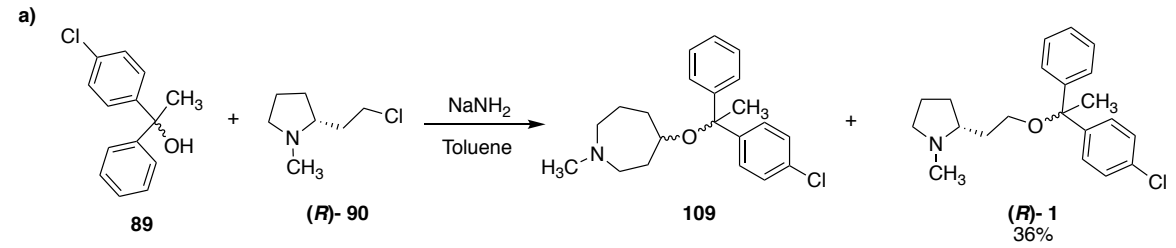

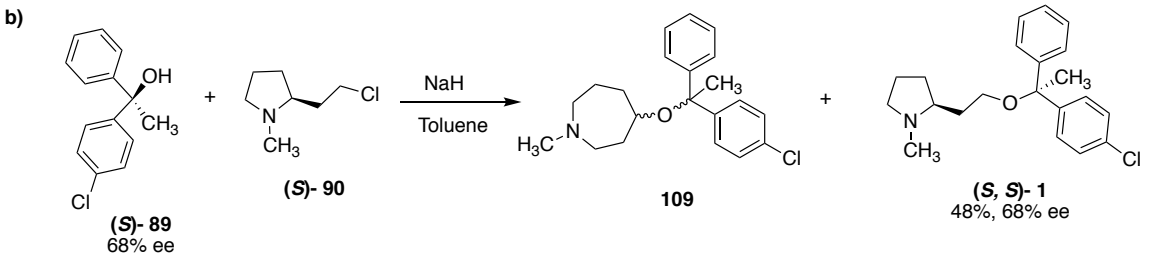

Scheme 11: Formation of clemastine 1 reported a) in US patent,[196] b) by Clayden *et al.*[201]

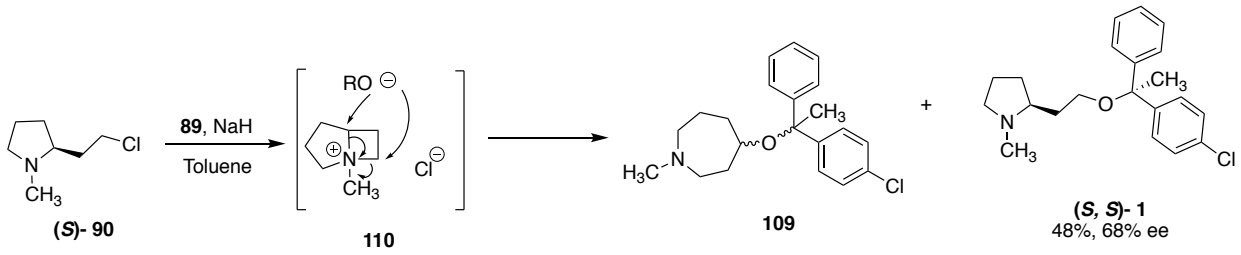

Scheme 12: Etherification *via* bicyclic cation 110[201]

2.7. Clemastine analogues

Inhibitors from the screen described in section 2.5. exhibited narrow chemical diversity. Therefore, previous work in the group developed a synthetic route to a small library of clemastine analogues based on the literature routes to clemastine reported in section 2.6. The development of this synthetic route by Brown[191] will be discussed in this section, along with the biological results which demonstrate the requirements for activity of clemastine against *Lmj*IPCS.

2.7.1 Synthesis of head and tail groups

An initial concern was the quaternary methyl group on the benzhydyl carbon of **89**. Previous research in the group demonstrated that tertiary alcohol **89** was unstable and prone to water elimination forming phenyl-styrene **111** (Scheme 13).

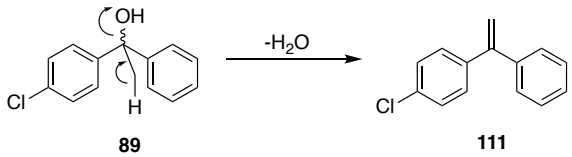

Scheme 13: Instability of tertiary alcohol

Therefore, the synthesis of a library of clemastine analogues lacking the quaternary methyl group on the benzhydryl carbon (nor-clemastine analogues) was investigated. Using the literature procedures outlined above, nor-clemastine analogue **(*R*)-112** was synthesised from benzhydrol tail group **113** and homoprolinol head group **(*R*)-108** (Scheme 14). The synthesis of both moieties and their coupling to form nor-clemastine analogues is described below.

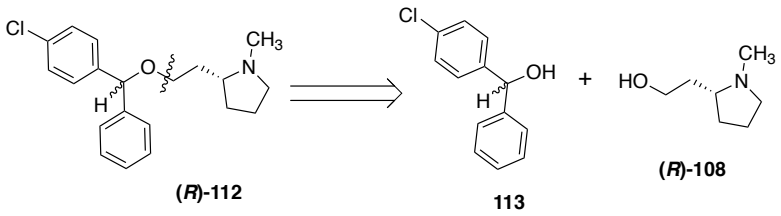

Scheme 14: Disconnection of nor-clemastine analogues

The synthesis of this tail group **113** was facile and used a Grignard reaction to furnish the desired benzhydrol tail group **113** in a good yield (Scheme 15).

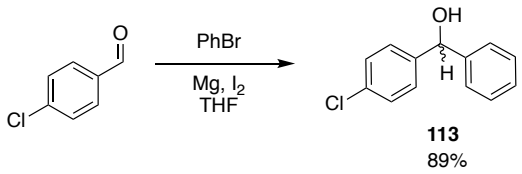

Scheme 15: Formation of benzhydrol 113

Initially, Brown attempted to access the Boc-protected homoprolinol head group **(*S*)-114** and this involved a straightforward homologation of proline as outlined in Scheme 16. It should be noted that tosylate **115** was very unstable and immediately displaced by the cyanide anion to form the desired nitrile **99**. The literature procedure was then modified and nitrile **99** was hydrolysed with the mild reagent Na_2O_2 which did not cleave the protecting group and afforded compound **(*S*)-116** in a good yield. Subsequent reduction using BH_3 then afforded the enantiomerically pure Boc-protected (*S*)-homoprolinol **(*S*)-114**. The overall yield was 33% over 5 steps and the route involved an unstable intermediate, therefore, other routes were explored.[191]

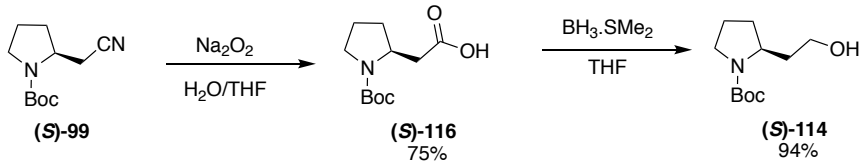

Scheme 16: Formation of (*S*)-homoprolinol from nitrile 99

Another procedure described by Brown involved using a Wittig homologation followed by a hydroboration as shown in Scheme 17. The oxidation of prolinol **(*S*)-117** to form

compound **(*S*)-118** was efficient on a gram-scale using a Parikh-Doeing oxidation, with SO_3.pyridine. However, the subsequent Wittig reaction formed **(*S*)-119** in a low yield and caused racemisation of the stereocentre. A hydroboration reaction followed by an oxidation with hydrogen peroxide furnished Boc-protected homoprolinol **(*S*)-114**.[191]

Although this route was successful it had a poor overall yield of 14% over 4 steps. In addition, there was a loss of enantiopurity and therefore was unsuitable for the synthesis of a nor-clemastine analogues.[191]

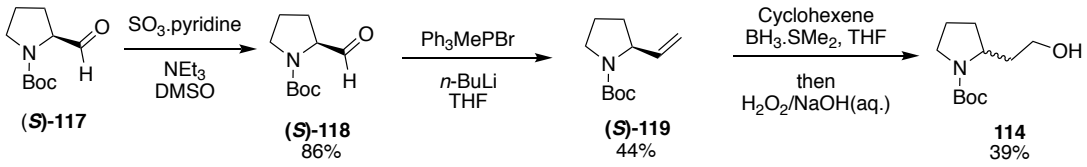

Scheme 17: Wittig reaction and subsequent hydroboration and oxidation to form Boc-protected homoprolinol 114

Brown found that the most efficient route was to access homoprolinol **108** *via* homologation of *N*-Cbz-proline using an Arndt-Eistert reaction described by Clayden *et al*. and outlined in Scheme 10.[202] This route retained stereochemistry and proved to be the most efficient, with overall yields of 62% for **(*S*)-108** and 43% for **(*R*)-108** over 4 steps.[191]

2.7.2. Etherification step to form nor-clemastine analogues

The final step of the synthetic route is a challenging etherification of a sterically hindered benzhydrol **113** and results in low-to-moderate yields of the final compound **112**. As described in section 2.6.3. and shown in Scheme 12, this reaction forms azepane by-product **109** *via* assistance of the amine group on chloroethylpyrolidine **90** to form the reactive bicyclic cation **110**. To try and circumvent this problem, Brown decreased the nucleophilicity of the nitrogen atom by using the Boc-protected homoprolinol **114**. The alcohol group of compound **114** was activated to a reaction with benzhydrol **113** *via* tosylation. However, tosylate **120** was unstable and degraded before it could be reacted with benzhydrol **113**. Brown suggests that the instability was due to an interaction between the carbamate and tosyl group (Scheme 18). Nevertheless, this route was abandoned and another explored.

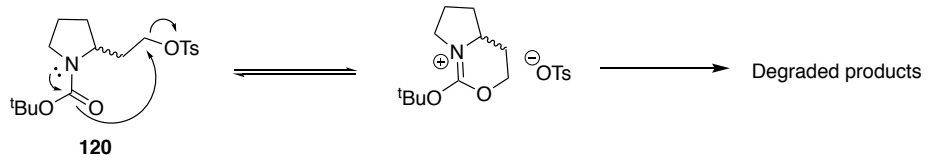

Scheme 18: Postulated degradation of compound 120[190]

Previous reports have demonstrated that benzhydrols can undergo acid-catalysed ether formation;[205, 206] therefore, benzhydrol **113** and Boc-protected alcohol **114** were refluxed with *p*-toluenesulfonic acid in the presence of 4 Å molecular sieves to afford the desired nor-clemastine analogue **121**. This general procedure was used to synthesise **121**, **(*S*)-112** and **(*R*)-112** in moderate yields of 66%, 34% and 57% respectively (Scheme 19).[191]

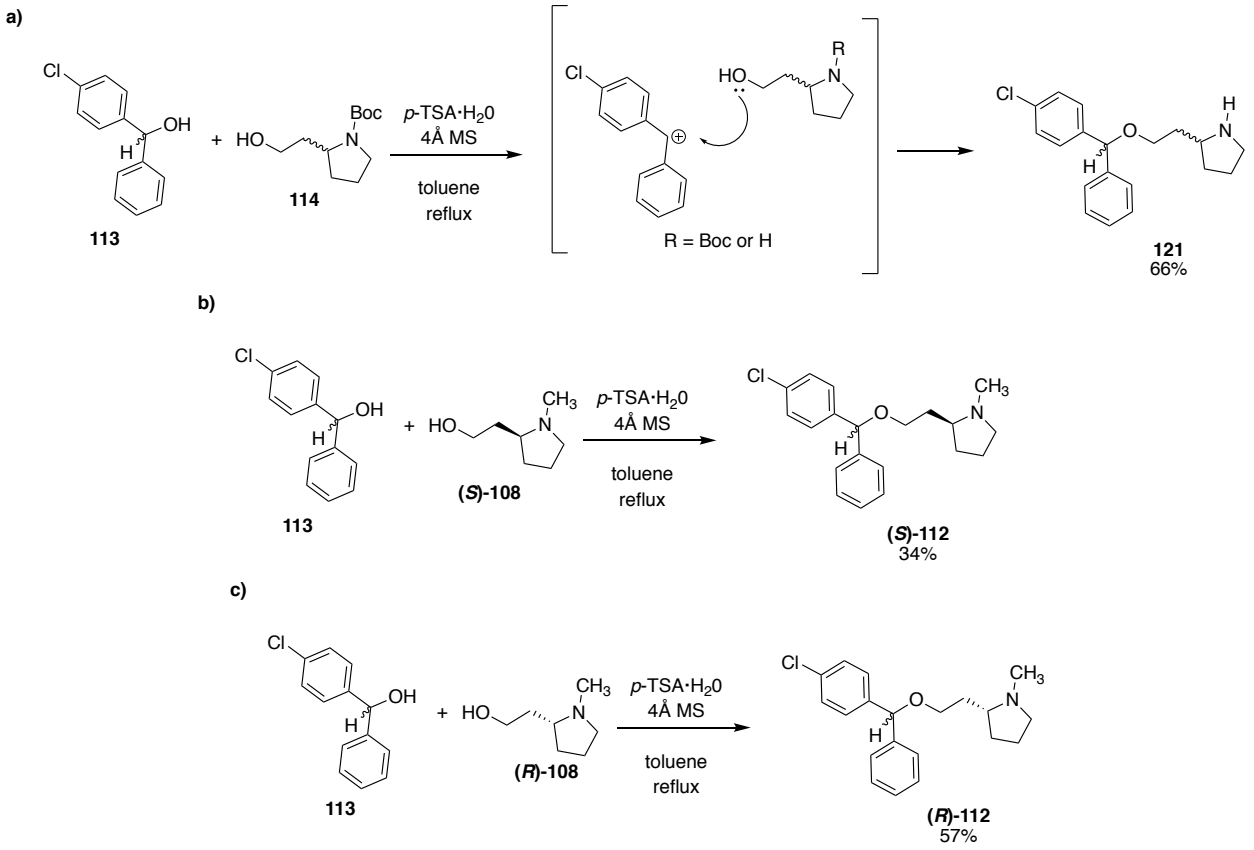

Scheme 19: Condensation of alcohols to form compounds 121, (*S*)-112 and (*R*)-112 (adapted from Brown with permission)[190]

2.7.3. SAR data for clemastine analogues

Molecules with different linker moieties were also synthesised and tested in addition to nor-clemastine analogues and the SAR data obtained by Brown is summarised in Figure 24. The synthetic routes to many of the analogues have not been included in this thesis as these changes had a detrimental effect on potency. Pleasingly, the quaternary methyl group on the benzhydryl carbon was not essential to activity, however, the methyl group on the amine improved potency.[191] The most active analogue of clemastine was nor-

clemastine **(*R*)-112** which retained activity in both the enzyme and parasite assays (Figure 25). Therefore, an initial focus of this project was to optimise the route to nor-clemastine analogues developed by Brown and synthesise analogues that would further explore the SAR (Chapter 4).

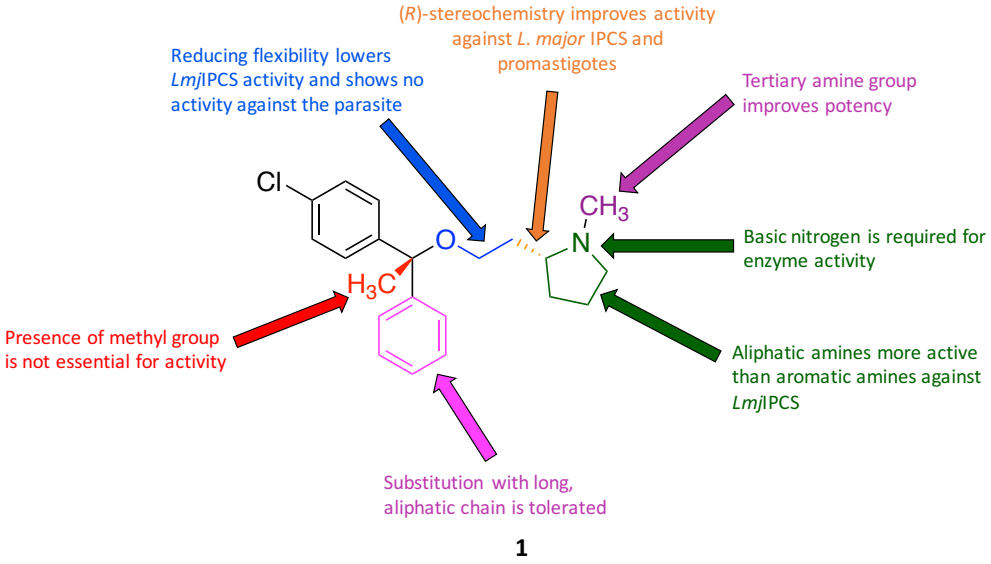

Figure 24: SAR of clemastine analogues (adapted from Brown with permission)[190]

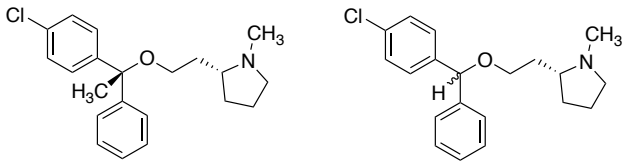

Figure 25: Enzyme and anti-promastigote activity of clemastine and analogue (*R*)-112[190]

2.8. Project objectives

The previous work discussed in this chapter identifies the overall aims of this project, which can be summarised as:

- Investigate the effects of clemastine in an animal model of cutaneous leishmaniasis and identify the most appropriate route of administration.
- Improve accessibility to clemastine analogues through the development of robust synthetic routes.
- Enhance potency and selectivity of these clemastine analogues towards *Leishmania*.
- Validate the on-target effects of clemastine and its analogues.

3. Clemastine activity

3.1. Anti-promastigote assays

Chapter 2 demonstrated the potential of clemastine **1** as a novel antileishmanial with its high activity against *Lmj*IPCS and *L. major* promastigotes and amastigotes. *L. major* is found in the Eastern hemisphere and manifests as CL, the most common form of the disease.[175] However, what is really essential is a drug that is active against all species of *Leishmania* and therefore has the potential to treat all forms of the disease around the globe. Thus, in addition to the *L. major* species clemastine **1** was tested against *L. amazonensis;* which also leads to CL but is found in the Western hemisphere;[207] *L. infantum* and *L. donovani,* which both manifest as the most fatal form of the disease, VL.[175]

Dose-response assays were performed for clemastine **1** against *L. major*, *L. amazonensis*, *L. donovani* and *L. infantum* promastigotes. In brief, promastigote parasites, in the log growth phase, were incubated with clemastine **1** for 48 h or 72 h prior to the addition of resazurin solution, and after 4 h the fluorescence was quantified to measure cell-viability.[192] In all cases, for each species standard growth curves were constructed to ensure that the parasite density and conditions were appropriate for the assay. Assays against *L. major* promastigotes were performed at Durham University using a 48 h protocol whereas assays using *L. amazonensis*, *L. donovani* and *L. infantum* promastigotes were carried out at Universidade Federal do Rio de Janeiro (UFRJ) using a 72 h protocol and adjusted materials (Chapter 8).

Figure 26 shows that *L. major* promastigotes incubated with 10 μM of clemastine **1** for 24 h become more rounded and less elongated in shape. This rounded morphology indicates that the parasites have started to die. The results from these assays show that clemastine **1** is 2-3 times more active against *L. major* (FV1) than previously reported,[191] presumably due to a longer incubation time of 48 h rather than performing a 24 h assay. Figure 27 and 28 clearly demonstrates that clemastine **1** has sub-micromolar activity across all of the *Leishmania* species tested. The differences in activity between the *L. major* and *L. donovani* species are interesting (Figure 28) as the sequence identity of IPCS is 93% and domains, D3 and D4, that contain the active residues possess 100% sequence identity. This suggests that the other IPCS domains are influencing binding affinities to the protein or that clemastine

1 has off-target effects. In addition, the EC_{50} value of clemastine **1** is particularly high against *L. infantum* compared to other *Leishmania* species. A possible explanation is that more of the target protein is being expressed in *L. infantum* compared to the other species; therefore, a higher dose of clemastine is needed to inhibit IPCS and cause parasite death. Clemastine **1** is most potent against *L. amazonensis* and *L. donovani* with an EC_{50} value in the nanomolar range (20 nM). Consequently, this compound has the potential be used as a therapy for both CL and VL. Having demonstrated broad spectrum activity, the next requirement was to assess activity in the clinically relevant amastigote form. This is described in the following section.

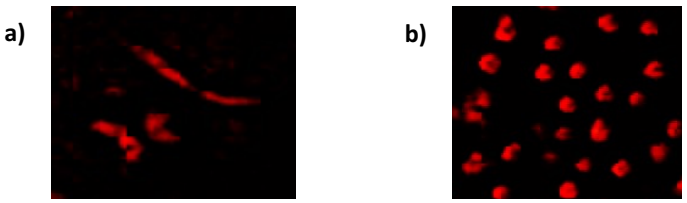

Figure 26: Images of *L. major* promastigotes a) untreated and b) treated with 10 μM clemastine 1 for 24 h.

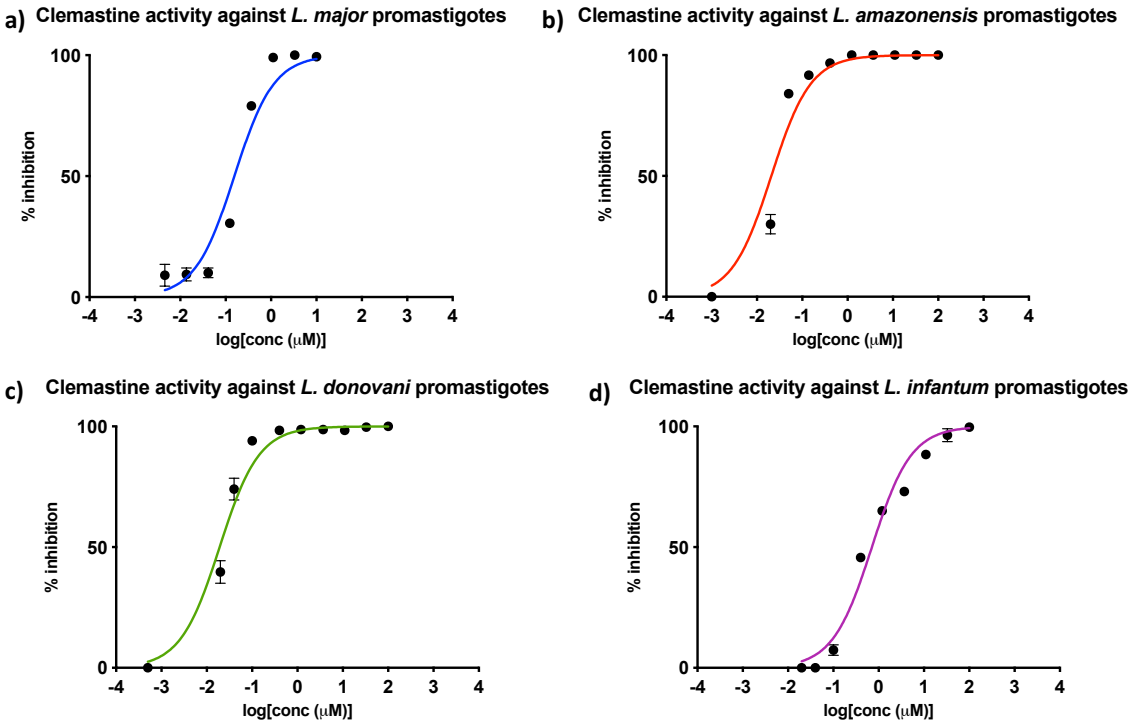

Figure 27: Dose-response curves of clemastine against *L. major, L. amazonensis, L. donovani* and *L. infantum* promastigotes; assays were performed in triplicate and each curve shows a representative experiment.

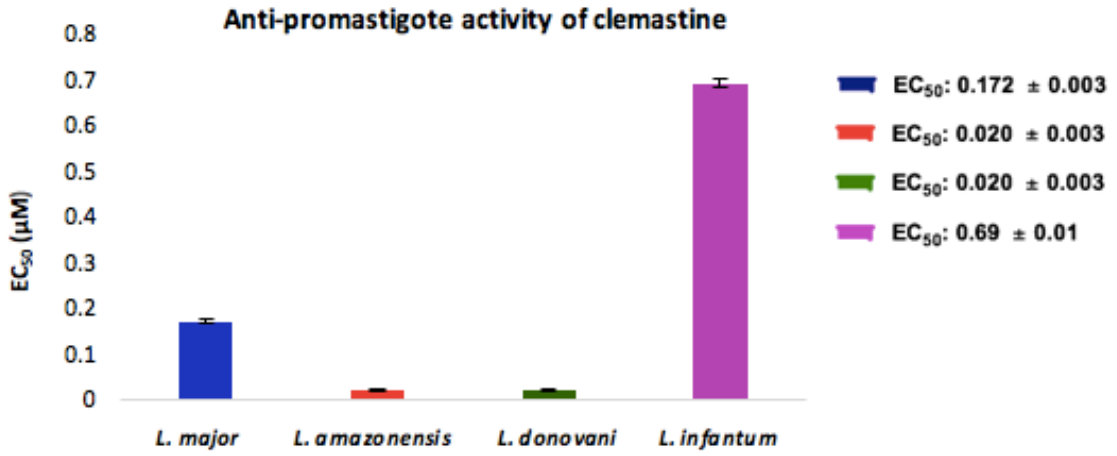

Figure 28: EC_{50} values of clemastine 1 against *L. major, L. amazonensis, L. donovani* and *L. infantum* promastigotes; EC_{50} values are mean ± 95% CI from at least three experiments.

3.2. Cytotoxicity to bone marrow derived macrophages (BMDM)

The cytotoxicity of clemastine **1** against peritoneal mouse macrophages (CC_{50} > 20 μM) was investigated in Chapter 2. Before an intramacrophage assay could be performed an accurate assessment of macrophage cytotoxicity using bone marrow-derived macrophages (BMDM) was required, as BMDM would be used in the following anti-amastigote assay. The benefit of BMDM over peritoneal macrophages is that more macrophages can be harvested per animal.[208] Briefly, 1×10^6 mL^{-1} BMDM were incubated with clemastine **1** for 48 h and, similarly to the anti-promastigote assay described above, resazurin solution was added and fluorescence quantified to measure cell-viability.[192] The result is shown in Figure 29 and was used to calculate a CC_{50} value of 20 ± 1 μM for uninfected BMDM. Therefore, clemastine **1** is more selective towards the promastigotes than mammalian cells (selectivity index, SI ≈ 117, 1247, 998 and 29 for *L. major*, *L. amazonensis*, *L. donovani* and *L. infantum*, respectively) and this compound was progressed into an intracellular amastigote assay.

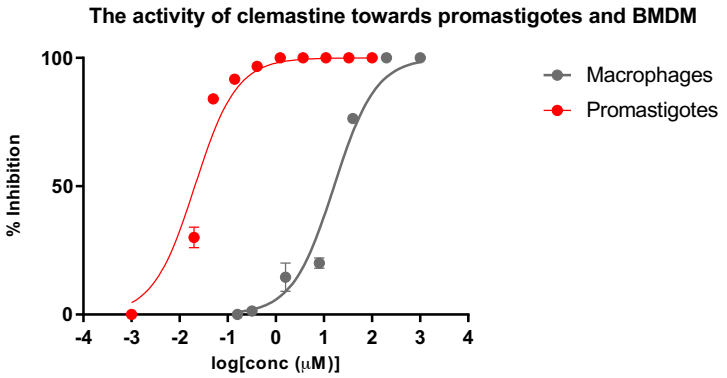

Figure 29: An example of dose-response curves of clemastine against macrophages (BMDM) and *L. amazonensis* promastigotes; assays were performed in triplicate and each curve shows a representative experiment.

3.3. Intramacrophage anti-amastigote assay

Clemastine **1** was tested against BMDM infected with *L. amazonensis* amastigotes, as depicted in Figure 30a *L. amazonensis* was chosen due to its sensitivity to clemastine **1**, infectivity towards BMDM and because it is responsible for many cases of CL and ML in South America.[209,207] Briefly, BMDM with cover slips were infected with *L. amazonensis* promastigotes (10:1). After 24 h, serial dilutions of clemastine **1** were added and incubated for 48 h. Cover slips were then stained with Giemsa modified solution and amastigotes were counted within 200 macrophages using an optical Nikon® microscope to generate the dose-response curve displayed in Figure 30b. This assay revealed that clemastine **1** exhibits sub-micromolar inhibition of *L. amazonensis* amastigote growth with an EC_{50} value of 0.40 ± 0.06 μM. In comparison with the CC_{50} value observed in the macrophage assay (20 ± 1 μM), clemastine **1** is 50 times more selective towards the parasite over the host macrophage (SI = 50).

In parallel with the results obtained in the anti-promastigote assay, the activity against *L. amazonensis* amastigotes was 7-8 times more effective than that observed against *L. major* amastigotes (Chapter 2),[191] EC_{50} = 0.40 ± 0.06 μM and EC_{50} = 3.06 μM respectively. However, no definite conclusions can be made due to the differences in the methods used for the anti-amastigote assays (such as different types of macrophages, incubation times and analysis technique).

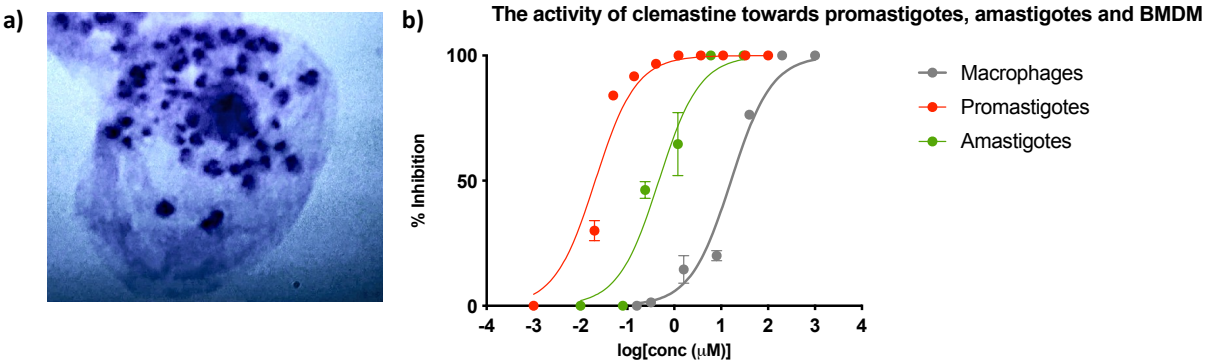

Figure 30: a) BMDM infected with *L. amazonensis* amastigotes stained with Giemsa modified solution and b) dose-response curves of clemastine 1 plotting the percentage of macrophage, promastigote and amastigote growth inhibition; assays were performed in triplicate and each curve shows a representative experiment.

Overall, these results, summarised in Table 3, show that clemastine **1** could be effective at a dose that does not cause any adverse side effects to the host. Before this hypothesis could be tested further with an *in vivo* infection study, additional tests were carried out to validate on-target effects and explore if clemastine **1** has macrophage modulatory activity, which could contribute to its intracellular activity.

Table 3: EC_{50} values of clemastine 1 against *L. amazonensis* promastigotes and amastigotes and CC_{50} value of clemastine 1 towards BMDM; values are mean ± 95% CI from at least three experiments.

Promastigote EC_{50} (μM)	Macrophages CC_{50} (μM)	Amastigotes EC_{50} (μM)
0.020 ± 0.003	20 ± 2	0.40 ± 0.06 μM

3.4. Macrophage modulation

Macrophages are important immune cells involved in the detection, phagocytosis and destruction of pathogens. Macrophages can destroy pathogens *via* two mechanisms and the first involves the generation of reactive oxygen species (ROS) and reactive nitrogen species (RNS). Upon microorganism invasion, the macrophages rely on the NADPH oxidase complex activity to generate superoxide radicals inside the phagosome. At the same time, the stimulation of nitric oxide synthase catalyses the production of nitric oxide in the cytosol which readily diffuses to the phagocytic vacuole. Inside the phagosome superoxide radicals and nitric oxides react to generate peroxynitrites, which are powerful oxidants capable of killing microorganisms.[210] The second mechanism occurs when the phagosome fuses with lysosome to become a phagolysosome. Formation of the acidified phagolysosome rapidly kills and degrades the pathogen.[211]

In the case of *Leishmania* parasites, amastigotes have adapted to survive in macrophage phagolysosomes by disrupting the generation of ROS.[212] However, in order to differentiate into amastigotes, the promastigotes must first survive antimicrobial activities of macrophages. A mechanism used to achieve this involves the inhibition of phagolysosome biogenesis. This leads to a decrease in the NADPH oxidase complex activity and reduces exposure to ROS. In addition, inhibition of phagosome maturation excludes the vesicular proton-ATPase (V-ATPase) from the phagosomes. The V-ATPase mediate phagosomal acidification which is essential for microbicidal properties and for optimal pathogen processing, as most lysosomal hydrolases are optimally active at acidic pH.[212] In summary, *Leishmania* parasites reduce the antimicrobial activities of macrophages enabling the parasite to proliferate inside these cells and cause the clinical manifestations. Therefore, a promising therapeutic approach for many diseases involves the modulation of macrophage activities.[213]

It was hypothesised that clemastine **1** was affecting the activity of the macrophage which was contributing to the observed antileishmanial activity. As described above nitric oxide (NO) is important as a toxic defence molecule against infectious organisms and is synthesised by many cell types involved in immunity and inflammation.[214] It was postulated that clemastine **1** could increase the synthesis of NO in host macrophages, which would be toxic to the intracellular parasites. In brief, uninfected macrophages were treated with serial dilutions of clemastine **1** and incubated for 48 h. Subsequently, supernatants were treated with the Griess reagent[3] and absorbance at 570 nm was quantified. The Griess Reagent System measures nitrite, a stable and non-volatile breakdown product of NO, and in our case a negative result was obtained. Therefore, NO cannot contribute to the observed antiparasitic activity.

Another mechanism of action by which immune response can contribute the antileishmanial activity is through the activation of the P2X7 receptor (P2X7R). The P2X7R is a membrane-bound protein with a ubiquitous distribution and is mostly highly expressed in immune cells. Activation of P2X7 by extracellular ATP opens a cation-specific ion channel which results in an influx of Na^+ and Ca^{2+} and efflux of K^+.[215] This leads to the secretion of pro-inflammatory cytokines, such as IL-1β and IL-18, and the production of reactive oxygen and nitrogen species.[216]

Significantly, it has been reported by Nörenberg *et al.* that clemastine **1** is an allosteric modulator of P2X7R, resulting in sensitisation of the receptor to lower ATP concentrations and facilitation of its pore dilation. The activity of clemastine **1** on P2X7R was confirmed in HEK293 cells stably transfected with human P2X7R, human monocyte-derived macrophages and murine bone marrow-derived macrophages. These assays measured the intracellular concentration of calcium using fluorescence as the cells were loaded with a calcium indicator.[217] Upon treatment with clemastine **1**, the human P2X7R is sensitised to extracellular ATP. This could stimulate an immune response and contribute to the antileishmanial activity. In support of this hypothesis, it has been reported by Rossi-Bergmann *et al.*[218] that macrophages infected with *L. amazonensis* display enhanced expression of P2X7R and are significantly more responsive to extracellular ATP. In fact, as low as 100 μM extracellular ATP diminishes the percentage of infected cells from BALB/c mice. It is unlikely that extracellular ATP is having a direct drug effect as it enhances axenic parasite growth.[218] Consistent with the results from the Griess Reagent assay, Rossi-Bergmann discovered that parasite death was unlikely due to NO production as this was unaltered with extracellular ATP concentrations. Hence, the mechanism of action is unknown but it was postulated that it involves host cell apoptosis.[218]

Collectively, this suggested that enhancement of the P2X7R, resulting from treatment with clemastine **1**, could contribute to the elimination of the parasites. To explore this idea, anti-amastigote assays were performed with macrophages from C57BL/6 WT mice and from C57BL/6 mice deficient in the P2X7 receptor ($P2X7R^-$). Analysis of the results obtained (Figure 31) revealed that clemastine **1** is 5-6 times more active against infected WT cells when a low concentration of extracellular ATP (100 μM) is added. In contrast, a similar experiment with $P2X7R^-$ macrophages did not show any effect with the addition extracellular ATP. This suggests that WT infected cells treated with clemastine **1** have an enhanced P2X7 receptor activity which is responsive to low concentrations of extracellular ATP with a downstream impact on intracellular parasite viability.

Overall, treatment of infected BMDM with clemastine **1**, results in sensitisation of the P2X7 receptor to extracellular ATP, which contributes to intracellular clearance (Figure 31). Therefore, the mechanism of action for antileishmanial activity of clemastine **1** may involve

modulation of macrophage activities as well as directly acting on the parasite by inhibition of IPCS. Whether or not IPCS inhibition and P2X7R expression are related events remains to be investigated.

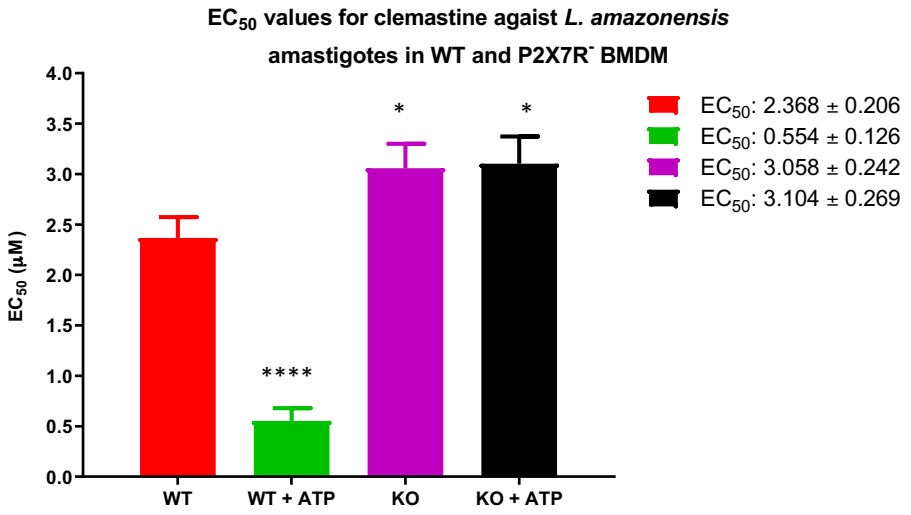

Figure 31: EC_{50} values of clemastine against *L. amazonensis* amastigotes in BMDM from WT and P2X7R⁻ C57BL/6 (KO) mice; results are from one experiment. Asterisks indicate that the difference between WT and WT + ATP and between WT and KO groups are statistically significant. * P ≤ 0.05, **** P ≤ 0.0001.

3.5. On-target validation

Clemastine **1** was identified as an inhibitor of *Lmj*IPCS from the biochemical assay described in Chapter 2. Further validation of this target came from metabolomic and lipidomic analyses, which showed a relative increase in *Lmj*IPCS substrate concentrations (ceramide and PI) after incubation with clemastine **1**. Collectively, this suggested that clemastine **1** functions as a *Lmj*IPCS inhibitor.

To confirm that the antileishmanial action of clemastine **1** occurred due to its activity as an *Lmj*IPCS inhibitor, assays were conducted with the sphingolipid-free *L. major* mutant (*Δ* LCB2). These parasites were created through targeted deletion of one SPT subunit, *Lm*LCB2.[179,178] Therefore, although these promastigotes have a functional IPCS they do not possess *de novo* synthesised ceramide which means IPCS is redundant. As a control, the *Δ* LCB2 cells were complemented by transfection with a plasmid encoding *Lm*LCB2 [pX NEO *Lm*LCB2] to generate an 'add-back' cell line termed PX. Ceramide and IPC synthesis were restored in these PX parasites.[178] Dose-response assays for clemastine **1** against *L. major* WT promastigotes, *Δ* LCB2 and PX cell lines were performed and EC_{50} values calculated. Results showed that the EC_{50} value of clemastine **1** against *Δ* LCB2 promastigotes was 0.45

± 0.07 μM, which is about 3 times less active compared to that observed for WT promastigotes. In addition, clemastine **1** shows similarly good levels of activity against the PX cell line as against the WT parasites (EC_{50} value of 0.08 ± 0.01 μM, Figure 32). By contrast the positive control, cycloheximide, maintained an EC_{50} value of 0.02 μM against mutant promastigotes and therefore acts *via* a separate mode of action.

Overall, the activity of clemastine **1** against *Δ* LCB2 parasites is lower than that observed against WT and PX parasites, which suggests that clemastine **1** is having an effect on the sphingolipid pathway. This result together with the positive IPCS biochemical assay and metabolomic and lipidomic results (Chapter 2) supports the hypothesis that clemastine **1** is having on-target effects.

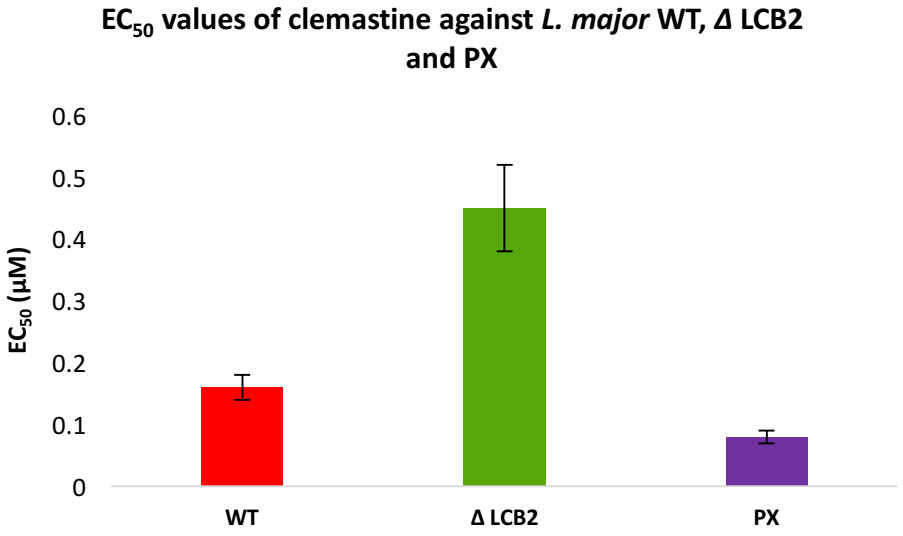

Figure 32: EC_{50} values of clemastine 1 against WT, *Δ* LCB2 and PX *L. major* promastigotes; values are mean ± 95% CI from at least three experiments

3.6. *In vivo* infection studies

It has been established that clemastine **1** is effective against *Leishmania* promastigotes and amastigotes, and that this antileishmanial action is due to its activity as an *Lmj*IPCS inhibitor, as well as potentially stimulating the immune system of the host. Therefore, the next step was to analyse the *in vivo* efficacy of clemastine **1** in the treatment of mice infected with *L. amazonensis*. Drugs can be administered to laboratory animals by a wide variety of routes[219] but initial investigations focused on the intralesional (IL) and oral routes of administration. The intralesional route was chosen as it is immediately absorbed at the site action and therefore the most effective means of delivering the drug. The oral route

was studied as an oral drug would be most accessible to those infected with leishmaniasis living in deprived communities, and also because clemastine is already orally available for humans as an antihistamine. A gavage was used for the oral administration of mice to ensure precise and accurate dosing.[219]

The first *in vivo* study used BALB/c mice infected with *L. amazonensis* expressing green fluorescent protein (GFP).[220] Treatment of the five groups was initiated one-week post infection: clemastine **1** (oral), miltefosine (oral), clemastine **1** (intralesional, IL), pentostam **2** (intralesional, IL) and untreated. Clemastine **1** was given to the mice at an oral dose of 30 mg kg^{-1} five times a week, which was calculated from the average human dose when used as an antihistamine.[221,222] Miltefosine was used as the positive control with an oral dose of 2.5 mg kg^{-1} five times a week. The intralesional dose of clemastine **1** was 217 μg kg^{-1}, 1.09 mM, over 100-fold higher than the *in vitro* anti-amastigote EC_{100} of 8 μM, and administered twice a week. The same intralesional dose of Pentostam **2** (217 μg kg^{-1} twice a week) was used for direct comparison and the untreated infected mice were used as the negative control group. Mice were treated for 28 days and weight variation and lesion size were measured at least once a week to monitor toxicity and the progression of the disease (Figure 33a and 33b). On day 45 the animals were sacrificed and the fluorescence measured (Figure 33c) and parasite load quantified using limiting dilution assay (LDA) (Figure 33d).[223] Lesion progression was analysed for statistical significance by using the Dunnett test (comparing every mean to a control mean) as part of the one-way ANOVA (GraphPad Prism 8 software).[224] A result was considered significant at $P \leq 0.05$.[225, 226]

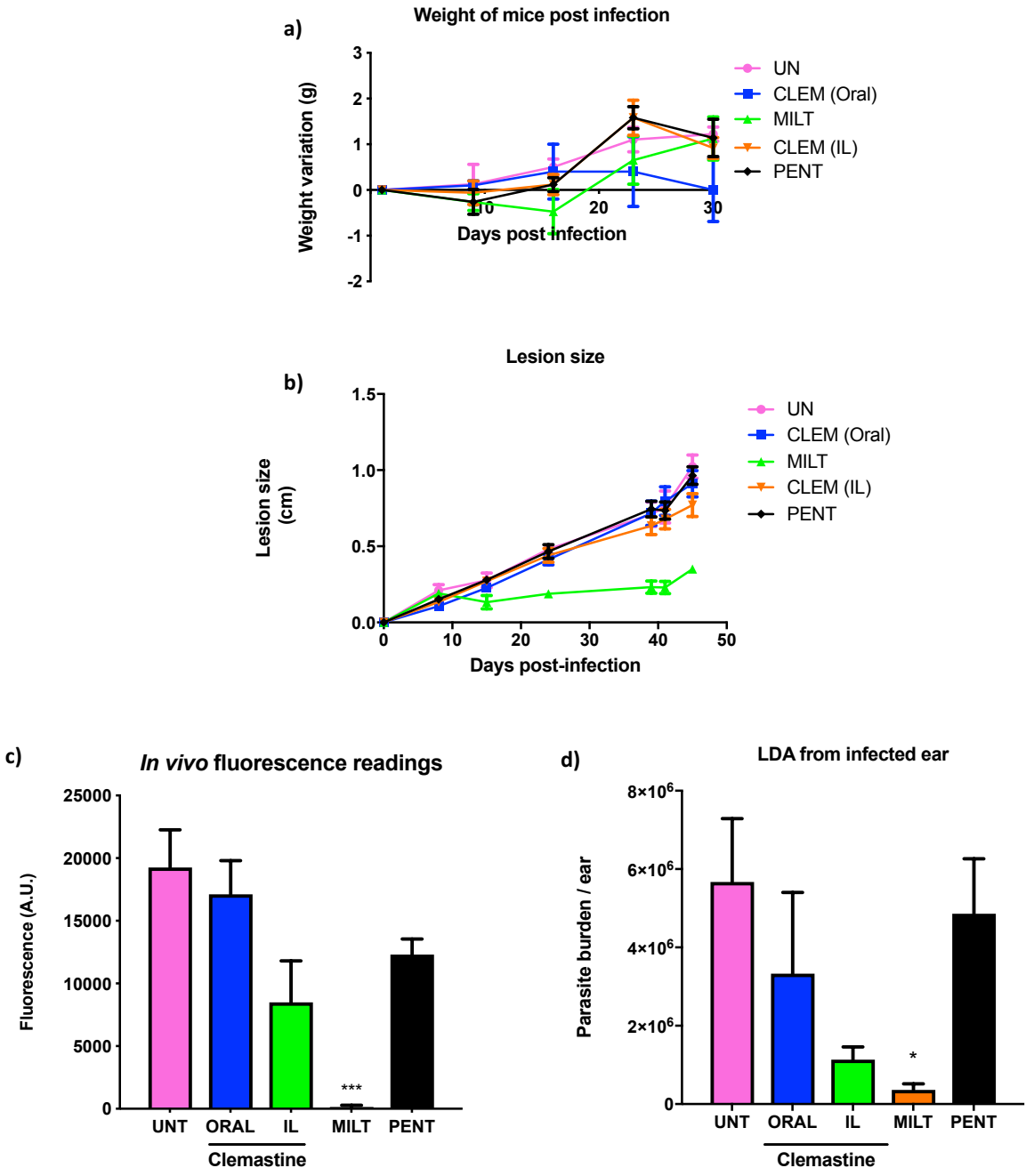

Figure 33: ***In vivo*** **study 1 from BALB/c mice infected with 2x10^6** ***L. amazonensis*** **GFP promastigotes in the right ear. Mice were divided into the following groups: oral clemastine (*n*=3), miltefosine (*n*=4), IL clemastine fumarate (*n*=5), IL pentostam (*n*=5) and untreated (*n*=4).** ***n*** **denotes the number of mice used in each group. During 28 days of treatment a) weight variation of mice and b) progression of lesion thickness were measured. After completion of treatment the parasite burden of the infected ear was evaluated by c) fluorescence measurements and d) LDA; asterisks indicate that the difference between control and drug-treated groups are statistically significant. * P ≤ 0.05, *** P ≤ 0.001.**

It should be noted that there were slight sedative effects for the oral clemastine **1** group directly after treatment but no long-lasting effects were observed and weight remained constant during treatment. The data from lesion size measurements and fluorescence readings were inconclusive. The LDA showed a reduction in parasite burden when clemastine **1** was given as an intralesional treatment; however, the reduction was not great

enough to show statistical significance between the clemastine **1** IL and the untreated groups (P= 0.08). In addition, the oral dose of clemastine **1** used in this *in vivo* assay was not effective. The lack of oral activity may be due to the poor aqueous solubility of clemastine **1** which makes dosing with the gavage difficult and results in insufficient drug absorption. Thus, despite a tendency of intralesional (and oral) clemastine in controlling parasite burden, the results were not statistically conclusive. Therefore, in the second *in vivo* study there was a 4-5 times increase in the dosage of oral clemastine **1** to try and increase drug absorption. Furthermore, the drug formulation consisted of a higher percentage of tween-80 to increase viscosity and therefore improve the drug suspension (Chapter 8).

The second *in vivo* study* involved treatment of BALB/c mice infected with *L. amazonensis* GFP which again was initiated one-week post infection. Animals were divided into the five groups plus a sixth group treated with a clemastine analogue which will be discussed in Chapter 5. The five groups discussed in this chapter: clemastine **1** (oral), clemastine **1** (intraperitoneal, IP), clemastine **1** (intralesional, IL), glucantime **3** solution (intraperitoneal, IP) and untreated. As mentioned previously, oral clemastine **1** was administered at a much higher dose of 134 mg kg^{-1} five times a week and the drug formulation was changed to produce a more evenly distributed suspension. Clemastine **1** was given as an IP injection at a dose of 11.65 mg kg^{-1} twice a week to give an insight into the pharmacokinetics of clemastine **1** as they should be similar to those observed by oral administration.[219] The previous *in vivo* study showed clemastine **1** had the potential to reduce the parasite burden as an IL therapy. With the aim of showing statistical significance, the IL dose was increased to 1.17 mg kg^{-1} twice a week. It should be noted that the IL dose is 10-fold less than the IP dose as the absorption of material delivered *via* IP is typically much smaller and slower than for IL. Finally, glucantime **3** solution was used as the positive control at an IP dose of 1.30 g kg^{-1} twice a week. Mice were treated for 28 days and weight variation and lesion size were measured at least once a week to monitor the progression of the disease. On day 41 the animals were sacrificed and the fluorescence measured and parasite load quantified using limiting dilution assay (LDA).

***Collaboration with Douglas Escrivani at UFRJ**

As before, there was little variation in weight of treated mice (Figure 34a) and the assay showed positive results. Figure 34b and 34c illustrate a significant reduction in lesion size between the untreated group and all clemastine-treated mice at day 35 post-infection. It should be noted that lesion sizes are typically larger for IL therapies as they cause inflammation to the ear. The animals were sacrificed on day 41 and the *in vivo* fluorescence measurements from the infected ear are shown in Figure 34d. There is a statistical significance between the untreated group and clemastine **1** administered *via* IP or IL ($P \leq 0.001$). However, fluorescence readings from the infected ear show no decrease in parasite burden when the untreated mice are compared with the oral clemastine group. Finally, results from the LDA show a statistical significance between the average parasite burden of the untreated group and the group treated with oral clemastine **1** ($P \leq 0.001$, Figure 34e). The LDA is a more sensitive and reliable technique than fluorescent measurements from *L. amazonensis* GFP which may account for the contrasting results for the oral clemastine group. In the LDA the greatest statistical significance was between the untreated group and the IP and IL clemastine groups ($P \leq 0.0001$).

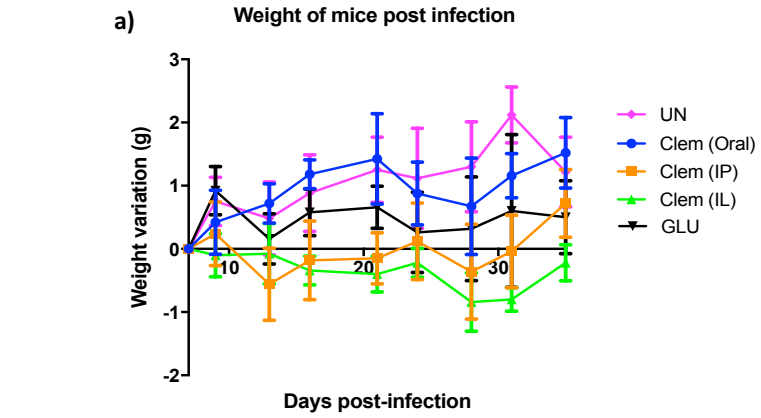

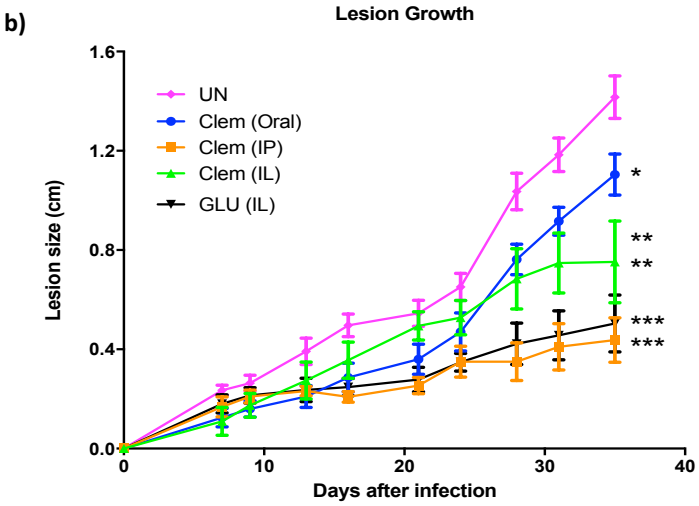

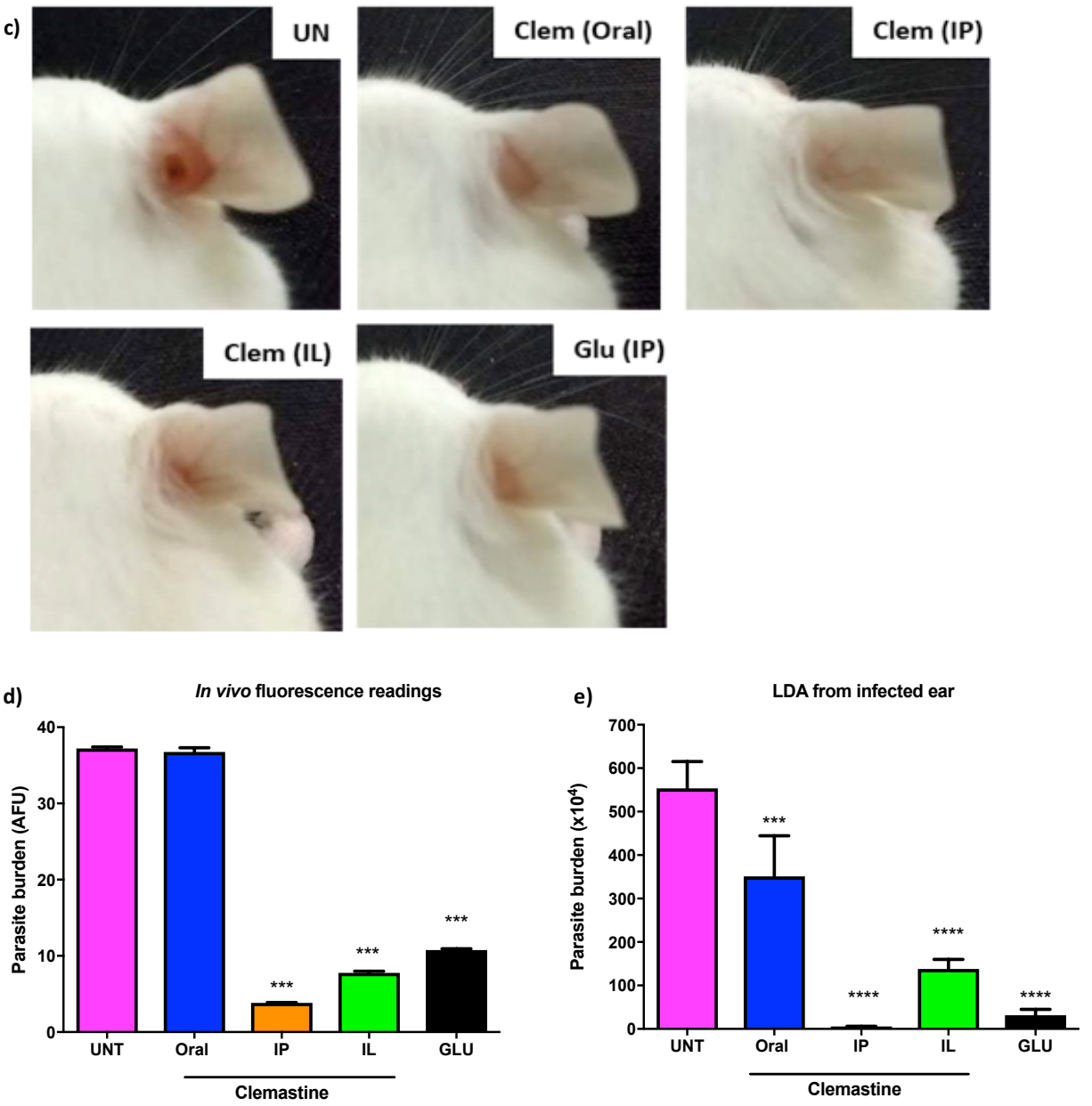

Figure 34: *In vivo* study 2 from BALB/c mice infected with 2x10^6 *L. amazonensis* GFP promastigotes in the right ear. Mice were divided into the following groups: oral clemastine (*n*=5), IP clemastine (*n*=5), IL clemastine (*n*=5), IP glucantime solution (*n*=5) and untreated (*n*=6). *n* denotes the number of mice used in each group. During 28 days of treatment a) weight variation of mice and b) progression of lesion thickness were measured. After completion of treatment, c) representative photographs of the infected ear for each group were taken and the parasite burden was evaluated by d) fluorescence measurements and e) LDA; Asterisks indicate that the difference between control and drug-treated groups are statistically significant. * P ≤ 0.05, ** P ≤ 0.01, *** P ≤ 0.001, **** P ≤ 0.0001.

The effectiveness of the IL therapy was not surprising given the *in vitro* efficacy of clemastine **1** as through this method the drug is immediately absorbed at the site of action. In addition, it was observed that IL treatment of clemastine **1** is more effective at the higher dose 1.17 mg kg^{-1} twice a week compared to the dose of 217 μg kg^{-1} used in the first *in vivo* study. By contrast, clemastine **1** administered *via* oral gavage was not as effective at reducing parasite burden even at the high dose administered. Achieving oral efficacy is challenging as the pathway to the site of action is accompanied by many barriers and

limitations; such as slower onset of action compared with parental delivery, reduced efficacy through hepatic first-pass elimination, lack of absorption and degradation by digestive enzymes and acids.[219]

Pleasingly, clemastine **1** administered *via* IP decreased the parasite burden to a greater extent than the antileishmanial drug, glucantime **3**. It should be noted that parasite burden was reduced by a much smaller concentration of 5.83 mM of clemastine **1** *via* IP compared with 819 mM, glucantime which corresponds to 221 mM of pentavalent antimonial. In addition, clemastine **1** administered *via* IP was more effective than the IL route which is surprising because the IP route delivers the drug slower than the IL route. Although IP delivery is considered a parental route of administration, the pharmacokinetics of substances administered intraperitoneally are more similar to those seen after oral administration as compounds are subjected to hepatic first-pass elimination.[227] Therefore, there is still potential for oral clemastine **1** to be used as a therapy for leishmaniasis but this may require investigation into other formulations and drug delivery vehicles such as cyclodextrins and nanocapsules.[228,229]

3.7. Conclusion

The work described in this chapter involved assessing the activity of clemastine **1** against a range of *Leishmania* species. Clemastine **1** showed sub-micromolar activity against all species of promastigotes and was selective for the parasite over mammalian macrophages. This compound was progressed into an intramacrophage anti-amastigote study where clemastine **1** retained its activity. Clemastine **1** causes sensitisation of the P2X7 receptors expressed in host macrophages which in turn trigger cellular responses and may contribute to the observed antileishmanial activity. The drug target of clemastine **1** was validated as *Lmj*IPCS through analyses of dose-response assays using *L. major* WT, *Δ* LCB2 and PX cell lines. Finally, *in vivo* studies showed that clemastine **1** can significantly decrease the parasite burden when administered intraperitoneally or intralesionally and future work will focus on achieving efficacy for the oral administration of clemastine **1**.

4. Nor-clemastine analogues

As discussed in Chapters 2, nor-clemastine analogues (lacking the methyl group on the benzhydryl carbon) were found to be more synthetically accessible than clemastine whilst still possessing activity and selectivity in both the enzyme and parasite assays. The initial goal was to develop a robust synthetic route to nor-clemastine analogues (Scheme 20a) with the aim of identifying a compound with improved antileishmanial activity.

4.1. Synthesis

4.1.1. Homoprolinol head group

The initial focus of this project was to use Clayden's protocol,[202,191] described in Chapter 2, to homologate N-carboxybenzyl (Cbz) proline **105** using an Arndt-Eistert reaction (Scheme 20b). Cbz-proline **(*R*)-105** was converted to the acid chloride with oxalyl chloride and without isolation, acid chloride was treated with trimethylsilyldiazomethane ($TMSCHN_2$) to produce diazoketone **(*R*)-106** as a yellow oil in a yield of 56%. Formation of the diazoketone **(*R*)-106** was confirmed by the appearance of the characteristic C***H***N_2 peaks at δ_H 5.48 and 5.25 ppm in the ^{1}H NMR spectrum which correspond to the two rotamers of diazoketone **(*R*)-106** and the presence of a C=N stretch at 2102 cm^{-1} in the IR spectrum. Subsequently, treatment of diazoketone **(*R*)-106** with silver benzoate in MeOH initiated the Wolff rearrangement to afford methyl ester **(*R*)-107** in a yield of 80%. The formation of the methyl ester **(*R*)-107** was verified by the presence of a methyl signal at δ_H 3.64 ppm in the ^{1}H NMR spectrum, and retention of stereochemistry in the majority of product, was confirmed *via* comparison of the optical rotation measurements with literature values ($[\alpha]_D$ (c = 1.00 g/100 mL, $CHCl_3$) +23.4° (lit.:[191] $[\alpha]_D$ (c = 1.00 g/100 mL, $CHCl_3$) +27.2°) for **(*R*)-107** and $[\alpha]_D$ (c = 1.00 g/100 mL, $CHCl_3$) -53.2° (lit.:[202] $[\alpha]_D$ (c = 1.02 g/100 mL, $CHCl_3$) -42.7°) for **(*S*)-107**.[202,191] Reduction of both the ester and the protecting group were performed using lithium aluminum hydride ($LiAlH_4$) in THF at room temperature (rt) to afford homoprolinol **(*R*)-108** in a 52% yield. This was confirmed by the loss of carbonyl signals at δ_C 171.9 (***C***O_2CH_3) and 154.8 (N***C***O_2) ppm in the ^{13}C NMR spectrum and the presence of a broad OH stretch at 3314 cm^{-1} in the IR spectrum. However, there were initial problems purifying homoprolinol **(*R*)-108** from the benzylalcohol by-product. In order to circumvent this

problem, an analogous procedure was followed using methyl carbonate protected proline. The overall yields starting from Cbz-proline **(*R*)-105** and methyl carbamate protected proline was 23% and 13% respectively. Therefore, the higher yields coupled with greater ease of analysis using the Cbz group did not warrant a change of protecting groups.

4.1.2. Benzhydrol tail group

The second fragment required for the synthesis of nor-clemastine analogues is a benzhydrol group, and the synthesis of 4-bromobenzhydrol **122** was initially investigated (Scheme 20c). Benzhydrol **122** was chosen as an analogue to test the synthetic route because the starting material, bromobenzaldehyde **123**, was already purchased and the bromo-substituent could act as handle providing access to further analogues *via* cross coupling reactions (e.g. Suzuki reaction, Heck reaction or Buchwald-Hartwig amination). Synthesis of substituted benzhydrol **122** was achieved using a Grignard reaction as illustrated in Scheme 20c. Treatment of bromobenzaldehyde **123** with phenylmagnesium bromide generated the desired alcohol **122** in a moderate yield of 66%. Formation of benzhydrol **122** was evident by the presence of the $Ar_2C\boldsymbol{H}$ peak at δ_H 5.76 ppm in the ^1H NMR spectrum. Complete formation of the Grignard reagent before addition of 4-bromobenzaldehyde **123** was essential, as residual magnesium led to debrominated product.

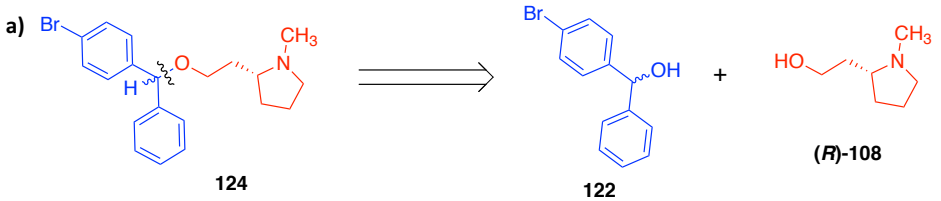

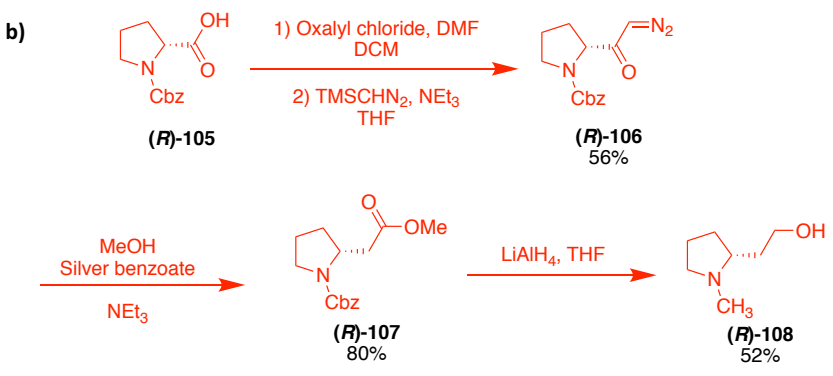

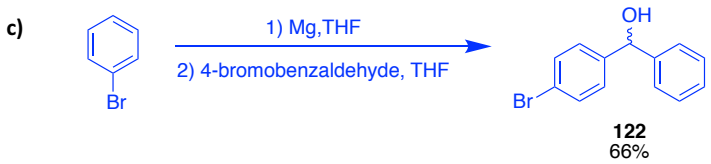

Scheme 20: a) Clemastine analogue 124 disconnection; b) Route to head group (*R*)-108; c) Route to tail group 122

4.1.3. Etherification step

As described in Chapter 2, substituted benzhydrols could form ethers under acidic conditions *via* an S_N1 reaction. However, yields varied and were generally low (~30%). It was initially decided to re-examine this reaction and ideally optimise the yields, but an attempt at the acid-catalysed condensation to produce ether **124** was unsuccessful (Scheme 21a). However, etherification was successful using a model substrate; benzhydrol **125** and 3-phenyl-1-propanol **126** were coupled to form diphenylmethyl ether **127** in a moderate yield of 48% (Scheme 21b). Formation of ether **127** was confirmed by the observation of the 2D HMBC correlations shown below in Scheme 21.

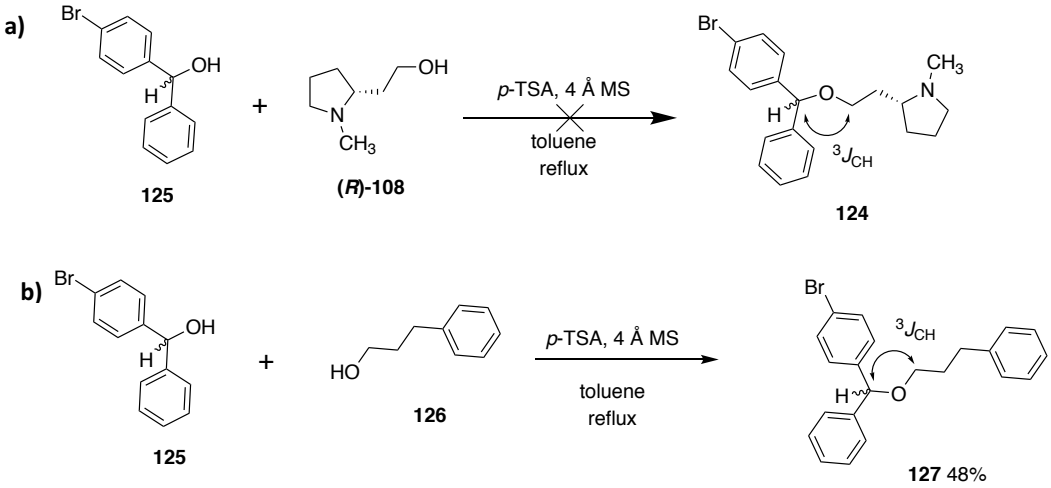

Scheme 21: Condensation reaction of benzhydrol 125 with a) homoprolinol (*R*)-108 and b) phenylpropanol 126

Further work was needed to find conditions for an etherification reaction that would produce good yields of clemastine analogues. Initial efforts focused on transforming the alcohol group of diphenylmethanol **125** into a better leaving group. In order to investigate this, mesylation of **125** was attempted using methanesulfonyl chloride in the presence of NEt_3 and DCM (Scheme 22a). Interestingly, this reaction formed chloride **128** instead of the mesylate as verified by the observation of the characteristic isotope pattern for bromine and chlorine *via* GC-MS *m/z* = 280 ($M(^{79}Br)(^{35}Cl)^+$), 282 ($M(^{79}Br)(^{37}Cl)^+$) and ($M(^{81}Br)(^{35}Cl)^+$), 284 ($M(^{81}Br)(^{37}Cl)^+$) with a peak intensity ratio of 3:4:1 respectively. This chloride **128** was

reacted with 3-pheny-1-propanol **126** using two different conditions (Scheme 22b), involving deprotonation of the primary alcohol using either NaH or Ag_2CO_3. Unfortunately, neither of these reactions generated the desired ether linkage as crude ^{1}H NMR and LC-MS showed only the presence of starting material.

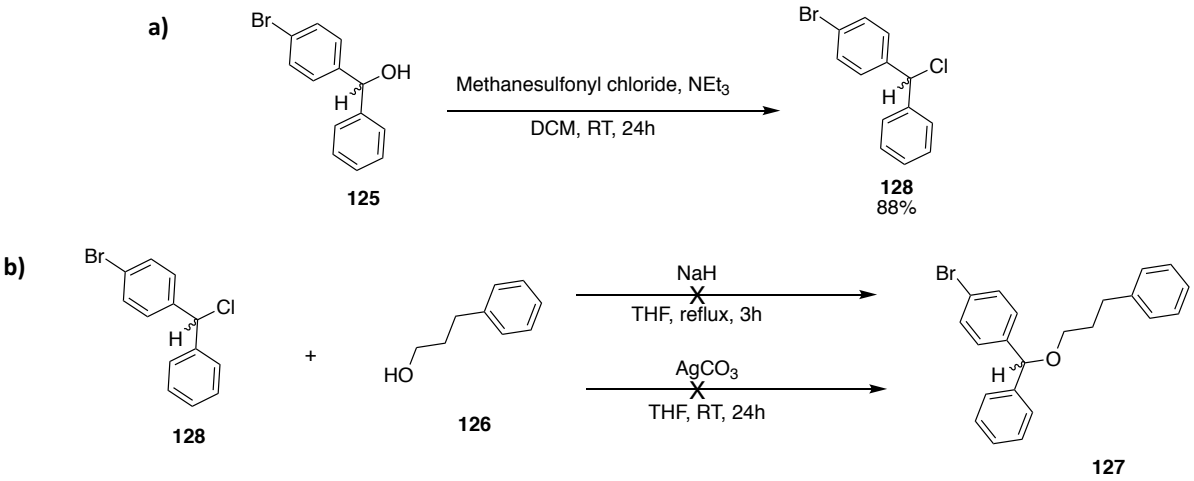

Scheme 22: a) Mesylation of benzhydrol 125 leads to formation of chloride 128 b) failed displacement attempt of chloride 128

Analysis of the literature showed that 0.1 equiv. of $PdCl_2$ catalysed the formation of benzhydryl ethers.[230] The conditions were used on the test reaction and produced benzhydryl ether **127** *via* a S_N1 reaction in a very high yield of 95% (Scheme 23).

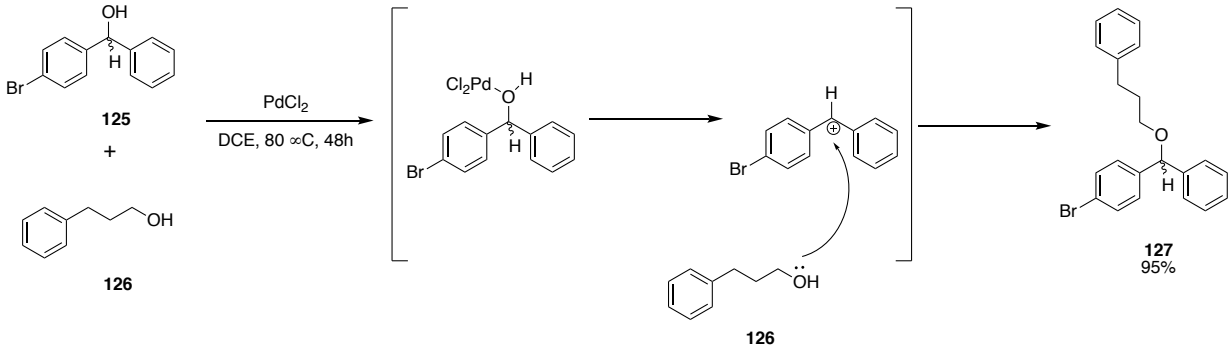

Scheme 23: $PdCl_2$-catalysed formation of benzhydryl ethers

In a second reaction, 2-dimethylaminoethanol **129** was coupled with benzhydrol **125** under Pd-catalysed conditions to discover whether the reaction would be successful in the presence of an amine. Unfortunately, LC-MS analysis showed no sign of product **130** after 48h, only starting material and some debrominated reagent could be detected (Scheme 24a). It is likely that the $PdCl_2$ does not activate the alcohol group of benzhydrol **125** but instead chelates to dimethylaminoethanol **129** reducing Pd(II) to Pd(0) (Scheme 24b).

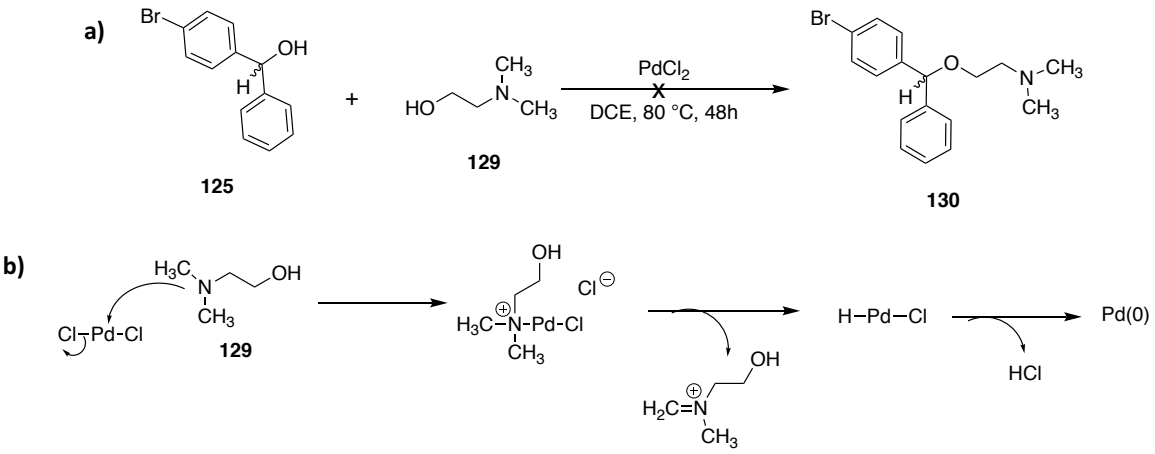

Scheme 24: a) $PdCl_2$-catalysed etherification in the presence of amine 129 b) generation of Pd(0) from Pd(II)

To try and avoid co-ordination of Pd(II) to the amino alcohol, the amine was protected as a carbamate **131**. Although the etherification to form compound **132** was possible (Scheme 25), the reaction proceeded with a poor yield of 24% which is consistent with possible chelation.

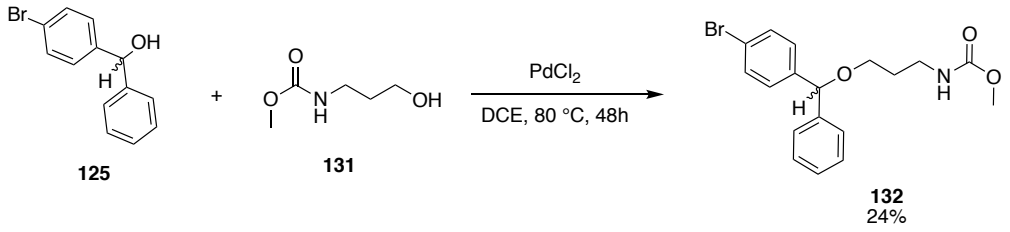

Scheme 25: $PdCl_2$-catalysed etherification to form compound 132 in the presence of protected amine 131

Based on this observation, it was speculated that palladium catalysed conditions should be tried with N-Cbz homoprolinol **(*R*)-108** as a more hindered tertiary amine may be less likely to bind to the palladium. To test this, a selective reduction of methyl ester **(*R*)-107** was first required to synthesise the carbamate protected homoprolinol **(*R*)-133**. Initial efforts employed Clayden's conditions of 3.5 equiv. of $LiBH_4$ at rt for 70 h to afford product **(*R*)-133** in a low yield of 35%.[202] Attempts to optimise this using either 5.5 equiv. of $LiBH_4$ or 3.5 equiv. of DIBAL were not productive. However, an improvement in yield was observed when the temperature was increased to 60 °C in the presence of 3.5 equiv. of $LiBH_4$, this led to the selective reduction of methyl ester **(*R*)-107** to N-Cbz homoprolinol **(*R*)-133** in a moderate yield of 58% (Scheme 26). Confirmation of the N-protected alcohol was obtained by the appearance of a characteristic OH stretch at 3440 cm^{-1} in the IR spectrum and the presence of only one carbonyl peak at 156.9 ppm in the ^{13}C NMR spectrum.

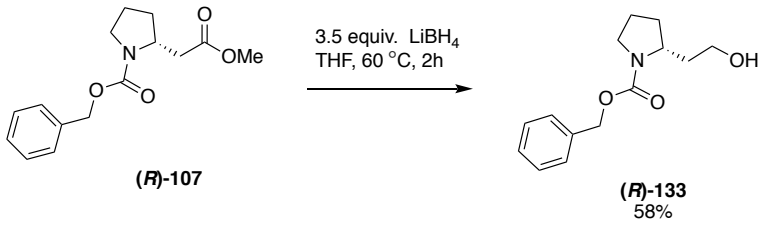

Scheme 26: Selective reduction of N-Cbz methyl ester (*R*)-107 to form N-Cbz homoprolinol 133

N-Cbz homoprolinol **(*R*)-133** was then used in the $PdCl_2$-catalysed etherification and produced the desired compound **(*R*)-134,** but in a low yield of 26 % (Scheme 27a). One hypothesis was that the $PdCl_2$ could be cleaving the carbamate protecting group. This theory was tested by heating N-Cbz homoprolinol **(*R*)-133** to 80 °C with $PdCl_2$; however, there was no sign of deprotection to form homoprolinol **(*R*)-135** after 24 h (Scheme 27b).

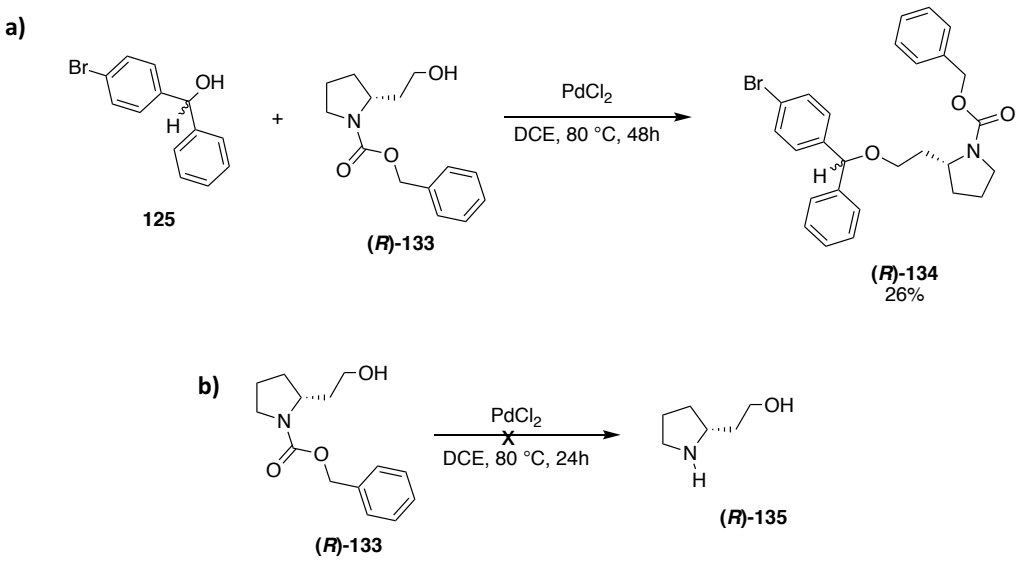

Scheme 27: a) $PdCl_2$-catalysed formation of clemastine analogue 134 b) attempt at Pd(II) cleavage of protecting group

Another hypothesis was that a stable 6-membered ring was being formed with Pd(II), complex **136**, through chelation to the alcohol and amine (Scheme 28). This means less Pd(II) is available to activate benzhydrol **125** and the nucleophilicity of amino alcohol **131** is reduced. Both these factors would result in a decrease in ether formation.

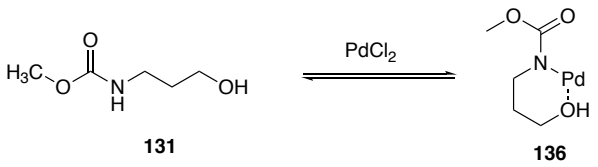

Scheme 28: Hypothesis for the co-ordination of Pd(II) to amino alcohol 131

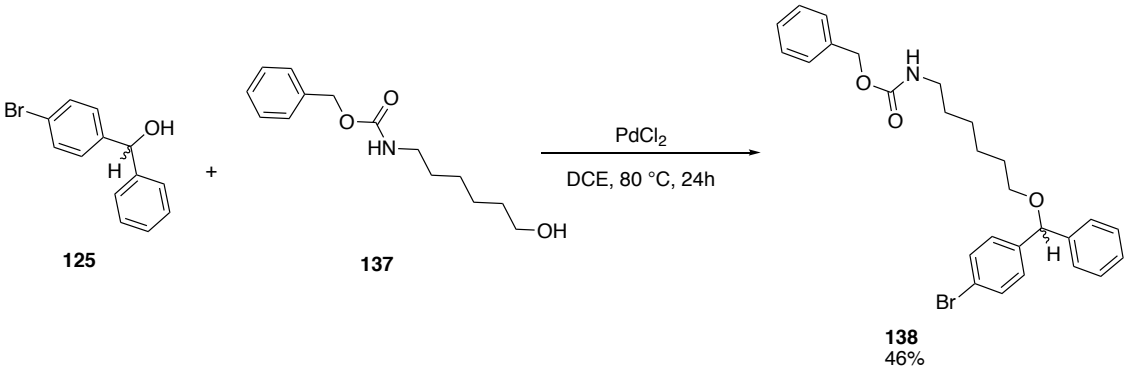

Scheme 29: $PdCl_2$-catalysed etherification of N-Cbz aminohexanol 137 and diphenylmethanol 125

To test this hypothesis a longer chain protected amino alcohol was reacted with benzhydrol **125** (Scheme 29). This reaction with N-Cbz aminohexanol **137** afforded the desired ether **138** in a yield of 46%, as chelation is less favourable, and therefore supports the hypothesis.

Other Lewis acids were explored with the aim of finding a catalyst which does not hinder the reaction *via* unfavourable co-ordination to the substrate. Eight condition sets using benzhydrol **125** and 3-phenyl-1-propanol **126** (Scheme 30) were screened in parallel with varying Lewis acids. The yields were estimated using integrals from GC-MS analysis with dodecane as the standard. The data showed that the etherification catalysed by AuCl led to the most efficient conversion to product **127** as shown in Figure 35.

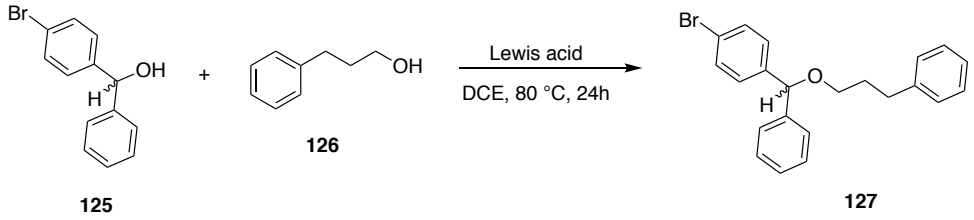

Scheme 30: Reaction employed for Lewis acid screen

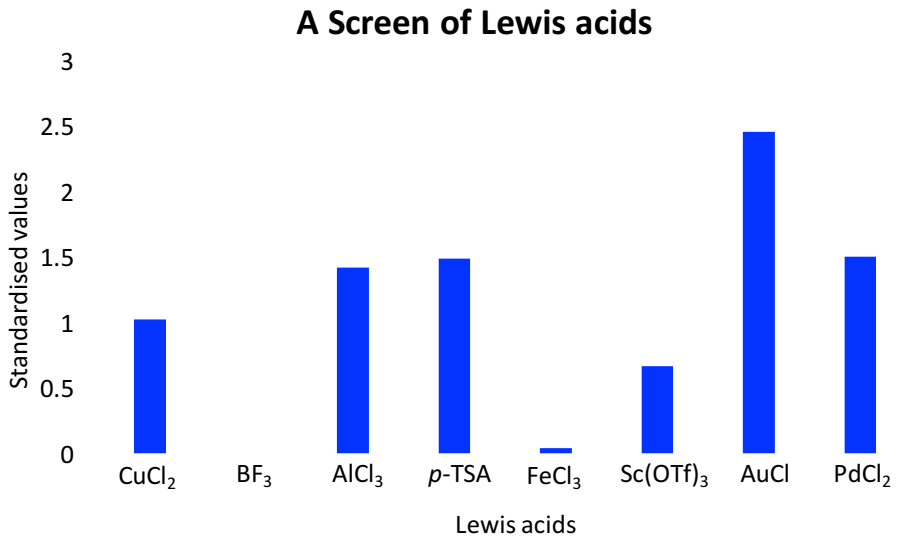

Figure 35: A screen of Lewis acids for etherification of diphenylmethanol 125 and 3-phenyl-1-propanol 126

The next step was to test the effect of a chelating group on the efficacy of Au(I) in the presence of an amine. Benzhydrol **125** with N-Cbz aminopropanol **139** were reacted in the presence of 0.1 equiv. of AuCl and DCE and produced the desired ether **140** in a good yield of 70% (Scheme 31). Au(I) is a softer transition metal ion than Pd(II) and therefore it is probable that N, O coordination to Au is weaker.

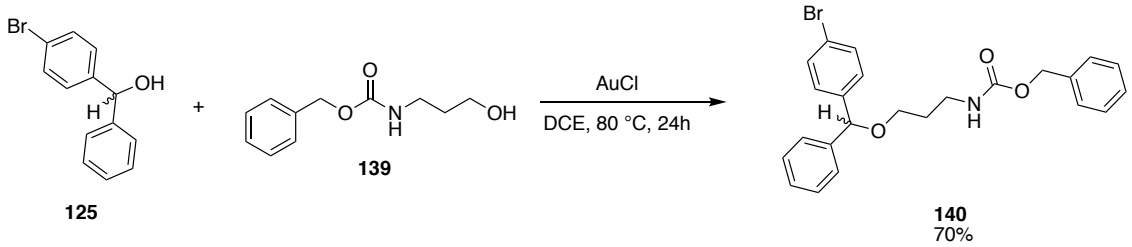

Scheme 31: AuCl-catalysed etherification of N-Cbz aminopropanol

The AuCl-catalysed reaction was then attempted using N-methyl homoprolinol **(*R*)-108** to form the clemastine analogue **(*R*)-124**. Unfortunately, no product was formed and only starting material could be recovered (Scheme 32). This suggests that the more electron rich unprotected amine can coordinate to Au(I).

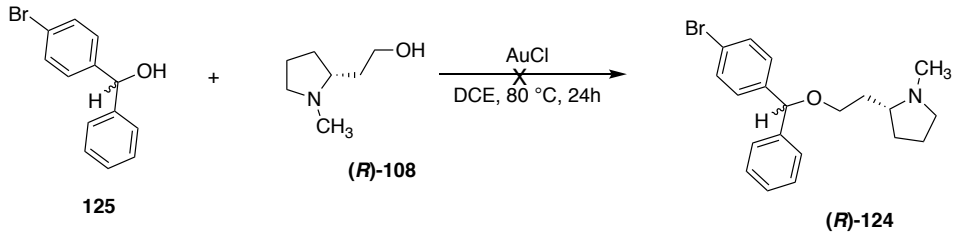

Scheme 32: S_N1 reaction of benzhydrol 125 and homoprolinol (*R*)-108 catalysed by AuCl

To verify this, the reaction was then performed using the N-Cbz homoprolinol **(*R*)-134** and benzhydrol **125** (Scheme 33). Gratifyingly, ether **(*R*)-134** was formed in a moderate yield of 63% which is consistent with the N-Cbz protected homoprolinol **(*R*)-134** exhibiting a weaker coordination to the Au(I) species.

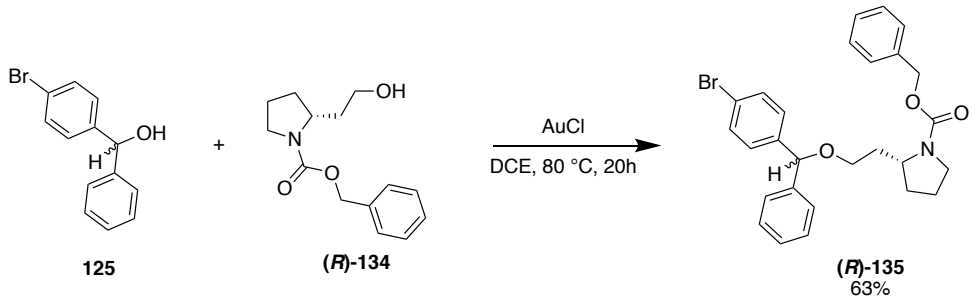

Scheme 33: AuCl-catalysed etherification with N-Cbz protected homoprolinol (*R*)-134 and benzhydrol 125

Having developed an efficient method to generate the key ether linkage the final step was to reduce the N-Cbz group to access the desired clemastine analogue **(*R*)-124**. Attempts to reduce compound **(*R*)-135** using $LiAlH_4$ in THF both at rt and reflux resulted in the formation of an intractable mixture containing the debrominated product **(*R*)-141** (Scheme 34), as identified by LC-MS analysis which contained a peak with (m/z 296 (MH^+)) lacking bromine isotope pattern.

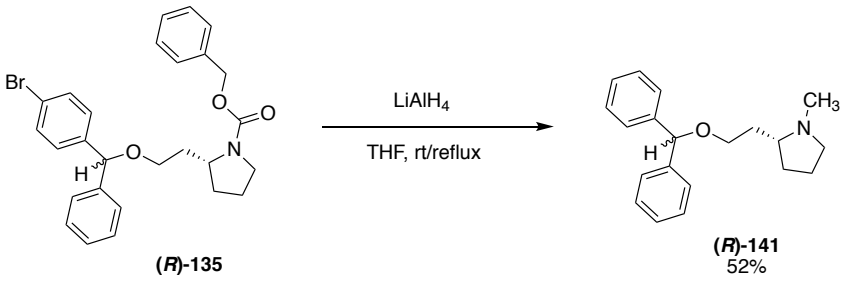

Scheme 34: Hydride reduction of N-Cbz clemastine (*R*)-135

However, this synthetic route did successfully access other desired clemastine analogues with substituents that were not prone to reduction with $LiAlH_4$ (Figure 36). The chlorine substituted analogue **(*R*)-112** was chosen because it closely resembles clemastine and was the most active analogue synthesised in previous work by Brown (Chapter 2).[191] The fluorine analogue **(*R*)-142** was investigated in order to understand the role of the halogen on antileishmanial activity and methoxy analogues, **(*R*)-143** and **(*R*)-144,** were explored with the aim of attaching a linker in the 4 or 3 position on the ring. Finally, clemastine analogue **(*R*)-145** was designed from two hit compounds in the NINDS screen (Chapter 2),

flunarizine **87** and pimozide **85**, which possess a 4,4'-difluorobenzhydyl tail fragment (Figure 20). The antileishmanial activity of these compounds will be discussed in section 4.2.

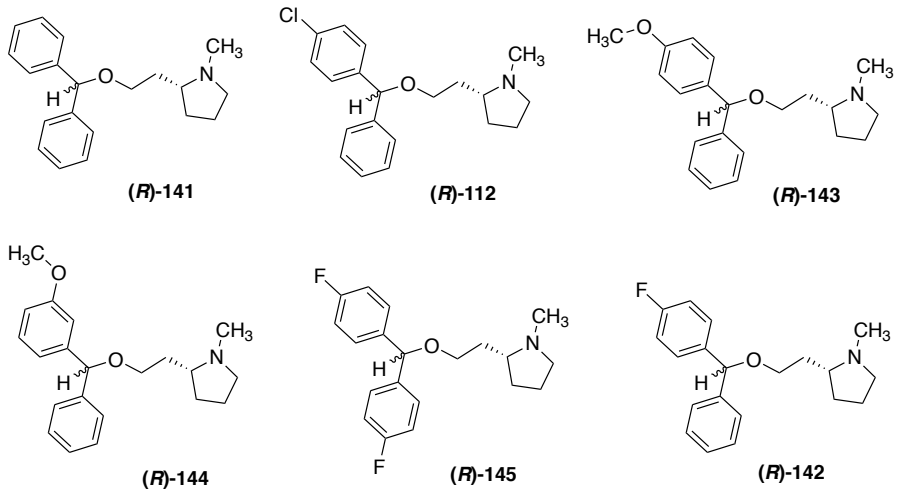

Figure 36: Structures of nor-clemastine analogues

4.2. In-vitro activity of nor-clemastine analogue

With the nor-clemastine analogues in hand (Figure 36), attention turned towards measuring their activity against *Leishmania* promastigotes. Dose response studies for nor-clemastine analogues investigated the growth inhibition of *L. major* and *L. amazonensis* promastigotes.

Brown previously showed that nor-clemastine **(*R*)-112** possesses a similar but slightly lower level of activity to clemastine **1** against *L. major* promastigotes (Chapter 2). Figure 37 and 38 supports these findings as nor-clemastine **(*R*)-112** is marginally less active than clemastine against both *L. major* and *L. amazonensis* promastigotes. As noted in Chapter 3, results from this assay are 2-3 times more active against *L. major* promastigotes than previously reported by Brown,[191] presumably due to the longer incubation time of 48 h rather than performing a 24 h assay. Overall, the absence of a quaternary methyl group on the benzhydryl carbon or the mixed stereochemistry at this position could be responsible for this lower activity and will be discussed further in section 4.3.

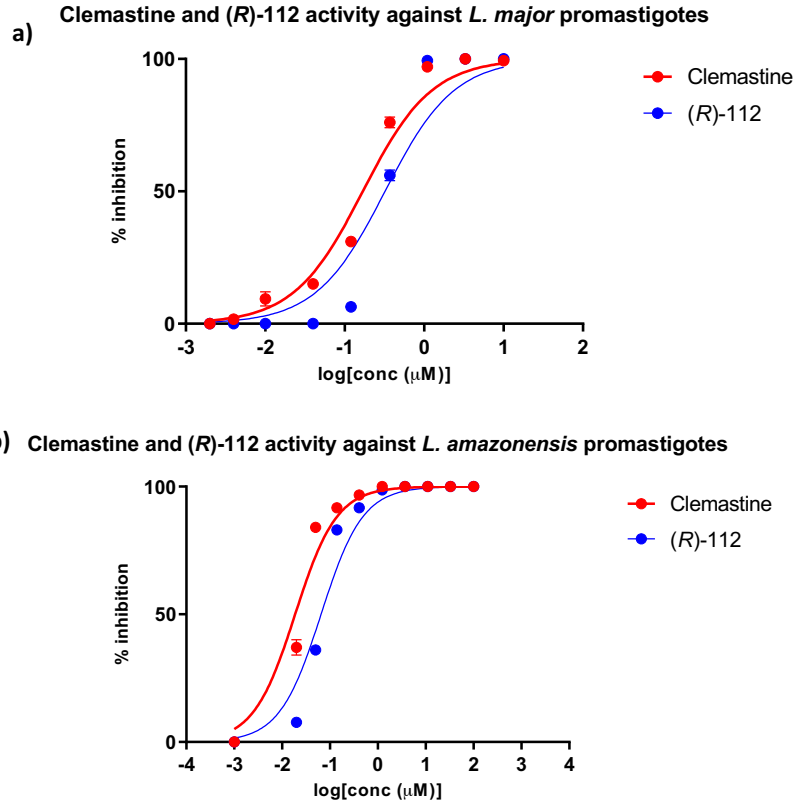

Figure 37: An example of dose response curves for clemastine and RC1248 against a) *L. major* b) *L. amazonensis*; assays were performed in triplicate and each curve shows a representative experiment.

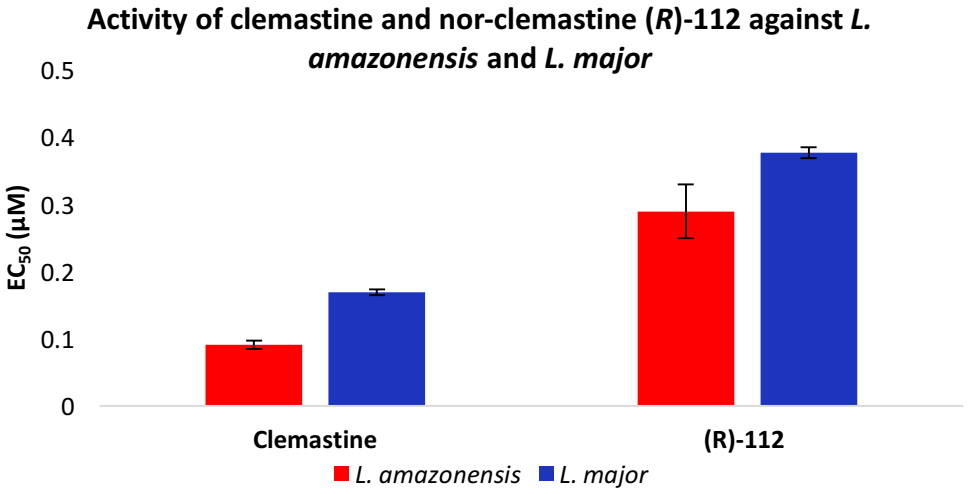

Figure 38: EC_{50} values for clemastine 1 and analogue (*R*)-112 against *L. amazonensis* and *L. major*; values are mean ± 95% CI from at least three experiments.

The unsubstituted and methoxy substituted nor-clemastine analogues, **(*R*)-141**, **(*R*)-143** and **(*R*)-144**, were more potent against *L. amazonensis* than *L. major* promastigotes (Figure 39). This variation in activity could be due to differences in the IPCS active site or off-target effects.

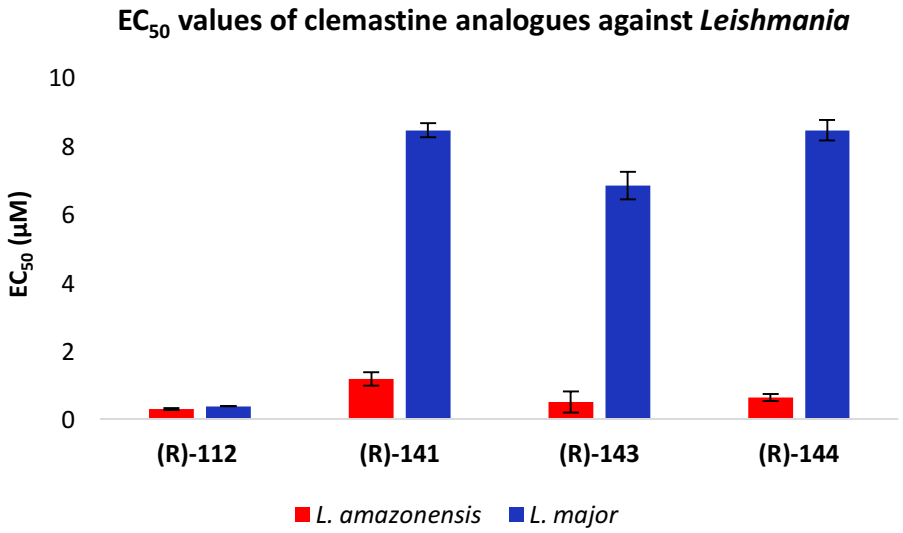

Figure 39: EC_{50} values of (*R*)-112, (*R*)-141, (*R*)-143 and (*R*)-144 against *L. amazonensis* and *L. major*; values are mean ± 95% CI from at least three experiments.

Nor-clemastine analogue **(*R*)-145** with a 4,4'-difluorobenzhydyl tail unit demonstrated a drop in potency when compared to analogue **(*R*)-112** which possessed sub-micromolar levels of activity. Although the mono-fluorinated analogue **(*R*)-142** regained some activity, the mono-chlorinated compound **(*R*)-112** remained the most active analogue (Figure 40).

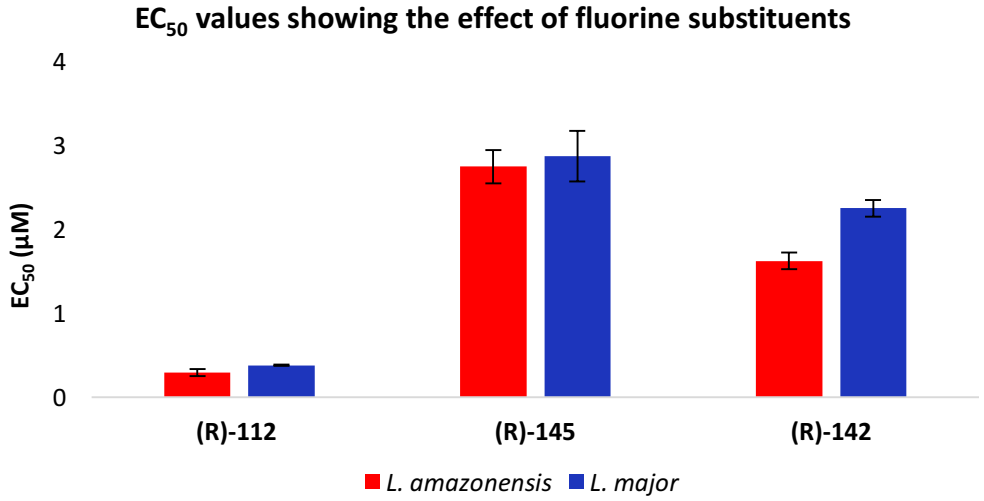

Figure 40: EC_{50} values for nor-clemastine analogues (*R*)-112, (*R*)-145 and (*R*)-142 against *L. amazonensis* and *L. major*; values are mean ± 95% CI from at least three experiments.

4.3. Role of stereochemistry

Analogue **(*R*)-112** is the most active nor-clemastine analogue and, like clemastine, analogue **(*R*)-112** possesses 2 stereocentres, therefore, the effect of stereochemistry was explored. Previous work in the group demonstrates the limited effect of varying pyrrolidinyl stereochemistry, with the (*R*)-configuration possessing slightly higher activity. This observation was confirmed by the preparation and testing of analogues **(*R*)-112** and **(*S*)-112** derived from (*R*)- and (*S*)-proline respectively. Having established the optimum pyrrolidinyl stereochemistry attention turned to the benzhydryl centre (Figure 41).

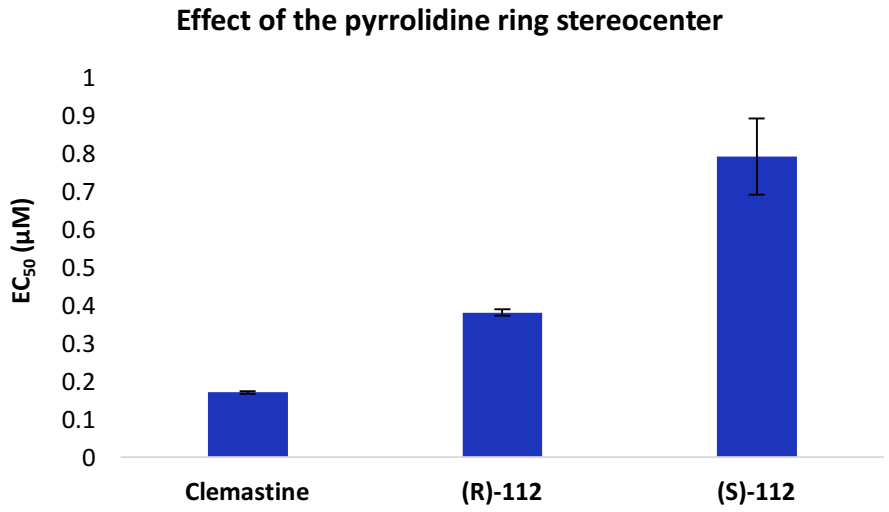

Figure 41: EC_{50} values for clemastine 1 and nor-clemastine analogues (*R*)-112 and (*S*)-112 against *L. major*; values are mean ± 95% CI from at least three experiments.

Compound **(*R*)-112** is made up of two diastereomers due to mixed stereochemistry at the benzhydryl carbon. Attempts to separate these using chiral HPLC (ChiralPak IA column) were undertaken. However, although there is literature precedent for using chiral preparatory HPLC to separate diastereomers of clemastine[197] these were not successful. As a result, an enantioselective synthetic route was developed.

4.3.1. Asymmetric synthesis of the benzhydrol tail group

A search of literature on how to form enantiopure benzhydrols, identified an asymmetric aryl transfer reaction.[231] Chiral pyrrolidindylmethanols were used as ligands in a zinc-catalysed addition of boronic acids to aldehydes (Scheme 35). The arylzinc species were generated *in situ* from boron-zinc exchange and the stereochemical course of the addition reaction to aldehydes was tentatively proposed by Soai *et al*.[232] Following this precedent,

the (*R*)-amino alcohol **(*R*)-146** and (*S*)-amino alcohol **(*S*)-146** were used to generate the respective enantiopure benzhydrols **(*R*)-125** and **(*S*)-125**. Overall, these reactions proceeded in good yields with high enantioselectivities as revealed by chiral HPLC analysis using a ChiralPak IA column as shown in Figure 42 and 43. Optical rotation measurements were compared with literature values to confirm the configuration of the benzhydrols ($[\alpha]_D$ (c = 1.00 g/100 mL, $CHCl_3$) -27.0 ° (lit.: $[\alpha]_D$ (c = 1.00 g/100 mL, $CHCl_3$) -16 °) for **(*R*)-125**, $[\alpha]_D$ (c = 1.00 g/100 mL, $CHCl_3$) +17.9 ° (lit.:[233] $[\alpha]_D$ (c = 1.00 g/100 mL, $CHCl_3$) +19°) for **(*S*)-125**.

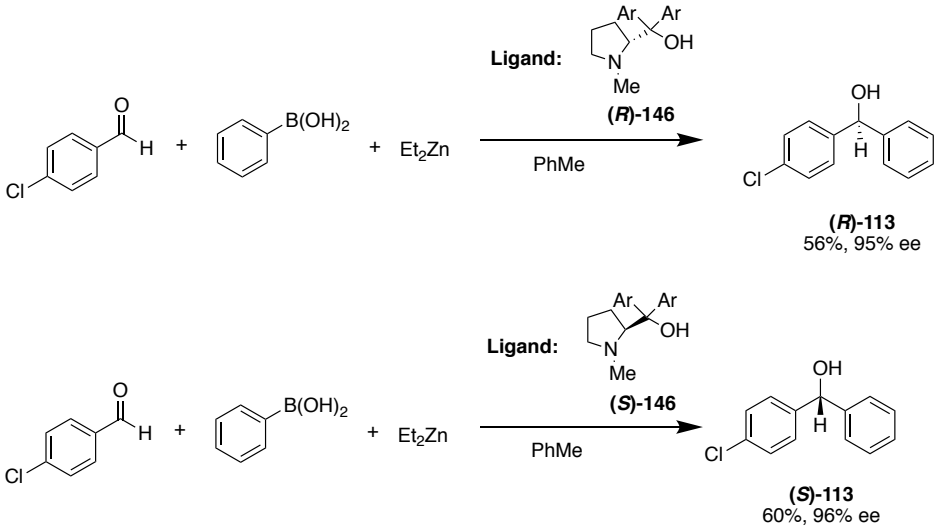

Scheme 35: Asymmetric arylation of aldehydes with arylboronic acids

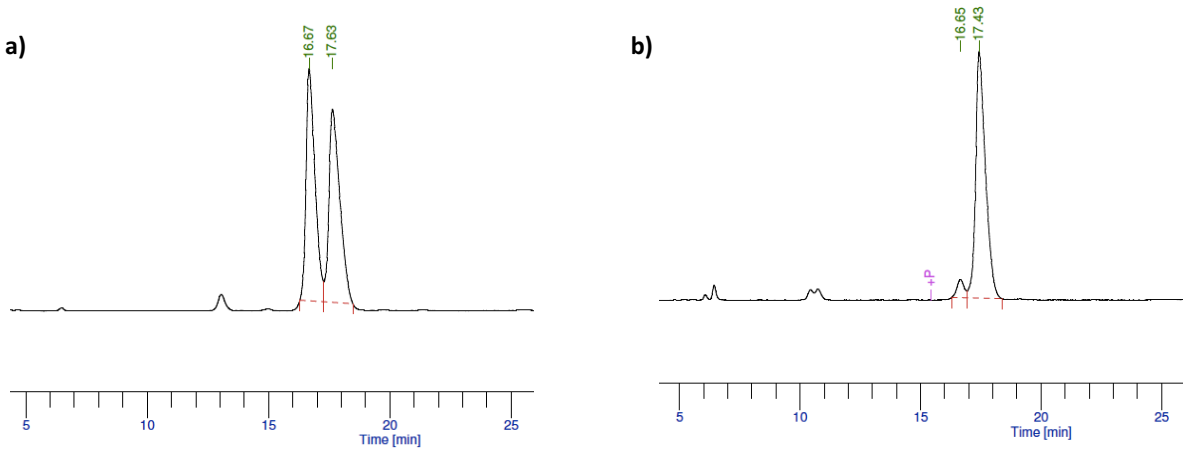

Figure 42: HPLC spectrum for a) Racemic mixture of benzhydrol 113 b) (*S*)-benzhydrol (*S*)-113

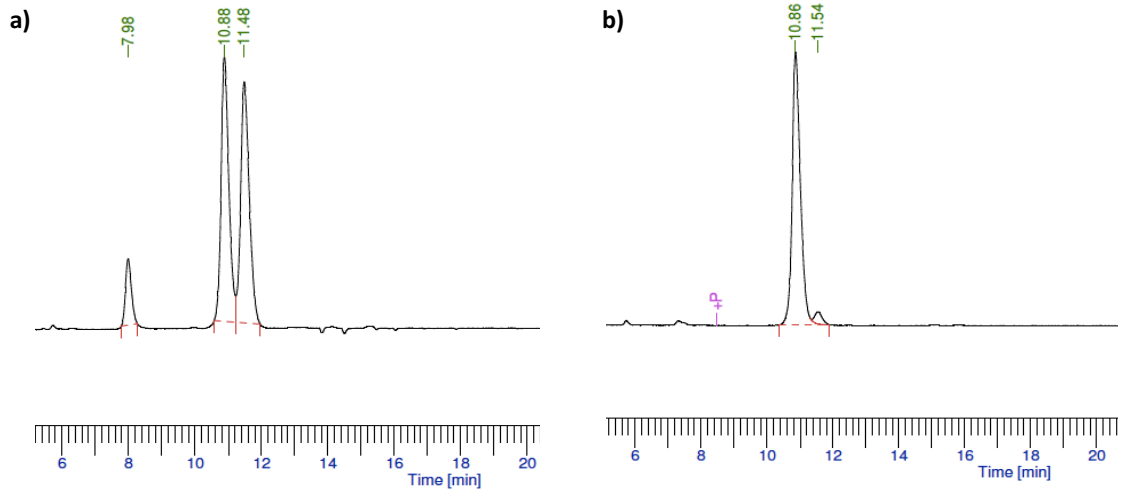

Figure 43: HPLC spectrum for a) Racemic mixture of benzhydrol 113 b) (*R*)-benzhydrol (*R*)-113

4.3.2. Etherification: retention of stereochemistry

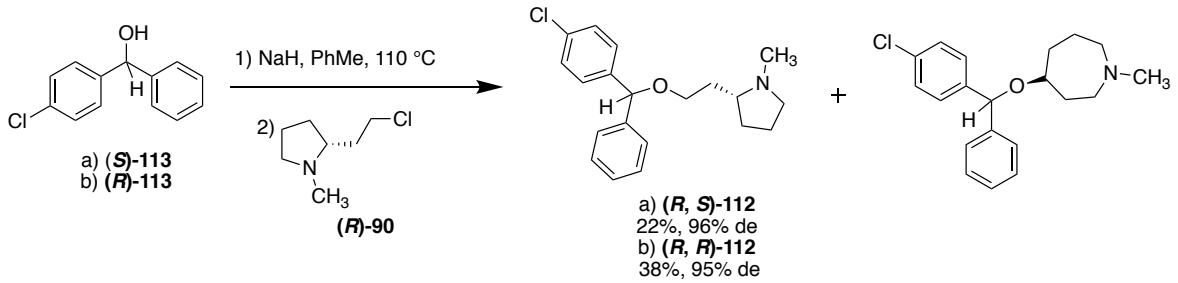

Scheme 36: Accessing enantiomerically pure diastereomers

With the enantiopure benzhydrol tail units, **(*R*)-113** and **(*S*)-113**, and head group **(*R*)-90** in hand attention was drawn to the etherification step. The previously developed S_N1 reaction could not be performed as it would generate mixed stereochemistry at the benzhydryl carbon. Therefore, the S_N2 reaction developed by Clayden *et al.*[202] was carried out to produce the enantiomerically pure diastereomers, using the slightly more active (*R*)-configuration on the pyrrolidine ring. This reaction involved harsh conditions as the free-based head group **(*R*)-90** and deprotonated tertiary alcohol (***R*)-113** were heated under reflux overnight to produce the desired product **(*R, R*)-112** albeit in a low yield of 38% (Scheme 36). The yields are low due to the formation of the azepane by-product and unidentified side reactions caused by the harsh conditions. The formation of the azepane by-product results in inversion of the azepane stereocentre to give the (*S*)-configuration, and this is likely due to attack at the less hindered face of the bicyclic cationic intermediate **110**. Analysis of the ^{13}C NMR spectrum confirms a single configuration at the azepane

stereocentre due to the presence of only one signal at 75.6 ppm. In addition, analysis of the ^{13}C NMR spectrum for compound **112** did not show any duplication of carbon peaks in the spectrum (Figure 44) confirming that the majority of the product was the desired **(*R, R*)-112** diastereomer.

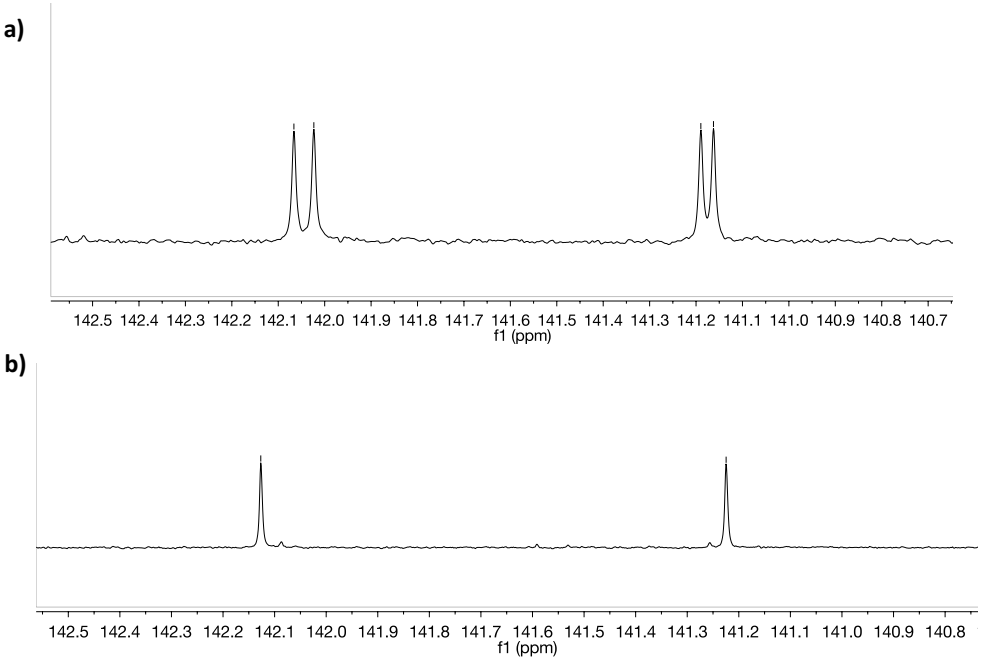

Figure 44: Section of ^{13}C NMR spectrum of the a) racemate compound (R)-112 and b) the single diastereomer (*R, R*)-112

4.4. Activity of diastereomers

With the single diastereomers in hand, the biological effect of the stereochemistry could be explored. Figure 45 shows the dose response curves for the nor-clemastine analogues **(*R*)-112**, **(*R, S*)-112** and **(*R, R*)-112** with *R*-configuration at the pyrrolidine ring. The most active stereochemistry at the benzhydryl carbon is the *R*-configuration, followed by the racemate and then the (*S*)-configuration. Figure 45 shows that nor-clemastine analogue **(*R, R*)-112** is equipotent to clemastine **1** with EC_{50} values of 0.026 ± 0.003 µM and 0.020 ± 0.003 µM against *L. amazonensis* and 0.13 ± 0.01 µM and 0.172 **±** 0.003 µM against *L. major* for nor-clemastine **(*R, R*)-112** and clemastine **1** respectively. This suggests that the quaternary methyl group on the benzhydryl carbon is not essential for activity but rather the stereochemistry at this position is important. Therefore, the most active isomer identified was **(*R, R*)-112** with the stereochemistry of the quaternary benzhydryl carbon determining activity to a greater extent than the stereocenter in the pyrrolidine ring. This indicates that the commercially available (*R, R*)-isomer of clemastine **1** would be the most active

antileishmanial. Interestingly, as described in Chapter 2 a similar trend in antihistamine activity is observed for the four diastereomers of clemastine where the (*R, R*)-isomer is also the most active.[199]

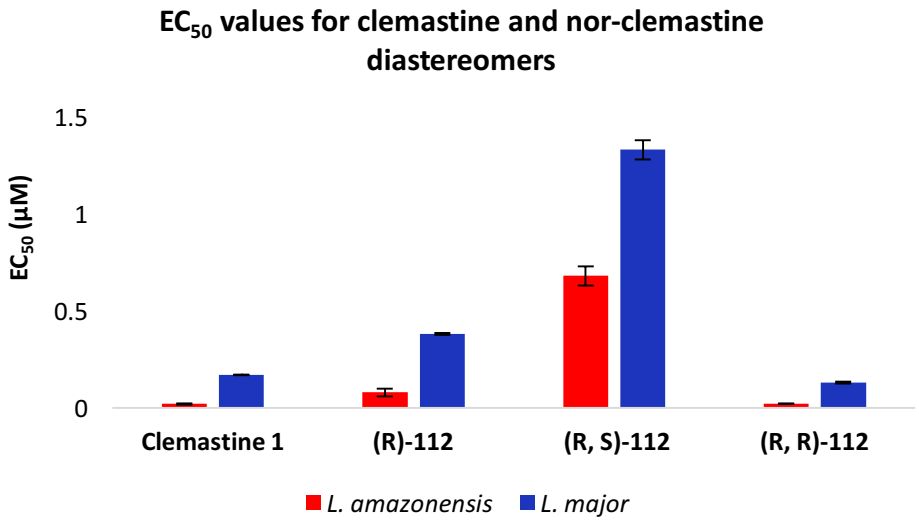

Figure 45: EC_{50} values of clemastine 1 and analogues (R)-112, (*R, S*)-112 and (*R, R*)-112 against *L. amazonensis* and *L. major* promastigotes; values are mean ± 95% CI from at least three experiments.

4.5. Cytotoxicity of nor-clemastine analogues

Having established the optimum stereochemistry for the nor-clemastine series it was of interest to investigate the macrophage cytotoxicity of these compounds. Consequently, the nor-clemastine analogues were tested against BMDM as previously described in Chapter 3. The CC_{50} values in Figure 46 shows that the quaternary methyl group on the benzhydryl carbon has a great influence on macrophage cytotoxicity, with the nor-clemastine analogues being on average 3-4 times less cytotoxic to the host than clemastine.

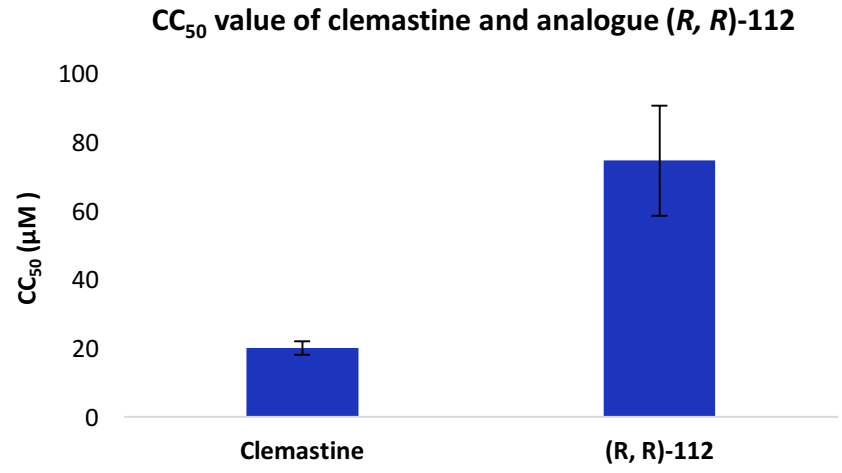

Figure 46: CC_{50} values of clemastine 1 and analogue (*R, R*)-112 against BMDM; values are mean ± 95% CI from at least three experiments.

4.6. Conclusion

The work described in this chapter involved developing a synthetic route to nor-clemastine analogues and in particular focused on forming the ether linkage. In addition, an enantioselective route to access two enantiopure diastereomers of nor-clemastine was developed and revealed the role of stereochemistry on antileishmanial activity. The analogue **(*R*, *R*)-112** was identified as the most active diastereomer and possessed greater selectivity towards the parasites over the murine macrophages (SI ≈ 2863 and 573 for *L. amazonensis* and *L. major* promastigotes respectively) than clemastine **1** (SI ≈ 1247 and 117 for *L. amazonensis* and *L. major* promastigotes respectively). Future work will aim to understand if the quaternary methyl group on the benzhydryl carbon in clemastine plays an important pharmacokinetic role. If analogue **(*R*, *R*)-112** possesses a good pharmacokinetic profile, it could be tested *in vivo* as an oral therapy.

5. N-linked clemastine analogues

As discussed in the previous chapter, some SAR data was obtained from the development of the nor-clemastine analogues that showed the quaternary methyl group on the benzhydryl carbon was not essential for activity but the stereochemistry at this position was important. However, in order to further develop this understanding of the SAR one remaining challenge was to efficiently synthesise a library of these compounds. A specific challenge arose in the synthesis of the head group **(*R*)-90**. This required four steps and produced **(*R*)-90** in a moderate overall yield. In addition, the final S_N2 reaction generated the desired analogue **(*R*)-112** but suffered from low yields. Therefore, an alternative more accessible series was explored in which the pyrrolidine nitrogen was moved round one position to form novel N-linked analogues such as analogue **(*R*)-147** (Figure 47).

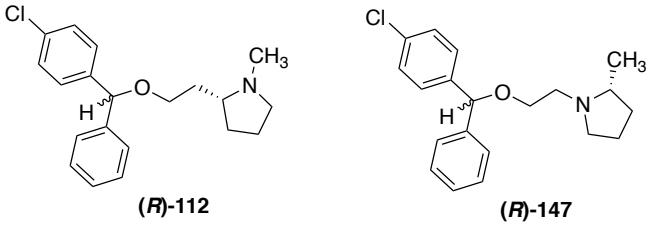

Figure 47: a) Compound (*R*)-112 from nor-clemastine library b) Compound (*R*)-147 from N-linked clemastine library.

5.1. Synthesis of N-linked analogues

The N-linked analogues were initially prepared, in 2 steps, using the Au(I) catalysed S_N1 reaction developed earlier (Chapter 4). For example, coupling of benzhydrol **113** with bromoethanol, followed by an alkylation with 2-methylpyrrolidine **(*R*)-148** at elevated temperature or at rt with KI as a catalyst gave N-linked analogue **(*R*)-147.** The higher overall yield for **(*R*)-147** of 57% compared favourably to the 15% yield for the synthesis of nor-clemastine **(*R*)-112**. Ether formation and N-alkylation was confirmed by analysis of the 2D HMBC correlations as illustrated in Scheme 37.

Pyrrolidinyl methanol **149** was synthesised to investigate the antileishmanial effects of expansion into the 2-position on the pyrrolidine ring and the potential to hydrogen bond in this position. Reduction of ester **150** using $LiAlH_4$ formed compound **149** in a moderate yield (Scheme 38). Confirmation of the pyrrolidinyl methanol **149** was obtained by a

characteristic OH stretch at 3408 cm^{-1} in the IR spectrum and the presence of ***C***H_2OH peaks in the ^{13}C NMR spectrum at 62.4(1) and 62.3(8) corresponding to the two diastereomers.

As discussed in Chapter 1, tamoxifen **20** has antileishmanial activity[82] and is likely to target *Lmj*IPCS.[84] Tamoxifen **20** possesses structural similarities to clemastine **1** and therefore the dimethylamine head group of tamoxifen was used to design clemastine analogue **151** (Scheme 37, Figure 48). The hypothesis was that this compound would have improved activity and be less expensive to synthesise and scale up as it benefits from only one stereocentre.

Overall, the desired N-linked analogues were attained quickly as head groups were commercially available. In addition, this synthetic route could be adapted for high throughput synthesis[234] to access a series of compounds in a short time; enhancing efforts in lead development.

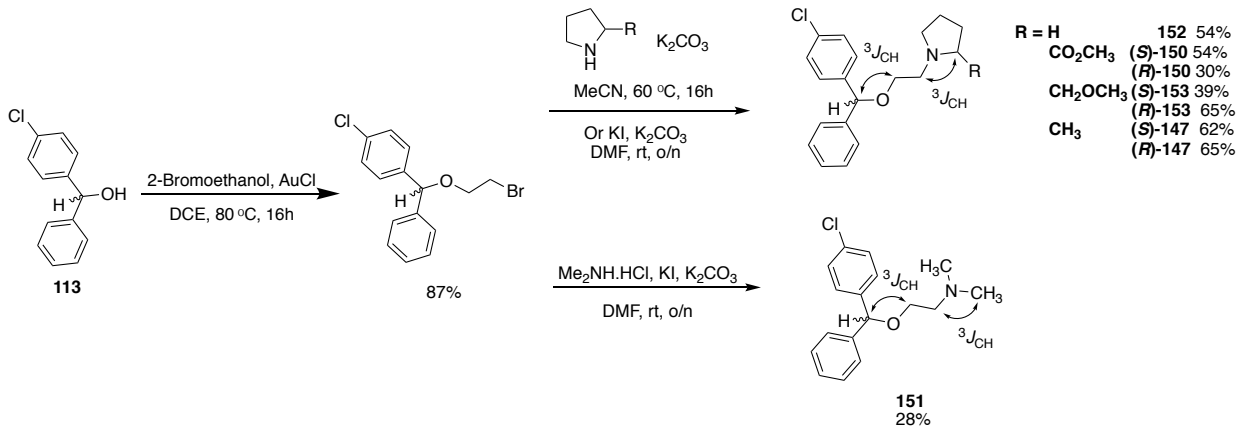

Scheme 37: Synthetic route N-linked analogues

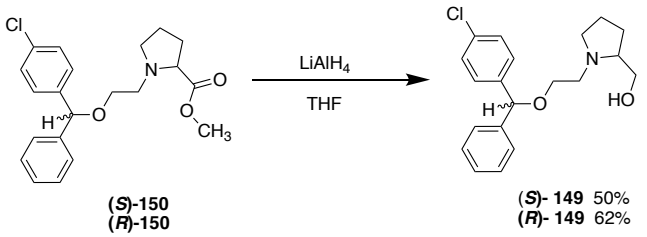

Scheme 38: Reduction of ester 150 to analogue 149

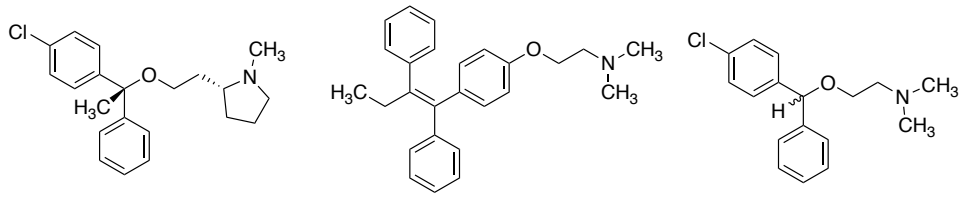

Clemastine **1** Tamoxifen **20** Analogue **151**

Figure 48: Related structures

5.2. Activity of N-linked analogues

With this initial set of analogues, the approach was validated by assaying the compounds against *L. major* promastigotes. Unfortunately, these more accessible analogues were not as active as nor-clemastine **(*R*)-112** showing micromolar as opposed to sub-micromolar potency (Appendix B). Hydrogen **152**, Ether **(*R*)- and (*S*)-153**, alcohol **(*R*)- and (*S*)-149** and methyl **(*R*)- and (*S*)-147** substituents on the head group have moderate levels of activity with EC_{50} values ranging from 2 – 15 μM against *L. major* promastigotes. Ester analogues **(*R*)- and (*S*)-150** had poor antileishmanial activity with EC_{50} values greater than 20 μM and analogue **151** was inactive against *L. major* promastigotes ($EC_{50} \geq 50$, Figure 49). The relationship between clemastine **1** and tamoxifen **20** and its effect on *Lmj*IPCS could be investigated further but it is outside the scope of this thesis. Overall, these compounds were not sufficiently active to be progressed into an anti-amastigote assay and therefore further development of these N-linked analogues was required to improve potency.

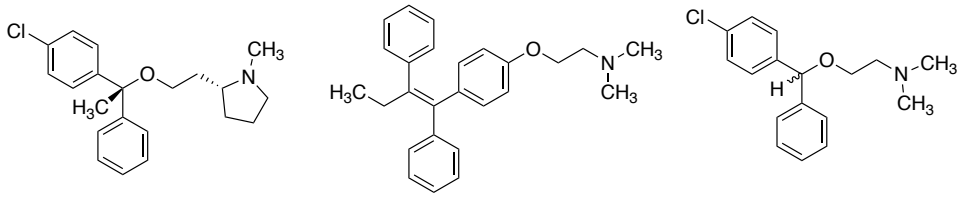

Clemastine **1**
L. major EC_{50} = 0.172 ± 0.003 μM

Tamoxifen **20**
L. major EC_{50} = 9.3 ± 0.3 μM

Analogue **151**
L. major EC_{50} = 70 ± 20 μM

Figure 49: Related structures and activities against *L. major* promastigotes

5.3. Role of stereochemistry

The previous chapter showed that one method to improve activity of clemastine analogues was to investigate the stereochemistry. N-linked compound **147**, R = Me, is structurally the closest related analogue to clemastine with moderate levels of activity. Therefore, the hypothesis was that the antileishmanial activity could be improved through synthesis of a

single diastereomer of compound **147**. It was discovered that similar to the nor-clemastine analogues, the stereocentre on the pyrrolidine ring has little effect on antileishmanial activity as both **(*R*)-147** and **(*S*)-147** have an activity of approximately 2 μM against *L. major* promastigotes (Appendix B).

The enantioselective synthesis illustrated in Scheme 39 was performed to access analogues which explore stereochemistry on the benzhydryl carbon. The enantiopure benzhydrol, **(*R*)-113** or **(*S*)-113**, was synthesised using the same procedure described in Chapter 2. The head group was prepared, in two steps, by carrying out an N-alkylation with 2-bromoethanol under reflux to afford compound **(*R*)-154** in a moderate yield of 48 %. The IR spectrum was used to confirm the formation of **(*R*)-155** with an OH signal at 3385 cm^{-1}. A subsequent chlorination with thionyl chloride formed head group **(*R*)-154** in a yield of 37 %. Formation of **(*R*)-154** was confirmed by the mass spectrum which showed a chlorine isotope pattern with an intensity ratio of 3:1 (*m/z* = 148 ($M(^{35}Cl)H^+$), 150 ($M(^{37}Cl)H^+$)). The final step was the S_N2 etherification, described in Chapter 4, to form analogue **(*R, R*)-147** or **(*R, S*)-147** in a moderate yield (Scheme 39). This provides access to N-linked clemastine analogues in higher yields as no by-product was formed, unlike the S_N2 reaction to form nor-clemastine **(*R, R*)-112** (Scheme 40a). This is because from bicyclic cation intermediate **156** the desired product is formed *via* both pathways as demonstrated in Scheme 40b.

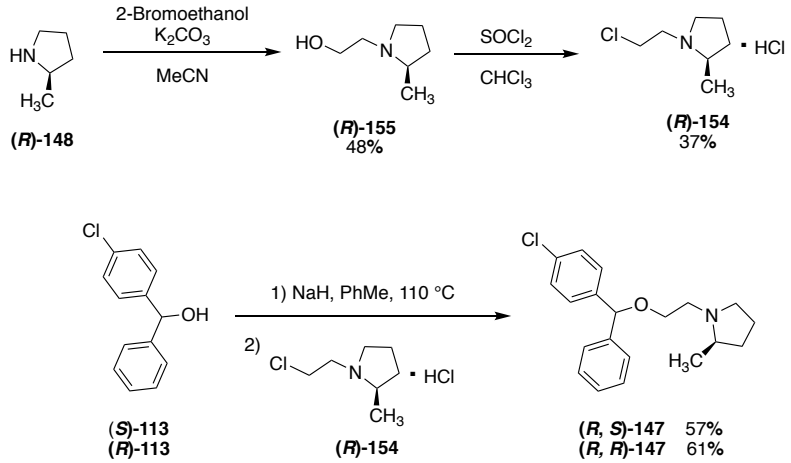

Scheme 39: Asymmetric synthetic route to N-linked clemastine analogues (*R, S*)-147 and (*R, R*)-147

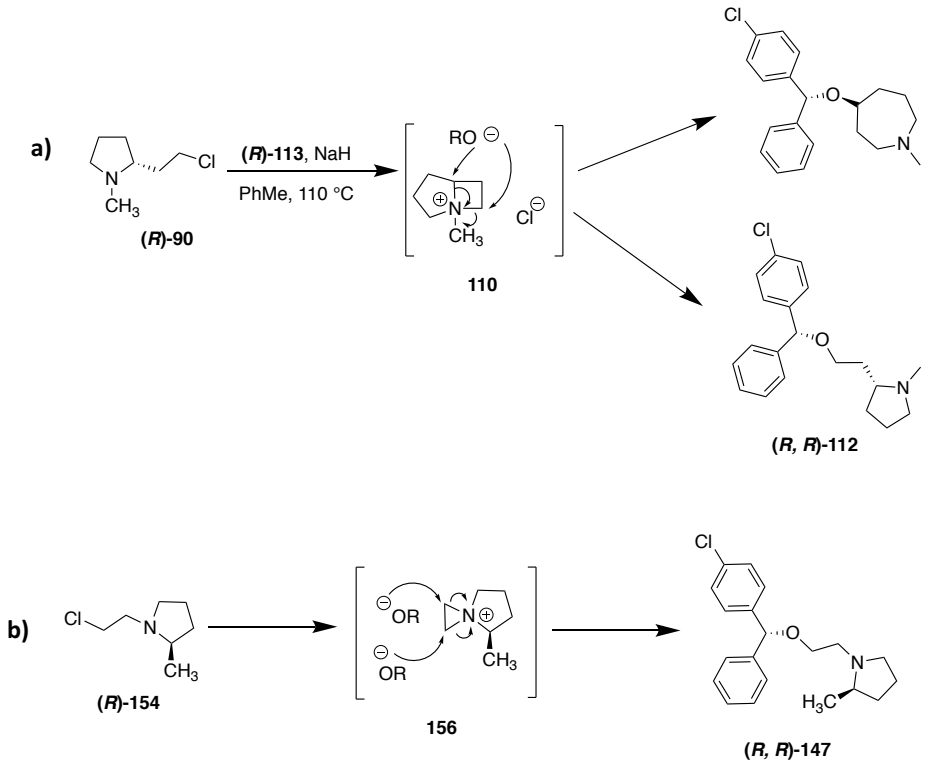

Scheme 40: Formation of ether linkage *via* bicyclic cation intermediate to afford a) nor-clemastine and by-product and b) n-linked analogue (*R, R*)-147.

These single diastereomer N-linked analogues were then tested against *L. major* promastigotes and demonstrate that the (*S*)-configuration on the benzhydryl carbon, **(*R, S*)-147**, is about 4 times less active than analogue **(*R*)-147** with mixed stereochemistry at this position (Figure 50). Hence, the benzhydryl stereocentre contributes to the antileishmanial activity to a greater extent than the chiral centre on the pyrrolidine ring. Similar to the nor-clemastine analogues, the (*R*)-configuration at the benzhydryl carbon in isomer **(*R, R*)-147** provided the highest activity (EC_{50} = 1.7 ± 0.3 μM) against *L. major* promastigotes. The EC_{50} value of racemate **(*R*)-147** is twice that of **(*R, R*)-147** whereas **(*R, S*)-147** is essentially inactive, which suggests that **(*R, R*)-147** is the only active compound. It can be summarised that the role stereochemistry plays in antileishmanial activity is similar for nor-clemastine and N-linked analogues, which indicates that they may have the same target. This will be investigated further in section 5.6.

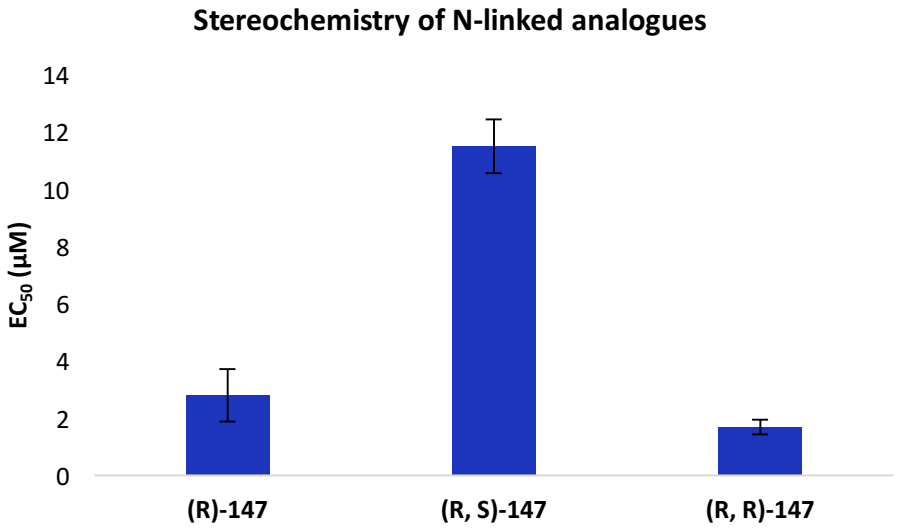

Figure 50: EC_{50} values of (*R*)-147, (*R, S*)-147 and (*R, R*)-147 against *L. major* promastigotes; values are mean ± 95% CI from at least three experiments.

Overall, section 5.2. shows that the most active N-linked analogue is **(*R, R*)-147**, R=Me, which is structurally the closest related analogue to clemastine **1** and possesses (*R*)-configuration at the benzhydryl carbon. However, unlike clemastine **1** and nor-clemastine **(*R, R*)-112**, this compound still does not show sub-micromolar potency. A potential reason for this lack of activity involves the positing of the nitrogen atom in space and this will be explored further in the following section.

5.4. Extending carbon linker

The more accessible N-linked analogues require optimisation to improve the antileishmanial activity. As mentioned above, the key difference between the nor-clemastine analogues and the N-linked compounds is that the nitrogen atom has moved position in space, which could affect the drugs interaction with the enzyme. It was hypothesised, that by extending the linker to 3 carbon units, to form analogue **(*S, R*)-157**, the nitrogen would be in a similar position as in clemastine **1**/nor-clemastine **(*S, R*)-112** improving the antileishmanial activity. In addition, it was postulated that if the chain is further extended to 4 carbon units, to form analogue **(*S, R*)-158**, the nitrogen would fall out of alignment and a drop in activity would be observed.

Results for analogues **(*R*)-147 and (*S*)-147** (section 5.3.) show that the stereocentre on the pyrrolidine ring has little effect on antileishmanial activity. The (*S*)-configuration in the

pyrrolidine ring of analogues **157** and **158**, with 3 and 4 carbon unit linker chains respectively, were synthesised with a racemic benzhydryl centre. Hence, **(*S*)-157** and **(*S*)-158** were synthesised by performing an S_N1 reaction on benzhydrol **113** with bromopropanol and bromobutanol respectively, followed by an alkylation with 2-methylpyrrolidine **148** (Scheme 41). This route is slightly shorter and benefits from higher overall yields compared to the enantioselective synthesis of N-linked analogues (Scheme 39).

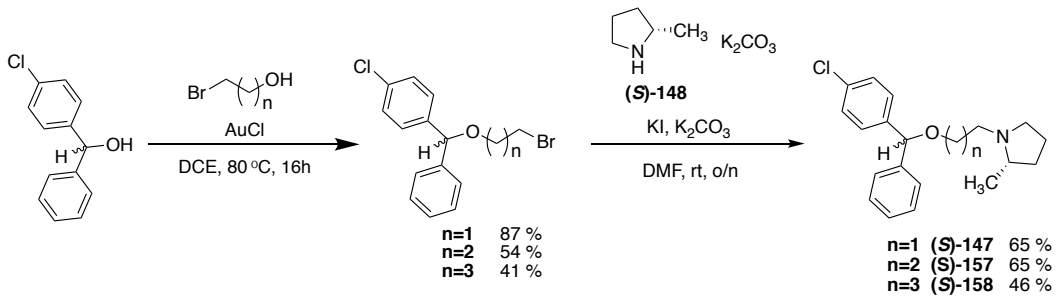

Scheme 41: Synthetic route to N-linked analogues (*S*)-147, (*S*)-157 and (*S*)-158

Gratifyingly, assaying these compounds against promastigotes generated dose response curves for N-linked analogues **(*S*)-147**, **(*S*)-157** and **(*S*)-158** (Figure 51) that support the above hypothesis showing that the optimum chain length was 3 carbons. For analogue **(*S*)-157** the antileishmanial activity drops to sub-micromolar (EC_{50} = 0.09 ± 0.02 μM), which is now equipotent to clemastine (EC_{50} = 0.172 ± 0.003 μM) and nor-clemastine **(*R, R*)-112** (EC_{50} = 0.13 ± 0.01 μM). To further build on this success, analogue **(*S*)-157** was then optimised through the synthesis of a single diastereomer section 5.5.

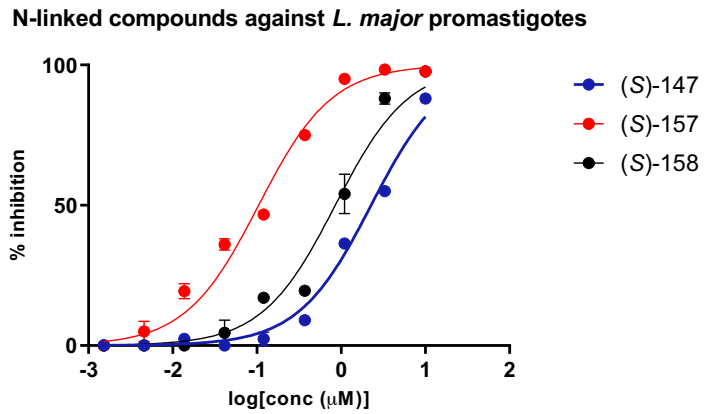

Figure 51: An example of dose response curves of (*S*)-147, (*S*)-157 and (*S*)-158 against *L. major* promastigotes; assays were performed in triplicate and each curve shows a representative experiment.

5.5. Activity of lead analogue

Based on the results in section 5.3. for analogue **147**, the stereocentre on the pyrrolidine ring has little effect on antileishmanial activity. However, **(*S*)-147** is marginally more active than **(*R*)-147** against *L. major* promastigotes, therefore **(*S*)-157** was prepared. In addition, it was proposed that the (*R*)-configuration on the benzhydryl carbon would result in the isomer with the highest activity. Therefore, the single diastereomer, analogue **(*S*, *R*)-157**, was synthesised following the same procedure as employed for the earlier enantiomeric compounds (Scheme 39). It should be noted, that in the interest of time the other three single diastereomers of compound **157** were not tested.

5.5.1. Anti-promastigote assays

Analogue **(*S*)-157** and **(*S*, *R*)-157** were then tested against *L. major* and *L. amazonensis* promastigotes. The EC_{50} values shown in Figure 52 demonstrate that analogue **(*S*, *R*)-157** is about three times more active against *L. major* promastigotes (EC_{50} = 0.058 ± 0.007 μM) than clemastine and equipotent to clemastine when tested against *L. amazonensis* promastigotes (EC_{50}= 0.02 ± 0.01 μM). In addition, the EC_{50} value for **(*S*)-157**, the racemic mixture of diastereomers, is approximately twice that of the value obtained for the single diastereomer **(*S*, *R*)-157** which is expected if **(*S*, *R*)-157** is the only active compound. Overall, the antileishmanial activity of N-linked analogue **(*S*, *R*)-157** was investigated further by testing against the clinically relevant amastigote form of the disease.

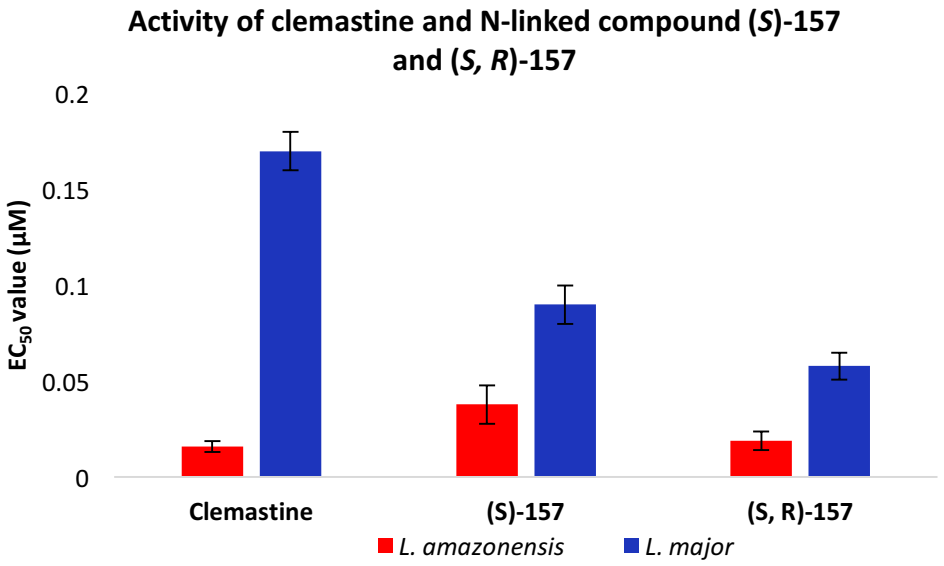

Figure 52: EC_{50} values of clemastine 1, and analogues (*S*)-157 and (*S, R*)-157 against *L. amazonensis* and *L. major* promastigotes; values are mean ± 95% CI from at least three experiments.

5.5.2. Cytotoxicity to BMDM

Before the anti-amastigote assay could be conducted the cytotoxicity of compound **(*S*, *R*)-157** against BMDM needed to be investigated using the resazurin-based cell-viability assay described earlier.[192] Pleasingly, analogue **(*S*, *R*)-157** proved to be 3-4 times less cytotoxic to host macrophages than clemastine (Figure 53). The low levels of cytotoxicity of analogue **(*S*, *R*)-157** to BMDM (CC_{50} = 73 ± 14 μM) suggest that this compound has the potential to be a more selective antileishmanial drug than clemastine. Interestingly, N-linked analogue **(*S*, *R*)-157** and nor-clemastine **(*R*, *R*)-112** are both less cytotoxic to host macrophages than clemastine and both lack a quaternary methyl group on the benzhydryl carbon. Therefore, the quaternary methyl group may be responsible for the higher levels of host cell cytotoxicity. One reason for this may involve the benzylic methyl group being subjected less to P450 mediated metabolism than the benzylic C-H bond. Therefore, clemastine would have a lower intrinsic clearance than nor-clemastine which may account for its higher host cell cytotoxicity.[235]

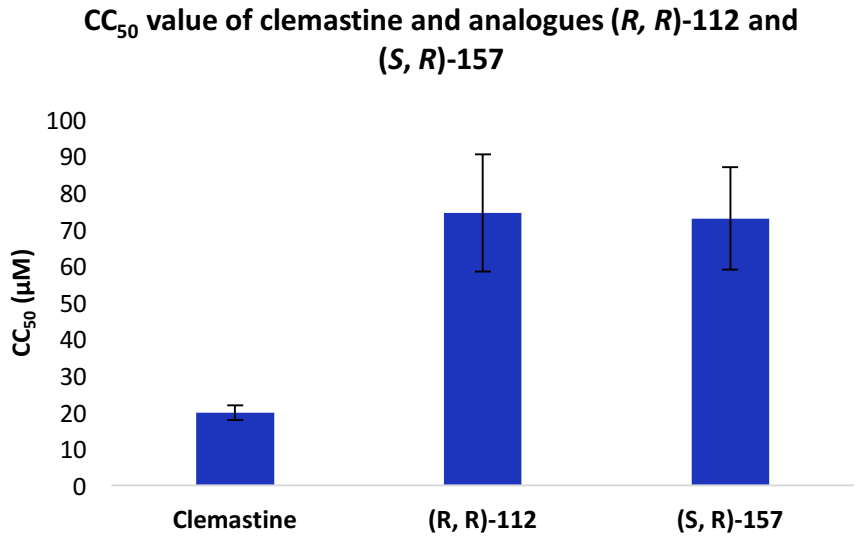

Figure 53: CC_{50} values of clemastine 1 and analogues (*R*, *R*)-112 and (*S*, *R*)-157 against BMDM; values are mean ± 95% CI from at least three experiments.

5.5.3. Intramacrophage anti-amastigote assay

As analogue **(*S*, *R*)-157** had a low level of host cell cytotoxicity it could be used to treat BMDM infected with *L. amazonensis,* this species was chosen as it is sensitive to analogue **(*S*, *R*)-157** and infective towards BMDM. As described in Chapter 3, the infected cells were adhered to cover slips and treated with analogue **(*S*, *R*)-157** for 48h. The cover slips were

then stained with Giemsa modified solution and amastigotes were counted within 200 macrophages. This assay generated the dose-response curve for analogue **(*S*, *R*)-157** (Figure 54) and showed that clemastine **1** and analogue **(*S*, *R*)-157** have similar levels of activity against intramacrophage amastigotes (EC_{50} = 0.40 ± 0.05 μM and 0.51 μM respectively). Overall, **(*S*, *R*)-157** is a more accessible and selective compound (SI = 146) than clemastine (SI = 50) and Table 4 summarises the data for this analogue. However, on-target effects of analogue **(*S*, *R*)-157** still required validation before it could be progressed into an animal model.

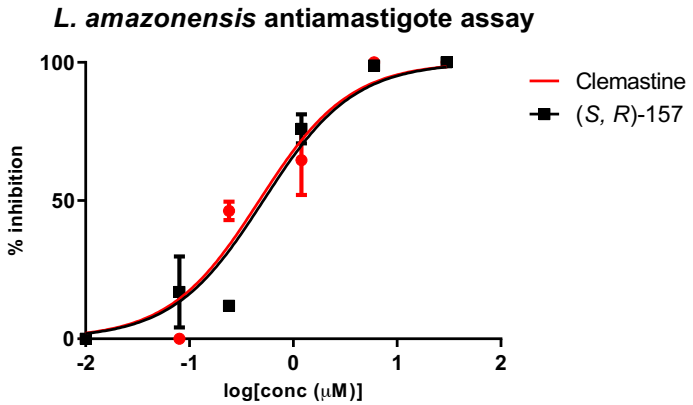

Figure 54: An example of dose response curves of clemastine 1 and analogue (*S, R*)-157 against intramacrophage amastigotes; each curve shows a representative experiment.

Table 4: EC_{50} values of analogue (*S, R*)-157 against *L. amazonensis* promastigotes and amastigotes and CC_{50} value of analogue (*S, R*)-157 towards BMDM; values are mean ± 95% CI from at least three experiments; no error for amastigote EC_{50} as only one assay was performed.

Promastigote EC_{50} (μM)	Macrophages CC_{50} (μM)	Amastigotes EC_{50} (μM)
0.02 ± 0.01	73 ± 14	0.51

5.6. On-target effects

As described in Chapter 3 for clemastine **1**, the dose-dependent growth inhibition of *L. major* WT, *Δ* LCB2 and PX cell line were assessed and compared to validate on target effects of N-linked analogue **(*S*, *R*)-157** (Figure 55). Using cycloheximide as a control these assays showed that, similar to clemastine **1**, analogue **(*S*, *R*)-157** is approximately 3 times more active against WT and PX cell lines than the mutant *Δ* LCB2 promastigotes. This suggested that both clemastine **1** and N-linked analogue **(*S*, *R*)-157** are disrupting the sphingolipid pathway.

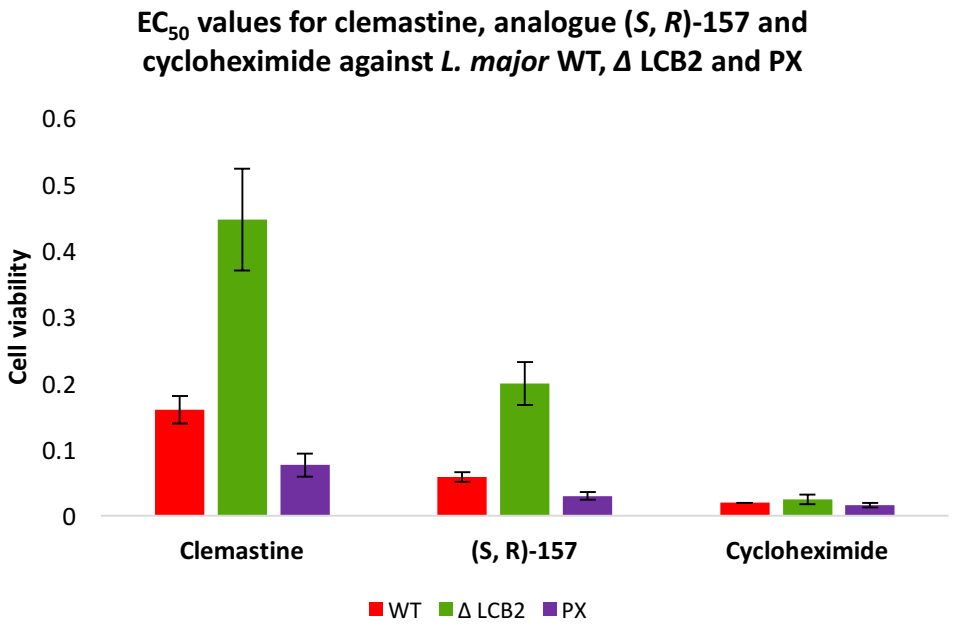

Figure 55: EC_{50} values of clemastine and analogue (*S*, *R*)-157 against WT, *Δ* LCB2 and PX *L. major* promastigotes; cycloheximide is used as a positive control; values are mean ± 95% CI from at least three experiments.

The mutant assay discussed above indicates that analogue **(*S*, *R*)-157** is having an effect on sphingolipid biosynthesis, however, IPCS still needs to be validated as the target. To achieve this, the biochemical assay[146] described in Chapter 2 was employed, in which NBD-C_6-ceramide **80** and NBD-C_6-IPC **81** were separated *via* HPTLC and analysed through fluorescence spectroscopy. This experiment demonstrated that **(*S*, *R*)-157** was a functional analogue of clemastine **1**, acting as an inhibitor of IPCS, because product IPC was not observed on the HPTLC plate (Figure 56).

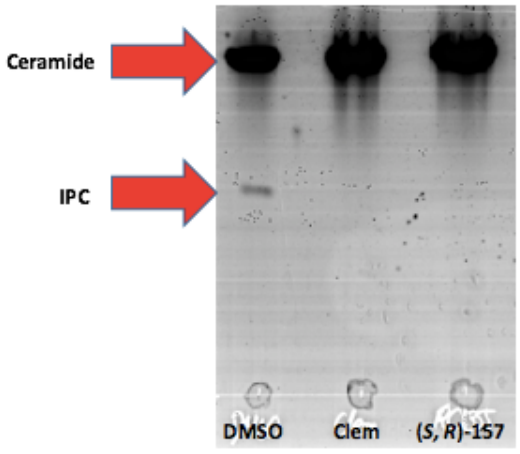

Figure 56: Separation of NBD-C_6-IPC 81 product from NBD-C_6-ceramide 80 substrate by HPTLC; Microsomes were treated with 5mM of analogue (*S, R*)-157 and negative and positive controls were DMSO and 5mM of clemastine 1.

5.7. *In vivo* infection study

As sub-micromolar activity has been observed for analogue **(*S*, *R*)-157** against *Leishmania in vitro*, it was hypothesised that this compound would be effective in an animal model infected with *L. amazonensis* parasites. Hence, analogue **(*S*, *R*)-157** was the sixth group in the second *in vivo* study* discussed in Chapter 3. Analogue **(*S*, *R*)-157** was administered at a dose of 1.17 mg kg^{-1} *via* IL injection twice a week. This was the same treatment regime as used in the clemastine IL group enabling the two therapies to be directly compared.

Similar to the other groups, there was little variation in the weight of mice treated with analogue **(*S*, *R*)-157** (Figure 57a). On day 35 post-infection, mice treated with analogue **(*S*, *R*)-157** IL showed a significant reduction in lesion size when compared to the untreated group. The lesion growth trend is similar for the groups treated with analogue **(*S*, *R*)-157** and clemastine **1** IL (Figure 57b). It should be noted that mice treated with glucantime **3** solution, positive control group, showed the greatest reduction in lesion size. This is partly due to glucantime **3** solution being administered as an IP therapy, whereas IL treatments can cause inflammation to the ear increasing lesion measurements. Images in Figure 57c show similar improvements in the appearance of the lesion for analogue **(*S*, *R*)-157** IL, clemastine **1** IL and glucantime **3** solution IP groups when compared to the untreated group.

The *in vivo* fluorescence measurements from the infected ear show a significant reduction in parasite burden for analogue **(*S*, *R*)-157** IL and clemastine **1** IL ($P \leq 0.001$) when compared to the untreated group (Figure 57d). Again, similar to clemastine **1** IL, results from the LDA showed statistical significance between the untreated group and analogue **(*S*, *R*)-157** IL group ($P \leq 0.0001$) (Figure 57e). This positive *in vivo* result supports the hypothesis that analogue **(*S*, *R*)-157** could be an effective treatment for CL in an animal model.

***Collaboration with Douglas Escrivani at UFRJ**

a)

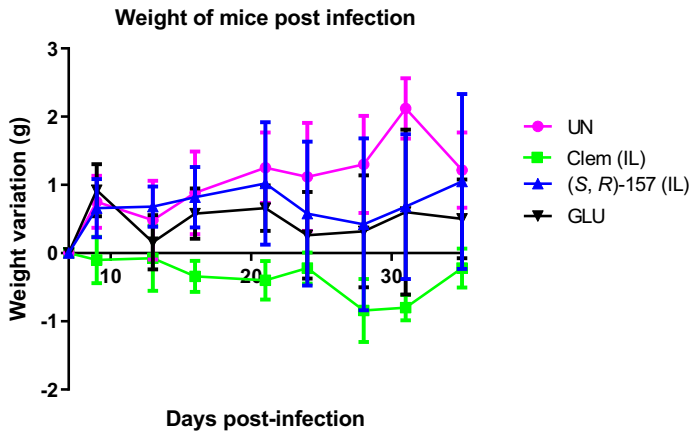
Weight of mice post infection
Weight variation (g)
Days post-infection
UN
Clem (IL)
(S, R)-157 (IL)
GLU

b)

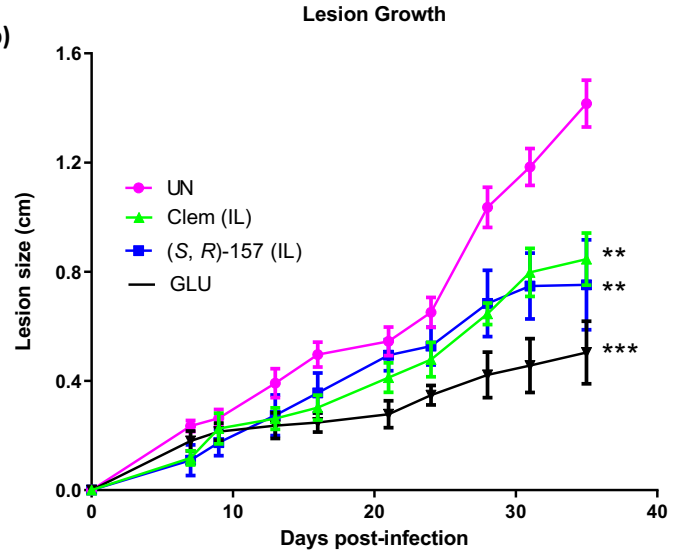
Lesion Growth
Lesion size (cm)
Days post-infection
UN
Clem (IL)
(S, R)-157 (IL)
GLU
**
**
***

c)

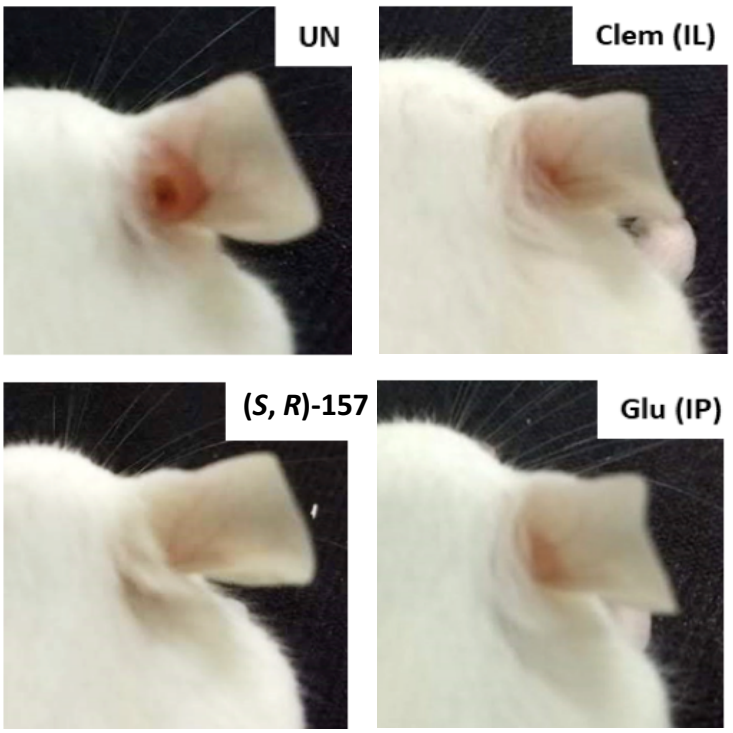
UN
Clem (IL)
(S, R)-157
Glu (IP)

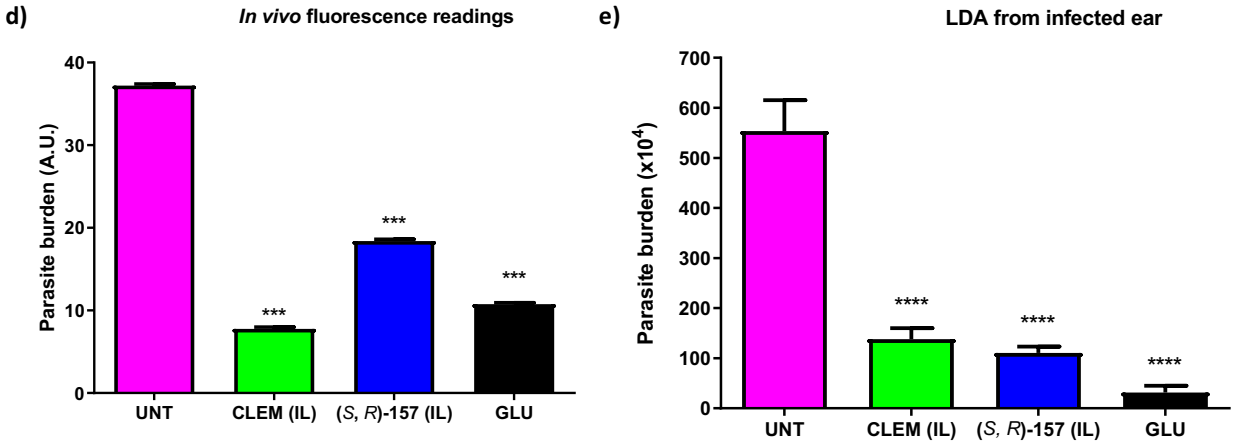

Figure 57: *In vivo* study 2 from BALB/c mice infected with 2x10^6 *L. amazonensis* GFP promastigotes in the right ear, mice were randomized into drug-treated and control groups of 5/6 mice each. During 28 days of treatment a) weight variation of mice and b) progression of lesion thickness were measured. After completion of treatment, c) representative photographs of the infected ear for each group were taken and the parasite burden was evaluated by d) fluorescence measurements and e) LDA; asterisks indicate that the difference between control and drug-treated groups are statistically significant. * P ≤ 0.05, ** P ≤ 0.01, *** P ≤ 0.001, **** P ≤ 0.0001.

5.8. Conclusion

The work described in this chapter involved developing simple synthetic routes to easily and quickly access N-linked analogues of clemastine. With a 3-carbon chain linker and the appropriate (*S*, *R*) stereochemistry, analogue **(*S*, *R*)-157**, was equipotent to clemastine **1** against *L. amazonensis* promastigotes and more active than clemastine **1** against *L. major* promastigotes. This compound was less toxic to macrophages than clemastine **1** and showed similar activity to clemastine **1** against *L. amazoneneisis* intramacrophage amastigotes. Therefore, analogue **(*S*, *R*)-157** was a more accessible and selective compound. The target of analogue **(*S*, *R*)-157** was validated as IPCS using mutant *Δ* LCB2 promastigotes and an *Lmj*IPCS biochemical HPTLC assay.[146] Analogue **(*S*, *R*)-157** was progressed into an *in vivo* infection study and showed efficacy as an IL therapy against CL. It could be hypothesised that the structural similarities of analogue **(*S*, *R*)-157** and clemastine **1** would result in similar immunological, antihistamine and CNS effects. Hence, future work would involve investigating these properties along with obtaining a pharmacokinetic profile of analogue **(*S*, *R*)-157**. Positive pharmacokinetic data could result in this novel compound being tested in an *in vivo* study as an IP and oral therapy.

6. Additional work

6.1. Fluorescent nor-clemastine analogue

As described previously, the antileishmanial target of clemastine **1** has been identified as IPCS. This target enzyme could be validated using chemical probes,[236] which may provide insight into the binding site and hence lead to the development of an efficacious drug with minimal side effects. Chemical probes based on clemastine analogues could be formed using the synthetic pathways discussed in Chapter 4 and 5. A starting point to probe development and the aim of this work was to design a fluorescent analogue of clemastine to image its localisation within the parasite.

6.1.1. Synthesis

Nitrobenzoxadiazole (NBD) has been used as fluorescent label for the lipids in the biochemical assay described in Chapter 2. There are literature reports using NBD labels to develop small molecule chemical probes.[237,238,239] Hence, the aim was to synthesise 4- and 3- benzoxadiazole analogues **(*R*)-159** and **(*R*)-160** using the same synthetic strategy employed for the nor-clemastine target molecules (Scheme 42).

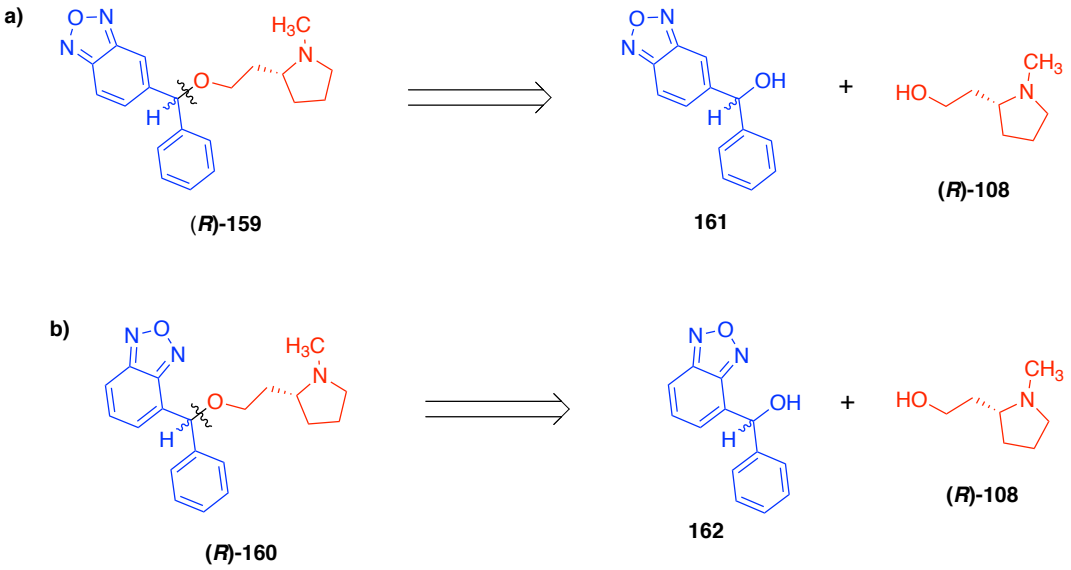

Scheme 42: Disconnection of benzoxadiazole analogue a) (*R*)-159 and b) (*R*)-160

Pleasingly, the tail groups **161** and **162** were formed in good yields *via* the Grignard procedure described in Chapter 4 for the synthesis of benzhydrols (Scheme 43).

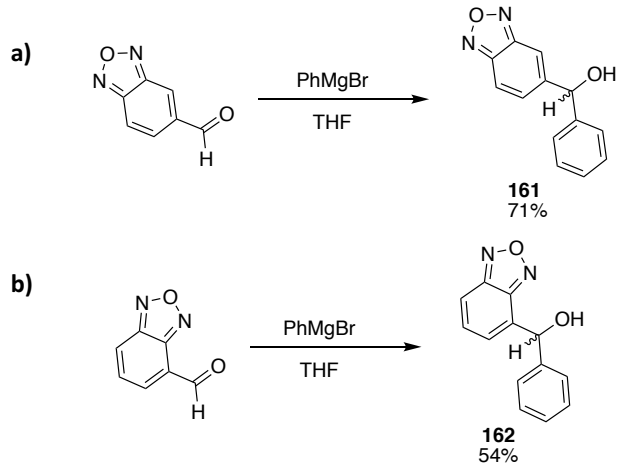

Scheme 43: Formation of tail groups 161 and 162 *via* Grignard reaction

Clayden's procedure (Scheme 20b, Chapter 4**)** was performed to access head group **(*R*)-108**. The challenging step with tail groups **161** and **162** was the etherification step. This reaction was unsuccessful with an acid catalyst (Scheme 44) which could be due to the instability of cation **163** caused by the electron withdrawing benzoxadiazole.

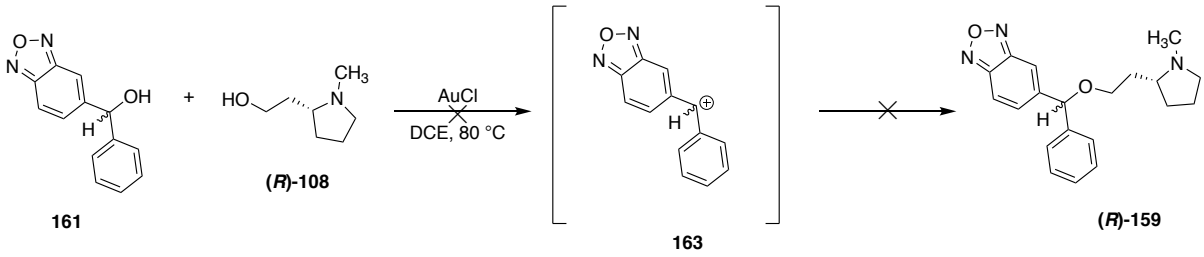

Scheme 44: Unsuccessful formation of analogue (*R*)-159 due to instability of benzoxadiazole cation 163

As a result, head group **(*R*)-90**, formed *via* chlorination of compound **(*R*)-108**, and tail group **161** were coupled together using NaH and high temperatures (Scheme 45). This afforded the desired analogue **(*R*)-159** and azepane by-product **(*S*)-164** in low yields of 16% and 9% respectively. However, sufficient material of both analogues, **(*R*)-159** and **(*S*)-164,** was isolated to analyse antileishmanial activity.

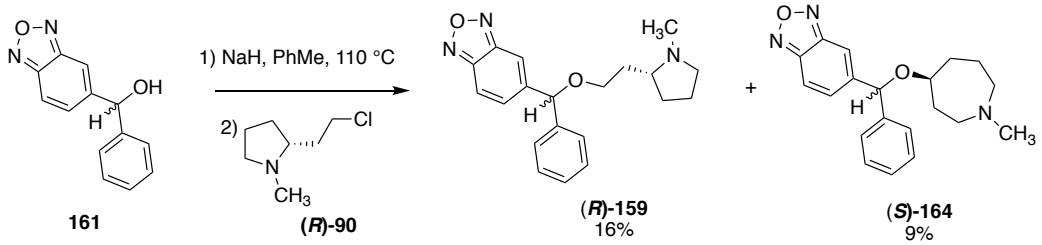

Scheme 45: Synthetic route to 4- benzoxadiazole nor-clemastine analogue (*R*)-159 and by-product (*S*)-164

Similar to alcohol **161** the 3- benzoxadiazole **162** could not undergo an acid catalysed etherification. In addition, the etherification with NaH to form analogue **(*R*)-160** was unsuccessful and this possibly could be due to the more sterically hindered nature of tail group **162** (Scheme 46). The synthesis of this compound was not investigated further due to time constraints and focus turned to analogue **(*R*)-159** and by-product **(*S*)-164.**

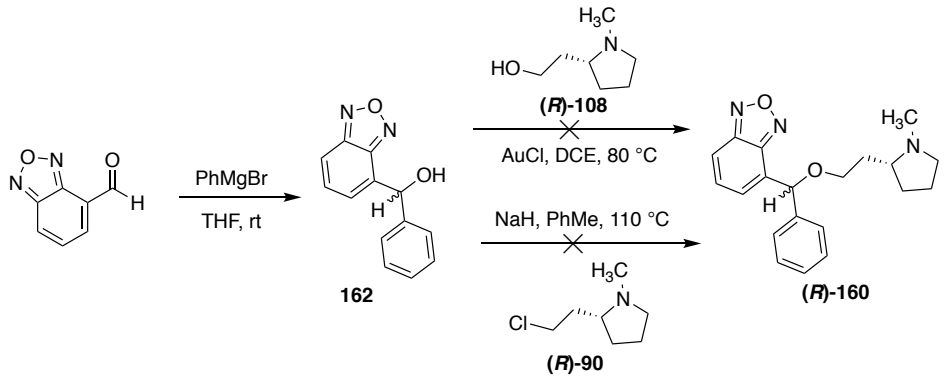

Scheme 46: Unsuccessful synthetic routes to 3-benzoxadiazole nor-clemastine analogue (*R*)-160

6.1.2. Anti-promastigote activity

With nor-clemastine analogue **(*R*)-159** and azepane by-product **(*S*)-164** in hand, the activity of these compounds against *Leishmania* promastigotes was assessed. Azepane by-product **(*S*)-164** showed poor activity against both *L. major* and *L. amazonensis* promastigotes (EC_{50} = 17 ± 1 μM and 6.0 ± 0.5 μM respectively). On the other hand, nor-clemastine analogue **(*R*)-159** showed sufficiently high levels of activity (EC_{50} = 2.80 ± 0.02 μM and 0.56 ± 0.03 μM against *L. major* and *L. amazonensis* promastigotes respectively) to be employed as a probe. Therefore, the fluorescence of compound **(*R*)-159** was investigated.

6.1.3. Fluorescence

Fluorescence for nor-clemastine analogue **(*R*)-159** was quantified (Figure 58) and shows low fluorescence intensity with an excitation wavelength at 445 nm and emission wavelength at 560 nm.

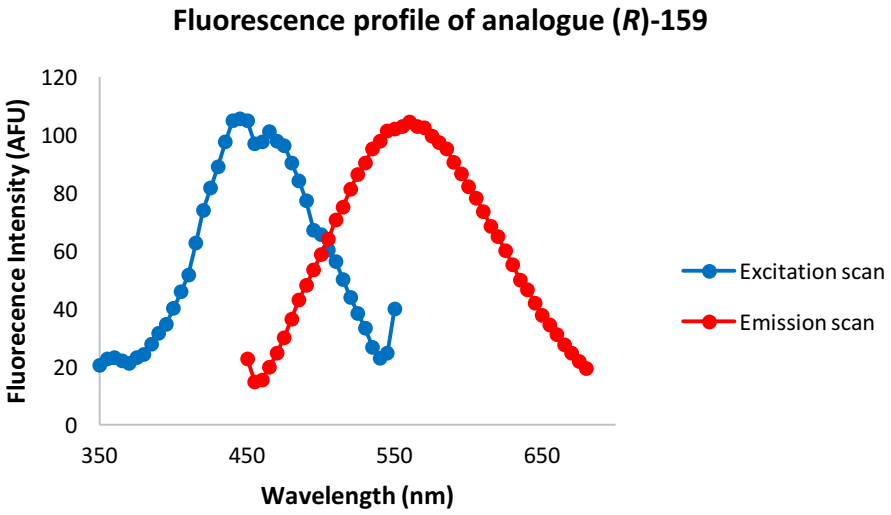

Figure 58: Excitation and Emission scan of 5 mM analogue (*R*)-159 in DMSO

The excitation and emission wavelengths observed for analogue **(*R*)-159** could theoretically be used for imaging. In this case, the aim was to use a microscope fitted with a filter cube (filter B-2A, Ex470/Em515) to image the localisation of analogue **(*R*)-159** in *L. amazonensis* promastigotes. The excitation and emission wavelengths of filter block B-2A did not directly correspond to the excitation and emission wavelengths of analogue **(*R*)-159** but the fluorescence signal was still strong enough to obtain images of this compound within the parasite (Figure 60-62).

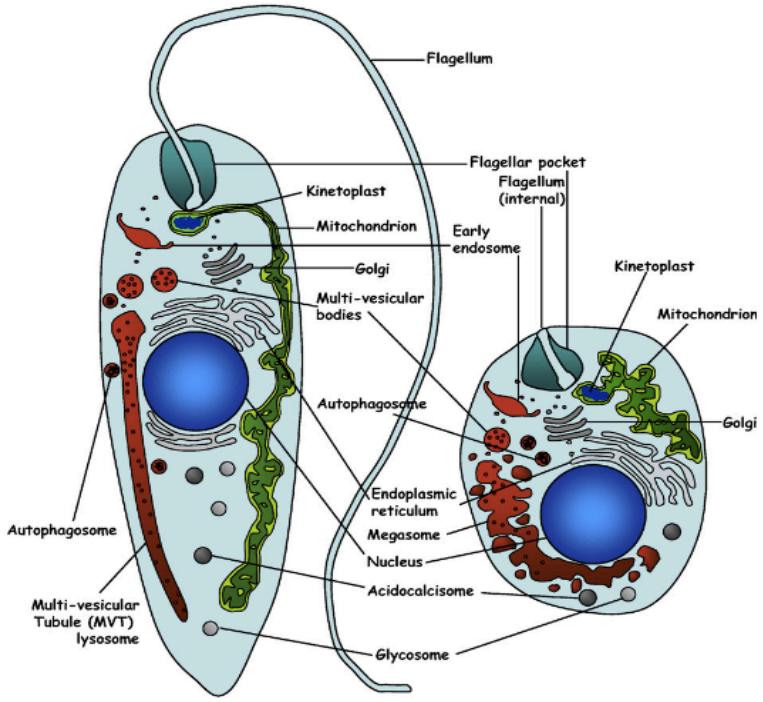

Figure 59: Schematic representation of the main intracellular organelles from *Leishmania* promastigotes (left) and amastigotes (right). Reprinted with permission.[6]

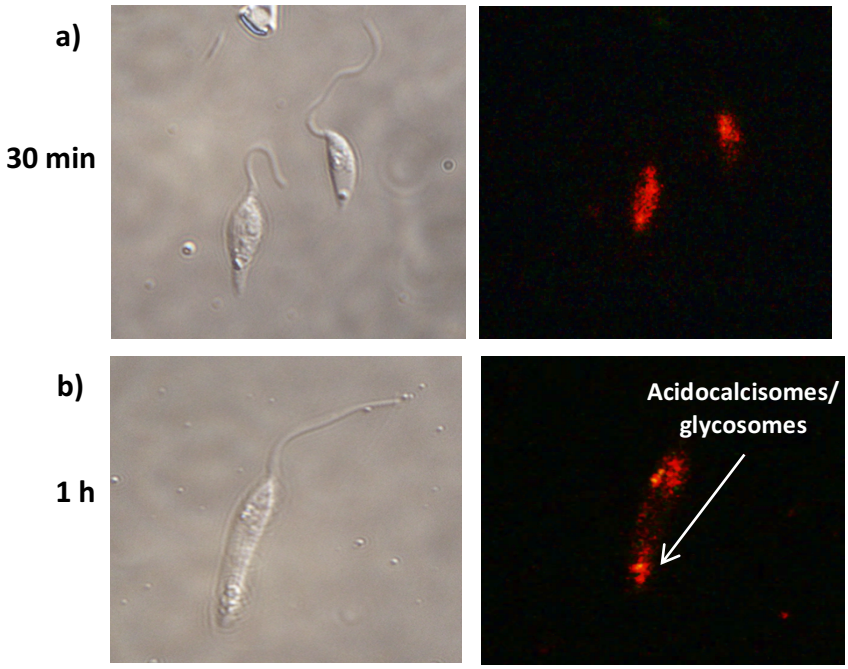

Figure 60: *L. amazonensis* WT promastigotes incubated with 100 µM of analogue (*R*)-159 in PBS for a) 30 min b) 1 h. Left column white light image, right column fluorescence image showing localisation of analogue 159 at the flagella pocket and possibly at the acidocalcisomes/glycosomes.

Figure 61: *L. amazonensis* GFP promastigote a) untreated b) incubated with 100 µM of analogue (*R*)-159 in PBS for 30 min. Left column white light image, right column fluorescence image of analogue 159 showing possible localisation at the acidocalcisomes/glycosomes.

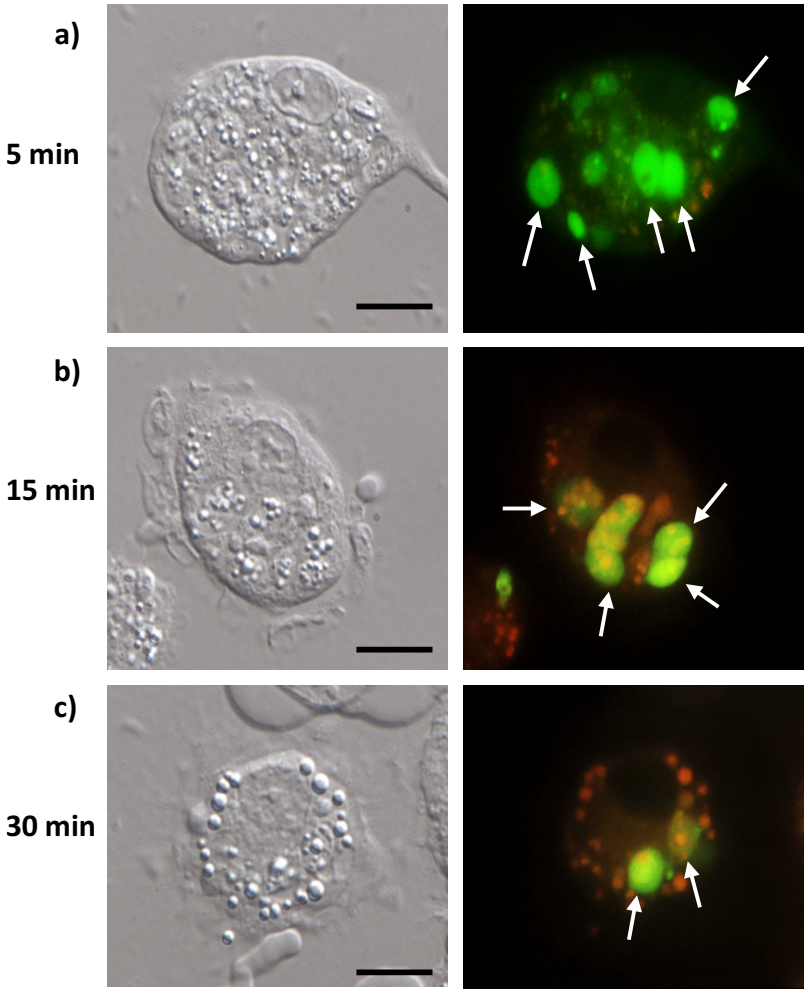

Figure 62: *L. amazonensis* GFP intramacrophage amastigotes incubated with 100 μM of analogue (*R*)-159 in PBS for a) 5 min b) 15 min c) 30 min. Left column white light image, right column fluorescence image showing internalisation of analogue (*R*)-159 into the macrophage. Arrows show typical amastigotes.

Figure 59 shows the main intracellular organelles in *Leishmania* promastigotes and amastigotes, the aim was to use this schematic to identify the possible targets of analogue **(*R*)-159** in the parasite. It was postulated that compound **(*R*)-159** would target *Leishmania* IPCS as it is an analogue of clemastine. However, IPCS is localised within the Golgi and the fluorescent images do not show localisation in this organelle.

Instead, the promastigotes incubated with analogue **(*R*)-159** for 30 min localise at the flagellar pocket, which is where the drug can enter the parasite (Figure 60a). After, 1 h the drug has moved to the posterior region. This assay was repeated with *L. amazonensis* GFP promastigotes to validate the internalisation of analogue **(*R*)-159**. Figure 61a is an image of the untreated parasite with no red fluorescence, this indicates that the observed fluorescence in the treated parasites is from the probe and not an artefact of

autofluorescence. After treatment of the parasite with 100 µM of analogue **(*R*)-159** for 30 min, there is again localisation of analogue **(*R*)-159** at the posterior region of the parasite.

Figure 62 shows BMDM infected with *L. amazonensis* GFP; after 5 min analogue **(*R*)-159** has started to enter the macrophage but not the amastigotes. At 15 and 30 min analogue **(*R*)-159** has fully accessed the macrophage but it is unclear as to whether or not it has penetrated the amastigotes.

The fluorescent images of treated promastigotes (Figure 60 and 61) show localisation of analogue **(*R*)-159** at the posterior of the parasite where organelle such as the acidocalcisomes and glycosomes reside. Acidocalcisomes are acidic organelle rich in calcium and polyphosphate and therefore involved in Ca^{2+} homeostasis. Chapter 1 shows examples of drugs with antileishmanial activity through disruption of intracellular Ca^{2+} homeostasis (e.g. amiodarone **48** and dronedarone **49**). In addition, glycosomes are a good drug target in kinetoplastids as glycolysis is the only source of energy for these parasites.[240,241] Hence, both of these organelles house viable antileishmanial drug targets.

Although this was an interesting study, it requires further investigation. For example, to improve the resolution of the image a molecule with an increased quantity of fluorescence, such as a nitro substituted analogue of **(*R*)-159,** could be synthesised. However, structural alterations to the probe could cause loss in activity against the parasite or off-target effects.

An alternative approach to improve the quality of the image is to use confocal laser scanning microscopy. This technique would enhance the resolution and contrast of the image through reduction of background signal.[242] Confocal microscopy could image analogue **(*R*)-159** in combination with a Golgi tracker to study colocalisation and may validate IPCS as the biological target.

Furthermore, knowing the localisation of the probe is only useful if it shares the same target as clemastine. This assumption can be validated *via* a competition assay, where promastigotes are pre-treated with clemastine, followed by the addition of the probe. If the image shows clemastine blocking the localisation of the probe, then this indicates that they target the same protein.

6.2. Conclusion

The work described in this chapter involved a preliminary study of a fluorescent analogue of nor-clemastine **(*R*)-159** which demonstrated micro-molar activity against *Leishmania* promastigotes. The fluorescent images from the microscope fitted with a filter cube are mostly inconclusive as to the localisation of analogue **(*R*)-159**. However, this study does provide a point for further investigation.

In addition, there are reports in literature of using photoaffinity probes, coupled with mass spectrometry analyses to identify and characterise biological targets.[236] Hence, future work could investigate the design and synthesis of a photoaffinity probe based on clemastine to validate the drug target. The general design of a photoaffinity probe is outlined in Figure 63 and involves the small molecule of interest, a photoreactivity moiety (e.g. phenylazides, phenyldiazirines and benzophenones) and a reporter tag (e.g. biotin). In response to activation by light this chemical probe will covalently bind to its target. The aim would be to validate the target of clemastine as IPCS and probe the location and structure of the binding site.[236]

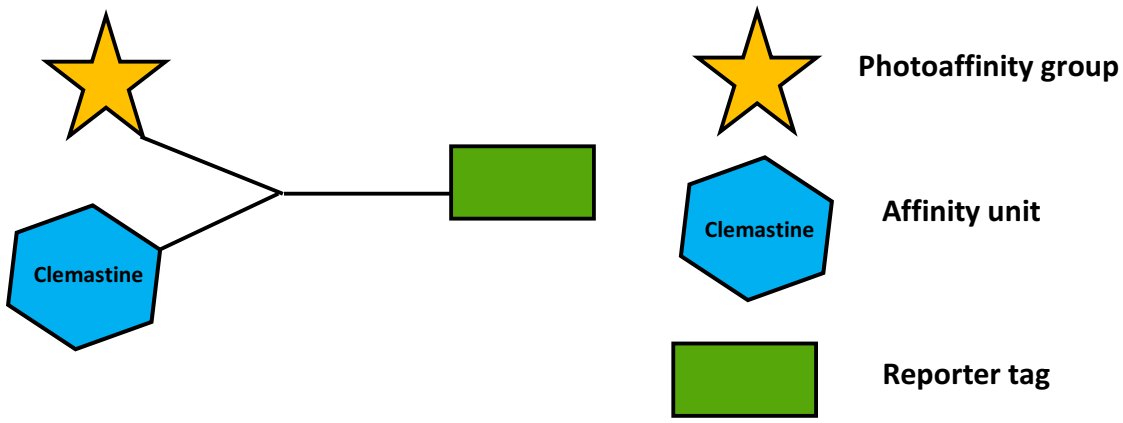

Figure 63: General designs for photoaffinity probes (adapted from *Collins et al*)[2]

7. Chemical experimental

7.1. General experimental details

SOLVENTS AND REAGENTS: All analytical grade solvents and commercially available regents were used as received from their respective suppliers or dried as required, using standard procedures. All reactions were performed under an inert atmosphere of argon unless otherwise stated.

CHARACTERISATION: Reactions were monitored by LC-MS, GC-MS or by TLC using aluminium backed plates. Methods to visualise the spots included ultra-violet light (254 nm) and colour reagents. The visualising stains used were potassium permanganate, phosphomolybdic acid or ninhydrin. Column chromatography was performed using a Teledyne Isco CombiFlash® System with RediSep® Rf normal-phase and C-18 reversed-phase columns. Both carbon and hydrogen NMR spectra were acquired at 295 K on Varian VNMRS 700 (^{1}H at 700 MHz, ^{13}C at 176 MHz), Varian VNMRS 600 (^{1}H at 600 MHz, ^{13}C at 151 MHz), with sample dissolved in the analytical solvent $CDCl_3$. 2D COSY, HSQC, HMBC and NOESY were run to aid assignment of peaks. Chemical shifts are reported in parts per million, ppm, to 2 decimal places; with the multiplicity of the signal reported as s, singlet; d, doublet; t, triplet; coupling constants, *J*, are quoted to the nearest ± 0.5 Hz. Ar refers to aryl resonances which could not be accurately assigned. Infrared (IR) spectra were acquired using a Perkin-Elmer Paragon 1000 FT-IR and absorption maxima (ν_{max}) are reported in wavenumbers (cm^{-1}) and assigned as strong (s), medium (m), weak (w) or broad (br). Mass spectra were recorded using Shimadzu gas chromatography *via* electron ionization (EI) or on a Waters TQD spectrometer coupled to an Acquity UPLC. Melting points are measured using Fisher ScientificTM IA9000 melting point apparatus.

7.2. Experimental procedures

General procedure A: Grignard reaction

Magnesium turnings (1.7 equiv.) were added to a 2-necked flask equipped with a reflux condenser and a dropping funnel containing dry THF (1 mL/ mmol) and a solution of bromobenzene (1.3 equiv.). About one quarter of the bromobenzene solution was added to the magnesium turnings and heated to 60 °C until the turbidity of the reaction increased.

Once the reaction started the remaining bromobenzene solution was added dropwise and the reaction was heated under reflux for 1 h. The solution was cooled to rt and a substituted benzaldehyde (1 equiv.) in THF (1 mL/ mmol) was added dropwise. The reaction was stirred overnight at rt and then quenched with saturated $NH_4Cl_{(aq.)}$. The mixture was washed with EtOAc (3 x 20 mL), dried over $MgSO_4$ and filtered. Solvent was removed under reduced pressure. [243]

General procedure B: Fieser's method for the workup of $LiAlH_4$ reactions

A reaction mixture of lithium aluminium hydride (X g) was cooled to 0 °C and diluted with ether. It was then carefully quenched with H_2O (X mL), followed by 3 M $NaOH_{(aq)}$ (3X mL) and finally H_2O (3X mL). This was warmed to rt and stirred for 15 min before the addition of anhydrous $MgSO_4$ and then stirring for another 5 min. The salts were then removed by filtration and solvent was removed *in vacuo* to afford the crude product.[244]

General procedure C: Pd-catalysed etherification

To a solution of alcohol (1 equiv.) and diphenylmethanol (1 equiv.) in DCE (5 mL $mmol^{-1}$) was added $PdCl_2$ (0.1 equiv.). The reaction mixture was heated at 80 °C for 48 h. The solvent was then removed under reduced pressure to afford the crude product.[230]

General procedure D: S_N2 reaction of 4-chlorobenzhydrol and alkyl chloride[202]

The 4-chlorobenzhydrol (1 equiv.) and NaH (60%, 3 equiv.) were dissolved in anhydrous toluene (5 mL $mmol^{-1}$) and heated under reflux for 3 h under nitrogen. The solution was cooled to rt and chloroethylpyrrolidine (1 equiv.) in toluene (2.5 mL $mmol^{-1}$) was added. The reaction mixture was then reacted under reflux overnight. The reaction mixture was cooled, quenched with H_2O and diluted with EtOAc. The aqueous layer was separated and extracted twice with EtOAc. The combined organic layers were then dried over Na_2SO_4, filtered, and then concentrated *in vacuo*.

7.3. Compound characterisation

4-Bromophenyl(phenyl)methanol[245] 122

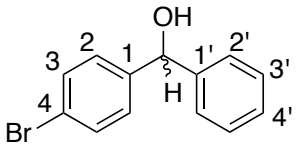

General procedure A was used with bromobenzene (2.60 mL, 24.84 mmol) and 4-bromobenzaldehyde (3.50 g, 18.92 mmol). The product was purified by column chromatography (0% → 20% ether in hexanes) to afford the title compound (2.99 g, 66%) as an off-white solid.

M.p. 64 – 65 °C (lit.:[245] 65 – 66 °C); ν_{max} (ATR) 3352 (br), 3063 (w), 2904 (w), 1906 (w), 1600 (w), 1481 (s), 1397 (m), 1190 (m), 1008 (s) cm^{-1}; δ_H (700 MHz, $CDCl_3$) 7.47 – 7.43 (2H, m, Ar***H***), 7.36 – 7.31 (4H, m, Ar***H***), 7.30 – 7.27 (1H, m, Ar***H***), 7.26 – 7.21 (2H, m, Ar***H***), 5.76 (1H, s, Ar_2C***H***), 2.39 (1H, s, O***H***); δ_C (176 MHz, $CDCl_3$) 143.5 (***C***-1'), 142.8 (***C***-1), 131.7 (Ar***C***), 128.8 (Ar***C***), 128.3 (Ar***C***), 128.0 (Ar***C***), 126.6 (Ar***C***), 121.5 (***C***-4), 75.8 (Ar_2***C***HO); *m/z* (LC-MS, ESI^+) 245 (M(^{79}Br)–OH^+), 247 (M(^{81}Br)–OH^+).

1-Bromo-4-[chloro(phenyl)methyl]benzene[246] 128

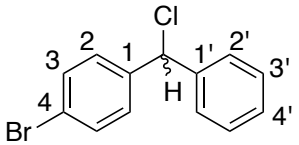

To a solution of 4-bromophenyl(phenyl)methanol **122** (150 mg, 0.57 mmol) and NEt_3 (0.16 mL, 1.15 mmol) in DCM (2.50 mL) at 0 °C was added methanesulfonyl chloride (0.10 mL, 1.29 mmol) dropwise and the reaction mixture was stirred overnight at rt. The mixture was then washed with H_2O (10 mL), 2M HCl (10 mL) and brine (10 mL) and dried over Na_2SO_4. The solvent was removed *in vacuo* to afford the title compound (142 mg, 88%) as a yellow oil which was carried forward without purification.

ν_{max} (ATR) 2982 (w), 1739 (w), 1590 (w), 1487 (s), 1453 (m), 1404 (m), 1316 (w), 1216 (w), 1173 (m), 1071 (s), 1010 (s); δ_H (700 MHz, $CDCl_3$) δ 7.49 – 7.46 (2H, m, Ar***H***), 7.40 - 7.37 (2H, m Ar***H***), 7.37 - 7.34 (2H, m, Ar***H***), 7.33 – 7.31 (1H, m, Ar***H***), 7.30 – 7.27 (2H, m, Ar***H***), 6.08 (1H, s, Ar_2C***H***); δ_C (176 MHz, $CDCl_3$) 140.6 (***C***-1'), 140.3 (***C***-1), 131.8 (Ar***C***), 129.6 (Ar***C***), 128.8

(Ar***C***), 128.4 (Ar***C***), 127.8 (Ar***C***), 122.3 (***C***-4), 63.6 (Ar_2***C***H); *m/z* (GC-MS, EI) 280 (M(^{79}Br)(^{35}Cl)$^+$), 282 (M(^{79}Br)(^{35}Cl)$^+$) and (M (^{81}Br)(^{37}Cl)$^+$), 284 (M(^{81}Br)(^{37}Cl)$^+$).

(2*R*)-1-[(benzyloxy)carbonyl]pyrrolidine-2-carboxylic acid[247] **(*R*)-105**

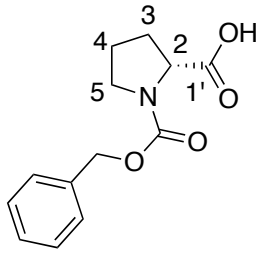

2M $NaOH_{(aq)}$ (65 mL, 130 mmol) was added to a three-neck round-bottom flask and cooled with an ice-salt bath. (*D*)-proline (15.0 g, 130 mmol) was added, followed by CbzCl (22 mL, 156 mmol) dropwise and 4M $NaOH_{(aq)}$ (46 mL, 182 mmol) over 20 min with vigorous stirring. The solution was slowly warmed to rt and left to stir overnight. The mixture was then washed with Et_2O and the aqueous solution was acidified to pH 2 by a dropwise addition of 3M $HCl_{(aq)}$. The resulting mixture was extracted with EtOAc (3 x 50 mL) and the extracts were combined and dried over $MgSO_4$. The volatiles were removed under reduced pressure to afford the title compound as a colourless oil (27.3 g, 84%) which was used without further purification.

$[\alpha]_D$ (c = 1.00 g/100 mL, $CHCl_3$) +84.3° (lit.:[248] $[\alpha]_D$ (c = 1.00 g/100 mL, $CHCl_3$) +69.7 °). ν_{max} (ATR) 2982 (w), 2884 (w), 1704 (s), 1662 (s), 1415 (s), 1357 (s), 1240 (m), 1168 (s), 1120 (s), 1089 (m) cm^{-1}; δ_H (700 MHz, $CDCl_3$, mixture of rotamers) 7.38 – 7.27 (5H, m, Ar***H***), 5.22 – 5.12 (2H, m, ArC***H₂***), 4.45 – 4.40 (0.6H, m, 2-***H***), 4.39 – 4.36 (0.4H, m, 2-***H***), 3.66 – 3.56 (1H, m, 5-***H***H'), 3.55 – 3.50 (0.4H, m, 5-H***H'***), 3.50 – 3.44 (0.6H, m, 5-H***H'***), 2.32 – 2.23 (1H, m, 3-***H***H'), 2.22 – 2.14 (1H, m, 3-H***H'***), 2.13 – 2.06 (1H, m, 4-***H***H'), 2.03 – 1.86 (1H, m, 4-H***H'***); δ_C (176 MHz, $CDCl_3$, mixture of rotamers) 178.1 (***C***-1'), 176.3 (***C***-1'), 156.0 (N***C***O_2), 154.6 (N***C***O_2), 136.6 (Ar***C***), 136.4 (Ar***C***), 128.6 (Ar***C***), 128.5 (Ar***C***), 128.3 (Ar***C***), 128.1 (Ar***C***), 128.0 (Ar***C***), 127.8 (Ar***C***), 67.7 (Ar***C***H_2), 67.3 (Ar*C*H_2), 59.4 (***C***-2), 58.8 (***C***-2), 47.1 (***C***-5), 46.8 (***C***-5), 31.0 (***C***-3), 29.4 (***C***-3), 24.4 (***C***-4), 23.6 (***C***-4); *m/z* (LC-MS, ESI^+) 250 (MH^+), 273 (MNa^+).

(2*S*)-1-[(benzyloxy)carbonyl]pyrrolidine-2-carboxylic acid[247] **(*S*)-105**

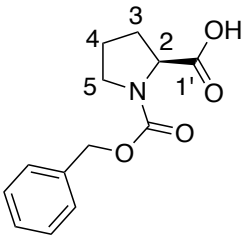

(*L*)-Proline (4.00g, 34.7 mmol) was reacted under the same conditions as the synthesis of **(*R*)-105**, furnishing the title compound as a colourless oil (8.46g, 98%).

$[\alpha]_D$ (c = 1.00 g/100 mL, $CHCl_3$) -71.4° (lit.:[248] $[\alpha]_D$ (c = 1.00 g/100 mL, $CHCl_3$) -69.7°). IR, NMR and mass spectra were consistent with the *R* enantiomer.

(2*R*)-1-(methoxycarbonyl)pyrrolidine-2-carboxylic acid[249] **(*R*)-165**

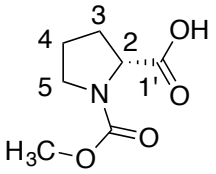

To a solution of (*D*)-proline (2.00 g, 17.36 mmol) in THF (26 mL) and saturated $NaHCO_{3(aq)}$ (26 mL), cooled to 0 °C, was added dropwise methyl chloroformate (2.6 mL, 34.72 mmol). The solution was allowed to warm to rt and then stirred overnight. The reaction mixture was then acidified with 2M HCl (20 mL) and extracted with CH_2Cl_2 (3 x 20 mL). The combined organic layers were dried over $MgSO_4$ and concentrated to afford the title compound (2.79g, 93%) as a colourless oil which was used without further purification.

ν_{max} (ATR) 2960 (w), 2886 (w), 1702 (s), 1662 (s), 1451 (s), 1386 (s), 1170 (s), 1125 (s), 1091 (m) cm^{-1}; δ_H (600 MHz, $CDCl_3$, mixture of rotamers) 9.15 (1H, s, O***H***), 4.41 – 4.37 (0.6H, m, 2-***H***), 4.34 – 4.29 (0.4H, m, *2-**H***), 3.74 (2H, s, C***H₃***), 3.69 (1H, s, C***H₃***), 3.62 – 3.56 (0.4H, m, 5-***H***H'), 3.55 – 3.47 (1H, m, 5-H***H'***), 3.45 – 3.38 (0.6H, m, 5-***H***H'), 2.32 – 2.22 (1H, m, 3-***H***H'), 2.21 – 2.14 (1H, m, 4-***HH'***), 2.13 – 2.06 (1H, m, 3-H***H'***), 2.02 – 1.88 (1H, m, 4-H***H'***); δ_C (151 MHz, $CDCl_3$, mixture of rotamers) 178.0 (***C***-1'), 176.3 (***C***-1'), 156.6 (N***C***O_2), 155.3 (N***C***O_2), 59.4 (***C***-2), 58.7 (***C***-2), 53.2 (***C***H_3), 52.9 (***C***H_3), 47.0 (***C***-5), 46.7 (***C***-5), 31.0 (***C***-3), 29.4 (***C***-3), 24.5 (***C***-4), 23.5 (***C***-4). *m/z* (LC-MS, ESI^+) 174 (MH^+), 196 (MNa^+).

Benzyl (2*R*)-2-(2-diazoacetyl)pyrrolidine-1-carboxylate[191] (*R*)-106

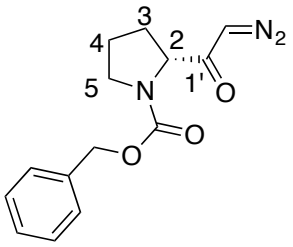

A solution of (2*R*)-1-[(benzyloxy)carbonyl]pyrrolidine-2-carboxylic acid **(*R*)-105** (1.05g, 4.01 mmol) in DCM (13 mL) was cooled to 0 °C and oxalyl chloride (0.46 mL, 5.41 mmol) was added dropwise, followed by DMF (7 drops). The mixture was stirred for 2 h at rt and then concentrated under reduced pressure before the addition of THF (16 mL) and MeCN (16 mL). After cooling the solution in an ice bath, NEt_3 (1.14 mL, 8.02 mmol) and $TMSCHN_2$ (2M solution in hexanes, 4.40 mL) were added and stirred for 4 h at rt. The reaction was then quenched with AcOH (1 mL), diluted with H_2O (31 mL) and concentrated under reduced pressure followed by the addition of EtOAc (30 mL) and washing with sat. $NaHCO_{3(aq)}$ (2 x 15 mL). The organic phase was then washed with brine (15 mL), dried over $MgSO_4$ and concentrated. Purification by column chromatography (0% → 80% EtOAC in hexanes) afforded the title compound (616 mg, 56%) as a yellow oil.

$[\alpha]_D$ (c = 1.00 g/100 mL, $CHCl_3$) +86.0° (lit.:[191] $[\alpha]_D$ (c = 1.00 g/100 mL, $CHCl_3$) +118.6°). ν_{max} (ATR) 3083 (w), 2955 (w), 2883 (w), 2102 (s), 1699 (s), 1645 (s), 1409 (s), 1351 (s), 1116 (s) cm^{-1}; δ_H (700 MHz, $CDCl_3$, mixture of rotamers) 7.41 – 7.27 (5H, m, Ar***H***), 5.48 (0.5H, s, C***H***N_2), 5.25 (0.5H, s, C***H***N_2), 5.21 - 5.04 (2H, m, ArC***H₂***), 4.35 (0.5H, s, 2-***H***), 4.28 (0.5H, s, 2-***H***), 3.60 – 3.45 (2H, m, 5-***H***$_2$), 2.23 – 2.15 (0.5H, m, 3-***H***H'), 2.13 – 2.01 (1.5H, m, 3-***H***H', 3-H***H'***,), 1.99 – 1.84 (2H, m, 4-C***H₂***); δ_C (176 MHz, $CDCl_3$, mixture of rotamers) 195.4 (***C***-1'), 194.5 (***C***-1'), 155.4 (N***C***O_2), 154.7 (N***C***O_2), 136.7 (Ar***C***), 136.5 (Ar***C***), 128.6(3) (Ar***C***), 128.5(9) (Ar***C***), 128.2(3) (Ar***C***), 128.1(7) (Ar***C***), 128.0(6) (Ar***C***), 67.4 (Ar***C***H_2), 64.2 (***C***-2), 53.5 (***C***HN_2), 52.8 (***C***HN_2), 47.5 (***C***-5), 47.1 (***C***-5), 31.4 (***C***-3), 29.8 (***C***-3), 24.5 (***C***-4), 23.7 (***C***-4); *m/z* (LC-MS, ESI^+) 246 ($M - N_2 + H^+$), 296 (MNa^+).

Benzyl (2*S*)-2-(2-diazoacetyl)pyrrolidine-1-carboxylate[202] (*S*)-106

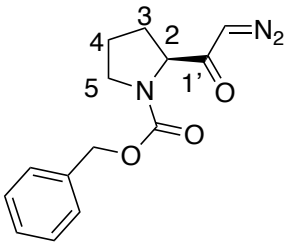

(2*S*)-1-[(benzyloxy)carbonyl]pyrrolidine-2-carboxylic acid (*S*)-105 was reacted under the same conditions as the synthesis of benzyl (2*R*)-2-(2-diazoacetyl)pyrrolidine-1-carboxylate (*R*)-106.

$[\alpha]_D$ (c = 1.00 g/100 mL, $CHCl_3$) -103.1 ° (lit.:[191] $[\alpha]_D$ (c = 1.00 g/100 mL, $CHCl_3$) = -135.8°). NMR and mass spectra were consistent with the *R* enantiomer.

Methyl (2*R*)-2-(2-diazoacetyl)pyrrolidine-1-carboxylate (*R*)-166

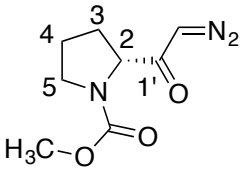

(2*R*)-1-(methoxycarbonyl)pyrrolidine-2-carboxylic acid **(*R*)-165** (1.20 g, 6.93 mmol) was reacted under the same conditions as the synthesis of benzyl (2*R*)-2-(2-diazoacetyl)pyrrolidine-1-carboxylate **(*R*)-106**, to afford the title compound (515 mg, 38%) as a yellow oil.

ν_{max} (ATR) 3083 (w), 2957 (w), 2883 (w), 2101 (s), 1697 (s), 1640 (s), 1447 (s), 1373 (s), 1119 (s) cm^{-1}; δ_H (700 MHz, $CDCl_3$, mixture of rotamers) 5.49 (0.5H, s C***H***N_2), 5.38 (0.5H, s, C***H***N_2), 4.31 (0.5H, s, 2-***H***), 4.23 (0.5H, s, 2-***H***), 3.70 (1.5H, s, C***H*****$_3$**), 3.67 (1.5H, s, C***H***$_3$), 3.58 – 3.46 (1.5H, m, 5-***H***H'***,*** 5-H***H'***), 3.45 – 3.39 (0.5H, m, 5-H***H'***), 2.22 - 2.10 (2H, m, 3-***H*****$_2$**), 1.94 – 1.84 (2H, m, 4-C***H*****$_2$**); δ_C (176 MHz, $CDCl_3$, mixture of rotamers) 195.5 (***C***-1'), 194.6 (***C***-1'), 156.0 (N***C***O_2Me), 155.5 (N***C***O_2 Me), 64.3 (***C***-2), 64.1 (***C***-2), 53.4 (***C***HN_2), 52.9 (***C***H_3), 52.8 (***C***H_3), 47.5 (***C***-5), 47.0 (***C***-5), 31.4 (***C***-3), 29.8 (***C***-3), 24.5 (***C***-4), 23.7 (***C***-4); *m/z* (LC-MS, ESI^+) 170 ($M - N_2 + H^+$). Accurate mass: Found MNa^+, 220.0715: $C_8H_{11}N_3O_3$ requires *M,* 220.0698.

Benzyl (2*R*)-2-(2-methoxy-2-oxoethyl)pyrrolidine-1-carboxylate[191] **(*R*)-107**

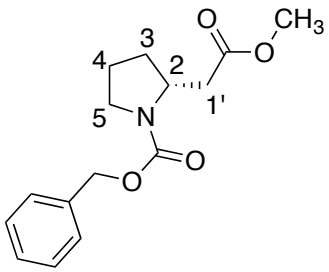

Benzyl (2*R*)-2-(2-diazoacetyl)pyrrolidine-1-carboxylate **(*R*)-106** (2.88 g, 10.50 mmol) in dry MeOH (34 mL) was treated dropwise with a solution of silver benzoate (243 mg, 1.06 mmol) in NEt_3 (4.40 mL, 31.50 mmol). The reaction mixture was stirred at rt for 3 h before being cooled in an ice bath and quenched with $Na_2S_2O_{5(aq.)}$ (20%, 33 mL). The reaction mixture was filtered through Celite and washed with EtOAc (3 x 30 mL) and the organic filtrate washed with brine (60 mL) and dried over $MgSO_4$. The solvent was removed under reduced pressure and purified by flash column chromatography (0% → 80% EtOAC in hexanes) to afford the title compound (2.32 g, 80%) as a colourless oil.

$[\alpha]_D$ (c = 1.00 g/100 mL, $CHCl_3$) +23.4° (lit.:[191] $[\alpha]_D$ (c = 1.00 g/100 mL, $CHCl_3$) +27.2°). ν_{max} (ATR) 2953 (w), 2881 (w), 1734 (m), 1697 (s), 1409 (s), 1357 (m), 1167 (m), 1095 (m) cm^{-1}. δ_H (700 MHz, $CDCl_3$, mixture of rotamers) 7.38 – 7.32 (4H, m, Ar***H***), 7.31 – 7.27 (1H, m, ArH), 5.16 – 5.09 (2H, m, ArC***H₂***), 4.27 – 4.20 (1H, m, 2-***H***), 3.64 (3H, s, C***H₃***), 3.48 – 3.38 (2H, m, 5-***H₂***), 3.05 – 2.90 (0.6H, m, 1'-***H***H' rotamer A), 2.86 – 2.73 (0.4H, m, 1'-***H***H' rotamer B), 2.38 – 2.31 (1H, m, 1-H***H'***), 2.12 – 2.03 (1H, m, 3-***H***H'), 1.93 – 1.80 (2H, m, 4-***H₂***), 1.80 – 1.72 (1H, m, 3-H***H'***). δ_C (176 MHz, $CDCl_3$, mixture of rotamers) 171.9 (***C***O_2CH_3), 154.8 (N***C***O_2), 137.0 (Ar***C***), 128.5 (Ar***C***), 128.0 (Ar***C***), 127.9 (Ar***C***), 66.8 (Ar***C***H_2), 54.7 (***C***-2), 54.1 (**C**-2), 51.7 (CO_2***C***H_3), 46.8 (***C***-5), 46.6 (***C***-5), 39.2 (***C***-1'), 38.3 (***C***-1'), 31.5 (***C***-3), 30.7 (***C***-3), 23.6 (***C***-4), 22.9 (***C***-4); *m/z* (LC-MS, ESI^+) 300 (MNa^+).

Benzyl (2*R*)-2-(2-methoxy-2-oxoethyl)pyrrolidine-1-carboxylate[202] (*S*)-107

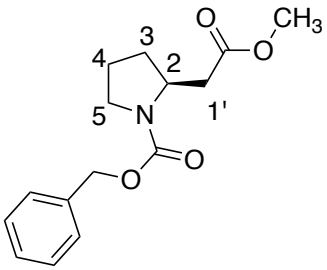

benzyl (2*S*)-2-(2-diazoacetyl)pyrrolidine-1-carboxylate **(*S*)-106** was reacted under the same conditions as the synthesis of benzyl (2*S*)-2-(2-methoxy-2-oxoethyl)pyrrolidine-1-carboxylate **(*R*)-107**.

$[\alpha]_D$ (c = 1.00 g/100 mL, $CHCl_3$) -53.2° (lit.:[202] $[\alpha]_D$ (c = 1.02 g/100 mL, $CHCl_3$) -42.7°). NMR and mass spectra were consistent with the *R* enantiomer.

Methyl (2*R*)-2-(2-methoxy-2-oxoethyl)pyrrolidine-1-carboxylate[249] (*R*)-167

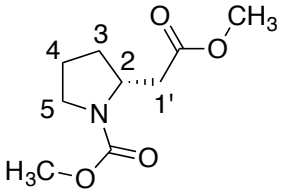

The conditions for the rearrangement of benzyl (2*R*)-2-(2-diazoacetyl)pyrrolidine-1-carboxylate **(*R*)-106** were applied to methyl (2*R*)-2-(2-diazoacetyl)pyrrolidine-1-carboxylate **(*R*)-166** (515 mg, 2.61 mmol) to afford the title compound (334 mg, 64%) as a yellow oil.

ν_{max} (ATR) 2956 (w), 2882 (w), 1734 (m), 1695 (s), 1449 (s), 1383 (s), 1194 (m), 1121 (m) cm^{-1}; δ_H (700 MHz, $CDCl_3$, mixture of rotamers) 4.22 – 4.11 (1H, m, 2-***H***), 3.71 – 3.61 (6H, m, 2 x $CO_2C\boldsymbol{H_3}$), 3.44 – 3.32 (2H, m, 5-$\boldsymbol{H_2}$), 2.98 – 2.90 (0.5H, m, 1'-***H***H' rotamer A), 2.78 – 2.71 (0.5H, m, 1'-***H***H' rotamer B), 2.35 – 2.26 (1H, m, 1'-H***H'***), 2.09 – 2.01 (1H, m, 3-***H***H'), 1.88 – 1.78 (2H, m, 4-$\boldsymbol{H_2}$), 1.77 – 1.69 (1H, m, 3-H***H'***); δ_C (176 MHz, $CDCl_3$, mixture of rotamers) 172.0 (***C***O_2CH_3), 171.9 (***C***O_2CH_3), 155.5 (N***C***O_2), 54.6 (***C***-2), 54.0 (***C***-2), 52.5 ($CO_2\boldsymbol{C}H_3$), 52.30 ($CO_2\boldsymbol{C}H_3$), 51.7 ($CO_2\boldsymbol{C}H_3$), 46.8 (***C***-5), 46.5 (***C***-5), 39.2 (***C***-1'), 38.3 (***C***-1'), 31.5 (***C***-3), 30.7 (***C***-3), 23.7 (***C***-4), 22.8 (***C***-4); *m/z* (LC-MS, ESI^+) 224 (MNa^+).

2-[(2*R*)-N-methylpyrrolidin-2'-yl]ethan-1'-ol[191] **(*R*)-108**

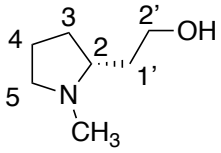

Procedure 1: To a solution of benzyl (2*R*)-2-(2-methoxy-2-oxoethyl)pyrrolidine-1-carboxylate **(*R*)-107** (349 mg, 1.74 mmol) in THF (6.0 mL) at 0 °C was slowly added $LiAlH_4$ (2.4M solution in THF, 2.2 mL, 5.23 mmol). This was allowed to warm to rt and left to stir for 3 h. The reaction mixture was then cooled in an ice bath and any reactive salts were quenched according to Fieser's method (general procedure B). Crude product was purified by column chromatography (0% → 10 % MeOH in $CHCl_3$ with 1% NEt_3) to afford the title compound (118 mg, 52%) as a colourless oil.

Procedure 2: The reduction was carried out using methyl (2*R*)-2-(2-methoxy-2-oxoethyl)pyrrolidine-1-carboxylate **(*R*)-167** (289 mg, 1.44 mmol) following the conditions for the reduction of Benzyl (2*R*)-2-(2-methoxy-2-oxoethyl)pyrrolidine-1-carboxylate **(*R*)-107** to afford the title compound (97 mg, 52%) as a colourless oil which was used without any further purification.

ν_{max} (ATR) 3314 (br), 2942 (w), 2872 (w), 2787 (w), 1667 (w), 1455 (m), 1371 (w), 1215 (w), 1057 (m), 1020 (m) cm^{-1}; δ_H (700 MHz, $CDCl_3$) 5.28 (1H, s, O***H***), 3.92 (1H, td, *J* = 10.5, 3.0 Hz, 2'-***H***H'), 3.68 – 3.56 (1H, m, 2'-H***H'***), 3.10 – 2.97 (1H, m, 5-***H***H'), 2.58 – 2.50 (1H, m, 2-***H***), 2.33 (3H, s, NC***H₃***), 2.19 – 2.09 (1H, m, 5'-H***H'***), 1.98 – 1.84 (2H, m, 3-***H***H', 1'-***H***H'), 1.82 – 1.67 (3H, m, 3'-H***H',*** 4-***H₂***), 1.52 – 1.47 (1H, m, 1'-H***H'***); δ_C (151 MHz, $CDCl_3$) 65.2 (***C***-2), 60.2 (***C***-2'), 57.0 (***C***-5), 40.9 (N***C***H_3), 31.7 (***C***-1'), 28.5 (***C***-3), 23.1 (***C***-4); *m/z* (LC-MS, ESI^+) 130 (MH^+).

Benzyl (2*R*)-2-(2'-hydroxyethyl)pyrrolidine-1-carboxylate (*R*)-133

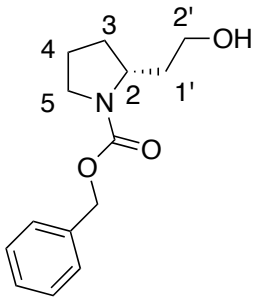

Benzyl (2*R*)-2-(2-methoxy-2-oxoethyl)pyrrolidine-1-carboxylate **(*R*)-107** (100 mg, 0.36 mmol) was dissolved in anhydrous THF (1.80 mL) and cooled to 0 °C. $LiBH_4$ (27 mg) was added and the reaction mixture was stirred for 2 h at 60 °C. It was then diluted with H_2O (5 mL) and extracted with EtOAc (2 x 5 mL). The combined organic layers were dried over Na_2SO_4 and the solvent was evaporated *in vacuo*. The crude product was purified by flash column chromatography (0% → 80% EtOAC in hexanes) to afford the title compound (52 mg, 58%) as a colourless oil.

$[\alpha]_D$ (c = 1.00 g/100 mL, $CHCl_3$) +4.7° (lit.:[250] $[\alpha]_D$ (c = 1.0 g/100 mL, $CHCl_3$) +7.2°). ν_{max} (ATR) 3440 (br), 2971 (m), 1700 (s), 1414 (s), 1359 (s), 1217 (m), 1103 (m) cm^{-1}; δ_H (600 MHz, $CDCl_3$) 7.39 - 7.35 (4H, m, Ar***H***), 7.34 – 7.30 (1H, m, Ar***H***), 5.16 – 5.13 (2H, m, ArC***H₂***), 4.27 – 4.18 (1H, m, 2-***H***), 3.66 – 3.53 (2H, m, 2'-***H₂***), 3.48 – 3.36 (2H, m, 5-***H₂***), 2.06 – 1.95 (1H, m, 3-***H***H'), 1.94 – 1.85 (2H, m, 4-***H₂***), 1.76 – 1.68 (1H, m, 1'-***H***H'), 1.67 – 1.62 (1H, m, 3-H***H'***), 1.55 – 1.47 (1H, m, 1'-H***H'***); δ_C (151 MHz, $CDCl_3$) 156.9 (***C***O), 136.8 (Ar***C***), 128.6 (Ar***C***), 128.2 (Ar***C***), 127.9 (Ar***C***), 67.2 (Ar***C***H_2), 59.2 (***C***-2'), 54.5 (***C***-2), 46.5 (***C***-5), 38.4 (***C***-1'), 31.3 (***C***-3), 23.7 (***C***-4); *m/z* (LC-MS, ESI^+) 250 (MH^+).

Benzyl (2*S*)-2-(2'-hydroxyethyl)pyrrolidine-1-carboxylate (*S*)-133

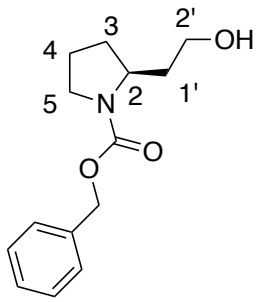

Benzyl (2*S*)-2-(2-methoxy-2-oxoethyl)pyrrolidine-1-carboxylate **(*S*)-107** (200 mg, 0.72 mmol) was reacted under the same conditions as the synthesis of benzyl (2*R*)-2-(2'-

hydroxyethyl)pyrrolidine-1-carboxylate **(*R*)-133** to afford the title compound (110 mg, 61%) as a colourless oil.

$[\alpha]_D$ (c = 1.00 g/100 mL, $CHCl_3$) -2.3 ° (lit.: $[\alpha]_D$ (c = 1.10 g/100 mL, $CHCl_3$) -7.6°). NMR and mass spectra were consistent with the *R* enantiomer.

1'-Bromo-4'-[phenyl(3-phenylpropoxy)methyl]benzene[230] 127

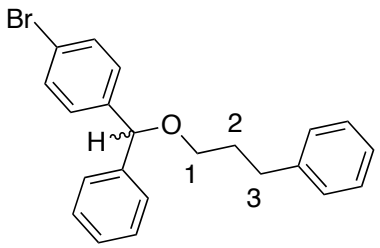

General procedure C was used in the reaction of 3-phenyl-1-propanol **126** (0.14 mL, 0.77 mmol) and (4-bromophenyl)(phenyl)methanol **122** (200 mg, 0.77 mmol). The crude product was purified by column chromatography (0% → 30% EtOAC in hexanes) to afford the title compound (293 mg, 95%) as a colourless oil.

ν_{max} (ATR) 3062 (w), 3026 (w), 2941 (w), 2859 (w), 1602 (w), 1495 (w), 1485 (m), 1453 (w), 1396 (w), 1295 (w), 1183 (w), 1095 (m), 1070 (m), 1010 (m) cm^{-1}; δ_H (600 MHz, $CDCl_3$) 7.48 - 7.42 (2H, m, Ar***H***), 7.40 – 7.30 (4H, m, Ar***H***), 7.32 – 7.20 (5H, m, Ar***H***), 7.22 – 7.15 (3H, m, Ar***H***), 5.28 (1H, s, Ar_2C***H***), 3.52 – 3.42 (2H, m, 1-***H₂***), 2.79 – 2.72 (2H, m, 2-***H₂***), 2.02 – 1.93 (2H, m, 3-***H₂***); δ_C (151 MHz, $CDCl_3$) 142.1(0) (Ar***C***), 142.0(6) (Ar***C***), 141.8 (Ar***C***), 131.6 (Ar***C***), 128.8 (Ar***C***), 128.6 (Ar***C***), 128.4 (Ar***C***), 127.7 (Ar***C***), 127.5 (Ar***C***), 127.1 (Ar***C***), 125.9 (Ar***C***), 121.3 (Ar***C***), 83.0 (Ar_2***C***H), 68.3 (***C***-1), 32.5 (***C***-2), 31.4 (***C***-3); *m/z* (LC-MS, ESI^+) 383 ($M(^{81}Br)H^+$), 381 ($M(^{79}Br)H^+$).

Benzyl N-(3-hydroxypropyl)carbamate[251] 139

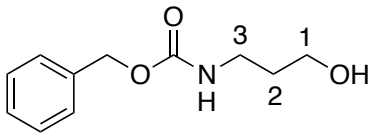

3-Aminopropanol (1.02 mL, 13.32 mmol) was dissolved in DCM (10 mL) and cooled to 0 °C. NEt_3 (0.91 mL, 6.50 mmol) and CbzCl (0.95 mL, 6.69 mmol) were added slowly and the solution then warmed to rt. The reaction mixture was stirred for 2 h and diethyl ether (10

mL) and H_2O (5 mL) were added and the product extracted with diethyl ether (3 x 5 mL). The combined organic extracts were then dried over Na_2SO_4, concentrated and the crude product purified by column chromatography (0%→ 80% EtOAC in hexanes) to afford the title compound (1.63 g, 61%) as a white solid.

M.p. 52 – 53 °C (lit.:[251] 51-52 °C); ν_{max} (ATR) 3324 (s), 3062 (w), 3039 (w), 2956 (w), 2886 (w), 1683 (s), 1530 (s), 1454 (m), 1326 (m), 1254 (s), 1243 (s), 1142 (m), 1061 (s), 1022 (s) cm^{-1}; δ_H (700 MHz, $CDCl_3$) 7.37-7.29 (5H, m, Ar***H***), 5.11 (2H, s, ArC***H***$_2$), 5.03 (1H, s, N***H***), 3.71 - 3.65 (2H, m, 1-***H*****$_2$**), 3.39 – 3.33 (2H, m, 3-***H*****$_2$**), 2.53 (1H, s, O***H***), 1.73 – 1.67 (2H, m, 2-***H*****$_2$**); δ_C (176 MHz, $CDCl_3$) 157.5 (***C***O), 136.6 (Ar***C***), 128.7 (Ar***C***), 128.3(3) (Ar***C***), 128.2(7) (Ar***C***), 67.0 (Ar***C***H_2), 59.7 (***C***-1), 37.9 (***C***-3), 32.8 (***C***-2); *m/z* (LC-MS, ESI^+) 232 (MNa^+).

Methyl N-(3-hydroxypropyl)carbamate[252] 131

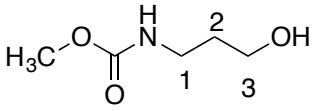

3-Aminopropanol (600 mg, 7.99 mmol) was dissolved in H_2O (4 mL) and a solution of K_2CO_3 (1.77 g, 12.78 mmol) in H_2O (4 mL) was added, followed by slow addition of methyl chloroformate (0.92 mL, 11.99 mmol) at 0 °C. Stirring was continued at 0 °C for 2 h. Then the reaction was extracted with CH_2Cl_2 (3 x 10 mL), the combined organic layers dried over Na_2SO_4 and concentrated *in vacuo* to afford the title compound (472 mg, 45%) as a colourless oil which was carried forward without purification.

ν_{max} (ATR) 3328 (br), 2948 (w), 1695 (s), 1533 (s), 1447 (w), 1261 (s), 1046 (s) cm^{-1} δ_H (600 MHz, $CDCl_3$) 5.25 (1H, s, N***H***), 3.66 - 3.61 (5H, m, C***H*****$_3$**, 3-***H*****$_2$**), 3.28 (2H, t, *J* = 6.0 Hz, 1-***H*****$_2$**), 3.11 (1H, s, O***H***), 1.67 (2H, p, *J* = 6.0 Hz, 2-***H*****$_2$**). δ_C (151 MHz, $CDCl_3$); 158.0 (***C***O), 59.7 (***C***-3), 52.3 (C***H*****$_3$**), 37.9 (***C***-1), 32.5 (***C***-2); *m/z* (LC-MS, ESI^+) 134 (MH^+), 116 (M - OH^+).

Benzyl N-(6-hydroxyhexyl)carbamate[253] 137

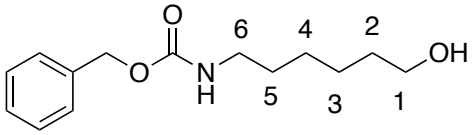

6-Aminopropanol (1.00 g, 8.53 mmol) was Cbz-protected under the same conditions as the synthesis of benzyl N-(3-hydroxypropyl)carbamate **139**, to afford the title compound (900 mg, 84%) as a white solid.

M.p. 82 – 83 °C (lit.:[253] 83 °C); ν_{max} (ATR) 3333 (m), 2941 (m), 2859 (w), 1685 (s), 1526 (s), 1453 (m), 1360 (m), 1288 (s), 1250 (s), 1218 (m), 1137 (m), 1110 (m), 1064 (m), 1036 (m), 1004 (s) cm^{-1}; δ_H (700 MHz, $CDCl_3$) 7.38 – 7.34 (4H, m, Ar***H***), 7.34 – 7.30 (1H, m, Ar***H***), 5.09 (2H, s, ArC***H₂***), 4.73 (1H, s, N***H***), 3.66 – 3.60 (2H, m, 1-***H***), 3.23 – 3.16 (2H, m, 6-***H***), 1.56 – 1.48 (4H, m, 2-***H₂***, 5-***H₂***), 1.42 – 1.28 (4H, m, 4-***H₂***, 3-***H₂***); δ_C (176 MHz, $CDCl_3$) 156.5 (***C***O), 136.8 (Ar***C***), 128.7 (Ar***C***), 128.2(8) (Ar***C***), 128.2(5) (Ar***C***), 66.8 (Ar***C***H_2), 62.9 (***C***-1), 41.1 (***C***-6), 32.7 (***C***-2), 30.1 (***C***-5), 26.5 (***C***-4), 25.4 (***C***-3); *m/z* (GC-MS, EI) 251 (M^+), 108 ($C_7H_8O^+$).

Methyl N-{3-[(4'-bromophenyl)(phenyl)methoxy]propyl}carbamate 132

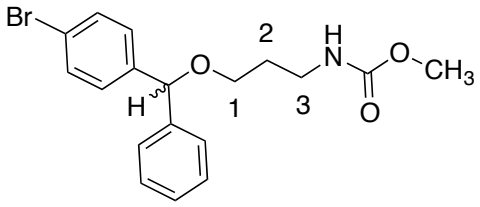

General procedure C was used in the reaction of protected methyl N-(3-hydroxypropyl)carbamate **131** (0.14 mL, 0.77 mmol) and (4-bromophenyl)(phenyl)methanol **122** (200 mg, 0.77 mmol). The crude product was purified by flash column chromatography (0% → 80% EtOAC in hexanes) to afford the title compound (65 mg, 24%) as a pale yellow oil.

ν_{max} (ATR) 3333 (w), 2951 (w), 1699 (s), 1521 (m), 1485 (m), 1449 (m), 1395 (w), 1260 (s), 1070 (s), 1010 (s) cm^{-1}; δ_H (600 MHz, $CDCl_3$) 7.45 – 7.41 (2H, m, Ar***H***), 7.34 – 7.23 (5H, m, Ar***H***), 7.21 – 7.17 (2H***,*** m, Ar***H***), 5.26 (1H, s, Ar_2C***H***), 4.94 (1H, s, N***H***), 3.63 (3H, s, C***H₃***), 3.49 (2H, t, *J* = 6.0 Hz, 1-***H***), 3.32 (2H, m, 3-***H***), 1.84 – 1.78 (2H, m, 2-***H***); δ_C (151 MHz, $CDCl_3$) 157.2

(***N***CO_2), 141.7 (Ar***C***), 141.4 (Ar***C***), 131.7 (Ar***C***), 128.7 (Ar***C***), 128.6 (Ar***C***), 127.9 (Ar***C***), 127.0 (Ar***C***), 121.5 (Ar***C***), 83.4 (Ar_2***C***H), 67.3 (***C***-1), 52.1 (***C***H_3), 39.2 (***C***-3), 29.9 (***C***-2); *m/z* (LC-MS, ESI^+) 402 ($M(^{81}Br)Na^+$), 400 ($M(^{79}Br)Na^+$). Accurate mass: Found MNa^+, 400.0523: $C_{18}H_{20}NO_3{}^{79}BrNa$ requires *M,* 400.0524.

Benzyl N-{6-[(4'-bromophenyl)(phenyl)methoxy]hexyl}carbamate 138

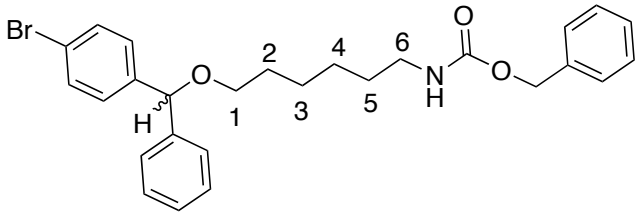

General procedure C was followed in the reaction of protected Benzyl N-(6-hydroxyhexyl)carbamate **137** (194 mg, 0.77 mmol) and (4-bromophenyl)(phenyl)methanol **122** (200 mg, 0.77 mmol). The crude product was purified by by flash column chromatography (0% → 50% EtOAC in hexanes) to afford the title compound (175 mg, 46%) as a colourless oil.

ν_{max} (ATR) 3338 (w), 2935 (w), 1699 (s), 1520 (m), 1485 (m), 1454 (m), 1249 (s), 1090 (m), 1070 (m), 1027 (m), 1010 (s) cm^{-1}; δ_H (700 MHz, $CDCl_3$) 7.45 – 7.41 (2H, m, Ar***H***), 7.37 – 7.34 (4H, m, Ar***H***), 7.33 – 7.29 (5H, m, Ar***H***), 7.27 - 7.23 (1H, m, Ar***H***), 7.23 – 7.20 (2H, m, Ar***H***), 5.27 (1H, s, Ar_2C***H***), 5.10 (2H, s, ArC***H_2***), 4.75 (1H, s, N***H***), 3.45 – 3.39 (2H, m, 1-***H_2***), 3.20 – 3.14 (2H, m, 6-***H_2***), 1.66 – 1.58 (2H, m, 5-***H_2***), 1.53 – 1.45 (2H, m, 2-***H_2***), 1.44 – 1.36 (2H, m, 4-***H_2***), 1.34 - 1.28 (2H, m, 3-***H_2***); δ_C (176 MHz, $CDCl_3$) 156.5 (***C***O), 142.1 (Ar***C***), 141.8 (Ar***C***), 136.8 (Ar***C***), 131.5 (Ar***C***), 128.7 (Ar***C***), 128.6(1) (Ar***C***), 128.5(6) (Ar***C***), 128.2(2) (Ar***C***), 128.1(8) (Ar***C***), 127.7 (Ar***C***), 127.0 (Ar***C***), 121.3 (Ar***C***), 83.1 (Ar_2***C***H), 69.2 (**C**-1), 66.7 (Ar***C***H_2), 41.1 (***C***-6), 30.0 (***C***-2), 29.8 (***C***-5), 26.7 (***C***-3), 26.0 (***C***-4); *m/z* (LC-MS, ESI^+) 520 ($M(^{81}Br)Na^+$), 518 ($M(^{79}Br)Na^+$); Accurate mass: Found MNa^+, 518.1311: $C_{27}H_{28}NO_3{}^{79}BrNa$ requires *M,* 518.1307.

Benzyl N-{3-[(4'-bromophenyl)(phenyl)methoxy]propyl}carbamate 140

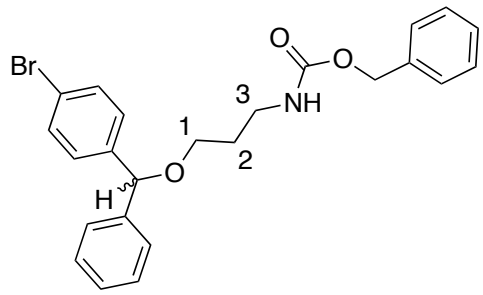

General procedure C was used with protected benzyl N-(3-hydroxypropyl)carbamate **139** (159 mg, 0.76 mmol) and (4-bromophenyl)(phenyl)methanol **122** (200 mg, 0.77 mmol) with the modification of AuCl (18 mg, 0.08 mmol) as the catalyst in the place of $PdCl_2$ with a reaction time of 20 h. The crude product was purified by flash column chromatography (0% → 40% EtOAc in hexanes) to afford the title compound (259 mg, 90%) as a colourless oil.

ν_{max} (ATR) 3334 (w), 2950 (w), 1699 (s), 1516 (m), 1485 (m), 1453 (m), 1395 (m), 1244 (s), 1070 (s), 1010 (s) cm^{-1}; δ_H (700 MHz, $CDCl_3$) 7.41 (2H, d, *J* = 8.0 Hz, Ar***H***), 7.38 – 7.27 (8H, m, Ar***H***), 7.26 – 7.23 (2H, m, Ar***H***), 7.19 (2H, d, *J* = 8.0 Hz, Ar***H***), 5.27 (1H, s, Ar_2C***H***), 5.09 (s, 2H, ArC***H₂***), 3.51 (2H, t, *J* = 6.0 Hz, 1-***H***), 3.39 - 3.31 (2H, m, 3-***H***), 1.84 (2H, p, *J* = 6.0 Hz, 2-***H***); δ_C (176 MHz, $CDCl_3$) 156.5 (***C***O), 141.7 (Ar**C**), 141.4 (Ar***C***), 136.8 (Ar***C***), 131.7 (Ar***C***), 128.7(2) **(**Ar***C*)**, 128.6(5) (Ar***C***), 128.6(2) (Ar***C***), 128.2(1) (Ar***C***), 128.1(8) (Ar***C***), 127.9 (Ar***C***), 127.0 (Ar***C***), 121.5 (Ar***C***), 83.5 (Ar_2***C***H), 67.5 (***C***-1), 66.7 (Ar***C***H_2), 39.4 (***C***-3), 29.8 (***C***-2); *m/z* (LC-MS, ESI^+) 478 ($M(^{81}Br)Na^+$), 476 ($M(^{79}Br)Na^+$); Accurate mass: Found MNa^+, 476.0855: $C_{27}H_{28}NO_3{}^{79}BrNa$ requires *M,* 476.0837.

Benzyl (2*R*)-2-{2'-[(4''-bromophenyl)(phenyl)methoxy]ethyl}pyrrolidine-1-carboxylate (*R*)-135

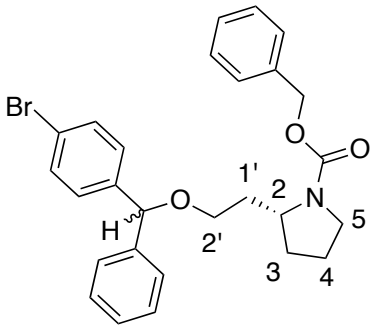

General procedure C was used with benzyl (2*R*)-2-(2'-hydroxyethyl)pyrrolidine-1-carboxylate **(*R*)-133** (80 mg, 0.32 mmol) and (4-bromophenyl)(phenyl)methanol **122** (84 mg, 0.32 mmol) with the modification of AuCl (8 mg, 0.03 mmol) as the catalyst in the place of $PdCl_2$ with a reaction time of 20 h. The crude product was then purified by flash column chromatography (0% → 20% EtOAc in hexanes) to afford the title compound (99 mg, 63%) as a colourless oil.

ν_{max} (ATR) 2872 (w), 1694 (s), 1484 (m), 1452 (w), 1408 (s), 1356 (m), 1183 (w), 1091 (s), 1070 (s), 1010 (s) cm^{-1}; δ_H (700 MHz, $CDCl_3$) 7.47 – 7.38 (2H, m, Ar***H***), 7.38 –7.13 (12H, m, Ar***H***), 5.36 – 5.18 (1H, m, Ar_2C***H***), 5.17 – 5.05 (2H, m, ArC***H₂***), 4.07 – 3.96 (1H, m, 2-***H***), 3.55 - 3.33 (4H, m, 2'-***H₂***, 5-***H***$_2$), 2.26 - 2.06 (1H, m, 1'-***H***H'), 1.99 – 1.90 (1H, m, 3-***H***H'), 1.90-1.80 (2H, m, 4-***H₂***), 1.79-1.72 (1H, m, 3-H***H'***), 1.70 - 1.56 (1H, m, 1'-H***H'***); δ_C (151 MHz, $CDCl_3$, mixture of diastereomers) 155.1 (***C***O), 142.0 (Ar***C***), 141.9 (Ar***C***), 141.7(6) (Ar***C***), 141.6(7) (Ar***C***), 137.2 (Ar***C***), 131.6 (Ar***C***), 131.5 (Ar***C***), 128.7 (Ar***C***), 128.5(9) (Ar***C***), 128.5(7) (Ar***C***), 128.0 (Ar***C***), 127.9 (Ar***C***), 127.8 (Ar***C***), 127.7 (Ar***C***), 127.0(2) (Ar***C***), 126.9(8) (Ar***C***), 121.3(4) (Ar***C***), 121.3(1) (Ar***C***), 83.1 (Ar_2***C***H), 83.0 (Ar_2***C***H), 66.7 (***C***-2'), 66.7 (Ar***C***H_2), 56.1 (***C***-2), 55.3 (***C***-2), 46.5 (***C***-5), 34.2 (***C***-1'), 30.8 (***C***-3), 23.3 (***C***-4); *m/z* (LC-MS, ESI^+) 516 (M(^{81}Br)Na^+), 518 (M(^{79}Br)Na^+); Accurate mass: Found MNa^+, 494.1319: $C_{27}H_{28}NO_3{}^{79}BrNa$ requires *M,* 494.1331.

(2*R*)-2-[2-(diphenylmethoxy)ethyl]-1-methylpyrrolidine[191] **(*R*)-141**

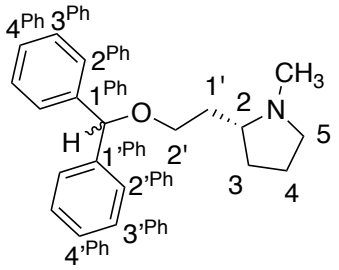

To a 0 °C solution of Benzyl (2R)-2-{2'-[(4''-bromophenyl)(phenyl)methoxy]ethyl}pyrrolidine-1-carboxylate **(*R*)-135** (256 mg, 0.52 mmol) in THF (6 mL) was slowly added $LiAlH_4$ (2.4M solution in THF, 0.54 mL, 1.30 mmol), before being heated under reflux for 16h. The reaction mixture was then cooled in an ice bath and any reactive salts were quenched according to Fieser's method (general procedure B). The crude product was purified by reversed phase column chromatography (5% → 100% MeCN in H_2O with 0.1% formic acid) to afford title compound (102 mg, 52%) as a yellow oil.

ν_{max} (ATR) 3028 (w), 2944 (w), 2869 (w), 2778 (w), 1697 (w), 1590 (w), 1485 (m), 1453 (m), 1346 (w), 1184 (w), 1091 (s), 1071 (s), 1010 (s) cm^{-1}; δ_H (600 MHz, $CDCl_3$) 7.34 - 7.29 (8H, m, Ar***H***), 7.27 – 7.23 (2H, m, Ar***H***), 5.32 (1H, m, Ar_2C***H***), 3.69 – 3.60 (2H, m, 2'-***H***H', 5-***H***H'), 3.53 – 3.46 (1H, m, 2'-H***H'***), 3.13 - 2.93 (1H, m, 2-***H***), 2.68 – 2.62 (4H, m, 5-H***H'***, NC***H₃***), 2.36 – 2.24 (1H, m, 1'-***H***H'), 2.18 – 1.99 (3H, m, 1'-H***H'***, 3-***H***H', 4-***H***H'), 1.96 – 1.76 (2H, m, 3-H***H'***, 4-H***H'***); δ_C (151 MHz, $CDCl_3$) 142.1 (***C***-1^{Ph}/$1'^{Ph}$), 142.0 (***C***-1^{Ph}/$1'^{Ph}$), 128.6 (***C***-4^{Ph}/$4'^{Ph}$), 127.8 (***C***-3^{Ph}/$3'^{Ph}$), 127.7 (***C***-3^{Ph}/$3'^{Ph}$), 127.0(3) (***C***-2^{Ph}/$2'^{Ph}$), 127.9(5) (***C***-2^{Ph}/$2'^{Ph}$), 84.1 (Ar_2***C***H), 66.3 (***C***-2), 65.9 (***C***-2'), 56.4 (***C***-5), 39.6 (N***C***H_3), 31.4 (***C***-1'), 30.1 (***C***-3), 21.8 (***C***-4); *m/z* (LC-MS, ESI^+) 296 (MH^+).

4-Chlorophenyl(phenyl)methanol[254] **113**

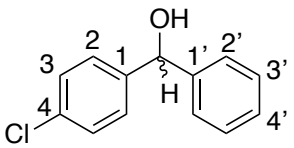

General procedure A was used with bromobenzene (2.6 mL, 24.8 mmol) and 4-chlorobenzaldehyde (3.5 mL, 19.10 mmol). The product was purified by column

chromatography (0% → 20% ether in hexanes) to afford the title compound (4.10g, 98%) as a white solid.

M.p. 59 – 60 °C (lit.:[254] 61 - 62 °C); ν_{max} (ATR) 3355 (br, m), 3065 (w), 3030 (w), 2981 (w), 1601 (w), 1486 (s), 1453 (m), 1402 (m), 1345 (w), 1319 (w), 1288 (w), 1273 (w), 1247 (w), 1192 (m), 1086 (m), 1034 (m), 1022 (s), 1011 (s) cm^{-1}. δ_H (700 MHz, $CDCl_3$) 7.36 – 7.26 (9H, m, Ar***H***), 5.81 (1H, s, Ar_2C***H***), 2.25 (1H, s, O***H***). δ_C (176 MHz, $CDCl_3$) 143.6 (Ar***C***), 142.3 (Ar***C***), 133.4 (Ar***C***), 128.8 (Ar***C***), 128.7 (Ar***C***), 128.0 (Ar***C***), 128.0 (Ar***C***), 126.7 (Ar***C***), 75.6 (Ar_2***C***). *m/z* (LC-MS, ESI^+) 218 ($M(^{35}Cl)H^+$), 220 ($M(^{37}Cl)H^+$).

Benzyl (2*R*)-2-{2-[(4-chlorophenyl)(phenyl)methoxy]ethyl}pyrrolidine-1-carboxylate (*R*)-168

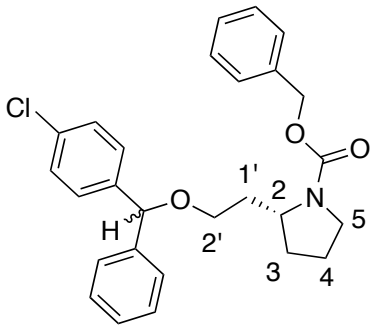

General Procedure C was followed using 4-chlorophenyl(phenyl)methanol **113** (311 mg, 1.42 mmol) and benzyl (2*R*)-2-(2'-hydroxyethyl)pyrrolidine-1-carboxylate **(*R*)-133** (353 mg, 1.42 mmol) with the modification of AuCl (33 mg, 0.14 mmol) as the catalyst in the place of $PdCl_2$ with a reaction time of 20 h. The crude product was purified by flash column chromatography (0 → 20 % EtOAc in hexanes) to afford title compound (514 mg, 80%).

ν_{max} (ATR) 2960 (w), 2874 (w), 1695 (s), 1489 (w), 1452 (w), 1409 (m), 1356 (m), 1335 (w), 1306 (w), 1260 (w), 1184 (w), 1090 (s), 1014 (m) cm^{-1}. δ_H (700 MHz, $CDCl_3$, mixture of diastereomers) 7.38 – 7.18 (14H, m, Ar***H***), 5.34 – 5.30 (0.5H, m, Ar_2C***H***), 5.22 - 5.18 (0.5H, m, Ar_2C***H***), 5.17 - 5.07 (2H, m, Ar***C*H₂**), 4.07 – 3.96 (1H, m, 2-***H***), 3.55 - 3.35 (4H, m, 2'-***H₂***, 5-***H₂***), 2.25 – 2.18 (0.5H, m, 1'-***H***H'), 2.16 – 2.08 (0.5H, m, 1'-***H***H'), 1.98 - 1.91 (1H, m, 3-***H***H'), 1.90 – 1.80 (2H, m, 4-***H₂***), 1.79 - 1.72 (1H, m, 3-H***H'***), 1.70 - 1.55 (1H, m, 1'-H***H'***); δ_C (176 MHz, $CDCl_3$, mixture of diastereomers) 155.1 (***C***O), 155.0 (***C***O), 142.1 (Ar***C***), 141.2 (Ar***C***), 137.2 (Ar***C***), 137.1 (Ar***C***), 133.1 (Ar***C***), 128.6(1) (Ar***C***), 128.5(8) (Ar***C***), 128.5(6) (Ar***C***), 128.4(1) (Ar***C***), 128.3(5) (Ar***C***), 128.3 (Ar***C***), 128.0 (Ar***C***), 127.9 (Ar***C***), 127.8 (Ar***C***), 127.7 (Ar***C***), 127.0

(Ar***C***), 126.9 (Ar***C***), 126.6(5) (Ar***C***), 83.0 (Ar_2***C***H), 66.8 (***C***-2'), 66.6 (Ar***C***H_2), 56.2 (***C***-2), 55.2 (***C***-2), 46.7 (***C***-5), 46.4 (***C***-5), 34.8 (***C***-1'), 34.1 (***C***-1'), 31.0 (***C***-3), 30.6 (***C***-3), 24.0 (***C***-4), 23.1 (***C***-4). *m/z* (LC-MS, ESI^+) 474 ($M(^{37}Cl)Na^+$), 472 ($M(^{35}Cl)Na^+$); Accurate mass: Found MH^+, 450.1826: $C_{27}H_{29}NO_3{}^{35}Cl$ requires *M,* 450.1836.

Benzyl (2*S*)-2-{2-[(4-chlorophenyl)(phenyl)methoxy]ethyl}pyrrolidine-1-carboxylate (*S*)-168

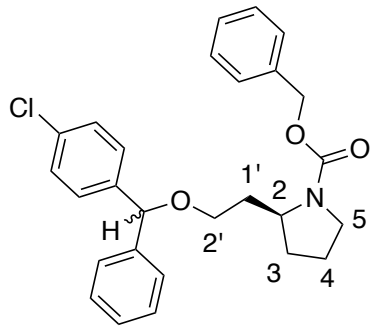

4-Chlorophenyl(phenyl)methanol **113** and benzyl (2*S*)-2-(2'-hydroxyethyl)pyrrolidine-1-carboxylate **(*S*)-133** were reacted together under the same conditions as the synthesis of benzyl (2*R*)-2-{2-[(4-chlorophenyl)(phenyl)methoxy]ethyl}pyrrolidine-1-carboxylate **(*R*)-168**.

ν_{max} (ATR) 3031 (w), 2954 (w), 2874 (w), 1695 (s), 1489 (m), 1452 (w), 1409 (s), 1357 (m), 1336 (m), 1185 (w), 1089 (s), 1029 (w), 1014 (m). δ_H (700 MHz, $CDCl_3$) 7.38 – 7.22 (14H, m, Ar***H***), 5.36 – 5.19 (1H, m, Ar_2C***H***), 5.17 – 5.06 (2H, m, Ar***C***H_2), 4.07 – 3.96 (1H, m, 2-***H***), 3.54 –3.35 (4H, m, 5-$\boldsymbol{H_2}$, 2'-$\boldsymbol{H_2}$), 2.27 – 2.07 (1H, m, 1'-***H***H'), 2.00 – 1.90 (1H, m, 3-***H***H'), 1.90 – 1.80 (2H, m, 4-$\boldsymbol{H_2}$), 1.80 – 1.72 (1H, m, 3-H***H'***), 1.71 – 1.57 (1H, m, 1'-H***H'***); δ_C (176 MHz, $CDCl_3$, mixture of diastereomers) 155.1 (***C***O), 142.1(0) (Ar***C***), 141.9(9) (Ar***C***), 141.2 (Ar***C***), 141.1 (Ar***C***), 137.2 (Ar***C***), 133.2 (Ar***C***), 133.1 (Ar***C***), 128.6(1) (Ar***C***), 128.5(8) (Ar***C***), 128.5(7) (Ar***C***), 128.3 (Ar***C***), 128.0 (Ar***C***), 127.9 (Ar***C***), 127.7(3) (Ar***C***), 127.6(9) (Ar***C***), 127.0(2) (Ar***C***), 126.9(7) (Ar***C***), 83.0(0) (Ar_2C***H***), 82.9(5) (Ar_2C***H***), 66.7 (***C***-2'), 66.7 (Ar***C***H_2), 56.2 (***C***-2), 55.2 (***C***-2), 46.5 (***C***-5), 34.7 (***C***-1'), 30.8 (***C***-3), 23.2 (***C***-4). *m/z* (LC-MS, ESI^+) 474 ($M(^{37}Cl)Na^+$), 472 ($M(^{35}Cl)Na^+$); Accurate mass: Found MH^+, 450.1816: $C_{27}H_{29}NO_3{}^{35}Cl$ requires *M,* 450.1836.

(2*R*)-2-{2-[(4-chlorophenyl)(phenyl)methoxy]ethyl}-1-methylpyrrolidine[191] **(*R*)-112**

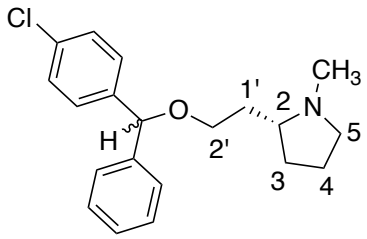

To a 0 °C solution of benzyl (2*R*)-2-{2-[(4-chlorophenyl)(phenyl)methoxy]ethyl}pyrrolidine-1-carboxylate **(*R*)-168** (305 mg, 0.68 mmol) in THF (8 mL) was slowly added $LiAlH_4$ (2.4M solution in THF, 0.7 mL, 1.70 mmol), before being heated to reflux for 16h. The reaction mixture was then cooled in an ice bath and any reactive salts were quenched according to Fieser's method (general procedure B). The crude product was purified by reversed phase column chromatography (5% → 100% MeCN in H_2O with 0.1% formic acid) to afford title compound (165 mg, 74%) as a yellow oil.

ν_{max} (ATR) 2955 (w), 1698 (s), 1599 (w), 1488 (w), 1453 (w), 1411 (m), 1357 (w), 1264 (w), 1100 (m), 1045 (w) cm^{-1}; δ_H (600 MHz, $CDCl_3$) 7.35 – 7.23 (9H, m, Ar***H***), 5.29 (1H, s, Ar_2C***H***), 3.55 – 3.49 (1H, m, 2'-***H***H'), 3.49 – 3.44 (1H, m, 2'-H***H'***), 3.18 – 3.08 (1H, m, 5-***H***H'), 2.34 (1.5H, s, NC$***H***_3$), 2.34 (1.5H, s, NC$***H***_3$), 2.31 – 2.24 (1H, m, 2-***H***), 2.23 – 2.17 (1H, m, 5-H***H'***), 2.14 – 2.07 (1H, m, 1'-***H***H'), 1.97 – 1.88 (1H, m, 3-***H***H'), 1.85 – 1.74 (1H, m, 4-***H***H'), 1.73 – 1.65 (1H, m, 4-H***H'***), 1.65 – 1.57 (1H, m, 1'-H***H'***), 1.56 – 1.46 (1H, m, 3-H***H'***); δ_C (151 MHz, $CDCl_3$, mixture of diastereomers) 142.1 (Ar***C***), 142.0 (Ar***C***), 141.1(9) (Ar***C***), 141.(6) (Ar***C***), 133.2(4) (Ar***C***), 133.2(1) (Ar***C***), 128.6(4) (Ar***C***), 128.6(3) (Ar***C***), 128.6(0) (Ar***C***), 128.4 (Ar***C***), 128.3 (Ar***C***), 127.8 (Ar***C***), 127.7 (Ar***C***), 127.0(2) (Ar***C***), 126.9(6) (Ar***C***), 83.2(4) (Ar_2***C***H), 83.2(2) (Ar_2***C***H), 67.1(1) (***C***-2'), 67.0(7) (***C***-2'), 64.2 (***C***-2), 57.2 (***C***-5), 40.5 (N***C***H_3), 33.8 (***C***-1'), 30.9(4) (***C***-3), 30.9(0) (***C***-3), 22.0(4) (***C***-4), 22.0(3) (***C***-4). *m/z* (LC-MS, ESI^+) 354 (M(^{37}Cl)Na^+), 352 (M(^{35}Cl)Na^+); Accurate mass: Found MH^+, 330.1627: $C_{20}H_{25}{}^{35}ClNO$ requires *M,* 330.1625.

(2*S*)-2-{2-[(4-chlorophenyl)(phenyl)methoxy]ethyl}-1-methylpyrrolidine[191] **(*S*)-112**

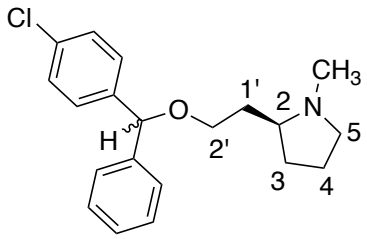

Benzyl (2*S*)-2-{2-[(4-chlorophenyl)(phenyl)methoxy]ethyl}pyrrolidine-1-carboxylate **(*S*)-168** was reduced under the same conditions as the synthesis of (2*R*)-2-{2-[(4-chlorophenyl)(phenyl)methoxy]ethyl}-1-methylpyrrolidine **(*R*)-112**.

ν_{max} (ATR) 2921 (w), 1489 (w), 1088 (w), 1014 (w). δ_H (700 MHz, $CDCl_3$) 7.35 – 7.23 (9H, m, Ar***H***), 5.29 (1H, s, Ar_2C***H***), 3.61 – 3.55 (1H, m, 2'-***H***H'), 3.51 – 3.44 (1H, m, 2'-H***H'***), 3.44 – 3.35 (1H, m, 5-***H***H'), 2.75 – 2.60 (1H, m, 2-***H***), 2.57 – 2.49 (3H, m, NC***H₃***), 2.48 – 2.39 (1H, m, 5-H***H'***), 2.26 – 2.17 (1H, m, 1-***H***H'), 2.10 – 1.91 (2H, m, 3-***H***H', 4-***H***H'), 1.90 – 1.76 (2H, m, 1'-H***H'***, 4-H***H'***), 1.74 – 1.62 (1H, m, 3-H***H'***). δ_C (176 MHz, $CDCl_3$, mixture of diastereomers) 141.8 (Ar***C***), 141.7 (Ar***C***), 140.9 (Ar***C***), 133.4(0) (Ar***C***), 133.3(6) (Ar***C***), 128.7(1) (Ar***C***), 128.6(9) (Ar***C***), 128.6(7) (Ar***C***), 128.3(4) (Ar***C***), 128.2(8) (Ar***C***), 127.9(4) (Ar***C***), 127.8(9) (Ar***C***), 127.0 (Ar***C***), 126.9 (Ar***C***), 83.4 (Ar_2***C***H), 83.3 (Ar_2***C***H), 66.5(3) (***C***-2'), 66.4(5) (***C***-2'), 65.3 (***C***-2), 56.7 (***C***-5), 40.0 (N***C***H_3), 32.4(7) (***C***-1'), 30.5(2) (***C***-1'), 30.4(3) (***C***-3), 21.9(2) (***C***-4), 21.8(9) (***C***-4). *m/z* (LC-MS, ESI^+) 332 ($M(^{37}Cl)H^+$), 330 ($M(^{35}Cl)H^+$); Accurate mass: Found MH^+, 330.1616: $C_{20}H_{25}{}^{35}ClNO$ requires *M,* 330.1625.

(3-methoxyphenyl)(phenyl)methanol[255] **169**

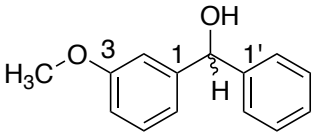

General procedure A was used with bromobenzene (3.01 mL, 28.64 mmol) and 3-methoxybenzaldehyde (2.70 mL, 22.03 mmol). The product was purified by flash column chromatography (0% → 30% ether in hexanes) to afford the title compound (2.99 g, 66%) as a yellow oil.

ν_{max} (ATR) 3404 (w), 1597 (m), 1585 (m), 1487 (m), 1453 (m), 1435 (m), 1314 (w), 1255 (s), 1186 (w), 1147 (m), 1021 (s) cm^{-1}. δ_H (700 MHz, $CDCl_3$) 7.40 - 7.37 (2H, m, Ar***H***), 7.36 - 7.33 (2H, m, Ar***H***), 7.30 – 7.24 (2H, m, Ar***H***), 6.98 – 6.95 (2H, m, Ar***H***), 6.83 – 6.80 (1H, m, Ar***H***), 5.79 (1H, s, Ar_2C***H***), 3.79 (3H, s, C***H***$_3$), 2.45 (1H, s, O***H***). δ_C (176 MHz, $CDCl_3$) 159.8 (***C***-3), 145.6 (***C***-1), 143.8 (***C***-1'), 129.6 (Ar***C***), 128.6 (Ar***C***), 127.7 (ArC), 126.6 (Ar***C***), 119.0 (Ar***C***), 113.1 (Ar***C***), 112.2 (Ar***C***), 76.2 (Ar_2***C***), 55.3 (***C***H_3). *m/z* (GC-MS, EI) 214 (M^+).

Benzyl (2*R*)-2-{2-[(3-methoxyphenyl)(phenyl)methoxy]ethyl}pyrrolidine-1-carboxylate (*R*)-170

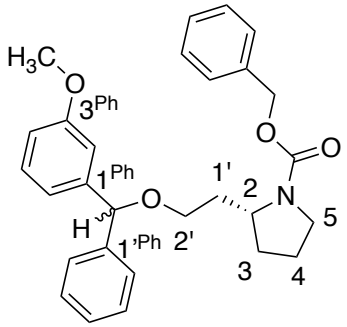

General Procedure C was used with (2*R*)-2-(2'-hydroxyethyl)pyrrolidine-1-carboxylate **(*R*)-133** (332 mg, 1.33 mmol) and (3-methoxyphenyl)(phenyl)methanol **169** (285 mg, 1.33 mmol) with the modification of AuCl (30 mg, 0.13 mmol) as the catalyst in the place of $PdCl_2$ with a reaction time of 20 h. The crude product was purified by flash column chromatography (0% → 20% EtOAc in hexanes) to afford the title compound (171 mg, 29%) as a yellow oil.

ν_{max} (ATR) 2955 (w), 1697 (w), 1598 (m), 1492 (m), 1452 (m), 1259 (m), 1152 (w), 1075 (w), 1040 (m) cm^{-1}. δ_H (700 MHz, $CDCl_3$) 7.40 – 7.28 (9H, m, Ar***H***), 7.25 - 7.20 (2H, m, Ar***H***), 6.97 -6.85 (2H, s, Ar***H***), 6.80 – 6.76 (1H, m, Ar***H***), 5.38 - 5.28 (0.5H, m, Ar_2C***H***), 5.27 - 5.19 (0.5H, m, Ar_2C***H***), 5.18 - 5.07 (2H, m, ArC***H***$_2$), 4.09 – 3.98 (1H, m, 2-***H***), 3.77 (3H, s, C***H$_3$***), 3.58 – 3.35 (4H, m, 2'-***H***$_2$, 5-***H$_2$***), 2.28 – 2.19 (0.5H, m, 1'-***H***H'), 2.18 – 2.08 (0.5H, m, 1'-***H***H'), 1.99 – 1.92 (1H, m, 4-***H***H'), 1.91 – 1.85 (1H, m, 3-***H***H'), 1.85 - 1.76 (2H, m, 4-H***H'***, 3-H***H'***), 1.72-1.56 (1H, m, 1'-H***H'***). δ_C (176 MHz, $CDCl_3$, mixture of diastereomers) 159.7(7) (***C***-3^{Ph}), 159.7(6) (***C***-3^{Ph}), 155.0 (***C***O), 144.2(4) (***C***-1^{Ph}), 144.1(5) (***C***-1^{Ph}), 142.5 (***C***-$1'^{Ph}$), 142.4 (***C***-$1'^{Ph}$), 137.2 (Ar***C***), 129.5 (Ar***C***), 129.4 (Ar***C***), 128.5 (Ar***C***), 128.4(4) (Ar***C***), 128.4(2) (Ar***C***), 127.9(1) (Ar***C***), 127.9(0) (Ar***C***), 127.4(8) (Ar***C***), 127.4(5), 126.9 (Ar***C***), 119.5 (Ar***C***), 112.8 (Ar***C***), 112.7 (Ar***C***), 83.6 (Ar_2***C***H), 66.6 (C-2'), 66.6 (***C***H_2Ar), 56.4 (***C***-2), 55.4 (***C***-2), 55.3 (***C***H_3), 46.6 (***C***-5), 46.4 (***C***-5), 34.8 (***C***-1'),

34.2 (***C***-1'), 31.0 (***C***-3), 30.7 (***C***-3), 23.9 (***C***-4), 23.1 (***C***-4). *m/z* (LC-MS, ESI^+) 468 (MNa^+); Accurate mass: Found MH^+, 446.2320: $C_{28}H_{32}NO_4$ requires *M,* 446.2331.

(2*R*)-2-{2-[(3-methoxyphenyl)(phenyl)methoxy]ethyl}-1-methylpyrrolidine (*R*)-144

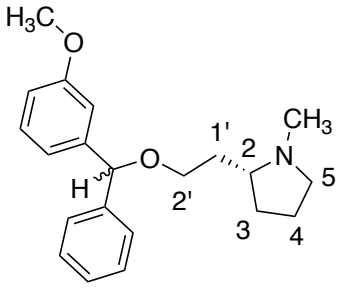

To a 0 °C solution of Benzyl (2*R*)-2-{2-[(3-methoxyphenyl)(phenyl)methoxy]ethyl}pyrrolidine-1-carboxylate **(*R*)-170** (143 mg, 0.32 mmol) in THF (4 mL) was slowly added $LiAlH_4$ (2.4M solution in THF, 0.33 mL, 0.80 mmol), before being heated to reflux for 16h. The reaction mixture was then cooled in an ice bath and any reactive salts were quenched according to Fieser's method (general procedure B). The crude product was purified by reversed phase column chromatography (5 → 100% MeCN in H_2O with 0.1% formic acid) to afford title compound (104 mg, 40%) as a colourless oil.

ν_{max} (ATR) 2946 (m), 1599 (m), 1488 (m), 1454 (m), 1265 (m), 1154 (w), 1095 (m), 1049 (m) cm^{-1}. δ_H (700 MHz, $CDCl_3$) 7.35 - 7.29 (4H, m, Ar***H***), 7.25 – 7.21 (2H, m, Ar***H***), 6.93 – 6.90 (2H, m, Ar***H***), 6.80 – 6.76 (1H, m, Ar***H***), 5.29 (1H, s, Ar_2C***H***), 3.78 (3H, s, OC***H₃***), 3.57 – 3.51 (1H, m, 2'-***H***H'), 3.51 – 3.45 (1H, m, 2'-H***H'***), 3.15 – 3.09 (1H, m, 5-***H***H'), 2.35 (3H, s, NC***H₃***), 2.32 – 2.24 (1H, m, 2-***H***), 2.22 – 2.16 (1H, m, 5-H***H'***), 2.15 – 2.09 (1H, m, 1'-***H***H'), 1.98 – 1.90 (1H, m, 3-***H***H'), 1.84 – 1.75 (1H, m, 4-***H***H'), 1.73 - 1.65 (1H, m, 4-H***H'***), 1.64 – 1.56 (1H, m, 1'-H***H'***), 1.55 – 1.46 (1H, m, 3-H***H'***). δ_C (176 MHz, $CDCl_3$, mixture of diastereomers) 159.8 (Ar***C***), 144.2(2) (Ar***C***), 144.2(0) (Ar***C***), 142.4(7) (Ar***C***), 142.4(3) (Ar***C***), 129.5 (Ar***C***), 128.5 (Ar***C***), 127.6 (Ar***C***), 127.5 (Ar***C***), 127.0(3) (Ar***C***), 126.9(8) (Ar***C***), 119.5(2) (Ar***C***), 119.4(7) (Ar***C***), 112.8(0) (Ar**C**), 112.7(6) (Ar**C**), 112.6(9) (Ar***C***), 112.6(5) (Ar***C***), 83.8 (Ar_2***C***H), 67.1 (***C***-2'), 64.2 (***C***-2), 57.2 (***C***-5), 55.3 (O***C***H_3), 40.5 (N***C***H_3), 33.9 (***C***-1'), 31.0 (***C***-3), 22.0 (***C***-4). *m/z* (LC-MS, ESI^+) 326 (MH^+). Accurate mass: Found MH^+, 326.2122: $C_{21}H_{28}NO_2$ requires *M,* 326.2120.

(4-Methoxyphenyl)(phenyl)methanol[256] **171**

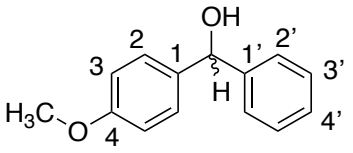

General procedure A was used with bromobenzene (2.60 mL, 24.80 mmol) and 4-methoxybenzaldehyde (2.32 mL, 19.10 mmol). The product was purified by flash column chromatography (0% → 80% ether in hexanes) to afford the title compound (1.73 g, 43%) as a white solid.

M.p. 63 – 64 °C (lit.:[256] 63 – 64 °C); ν_{max} (ATR) 3401 (br, w), 1610 (m), 1587 (w), 1510 (s), 1494 (s), 1445 (s), 1304 (w), 1249 (s), 1239 (s), 1172 (s), 1110 (w), 1031 (s), 1018 (s), 1008 (s) cm^{-1}. δ_H (700 MHz, $CDCl_3$) 7.40 - 7.36 (2H, m, Ar***H***), 7.36 - 7.32 (2H, m, Ar***H***), 7.32 – 7.26 (3H, m, Ar***H***), 6.89 – 6.86 (2H, m, Ar***H***), 5.83 – 5.80 (1H, m, Ar_2C***H***), 3.80 – 3.78 (3H, m, C***H***$_3$), 2.19 – 2.17 (1H, m, O***H***). δ_C (176 MHz, $CDCl_3$) 159.2 (Ar***C***), 144.2 (Ar***C***), 136.3 (Ar***C***), 128.6 (Ar***C***), 128.1 (Ar***C***), 127.6 (Ar***C***), 126.5 (Ar***C***), 114.0 (Ar***C***), 76.0 (Ar_2***C***), 55.4 (***C***H_3). *m/z* (GC-MS, EI) 214 (M^+).

Benzyl (2*R*)-2-{2-[(4-methoxyphenyl)(phenyl)methoxy]ethyl}pyrrolidine-1-carboxylate (*R*)-172

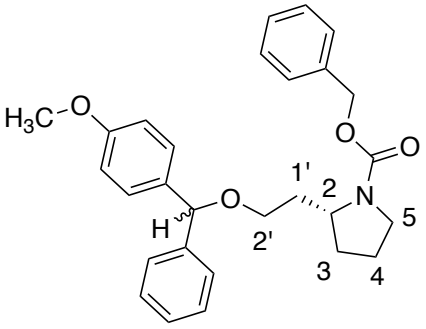

General Procedure C was used with (2*R*)-2-(2'-hydroxyethyl)pyrrolidine-1-carboxylate **(*R*)-133** (332 mg, 1.33 mmol) (257 mg, 1.03 mmol) and (4-methoxyphenyl)(phenyl)methanol **171** (221 mg, 1.03 mmol) with the modification of AuCl (30 mg, 0.13 mmol) as the catalyst in the place of $PdCl_2$ with a reaction time of 20 h. The product was purified by flash column chromatography (0 → 30% EtOAc in hexanes) to afford the title compound (205 mg, 45%).

ν_{max} (ATR) 2953 (w), 1698 (s), 1610 (w), 1510 (s), 1452 (w), 1412 (s), 1357 (m), 1303 (w), 1247 (s), 1173 (m), 1097 (s), 1032 (m). δ_H (700 MHz, $CDCl_3$, mixture of diastereomers) 7.40–

7.27 (10H, m, Ar***H***), 7.25 - 7.21 (1H, m, Ar***H***), 6.89 - 6.85 (1H, m, Ar***H***), 6.85 – 6.81 (2H, m, Ar***H***), 5.32 – 5.30 (0.5H, m, Ar_2C***H***), 5.23 – 5.19 (0.5H, m, Ar_2C***H***), 5.16 - 5.07 (2H, m, ArC***H***$_2$), 4.07 - 3.96 (1H, m, 2-***H***), 3.80–3.77 (3H, m, C***H₃***), 3.54–3.32 (4H, m, 2'-***H₂***, 5-***H₂***), 2.25 – 2.18 (0.5H, m, 1'-***H***H'), 2.15 - 2.08 (0.5H, m, 1'-***H***H'), 1.97– 1.90 (1H, m, 3-***H***H'), 1.90-1.74 (3H, m, 4-***H₂***, 3-H***H'***), 1.70 – 1.64 (1H, m, 1'-H***H'***). δ_C (176 MHz, $CDCl_3$, mixture of diastereomers) 159.2 (Ar***C***), 159.0 (Ar***C***), 144.2 (Ar***C***), 136.3 (Ar***C***), 128.6 (Ar***C***), 128.4(1) (Ar***C***), 128.3(6) (Ar***C***), 128.0 (Ar***C***), 127.9 (Ar***C***), 127.6 (Ar***C***), 127.3 (Ar***C***), 126.9(4) (Ar***C***), 126.8(6) (Ar***C***), 126.5 (Ar***C***), 114.0 (Ar***C***), 113.8(6) (Ar***C***), 113.8(5) (Ar***C***), 83.3 (Ar_2***C***H), 83.2 (Ar_2***C***H), 66.8 (***C***-2'), 66.6 (***C***H_2Ar), 56.4 (***C***-2), 55.4 (***C***H_3), 46.7 (***C***-5), 46.4 (***C***-5), 34.8 (***C***-1'), 34.1 (***C***-1'), 31.0 (***C***-3), 30.6 (***C***-3), 24.0 (***C***-4), 23.2 (***C***-4). *m/z* (LC-MS, ESI^+) 468 (MNa^+). Accurate mass: Found MNa^+, 468.2130: $C_{28}H_{31}NO_4Na$ requires *M,* 468.2151.

(2*R*)-2-{2-[(4-Methoxyphenyl)(phenyl)methoxy]ethyl}-1-methylpyrrolidine (*R*)-143

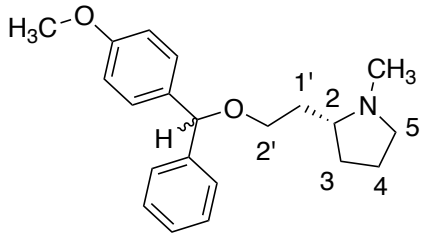

To a 0 °C solution of Benzyl (2*R*)-2-{2-[(4-methoxyphenyl)(phenyl)methoxy]ethyl}pyrrolidine-1-carboxylate **(*R*)-172** (148 mg, 0.33 mmol) in THF (4 mL) was slowly added $LiAlH_4$ (2.4M solution in THF, 0.35 mL, 0.83 mmol), before being heated to reflux for 16h. The reaction mixture was then cooled in an ice bath and any reactive salts were quenched according to Fieser's method (general procedure B). The crude product was purified by reversed phase column chromatography (5 → 100% MeCN in H_2O with 0.1% formic acid) to afford title compound (47 mg, 44%) as a colourless oil.

ν_{max} (ATR) 2961 (w), 1611(w), 1510 (m), 1453 (w), 1247 (m), 1172 (w), 1090 (m), 1031 (m) cm^{-1}. δ_H (700 MHz, $CDCl_3$) 7.32 - 7.12 (7H, m, Ar***H***), 6.83 – 6.77 (2H, m, Ar***H***), 5.23 (1H, s, Ar_2C***H***), 3.72 (3H, s, OC***H₃***), 3.55 – 3.49 (1H, m, 2'-***H***H'), 3.48 – 3.38 (2H, m, 2'-H***H'***, 5-***H***H'), 2.77 – 2.69 (1H, m, 2-***H***), 2.50 (3H, s, NC***H₃***), 2.47 – 2.40 (1H, m, 5-H***H'***), 2.21 – 2.12 (1H, m, 1'-***H***H'), 2.05 – 1.96 (1H, m, 3-***H***H'), 1.95 – 1.85 (1H, m, 4-***H***H'), 1.82 – 1.71 (2H, m, 1'-H***H'***, 4-H***H'***), 1.68 - 1.59 (1H, m, 3-H***H'***). δ_C (176 MHz, $CDCl_3$, mixture of diastereomers) 159.0(4)

(Ar***C***), 159.0(1) (Ar***C***), 142.5 (Ar***C***), 142.4 (Ar***C***), 134.3(4) (Ar***C***), 134.2(9) (Ar***C***), 128.4 (Ar***C***), 128.3 (Ar***C***), 128.2 (Ar***C***), 127.4(4) (Ar***C***), 127.3(9) (Ar***C***), 126.8 (Ar***C***), 126.7 (Ar***C***), 113.8 (Ar***C***), 83.5 (Ar_2***C***), 83.4 (Ar_2***C***), 66.1(0) (***C***-2'), 66.0(6) (***C***-2'), 65.0 (***C***-2), 56.0 (***C***-5), 55.3 (O***C***H_3), 39.5 (N***C***H_3), 31.8(4) (***C***-1'), 31.8(1) (***C***-1'), 30.2(3) (***C***-3), 30.2(0) (***C***-3), 21.7 (***C***-4). *m/z* (LC-MS, ESI^+) 326 (MH^+). Accurate mass: Found MH^+, 326.2129: $C_{21}H_{28}NO_2$ requires *M,* 326.2120.

(3-Chlorophenyl)(phenyl)methanol[257] **173**

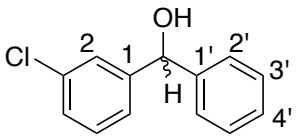

General procedure A was used with bromobenzene (3.01 mL, 28.64 mmol) and 3-chlorobenzaldehyde (2.15 mL, 19.10 mmol). The product was purified by flash column chromatography (0% → 30% ether in hexanes) to afford the title compound (700 mg, 17%) as a yellow oil.

ν_{max} (ATR) 3335 (br, m), 3064 (w), 1596 (m), 1575 (m), 1495 (m), 1475 (m), 1454 (m), 1429 (m), 1184 (m), 1021 (m) cm^{-1}. δ_H (700 MHz, $CDCl_3$) 7.41 – 7.22 (9H, m, Ar***H***), 5.76 (1H, s, Ar_2C***H***), 2.48 (1H, s, O***H***). δ_C (176 MHz, $CDCl_3$) 145.8 (Ar***C***), 143.3 (Ar***C***), 134.5 (Ar***C***), 129.8 (Ar***C***), 128.8 (Ar***C***), 128.0 (Ar***C***), 127.7 (Ar***C***), 126.7 (Ar***C***), 124.7 (Ar***C***), 75.8 (Ar_2***C***). *m/z* (LC-MS, ESI^+) 201 ($M(^{35}Cl)–OH^+$), 203 ($M(^{37}Cl)–OH^+$).

Benzyl (2*R*)-2-{2-[(3-chlorophenyl)(phenyl)methoxy]ethyl}pyrrolidine-1-carboxylate (R)-174

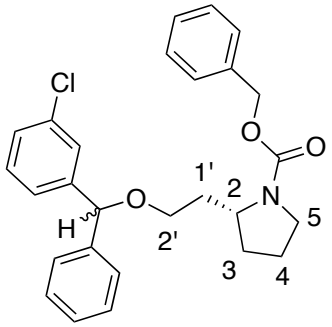

General Procedure C was used with (2*R*)-2-(2'-hydroxyethyl)pyrrolidine-1-carboxylate **(*R*)-133** (269 mg, 1.08 mmol) and compound (3-chlorophenyl)(phenyl)methanol **173** (237 mg, 1.08 mmol) with the modification of AuCl (25 mg, 0.11 mmol) as the catalyst in the place of $PdCl_2$ with a reaction time of 20 h. The crude product was purified by flash column

chromatography (0 → 30% EtOAc in hexanes) to afford the title compound as a colourless oil (172 mg, 38%).

ν_{max} (ATR) 2950 (w), 2875 (w), 1695 (s), 1595 (w), 1574 (w), 1495 (w), 1454 (w), 1411 (s), 1357 (m), 1335 (w), 1184 (w), 1100 (s), 1078 (s), 1029 (w) cm^{-1}. δ_H (700 MHz, $CDCl_3$, mixture of diastereomers) 7.42 -7.05 (14H, m, Ar***H***), 5.31 (0.5H, s, Ar_2C***H***), 5.21 – 5.17 (0.5H, m, Ar_2C***H***), 5.16 – 5.04 (2H, m, OC***H***$_2$), 4.09 – 3.94 (1***H***, m, 2***H***), 3.56 – 3.31 (4H, m, 2'-***H*****$_2$**, 5-***H*****$_2$**), 2.21 (0.5H, s, 1'-***H***H'), 2.12 (0.5H, s, 1'-***H***H'), 1.99 - 1.91 (1H, m, 3-***H***H'), 1.91 – 1.72 (3H, m, 4-***H*****$_2$**, 3-H***H'***), 1.71 - 1.64 (1H, m, 1'-H***H'***); δ_C (176 MHz, $CDCl_3$, mixture of diastereomers) 155.1 (***C***O), 155.0 (***C***O), 144.8 (Ar***C***), 141.9 (Ar***C***), 137.3 (Ar***C***), 137.1 (Ar***C***), 134.4(0) (Ar***C***), 134.3(7) (Ar***C***), 128.6(2) (Ar***C***), 128.6(0) (Ar***C***), 128.5(8) (Ar***C***), 128.0 (Ar***C***), 127.9 (Ar***C***), 127.8 (Ar***C***), 127.7 (Ar***C***), 127.6 (Ar***C***), 127.1 (Ar***C***), 127.0 (Ar***C***), 125.2 (Ar***C***), 125.0 (Ar***C***), 83.1 (Ar_2C***H***), 83.0 (Ar_2C***H***), 67.1 (***C***-2'), 66.9 (Ar***C***H_2), 66.7 (Ar***C***H_2), 66.6 (***C***-2'), 56.3 (***C***-2), 55.3 (***C***-2), 46.7 (***C***-5), 46.4 (***C***-5), 34.8 (***C***-1'), 34.2 (***C***-1'), 31.0 (***C***-3), 30.7 (***C***-3), 24.0 (***C***-4), 23.2 (***C***-4). *m/z* (LC-MS, ESI^+) 450 ($M(^{35}Cl)H^+$), 452 ($M(^{37}Cl)H^+$). Accurate mass: Found ($M(^{35}Cl)H^+$), 450.1853: $C_{27}H_{29}{}^{35}ClNO_3$ requires *M*, 450.1836.

(4-Fluorophenyl)(phenyl)methanol[258] 175

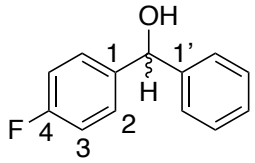

General procedure A was used with bromobenzene (2.60 mL, 24.80 mmol) and 4-fluorobenzaldehyde (2.05 mL, 19.10 mmol). The product was purified by flash column chromatography (0 → 20% EtOAc in hexanes) to afford the title compound (3.82 g, 99%) as a white solid.

M.p. 48– 49 °C (lit.:[259] 48 °C); ν_{max} (ATR) 3378 (br, m), 1602 (m), 1508 (s), 1494 (s), 1447 (m), 1419 (w), 1335 (w), 1270 (w), 1227 (s), 1173 (m), 1159 (m), 1097 (w), 1014 (s). δ_H (700 MHz, $CDCl_3$) 7.38 – 7.28 (7H, m, Ar***H***), 7.04 – 7.00 (2H, m, Ar***H***), 5.77 (1H, s, Ar_2C***H***), 2.64 (1H, s, O***H***). δ_C (176 MHz, $CDCl_3$) 162.2 (d, *J* = 245.5 Hz, ***C***-4), 143.7 (***C***-1'), 139.7 (d, *J* = 3.0 Hz, ***C***-1), 128.7 (Ar***C***), 128.3 (d, *J* = 8.0 Hz, ***C***-2), 127.8 (Ar***C***), 126.6 (Ar***C***), 115.4 (d, *J* = 21.5 Hz, ***C***-3), 75.6 (Ar_2***C***H). δ_F (376 MHz, $CDCl_3$) - 115.06 (s, 4-***F***). m/z (GC-MS, EI) 214 (M^+).

Benzyl (2*R*)-2-{2-[(4-fluorophenyl)(phenyl)methoxy]ethyl}pyrrolidine-1-carboxylate (*R*)-176

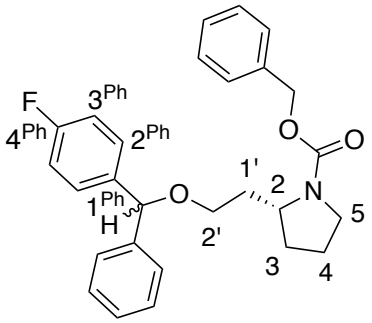

General Procedure C was used with (2*R*)-2-(2'-hydroxyethyl)pyrrolidine-1-carboxylate **(*R*)-133** (250 mg, 1.00 mmol) and (4-fluorophenyl)(phenyl)methanol **175** (202 mg, 1.00 mmol) with the modification of AuCl (24 mg, 0.1 mmol) as the catalyst in the place of $PdCl_2$ with a reaction time of 20 h. The crude product was purified by flash column chromatography (0 → 30% EtOAc in hexanes) to afford the title compound (305 mg, 70%) as a colourless oil.

ν_{max} (ATR) 3032 (w), 2954 (w), 2875 (w), 1694 (s), 1604 (w), 1507 (m), 1409 (s), 1356 (m), 1335 (m), 1220 (m), 1156 (w), 1089 (s), 1028 (w), 1014 (w). δ_H (700 MHz, $CDCl_3$, mixture of diastereomers) 7.38 – 7.20 (7H, m, Ar***H***), 7.02 – 6.94 (2H, m, 3^{Ph}-***H***), 5.36 – 5.31 (0.5H, m, Ar_2C***H***), 5.24 – 5.19 (0.5H, m, Ar_2C***H***), 5.18 – 5.06 (2H, m, OC***H₂***Ar), 4.08 – 3.96 (1H, m, 2-***H***), 3.55 – 3.33 (4H, m, 2'-***H₂***, 5-***H₂***), 2.26 – 2.17 (0.5H, m, 1'-***H***H'), 2.16 – 2.08 (0.5H, m, 1'-***H***H'), 2.00 – 1.90 (1H, m, 3-***H***H'), 1.90 - 1.79 (2H, m, 4-***H₂***), 1.79 – 1.72 (1H, m, 3-H***H'***), 1.71 – 1.56 (1H, m, 1' - H***H'***); δ_C (176 MHz, $CDCl_3$, mixture of diastereomers) 162.1(9) (***C***-4^{Ph}, d, *J* = 242.5 Hz), 162.1(7) (***C***-4^{Ph}, d, *J* = 242.5 Hz), 155.1 (***C***O), 142.4 (Ar***C***), 138.5 (Ar***C***), 137.2 (Ar***C***), 128.7 (***C***-2^{Ph}, d, J = 8.3 Hz), 128.6 (Ar***C***), 128.5(4) (Ar***C***), 128.5(3) (Ar***C***), 128.0 (Ar***C***), 127.9 (Ar***C***), 127.6 (Ar***C***), 127.0 (Ar***C***), 126.9 (Ar***C***), 115.2(8) (***C***-3^{Ph}, d, *J* = 21.5 Hz), 115.2(5) (***C***-3^{Ph}, d, *J* = 21.5 Hz), 83.0 (Ar_2***C***H), 66.8 (***C***-2'), 66.6 (Ar***C***H_2), 56.3 (***C***-2), 55.3 (***C***-2), 46.7 (***C***-5), 46.4 (***C***-5), 34.9 (***C***-1'), 34.2 (***C***-1'), 31.0 (***C***-3), 30.6 (***C***-3), 24.0 (***C***-4), 23.1 (***C***-4). δ_F (376 MHz, $CDCl_3$, mixture of rotamers) -115.10- -115.62 (m, 4-***F***). *m/z* (LC-MS, ESI^+) 456 (MNa^+), Accurate mass: Found (MNa^+), 456.1969: $C_{27}H_{28}NO_3NaF$ requires *M*, 456.1951.

(2*R*)-2-{2-[(4-fluorophenyl)(phenyl)methoxy]ethyl}-1-methylpyrrolidine (*R*)-142

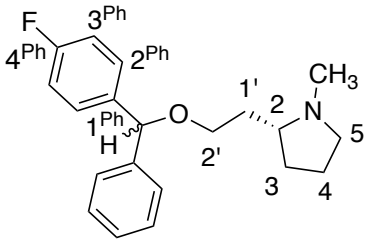

To a 0 °C solution of benzyl (2*R*)-2-{2-[(3-Fluorophenyl)(phenyl)methoxy]ethyl}pyrrolidine-1-carboxylate **(*R*)-176** (206 mg, 0.48 mmol) in THF (7 mL) was slowly added $LiAlH_4$ (2.4M solution in THF, 0.50 mL, 1.19 mmol), before being heated under reflux overnight. The reaction mixture was then cooled in an ice bath and any reactive salts were quenched according to Fieser's method (general procedure B). The crude product was purified by reversed phase column chromatography (5 → 100% MeCN in H_2O with 0.1% formic acid) to afford title compound (74 mg, 49%) as a yellow oil.

ν_{max} (ATR) 2942, 2870, 2777, 1604, 1508, 1454, 1348, 1294, 1221, 1184, 1156, 1090, 1029, 1016. δ_H (700 MHz, $CDCl_3$, mixture of diastereomers) 7.35 – 7.23 (7H, m, Ar***H***), 7.02 – 6.97 (2H, m, 3^{Ph}-***H₂***), 5.31 (1H, s, Ar_2C***H***), 3.55 – 3.49 (1H, m, 2'-***H***H'), 3.49 – 3.43 (1H, m, 2'-H***H'***), 3.14 – 3.08 (1H, m, 5-***H***H'), 2.34 (1.5H, s, NC***H₃***), 2.34 (1.5H, s, NC***H₃***), 2.29 – 2.21 (1H, m, 2-***H***), 2.21 – 2.15 (1H, m, 5-***H***H'), 2.14 – 2.06 (1H, m, 1'-***H***H'), 1.96 – 1.88 (1H, m, 3-***H***H'), 1.83 – 1.73 (1H, m, 4-***H***H'), 1.72 – 1.64 (1H, m, 4-H***H'***), 1.63 – 1.55 (1H, m, 1'-H***H'***), 1.53 – 1.44 (1H, m, 3-H***H'***). δ_C (176 MHz, $CDCl_3$, mixture of diastereomers) 162.2(1) (***C***-4^{Ph}, d, *J* = 245.3), 162.1(9) (***C***-4^{Ph}, d, *J* = 245.3 Hz), 142.4 (Ar***C***), 142.3 (Ar***C***), 138.4(5) (***C***-1^{Ph}, d, *J* = 3.0 Hz), 138.4(2) (***C***-1^{Ph}, d, *J* = 3.0 Hz), 128.7(0) (Ar***C***), 128.6(5) (Ar***C***), 128.5(9) (Ar***C***), 128.5(5) (Ar***C***), 127.7 (Ar***C***), 127.6 (Ar***C***), 127.0 (***C***-2^{Ph}, d, *J* = 9.0 Hz), 115.3(0) (***C***-3^{Ph}, d, *J* = 21.4 Hz), 115.2(9) (***C***-3^{Ph}, d, *J* = 21.4 Hz), 83.2 (Ar_2***C***H), 66.1(0) (***C***-2'), 66.0(8) (***C***-2'), 64.1(2) (***C***-2), 64.1(1) (***C***-2), 57.2 (***C***-5), 40.5 (***C***H_3), 33.9 (***C***-1'), 31.0 (***C***-3), 30.9 (***C***-3), 22.1 (***C***-4). δ_F (376 MHz, $CDCl_3$) -115.3(2) (s, 4-***F***, isomer 1), -115.3(8) (s, 4^{Ph}-***F***, isomer 2). *m/z* (LC-MS, ESI^+) 314 (MH^+). Accurate mass: Found (MH^+), 314.1909: $C_{20}H_{25}NOF$ requires *M*, 314.1920.

Bis(4-fluorophenyl)methanol[260] 177

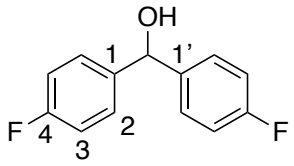

General procedure A was used and the product was purified by flash column chromatography (0% → 40% ether in hexanes) to afford the title compound (2.99g, 71%).

M.p. 46 - 47 °C (lit.:[261] 47 – 49 °C); ν_{max} (ATR) 3247 (br, m), 1603 (m), 1506 (s), 1416 (w), 1326 (w), 1299 (w), 1218 (s), 1182 (m), 1155 (m), 1023 (m), 1011 (m). δ_H (700 MHz, $CDCl_3$) 7.34 – 7.29 (4H, m, 2-***H***), 7.06 – 6.99 (4H, m, 3-***H***), 5.79 (1H, s, $Ar_2C\boldsymbol{H}$). δ_C (176 MHz, $CDCl_3$) 162.4 (***C***-4, d, *J* = 246.0 Hz), 139.5 (***C***-1, d, *J* = 3.0 Hz), 128.3 (***C***-2, d, *J* = 8.0 Hz), 115.5 (***C***-3, d, *J* = 21.5 Hz), 75.1 ($Ar_2\boldsymbol{C}H$). δ_F (376 MHz, $CDCl_3$) -114.70 (4-***F***). *m/z* (LC-MS, ESI^+) 203 ($M–OH^+$). Accurate mass: Found ($M–OH^+$), 203.0678: $C_{13}H_9F_2$ requires *M*, 203.0672.

Benzyl (2*R*)-2-{2-[bis(4-fluorophenyl)methoxy]ethyl}pyrrolidine-1-carboxylate (*R*)-178

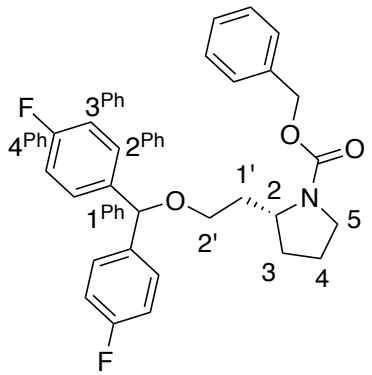

General Procedure C was used with (2*R*)-2-(2'-hydroxyethyl)pyrrolidine-1-carboxylate **(*R*)-133** (150 mg, 0.60 mmol) and bis(4-fluorophenyl)methanol **177** (132 mg, 0.60 mmol) with the modification of AuCl (14 mg, 0.05 mmol) as the catalyst in the place of $PdCl_2$ with a reaction time of 20 h. The crude product was purified by flash column chromatography (0 → 40% EtOAc in hexanes) to afford the title compound (210 mg, 77%) as a colourless oil.

ν_{max} (ATR) 2956 (w), 2876 (w), 1694 (s), 1603 (w), 1506 (s), 1410 (s), 1357 (m), 1335 (w), 1220 (s), 1182 (w), 1154 (m), 1088 (s), 1014 (w). δ_H (700 MHz, $CDCl_3$) 7.39 - 7.28 (5H, m, Ar***H***), 7.27 - 7.18 (5H, m, Ar***H***), 7.06 - 6.95 (3H, m, Ar***H***), 5.34 - 5.17 (1H, m, $Ar_2C\boldsymbol{H}$), 5.17 - 5.07 (2H, m, $ArC\boldsymbol{H_2}$), 4.04 - 3.97 (1H, m, 2-***H***), 3.53 - 3.41 (3H, m, 2'-$\boldsymbol{H_2}$, 5-H***H'***), 3.41-3.35 (1H, m, 5-H***H'***), 2.25 - 2.07 (1H, m, 1'-***H***H'), 1.98 - 1.78 (3H, m, 3-***H***H', 4-$\boldsymbol{H_2}$), 1.77 -1.71 (1H,

m, 3-H***H'***), 1.70 - 1.54 (1H, m, 1'-H***H'***). δ_C (176 MHz, $CDCl_3$, mixture of rotamers) 162.2(7) (***C***-4^{Ph}, d, *J* = 245.5 Hz), 162.2(5) (***C***-4^{Ph}, d, *J* = 245.5 Hz), 155.1 (***C***O), 138.2 (***C***-1^{Ph}), 138.1 (***C***-1^{Ph}), 137.2 (Ar***C***), 128.7 (Ar***C***), 128.7 (***C***-2^{Ph}, d, *J* = 9.0 Hz), 128.0 (***C***-2^{Ph}, d, *J* = 9.0 Hz), 128.5(8) (Ar**C**), 128.0 (Ar**C**), 127.9 (Ar**C**), 115.5 (***C***-3^{Ph}, d, *J* = 21.5), 115.3 (***C***-3^{Ph}, d, *J* = 21.5), 82.3 (Ar_2***C***H), 66.7(5) (***C***-2'), 66.7(3) (Ar***C***H_2), 46.5 (***C***-5), 34.8 (***C***-1'), 30.9 (***C***-3), 23.5 (***C***-4). δ_F (376 MHz, $CDCl_3$, mixture of rotamers) -114.73- -115.41 (m, 4^{Ph}-***F***). *m/z* (LC-MS, ESI^+) 474 (MNa^+). Accurate mass: Found (MH^+), 452.2048: $C_{27}H_{28}NO_3F_2$ requires *M*, 452.2037.

(2*R*)-2-{2-[bis(4-fluorophenyl)methoxy]ethyl}-1-methylpyrrolidine (*R*)-145

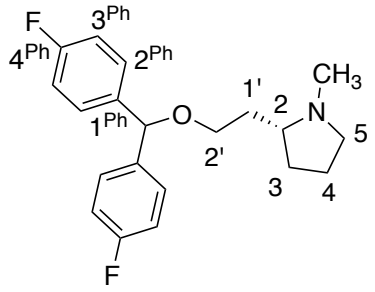

To a 0 °C solution of Benzyl (2R)-2-{2-[bis(4-fluorophenyl)methoxy]ethyl}pyrrolidine-1-carboxylate **(*R*)-178** (210 mg, 0.47 mmol) in THF (4 mL) was slowly added $LiAlH_4$ (2.4M solution in THF, 0.49 mL, 1.18 mmol), before being stirred at rt for 4 h. The reaction mixture was then cooled in an ice bath and any reactive salts were quenched according to Fieser's method (general procedure B).[116] The crude product was purified by reversed phase column chromatography (5 → 100% MeCN in H_2O) to afford title compound (99 mg, 63%) as a colourless oil.

ν_{max} (ATR) 2946 (w), 2871 (w), 1603 (w), 1506 (s), 1220 (s), 1154 (w), 1086 (w). δ_H (700 MHz, $CDCl_3$) 7.28 - 7.24 (4H, m, 2^{Ph}-***H***), 7.02 - 6.98 (4H, m, 3^{Ph}-***H***), 5.28 (1H, s, Ar_2C***H***), 3.53 - 3.49 (1H, m, 2'-***H***H'), 3.46 - 3.42 (1H, m, 2'-H***H'***), 3.21 - 3.15 (1H, m, 5-***H***H'), 2.38 (3H, s, C***H₃***), 2.37 - 2.32 (1H, m, 2-***H***), 2.29 - 2.22 (1H, m, 5-H***H'***), 2.14 - 2.09 (1H, m, 1-***H***H'), 1.97 - 1.90 (1H, m, 4-***H***H'), 1.87 - 1.78 (1H, m, 3-***H***H'), 1.75 - 1.62 (2H, m, 3-H***H'***, 1'-H***H'***), 1.58 - 1.49 (1H, m, 4-H***H'***). δ_C (176 MHz, $CDCl_3$) 162.2(6) (***C***-4^{Ph}, d, *J* = 245.5 Hz), 162.2(4) (***C***-4^{Ph}, d, *J* = 245.5 Hz), 138.0(9) (***C***-1^{Ph}, d, *J* = 3.0), 138.0(6) (***C***-1^{Ph}, d, *J* = 3.0), 128.6(2) (***C***-2^{Ph}, d, *J* = 8.0 Hz), 128.5(6) (***C***-2^{Ph}, d, *J* = 8.0 Hz), 115.4(1) (***C***-3^{Ph}, d, *J* = 21.5), 115.3(9) (***C***-3^{Ph}, d, *J* = 21.5), 82.5 (Ar_2***C***H), 66.9 (***C***-2'), 64.4 (***C***-2), 57.0 (***C***-5), 40.4 (***C***H_3), 33.4 (***C***-1'), 30.8 (***C***-4), 22.0 (***C***-3). δ_F (376 MHz,

$CDCl_3$) -115.01- -115.11 (m, 4^{Ph}-***F***). *m/z* (LC-MS, ESI^+) 332 (MH^+). Accurate mass: Found (MH^+), 332.1828: $C_{20}H_{24}F_2NO$ requires *M*, 332.1826.

(2*R*)-2-(2-chloroethyl)-1-methylpyrrolidine hydrochloride[202] (*R*)-90

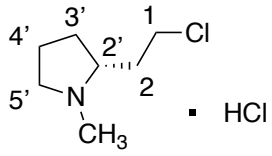

To a solution of 2-[(2*R*)-N-methylpyrrolidin-2'-yl]ethan-1'-ol **(*R*)-108** (77 mg, 0.59 mmol) in chloroform (1.2 mL), a solution of thionyl chloride (0.12 mL) in chloroform (0.4 ml) was added dropwise at 0 °C, and the resulting mixture was refluxed for 2h and concentrated under reduced pressure to afford the crude product as an brown oil. This was recrystalised from ethanol-diethylether to provide product (63 mg, 72%) as a brown solid.

$[\alpha]_D$ (c = 1.00 g/100 mL, $CHCl_3$) +47.0° (lit.:[233] $[\alpha]_D$ (c = 1.00 g/100 mL, $CHCl_3$) -49.8°). M.p. 126 - 127 °C (lit.[202]: 119 – 121 °C); ν_{max} (ATR) 3410 (br, w), 2959 (w), 2550 (br, w), 1495 (w). δ_H (700 MHz, $CDCl_3$) 12.56 – 12.44 (1H, s, N^+H), 3.92 - 3.84 (2H, m, 5'-***H***H', 1-***H***H'), 3.58 - 3.53 (1H, m, 1-H***H'***), 3.41 - 3.34 (1H, m, 2'-***H***), 2.91 - 2.85 (1H, m, 5'-H***H'***), 2.84 (3H, d, *J* = 5.0 Hz, C***H*****3**), 2.57 - 2.51 (1H, m, 2-***H***H'), 2.49 - 2.42 (1H, m, 2-H***H'***), 2.38 - 2.31 (1H, m, 3'-***H***H'), 2.30 - 2.23 (1H, m, 4'-***H***H'), 2.11 - 2.03 (1H, m, 4'-H***H'***), 2.02 - 1.95 (1H, m, 3'-H***H'***). δ_C (176 MHz, $CDCl_3$) 66.6 (***C***-2'), 56.4 (***C***-5'), 41.7 (***C***-1), 39.6 (***C***H_3), 32.6 (***C***-2), 29.4 (***C***-3'), 21.7 (***C***-4'). *m/z* (LC-MS, ESI^+)148 (MH+).

(*R*)-(4-chlorophenyl)(phenyl)methanol[231] (*R*)-113

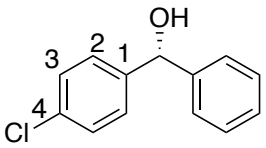

Et_2Zn (2.4 mL, 3.6 mmol) was added dropwise to a solution of phenylboronic acid (146 mg, 1.2 mmol) in toluene (3 mL) under an argon atmosphere. After stirring for 12 h at 60 °C, the mixture is cooled to 0 °C and a toluene solution of [(2*R*)-1-methylpyrrolidin-2-yl]diphenylmethanol (27 mg, 0.1 mmol) was introduced. The reaction was stirred for an additional 15 min and the 4-chlorobenzaldehyde (70 mg, 0.5 mmol) then added. After stirring for 12 h at 0 °C the reaction was quenched with H_2O (2 mL) and extracted with DCM

(3 x 5 mL). The combined organic layers were dried over $MgSO_4$, filtered, and solvent evaporated. Purification by chromatography (10% EtOAc in hexanes) to afford the desired product (77 mg, 56%) as a white solid.

$[\alpha]_D$ (c = 1.00 g/100 mL, $CHCl_3$) -27.0 ° (lit.: $[\alpha]_D$ (c = 1.00 g/100 mL, $CHCl_3$) -16 °); 95 % ee (determined by chiral HPLC analysis). ν_{max} (ATR) 3347 (br, m), 1489 (s), 1453 (m), 1089 (s), 1012 (s). δ_H (400 MHz, $CDCl_3$) 7.41 - 7.28 (9H, m, Ar***H***), 5.81 (1H, s, Ar_2C***H***), 2.42 (1H, s, O***H***). δ_C (101 MHz, $CDCl_3$) 143.5 (Ar***C***), 142.3 (Ar***C***), 133.4 (Ar***C***), 128.8 (Ar***C***), 128.7 (Ar***C***), 127.9(9) (Ar***C***), 127.9(6) (Ar***C***), 126.6 (Ar***C***), 75.7 (Ar_2***C***H). *m/z* (LC-MS, ESI^+) 201 (M(^{35}Cl)–OH^+), 203 (M(^{37}Cl)–OH+).

(*S*)-(4-chlorophenyl)(phenyl)methanol[231] **(*S*)-113**

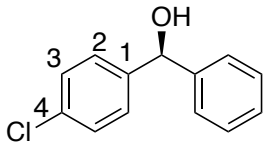

Et_2Zn (2.4 mL, 3.6 mmol) was added dropwise to a solution of phenylboronic acid (146 mg, 1.2 mmol) in toluene (3 mL) under an argon atmosphere. After stirring for 12 h at 60 °C, the mixture is cooled to 0 °C and a toluene solution of [(2S)-1-methylpyrrolidin-2-yl]diphenylmethanol (27 mg, 0.1 mmol) was introduced. The reaction was stirred for an additional 15 min and the 4-chlorobenzaldehyde (70 mg, 0.5 mmol) then added. After stirring for 12 h at 0 °C the reaction was quenched with H_2O (2 mL) and extracted with DCM (3 x 5 mL). The combined organic layers were dried over $MgSO_4$, filtered, and solvent evaporated. Purification by chromatography (10% EtOAc in hexanes) to afford the desired product (134 mg, 97%) as a white solid.

$[\alpha]_D$ (c = 1.00 g/100 mL, $CHCl_3$) +17.9 ° (lit.:[233] $[\alpha]_D$ (c = 1.00 g/100 mL, $CHCl_3$) +19°); 96 % ee (determined by chiral HPLC analysis). ν_{max} (ATR) 3347 (br, m), 1489 (s), 1453 (m), 1089 (s), 1012 (s). NMR and mass spectra were consistent with the *R* enantiomer.

(2*R*)-2-(2-[(*S*)-(4-chlorophenyl)(phenyl)methoxy]ethyl)-1-methylpyrrolidine (*R*, *S*)-112

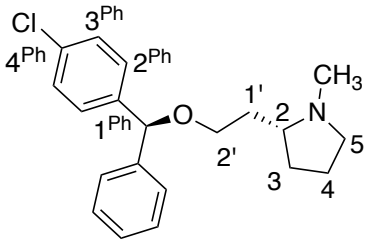

General procedure D was used in the reaction of (*S*)-4-chlorophenyl(phenyl)methanol **(*S*)-113** (105 mg, 0.38 mmol) and (2*R*)-2-(2-chloroethyl)-1-methylpyrrolidine **(*R*)-90** (58 mg, 0.39 mmol). The crude product was purified by column chromatography (0 → 100% EtOAc in hexanes with 1% NEt_3) to afford the title compound as a colourless oil (27 mg, 22%).

ν_{max} (ATR) 2943 (w), 2870 (w), 2776 (w), 1490 (m), 1453 (w), 1088 (s), 1015 (m). δ_H (700 MHz, $CDCl_3$) 7.32 – 7.22 (9H, m, Ar***H***), 5.28 (1H, s, Ar_2C***H***), 3.51 - 3.42 (2H, m, 2'-***H*****2**), 3.05 - 3.01 (1H, m, 5-***H***H'), 2.29 (3H, s, C***H*****3**), 2.17 - 2.03 (3H, m, 1'-***H***H', 2-***H***, 5-H***H'***), 1.91 - 1.84 (1H, m, 3-***H***H'), 1.77 - 1.69 (1H, m, 4-***H***H'), 1.67 - 1.60 (1H, m, 4-H***H'***), 1.56 - 1.50 (1H, m, 1'-H***H'***), 1.46 - 1.40 (1H, m, 3-H***H'***). δ_C (176 MHz, $CDCl_3$) 142.1 (Ar***C***), 141.3 (Ar***C***), 133.2 (Ar***C***), 128.6(2) (Ar***C***), 128.5(9) (Ar***C***), 128.3 (Ar***C***), 127.7 (Ar***C***), 127.0 (Ar***C***), 83.2 (Ar_2***C***H), 67.3 (***C***-2'), 63.9 (***C***-2), 57.3 (***C***-5), 40.6 (NC***H*****3**), 34.2 (***C***-1'), 31.1 (***C***-3), 22.1 (***C***-4). *m/z* (LC-MS, ESI^+) 330 ($M(^{35}Cl)H^+$), 332 ($M(^{37}Cl)H^+$). Accurate mass: Found (MH^+), 330.1643: $C_{20}H_{25}NO^{35}Cl$ requires *M*, 330.1625.

(2*R*)-2-{2-[(*R*)-(4-chlorophenyl)(phenyl)methoxy]ethyl}-1-methylpyrrolidine (*R*, *R*)-112

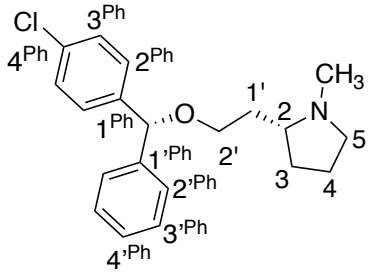

General procedure D was followed in the reaction of (*R*)-4-chlorophenyl(phenyl)methanol **(*R*)-113** (120 mg, 0.43 mmol) and (2*R*)-2-(2-chloroethyl)-1-methylpyrrolidine **(*R*)-90** (63mg, 0.43 mmol). The crude product was purified by column chromatography (0 → 100% EtOAc in hexanes with 1% NEt_3) to afford title compound **(*R*, *R*)-112** as a colourless oil (53 mg, 38%) and by-product **(*S*, *R*)-179** (6 mg, 4%) as a colourless oil.

R_f = 0.32 (80% EtOAc in hexanes with 1% NEt_3). ν_{max} (ATR) 2943 (w), 2776 (w), 1489 (w), 1453 (w), 1088 (m), 1015 (m). δ_H (700 MHz, $CDCl_3$) 7.32 – 7.29 (4H, m, 2^{Ph}-***H***, 3^{Ph}-***H***), 7.29 – 7.22 (5H, m, $2'^{Ph}$-***H***, $3'^{Ph}$-***H***, $4'^{Ph}$-***H***), 5.28 (1H, s, Ar_2C***H***), 3.53 – 3.48 (1H, m, 2'-***H***H'), 3.47 - 3.42 (1H, m, 2'-H***H'***), 3.08 – 3.01 (1H, m, 5-***H***H'), 2.30 (3H, s, C***H₃***), 2.19 – 2.04 (3H, m, 1'-***H***H', 2-***H***, 5-H***H'***), 1.93 – 1.86 (1H, m, 3-***H***H'), 1.79 – 1.70 (1H, m, 4-***H***H'), 1.69 - 1.61 (1H, m, 4-H***H'***), 1.58 – 1.50 (1H, m, 1'-H***H'***), 1.49 -1.40 (1H, m, 3-H***H'***). δ_C (151 MHz, $CDCl_3$) 142.1 (Ar***C***), 141.2 (Ar***C***), 133.2 (Ar***C***), 128.6(0) (Ar***C***), 128.5(6) (Ar***C***), 128.4 (Ar***C***), 127.7 (Ar***C***), 127.0 (Ar***C***), 83.2 (Ar_2C***H***), 67.3 (***C***-2'), 63.9 (***C***-2), 57.3 (***C***-5), 40.6 (***C***H_3), 34.1 (***C***-1'), 31.0 (***C***-3), 22.1 (***C***-4). *m/z* (LC-MS, ESI^+) 330 ($M(^{35}Cl)H^+$), 332 ($M(^{37}Cl)H^+$). Accurate mass: Found (MH^+), 330.1608: $C_{20}H_{25}NO^{35}Cl$ requires *M*, 330.1625.

(4S)-4-[(R)-(4-chlorophenyl)(phenyl)methoxy]-1-methylazepane (*S*, *R*)-179

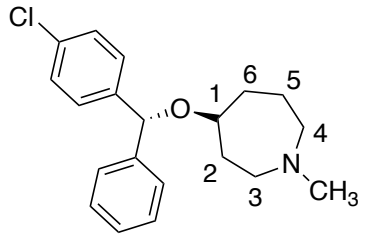

R_f = 0.27 (80% EtOAc in hexanes with 1% NEt_3). ν_{max} (ATR) 2936 (w), 1489 (w). δ_H (700 MHz, $CDCl_3$) 7.32 – 7.22 (9H, m, Ar***H***), 5.40 (1H, s, Ar_2C***H***), 3.67 – 3.61 (1H, m, 1-***H***), 2.81 - 2.72 (1H, m, 3-***H***H'), 2.69 – 2.63 (1H, m, 4-***H***H'), 2.62 – 2.56 (1H, m, 4-H***H'***), 2.54 – 2.47 (1H, m, 3-H***H'***), 2.36 (3H, s, C***H₃***), 2.07 – 2.00 (1H, m, 2-***H***H'), 1.98 – 1.89 (2H, m, 2-H***H'***, 6-***H***H'), 1.85 – 1.77 (2H, m, 6-H***H'***, 5-***H***H'), 1.60 – 1.52 (1H, m, 5-H***H'***). δ_C (176 MHz, $CDCl_3$) 142.5 (Ar***C***), 141.6 (Ar***C***), 133.2 (Ar***C***), 128.6(3) (Ar***C***), 128.5(8) (Ar***C***), 128.5 (Ar***C***), 127.7 (Ar***C***), 127.1 (Ar***C***), 79.9 (Ar_2***C***H), 75.6 (***C***-1), 58.9 (***C***-4), 52.7 (***C***-3), 47.0 (***C***H_3), 33.1 (***C***-2), 32.9 (***C***-6), 23.0 (***C***-5). *m/z* (LC-MS, ESI^+) 330 ($M(^{35}Cl)H^+$), 332 ($M(^{37}Cl)H^+$). Accurate mass: Found (MH^+), 330.1620: $C_{20}H_{25}NO^{35}Cl$ requires *M,* 330.1625.

(2,1,3-benzoxadiazol-5-yl)(phenyl)methanol 161

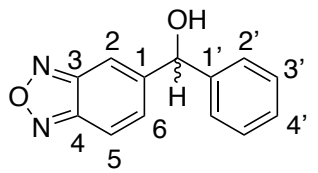

2,1,3-benzoxadiazole-5-carbaldehyde (296 mg, 2.00 mmol) was dissolved in THF (2 mL) and put on ice. Phenyl magnesium bromide (1.14 mL, 3.20 mmol) was then added dropwise

and the reaction mixture was warmed to rt and stirred for 4 h. The reaction was quenched with NH_4Cl (5 mL) and the product was extracted with EtOAc (3 x 5 mL) and dried over $MgSO_4$. The crude product was purified by column chromatography (0 → 40% Et_2O in hexanes) to afford the title compound (323 mg, 71%) as a red oil

ν_{max} (ATR) 3408 (br, m), 3064 (w), 2878 (w), 1634 (w), 1539 (w), 1493 (w), 1453 (m), 1138 (m), 1025 (m) 1040 (m), 1008 (m). δ_H (700 MHz, $CDCl_3$) 7.96 – 7.95 (1H, m, 2-***H***), 7.71 (1H, dd, *J* = 9.5, 1.5 Hz, 5-***H***), 7.40 – 7.37 (4H, m, 2'-***H***, 3'-***H***), 7.36 – 7.32 (1H, m, 4'-***H***), 7.29 (1H, dd, *J* = 9.5, 1.5 Hz, 6-***H***), 5.86 (1H, s, Ar_2C***H***), 2.50 (1H, s, O***H***). δ_C (176 MHz, $CDCl_3$) 149.4 (***C***-3), 148.9 (***C***-4), 147.3 (***C***-1), 141.6 (***C***-1'), 131.6 (***C***-6), 129.2 (***C***-3'), 128.8 (***C***-4'), 127.1 (***C***-2'), 116.6 (***C***-5), 112.1 (***C***-2), 75.8 (Ar_2***C***H). *m/z* (LC-MS, ESI^+) 227 (MH^+). Accurate mass: Found (MH^+), 227.0818: $C_{13}H_{11}N_2O_2$ requires *M*, 227.0821.

(2,1,3-benzoxadiazol-4-yl)(phenyl)methanol 162

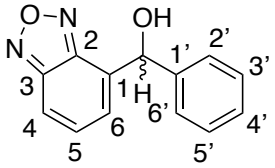

4-Formyl-2,1,3-benzoxadiazole (296 mg, 2.00 mmol) was dissolved in THF (2 mL) and put on ice. Phenyl magnesium bromide (1.14 mL, 3.20 mmol) was then added dropwise and the reaction mixture was warmed to rt and stirred for 4 h. The reaction was quenched with NH_4Cl (5 mL) and the product was extracted with EtOAc (3 x 5 mL) and dried over $MgSO_4$. The crude product was purified by column chromatography (0 → 40% Et_2O in hexanes) to afford the title compound as a red oil (244 mg, 54%).

ν_{max} (ATR) 3399 (br, m). δ_H (700 MHz, $CDCl_3$) 7.71 (1H, d, *J* = 9.0 Hz, 6-***H***), 7.53 – 7.50 (3H, m, 6'-***H***, 2'-***H***), 7.50– 7.49 (1H, m, 4-***H***), 7.40 (1H, dd, *J* = 9.0, 6.5 Hz, 5-***H***), 7.37 – 7.33 (2H, m, 3'-***H***, 5'-***H***), 7.32 – 7.28 (1H, m, 4'-***H***), 6.31 (1H, s, Ar_2C***H***), 2.90 (1H, s, O***H***). δ_C (176 MHz, $CDCl_3$) 149.5 (***C***-3), 147.7 (***C***-2), 141.4 (***C***-1'), 133.2 (***C***-1), 131.7 (***C***-5), 128.9 (***C***-3', ***C***-5'), 128.6 (***C***-4'), 127.0 (***C***-2', ***C***-6'), 126.7 (***C***-4), 115.5 (***C***-6), 73.1 (Ar_2***C***H). *m/z* (LC-MS, ESI^+) 209 ($M–OH^+$). Accurate mass: Found (MH^+), 227.0841: $C_{13}H_{11}N_2O_2$ requires *M*, 227.0821.

5-({2-[(2*R*)-1-methylpyrrolidin-2-yl]ethoxy}(phenyl)methyl)-2,1,3-benzoxadiazole (*R*)-159

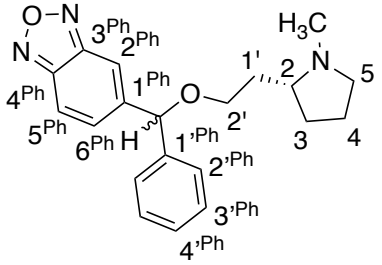

General procedure D was used in the reaction of (2,1,3-benzoxadiazol-5-yl)(phenyl)methanol **161** (90 mg, 0.40 mmol) and (2*R*)-1-(2-chloroethyl)-2-methylpyrrolidine **(*R*)-90** (83 mg, 0.56 mmol). The crude product was purified by flash column chromatography (0 → 100% EtOAc in hexanes with 1% NEt_3) to afford the title compound **(*R*)-159** (23 mg, 16%) as a brown/orange oil and by-product **(*S*)-164** (12 mg, 9%) as a brown oil.

R_f = 0.30 (80% EtOAc in hexanes with 1% NEt_3). ν_{max} (ATR) 2947 (w), 1095 (w). δ_H (600 MHz, $CDCl_3$, mixture of diastereomers) 7.88 – 7.85 (1H, m, 2^{Ph}-***H***), 7.73 - 7.69 (1H, m, 6^{Ph}-***H***), 7.39 – 7.34 (4H, m, $2'^{Ph}$-***H***, $3'^{Ph}$-***H***), 7.33 – 7.30 (1H, m, $4'^{Ph}$-***H***), 7.30 – 7.27 (1H, m, 5^{Ph}-***H***), 5.35 (1H, s, Ar_2C***H***), 3.61 – 3.49 (2H, m, 2'-***H*****$_2$**), 3.16 – 3.09 (1H, m, 5-***H***H'), 2.37 (1.5H, s, C***H*****$_3$**), 2.35 (1.5H, s, C***H*****$_3$**), 2.32 – 2.24 (1H, m, 2-***H***), 2.23 – 2.17 (1H, m, 5-H***H'***), 2.16 – 2.08 (1H, m, 1'-***H***H'), 2.01 – 1.87 (1H, m, 3-***H***H'), 1.84 - 1.74 (1H, m, 4-***H***H'), 1.74 – 1.60 (2H, m, 4-H***H'***, 1'-H***H'***), 1.58 – 1.45 (1H, m, 3-H***H'***). δ_C (151 MHz, $CDCl_3$, mixture of diastereomers) 149.4 (***C***-4^{Ph}), 149.0 (***C***-3^{Ph}), 146.4(2) (***C***-1^{Ph}), 146.4(0) (***C***-1^{Ph}), 139.9(3) (***C***-$1'^{Ph}$), 139.8(8) (***C***-$1'^{Ph}$), 131.7(0) (***C***-5^{Ph}), 131.6(7) (***C***-5^{Ph}), 129.0 (***C***-$2'^{Ph}$/***C***-$3'^{Ph}$), 128.6 (***C***-$4'^{Ph}$), 128.5 (***C***-$4'^{Ph}$), 127.4 (***C***-$2'^{Ph}$/***C***-$3'^{Ph}$), 127.3 (***C***-$2'^{Ph}$/***C***-$3'^{Ph}$), 116.5(8) (***C***-6^{Ph}), 116.5(5) (***C***-6^{Ph}), 112.6(3) (***C***-2^{Ph}), 112.5(5) (***C***-2^{Ph}), 83.2 (Ar_2***C***H), 83.1 (Ar_2***C***H), 67.4 (***C***-2'), 67.3 (***C***-2'), 64.2 (***C***-2), 64.1 (***C***-2), 57.2 (***C***-5), 40.6 (C***H***$_3$), 33.8(1) (***C***-1'), 33.7(5) (***C***-1'), 31.0(3) (***C***-3), 30.8(8) (***C***-3), 22.0(8) (***C***-4), 22.0(5) (***C***-4). *m/z* (LC-MS, ESI^+) 338 (MH^+). Accurate mass: Found (MH^+), 338.1881: $C_{20}H_{24}N_3O_2$ requires *M*, 338.1869.

5-({[(4*S*)-1-methylazepan-4-yl]oxy}(phenyl)methyl)-2,1,3-benzoxadiazole (*S*)-164

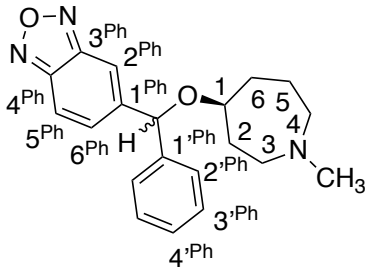

R_f = 0.26 (80% EtOAc in hexanes with 1% NEt_3). ν_{max} (ATR) 2935 (w), 1065 (w). δ_H (600 MHz, $CDCl_3$) 7.85 – 7.82 (1H, m, 2^{Ph}-***H***), 7.70 (1H, dd, *J* = 9.5, 1.0 Hz, 6^{Ph}-***H***), 7.37 – 7.34 (4H, m, $2'^{Ph}$-***H***, $3'^{Ph}$-***H***), 7.33 – 7.28 (2H, m, 5^{Ph}-***H***), 5.47 - 5.46 (1H, m, Ar_2C***H***), 3.76 – 3.69 (1H, m, 1-***H***), 2.81 – 2.73 (1H, m, 3-***H/***4-***H***), 2.71 – 2.57 (2H, m, 3-***H/***4-***H***), 2.56 – 2.48 (1H, m, 3-***H***/4-***H***), 2.38 (3H, s, C***H₃***), 2.15 – 1.78 (2H, m, 2-H_2, 6-H_2, 5-***H***H'), 1.63 – 1.53 (1H, m, 5-H***H'***). δ_C (151 MHz, $CDCl_3$, mixture of diastereomers) 149.3(9) (***C***-4^{Ph}), 149.3(9) (***C***-4^{Ph}), 149.0 (***C***-3^{Ph}), 146.9(0) (***C***-1^{Ph}), 146.8(6) (***C***-1^{Ph}), 140.3(8) (***C***-$1'^{Ph}$), 140.3(5) (***C***-$1'^{Ph}$), 131.9(3) (***C***-5^{Ph}), 131.9(2) (***C***-5^{Ph}), 128.9(4) (***C***-$3'^{Ph}$), 128.9(2) (***C***-$3'^{Ph}$), 128.5 (***C***-$4'^{Ph}$), 128.4 (***C***-$4'^{Ph}$), 127.4(0) (***C***-$2'^{Ph}$), 127.3(6) (***C***-$2'^{Ph}$), 116.5(2) (***C***-6^{Ph}), 116.4(9) (***C***-6^{Ph}), 112.7(1) (***C***-2^{Ph}), 112.6(5) (***C***-2^{Ph}), 80.0 (Ar_2C***H***), 79.9 (Ar_2C***H***), 76.1 (***C***-1), 60.0 (***C***-3/***C***-4), 58.9 (***C***-3/***C***-4), 52.7 (***C***-3/***C***-4), 47.1 (***C***H_3), 33.0 (***C***-2/***C***-6), 32.5 (***C***-2/***C***-6), 23.0 (***C***-5). *m/z* (LC-MS, ESI^+) 338 (MH^+). Accurate mass: Found (MH^+), 338.1883: $C_{20}H_{24}N_3O_2$ requires *M*, 338.1869.

1-[(2-Bromoethoxy)(phenyl)methyl]-4-chlorobenzene[262] 180

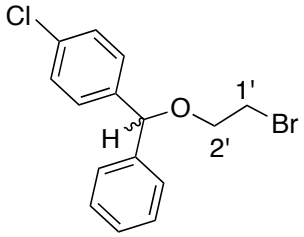

General Procedure C was followed with 2-bromoethanol (0.1 mL, 1.41 mmol) and (4-chlorophenyl)(phenyl)methanol **113** (218 mg, 1.00 mmol) with the modification of AuCl (24 mg, 0.14 mmol) as the catalyst in the place of $PdCl_2$ with a reaction time of 20 h. The product was purified by flash column chromatography (0 → 20 % EtOAc in hexanes) to afford the title compound (282 mg, 87%) as a colourless oil.

ν_{max} (ATR) 2858 (w), 1490 (m), 1453 (w), 1276 (w), 1185 (w), 1089 (m), 1029 (w), 1015 (m) cm^{-1}. δ_H (700 MHz, $CDCl_3$) 7.37 – 7.33 (4H, m, Ar***H***), 7.32 – 7.27 (5H, m, Ar***H***), 5.41 (1H, s,

Ar_2CH), 3.82 – 3.74 (2H, m, 2'-***H***), 3.53 (2H, t, *J* = 6.0 Hz, 1'-***H***). δ_C (176 MHz, $CDCl_3$) 141.3 (Ar***C***), 140.5 (Ar***C***), 133.5 (Ar***C***), 128.7(2) (Ar***C***), 128.7(1) (Ar***C***), 128.4(5) (Ar***C***), 128.0 (Ar***C***), 127.1 (Ar***C***), 83.4 (Ar_2CH), 69.1 (***C***-2'), 30.7 (***C***-1'). *m/z* (LC-MS, ESI^+) 347 ($M(^{35}Cl)(^{79}Br)\ Na^+$), 349 ($M(^{37}Cl)(^{79}Br)\ Na^+$) ($M(^{35}Cl)(^{81}Br)\ Na^+$), 351 ($M(^{37}Cl)(^{81}Br)\ Na^+$).

1-{2-[(4-Chlorophenyl)(phenyl)methoxy]ethyl}pyrrolidine[263] 152

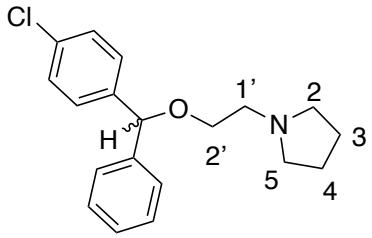

1-[(2-Bromoethoxy)(phenyl)methyl]-4-chlorobenzene **180** (117 mg, 0.36 mmol) is dissolved in MeCN (3 mL) and pyrollidine (0.04 mL, 0.43 mmol) and K_2CO_3 (69 mg, 0.50 mmol) are added. The reaction is heated to 60 °C and left to stir overnight. The reaction was extracted with EtOAc (3 x 5 mL) and washed with H_2O (5 mL) and dried over Na_2SO_4. The crude product was purified by reversed phase column chromatography (5 → 100% MeCN in H_2O with 0.1% formic acid) to afford the title compound (61 mg, 54%) as a yellow oil.

ν_{max} (ATR) 2962 (w), 2787 (w), 1490 (m), 1453 (w), 1088 (s), 1015 (m) cm^{-1}. δ_H (700 MHz, $CDCl_3$) 7.33 – 7.23 (9H, m, Ar***H***), 5.35 (1H, s, Ar_2CH), 3.62 (2H, t, *J* = 6.0 Hz, 2'-***H₂***), 2.82 (2H, t, *J* = 6.0 Hz, 1'-***H₂***), 2.66 – 2.61 (4H, m, 2-***H₂***, 5-***H₂***), 1.82 – 1.76 (4H, m, 3-***H₂***, 4-***H₂***). δ_C (176 MHz, $CDCl_3$) 141.8 (Ar***C***), 141.0 (Ar***C***), 133.3 (Ar***C***), 128.6(2) (Ar***C***), 128.5(9) (Ar***C***), 128.4 (Ar***C***), 127.8 (Ar***C***), 127.1 (Ar***C***), 83.4 (Ar_2CH), 68.2 (***C***-2'), 55.7 (***C***-1'), 54.8 (***C***-2, ***C***-5), 23.6 (***C***-3, ***C***-4). *m/z* (LC-MS, ESI^+) 316 ($M(^{35}Cl)H^+$), 318 ($M(^{37}Cl)H^+$). Accurate mass: Found ($M(^{35}Cl)H^+$), 316.1461: $C_{19}H_{23}{}^{35}ClNO$ requires *M*, 316.1468.

Methyl (2*S*)-1-{2-[(4-chlorophenyl)(phenyl)methoxy]ethyl}pyrrolidine-2-carboxylate (*S*)-150

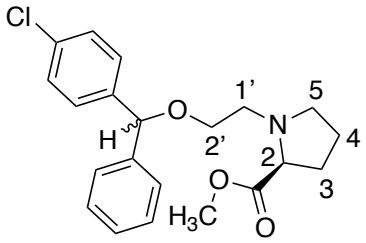

1-[(2-Bromoethoxy)(phenyl)methyl]-4-chlorobenzene **180** (170 mg, 0.52 mmol) is dissolved in MeCN (5 mL) and *L*-proline methyl ester hydrochloride (104 mg, 0.63 mmol) and K_2CO_3 (144 mg, 1.04 mmol) are added. The reaction is heated to 60 °C and left to stir overnight. The reaction was extracted with EtOAc (3 x 5 mL) and washed with H_2O (5 mL) and dried over Na_2SO_4. The crude product was purified by reversed phase column chromatography (5 → 100% MeCN in H_2O with 0.1% formic acid) to afford the title compound (104 mg, 54%) as a colourless oil.

ν_{max} (ATR) 2950 (w), 1732 (m), 1489 (m), 1452 (w), 1435 (w), 1262 (w), 1170 (m), 1087 (s), 1014 (m) cm^{-1}. δ_H (700 MHz, $CDCl_3$) 7.32 – 7.20 (9H, m, Ar***H***), 5.31 (0.5H, s, Ar_2C***H***), 5.30 (0.5H, s, Ar_2C***H***), 3.61 – 3.56 (2H, m, 2'-***H*****$_2$**), 3.55 (3H, s, OC***H*****$_3$**), 3.42 – 3.33 (1H, m, 2-***H***), 3.24 – 3.15 (1H, m, 1'-***H***H'), 3.01 – 2.91 (1H, m, 5-***H***H'), 2.89 – 2.80 (1H, m, 5-H***H'***), 2.61 – 2.49 (1H, m, 1'-H***H'***), 2.19 – 2.09 (1H, m, 3***H***H'), 1.95 – 1.84 (2H, m, 4***H*****$_2$**), 1.84 – 1.75 (1H, m, 3H***H'***). δ_C (176 MHz, $CDCl_3$, mixture of diastereomers) 174.5(4) (***C***O), 174.4(9) (***C***O), 141.9 (Ar***C***), 141.0(2) (Ar***C***), 141.0(0) (Ar***C***), 133.3 (Ar***C***), 133.2 (Ar***C***), 128.6(1) (Ar***C***), 128.5(9) (Ar***C***), 128.5(6) (Ar***C***), 128.5(5) (Ar***C***), 128.5 (Ar***C***), 128.3 (Ar***C***), 127.8 (Ar***C***), 127.7 (Ar***C***), 127.1 (Ar***C***), 126.9 (Ar***C***), 83.4 (Ar_2***C***H), 68.1 (***C***-2'), 65.9 (***C***-2), 54.5(1) (***C***-5), 54.4(9) (***C***-5), 54.0 (***C***-1'), 53.9 (***C***-1'), 51.7(8) (OC***H*****$_3$**), 51.7(7) (OC***H*****$_3$**), 29.7 (***C***-3), 29.6 (***C***-3), 23.3 (***C***-4). *m/z* (LC-MS, ESI^+) 396.105 (M(^{35}Cl)Na^+), 398.016 (M(^{37}Cl)Na^+). Accurate mass: Found (M(^{35}Cl)H^+), 374.1516: $C_{21}H_{25}{}^{35}ClNO_3$ requires *M*, 374.1523.

Methyl (2*R*)-1-{2-[(4-chlorophenyl)(phenyl)methoxy]ethyl}pyrrolidine-2-carboxylate (*R*)-150

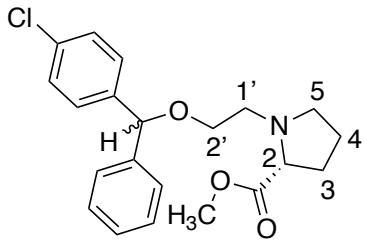

1-[(2-Bromoethoxy)(phenyl)methyl]-4-chlorobenzene **180** (462 mg, 1.42 mmol) is dissolved in MeCN (7 mL) and D-proline methyl ester hydrochloride (282 mg, 1.70 mmol) and K_2CO_3 (471 mg, 3.41 mmol) are added. The reaction is heated to 60 °C and left to stir overnight. The reaction was extracted with EtOAc (3 x 10 mL) and washed with H_2O (10 mL) and dried over Na_2SO_4. The crude product was purified by reversed phase column chromatography (5 → 100% MeCN in H_2O with 0.1% formic acid) to afford the title compound (161 mg, 30%) as a colourless oil.

ν_{max} (ATR) 2950 (w), 2870 (w), 1733 (m), 1489 (m), 1455 (w), 1435 (w), 1196 (m), 1169 (m), 1087 (s), 1072 (m), 1012 (m) cm^{-1}. δ_H (700 MHz, $CDCl_3$) 7.32 – 7.20 (9H, m, Ar***H***), 5.31 – 5.29 (1H, m, Ar_2C***H***), 3.58 – 3.53 (5H, m, 2'-***H₂***, OC***H₃***), 3.35 – 3.30 (1H, m, 2-***H***), 3.21 – 3.16 (1H, m, 1'-***H***H'), 2.97 – 2.91 (1H, m, 5-***H***), 2.84 – 2.78 (1H, m, 5-***H***), 2.53 – 2.46 (1H, m, 1'-H***H'***), 2.15 – 2.06 (1H, m, 3-***H***H'), 1.93 – 1.83 (2H, m, 4-***H₂***), 1.81 – 1.74 (1H, m, 3-H***H'***). δ_C (176 MHz, $CDCl_3$, mixture of diastereomers) 174.6(8) (***C***O), 174.6(5) (***C***O), 141.8(8) (Ar***C***), 141.8(5) (Ar***C***), 141.1 (Ar***C***), 141.0 (Ar***C***), 133.2 (Ar***C***), 133.1 (Ar***C***), 128.5(7) (Ar***C***), 128.5(5) (Ar***C***), 128.5(2) (Ar***C***), 128.5(0) (Ar***C***), 128.4 (Ar***C***), 128.3 (Ar***C***), 127.7(3) (Ar***C***), 127.6(5) (Ar***C***), 127.1 (Ar***C***), 126.9 (Ar***C***), 83.3 (Ar_2***C***H), 68.2(1) (***C***-2'), 68.1(8) (***C***-2'), 65.9(4) (***C***-2), 65.9(2) (***C***-2), 54.5 (***C***-5), 54.0(3) (***C***-1'), 53.9(9) (***C***-1'), 51.7 (O***C***H_3), 29.7 (***C***-3), 29.6 (***C***-3), 23.4(0) (***C***-4), 23.3(9) (***C***-4). *m/z* (LC-MS, ESI^+) 396.343 (M(^{35}Cl)Na^+), 398.256 (M(^{37}Cl)Na^+). Accurate mass: Found (M(^{35}Cl)H^+), 374.1530: $C_{21}H_{25}{}^{35}ClNO_3$ requires *M*, 374.1523.

[(2*S*)-1-{2-[(4-Chlorophenyl)(phenyl)methoxy]ethyl}pyrrolidin-2-yl]methanol (*S*)-149

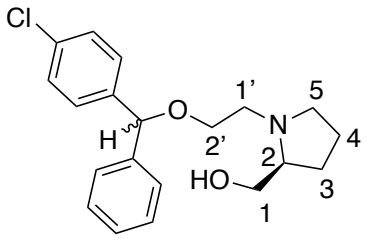

To a 0 °C solution of methyl (2*S*)-1-{2-[(4-chlorophenyl)(phenyl)methoxy]ethyl}pyrrolidine-2-carboxylate **(*S*)-150** (50 mg, 0.13 mmol) in THF (2 mL) was slowly added $LiAlH_4$ (2.4 M solution in THF, 0.14 mL, 0.33 mmol), before being warmed to rt and stirred for 3h. The reaction mixture was then cooled in an ice bath and any reactive salts were quenched according to Fieser's method (general procedure B). The product was purified by reversed phase column chromatography (5 → 100% MeCN in H_2O with 0.1% formic acid). To afford the title compound (22.5 mg, 50%) as a yellow oil.

ν_{max} (ATR) 3408 (br, w), 2870 (w), 1490 (m), 1088 (s) cm^{-1}. δ_H (700 MHz, $CDCl_3$) 7.34 - 7.23 (9H, m, Ar***H***), 5.33 (1H, s, Ar_2C***H***), 3.65 – 3.60 (1H, m, HOC***H***H'), 3.58 – 3.52 (2H, m, 2'-***H₂***), 3.41 – 3.36 (1H, m, HOCH***H'***), 3.21 – 3.14 (1H, m, 5–***H***H'), 3.10 – 3.02 (1H, m, 1'-***H***H'), 2.77 – 2.69 (1H, m, 2-***H***), 2.66 – 2.59 (1H, m, 1-H***H'***), 2.42 – 2.34 (1H, m, 5-H***H'***), 1.90 – 1.82 (1H, m, 4-***H***H'), 1.77 – 1.68 (3H, m, 4-H***H'***, 3-***H₂***). δ_C (176 MHz, $CDCl_3$, mixture of diastereomers) 141.8(3) (Ar***C***), 141.7(7) (Ar***C***), 141.0 (Ar***C***), 140.9 (Ar***C***), 133.3(3) (Ar***C***), 133.3(1) (Ar***C***), 128.7(0) (Ar***C***), 128.6(7) (Ar***C***), 128.3(2) (Ar***C***), 128.3(0) (Ar***C***), 127.9 (Ar***C***), 127.8 (Ar***C***), 127.0(0) (Ar***C***), 126.9(5) (Ar***C***), 83.5(2) (Ar_2C***H***), 83.4(9) (Ar_2C***H***), 68.2(4) (***C***-2'), 68.1(9) (***C***-2'), 65.2 (***C***-2), 62.6 (***C***H_2OH), 62.5 (***C***H_2OH), 55.2 (***C***-5), 55.1 (***C***-5), 54.3(6) (***C***-1'), 54.3(5) (***C***-1'), 27.6 (***C***-3), 24.1 (***C***-4). *m/z* (LC-MS, ESI^+) 368 (M(^{35}Cl)Na^+), 370 (M(^{37}Cl)Na^+). Accurate mass: Found (M(^{35}Cl)H^+), 346.1571: $C_{20}H_{25}{}^{35}ClNO_2$ requires *M*, 346.1574

[(2*R*)-1-{2-[(4-Chlorophenyl)(phenyl)methoxy]ethyl}pyrrolidin-2-yl]methanol (*R*)-149

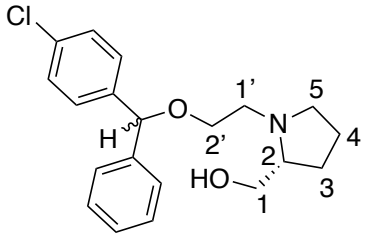

To a 0 °C solution of methyl (2*R*)-1-{2-[(4-chlorophenyl)(phenyl)methoxy]ethyl}pyrrolidine-2-carboxylate **(*R*)-150** (115 mg, 0.30 mmol) in THF (4 mL) was slowly added $LiAlH_4$ (2.4M

solution in THF, 0.31 mL, 0.75 mmol), before being warmed to rt and stirred for 3h. The reaction mixture was then cooled in an ice bath and any reactive salts were quenched according to Fieser's method (general procedure B). The product was purified by reversed phase column chromatography (5 → 100% MeCN in H_2O with 0.1% formic acid). To afford the title compound (64 mg, 62%) as a yellow oil.

ν_{max} (ATR) 3392 (br, w), 2946 (w), 2870 (w), 1489 (m), 1453 (w), 1403 (w), 1295 (w), 1185 (w), 1086 (s), 1028 (m), 1014 (s) cm^{-1}. δ_H (700 MHz, $CDCl_3$) 7.35 - 7.23 (9H, m, Ar***H***), 5.35 (1H, s, Ar_2C***H***), 3.68 – 3.63 (1H, m, HOC***H***H'), 3.63 – 3.56 (2H, m, 2'-***H₂***), 3.45 – 3.40 (1H, m, HOCH***H'***), 3.27 – 3.18 (1H, m, 5–***H***H'), 3.14 – 3.06 (1H, m, 1'-***H***H'), 2.85 – 2.75 (1H, m, 2-***H***), 2.71 – 2.65 (1H, m, 1-H***H'***), 2.48 – 2.38 (1H, m, 5-H***H'***), 1.93 – 1.85 (1H, m, 4-***H***H'), 1.81 – 1.70 (3H, m, 4-H***H'***, 3-***H₂***). δ_C (176 MHz, $CDCl_3$, mixture of diastereomers) 141.7 (Ar***C***), 141.6 (Ar***C***), 140.9 (Ar***C***), 140.8 (Ar***C***), 133.4 (Ar***C***), 133.3 (Ar***C***), 128.6(9) (Ar***C***), 128.6(8) (Ar***C***), 128.6(6) (Ar***C***), 128.3(2) (Ar***C***), 128.2(8) (Ar***C***), 127.9 (Ar***C***), 127.8 (Ar***C***), 127.0 (Ar***C***), 126.9 (Ar***C***), 83.5(3) (Ar_2C***H***), 83.5(1) (Ar_2C***H***), 67.9(5) (***C***-2'), 67.8(9) (***C***-2'), 65.7 (***C***-2), 62.4(1) (***C***H_2OH), 62.3(8) (***C***H_2OH), 55.1(8) (***C***-5), 55.1(6) (***C***-5), 54.5 (***C***-1'), 27.5 (***C***-3), 24.1 (***C***-4). *m/z* (LC-MS, ESI^+) 368 ($M(^{35}Cl)Na^+$), 370 ($M(^{37}Cl)Na^+$). Accurate mass: Found ($M(^{35}Cl)H^+$), 346.1579: $C_{20}H_{25}{}^{35}ClNO_2$ requires *M*, 346.1574.

(2*R*)-1-{2-[(4-chlorophenyl)(phenyl)methoxy]ethyl}-2-(methoxymethyl)pyrrolidine (*R*)-153

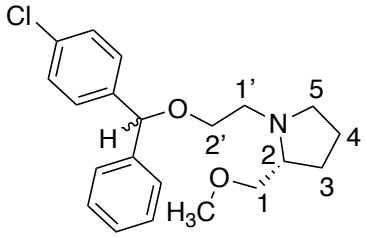

1-[(2-bromoethoxy)(phenyl)methyl]-4-chlorobenzene **180** (160 mg, 0.49 mmol) in DMF (0.8 mL) was added dropwise to a suspension of the (*R*)-methoxymethylpyrrolidine (0.06 mL, 0.49 mmol), KI (8.3 mg, 0.08 mmol) and K_2CO_3 (135 mg, 0.98 mmol) in DMF (0.5 mL). The reaction mixture was stirred at rt for 4 h. Following the addition of H_2O (5 mL) and extraction with EtOAc (3 x 5mL), the combined organic layers were dried over Na_2SO_4 and concentrated *in vacuo*. The crude product was purified by column chromatography (10% MeOH in $CHCl_3$) to afford the title compound (114 mg, 65 %) as a brown oil.

ν_{max} (ATR) 2871 (w), 2810 (w), 1489 (m), 1453 (w), 1185 (w), 1088 (s), 1015 (m). δ_H (700 MHz, $CDCl_3$) 7.33 – 7.23 (9H, m, Ar***H***), 5.37 (1H, s, Ar_2C***H***), 3.74 – 3.57 (2H, m, 2'-***H₂***), 3.56 - 3.41 (1H, m, 1-***H***H'), 3.37 – 3.29 (4H, m, C***H₃***, 1-H***H'***), 3.29 – 3.11 (2H, m, 1'-***H***H', 5-***H***H'), 2.95 – 2.60 (2H, m, 1'-H***H'***, 2-***H***), 2.58 – 2.32 (1H, m, 5-H***H'***), 1.97 – 1.86 (1H, m, 3-***H***H'), 1.86 – 1.70 (2H, m, 4-***H₂***), 1.70 – 1.57 (1H, m, 3-H***H'***). δ_C (176 MHz, $CDCl_3$, mixture of diastereomers) 141.8 (Ar***C***), 141.7 (Ar***C***), 141.0 (Ar***C***), 140.9 (Ar***C***), 133.3 (Ar***C***), 133.2 (Ar***C***), 128.6(3) (Ar***C***), 128.6(1) (Ar***C***), 128.5(9) (Ar***C***), 128.4(4) (Ar***C***), 128.3(8) (Ar***C***), 127.8(2) (Ar***C***), 127.7(7) (Ar***C***), 127.1 (Ar***C***), 127.0 (Ar***C***), 83.4 (Ar_2***C***H), 75.4 (***C***-1), 67.8 (***C***-2'), 64.3 (***C***-2), 59.2 (***C***H_3), 55.6 (***C***-5), 55.5 (***C***-5), 54.9 (***C***-1'), 28.0 (***C***-3), 23.2 (***C***-4). *m/z* (LC-MS, ESI^+) 382 ($M(^{35}Cl)Na^+$), 384 ($M(^{37}Cl)Na^+$). Accurate mass: Found (MH^+), 360.1734: $C_{21}H_{27}NO_2{}^{35}Cl$ requires *M*, 360.1730.

(2*S*)-1-{2-[(4-chlorophenyl)(phenyl)methoxy]ethyl}-2-(methoxymethyl)pyrrolidine (*S*)-153

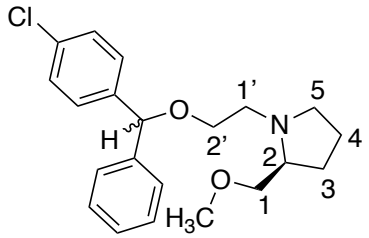

1-[(2-bromoethoxy)(phenyl)methyl]-4-chlorobenzene **180** (160 mg, 0.49 mmol) in DMF (0.8 mL) was added dropwise to a suspension of the (*S*)-methoxymethylpyrrolidine (0.06 mL, 0.49 mmol), KI (8.3 mg, 0.08 mmol) and K_2CO_3 (135 mg, 0.98 mmol) in DMF (0.5 mL). The reaction mixture was stirred at rt for 4 h. Following the addition of H_2O (5 mL) and extraction with EtOAc (3 x 5mL), the combined organic layers were dried and concentrated *in vacuo*. The crude product was purified by flash column chromatography (10% MeOH in $CHCl_3$) to afford the title compound (68 mg, 39 %) as a brown oil.

ν_{max} (ATR) 2871 (w), 2811 (w), 1489 (m), 1452 (w), 1185 (m), 1087 (s), 1014 (m). δ_H (700 MHz, $CDCl_3$) 7.33 - 7.30 (4H, m, Ar***H***), 7.30 – 7.26 (4H, m, Ar***H***), 7.26 -7.23 (1H, m, Ar***H***), 5.36 (1H, s, Ar_2C***H***), 3.67 - 3.55 (2H, m, 2'-***H₂***), 3.53 - 3.38 (1H, m, 1-***H***H'), 3.33 – 3.27 (4H, m, C***H₃***, 1-H***H'***), 3.25 – 3.14 (2H, m, 1'-***H***H', 5-***H***H'), 2.80 - 2.63 (2H, m, 1'-H***H'***, 2-***H***), 2.45 – 2.30 (1H, m, 5-H***H'***), 1.94 – 1.85 (1H, m, 3-***H***H'), 1.84 – 1.68 (2H, m, 4-***H₂***), 1.66 – 1.57 (1H, m, 3-H***H'***).

δ_C (176 MHz, $CDCl_3$, mixture of diastereomers) 141.9 (Ar***C***), 141.8 (Ar***C***), 141.1 (Ar***C***), 141.0 (Ar***C***), 133.2(2) (Ar***C***), 133.1(9) (Ar***C***), 128.5(9) (Ar***C***), 128.5(8) (Ar***C***), 128.5(7) (Ar***C***), 128.5(6), 128.4(2) (Ar***C***), 128.3(8) (Ar***C***), 127.8 (Ar***C***), 127.7 (Ar***C***), 127.1 (Ar***C***), 127.0 (Ar***C***), 83.3 (Ar_2C***H***), 75.8 (***C***-1), 68.2 (***C***-2'), 64.2 (***C***-2), 59.2 (***C***H_3), 55.5(1) (***C***-5), 55.4(5) (***C***-5), 54.9 (C-1'), 28.1 (***C***-3), 23.2 (***C***-4). *m/z* (LC-MS, ESI^+) 382 ($M(^{35}Cl)Na^+$), 384 ($M(^{37}Cl)Na^+$). Accurate mass: Found (MH^+), 360.1732: $C_{21}H_{27}NO_2{}^{35}Cl$ requires *M*, 360.1730.

(2*R*)-1-{2-[(4-Chlorophenyl)(phenyl)methoxy]ethyl}-2-methylpyrrolidine (*R*)-147

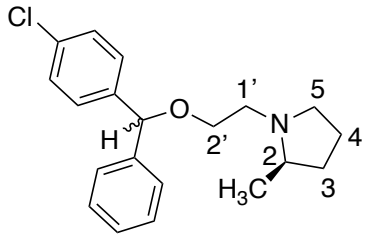

1-[(2-bromoethoxy)(phenyl)methyl]-4-chlorobenzene **180** (326 mg, 1.03 mmol) in DMF (1 mL) was added dropwise to a suspension of the (*R*)-2-methyl-pyrrolidine hydrochloride (125 mg, 1.03 mmol), KI (17 mg, 0.10 mmol) and K_2CO_3 (285 mg, 2.06 mmol) in DMF (1.5 mL). The reaction mixture was stirred at rt for 24 h. Following the addition of H_2O (5 mL) and extraction with EtOAc (3 x 5 mL), the combined organic layers were dried and concentrated *in vacuo*. The crude product was purified by column chromatography (10% MeOH in $CHCl_3$) to afford the title compound (217 mg, 65 %) as a brown oil.

ν_{max} (ATR) 2962 (w), 2869 (w), 2786 (w), 1490 (m), 1453 (w), 1375 (w), 1185 (w), 1088 (s) 1015 (m). δ_H (700 MHz, $CDCl_3$, mixture of diastereomers) 7.33 – 7.23 (9H, m, ArH), 5.36 (1H, s, Ar_2***H***), 3.62 – 3.55 (2H, m, 2'-***H₂***), 3.16 – 3.11 (1H, m, 5-***H***H'), 3.09 – 3.03 (1H, m, 1'-***H***H'), 2.44 - 2.38 (1H, m, 5-H***H'***), 2.38 – 2.31 (1H, m, 2-***H***), 2.24 – 2.16 (1H, m, 1' –H***H'***), 1.93 – 1.85 (1H, m, 3-***H***H'), 1.80 – 1.62 (2H, m, 4-***H₂***), 1.43 – 1.34 (1H, m, 3-H***H'***), 1.09 (1.5H, d, *J* = 6.0 Hz, C***H₃***), 1.08 (1.5H, d, *J* = 6.0 Hz, C***H₃***). δ_C (176 MHz, $CDCl_3$, mixture of diastereomers) 142.0(2) (Ar***C***), 141.9(6) (Ar***C***), 141.2 (Ar***C***), 141.1 (Ar***C***), 133.2(2) (Ar***C***), 133.1(9) (Ar***C***), 128.6(2) (Ar***C***), 128.5(7) (Ar***C***), 128.5 (Ar***C***), 128.4 (Ar***C***), 127.8 (Ar***C***), 127.7 (Ar***C***), 127.1(0) (Ar***C***), 127.0(6) (Ar***C***), 83.4 (Ar_2***C***H), 68.6(0) (***C***-2'), 68.5(6) (***C***-2'), 60.4(3) (***C***-2), 60.4(0) (***C***-2), 55.0 (***C***-5), 54.9 (***C***-5), 53.5 (***C***-1'), 53.4 (***C***-1'), 32.6 (***C***-3), 22.0 (***C*-4**), 19.2 (***C***H_3). *m/z* (LC-MS, ESI^+) 330 ($M(^{35}Cl)Na^+$), 332 ($M(^{37}Cl)Na^+$). Accurate mass: Found ($M(^{35}Cl)H^+$), 330.1630: $C_{20}H_{25}{}^{35}ClNO$ requires *M*, 330.1625.

(2*S*)-1-{2-[(4-Chlorophenyl)(phenyl)methoxy]ethyl}-2-methylpyrrolidine (*S*)-147

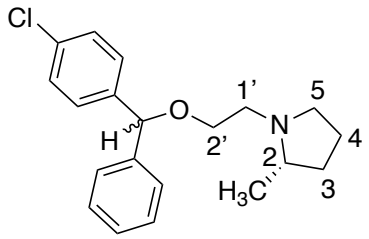

1-[(2-bromoethoxy)(phenyl)methyl]-4-chlorobenzene **180** (310 mg, 0.95 mmol) in DMF (1 mL) was added dropwise to a suspension of the (*S*)-2-methyl-pyrrolidine hydrochloride (115 mg, 0.95 mmol), KI (17 mg, 0.10 mmol) and K_2CO_3 (263 mg, 1.90 mmol) in DMF (1.5 mL). The reaction mixture was stirred at rt for 24 h. Following the addition of H_2O (5 mL) and extraction with EtOAc (3 x 5 mL), the combined organic layers were dried and concentrated *in vacuo*. The crude product was purified by column chromatography (10% MeOH in $CHCl_3$) to afford the title compound (195 mg, 62 %) as a brown oil.

ν_{max} (ATR) 2962 (w), 2869 (w), 2785 (w), 1489 (m), 1453 (w), 1375 (w), 1293 (w), 1184 (w), 1087 (s), 1014 (m). δ_H (700 MHz, $CDCl_3$) 7.32 - 7.22 (9H, m, Ar***H***), 5.36 (1H, s, Ar_2C***H***), 3.65 – 3.55 (2H, m, 2'-***H*****$_2$**), 3.20 – 3.13 (1H, m, 5-***H***H'), 3.10 – 3.04 (1H, m, 1'-***H***H'), 2.47 – 2.35 (2H, m, 5-H***H'***, 2-***H***), 2.28 – 2.20 (1H, m, 1' –H***H'***), 1.94 – 1.85 (1H, m, 3-***H***H'), 1.81 - 1.72 (1H, m, 4-***H***H'), 1.71 – 1.63 (1H, m, 4-H***H'***), 1.46 – 1.36 (1H, m, 3-H***H'***), 1.10 (3H, d, *J* = 6.0, C***H*****$_3$**). δ_C (176 MHz, $CDCl_3$, mixture of diastereomers) 141.9(3) (Ar***C***), 141.8(6) (Ar***C***), 141.1 (Ar***C***), 141.0 (Ar***C***), 133.2(2) (Ar***C***), 133.1(9) (Ar***C***), 128.6(0) (Ar***C***), 128.5(8) (Ar***C***), 128.5(5) (Ar***C***), 128.4(2) (Ar***C***), 128.3(8) (Ar***C***), 127.8 (Ar***C***), 127.7 (Ar***C***), 127.1 (Ar***C***), 127.0 (Ar***C***), 83.4 (Ar_2***C***H), 68.3(2) (***C***-2'), 68.2(9) (***C***-2'), 60.5(9) (***C***-2), 60.5(6) (***C***-2), 54.9 (***C***-5), 54.8 (***C***-5), 53.4 (***C***-1'), 53.3 (***C***-1'), 32.5 (***C***-3), 32.4 (***C***-3), 22.0(0) (***C***-4), 21.9(9) (***C***-4), 18.9(3) (***C***H_3), 18.9(1) (***C***H_3). *m/z* (LC-MS, ESI^+) 330 (M(^{35}Cl)Na^+), 332 (M(^{37}Cl)Na^+). Accurate mass: Found (M(^{35}Cl)H^+), 330.1636: $C_{20}H_{25}{}^{35}ClNO$ requires *M*, 330.1625.

1-[(2-Bromoethoxy)(phenyl)methyl]-4-fluorobenzene 181

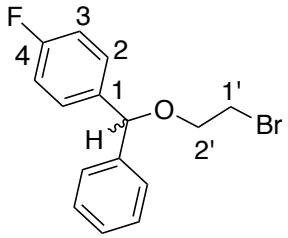

General Procedure C was followed with 2-bromoethanol (0.1 mL, 1.41 mmol) and (4-fluorophenyl)(phenyl)methanol **175** (300 mg, 1.48 mmol) with the modification of AuCl (35 mg, 0.15 mmol) as the catalyst in the place of $PdCl_2$ with a reaction time of 3 h. The product was purified by flash column chromatography (0 → 20 % EtOAc in hexanes) to afford the title compound contaminated with 20% fluorodiphenylmethane and 16% 4-fluorobenzophenone (272 mg, 62%) as a colourless oil.

ν_{max} (ATR) 3030 (w), 2858 (w), 1660 (w), 1603 (m), 1507 (s), 1452 (m), 1276 (w), 1221 (s), 1184 (w), 1156 (m), 1096 (m), 1014 (m). δ_H (400 MHz, $CDCl_3$, shows 20% fluorodiphenylmethane, 16% 4-fluorobenzophenone) 7.38 – 7.27 (7H, m, Ar***H***), 7.06 – 7.01 (2H, m, 3-***H***), 5.43 (1H, s, Ar_2C***H***), 3.79 (2H, td, *J* = 6.0, 2.5 Hz, 2'-***H₂***), 3.53 (2H, t, *J* = 6.0 Hz, 1'-***H₂***) δ_C (176 MHz, $CDCl_3$, shows 20% fluorodiphenylmethane, 16% 4-fluorobenzophenone) 162.4 (d, *J* = 246.0 Hz, ***C***-4), 141.5 (Ar***C***), 137.7 (d, *J* = 3.0 Hz, ***C***-1), 128.8 (d, *J* = 8.0 Hz, ***C***-2), 128.7 (Ar***C***), 128.0 (Ar***C***), 127.1 (Ar***C***), 115.4 (d, *J* = 21.5 Hz, ***C***-3), 83.4 (Ar_2***C***), 69.0 (***C***-2'), 30.7 (***C***-1'). δ_F (376 MHz, $CDCl_3$, shows 20% fluorodiphenylmethane, 16% 4-fluorobenzophenone) -114.68- -114.75 (m, 4-***F***). *m/z* (GC-MS, EI) 308 ($M(^{79}Br)^+$), 310 ($M(^{81}Br)^+$).

(2*R*)-1-{2-[(4-Fluorophenyl)(phenyl)methoxy]ethyl}-2-methylpyrrolidine (*R*)-182

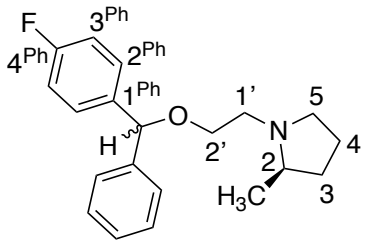

1-[(2-Bromoethoxy)(phenyl)methyl]-4-fluorobenzene **181** (151 mg, 0.49 mmol) in DMF (0.8 mL) was added dropwise to a suspension of the (*R*)-2-methyl-pyrrolidine hydrochloride (60 mg, 0.49 mmol), KI (8.3 mg, 0.08 mmol) and K_2CO_3 (135 mg, 0.98 mmol) in DMF (0.5 mL). The reaction mixture was stirred at rt for 4 h. Following the addition of H_2O (5 mL) and

extraction with EtOAc (3 x 5 mL), the combined organic layers were dried and concentrated *in vacuo*. The crude product was purified by flash column chromatography (10% MeOH in $CHCl_3$) to afford the title compound as a brown oil (56 mg, 35 %).

ν_{max} (ATR) 2962 (m), 2870 (w), 2786 (w), 1604 (m), 1508 (s), 1454 (m), 1376 (w), 1295 (w), 1222 (s), 1156 (m), 1089 (s), 1015 (w). δ_H (700 MHz, $CDCl_3$) 7.34 – 7.29 (6H, m, Ar***H***), 7.27 – 7.23 (1H, m, Ar***H***), 7.02 – 6.97 (2H, m, 3^{Ph}-***H***), 5.38 (1H, s, Ar_2C***H***), 3.67 – 3.57 (2H, m, 2'-***H***H), 3.22 – 3.16 (1H, m, 5-***H***H'), 3.13 – 3.06 (1H, m, 1'-***H***H'), 2.51 – 2.40 (2H, m, 5-H***H'***, 2-***H***), 2.33 – 2.24 (1H, m, 1'-H***H'***), 1.96 – 1.86 (1H, m, 3-***H***H'), 1.83 – 1.75 (1H, m, 4-***H***H'), 1.73 – 1.66 (1H, m, 4-H***H'***), 1.48 – 1.38 (1H, m, 3-H***H'***), 1.13 (3H, d, *J* = 6.0 Hz, C***H₃***). δ_C (176 MHz, $CDCl_3$, mixture of diastereomers) 162.2(3) (***C***-4^{Ph}, d, *J* = 245.5 Hz), 162.2(0) (***C***-4^{Ph}, d, *J* = 245.5 Hz), 142.2 (Ar***C***), 142.1 (Ar***C***), 138.2(6) (***C***-1^{Ph}, d, *J* = 3.0 Hz), 138.2(4) (***C***-1^{Ph}, d, *J* = 3.0 Hz), 128.7(3) (***C***-2^{Ph}, d, *J* = 16.5 Hz), 128.7(3) (Ar***C***), 128.6 (Ar***C***), 128.5 (Ar***C***), 127.7 (Ar***C***), 127.6 (Ar***C***), 127.1 (Ar***C***), 127.0 (Ar***C***), 115.3(0) (***C***-3^{Ph}, d, *J* = 21.5 Hz), 115.2(7) (***C***-3^{Ph}, d, *J* = 21.5 Hz), 83.4 (Ar_2***C***H), 68.1 (***C***-2'), 60.7 (***C***-2), 54.8(2) (***C***-5), 54.7(8) (***C***-5), 53.3(4) (***C***-1'), 53.3(2) (***C***-1'), 32.4(2) (***C***-3), 32.4(1) (***C***-3), 22.0 (***C***-4), 18.8 (***C***H_3). δ_F (376 MHz, $CDCl_3$) -115.30 (s, 4-***F***, isomer 1), -115.36 (s, 4-***F***, isomer 2). *m/z* (LC-MS, ESI^+) 314 (MH^+). Accurate mass: Found (MH^+), 314.1930: $C_{20}H_{25}NOF$ requires *M*, 314.1920.

2-((2*R*)-2-methylpyrrolidin-1-yl)ethan-1-ol[264] (*R*)-155

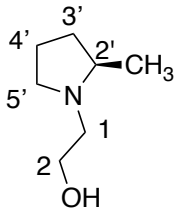

2-Bromoethanol (0.23 mL, 3.20 mmol) in dry MeCN (2 mL) was added dropwise to a mixture of (*R*)-2-methylpyrrolidine (415mg, 3.32 mmol) and K_2CO_3 (918 mg, 6.64 mmol) in dry MeCN (2 mL) heated under reflux. After 15 h the mixture was cooled to rt, filtered and concentrated. Et_2O (5 mL) was then added and the product extracted with 1M HCl (2 x 5 mL). The aqueous phase was made basic with solid NaOH, then extracted with DCM (3 x 5 mL). The organic layers were combined, dried over Na_2SO_4, filtered and concentrated to afford the product (200 mg, 48%) as a colourless oil. Carried through without further purification.

$[\alpha]_D$ (c = 1.00 g/100 mL, $CHCl_3$) -58.8°. ν_{max} (ATR) 3385 (br, m), 2963 (m), 2875 (m), 2806 (m), 1677 (m), 1416 (m), 1509 (m). δ_H (400 MHz, $CDCl_3$) 4.03 – 3.86 (3H, m, 2-***H***$_2$, 5'-***H***H'), 3.42 – 3.35 (1H, m, 1-***H***H'), 3.33 – 3.23 (1H, m, 2'-***H***), 3.01 – 2.91 (2H, m, 1-H***H'***, 5'-H***H'***), 2.29 – 2.18 (2H, m, 3'-***H***H', 4-***H***H'), 2.08 – 1.98 (1H, m, 4-H***H'***), 1.97 - 1.87 (2H, m, 3'-H***H'***), 1.54 (3H, d, *J* = 6.5 Hz, C***H*****$_3$**). δ_C (176 MHz, $CDCl_3$) 64.6 (***C***-2'), 57.6 (***C***-2), 57.2 (***C***-5'), 54.6 (***C***-1), 31.4 (***C***-3'), 21.7 (***C***-4'), 15.9 (***C***H_3). *m/z* (LC-MS, ESI^+) 130 (MH+). Accurate mass: Found (MH^+), 130.1232: $C_7H_{16}NO$ requires *M*, 130.1232.

2-((2S)-2-methylpyrrolidin-1-yl)ethan-1-ol[264] **(*S*)-155**

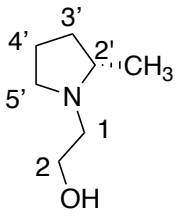

2-Bromoethanol (0.14 mL, 1.93 mmol) in dry MeCN (1 mL) was added to a refluxing mixture of (*S*)-2-methylpyrrolidine (257 mg, 2.00 mmol), K_2CO_3 (535 mg, 3.87 mmol) in dry MeCN (2 mL). After 15 h the mixture was cooled to rt, filtered and concentrated. Et_2O (5 mL) was then added and the product extracted with 1M HCl (2 x 5 mL). The aqueous phase was made basic with solid NaOH, then extracted with DCM (3 x 5 mL). The organic layers were dried over Na_2SO_4, filtered and concentrated to afford the product (200 mg, 48%) as a colourless oil. Carried through without further purification.

$[\alpha]_D$ (c = 1.00 g/100 mL, $CHCl_3$) +60.0°. ν_{max} (ATR) 3337 (br, m), 2948 (m), 2657 (m), 1451 (m), 1053 (m). NMR and mass spectra were consistent with the *R* enantiomer.

(2*R*)-1-(2-chloroethyl)-2-methylpyrrolidine hydrochloride (*R*)-154

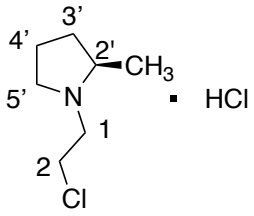

A solution of thionyl chloride (0.57 mL, 7.87 mmol) in chloroform (3 mL) was added dropwise to a solution of 2-((2*R*)-2-methylpyrrolidin-1-yl)ethan-1-ol **(*R*)-155** (377 mg, 2.92 mmol) in chloroform (4 mL) at 0 °C. The resulting mixture was heated under reflux for 2 h

and then concentrated under reduced pressure. Precipitation from a mixture of EtOH and Et_2O afforded the title compound contaminated with 19% 2-((2*R*)-2-methylpyrrolidin-1-yl)ethan-1-ol hydrochloride (353 mg, 35%) as a brown semi-solid.

$[\alpha]_D$ (c = 1.00 g/100 mL, $CHCl_3$) -23.7°. ν_{max} (ATR) 3392 (br, m), 2974 (m), 2554 (m), 2453 (m), 1452 (m), 1422 (m), 1393 (m). δ_H (700 MHz, $CDCl_3$, 19% 2-((2R)-2-methylpyrrolidin-1-yl)ethan-1-ol hydrochloride) 12.56 (1H, s, N***H*****⁺**), 4.15 – 4.10 (1H, m, 4'-***H***H'), 4.05 – 3.99 (1H, m, 4-H***H'***), 3.97 – 3.90 (1H, m, 5'-***H***H'), 3.72 – 3.66 (1H, m, 3'-***H***H'), 3.31 – 3.24 (1H, m, 2'-***H***), 3.12 – 3.05 (1H, m, 3'-H***H'***), 3.04 – 2.97 (1H, m, 5'-H***H'***), 2.30 – 2.17 (2H, m, 2-***H*****₂**), 2.08 – 1.95 (2H, m, 1-***H*****₂**), 1.64 (3H, d, *J* = 6.5 Hz, C***H*****₃**). δ_C (176 MHz, $CDCl_3$, 19% 2-((2R)-2-methylpyrrolidin-1-yl)ethan-1-ol hydrochloride) 65.3 (***C***-2'), 54.0 (***C***-3'), 53.8 (***C***-5'), 37.6 (***C***-4'), 31.1 (***C***-2), 21.6 (***C***-1), 15.7 (***C***H_3). *m/z* (LC-MS, ESI^+) 148 ($M(^{35}Cl)H^+$), 150 ($M(^{37}Cl)H^+$).

(2*S*)-1-(2-chloroethyl)-2-methylpyrrolidine hydrochloride (*S*)-154

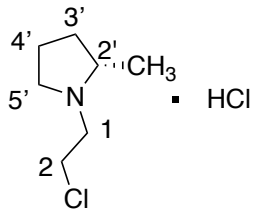

A solution of thionyl chloride (0.87 mL, 12 mmol) in chloroform (5 mL) was added dropwise to a solution of 2-((2*S*)-2-methylpyrrolidin-1-yl)ethan-1-ol **(*S*)-155** (575 mg, 4.45 mmol) in chloroform (5 mL) at 0 °C. The resulting mixture was heated under reflux for 2 h and then concentrated under reduced pressure. Precipitation from a mixture of EtOH and Et_2O afforded the title compound contaminated with 19% 2-((2*S*)-2-methylpyrrolidin-1-yl)ethan-1-ol hydrochloride (302 mg, 37%) as a brown semi-solid.

$[\alpha]_D$ (c = 1.00 g/100 mL, $CHCl_3$) +20.4°. ν_{max} (ATR) 3389 (br, m), 2974 (m), 2557 (m), 2461 (m), 1452 (m), 1423 (m), 1393 (m). NMR and mass spectra were consistent with the *R* enantiomer.

(2*S*)-1-{2-[(*S*)-(4-chlorophenyl)(phenyl)methoxy]ethyl}-2-methylpyrrolidine (*S*, *S*)-147

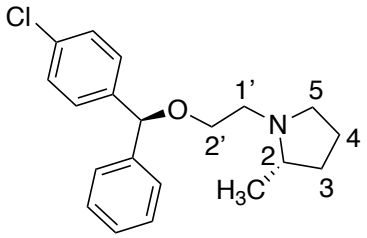

General procedure D was used in the reaction of (*S*)-4-chlorophenyl(phenyl)methanol **(*S*)-113** (119 mg, 0.43 mmol) and (2*S*)-1-(2-chloroethyl)-2-methylpyrrolidine **(*S*)-154** (63 mg, 0.43 mmol). The crude product was purified by flash column chromatography (0 → 100% EtOAc in hexanes with 1% NEt_3) to afford the title compound (78mg, 55%) as a colourless oil.

ν_{max} (ATR) 2962 (w), 2869 (w), 2787 (w), 1489 (m), 1453 (w), 1375 (w), 1086 (s), 1014 (m). δ_H (700 MHz, $CDCl_3$) 7.31 - 7.22 (9H, m, Ar***H***), 5.34 (1H, s, Ar_2C***H***), 3.57 (2H, t, *J* = 6.5 Hz, 2'-***H*₂**), 3.15 – 3.09 (1H, m, 5-***H***H'), 3.04 (1H, dt, *J* = 12.5, 6.5 Hz, 1'-***H***H'), 2.39 (1H, dt, *J* = 12.5, 6.5 Hz, 1'-H***H'***), 2.36 – 2.30 (1H, m, 2-***H***), 2.22 – 2.16 (1H, m, 5-H***H'***), 1.91 – 1.84 (1H, m, 3-***H***H'), 1.78 – 1.69 (1H, m, 4-***H***H'), 1.69 - 1.61 (1H, m, 4-H***H'***), 1.41 - 1.33 (1H, m, 3-***H***H'), 1.07 (3H, d, *J* = 6.0 Hz, CH_3). δ_C (176 MHz, $CDCl_3$) 142.0 (Ar***C***), 141.2 (Ar***C***), 133.2 (Ar***C***), 128.6(1) (Ar***C***), 128.6(0) (Ar***C***), 128.4 (Ar***C***), 127.8 (Ar***C***), 127.1 (Ar***C***), 83.4 (Ar_2C***H***), 68.6 (***C***-2'), 60.5 (***C***-2), 54.9 (***C***-5), 53.4 (***C***-1'), 32.6 (***C***-3), 22.0 (***C***-4), 19.1 (***C***H_3). *m/z* (LC-MS, ESI^+) 330 ($M(^{35}Cl)H^+$), 332 ($M(^{37}Cl)H^+$). Accurate mass: Found (MH^+), 330.1624: $C_{20}H_{25}NO^{35}Cl$ requires *M*, 330.1625.

(2*R*)-1-{2-[(S)-(4-chlorophenyl)(phenyl)methoxy]ethyl}-2-methylpyrrolidine (*R*, *S*)-147

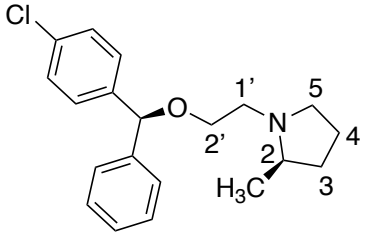

General procedure D was used in the reaction of (*S*)-4-chlorophenyl(phenyl)methanol **(*S*)-113** (67 mg, 0.24 mmol) and (2*R*)-1-(2-chloroethyl)-2-methylpyrrolidine (***R*)-154** (12 mg, 0.08 mmol). The crude product was purified by flash column chromatography (0 → 100% EtOAc in hexanes with 1% NEt_3) to afford the title compound (15 mg, 57 %) as a colourless oil.

ν_{max} (ATR) 2963 (w), 2870 (w), 2789 (w), 1490 (w), 1453 (w), 1375 (w), 1089 (m), 1015 (w). δ_H (700 MHz, $CDCl_3$) 7.33 – 7.29 (4H, m, Ar***H***), 7.29 - 7.27 (4H, m, Ar***H***), 7.26 – 7.23 (1H, m, Ar***H***), 5.36 (1H, s, Ar_2C***H***), 3.69 – 3.54 (2H, m, 2'-***H₂***), 3.22 - 3.14 (1H, m, 5-***H***H'), 3.12 – 3.05 (1H, m, 1'-***H***H'), 2.54 – 2.36 (2H, m, 1-H***H'***, 2-***H***), 2.34 – 2.22 (1H, m, 5-H***H'***), 1.98 – 1.86 (1H, m, 3-***H***H'), 1.84 – 1.74 (1H, m, 4-***H***H'), 1.73 – 1.64 (1H, m, 4-H***H'***), 1.49 – 1.36 (1H, m, 3-H***H'***), 1.12 (3H, d, *J* = 6.0 Hz, C***H₃***). δ_C (176 MHz, $CDCl_3$) 141.9 (Ar***C***), 141.0 (Ar***C***), 133.3 (Ar***C***), 128.7 (Ar***C***), 128.6 (Ar***C***), 128.5 (Ar***C***), 127.8 (Ar***C***), 127.1 (Ar***C***), 83.5 (Ar_2***C***H), 68.2 (***C***-2'), 60.7 (***C***-2), 54.8 (***C***-5), 53.4 (***C***-1'), 32.4 (***C***-3), 22.0 (***C***-4), 18.9 (***C***H_3). *m/z* (LC-MS, ESI^+) 330 ($M(^{35}Cl)H^+$), 332 ($M(^{37}Cl)H^+$). Accurate mass: Found (MH^+), 330.1634: $C_{20}H_{25}NO^{35}Cl$ requires *M*, 330.1625.

(2*R*)-1-{2-[(*R*)-(4-chlorophenyl)(phenyl)methoxy]ethyl}-2-methylpyrrolidine (*R*, *R*)-147

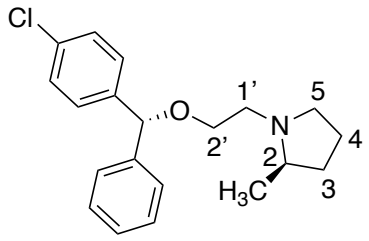

General procedure D was used in the reaction of (*R*)-4-chlorophenyl(phenyl)methanol **(*R*)-113** (100 mg, 0.36 mmol) and (2*R*)-1-(2-chloroethyl)-2-methylpyrrolidine (***R*)-154** (53 mg, 0.36 mmol). The crude product was purified by flash column chromatography (0 → 100% EtOAc in hexanes with 1% NEt_3) to afford the title compound as a colourless oil (72 mg, 61%).

ν_{max} (ATR) 2962 (w), 2869 (w), 2788 (w), 1490 (w), 1088 (m), 1015 (w). δ_H (700 MHz, $CDCl_3$) 7.32 - 7.20 (9H, m, Ar***H***), 5.35 (1H, s, Ar_2C***H***), 3.61 – 3.55 (2H, m, 2'-***H₂***), 3.16 – 3.12 (1H, m, 5-***H***H'), 3.06 (1H, dt, *J* = 12.5, 6.5 Hz, 1'-***H***H'), 2.41 (1H, dt, *J* = 12.5, 6.5 Hz, 1'-H***H'***), 2.38 – 2.32 (1H, m, 2-***H***), 2.24 – 2.18 (1H, m, 5-H***H'***), 1.91 – 1.85 (1H, m, 3-***H***H'), 1.80 – 1.71 (1H, m, 4-***H***H'), 1.70 - 1.63 (1H, m, 4-H***H'***), 1.42-1.35 (1H, m, 3-H***H'***), 1.09 (3H, d, *J* = 6.0 Hz, C***H₃***). δ_C (176 MHz, $CDCl_3$) 141.9 (Ar***C***), 141.1 (Ar***C***), 133.2 (Ar***C***), 128.5(8) (Ar***C***), 128.5(7) (Ar**C**), 128.4 (Ar***C***), 127.7 (Ar***C***), 127.1 (Ar***C***), 83.4 (Ar_2***C***H), 68.5 (***C***-2'), 60.5 (***C***-2), 54.9 (***C***-5), 53.4 (***C***-1'), 32.5 (***C***-3), 22.0 (***C***-4), 19.1 (***C***H_3). m/z (LC-MS, ESI^+) 330 ($M(^{35}Cl)H^+$), 332 ($M(^{37}Cl)H^+$). Accurate mass: Found (MH^+), 330.1632: $C_{20}H_{25}NO^{35}Cl$ requires *M*, 330.1625.

{2-[(4-chlorophenyl)(phenyl)methoxy]ethyl}dimethylamine[265] 151

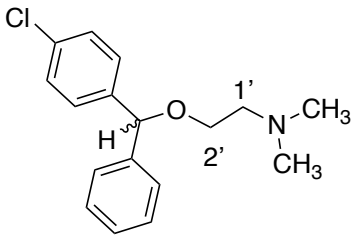

1-[(2-Bromoethoxy)(phenyl)methyl]-4-chlorobenzene **180** (170 mg, 0.50 mmol) in DMF (1 mL) was added dropwise to a suspension of dimethylamine hydrochloride (41 mg, 0.50 mmol), KI (8 mg, 0.05 mmol) and K_2CO_3 (138 mg, 1.00 mmol) in DMF (1 mL). The reaction mixture was stirred at rt for 4 h and then further portions of dimethylamine hydrochloride (82 mg, 1.00 mmol) and K_2CO_3 (207 mg, 1.5 mmol) were added and the mixture was stirred at rt for a further 24 h. Following the addition of H_2O (5 mL) and extraction with EtOAc (3 x 5 mL), the combined organic layers were dried and concentrated *in vacuo.* The crude product was purified by column chromatography (0 → 100% EtOAc in hexanes with 1% NEt_3) to afford the title compound (41 mg, 28 %) as a brown oil.

ν_{max} (ATR) 2942 (w), 2862 (w), 2819 (w), 1490 (w), 1454 (w), 1089 (w), 1015 (w). δ_H (600 MHz, $CDCl_3$) 7.33 -7.23 (9H, m, Ar***H***), 5.34 (1H, s, Ar_2C***H***), 3.58 – 3.52 (2H, m, 2'-***H₂***), 2.59 (2H, t, *J* = 6.0 Hz, 1'-***H₂***), 2.27 (6H, s, 2 x C***H₃***). δ_C (151 MHz, $CDCl_3$) 141.9 (Ar***C***), 141.1 (Ar***C***), 133.2 (Ar***C***), 128.6(2) (Ar***C***), 128.6(0) (Ar***C***), 128.5 (Ar***C***), 127.8 (Ar***C***), 127.1 (Ar***C***), 83.5 (Ar_2C***H***), 67.8 (***C***-2'), 59.1 (***C***-1'), 46.2 (***C***H_3). *m/z* (LC-MS, ESI^+) 290 ($M(^{35}Cl)H^+$), 292 ($M(^{37}Cl)H^+$). Accurate mass: Found ($M(^{35}Cl)H^+$), 290.1334: $C_{17}H_{21}NO^{35}Cl$ requires *M*, 290.1312.

1-[(3-bromopropoxy)(phenyl)methyl]-4-chlorobenzene 183

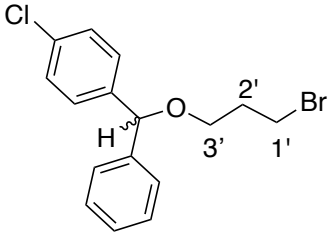

To a solution of 4-chlorophenyl(phenyl)methanol **113** (500 mg, 2.29 mmol) and AuCl (33 mg, 0.23 mmol) in DCE was added 3-bromopropanol (318 mg, 2.29 mmol). This reaction was heated to 80 °C for 16 h. The solvent was then removed under reduced pressure and

purified by flash column chromatography (0 → 20% EtOAc in hexanes) to afford the product as a colourless oil (244 mg, 54%).

ν_{max} (ATR) 3029 (w), 2866 (w), 1489 (m), 1088 (s), 1014 (m). δ_H (700 MHz, $CDCl_3$) 7.37 – 7.27 (9H, m, Ar***H***), 5.5 (1H, s, Ar_2C***H***), 3.61 – 3.56 (4H, m, 3'-***H***$_2$, 1'-***H*****$_2$**), 2.18 (2H, p, *J* = 6.0 Hz, 2'-***H*****$_2$**). δ_C (176 MHz, $CDCl_3$) 141.8 (Ar***C***), 140.9 (Ar***C***), 133.3 (Ar***C***), 128.7 (Ar***C***), 128.6 (Ar***C***), 128.4 (Ar***C***), 127.9 (Ar***C***), 127.0 (Ar***C***), 83.3 (Ar_2***C***H), 66.6 (***C***-3'), 33.1 (***C***-2'), 30.8 (***C***-1'). *m/z* (LC-MS, ESI^+) 201 ($M(^{35}Cl)$-$OC_3H_6Br^+$), 203 ($M(^{37}Cl)$- $OC_3H_6Br^+$). Accurate mass: Found (M-$OC_3H_6Br^+$), 201.0474: $C_{13}H_{10}{}^{35}Cl$ requires *M,* 201.0471.

(2*S*)-1-{3-[(4-chlorophenyl)(phenyl)methoxy]propyl}-2-methylpyrrolidine (*S*)-157

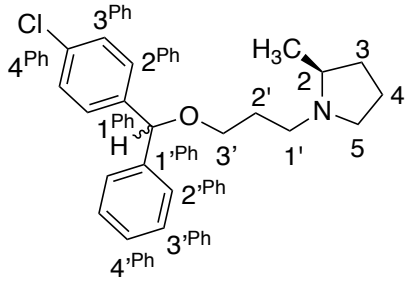

1-[(3-bromopropoxy)(phenyl)methyl]-4-chlorobenzene **183** (320 mg, 0.94 mmol) in DMF (5 mL) was added dropwise to a suspension of (2*S*)-2-methylpyrrolidine hydrochloride (115 mg, 0.94 mmol), KI (17g, 0.1 mmol) and K_2CO_3 (210mg, 1.88 mmol) in DMF (10 mL). The reaction was then stirred at rt for 24 h. Following the addition of EtOAc (10 mL), the organic layer was washed with H_2O (5 x 10 mL), dried over Na_2SO_4, filtered and concentrated *in vacuo*. The crude product was purified by column chromatography (10% MeOH in $CHCl_3$) to afford the title compound (217 mg, 65 %) as a colourless oil.

ν_{max} (ATR) 2960 (w), 2869 (w), 2789 (w), 1489 (m), 1087 (s), 1014 (m). δ_H (600 MHz, $CDCl_3$, mixture of diastereomers) 7.32 – 7.29 (4H, m, Ar***H***), 7.28 – 7.26 (4H, m, Ar***H***), 7.26 – 7.22 (1H, m, Ar***H***), 5.30 (1H, s, Ar_2C***H***), 3.51 – 3.47 (2H, m, 3'-***H*****$_2$**), 3.17 – 3.09 (1H, m, 5-***H***H***'***), 2.95 – 2.86 (1H, m, 1'-***H***H'), 2.31 – 2.22 (1H, m, 2-***H***), 2.16 – 2.10 (1H, m, 1'-H***H'***), 2.10 – 2.04 (1H, m, 5-H***H'***), 1.93 – 1.81 (3H, m, 2'-***H*****$_2$**, 3-***H***H'), 1.80 – 1.71 (1H, m, 4-***H***H'), 1.70 – 1.62 (1H, m, 4-H***H'***), 1.46 – 1.36 (1H, m, 3-H***H'***), 1.08 (1.5H, d, *J* = 6.0, C***H*****$_3$**), 1.08 (1.5H, d, *J* = 6.0, C***H*****$_3$**). δ_C (151 MHz, $CDCl_3$, mixture of diastereomers) 142.2 (***C***-$1'^{Ph}$), 141.2(8) (***C***-1^{Ph}), 141.2(8) (***C***-1^{Ph}), 133.1(3) (***C***-4^{Ph}), 133.1(2) (***C***-4^{Ph}), 128.5(7) (Ar***C***), 128.5(5) (Ar***C***), 128.5(4) (Ar***C***), 128.5(2)

(Ar***C***), 128.4 (Ar***C***), 127.6(6) (***C***-4'^{Ph}), 127.6(5) (***C***-4'^{Ph}), 127.0 (Ar***C***), 83.0 (Ar_2***C***H), 67.8(3) (***C***-3'), 67.8(0) (***C***-3'), 60.3 (***C***-2), 54.0(7) (***C***-5), 54.0(6) (***C***-5), 51.3 (***C***-1'), 51.2 (***C***-1'), 32.8 (***C***-3), 29.2 (***C***-2'). 21.7 (***C***-4), 19.1 (***C***H_3). m/z (LC-MS, ESI^+) 344 (M(^{35}Cl)H^+), 346 (M(^{37}Cl)H^+). Accurate mass: Found (M(^{35}Cl)H^+), 344.1784: $C_{21}H_{27}{}^{35}ClNO$ requires *M,* 344.1781.

3-[(2*S*)-2-methylpyrrolidin-1-yl]propan-1-ol (*S*)-184

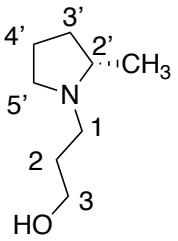

3-Bromopropanol (0.72 mL, 7.9 mmol) in dry MeCN (5 mL) was added dropwise to a mixture of (*S*)-2-methylpyrrolidine (1 g, 8.2 mmol) and K_2CO_3 (2.27g, 16.4 mmol) in dry MeCN (5 mL) heated under reflux. After 15 h the mixture was cooled to rt, filtered and concentrated. Et_2O (10 mL) was then added and the product extracted with 1M HCl (2 x 10 mL). The aqueous phase was made more basic with solid NaOH, then extracted with DCM (3 x 10 mL). The organic layers were combined, dried over Na_2SO_4, filtered and concentrated to afford product (620 mg, 55%) as a colourless oil. Carried through without further purification.

ν_{max} (ATR) 3372 (br), 2961 (m), 2872 (w), 1114 (w). δ_H (400 MHz, $CDCl_3$) 3.81 – 3.72 (2H, m, 3-***H*****$_2$**), 3.35 – 3.26 (1H, m, 1-***H***H'), 3.02 – 2.91 (1H, m, 5'-***H***H'), 2.43 – 2.34 (1H, m, 5'-H***H'***), 2.33 – 2.23 (1H, m, 2'-***H***H'), 2.13 - 2.02 (1H, m, 1-H***H'***), 2.01 - 1.81 (2H, m, 2-***H***H', 3'-***H***H'), 1.79 – 1.60 (2H, m, 4'-***H*****$_2$**), 1.58 - 1.46 (1H, m, 2-H***H'***), 1.43 - 1.29 (1H, m, 3'-H***H'***), 1.11 (3H, d, *J* = 6.0 Hz, C***H*****$_3$**). δ_C (176 MHz, $CDCl_3$) 69.3 (***C***-2'), 61.9 (***C***-5'), 54.0 (***C***-1), 50.9 (***C***-3), 32.2 (***C***-3'), 27.3 (***C***-2), 21.6 (***C***-4'), 18.1 (***C***H_3). *m/z* (LC-MS, ESI^+) 144 (MH^+). Accurate mass: Found (MH^+), 144.1393: $C_8H_{18}NO$ requires *M,* 144.1388.

(2*S*)-1-(3-chloropropyl)-2-methylpyrrolidine hydrochloride (*S*)-185

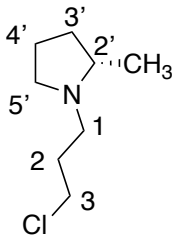

. HCl

A solution of thionyl chloride (0.74 mL, 10.24 mmol) in chloroform (2 mL) was added dropwise to a solution of 3-[(2*S*)-2-methylpyrrolidin-1-yl]propan-1-ol **(*S*)-184** (491 mg, 3.43 mmol) in chloroform (6 mL) at 0 °C. The mixture was heated to reflux for 2 h and concentrated under reduced pressure. The product was precipitated from ethanol and diethylether to afford the title compound (172 mg, 25%) contaminated with 19% 3-[(2*S*)-2-methylpyrrolidin-1-yl]propan-1-ol hydrochloride.

ν_{max} (ATR) 3404 (br), 2964 (m), 2600 (w), 2511 (w), 1633 (w), 1453 (w), 1063 (w). M.p. 125 – 127 °C (lit.[266]: 150.5 – 152.0 °C). δ_H (700 MHz, $CDCl_3$, 19% 3-[(2*S*)-2-methylpyrrolidin-1-yl]propan-1-ol hydrochloride) 12.15 (1H, s, N^+H), 3.93 - 3.83 (1H, m, 5'-***H***H'), 3.74 – 3.62 (2H, m, 3-***H*~2~**), 3.44 - 3.37 (1H, m, 1-***H***H'), 3.24 – 3.12 (1H, m, 2'-***H***), 3.00 – 2.92 (1H, m, 1-***H***H'), 2.89 – 2.79 (1H, m, 5'-H***H'***), 2.72 – 2.61 (1H, m, 2-***H***H'), 2.29 - 2.16 (3H, m, 3'-***H***H', 4'-***H***H', 2-H***H'***), 2.11 – 1.96 (2H, m, 3'-H***H'***, 4'- H***H'***), 1.64 (3H, d, *J* = 6.5 Hz, C***H*~3~**). δ_C (176 MHz, $CDCl_3$, 19% 3-[(2S)-2-methylpyrrolidin-1-yl]propan-1-ol hydrochloride) 65.3 (***C***-2'), 53.5 (***C***-5'), 51.4 (***C***-1), 42.1 (***C***-3), 31.5 (***C***-3'), 28.2 (***C***-2), 21.5 (***C***-4'), 15.7 (***C***H_3). *m/z* (LC-MS, ESI^+) 162 ($M(^{35}Cl)H^+$), 164 ($M(^{37}Cl)H^+$). Accurate mass: Found (MH^+), 162.1041: $C_8H_{17}N^{35}Cl$ requires *M,* 162.1050.

(2*S*)-1-{3-[(R)-(4-chlorophenyl)(phenyl)methoxy]propyl}-2-methylpyrrolidine (*S*, *R*)-157

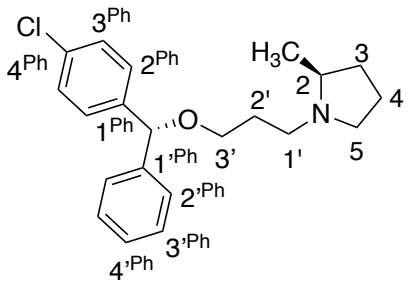

General procedure D was used for the reaction of (*R*)-4-chlorophenyl(phenyl)methanol **113** (76 mg, 0.27 mmol) and (2*R*)-1-(2-chloropropyl)-2-methylpyrrolidine **(*S*)-185** (101 mg, 0.62

mmol). The crude product was purified by flash column chromatography (0 → 100% EtOAc in hexanes with 1% NEt_3) to afford the title compound (78 mg, 55%) as a colourless oil.

ν_{max} (ATR) 2960 (w), 1489 (w), 1089 (w**).** δ_H (700 MHz, $CDCl_3$) 7.32 – 7.29 (4H, m, Ar***H***), 7.27 – 7.22 (5H, m, Ar***H***), 5.30 (1H, s, Ar_2C***H***), 3.49 (2H, td, *J* = 6.0, 1.5 Hz, 3'-***H₂***), 3.21 – 3.15 (1H, m, 5-***H***H'), 2.98 – 2.90 (1H, m, 1'-***H***H'), 2.39 – 2.31 (1H, m, 2-***H***), 2.22 – 2.10 (2H, m, 1'-H***H'***, 5-H***H'***), 1.96 – 1.85 (3H, m, 2'-***H₂***, 3-***H***H'), 1.83 – 1.75 (1H, m, 4-***H***H'), 1.73 – 1.65 (1H, m, 4-H***H'***), 1.50 – 1.42 (1H, m, 3-H***H'***), 1.12 (3H, d, *J* = 6.0 Hz, C***H₃***). δ_C (176 MHz, $CDCl_3$) 142.1 (***C***-$1'^{Ph}$), 141.2 (***C***-1^{Ph}), 133.2 (***C***-4^{Ph}), 128.5(7) (Ar***C***), 128.5(6) (Ar***C***), 128.4 (Ar***C***), 127.7 (***C***-$4'^{Ph}$), 127.0 (Ar***C***), 83.0 (Ar_2***C***H), 67.6 (***C***-3'), 60.7 (***C***-2), 53.9 (***C***-5), 51.2 (***C***-1'), 32.7 (***C***-3), 28.9 (***C***-2'), 21.7 (***C***-4), 18.7 (***C***H_3). *m/z* (LC-MS, ESI^+) 344 ($M(^{35}Cl)H^+$), 346 ($M(^{37}Cl)H^+$). Accurate mass: Found (MH^+), 344.1783: $C_{21}H_{27}NO^{35}Cl$ requires *M,* 344.1781.

1-[(4-bromobutoxy)(phenyl)methyl]-4-chlorobenzene 186

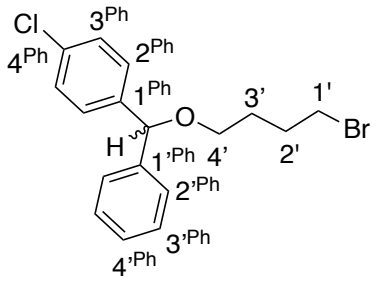

General procedure C was used for 4-chlorophenyl(phenyl)methanol **113** (531 mg, 2.43 mmol) and 4-bromobutanol (372 mg, 2.43 mmol) with the modification of AuCl (56 mg, 0.24 mmol) as the catalyst in the place of $PdCl_2$ with a reaction time of 20 h. The crude product was purified by column chromatography (0 → 20% EtOAc in hexanes) to afford the title compound (350 mg, 41%) as a colourless oil.

ν_{max} (ATR) 3029 (w), 2941 (w), 2863 (w), 1489 (m), 1086 (s), 1014 (m). δ_H (600 MHz, $CDCl_3$) 7.36 – 7.24 (9H, m, Ar***H***), 5.30 (1H, s, Ar_2C***H***), 3.47 (2H, t, *J* = 6.5 Hz, 4'-***H₂***), 3.43 (2H, t, *J* = 6.5 Hz, 1'-***H₂***), 2.00 (2H, p, *J* = 6.5 Hz, 2'-***H***), 1.79 (2H, p, *J* = 6.5 Hz, 3'-***H***). δ_C (176 MHz, $CDCl_3$) 142.0 (***C***-1^{Ph}), 141.1 (***C***-$1'^{Ph}$), 133.2 (***C***-4^{Ph}), 128.6(4) (***C***-$3'^{Ph}$), 128.6(1) (***C***-3^{Ph}), 128.3 (***C***-2^{Ph}), 127.8 (***C***-$4'^{Ph}$), 127.0 (***C***-$2'^{Ph}$), 83.1 (Ar_2***C***H), 68.1 (***C***-4'), 33.8 (***C***-1'), 29.9 (***C***-2'), 28.5 (***C***-3'). *m/z* (LC-MS, ESI^+) 201 ($M(^{35}Cl)$-$OC_4H_8Br]^+$), 203 ($M(^{37}Cl)$-$OC_4H_8Br]^+$). Accurate mass: Found ($[M-OC_4H_8Br]^+$), 201.0480: $C_{13}H_{10}{}^{35}Cl$ requires *M,* 201.0471.

(2*S*)-1-{4-[(4-chlorophenyl)(phenyl)methoxy]butyl}-2-methylpyrrolidine (*S*)-158

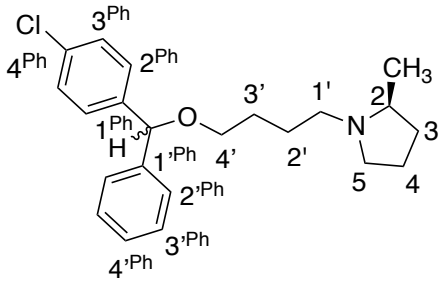

1-[(4-bromobutoxy)(phenyl)methyl]-4-chlorobenzene **186** (106 mg, 0.3 mmol) in DMF (0.5 mL) was added dropwise to a suspension of (2*R*)-2-methylpyrrolidine hydrochloride (46 mg, 0.38 mmol), KI (7 mg, 0.04 mmol) and K_2CO_3 (105 mg, 0.76 mmol) in DMF (1 mL). The reaction was stirred at rt for 24 h. Following the addition of EtOAc (10 mL), the organic layer was washed with H_2O (5 x 10 mL), dried over Na_2SO_4, filtered and concentrated *in vacuo*. The crude product was purified by column chromatography (0 → 100% EtOAc in hexanes with 1% NEt_3) to afford the title compound as a colourless oil (49 mg, 46 %).

ν_{max} (ATR) 2954 (w), 2867 (w), 2789 (w), 1490 (m), 1453 (w), 1089 (s), 1015 (m). δ_H (600 MHz, $CDCl_3$) 7.31 – 7.28 (4H, m, Ar***H***), 7.27 - 7.21 (5H, m, Ar***H***), 5.28 (1H, s, Ar_2C***H***), 3.47 – 3.41 (2H, m, 3'-***H₂***), 3.18 – 3.12 (1H, m, 5-***H***H'), 2.81 – 2.74 (1H, m, 1'-***H***H'), 2.29 – 2.19 (1H, m, 2-***H***), 2.09 –1.96 (2H, m, 5-H***H'***, 1'-H***H'***), 1.93 – 1.85 (1H, m, 3-***H***H'), 1.81 – 1.72 (1H, m, 4-***H***H'), 1.72 – 1.55 (5H, m, 4-H***H'***, 3'-***H₂***, 2'-***H***$_2$), 1.45 – 1.38 (1H, m, 3-H***H'***), 1.07 (3H, d, *J* = 6.0, C***H₃***). δ_C (176 MHz, $CDCl_3$, mixture of diastereomers) 142.2(1) (***C***-1'^{Ph}), 142.2(0) (***C***-1'^{Ph}), 141.3 (***C***-1^{Ph}), 133.2 (***C***-4^{Ph}), 128.6(0) (Ar***C***), 128.5(9) (Ar***C***), 128.5(7) (Ar***C***), 128.5(6) (Ar***C***), 128.3(9) (Ar***C***), 128.3(8) (Ar***C***), 127.7 (***C***-4'^{Ph}), 127.0(3) (Ar***C***), 127.0(1) (Ar***C***), 83.1 (Ar_2***C***H), 69.1(6) (***C***-4'), 69.1(5) (***C***-4'), 60.5 (***C***-2), 54.3 (***C***-1'), 54.2 (***C***-1'), 54.1 (***C***-5), 32.8 (***C***-3), 28.2(4) (***C***-2'), 28.2(3) (***C***-2'), 25.7 (***C***-3'), 21.7 (***C***-4), 19.0 (***C***H_3). *m/z* (LC-MS, ESI^+) 358 (M(^{35}Cl)H^+), 360 (M(^{37}Cl)H^+). Accurate mass: Found (MH^+), 358.1949: $C_{22}H_{28}{}^{35}ClNO$ requires *M,* 358.1938.

7.4. Additional compound

Diphenylmethanol[267] 187

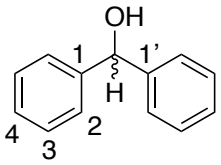

General procedure A was used with bromobenzene (2.60 mL, 24.80 mmol) and benzaldehyde (1.95 mL, 19.10 mmol). The product was purified by column chromatography (0 → 20% EtOAc in hexanes) to afford the title compound (1.35 g, 38 %) as colourless oil.

ν_{max} (ATR) 3371 (br, m), 1596 (w), 1494 (m), 1455 (m), 1494 (m), 1351 (w), 1269 (m), 1182 (m), 1171 (m), 1031 (m), 1017 (s). M.p. 60– 61 °C (lit.:[268] 63 - 64 °C); δ_H (600 MHz, $CDCl_3$) 7.40 – 7.37 (4H, m, 2-***H***), 7.36 – 7.32 (4H, m, 3-***H***), 7.29 – 7.26 (2H, m, 4-***H***), 5.86 (1H, s, Ar_2C***H***). δ_C (151 MHz, $CDCl_3$) 143.9 (***C***-1), 128.7 (***C***-3), 127.7 (***C***-4), 126.7 (***C***-2), 76.4 (Ar_2***C***H). m/z (LC-MS, ESI^+) 314 ($M\text{-}OH^+$).

N-(4-bromophenyl)-N,2-diphenylacetamide 188

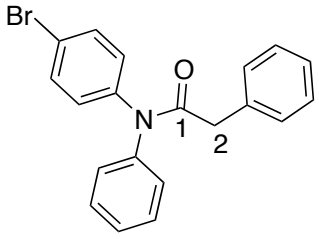

Diarylamine (248 mg, 1.00 mmol) was dissolved in dioxane (3 mL) and phenacetylchloride (0.26 mL, 2.00 mmol) was added dropwise at rt. Then, the mixture was refluxed for 1h. After cooling, the mixture was poured in ice-water (10 mL) and extracted with EtOAc (3 x 5 mL). The combined organics were washed with brine (10 mL) and dried over Na_2SO_4. Crude product was purified by flash column chromatography (0 → 30% EtOAc in hexanes) to afford the title compound (221 mg, 60%) as a white solid.

M.p. 73 – 75 °C; ν_{max} (ATR) 3030 (w), 1668 (s), 1593 (w), 1486 (s), 1453 (w), 1349 (m), 1263 (m), 1206 (w), 1139 (w), 1100 (w), 1069 (m), 1030 (w), 1011 (m) cm^{-1}. δ_H (700 MHz, $CDCl_3$) 7.49 – 7.32 (4H, m, Ar***H***), 7.29 – 7.21 (4H, m, Ar***H***), 7.19 – 7.15 (2H, m, Ar***H***), 7.14 – 7.05 (4H, m, Ar***H***), 3.65 (2H, s, $ArC\boldsymbol{H}_2$). δ_C (176 MHz, $CDCl_3$) 171.1 (***C***O), 142.4 (Ar***C***), 141.9 (Ar***C***), 134.9

(Ar***C***), 132.8 (Ar***C***), 132.1 (Ar***C***), 129.9 (Ar***C***), 129.1 (Ar***C***), 128.6 (Ar***C***), 127.9 (Ar***C***), 127.0 (Ar***C***), 126.6 (Ar***C***), 119.4 (Ar***C***), 42.3 (Ar***C***H_2). *m/z* (LC-MS, ESI^+) 367 ($M(^{81}Br)H^+$), 369 ($M(^{79}Br)H^+$); Accurate mass: Found ($M(^{79}Br)H^+$), 366.0486: $C_{20}H_{17}NO^{79}Br$ requires *M,* 366.0494.

4-Bromo-N-phenyl-N-(2-phenylethyl)aniline 189

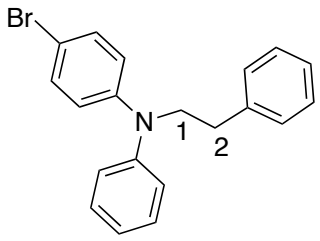

To a 5 °C solution of N-(4-bromophenyl)-N,2-diphenylacetamide **188** (1.55 g, 4.22 mmol) in THF (17 mL) was added borane dimethyl sulfide complex (2.10 mmol, 22 mmol) gradually and the reaction mixture was stirred at rt for 4 h. Then, 10 % acetic acid in MeOH (26 mL) was added and the resulting solution was stirred for 20 h. The solvent was removed by evaporation and product was extracted with EtOAc (3 x 10mL) in H_2O (10 mL). The combined organics were dried over Na_2SO_4 and the crude product was purified by column chromatography (0 → 30% EtOAc in hexanes) to afford title compound (280 mg, 19%) as a colourless oil.

ν_{max} (ATR) 3026 (w), 2930 (w), 1581 (m), 1486 (s), 1355 (m), 1244 (m), 1178 (m), 1072 (m), 1024 (w), 1008 (w) cm^{-1}. δ_H (700 MHz, $CDCl_3$) 7.35 – 7.29 (6H, m, Ar***H***), 7.26 – 7.23 (1H, m, Ar***H***), 7.21 - 7.18 (2H, m, Ar***H***), 7.06 - 7.00 (3H, m, Ar***H***), 6.82 - 6.77 (2H, m, Ar***H***), 3.95 -3.90 (2H, m, 1-***H₂***), 2.98 – 2.93 (2H, m, 2-***H₂***). δ_C (176 MHz, $CDCl_3$) 147.4 (Ar***C***), 147.1 (Ar***C***), 139.3 (Ar***C***), 132.2 (Ar***C***), 129.7 (Ar***C***), 128.9 (Ar***C***), 128.7 (Ar***C***), 126.5 (Ar***C***), 122.7 (Ar***C***), 122.5 (Ar***C***), 121.3 (Ar***C***), 112.8 (Ar***C***), 54.2 (***C***-1), 33.7 (***C***-2). *m/z* (LC-MS, ESI^+) 354 ($M(^{81}Br)H^+$), 352 ($M(^{79}Br)H^+$); Accurate mass: Found ($M(^{79}Br)H^+$), 352.0680: $C_{20}H_{19}N^{79}Br$ requires *M,* 352.0701.

[1-(3-phenylpropoxy)ethyl]benzene[269] 190

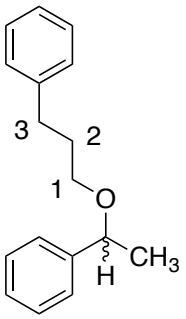

General procedure C was used with phenyl propanol (136 mg, 1.00 mmol) and 1-phenyl ethanol (122 mg, 1.00 mmol) with the modification of AuCl (23 mg, 0.10 mmol) as the catalyst in the place of $PdCl_2$ with a reaction time of 20 h. The crude product was purified by flash column chromatography (0% → 20% EtOAc in hexanes) to afford title compound (116 mg, 48%) as a colourless oil.

ν_{max} (ATR) 2927 (w), 1494 (w), 1453 (w), 1104 (m) cm^{-1}. δ_H (700 MHz, $CDCl_3$) 7.38 – 7.15 (10H, m, Ar***H***), 4.40 (1H, q, *J* = 6.5 Hz, ArC***H***CH_3), 3.37 – 3.31 (2H, m, 1-***H***$_2$), 2.78 – 2.59 (2H, m, 3-***H***$_2$), 1.93 – 1.84 (2H, m, 2-***H***$_2$), 1.47 (3H, d, *J* = 6.5 Hz). δ_C (151 MHz, $CDCl_3$) 144.3 (Ar***C***), 142.2 (Ar***C***), 128.6 (Ar***C***), 128.5 (Ar***C***), 128.4 (Ar***C***), 127.5 (Ar***C***), 126.3 (Ar***C***), 125.8 (Ar***C***), 78.1 (ArC***H***CH_3), 68.0 (***C***-1), 32.6 (***C***-3), 31.7 (***C***-2), 24.3 (***C***H_3); *m/z* (LC-MS, ESI^+) 263 (MNa^+).

1-(4-bromophenyl)-1-phenylethan-1-ol[270] 191

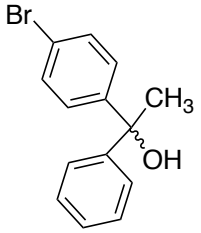

General procedure A was used with bromobenzene (2.40 mL, 22.67 mmol) and 4-bromoacetophenone (3.00 g, 15.10 mmol). The product was purified by flash column chromatography (0% → 20% ether in hexanes) to afford the title compound (1.20 g, 29%) as a colourless oil.

ν_{max} (ATR) 3434 (br, w), 2977 (w), 1590 (w), 1485 (m), 1446 (m), 1394 (m), 1372 (m), 1328 (m), 1224 (w), 1120 (w), 1173 (w), 1120 (w), 1027 (w), 1070 (m), 1008 (s) cm^{-1}. δ_H (700 MHz, $CDCl_3$) 7.45 – 7.41 (2H, m, Ar***H***), 7.40 - 7.38 (2H, m, Ar***H***), 7.35 - 7.31 (2H, m, Ar***H***), 7.40 -

7.38 (3H, m, Ar***H***), 1.92 (3H, s, C***H₃***). δ_C (176 MHz, $CDCl_3$) 147.5 (Ar***C***), 147.2 (Ar***C***), 131.3 (Ar***C***), 128.4 (Ar***C***), 127.8 (Ar***C***), 127.4 (Ar***C***), 125.9 (Ar***C***), 121.0 (ArC), 76.1 (Ar_2***C***H), 30.8 (***C***H_3); *m/z* (GC-MS, EI) 278 ((^{81}Br)M^+), 276 ((^{79}Br)M^+).

1-bromo-4-(1-phenylethenyl)benzene[271] **192**

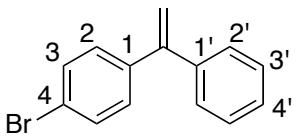

General Procedure C was used with benzyl (2*R*)-2-(2'-hydroxyethyl)pyrrolidine-1-carboxylate **(*R*)-133** (216 mg, 0.87 mmol) and 1-(4-bromophenyl)-1-phenylethan-1-ol **191** (241 mg, 0.87 mmol) with the modification of AuCl (20 mg, 0.09 mmol) as the catalyst in the place of $PdCl_2$ with a reaction time of 20 h. The crude product was purified by flash column chromatography (0% → 10% ether in hexanes) to afford the title compound (163 mg, 72%) as a colourless oil.

ν_{max} (ATR) 1660 (w), 1587 (w), 1485 (w), 1447 (w), 1394 (w), 1316 (w), 1281 (w), 1270 (w), 1071 (w), 1010 (m) cm^{-1}. δ_H (700 MHz, $CDCl_3$) 7.49 - 7.46 (2H, m, Ar***H***), 7.38 - 7.31 (5H, m, Ar***H***), 7.25 – 7.21 (2H, m, Ar***H***), 5.49 (1H, s, C***H***H'), 5.47 (1H, s, CH***H'***). δ_C (176 MHz, $CDCl_3$) 149.2 (Ar_2***C***), 141.1 (Ar***C***), 140.6 (Ar***C***), 131.5 (Ar***C***), 130.0 (Ar***C***), 128.4 (Ar***C***), 128.3 (Ar***C***), 128.1 (Ar***C***), 121.9 (Ar***C***), 114.9 (C***H₂***). *m/z* (GC-MS, EI) 260 ((^{81}Br)M^+), 258 ((^{79}Br)M^+).

8. Biological experimental

8.1. General experimental details

MATERIALS: Biological grade materials, solvents, reagents and media components were purchased from commercial suppliers and used as provided. NBD-C_6-ceramide **80** was from Invitrogen and AG 4-X4 ion exchange resin was from Bio-Rad. Reactions and media were prepared using ultrapure water from Milli-Q® water purification system. FBS refers to heat-inactivated foetal bovine serum. Solutions of test compounds were made up in DMSO, unless otherwise stated.

INSTRUMENTS AND EQUIPMENT: 1.5 mL Eppendorfs were used during the preparation of serial dilutions. Media were filter-sterilised using a vacuum filter with a 0.22 µm pore CA membrane. Centrifugation steps were carried out using Sorvall® Legend *RT* centrifuge, Sorvall® Legend Micro 17R centrifuge, Beckman Coulter® centrifuges and ultracentrifuges. Eppendorf tubes were centrifuged using Sigma 1-14 microfuge. Disruption of yeast cells was performed using an IKA® Vortex Genius 3. Protein content and optical density (OD) were determined using a Boeco S-32 spectrophotometer. Eppendorf contents were dried using an Eppendorf Vacuum Concentrator 5301. Cells were counted using a Neubauer haemocytometer. 96-well plates used were Nest Biotechnology Co., Ltd cell culture plates (clear); Corning® Costar® cell culture plates (clear); Corning® V-bottom (clear); MultiScreen® Solvinert filter plates (Merck Millipore) and PerkinElmer OptiPlate-96 (black). 24-well plates were supplied by Nest Biotechnology Co., Ltd and cover slips from Thomas Scientific®. Fluorescence quantification was carried out using SpectraMax® microplate reader with SoftMax® Pro 6.4 data analysis software from Molecular Devices and Synergy H4 and FLx800 microplate readers with Gen5® 1.08 data analysis software from Biotek. HPTLC silica plates were from Merck Millipore and imaged using a Fuji FLA-3000 plate reader with AIDA image analyser® (version 3.52).

8.2. Solutions, buffers and media compositions

Buffer/Solutions	Vol./Mass	Stock
STE Buffer (50 mL)	1.25 mL 12.5 mL 0.5 mL 1 tablet 36.15 mL	Tris-HCl (1 M, pH 7.4) Sucrose (1 M) EDTA (0.5 M, pH 8) Complete® Protease Inhibitor Cocktail H_2O
Storage Buffer (50 mL)	2.5 mL 6.25 mL 0.25 mL 1 tablet 41 mL	Tris/HCl Glycerol (80% w/v) $MgCl_2$ (1 M) Complete® Protease Inhibitor Cocktail H_2O
Phosphate Buffer (1L, 71.4 mM, pH 7.0)	3.77 g 7.71 g 1L	KH_2PO_4 K_2HPO_4 H_2O
Resazurin Solution	5 mg 40 mL	Resazurin sodium salt PBS

Growth Media	Vol./Mass	Stock
SGR-W-L (1 L)	1 g 10 g 5 g 1.93 g 640 mg 1L	Galactose Raffinose pentahydrate $(NH_4)_2SO_4$ Yeast Nitrogen Base – Amino acids – $(NH_4)_2SO_4$ LoFlo Amino acids Drop-Out Supplement -W-L H_2O

Schneider's Insect Medium, Merck® (stock) (1L, pH 7.0)	24.5 g 0.4 g 0.6 g 1 L	Schneider's Insect Medium $NaHCO_3$ $CaCl_2$ HCl (for pH adjustment) NaOH (for pH adjustment) H_2O
Schneider's Insect Medium (50 mL, pH 7.0)	42.5 mL 7.5 mL 0.5 mL	Schneider's Insect Medium (stock) FBS Penicillin Steptomycin (Pen Strep|)
Medium 199, Cultilab® (50 mL, pH 6.5)	250 µg 1 mL 5 mL 0.5 mL	Hemin Urine FBS Penicillin Steptomycin (Pen Strep|)
RPMI 1640 Medium, Cultilab® (50 mL, pH 7)	5 mL 0.5 mL	FBS HCl (for pH adjustment) Penicillin Steptomycin (Pen Strep|)

8.3. Protocols

All of the following biological procedures were carried out under sterile conditions unless otherwise stated.

8.3.1. *Leishmania* culture

Leishmania amazonensis (MHOM/Br/75/JOSEFA), *Leishmania donovani* (LV9) and *Leishmania infantum* (NCL) promastigotes were maintained at 26 °C in Medium 199, supplemented with 15% FBS. *Leishmania amazonensis* (MHOM/Br/75/JOSEFA), *Leishmania major* (FV1) WT and Δ *LCB2* promastigotes were maintained at 26 °C in Schneider's insect medium at pH 7, supplemented with 15% FBS. *Leishmania major* (FV1) PX promastigotes were maintained at 26 °C in Schneider's insect medium at pH 7, supplemented with 15% FBS and 40 µg mL^{-1} G418 (Gibco BRL). *Leishmania amazonensis*-

GFP were selected for bright green fluorescence by 48 h-incubation in the presence of 1000 μg mL^{-1} G418 (Gibco BRL).

8.3.2. Animals and ethics statement

All mice used in the experiments were maintained under controlled temperature, filtered air and water, autoclave bedding, and commercial food at the animal facilities at Federal University of Rio de Janeiro.

The animal protocols for this study were approved by the Federal University of Rio de Janeiro Institutional Animal Care and Use Committee under the number 030/17. The research was conducted in compliance with the principles stated in the *Guide for the Care and Use of Laboratory Animals* (NIH).[272]

8.3.3. Isolation of Bone Marrow Derived Macrophages (BMDM)

BMDM were differentiated from bone marrow of BALB/C, C57BL/6 and knock out C57BL/6 mice using L929-cell conditioned medium (LCCM) as a source of macrophage colony-stimulating factor (M-CSF) as described by Zamboni *et al.*[273] Briefly, bone marrow was extracted from the femurs and tibias and re-suspended in bone marrow differentiated media (which is RPMI 1640 medium supplemented with 20% LCCM) in Petri dishes for 7 days at 37 °C with 5% CO_2. After, the plates were washed with warm PBS to remove detached cells, the adherent BMDM were gently scraped off the surface and re-suspended in RPMI (without LCCM). These cells are ready to use in the assays described in section 8.4.2. and 8.4.3.

8.3.4. Drugs

Clemastine fumarate, miltefosine, pentostam, amphotericin B and cycloheximide were purchased from Sigma-Aldrich. Glucantime solution (meglumine antimoniate, 300 mg mL^{-1}) was a gift from Sanofi Aventis. Clemastine derivatives were synthesised using the procedure outline in the previous section. Stock solutions of clemastine and its derivatives (10 mM) were prepared in dimethyl sulfoxide (DMSO) and kept at 0 - 4° C. Subsequent dilutions were done in culture media. For *in vitro* assays, all drugs were serially diluted in

100% DMSO, and then diluted 1:100 in culture medium, so that all final drug concentrations contained 1% DMSO.

***In vivo* assay 1**: clemastine fumarate (oral) and miltefosine (oral) were dissolved in vehicle composed of sodium carboxymethylcellulose 0.5% w/v, benzyl alcohol 0.5% v/v, Tween-80 0.4% v/v diluted in 0.9% aqueous NaCl solution. The vehicle for clemastine (IL) and pentostam was PBS.

In vivo assay 2: clemastine fumarate (oral) was dissolved in ORA-PLUS (Perrigo). ORA-PLUS is composed of purified water, microcrystalline cellulose, carboxymethylcellulose sodium, xanthan gum, carrageenan, calcium sulfate, trisodium phosphate, citric acid and sodium phosphate as buffers, dimethicone antifoam emulsion. Preserved with methylparaben and potassium sorbate.

8.3.5. Fluorescence quantification

The fluorescence spectra of analogue **(*R*)-159** were quantified using the above SpectraMax® microplate reader. Images were taken using Nikon® microscope and B-2A filter cube (Ex470/Em515).

8.3.6. Preparation of *Lmj*IPCS microsomal material

Auxotrophic AUR1 mutant *S. cerevisiae* was complemented by the expression of the *L. major* IPCS to create YPH499-HIS-GAL-AUR1 pRS246 *Lmj*IPCS.[184] These steps were carried out under non-sterile conditions.

Step 1: Preparation of cell extract

Crude membranes from this mutant *S. cerevisiae* were prepared as described by Fischl *et al.*[274] The complemented yeast cells were propagated in SGR-W-L media until OD ≥ 0.8. Cells were harvested by centrifugation (4,000 x g, 4 °C, 10 min) and washed with cold PBS (3 x 20 mL). The cell pellet was weighed and re-suspended in STE buffer (1.5 mL per 1g wet cell mass (WCM)). The yeast cells were disrupted using pre-chilled, acid washed glass beads (425-600 μm, 1.5 mL per 1g WCM), using a vortex mixer. Disruption step involved 30 cycles of 1 min vortex mixing followed by a 1 min rest on ice. Glass beads, unbroken cells and cell-wall debris were pelleted by centrifugation (3,800 x g, 4 °C, 15 min) to obtain cell extract (supernatant) which was removed and stored on ice. The pellet was re-suspended in STE

buffer (0.5 mL per 1g WCM) and subjected to 20 further disruption cycles. Following centrifugation (3,800 x g, 4 °C, 15 min), the supernatant was removed and cell extracts combined.

Step 2: Preparation of crude microsomal membrane fraction

The microsomal membrane faction, enriched in IPCS, was isolated from the cell extract by differential centrifugation. An initial centrifugation of the cell extract (23,000 x g, 4 °C, 15 min) pelleted large organelles and cell debris. The supernatant was removed and re-centrifuged (150,000 x g, 4 °C, 90 min) to obtain a pellet enriched with microsomal membranes. The pellet was re-suspended in storage buffer (approximately 100 μL) and the protein content was determined according to Bradford's protocol.[275] The concentration was adjusted to 20 mg ml^{-1} and 100 μL aliquots were stored in LoBind Eppendorf tubes at -80 °C.

Step 3: Preparation of washed microsomal membranes

The crude microsomal membranes were adjusted to a concentration of 10 mg mL^{-1} using STE buffer. Equal volume of the microsomal membranes and 2.5% CHAPS solution were mixed together and kept on ice for 1 h without shaking. The mixture was centrifuged (150,000 x g, 4 °C, 90 min) and the pellet re-suspended in storage buffer. The protein content was quantified according to Bradford's protocol[275] and the membranes were stored in LoBind Eppendorf tubes at -80 °C.

Step 4: Determination of the Protein Content in Enzyme Units

To standardise the assay and remove variability from sample preparation, microsome samples were normalised with respect to active enzyme content. The data is presented in enzyme units (U), where one unit (U) of enzyme converts 1 pmol of substrate per minute under the conditions described (1U = 1 pmol(product) min^{-1}).

A stock solution of NBD-C_6-ceramide **80** at a concentration of 10 pmol μL^{-1} was used to produce a standard curve ranging from 0.2 pmol to 80 pmol. The volumes were adjusted to 200 μL with 1M potassium formate in MeOH and the fluorescence was read (Ex460/Em540).

Samples of the washed microsomal membranes were incubated with NBD-C_6-ceramide **80** and PI under assay conditions 8.4.7. and the product fluorescence measured (Ex460/Em540). Correlation with the standard curve allowed the activity of the microsome preparation to be determined in U μL^{-1}. The membranes were adjusted to 1.5 U μL^{-1} with storage buffer and stored in LoBind Eppendorf tubes at -80 °C.

8.4. Assays

8.4.1. Anti-promastigote assays

L. major promastigotes in Schneider's insect medium (100 µL at 1×10^6 mL^{-1}) were incubated in 96-well plates with compounds in triplicate (amphotericin B and cycloheximide were used as positive controls, and untreated parasites with 1% DMSO as a negative control) at 26 °C for 48 h. Resazurin Solution (10 µL) was then added and the plate incubated at 26 °C for 4 h prior to measurement using a fluorescence plate reader (555 - 585 nm). EC_{50} values were calculated using sigmoidal regression analysis (GraphPad Prism).

Protocol 1: *L. amazonensis* promastigotes in Medium 199 (100 µL at 5×10^5 mL^{-1}) were incubated in 96-well plates with compounds in triplicate (amphotericin B was used as a positive control, and untreated parasites with DMSO as a negative control) at 26 °C for 72 h. Resazurin Solution (10 µL) was then added and the plate incubated at 26 °C for 4 h prior to measurement using a fluorescence plate reader (555 - 585 nm). EC_{50} values were calculated using sigmoidal regression analysis (GraphPad Prism).
Protocol 2: Same procedure as above with the modification of a 48 h incubation time as opposed to 72 h and *Leishmania amazonensis* (MHOM/Br/75/JOSEFA) in Schneider's insect medium in the place of *Leishmania amazonensis* (MHOM/Br/75/JOSEFA) in Medium 199.

L. donovani promastigotes in Medium 199 (100 µL at 2×10^6 mL^{-1}) were incubated in 96-well plates with compounds in triplicate (amphotericin B was used as a positive control, and untreated parasites with DMSO as a negative control) at 26 °C for 72 h. Resazurin Solution (10 µL) was then added and the plate incubated at 26 °C for 4 h prior to measurement using a fluorescence plate reader (555 - 585 nm). EC_{50} values were calculated using sigmoidal regression analysis (GraphPad Prism).

L. infantum promastigotes in Medium 199 (100 µL at 2 × 10^6 mL^{-1}) were incubated in 96-well plates with compounds in triplicate (amphotericin B was used as a positive control, and untreated parasites with DMSO as a negative control) at 26 °C for 72 h. Resazurin Solution (10 µL) was then added and the plate incubated at 26 °C for 4 h prior to measurement using a fluorescence plate reader (555 - 585 nm). EC_{50} values were calculated using sigmoidal regression analysis (GraphPad Prism).

8.4.2. Anti-amastigote intramacrophage assay

Bone marrow derived macrophages obtained as in 8.3.3. were diluted in RPMI 1640 medium to a concentration of 2 x 10^5 $well^{-1}$ in a 24-well plate with round cover slips and incubated for 24 h at 37 °C and 5% CO_2. They were infected with *L. amazonensis* promastigotes (10:1) at 37 °C for 4 h. Then washed with PBS twice to remove extracellular promastigotes and fresh RPMI medium supplemented with 5% FBS was added. After 24 h serial dilutions of the test compounds in RPMI medium (350 µL) were added and the cells were incubated at 37 °C for 48 h. The adherent infected cells were then stained with Giemsa modified solution and amastigotes were counted using an optical Nikon® microscope.

8.4.3. Macrophage cytotoxicity assay

Bone marrow derived macrophages in RPMI 1640 medium were seeded (1 × 10^6 mL^{-1}, 100 µL $well^{-1}$) in 96-well plates and incubated for 24 h at 37 °C and 5% CO_2. Following removal of media, serial dilutions of the test compounds in fresh RPMI medium (100 µL) were added and the cells were incubated for 48 h at 37 °C and 5% CO_2. Aliquots of resazurin solution (10 µL) were then added and the cells were incubated at 37 °C and 5% CO_2 for 4 h. Cell-viability measurement was carried out using a fluorescence plate reader. Triton was used as a reference compound. EC_{50} values were calculated using sigmoidal regression analysis.

8.4.4. NO assay

The generation of nitrite in bone marrow derived macrophages was assessed by the Griess Reagent System (1% sulfanilamide / 0.1% N-(1-naphthyl)-ethylenediaminedihydrochloride/ 2.5% H_3PO_4). Uninfected macrophages (1 × 10^6 mL^{-1}, 100 µL $well^{-1}$) in 96-well plates were

incubated for 24 h at 37 °C and 5% CO_2. Following removal of media, serial dilutions of the test compounds in fresh RPMI medium (100 µL) were added and the plate was incubated for 48 h at 37 °C and 5% CO_2. The plates were centrifuged at 500 g/5 min and culture supernatants were then incubated with the Griess Reagent for 30 min at 37 °C. The absorbance was measured at 570 nm, and the nitrite concentration was determined using a standard curve of sodium nitrite (0 to 50 µM). The positive control was macrophages incubated with 1 µg mL^{-1} of LPS (Sigma-Aldrich, Brazil) and 10% conditioned medium of lymphocytes as a source of IFN. Negative controls were cells treated with DMSO and untreated cells.

8.4.5. *In vivo* assay

Assay 1:

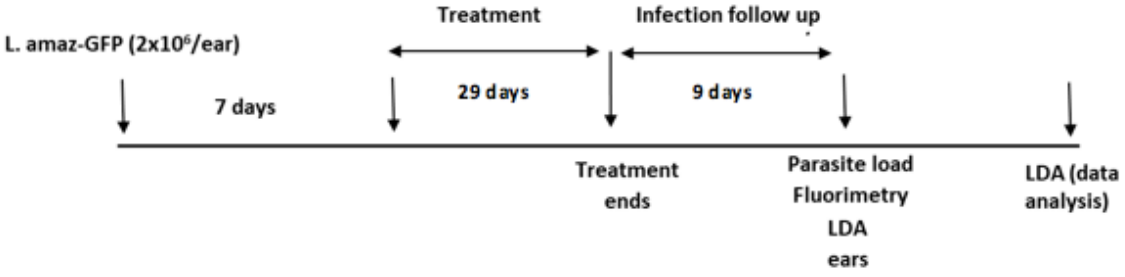

3 month old BALB/c female mice, weighing 20–25 g and of approximately the same age were used for the study. For infection of mice, stationary phase GFP *L. amazonensis* promastigotes were collected, washed and suspended in sterile PBS. A volume of 10 µl of sterile PBS containing 2 x 10^6 parasites was injected into the right ear. On day seven of infection, animals were randomly distributed into 5 groups; oral clemastine fumarate (3 animals), miltefosine (4 animals), IL clemastine fumarate (5 animals), pentostam (5 animals) and untreated (4 animals). Mice were treated with clemastine fumarate at a dose of 30 mg kg^{-1} and miltefosine at a dose of 2.5 mg kg^{-1} by oral gavage five times a week for 29 days. Mice were treated with clemastine fumarate and pentostam at a dose of 0.22 mg kg^{-1} by intralesional injection twice a week for 28 days. Infected ear thicknesses were measured once or twice a week with a caliper gauge, and the lesion sizes were expressed as the difference between the thickness of infected and non-infected ear. On day 45 animals were sacrificed and the fluorescence measured (485 - 528 nm) and parasite load quantified using a limiting dilution assay (LDA).

Assay 2:*

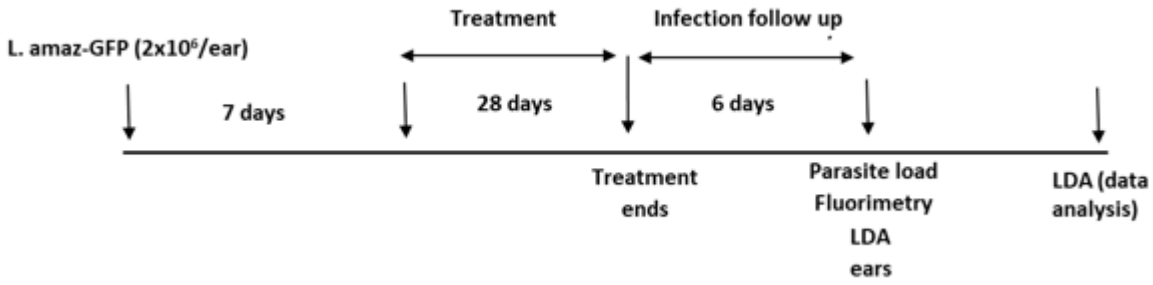

Two month old BALB/c female mice, weighing 20 - 25 g and of approximately the same age were used for the study. For infection of mice, stationary phase GFP *L. amazonensis* promastigotes were collected, washed and suspended in sterile PBS. A volume of 10 µl of sterile PBS containing 2 x 10^6 parasites was injected into the right ear. On day seven of infection, animals were randomly distributed into 5 groups; oral clemastine fumarate (5 animals), IP clemastine fumarate (5 animals), IL clemastine fumarate (5 animals), IP glucantime solution (5 animals) and untreated (6 animals). Mice were treated with clemastine fumarate at a dose of 134 mg kg^{-1} by oral gavage five times a week for 28 days. Mice were treated with clemastine fumarate and glucantime solution at a dose of 11.65 mg kg^{-1} and 1.30 g kg^{-1} respectively, by intraperitoneal injection twice a week for 28 days. Mice were treated with clemastine fumarate at a dose of 1.17 mg kg^{-1} by intralesional injection twice a week for 28 days. Infected ear thicknesses were measured once or twice a week with a caliper gauge, and the lesion sizes were expressed as the difference between the thickness of infected and non-infected ear. On day 41 animals were sacrificed and the fluorescence measured (485 - 528 nm) and parasite load quantified using a limiting dilution assay (LDA).

Data on lesion progression were analysed for statistical significance by using the Dunnett test as part of the one-way ANOVA (GraphPad Prism 8 software). A result was considered significant at * $P \leq 0.05$, ** $P \leq 0.01$, *** $P \leq 0.001$, **** $P \leq 0.0001$.[226]

***Collaboration with Douglas Escrivani at UFRJ**

8.4.6. High performance thin layer chromatography (HPTLC) based *Lmj*IPCS assay

The following protocol was adapted from a literature procedure and carried out under non-sterile conditions.[146]

Stock 1: Dry PI (1 mM, 30 μL) in a LoBind Eppendorf tube using a vacuum concentrator. To the dried PI, phosphate buffer (71.4 mM , pH 7.0, 105 μL), CHAPS (3 mM, 30 μL) and NBD-C_6-ceramide **80** (200 μM, 1.7 μL) was added. The solution was mixed by vortex and stored on ice.

Stock 2: Phosphate buffer (71.4 mM , pH 7.0, 105 μL), CHAPS (3 mM, 30 μL), storage buffer (6 μL) and microsomal membranes (1.5 μL) were combined in a LoBind Eppendorf tube.

Stock 2 (23.75 μL) was added to n LoBind Eppendorf tubes (where n is the number of test compounds + controls), followed by the addition test compounds in DMSO (5 mM, 1 μL). After pre-incubation at 30 °C for 20 min, the reaction was started by the addition of stock 1 (23.75 μL) to each tube and incubation at 30 °C for 30 min. The reaction mixtures were quenched with $CHCl_3$:MeOH:H_20 (10:10:3, 150 μL).

The mixtures were centrifuged to separate phases, the organic layer was removed and dried using a vacuum concentrator. The residue was re-suspended in $CHCl_3$:MeOH:H_20 (10:10:3, 20 μL) and loaded (3 x 3 μL) onto HPTLC plates (silica gel 60 F_{254}). This was run using the solvent system $CHCl_3$:MeOH:0.25% $KCl_{(aq)}$ (55:45:10) and the R_f values for the excess NBD-C_6-ceramide **80** and the product NBD- C_6-IPC **81** were 0.96 and 0.57 respectively. Product quantification was carried out using a fluorescence plate reader (Ex473/Em520).

8.4.7. 96-well plate–based *Lmj*IPCS assay

The following protocol was adapted from a literature procedure and carried out under non-sterile conditions.[146]

Stock 1: Dry PI (1 mM, 48 μL) in a glass vial using a vacuum concentrator. To the dried PI, phosphate buffer (71.4 mM , pH 7.0, 1680 μL), CHAPS (3 mM, 480 μL) and NBD-C_6-ceramide **80** (200 μM, 120 μL) was added. The solution was mixed by vortex and stored on ice.
Stock 2: Phosphate buffer (71.4 mM , pH 7.0, 1680 μL), CHAPS (3 mM, 480 μL), storage buffer (72 μL) and CHAPS-washed microsomal membranes (0.6 U) were combined in a glass vial. The solution was mixed by vortex and stored on ice.

In a V-bottom 96-well plate, stock 1 (19 μL $well^{-1}$) and test compounds (0.8 μL) were added. The reaction was initiated by the addition of stock 2 (20 μL $well^{-1}$) and was incubated at 30 °C for 25 min before quenching with MeOH (200 μL $well^{-1}$).

Separation of the reaction product, NBD-C_6-ceramide **80**, from the starting material, IPC-C_6-caramide **81**, was achieved using anion exchange chromatography. 20% w/v AG4-X4 resin in EtOH (200 μL $well^{-1}$) was added to a 96-well filter plate and centrifuged (2,450 x g, rt, 27 seconds). The resin was incubated with formic acid (50 μL $well^{-1}$) for 5 minutes before being centrifuged (2,450 x g, rt, 27 seconds). The resin was then washed with water and dried by centrifugation (2,450 x g, rt, 27 seconds).

The reaction mixture (200 μL) was loaded onto the resin and the starting material, NBD-C_6-ceramide **80**, removed by centrifugation (2,450 x g, rt, 1 min). The resin was washed with MeOH (5 x 200 μL) and subsequent centrifugation (2,450 x g, rt, 1 min). The product, NBD-C_6-IPC **81**, was eluted into black plates with potassium formate in MeOH (1M, 4 x 50 μL) followed by centrifugation (2,450 x g, rt, 1 min). Product quantification was carried out using a fluorescence plate reader (Ex460/Em540) and IC_{50} values were calculated using sigmoidal regression analysis (GraphPad Prism).

8.4.8. Error calculations

Each dose response curve is representative of one experiment and error bars represent the dose in triplicate. Errors for EC_{50} and CC_{50} values against promastigotes (Appendix B), amastigotes and macrophages (Appendix B) are reported as 95% confidence intervals (95% CI).

References

1 R. L. Charlton, B. Rossi-Bergmann, P. W. Denny and P. G. Steel, *Parasitology*, 2018, **145**, 219–236.
2 M. Guha, *Pharm. J.*, 2015, **294**, 7867.
3 S. M. Paul, D. S. Mytelka, C. T. Dunwiddie, C. C. Persinger, B. H. Munos, S. R. Lindborg and A. L. Schacht, *Nat. Rev. Drug Discov.*, 2010, **9**, 203–214.
4 T. T. Ashburn and K. B. Thor, *Nat. Rev. Drug Discov.*, 2004, **3**, 673–683.
5 T. I. Oprea and J. Mestres, *AAPS J.*, 2012, **14**, 759–763.
6 J. Aubé, *ACS Med. Chem. Lett.*, 2012, **3**, 442–444.
7 K. T. Andrews, G. Fisher and T. S. Skinner-Adams, *Int. J. Parasitol. Drugs Drug Resist.*, 2014, **4**, 95–111.
8 D. M. Klug, M. H. Gelb and M. P. Pollastri, *Bioorg. Med. Chem. Lett.*, 2016, **26**, 2569–2576.
9 V. Jain, A. Sharma, G. Singh, M. Yogavel and A. Sharma, *ACS Infect. Dis.*, 2017, **3**, 281–292.
10 S. Pushpakom, F. Iorio, P. A. Eyers, K. J. Escott, S. Hopper, A. Wells, A. Doig, T. Guilliams, J. Latimer, C. McNamee, A. Norris, P. Sanseau, D. Cavalla and M. Pirmohamed, *Nat. Rev. Drug Discov.*, 2019, **18**, 41–58.
11 M. T. M. Roberts, *Br. Med. Bull.*, 2006, **75–76**, 115–130.
12 L. Kedzierski, *J. Glob. Infect. Dis.*, 2010, **2**, 177–185.
13 http://www.who.int/entity/mediacentre/factsheets/fs375/en/index.html, (Accessed 26 December 2018).
14 C. Bern, J. H. Maguire and J. Alvar, *PLoS Negl. Trop. Dis.*, 2008, **2**, 10.
15 C. R. Davies, P. Kaye, S. L. Croft and S. Sundar, *BMJ*, 2003, **326**, 377–382.
16 J. Alvar, P. Aparicio, A. Aseffa, M. Den Boer, C. Cañavate, J.-P. Dedet, L. Gradoni, R. Ter Horst, R. López-Vélez and J. Moreno, *Clin. Microbiol. Rev.*, 2008, **21**, 334–359.
17 J. Alvar, I. D. Vélez, C. Bern, M. Herrero, P. Desjeux, J. Cano, J. Jannin and M. den Boer, *PLoS ONE*, 2012, **7**, 5.
18 L. Gradoni, *Eurosurveillance*, 2013, **18**, 20539.
19 L. Solano-Gallego, G. Miró, A. Koutinas, L. Cardoso, M. Pennisi, L. Ferrer, P. Bourdeau, G. Oliva and G. Baneth, *Parasit. Vectors*, 2011, **4**, 86.
20 M. Akhoundi, K. Kuhls, A. Cannet, J. Votýpka, P. Marty, P. Delaunay and D. Sereno, *PLoS Negl. Trop. Dis.*, 2016, **10**, 3.
21 https://www.cdc.gov/parasites/leishmaniasis/health_professionals/, (Accessed 28 January 2019).
22 L. Kedzierski, A. Sakthianandeswaren, J. Curtis, P. Andrews, P. Junk and K. Kedzierska, *Curr. Med. Chem.*, 2009, **16**, 599–614.
23 P. Shaked-Mishan, N. Ulrich, M. Ephros and D. Zilberstein, *J. Biol. Chem.*, 2001, **276**, 3971–3976.
24 R. L. Krauth-Siegel and M. A. Comini, *Biochim. Biophys. Acta*, 2008, **1780**, 1236–1248.
25 S. Sundar and J. Chakravarty, *Int. J. Environ. Res. Public. Health*, 2010, **7**, 4267–4277.
26 S. L. Croft, S. Sundar and A. H. Fairlamb, *Clin. Microbiol. Rev.*, 2006, **19**, 111–126.
27 D. Lockwood and E. Moore, *J. Glob. Infect. Dis.*, 2010, **2**, 151.
28 J. H. No, *Acta Trop.*, 2016, **155**, 113–123.
29 D. M. Kamiński, *Eur. Biophys. J. EBJ*, 2014, **43**, 453–467.
30 J. P. B. de Menezes, C. E. S. Guedes, A. Petersen, D. Fraga and P. Veras, *BioMed Res. Int.*, 2015, **2015**, 11.
31 S. Sundar and A. Singh, *Ther. Adv. Infect. Dis.*, 2016, **3**, 98–109.
32 S. Sundar and J. Chakravarty, *Expert Opin. Pharmacother.*, 2015, **16**, 237–252.

33 A. M. Musa, B. Younis, A. Fadlalla, C. Royce, M. Balasegaram, M. Wasunna, A. Hailu, T. Edwards, R. Omollo, M. Mudawi, G. Kokwaro, A. El-Hassan and E. Khalil, *PLoS Negl. Trop. Dis.*, 2010, **4**, e855.
34 M. M. Fernández, E. L. Malchiodi and I. D. Algranati, *Antimicrob. Agents Chemother.*, 2011, **55**, 86–93.
35 S. Sundar, T. K. Jha, C. P. Thakur, P. K. Sinha and S. K. Bhattacharya, *N. Engl. J. Med.*, 2007, **356**, 2571–2581.
36 A. Hailu, A. Musa, M. Wasunna, M. Balasegaram, S. Yifru, G. Mengistu, Z. Hurissa, W. Hailu, T. Weldegebreal, S. Tesfaye, E. Makonnen, E. Khalil, O. Ahmed, A. Fadlalla, A. El-Hassan, M. Raheem, M. Mueller, Y. Koummuki, J. Rashid, J. Mbui, G. Mucee, S. Njoroge, V. Manduku, A. Musibi, G. Mutuma, F. Kirui, H. Lodenyo, D. Mutea, G. Kirigi, T. Edwards, P. Smith, L. Muthami, C. Royce, S. Ellis, M. Alobo, R. Omollo, J. Kesusu, R. Owiti and J. Kinuthia, *PLOS Negl Trop Dis*, 2010, **4**, e709.
37 J. Soto and J. Berman, *Trans. R. Soc. Trop. Med. Hyg.*, 2006, **100**, S34–S40.
38 T. P. C. Dorlo, M. Balasegaram, J. H. Beijnen and P. J. de Vries, *J. Antimicrob. Chemother.*, 2012, **67**, 2576–2597.
39 K. Seifert, S. Matu, F. Javier Pérez-Victoria, S. Castanys, F. Gamarro and S. L. Croft, *Int. J. Antimicrob. Agents*, 2003, **22**, 380–387.
40 K. A. Bahamdan, T. M. Tallab, H. Johargi, M. M. Nourad, K. Ibrahim, A. H. el Sherbini, E. Karkashan, A. K. Khare and M. M. Nauri, *Int. J. Dermatol.*, 1997, **36**, 59–60.
41 A. A. Alrajhi, E. A. Ibrahim, E. B. De Vol, M. Khairat, R. M. Faris and J. H. Maguire, *N. Engl. J. Med.*, 2002, **346**, 891–895.
42 A. Z. Momeni, M. R. Reiszadae and M. Aminjavaheri, *Int. J. Dermatol.*, 2002, **41**, 441–443.
43 https://clinicaltrials.gov/show/NCT01790659, (Accessed 15 May 2016).
44 S. Sundar, P. K. Sinha, S. A. Dixon, R. Buckley, A. K. Miller, K. Mohamed and M. Al-Banna, *Am. J. Trop. Med. Hyg.*, 2011, **84**, 892–900.
45 B. B. Mishra, R. K. Singh, A. Srivastava, V. J. Tripathi and V. K. Tiwari, *Mini Rev. Med. Chem.*, 2009, **9**, 107–123.
46 B. B. Mishra, R. R. Kale, R. K. Singh and V. K. Tiwari, *Fitoterapia*, 2009, **80**, 81–90.
47 E. R. da Silva, C. do C. Maquiaveli and P. P. Magalhães, *Exp. Parasitol.*, 2012, **130**, 183–188.
48 B. Mittra, A. Saha, A. R. Chowdhury, C. Pal, S. Mandal, S. Mukhopadhyay, S. Bandyopadhyay and H. K. Majumder, *Mol. Med.*, 2000, **6**, 527–541.
49 T. F. P. de Mello, H. R. Bitencourt, R. B. Pedroso, S. M. A. Aristides, M. V. C. Lonardoni and T. G. V. Silveira, *Exp. Parasitol.*, 2014, **136**, 27–34.
50 J. C. Aponte, D. Castillo, Y. Estevez, G. Gonzalez, J. Arevalo, G. B. Hammond and M. Sauvain, *Bioorg. Med. Chem. Lett.*, 2010, **20**, 100–103.
51 M. Chen, S. B. Christensen, T. G. Theander and A. Kharazmi, *Antimicrob. Agents Chemother.*, 1994, **38**, 1339–1344.
52 P. Boeck, C. A. Bandeira Falcão, P. C. Leal, R. A. Yunes, V. C. Filho, E. C. Torres-Santos and B. Rossi-Bergmann, *Bioorg. Med. Chem.*, 2006, **14**, 1538–1545.
53 S. do Socorro, R. R. Mendonca-Filho, H. R. Bizzo, I. d. A. Rodrigues, R. M. A. Soares, T. Souto-Padron, C. S. Alviano and A. H. C. S. Lopes, *Antimicrob. Agents Chemother.*, 2003, **47**, 1895–1901.
54 E. C. Torres-Santos, D. Lopes, R. R. Oliveira, J. P. P. Carauta, C. A. B. Falcao, M. A. C. Kaplan and B. Rossi-Bergmann, *Phytomedicine Int. J. Phytother. Phytopharm.*, 2004, **11**, 114–120.

55 D. C. Arruda, F. L. D'Alexandri, A. M. Katzin and S. R. B. Uliana, *Antimicrob. Agents Chemother.*, 2005, **49**, 1679–1687.
56 N. Mazoir, A. Benharref, M. Bailén, M. Reina, A. González-Coloma and R. A. Martínez-Díaz, *Z. Naturforschung C J. Biosci.*, 2011, **66**, 360–366.
57 T. J. Schmidt, S. A. Khalid, A. J. Romanha, T. M. Alves, M. W. Biavatti, R. Brun, F. B. Da Costa, S. L. de Castro, V. F. Ferreira, M. V. G. de Lacerda, J. H. G. Lago, L. L. Leon, N. P. Lopes, R. C. das Neves Amorim, M. Niehues, I. V. Ogungbe, A. M. Pohlit, M. T. Scotti, W. N. Setzer, M. de N C Soeiro, M. Steindel and A. G. Tempone, *Curr. Med. Chem.*, 2012, **19**, 2176–2228.
58 N. Singh, B. B. Mishra, S. Bajpai, R. K. Singh and V. K. Tiwari, *Bioorg. Med. Chem.*, 2014, **22**, 18–45.
59 S. R. Bortolin Uliana and M. A. Barcinski, *Science*, 2009, **326**, 935–935.
60 M.- Klinkert and V. Heussler, *Mini-Rev. Med. Chem.*, 2006, **6**, 131–143.
61 R. Diaz-Gonzalez, F. M. Kuhlmann, C. Galan-Rodriguez, L. M. da Silva, M. Saldivia, C. E. Karver, A. Rodriguez, S. M. Beverley, M. Navarro and M. P. Pollastri, *PLOS Negl Trop Dis*, 2011, **5**, e1297.
62 G. Patel, N. E. Roncal, P. J. Lee, S. E. Leed, J. Erath, A. Rodriguez, R. J. Sciotti and M. P. Pollastri, *MedChemComm*, 2014, **5**, 655–658.
63 G. De Muylder, K. K. H. Ang, S. Chen, M. R. Arkin, J. C. Engel and J. H. McKerrow, *PLoS Negl. Trop. Dis.*, 2011, **5**, e1253.
64 M. W. Karaman, S. Herrgard, D. K. Treiber, P. Gallant, C. E. Atteridge, B. T. Campbell, K. W. Chan, P. Ciceri, M. I. Davis, P. T. Edeen, R. Faraoni, M. Floyd, J. P. Hunt, D. J. Lockhart, Z. V. Milanov, M. J. Morrison, G. Pallares, H. K. Patel, S. Pritchard, L. M. Wodicka and P. P. Zarrinkar, *Nat. Biotechnol.*, 2008, **26**, 127–132.
65 I. Peña, M. Pilar Manzano, J. Cantizani, A. Kessler, J. Alonso-Padilla, A. I. Bardera, E. Alvarez, G. Colmenarejo, I. Cotillo, I. Roquero, F. de Dios-Anton, V. Barroso, A. Rodriguez, D. W. Gray, M. Navarro, V. Kumar, A. Sherstnev, D. H. Drewry, J. R. Brown, J. M. Fiandor and J. Julio Martin, *Sci. Rep.*, 2015, **5**, 8771.
66 L. Sanderson, V. Yardley and S. L. Croft, *J. Antimicrob. Chemother.*, 2014, **69**, 1888–1891.
67 D. M. Wetzel, D. McMahon-Pratt and A. J. Koleske, *Mol. Cell. Biol.*, 2012, **32**, 3176–3186.
68 Q. Wang, B. A. Rosa, B. Nare, K. Powell, S. Valente, D. Rotili, A. Mai, G. R. Marshall and M. Mitreva, *PLoS Negl. Trop. Dis.*, 2015, **9**, e0004026.
69 V. Patil, W. Guerrant, P. C. Chen, B. Gryder, D. B. Benicewicz, S. I. Khan, B. L. Tekwani and A. K. Oyelere, *Bioorg. Med. Chem.*, 2010, **18**, 415–425.
70 P. Kapoor, M. Sachdeva and R. Madhubala, *FEMS Microbiol. Lett.*, 1999, **176**, 429–435.
71 L. Moulay, M. Robert-Gero, S. Brown, M. C. Gendron and F. Tournier, *Exp. Cell Res.*, 1996, **226**, 283–291.
72 R. J. Wheeler, E. Gluenz and K. Gull, *Mol. Microbiol.*, 2011, **79**, 647–662.
73 H. Martinez-Rojano, J. Mancilla-Ramirez, L. Quiñonez-Diaz and N. Galindo-Sevilla, *Antimicrob. Agents Chemother.*, 2008, **52**, 3642–3647.
74 J. Tavares, M. Ouaissi, A. Ouaissi and A. Cordeiro-da-Silva, *Acta Trop.*, 2007, **103**, 133–141.
75 S. Kaur, H. Sachdeva, S. Dhuria, M. Sharma and T. Kaur, *Parasitol. Int.*, 2010, **59**, 62–69.
76 M. Sharma, R. Sehgal and S. Kaur, *PLoS Negl. Trop. Dis.*, 2012, **6**, 5.
77 J. Akhtari, R. Faridnia, H. Kalani, R. Bastani, A. Kazemi Beydokhti, H. Rezvan and M. Fakhar, *J. Glob. Antimicrob. Resist.*, 2018, **16**, 11–16.
78 S. Kansal, R. Tandon, P. Dwivedi, P. Misra, P. R. P. Verma, A. Dube and P. R. Mishra, *J. Antimicrob. Chemother.*, 2012, **67**, 2650–2660.

79 J. Q. Reimao, D. C. Miguel, N. N. Taniwaki, C. T. Trinconi, J. K. U. Yokoyama-Yasunaka and S. R. B. Uliana, *PLoS Negl. Trop. Dis.*, 2014, **8**, e2842.
80 C. T. Trinconi, J. Q. Reimão, A. C. Coelho and S. R. B. Uliana, *J. Antimicrob. Chemother.*, 2016, **71**, 1314–1322.
81 M. Doroodgar, M. Delavari, M. Doroodgar, A. Abbasi, A. A. Taherian and A. Doroodgar, *Korean J. Parasitol.*, 2016, **54**, 9–14.
82 D. C. Miguel, J. K. U. Yokoyama-Yasunaka, W. K. Andreoli, R. A. Mortara and S. R. B. Uliana, *J. Antimicrob. Chemother.*, 2007, **60**, 526–534.
83 D. C. Miguel, J. K. U. Yokoyama-Yasunaka and S. R. B. Uliana, *PLoS Negl. Trop. Dis.*, 2008, **2**, 6.
84 C. T. Trinconi, D. C. Miguel, A. M. Silber, C. Brown, J. G. M. Mina, P. W. Denny, N. Heise and S. R. B. Uliana, *Int. J. Parasitol. Drugs Drug Resist.*, 2018, **8**, 475–487.
85 S. Sundar and J. Chakravarty, *J. Glob. Infect. Dis.*, 2010, **2**, 159–166.
86 W. de Souza and J. C. F. Rodrigues, *Interdiscip. Perspect. Infect. Dis.*, 2009, **2009**, 19.
87 M. Emad, F. Hayati, M. K. Fallahzadeh and M. R. Namazi, *J. Am. Acad. Dermatol.*, 2011, **64**, 606–608.
88 https://clinicaltrials.gov/ct2/show/NCT01953744, (Accessed 28 January 2017).
89 S. Farajzadeh, I. Esfandiarpour, A. A. Haghdoost, S. Mohammadi, A. Mohebbi, E. Mohebbi and M. Mostafavi, *Iran. J. Parasitol.*, 2015, **10**, 1–8.
90 A. Bezerra-Souza, E. S. Yamamoto, M. D. Laurenti, S. P. Ribeiro and L. F. D. Passero, *Parasitol. Int.*, 2016, **65**, 702–707.
91 J. T. Mesquita, T. A. da Costa-Silva, S. E. T. Borborema and A. G. Tempone, *Mol. Cell. Biochem.*, 2014, **389**, 293–300.
92 https://pubs.acs.org/doi/pdf/10.1021/jm300070h, (Accessed 17 November 2018).
93 E. Iniguez, A. Varela-Ramirez, A. Martínez, C. L. Torres, R. A. Sánchez-Delgado and R. A. Maldonado, *Acta Trop.*, 2016, **164**, 402–410.
94 L. H. Freitas-Junior, E. Chatelain, H. A. Kim and J. L. Siqueira-Neto, *Int. J. Parasitol. Drugs Drug Resist.*, 2012, **2**, 11–19.
95 M. Khraiwesh, S. Leed, N. Roncal, J. Johnson, R. Sciotti, P. Smith, L. Read, R. Paris, T. Hudson, M. Hickman and M. Grogl, *Am. J. Trop. Med. Hyg.*, 2016, **94**, 340–347.
96 J. T. Mesquita, E. G. Pinto, N. N. Taniwaki, A. J. Galisteo Jr and A. G. Tempone, *Acta Trop.*, 2013, **128**, 666–673.
97 R. Zhang, L. Shang, H. Jin, C. Ma, Y. Wu, Q. Liu, Z. Xia, F. Wei, X.-Q. Zhu and H. Gao, *Parasitol. Res.*, 2010, **107**, 475–479.
98 C. Nava-Zuazo, F. Chavez-Silva, R. Moo-Puc, M. Jesus Chan-Bacab, B. Otto Ortega-Morales, H. Moreno-Diaz, D. Diaz-Coutino, E. Hernandez-Nunez and G. Navarrete-Vazquez, *Bioorg. Med. Chem.*, 2014, **22**, 1626–1633.
99 S. Patterson and S. Wyllie, *Trends Parasitol.*, 2014, **30**, 289–298.
100 S. Wyllie, S. Patterson, L. Stojanovski, F. R. C. Simeons, S. Norval, R. Kime, K. D. Read and A. H. Fairlamb, *Sci. Transl. Med.*, 2012, **4**, 119re1.
101 https://clinicaltrials.gov/show/NCT01980199, (Accessed 14 May 2016).
102 http://www.dndi.org/diseases-projects/portfolio/fexinidazole-vl/, (Accessed 18 October 2016).
103 E. Hsu, *Br. J. Clin. Pharmacol.*, 2006, **61**, 666–670.
104 P. L. Olliaro, R. K. Haynes, B. Meunier and Y. Yuthavong, *Trends Parasitol.*, 2001, **17**, 122–126.
105 D. M. Yang and F. Y. Liew, *Parasitology*, 1993, **106**, 7–11.

106 L. E. Mesa, D. Vasquez, P. Lutgen, I. D. Vélez, A. M. Restrepo, I. Ortiz, S. M. Robledo, L. E. Mesa, D. Vasquez, P. Lutgen, I. D. Vélez, A. M. Restrepo, I. Ortiz and S. M. Robledo, *Rev. Soc. Bras. Med. Trop.*, 2017, **50**, 52–60.
107 R. Sen, S. Bandyopadhyay, A. Dutta, G. Mandal, S. Ganguly, P. Saha and M. Chatterjee, *J. Med. Microbiol.*, 2007, **56**, 1213–1218.
108 V. P. C. Rocha, F. R. Nonato, E. T. Guimarães, L. A. Rodrigues de Freitas and M. B. P. Soares, *J. Med. Microbiol.*, 2013, **62**, 1001–1010.
109 G. Goldstein, *J. Rheumatol. Suppl.*, 1978, **4**, 143–148.
110 P. G. Butler, *J. Trop. Med. Hyg.*, 1978, **81**, 221–224.
111 F. H. Rodrigues, S. R. Afonso-Cardoso, M. A. B. Gomes, M. E. Beletti, A. Rocha, A. H. B. Guimarães, I. Candeloro and M. A. de Souza, *Vet. Parasitol.*, 2006, **139**, 37–46.
112 F. Beltran, M. Gutierrez and F. Biagi, *Bull. Soc. Pathol. Exot. Filiales*, 1967, **60**, 61–64.
113 P. I. Long, *JAMA*, 1973, **223**, 1378–1379.
114 W. A. D. Griffiths and M. Sodeify, *Arch. Dermatol.*, 1976, **112**, 1791–1791.
115 J. S. Keithly and S. G. Langreth, *Am. J. Trop. Med. Hyg.*, 1983, **32**, 485–496.
116 M. A. Mapar and M. Omidian, *Jundishapur J Microbiol*, 2010, **3**, 79–83.
117 A. Belehu, B. Naafs and E. Touw-Langendijk, *Br. J. Dermatol.*, 1978, **99**, 421–422.
118 A. Krolewiecki, S. Leon, P. Scott and D. Abraham, *Am. J. Trop. Med. Hyg.*, 2002, **67**, 273–277.
119 E. I. Amer, M. M. Eissa and S. F. Mossallam, *J. Parasit. Dis. Off. Organ Indian Soc. Parasitol.*, 2016, **40**, 475–484.
120 F. de Oliveira-Silva, E. de Morais-Teixeira and A. Rabello, *Am. J. Trop. Med. Hyg.*, 2008, **78**, 745–749.
121 A. Sinagra, C. Luna, D. Abraham, M. del C. Iannella, A. Riarte and A. J. Krolewiecki, *Rev. Soc. Bras. Med. Trop.*, 2007, **40**, 627–630.
122 A. T. Evans, S. L. Croft, W. Peters and R. A. Neal, *Ann. Trop. Med. Parasitol.*, 2016, **83**, 447–454.
123 M. R. Namazi, L. Dastgheib, J. Mazandarani and F. Jowkar, *J. Am. Acad. Dermatol.*, 2010, **62**, 890–892.
124 I. C. Bygbjerg, L. Knudsen, M. Kieffer and A. H. Mehregan, *Arch. Dermatol.*, 1980, **116**, 988–989.
125 R. Livshin, L. Weinrauch, Z. Even-Paz and J. El-On, *Int. J. Dermatol.*, 1987, **26**, 55–59.
126 S. S. Pareek, *Int. J. Dermatol.*, 1984, **23**, 70–71.
127 S. Patterson, S. Wyllie, S. Norval, L. Stojanovski, F. R. C. Simeons, J. L. Auer, M. Osuna-Cabello, K. D. Read and A. H. Fairlamb, *Elife*, 2016, **5**, e09744.
128 A. M. Thompson, P. D. O'Connor, A. Blaser, V. Yardley, L. Maes, S. Gupta, D. Launay, D. Martin, S. G. Franzblau, B. Wan, Y. Wang, Z. Ma and W. A. Denny, *J. Med. Chem.*, 2016, **59**, 2530–2550.
129 S. Patterson, S. Wyllie, L. Stojanovski, M. R. Perry, F. R. C. Simeons, S. Norval, M. Osuna-Cabello, M. D. Rycker, K. D. Read and A. H. Fairlamb, *Antimicrob. Agents Chemother.*, 2013, **57**, 4699–4706.
130 S. Gupta, V. Yardley, P. Vishwakarma, R. Shivahare, B. Sharma, D. Launay, D. Martin and S. K. Puri, *J. Antimicrob. Chemother.*, 2015, **70**, 518–527.
131 U. Manjunatha, H. I. M. Boshoff and C. E. Barry, *Commun. Integr. Biol.*, 2009, **2**, 215–218.
132 http://www.dndi.org/diseases-projects/portfolio/completed-projects/vl-2098/, (Accessed 5 November 2016).

133 A. Gori, D. Trabattoni, A. Bandera, M. Saresella, G. Marchetti, L. Gazzola, M. Biasin, J. Rhodes, H. McDade, R. Panebianco, M. Galli, M. Moroni, P. Ferrante, N. Thomas, F. Franzetti, D. Bray and M. Clerici, *Antivir. Ther.*, 2004, **9**, 603–614.
134 https://clinicaltrials.gov/ct2/show/study/NCT00343941?term=Tucaresol&rank=1, (Accessed 9 April 2017).
135 A. C. Smith, V. Yardley, J. Rhodes and S. L. Croft, *Antimicrob. Agents Chemother.*, 2000, **44**, 1494–1498.
136 S. Buates and G. Matlashewski, *J. Infect. Dis.*, 1999, **179**, 1485–1494.
137 J. Seeberger, S. Daoud and J. Pammer, *Int. J. Dermatol.*, 2003, **42**, 576–579.
138 C. Miranda-Verástegui, A. Llanos-Cuentas, I. Arévalo, B. J. Ward and G. Matlashewski, *Clin. Infect. Dis.*, 2005, **40**, 1395–1403.
139 E. A. Cruz, S. a. G. Da-Silva, M. F. Muzitano, P. M. R. Silva, S. S. Costa and B. Rossi-Bergmann, *Int. Immunopharmacol.*, 2008, **8**, 1616–1621.
140 E. A. Cruz, S. Reuter, H. Martin, N. Dehzad, M. F. Muzitano, S. S. Costa, B. Rossi-Bergmann, R. Buhl, M. Stassen and C. Taube, *Phytomedicine Int. J. Phytother. Phytopharm.*, 2012, **19**, 115–121.
141 M. F. Muzitano, C. A. B. Falcão, E. A. Cruz, M. C. Bergonzi, A. R. Bilia, F. F. Vincieri, B. Rossi-Bergmann and S. S. Costa, *Planta Med.*, 2009, **75**, 307–311.
142 D. C. O. Gomes, M. F. Muzitano, S. S. Costa and B. Rossi-Bergmann, *Parasitology*, 2010, **137**, 613–618.
143 J. Mlcek, T. Jurikova, S. Skrovankova and J. Sochor, *Mol. Basel Switz.*, 2016, **21**, 623.
144 E. G. Pinto, T. A. da Costa-Silva and A. G. Tempone, *Acta Trop.*, 2014, **137**, 206–210.
145 J. Q. Reimão, M. T. Scotti and A. G. Tempone, *Bioorg. Med. Chem.*, 2010, **18**, 8044–8053.
146 J. G. Mina, J. A. Mosely, H. Z. Ali, H. Shams-Eldin, R. T. Schwarz, P. G. Steel and P. W. Denny, *Int. J. Biochem. Cell Biol.*, 2010, **42**, 1553–1561.
147 J. G. Mina, J. A. Mosely, H. Z. Ali, P. W. Denny and P. G. Steel, *Org. Biomol. Chem.*, 2011, **9**, 1823–1830.
148 J. D. Planer, M. A. Hulverson, J. A. Arif, R. M. Ranade, R. Don and F. S. Buckner, *PLoS Negl. Trop. Dis.*, 2014, **8**, e2977.
149 L. M. Johansen, L. E. DeWald, C. J. Shoemaker, B. G. Hoffstrom, C. M. Lear-Rooney, A. Stossel, E. Nelson, S. E. Delos, J. A. Simmons, J. M. Grenier, L. T. Pierce, H. Pajouhesh, J. Lehár, L. E. Hensley, P. J. Glass, J. M. White and G. G. Olinger, *Sci. Transl. Med.*, 2015, **7**, 290ra89.
150 A. Marcu, U. Schurigt, K. Müller, H. Moll, R. L. Krauth-Siegel and H. Prinz, *Eur. J. Med. Chem.*, 2016, **108**, 436–443.
151 R. D. Pearson, A. A. Manian, D. Hall, J. L. Harcus and E. L. Hewlett, *Antimicrob. Agents Chemother.*, 1984, **25**, 571–574.
152 J. El-On, N. Rubinstein, S. Kernbaum and L. F. Schnur, *Ann. Trop. Med. Parasitol.*, 1986, **80**, 509–517.
153 S. Parveen, M. O. F. Khan, S. E. Austin, S. L. Croft, V. Yardley, P. Rock and K. T. Douglas, *J. Med. Chem.*, 2005, **48**, 8087–8097.
154 M. O. F. Khan, S. E. Austin, C. Chan, H. Yin, D. Marks, S. N. Vaghjiani, H. Kendrick, V. Yardley, S. L. Croft and K. T. Douglas, *J. Med. Chem.*, 2000, **43**, 3148–3156.
155 D. Zilberstein and D. M. Dwyer, *Science*, 1984, **226**, 977–979.
156 E. F. Cunha-Júnior, V. V. Andrade-Neto, M. L. Lima, T. A. da Costa-Silva, A. J. G. Junior, M. A. Abengózar, C. Barbas, L. Rivas, E. E. Almeida-Amaral, A. G. Tempone and E. C. Torres-Santos, *PLoS Negl. Trop. Dis.*, 2017, **11**, e0005281.

157 S. Mukherjee, B. Mukherjee, R. Mukhopadhyay, K. Naskar, S. Sundar, J. C. Dujardin, A. K. Das and S. Roy, *PLoS Negl. Trop. Dis.*, 2012, **6**, e1987.
158 V. V. Andrade-Neto, T. M. Pereira, M. do Canto-Cavalheiro and E. C. Torres-Santos, *Parasit. Vectors*, 2016, **9**, 183.
159 S. Singh, N. Dinesh, P. K. Kaur and B. Shamiulla, *Parasitol. Res.*, 2014, **113**, 2161–2168.
160 N. Dinesh, P. K. Kaur, K. K. Swamy and S. Singh, *Exp. Parasitol.*, 2014, **144**, 84–90.
161 P. Palit and N. Ali, *J. Antimicrob. Chemother.*, 2008, **61**, 1120–1124.
162 M. L. Lima, M. A. Abengózar, M. Nácher-Vázquez, M. P. Martínez-Alcázar, C. Barbas, A. G. Tempone, Á. López-Gonzálvez and L. Rivas, *Antimicrob. Agents Chemother.*, 2018, AAC.01928-18.
163 G. A. Kumar, S. Roy, M. Jafurulla, C. Mandal and A. Chattopadhyay, *Biochim. Biophys. Acta*, 2016, **1858**, 2088–2096.
164 S. P. Parihar, M.-A. Hartley, R. Hurdayal, R. Guler and F. Brombacher, *Sci. Rep.*, 2016, **6**, 33458.
165 N. Dinesh, N. Soumya and S. Singh, *Parasitol. Res.*, 2015, **114**, 3873–3883.
166 X. Serrano-Martin, Y. Garcia-Marchan, A. Fernandez, N. Rodriguez, H. Rojas, G. Visbal and G. Benaim, *Antimicrob. Agents Chemother.*, 2009, **53**, 1403–1410.
167 X. Serrano-Martín, G. Payares, M. De Lucca, J. C. Martinez, A. Mendoza-León and G. Benaim, *Antimicrob. Agents Chemother.*, 2009, **53**, 5108–5113.
168 G. Benaim, P. Casanova, V. Hernandez-Rodriguez, S. Mujica-Gonzalez, N. Parra-Gimenez, L. Plaza-Rojas, J. L. Concepcion, Y.-L. Liu, E. Oldfield, A. Paniz-Mondolfi and A. I. Suarez, *Antimicrob. Agents Chemother.*, 2014, **58**, 2295–2303.
169 J. Q. Reimão, F. A. Colombo, V. L. Pereira-Chioccola and A. G. Tempone, *Exp. Parasitol.*, 2011, **128**, 111–115.
170 P. Palit and N. Ali, *Antimicrob. Agents Chemother.*, 2008, **52**, 374–377.
171 P. S. de Sousa Araújo, S. S. C. de Oliveira, C. M. d'Avila-Levy, A. L. S. dos Santos and M. H. Branquinha, *Parasitol. Res.*, 2018, **117**, 2085–2094.
172 V. Ennes-Vidal, R. F. S. Menna-Barreto, M. H. Branquinha, A. L. S. D. Santos and C. M. D'avila-Levy, *Parasitology*, 2017, **144**, 117.
173 R. Firdessa, L. Good, M. C. Amstalden, K. Chindera, N. F. Kamaruzzaman, M. Schultheis, B. Roeger, N. Hecht, T. A. Oelschlaeger, L. Meinel, T. Luehmann and H. Moll, *PLoS Negl. Trop. Dis.*, 2015, **9**, e0004041.
174 M. Witschel, M. Rottmann, M. Kaiser and R. Brun, *PLOS Negl Trop Dis*, 2012, **6**, e1805.
175 J. A. L. Lindoso, J. M. L. Costa, I. T. Queiroz and H. Goto, *Res Rep Trop Med*, 2012, **3**, 69–77.
176 R. C. Dickson and R. L. Lester, *Biochim. Biophys. Acta BBA - Mol. Cell Biol. Lipids*, 2002, **1583**, 13–25.
177 A. H. Merrill, *Chem. Rev.*, 2011, **111**, 6387–6422.
178 P. W. Denny, D. Goulding, M. A. J. Ferguson and D. F. Smith, *Mol. Microbiol.*, 2004, **52**, 313–327.
179 K. Zhang, M. Showalter, J. Revollo, F.-F. Hsu, J. Turk and S. M. Beverley, *EMBO J.*, 2003, **22**, 6016–6026.
180 K. Zhang, F.-F. Hsu, D. A. Scott, R. Docampo, J. Turk and S. M. Beverley, *Mol. Microbiol.*, 2005, **55**, 1566–1578.
181 T. P. Levine, C. A. R. Wiggins and S. Munro, *Mol. Biol. Cell*, 2000, **11**, 2267–2281.
182 M. M. Nagiec, E. E. Nagiec, J. A. Baltisberger, G. B. Wells, R. L. Lester and R. C. Dickson, *J. Biol. Chem.*, 1997, **272**, 9809–9817.
183 A. K. Tanaka, V. B. Valero, H. K. Takahashi and A. H. Straus, *J. Antimicrob. Chemother.*, 2007, **59**, 487–492.

184 P. W. Denny, H. Shams-Eldin, Helen. P. Price, D. F. Smith and R. T. Schwarz, *J. Biol. Chem.*, 2006, **281**, 28200–28209.
185 Y. J. Sigal, M. I. McDERMOTT and A. J. Morris, *Biochem. J.*, 2005, **387**, 281–293.
186 Home - Protein - NCBI, https://www.ncbi.nlm.nih.gov/protein, (accessed 10 June 2019).
187 M. A. Goren, B. G. Fox and J. D. Bangs, *Biochemistry*, 2011, **50**, 8853–8861.
188 G. Walsh, in *Proteins*, John Wiley & Sons, Ltd, 2015, pp. 91–140.
189 B. Alberts, A. Johnson, J. Lewis, M. Raff, K. Roberts and P. Walter, *Mol. Biol. Cell 4th Ed.*
190 E. P. Carpenter, K. Beis, A. D. Cameron and S. Iwata, *Curr. Opin. Struct. Biol.*, 2008, **18**, 581–586.
191 C. Brown, Durham University, 2015.
192 H. L. Bolt, G. A. Eggimann, P. W. Denny and S. L. Cobb, *MedChemComm*, 2016, **7**, 799–805.
193 N. C. Thomson and J. W. Kerr, *Thorax*, 1980, **35**, 428–434.
194 A. J. Green, J. M. Gelfand, B. A. Cree, C. Bevan, W. J. Boscardin, F. Mei, J. Inman, S. Arnow, M. Devereux, A. Abounasr, H. Nobuta, A. Zhu, M. Friessen, R. Gerona, H. C. von Büdingen, R. G. Henry, S. L. Hauser and J. R. Chan, *Lancet Lond. Engl.*, 2017, **390**, 2481–2489.
195 S. Budavari, in *The Merck Index - Encyclopedia of Chemicals, Drugs and Biologicals*, Merck and Co. Inc., Rahway, NJ, 1989, p. 366.
196 E. R. Derbyshire, M. Prudêncio, M. M. Mota and J. Clardy, *Proc. Natl. Acad. Sci.*, 2012, **109**, 8511–8516.
197 US Pat., 2009203763, 2009.
198 H. F. Schran, L. Petryk, C.-T. Chang, R. O'Connor and M. B. Gelbert, *J. Clin. Pharmacol.*, 1996, **36**, 911–922.
199 A. Ebnöther and H. P. Weber, *Helv. Chim. Acta*, 1976, **59**, 2462–2468.
200 S. Y. Lee, J. W. Jung, T.-H. Kim and H.-D. Kim, *Arch. Pharm. Res.*, 2015, **38**, 2131–2136.
201 CN. Pat., 107011228, 2017.
202 A. M. Fournier, R. A. Brown, W. Farnaby, H. Miyatake-Ondozabal and J. Clayden, *Org. Lett.*, 2010, **12**, 2222–2225.
203 T. Nikiforov, S. Stanchev, B. Milenkov and V. Dimitrov, *Synth. Commun.*, 1990, **20**, 1977–1981.
204 S. J. Kim, M. Chang and H.-D. Kim, *Tetrahedron Asymmetry*, 2011, **22**, 1901–1905.
205 S.-W. Choi, D. R. Elmaleh, R. N. Hanson and A. J. Fischman, *J. Med. Chem.*, 1999, **42**, 3647–3656.
206 L. Winfield, C. Zhang, C. A. Reid, E. D. Stevens, M. L. Trudell, S. Izenwasser and D. Wade, *J. Heterocycl. Chem.*, 2003, **40**, 827–832.
207 V. S. Amato, F. F. Tuon, H. A. Bacha, V. A. Neto and A. C. Nicodemo, *Acta Trop.*, 2008, **105**, 1–9.
208 F. M. Marim, T. N. Silveira, D. S. L. Jr and D. S. Zamboni, *PLOS ONE*, 2010, **5**, e15263.
209 N. B. Norsworthy, J. Sun, D. Elnaiem, G. Lanzaro and L. Soong, *Infect. Immun.*, 2004, **72**, 1240–1247.
210 C. Prolo, M. N. Álvarez and R. Radi, *BioFactors*, 2014, **40**, 215–225.
211 J. M. Slauch, *Mol. Microbiol.*, 2011, **80**, 580–583.
212 N. Moradin and A. Descoteaux, *Front. Cell. Infect. Microbiol.*, , DOI:10.3389/fcimb.2012.00121.
213 P. Italiani, E. Töpfer and D. Boraschi, in *Immune Rebalancing*, eds. D. Boraschi and G. Penton-Rol, Academic Press, 2016, pp. 123–149.
214 J. W. Coleman, *Int. Immunopharmacol.*, 2001, **1**, 1397–1406.

215 The Role of the P2X7 Receptor in Infectious Diseases, https://journals.plos.org/plospathogens/article?id=10.1371/journal.ppat.1002212, (accessed 21 June 2019).
216 L. E. B. Savio, P. de Andrade Mello, C. G. da Silva and R. Coutinho-Silva, *Front. Pharmacol.*, , DOI:10.3389/fphar.2018.00052.
217 W. Nörenberg, C. Hempel, N. Urban, H. Sobottka, P. Illes and M. Schaefer, *J. Biol. Chem.*, 2011, **286**, 11067–11081.
218 S. P. Chaves, E. C. Torres-Santos, C. Marques, V. R. Figliuolo, P. M. Persechini, R. Coutinho-Silva and B. Rossi-Bergmann, *Microbes Infect.*, 2009, **11**, 842–849.
219 P. V. Turner, T. Brabb, C. Pekow and M. A. Vasbinder, *J. Am. Assoc. Lab. Anim. Sci. JAALAS*, 2011, **50**, 600–613.
220 S. dos S. Costa, M. de Assis Golim, B. Rossi-Bergmann, F. T. M. Costa and S. Giorgio, *Korean J. Parasitol.*, 2011, **49**, 357–364.
221 Clemastine Dosage Guide with Precautions - Drugs.com, https://www.drugs.com/dosage/clemastine.html, (accessed 21 August 2017).
222 A. B. Nair and S. Jacob, *J. Basic Clin. Pharm.*, 2016, **7**, 27–31.
223 R. G. Titus, M. Marchand, T. Boon and J. A. Louis, *Parasite Immunol.*, 1985, **7**, 545–555.
224 GraphPad Statistics Guide, https://www.graphpad.com/guides/prism/7/statistics/index.htm?stat_the_methods_of_tukey_and_dunne.htm, (accessed 3 June 2019).
225 S. P. Wright, *Biometrics*, 1992, **48**, 1005–1013.
226 What is the meaning of * or ** or *** in reports of statistical significance from Prism or InStat? - FAQ 978 - GraphPad, https://www.graphpad.com/support/faq/what-is-the-meaning-of--or--or--in-reports-of-statistical-significance-from-prism-or-instat/, (accessed 30 May 2019).
227 V. Claassen, Ed., in *Techniques in the Behavioral and Neural Sciences*, Elsevier, 1994, vol. 12, pp. 46–58.
228 C. Demicheli, R. Ochoa, J. B. B. da Silva, C. A. B. Falcão, B. Rossi-Bergmann, A. L. de Melo, R. D. Sinisterra and F. Frézard, *Antimicrob. Agents Chemother.*, 2004, **48**, 100–103.
229 A. J. Sousa-Batista, F. S. Poletto, C. I. M. S. Philipon, S. S. Guterres, A. R. Pohlmann and B. Rossi-Bergmann, *Parasitology*, 2017, 1–6.
230 Y. Bikard, J.-M. Weibel, C. Sirlin, L. Dupuis, J.-P. Loeffler and P. Pale, *Tetrahedron Lett.*, 2007, **48**, 8895–8899.
231 A. L. Braga, D. S. Lüdtke, P. H. Schneider, F. Vargas, A. Schneider, L. A. Wessjohann and M. W. Paixão, *Tetrahedron Lett.*, 2005, **46**, 7827–7830.
232 K. Soai, A. Ookawa, T. Kaba and K. Ogawa, *J. Am. Chem. Soc.*, 1987, **109**, 7111–7115.
233 Y.-X. Yang, Y. Liu, L. Zhang, Y.-E. Jia, P. Wang, F.-F. Zhuo, X.-T. An and C.-S. Da, *J. Org. Chem.*, 2014, **79**, 10696–10702.
234 A. Chighine, G. Sechi and M. Bradley, *Drug Discov. Today*, 2007, **12**, 459–464.
235 Z. Zhang and W. Tang, *Acta Pharm. Sin. B*, 2018, **8**, 721–732.
236 E. Smith and I. Collins, *Future Med. Chem.*, 2015, **7**, 159–183.
237 K. Teruya, K. F. Tonissen and S.-A. Poulsen, *MedChemComm*, 2016, **7**, 2045–2062.
238 W. Jiang, Q. Fu, H. Fan and W. Wang, *Chem. Commun.*, 2007, 259–261.
239 L. Yi and Z. Xi, *Org. Biomol. Chem.*, 2017, **15**, 3828–3839.
240 Glycosome - an overview | ScienceDirect Topics, https://www.sciencedirect.com/topics/neuroscience/glycosome, (accessed 8 July 2019).
241 B. Chawla and R. Madhubala, *J. Parasit. Dis. Off. Organ Indian Soc. Parasitol.*, 2010, **34**, 1–13.

242 J. Pawley, *Handbook of Biological Confocal Microscopy*, Springer Science & Business Media, 2010.
243 H. Li, R.-Y. Zhu, W.-J. Shi, K.-H. He and Z.-J. Shi, *Org. Lett.*, 2012, **14**, 4850–4853.
244 L. F. Fieser and M. Fieser, *Reagents of Organic Synthesis*, John Wiley and Sons Inc., New York, 1967.
245 S. Nishida, *J. Org. Chem.*, 1967, **32**, 2692–2695.
246 G. A. Holloway, J. P. Parisot, P. M. Novello, K. G. Watson, T. Armstrong, R. C. A. Thompson, I. P. Street and J. B. Baell, *Bioorg. Med. Chem. Lett.*, 2010, **20**, 1816–1818.
247 E. J. Corey, S. Shibata and R. K. Bakshi, *J. Org. Chem.*, 1988, **53**, 2861–2863.
248 C. Mazzini, L. Sambri, H. Regeling, B. Zwanenburg and G. J. F. Chittenden, *J. Chem. Soc. Perkin 1*, 1997, **0**, 3351–3356.
249 M. J. e Silva, Cottier, Louis, D. Sinou and R. M. Srivastava, *J. Braz. Chem. Soc.*, 2005, **16**, 995–1000.
250 E. C. Carlson, L. K. Rathbone, H. Yang, N. D. Collett and R. G. Carter, *J. Org. Chem.*, 2008, **73**, 5155–5158.
251 D. J. Miller, M. B.-U. Surfraz, M. Akhtar, D. Gani and R. K. Allemann, *Org. Biomol. Chem.*, 2004, **2**, 671–688.
252 G. Xu, M. Micklatcher, M. A. Silvestri, T. L. Hartman, J. Burrier, M. C. Osterling, H. Wargo, J. A. Turpin, Buckheit Robert W. and M. Cushman, *J. Med. Chem.*, 2001, **44**, 4092–4113.
253 T. Iwasaki, K. Agura, Y. Maegawa, Y. Hayashi, T. Ohshima and K. Mashima, *Chem. – Eur. J.*, 2010, **16**, 11567–11571.
254 H. Zhao, M. Cheng, T. Zhang and M. Cai, *J. Organomet. Chem.*, 2015, **777**, 50–56.
255 T. Lee, T. W. Wilson, R. Berg, P. Ryberg and J. F. Hartwig, *J. Am. Chem. Soc.*, 2015, **137**, 6742–6745.
256 T. Matsuda, K. Mizuno and S. Watanuki, *J. Organomet. Chem.*, 2014, **765**, 64–67.
257 C.-H. Xing and Q.-S. Hu, *Tetrahedron Lett.*, 2010, **51**, 924–927.
258 K. M. Liu, J. Wei and X. F. Duan, *Chem. Commun.*, 2015, **51**, 4655–4658.
259 W. E. Bachmann, R. Hoffman and F. Whitehead, *J. Org. Chem.*, 1943, **08**, 320–330.
260 M. Padmanaban, A. T. Biju and F. Glorius, *Org. Lett.*, 2011, **13**, 98–101.
261 V. J. Forrat, D. J. Ramón and M. Yus, *Tetrahedron Asymmetry*, 2007, **18**, 400–405.
262 M. L. Burdeinyi, S. V. Popkov and M. V. Kharchevnikova, *Russ. Chem. Bull.*, 2009, **58**, 936–939.
263 S. Stanchev, R. Rakovska, N. Berova and G. Snatzke, *Tetrahedron Asymmetry*, 1995, **6**, 183–198.
264 US Pat., JP2018203751, 2018.
265 C. Wolf and W. Schunack, *Arch. Pharm. (Weinheim)*, 1996, **329**, 87–94.
266 H. G. Kolloff, J. H. Hunter, E. H. Woodruff and R. Bruce. Moffett, *J. Am. Chem. Soc.*, 1949, **71**, 3988–3990.
267 C. S. A. Kumar, S. B. B. Prasad, K. Vinaya, S. Chandrappa, N. R. Thimmegowda, Y. C. S. Kumar, S. Swarup and K. S. Rangappa, *Eur. J. Med. Chem.*, 2009, **44**, 1223–1229.
268 N. J. Findlay, S. R. Park, F. Schoenebeck, E. Cahard, S. Zhou, L. E. A. Berlouis, M. D. Spicer, T. Tuttle and J. A. Murphy, *J. Am. Chem. Soc.*, 2010, **132**, 15462–15464.
269 Q. Xu, H. Xie, P. Chen, L. Yu, J. Chen and X. Hu, *Green Chem.*, 2015, **17**, 2774–2779.
270 S. Zhou, K.-H. Wu, C.-A. Chen and H.-M. Gau, *J. Org. Chem.*, 2009, **74**, 3500–3505.
271 G. Wu, X. Zhao, W. Ji, Y. Zhang and J. Wang, *Chem. Commun.*, 2016, **52**, 1961–1963.
272 National Research Council (US) Committee for the Update of the Guide for the Care and Use of Laboratory Animals, *Guide for the Care and Use of Laboratory Animals*, National Academies Press (US), Washington (DC), 8th edn., 2011.

273 A Method for Generation of Bone Marrow-Derived Macrophages from Cryopreserved Mouse Bone Marrow Cells, https://journals.plos.org/plosone/article?id=10.1371/journal.pone.0015263, (accessed 23 April 2019).
274 A. S. Fischl, Y. Liu, A. Browdy and A. E. Cremesti, in *Methods in Enzymology*, Academic Press, 2000, vol. 311, pp. 123–130.
275 M. M. Bradford, *Anal. Biochem.*, 1976, **72**, 248–254.
276 J. D. Berman and J. V. Gallalee, *J. Parasitol.*, 1987, **73**, 671–673.
277 H. A. Zakai and S. K. Zimmo, *Ann. Trop. Med. Parasitol.*, 2000, **94**, 787–791.
278 A. Shokri, S. Emami, M. Fakhar, S. H. Teshnizi and M. Keighobadi, *Acta Trop.*, 2017, **167**, 73–78.
279 S. T. de Macedo-Silva, J. A. Urbina, W. de Souza and J. C. F. Rodrigues, *PLOS ONE*, 2013, **8**, e83247.
280 W. Peters, J. J. Shaw, R. Lainson, B. L. Robinson and A. F. Leão, *The Lancet*, 1981, **317**, 1122–1124.
281 J. El-On, E. Bazarsky and R. Sneir, *Exp. Parasitol.*, 2007, **116**, 156–162.
282 C. Chan, H. Yin, J. Garforth, J. H. McKie, R. Jaouhari, P. Speers, K. T. Douglas, P. J. Rock, V. Yardley, S. L. Croft and A. H. Fairlamb, *J. Med. Chem.*, 1998, **41**, 148–156.
283 A. T. Evans and S. L. Croft, *Biochem. Pharmacol.*, 1994, **48**, 613–616.

Appendix A

List of drugs in Chapter 1 and their activities

Drug	Species	*In vitro* form	EC_{50} (μM)	Selectivity index	Animal study	References
9	*L. major*	Promastigotes	0.11	-	Y	[61]
	L. donovani	Promastigotes	0.14		N	
		Axenic amastigotes	0.07			
10	*L. major*	Promastigotes	0.12	0.08	N	[62]
		Axenic amastigotes	2.37			
11	*L. donovani*	Intracellular amastigotes	1.08	7.04	Y	[66]
	L. mexicana	Intracellular amastigotes	2.63	2.89	N	
12	*L. donovani*	Intracellular amastigotes	3.73	1.88	Y	
	L. amazonensis	Intracellular amastigotes	6.87	1.02	N	
	L. mexicana	Intracellular amastigotes	4.72	1.48	N	
	L. major	Intracellular amastigotes	3.77	1.86	N	
13	*L. donovani*	Intracellular amastigotes	2.49	2.41	Y	
14	*L. amazonensis*	-	-	-	Y	[67]
15	*L. donovani*	Axenic amastigotes	0.47	10	N	[68]
16	*L. donovani*	Promastigotes	0.035	-	N	[70]
		Intracellular amastigotes	Active			
17	*L. mexicana*	Promastigotes	0.2	>6666	N	[73]
		Intracellular amastigotes	0.65			
18	*L. infantum*	Promastigotes	7.73	2.69	N	[74]
		Axenic amastigotes	1.88			

		Intracellular amastigotes	1.85			
	L. donovani	-	-	-	Y	[75]
	L. major	Promastigotes	1.75	6.53	N	[77]
		Intracellular amastigotes	0.76			
MWCNT-18	*L. major*	Promastigotes	0.24	12.54	N	
		Intracellular amastigotes	0.11			
19	*L. donovani*	Intracellular amastigotes	1.27	-	Y	[78]
NCs-19	*L. donovani*	Intracellular amastigotes	0.72	-		
20	*L. amazonensis*	Promastigotes	13.51	-	Y	[80]
		Intracellular amastigotes	4.25			
21	*L. amazonensis*	Promastigotes	30.2	1.77	Y	[79]
		Intracellular amastigotes	16.2			
22	*L. major*	Intracellular amastigotes	>105	-	Y	[276]
23	*L. major*	-	-	-	Y	[277]
24	*L. major*	Promastigotes	136	1.82	Y	[278]
		Intracellular amastigotes	24			
25	*L. amazonensis*	Promastigotes	0.44	187.5	Y	[279, 277]
		Intracellular amastigotes	0.08			

26	*L. amazonensis*	Promastigotes	34.10	3.28	N	[90]
		Intracellular amastigotes	29.81			
	L. braziliensis	Promastigotes	81.25	2.27	N	
		Intracellular amastigotes	38.43			
27	*L. amazonensis*	Promastigotes	2.74	12.2	Y	[279]
		Intracellular amastigotes	1.63			
28	*L. infantum*	Promastigotes	5.36	3.6	N	[91]
		Intracellular amastigotes	11.95			
29	*L. infantum*	Promastigotes	8.97	-	N	
30	*L. infantum*	Promastigotes	2.81			
31	*L. major*	Intracellular amastigotes	0.015	>407	N	[95]
32			0.061	>100		
33			0.091	14.2		
34			0.13	>45.4		
35	*L. infantum*	*Promastigotes*	139	3.09	N	[96]
		Intracellular amastigotes	22			
	L. donovani	-	-	-	Y	[97]
	L. amazonensis	*Promastigote*	7.2	115	N	[98]
36	*L. donovani*	Promastigotes	5.6	>17.9	Y	[100]
		Axenic amastigotes	2.8			
		Intracellular amastigotes	Inactive	-		
37	*L. major*	Promastigotes	0.75	>3.33	Y	[105]
		Intracellular amastigotes	30			
	L. donovani	Promastigotes	160	>22	N	[107]
		Intracellular amastigotes	22			
38	*L. amazonensis*	Promastigotes	8.4	7.66	Y	[108]

		Intracellular amastigotes	1.56			
39	*L. amazonensis*	Promastigotes	>50	138.61	Y	
		Intracellular amastigotes	0.78			
40	*L. amazonensis*	Promastigotes	>50	209.85	N	
		Intracellular amastigotes	0.67			
41	*L. amazonensis*	-	-	-	Y	[111]
42	*L. amazonensis*	-	-	-	Y	[111]
43	*L. mexicana*	-	-	-	Y	[115]
	L. donovani	-	-	-	Y	
44	*L. major*	Intracellular amastigotes	16	-	Y	[118, 119]
	L. amazonensis	Promastigotes	1000	-	Y	[120, 121]
		Intracellular amastigotes	20.83			
	L. braziliensis	Promastigotes	590	-	Y	[120, 121]
		Intracellular amastigotes	2.18			
	L. chagasi	Promastigotes	1500	-	N	[120]
		Intracellular amastigotes	6.12			
45	*L. amazonensis*	Intracellular amastigotes	4.86	-	Y	[122]
	L. donovani	Intracellular amastigotes	2.96	-	Y	
	L. major	Intracellular amastigotes	1.06	-	Y	
46	*L. amazonensis*	-	-	-	Y	[280]
47	*L. donovani*	Promastigotes	0.9	>10	Y	[129]
		Intracellular amastigotes	4.92			
47	*L. donovani*	Promastigotes	0.16	>54	Y	[129]
		Intracellular amastigotes	0.93			

48	*L. donovani*	Promastigotes	0.020	>3125	Y	[127]
		Axenic amastigotes	0.005	>10000		
		Intracellular amastigotes	0.087	>575		
49	*L. donovani*	Intracellular amastigotes	Inactive	-	Y	[135]
50	*L. donovani*	Promastigotes	Inactive	-	N	[136]
		Axenic amastigotes	Inactive	-		
		Intracellular amastigotes	Active	-		
	L. major	Intracellular amastigotes	21-42	-	Y	[281]
51	*L. infantum*	Promastigotes	34	4.14	Y	[144]
		Intracellular amastigotes	21			
1	*L. amazonensis*	Promastigotes	0.023	49.9	Y	-
		Intracellular amastigotes	0.40			
	L. major	Promastigotes	0.17	-	N	
		Intracellular amastigotes	3.06	>6.5		
	L. donovani	Promastigotes	0.023	-	Y	
	L. infantum	Promastigotes	0.69	-	N	
52	*L. donovani*	Intracellular amastigotes	4.90	-	Y	[282]
53	*L. donovani*	Intracellular amastigotes	8.60	0.55	N	[153]
54	*L. infantum*	Promastigotes	14.5	-	Y	[156]
		Intracellular amastigotes	12.6	-		
55	*L. donovani*	Promastigotes	22.38	>5.50	Y	[157, 283]

		Intracellular amastigotes	16.2			
	L. amazonensis	Promastigotes	28.63	>3.75	N	[158]
		Intracellular amastigotes	13.32			
56		Intracellular amastigotes	13.32			
		Axenic amastigotes	>50			
		Intracellular amastigotes	3.45			
57	*L. donovani*	Promastigotes	17.30	3.02	N	[63]
		Axenic amastigotes	>50			
		Intracellular amastigotes	5.40			
58	*L. donovani*	Promastigotes	37	3.51	N	[159]
		Intracellular amastigotes	28			
59	*L. donovani*	Promastigotes	21	2.16	N	[160]
		Intracellular amastigotes	46			
60	*L. donovani*	Promastigotes	7.2	-	Y	[161]
		Intracellular amastigotes	7.5			
	L. infantum	Promastigotes	2.0	>20	N	[162]
		Intracellular amastigotes	3.9			
61	*L. donovani*	Promastigotes	23.8	>13	N	[165]
		Intracellular amastigotes	7.5			
62	*L. mexicana*	Promastigotes	0.9	-	Y	[166]

		Intracellular amastigotes	0.008			
63	*L. mexicana*	Promastigotes	0.115	-	N	[168]
		Intracellular amastigotes	0.0007			
64	*L. chagasi*	Promastigotes	3.81	3.12	Y	[169]
		Intracellular amastigotes	21.55			
	L. amazonensis	Promastigotes	4.71	-		
	L. major	Promastigotes	7.33	-		
	L. braziliensis	Promastigotes	3.54	-		
65	*L. donovani*	Promastigotes	2.14	>69.0	Y	[170]
		Intracellular amastigotes	5.14			
66	*L. donovani*	Promastigotes	3.18	>53.6	Y	
		Intracellular amastigotes	6.15			
67	*L. amazonensis*	Promastigotes	6.0	22.8	N	[171]
		Intracellular amastigotes	4.9			
	L. braziliensis	Promastigotes	4.0	39.8	N	
		Intracellular amastigotes	2.8			
	L. chagasi	Promastigotes	8.1	16.0		
		Intracellular amastigotes	7.0			
	L. donovani	Promastigotes	8.8	17.2		
		Intracellular amastigotes	6.5			
	L. major	Promastigotes	4.7	23.2		
		Intracellular amastigotes	4.8			

	L. mexicana	Promastigotes	9.3	13.1		
		Intracellular amastigotes	8.5			
68	*L. major*	Promastigotes	0.41	1	N	[173]
		Intracellular amastigotes	4			
69	*L. donovani*	Promastigotes	0.25	-	N	[174]

Appendix B

List of compounds synthesised in this project and their activities

Column	A	B	C	D	E
Structure	***L. amazonensis*** **promastigote EC_{50} (µM) (95% CI)**	***L. major*** **promastigote EC_{50} (µM) (95% CI)**	***L. donovani*** **promastigote EC_{50} (µM) (95% CI)**	***L. infantum*** **promastigote EC_{50} (µM) (95% CI)**	**Cytotoxicity against mammalian macrophages CC_{50} (µM) (95% CI)**
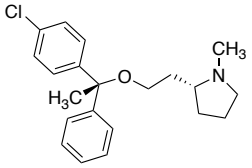 Clemastine **1**	0.020 ± 0.003 0.09 ± 0.01*	0.172 ± 0.003*	0.020 ± 0.003	0.69 ± 0.01	20 ± 2
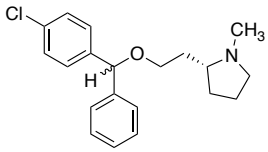 ***(R)*-112**	0.08 ± 0.03 0.29 ± 0.04*	0.38 ± 0.01*	0.06 ± 0.02	2.75 ± 1	62 ± 20
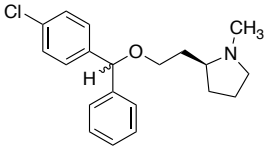 ***(S)*-112**	0.80 ± 0.1*	0.79 ± 0.1*			
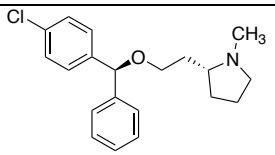 **(*R, S*)-112**	0.53 ± 0.2 1.40 ± 0.2*	1.33 ± 0.1*			
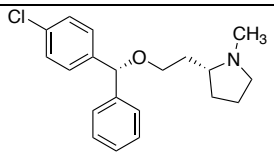 **(*R, R*)-112**	0.026 ± 0.003 0.13 ± 0.01*	0.13 ± 0.01*			75 ± 16
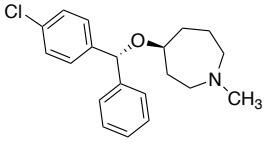 **(*S, R*)-179**	1.50 ± 0.5*	1.35 ± 0.1*			

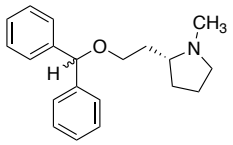 (*R*)-141	0.94 ± 0.2 1.17 ± 0.3*	8.44 ± 0.2*	0.52 ± 0.3	28.66 ± 5	80 ± 10
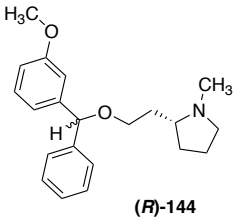 (*R*)-144	0.35 ± 0.1 0.63 ± 0.6*	8.44 ± 0.3*	0.82 ± 0.3	19.15 ± 3	85 ± 10
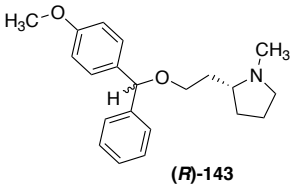 (*R*)-143	0.50 ± 0.3 0.50 ± 0.3*	6.83 ± 0.4*	1.02 ± 0.15	17.29 ± 3	70 ± 20
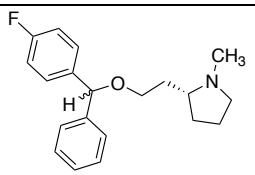 (*R*)-142	1.62 ± 0.2*	2.25 ± 0.1*			
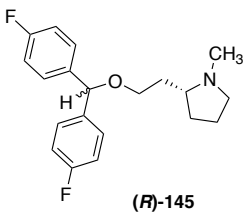 (*R*)-145	2.74 ± 0.4*	2.87 ± 0.4*			
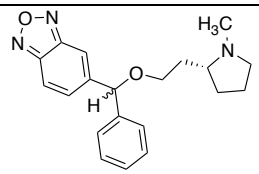 (*R*)-159	0.56 ± 0.03 1.30 ± 0.3*	2.80 ± 0.02*			
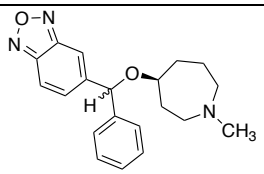 (*S*)-164	6.0 ± 0.5*	17.33 ± 1*			
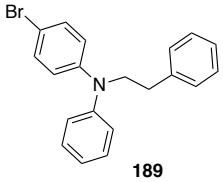 189	21.73 ± 1	-	-	-	-

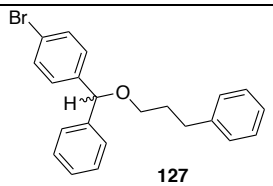 **127**	19.18 ± 3	-	-	-	-
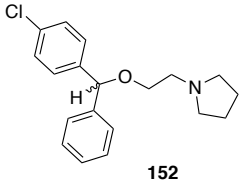 **152**	3.27 ± 0.7	-	2.30 ± 1	30.35 ± 2	57± 20
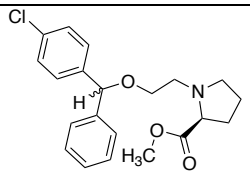 (***S***)-150	10.16 ± 2 9.75 ± 2*	49.2 ± 2*	-	-	-
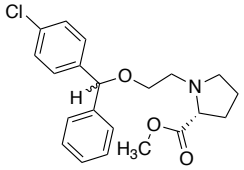 (***R***)-150	17.39 ± 0.7	23.83 ± 10*			
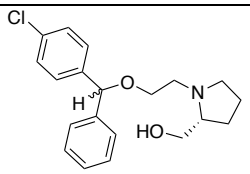 (***R***)-149	3.20 ± 0.7*	5.88 ± 2*			
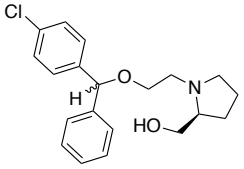 (***S***)-149	1.47 ± 0.6 3.37 ± 1*	2.76 ± 0.6*	1.71 ± 0.8	28.25 ± 20	60 ± 20
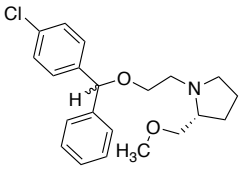 (***R***)-153	12.35 ± 3*	14.41 ± 4*			
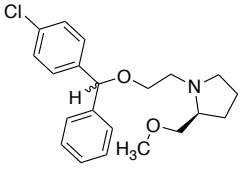 (***S***)-153	6.33 ± 2*	4.68 ± 2*			
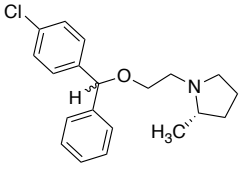 (***S***)-147	1.35 ± 0.8 3.40 ± 0.9*	2.05 ± 0.2*			

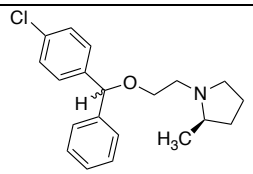 (*R*)-147	4.10 ± 1*	2.65 ± 1*			
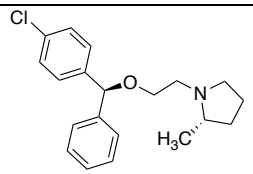 (*S, S*)-147	-	7.05 ± 0.5*			
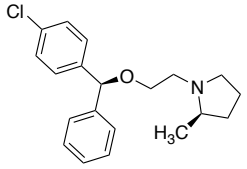 (*R, S*)-147	-	11.5 ± 0.9*			
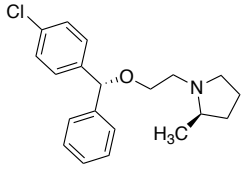 (*R, R*)-147	-	1.7 ± 0.3*			
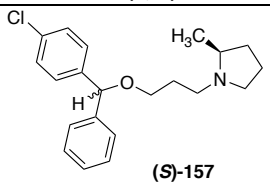 (*S*)-157	0.038 ± 0.02	0.09 ± 0.02*			81 ± 12
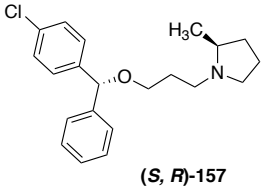 (*S, R*)-157	0.02 ± 0.01	0.058 ± 0.007*			73 ± 14
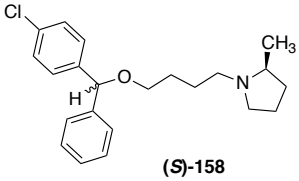 (*S*)-158	0.52 ± 0.1	1.21 ± 0.5*			46 ± 14
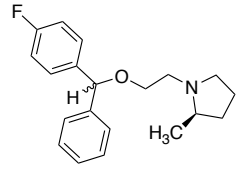 (*R*)-182	23.17 ± 4*	26.80 ± 6*			
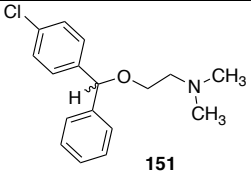 151	51 ± 1*	70 ± 20*			

***Tested at Durham University (*L. major* protocol and *L. amazonensis* protocol 2, see Chapter 8)**

Appendix C

NMR spectra

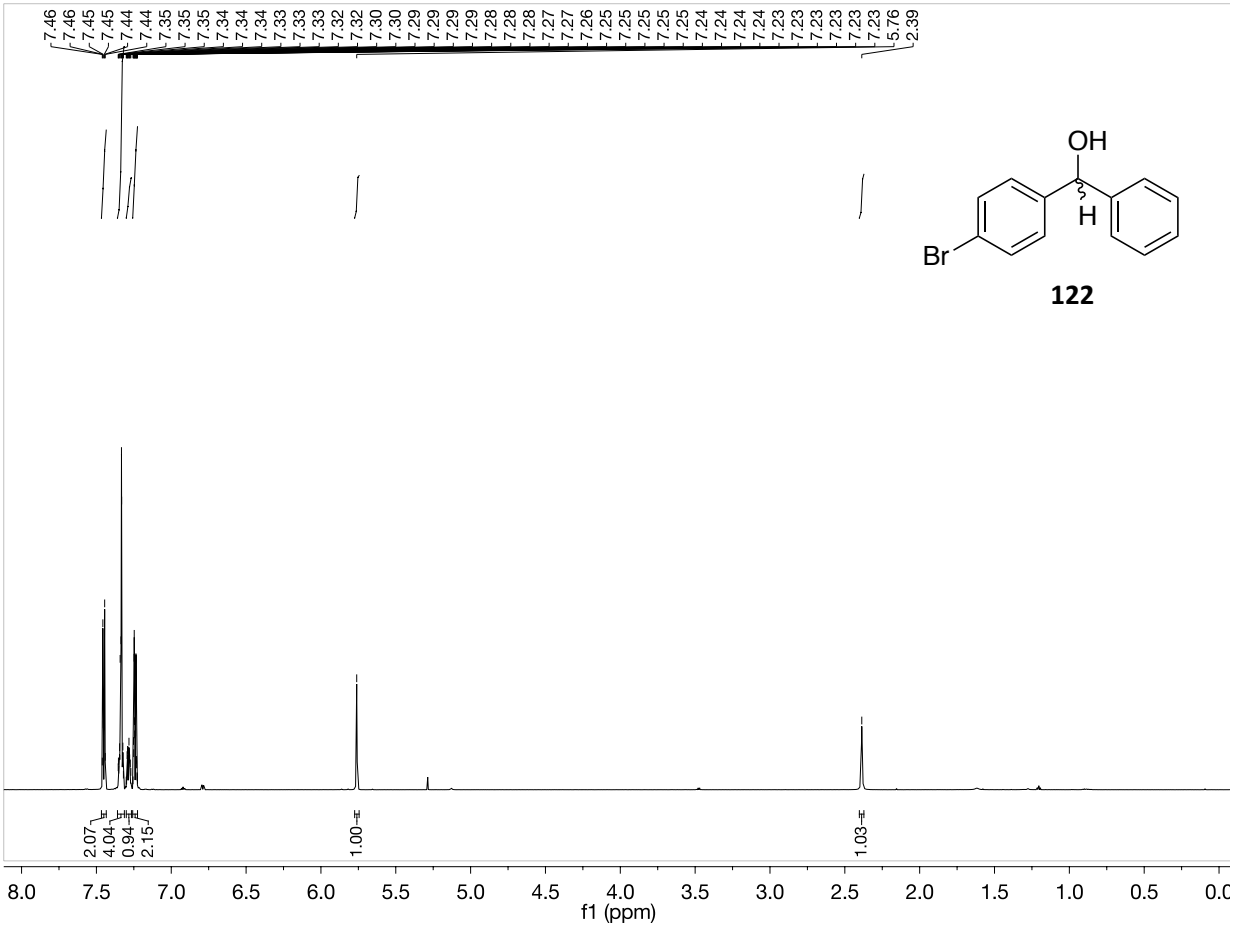
7.46
7.46
7.45
7.45
7.44
7.44
7.35
7.35
7.35
7.34
7.34
7.34
7.33
7.33
7.33
7.32
7.32
7.30
7.30
7.29
7.29
7.29
7.29
7.28
7.28
7.28
7.27
7.27
7.26
7.25
7.25
7.25
7.25
7.24
7.24
7.24
7.23
7.23
7.23
7.23
7.23
5.76
2.39
OH
H
Br
2.07
4.04
0.94
2.15
1.00
1.03
8.0
7.5
7.0
6.5
6.0
5.5
5.0
4.5
4.0
3.5
3.0
2.5
2.0
1.5
1.0
0.5
f1 (ppm)

122

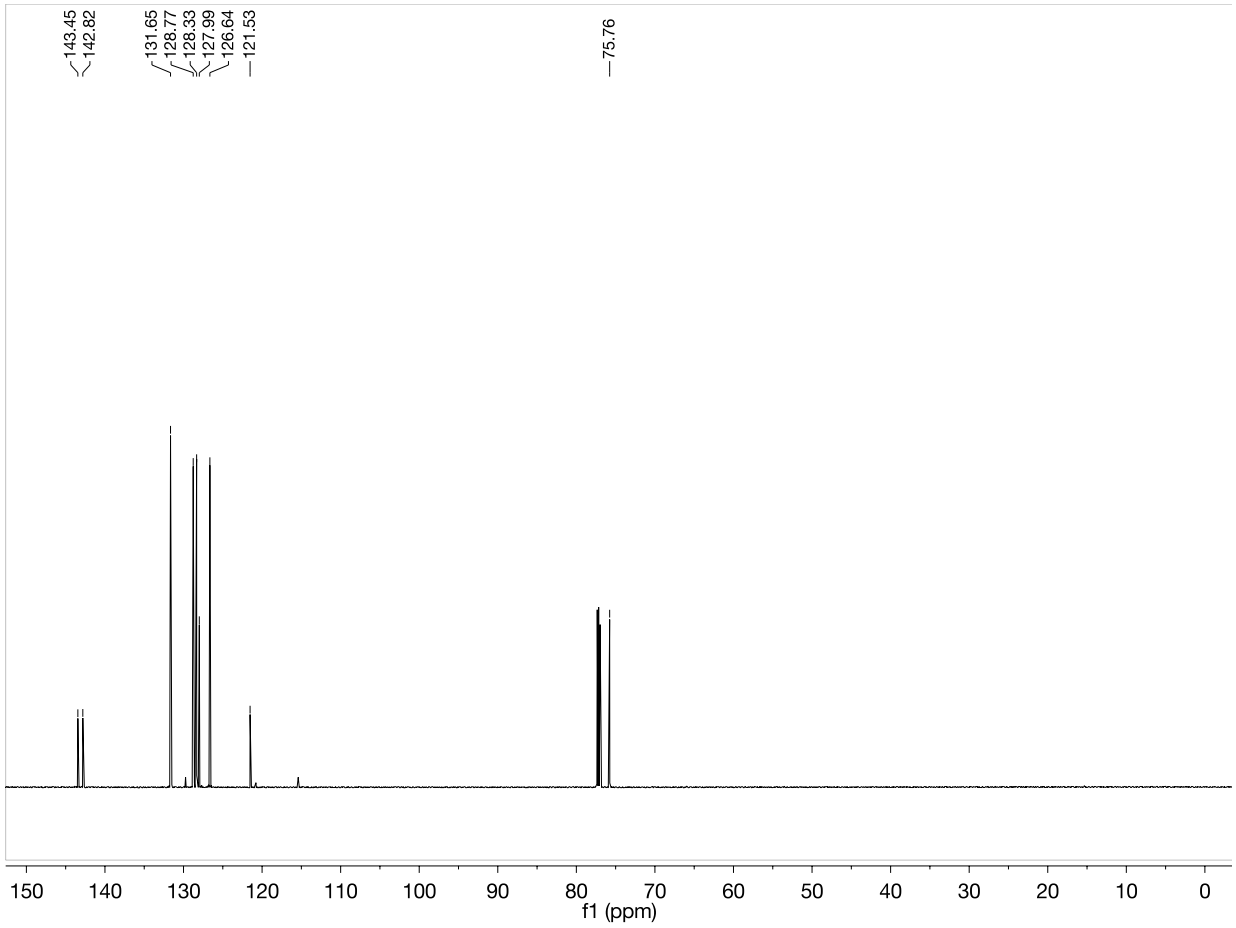
143.45
142.82
131.65
128.77
128.33
127.99
126.64
121.53
75.76
150
140
130
120
110
100
90
80
70
60
50
40
30
20
10
0
f1 (ppm)

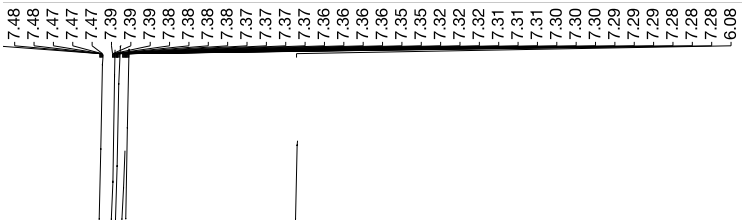
7.48
7.48
7.47
7.47
7.47
7.39
7.39
7.38
7.38
7.38
7.37
7.37
7.37
7.37
7.36
7.36
7.36
7.35
7.35
7.32
7.32
7.31
7.31
7.30
7.30
7.30
7.29
7.29
7.29
7.28
7.28
7.28
6.08

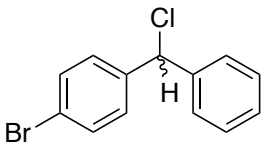
Cl
H
Br

128

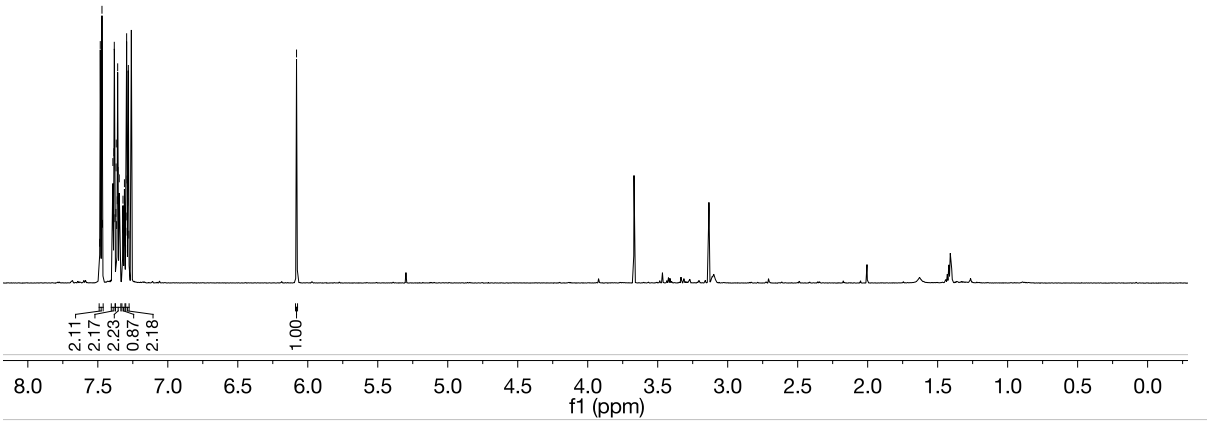
2.11
2.17
2.23
0.87
2.18
1.00
8.0
7.5
7.0
6.5
6.0
5.5
5.0
4.5
4.0
3.5
3.0
2.5
2.0
1.5
1.0
0.5
0.0
f1 (ppm)

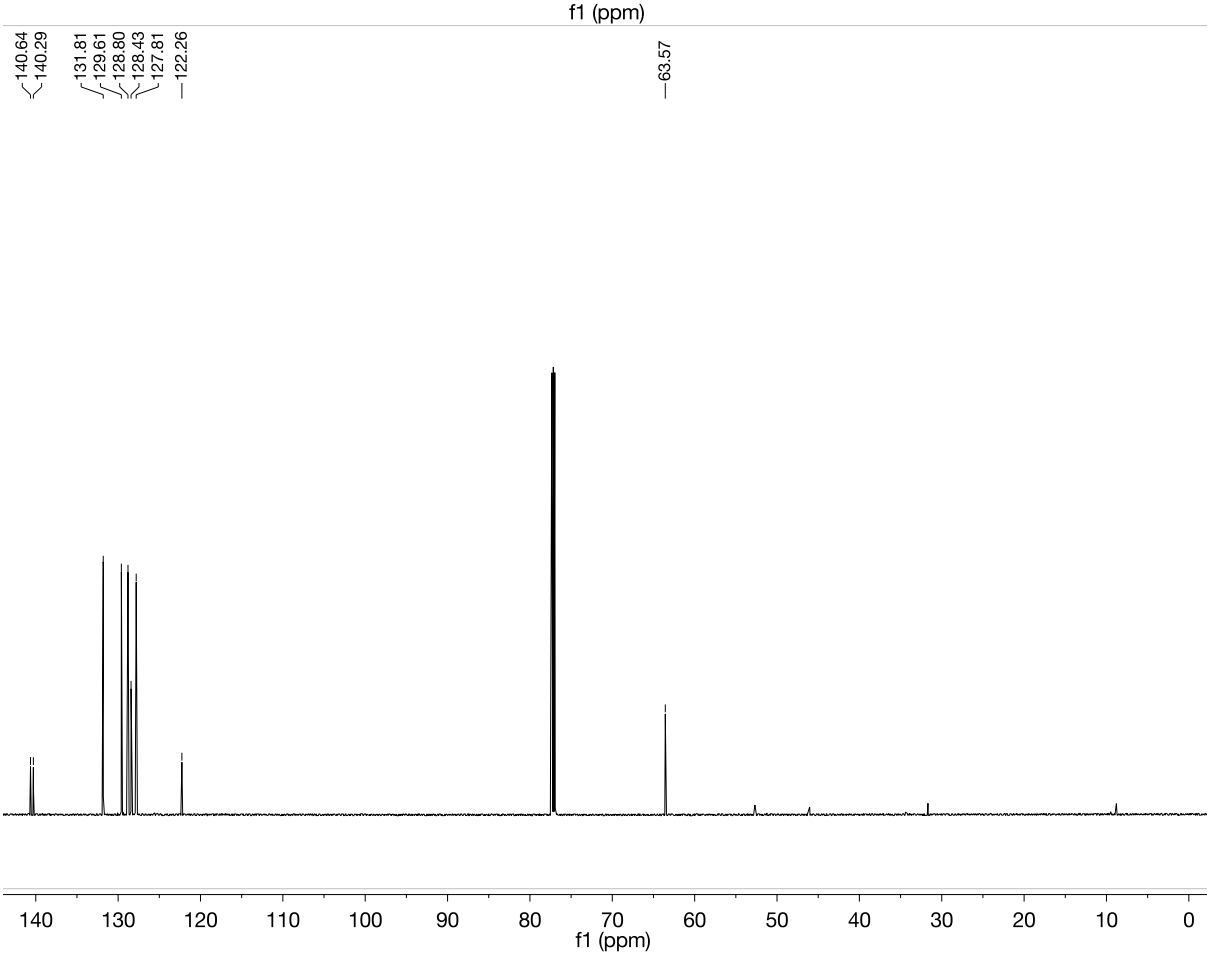
140.64
140.29
131.81
129.61
128.80
128.43
127.81
122.26
63.57
140
130
120
110
100
90
80
70
60
50
40
30
20
10
0
f1 (ppm)

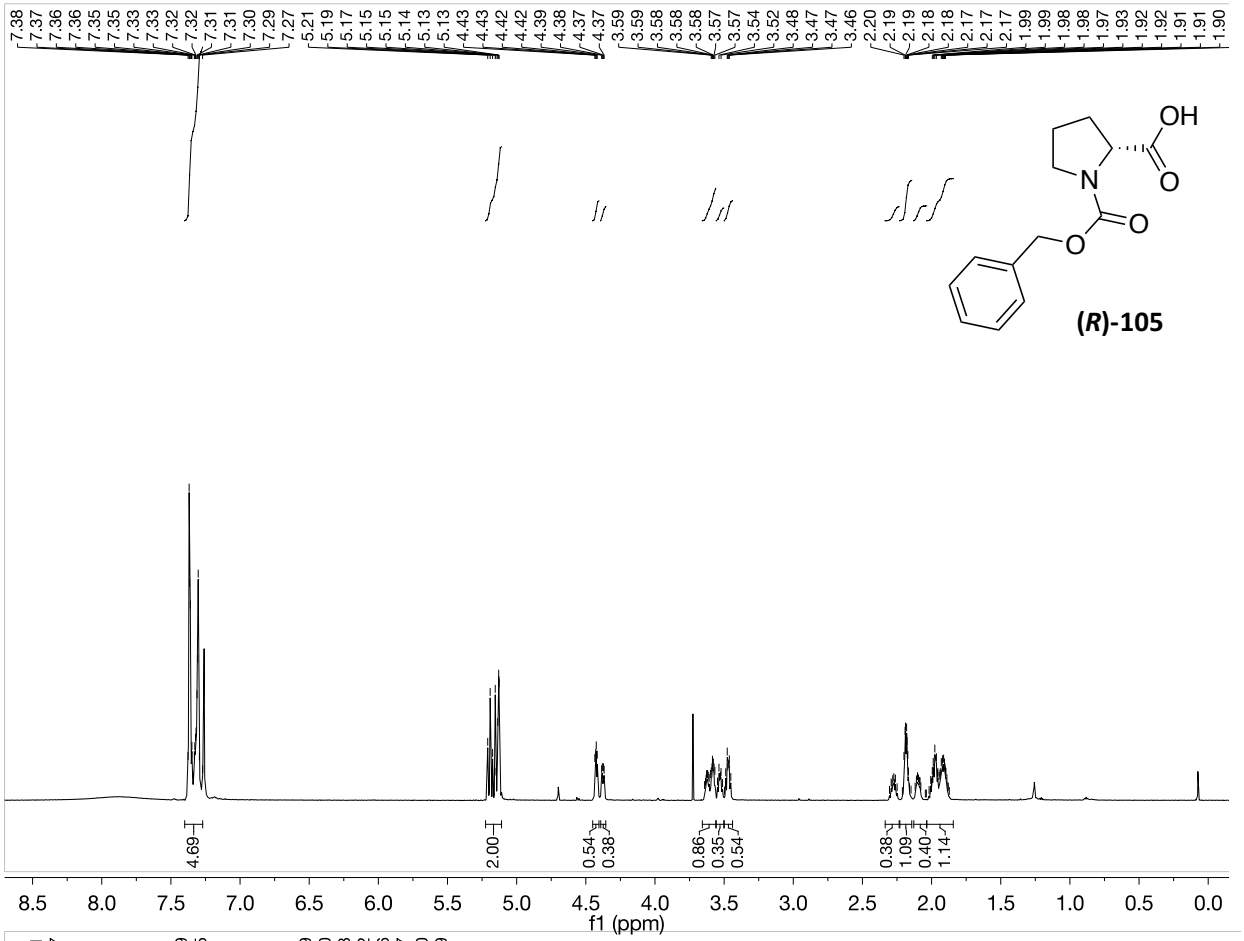
7.38 7.37 7.36 7.36 7.35 7.35 7.33 7.33 7.32 7.32 7.31 7.31 7.30 7.29 7.27
5.21 5.19 5.17 5.15 5.15 5.14 5.13 5.13 4.43 4.43 4.42 4.42 4.39 4.38 4.37 4.37
3.59 3.59 3.58 3.58 3.57 3.57 3.54 3.52 3.48 3.47 3.47 3.46
2.20 2.19 2.19 2.18 2.18 2.17 2.17 2.17 1.99 1.99 1.98 1.98 1.97 1.93 1.92 1.92 1.91 1.91 1.90
OH
O
N
O
O
4.69
2.00
0.54
0.38
0.86
0.35
0.54
0.38
1.09
0.40
1.14
8.5 8.0 7.5 7.0 6.5 6.0 5.5 5.0 4.5 4.0 3.5 3.0 2.5 2.0 1.5 1.0 0.5 0.0
f1 (ppm)

(*R*)-105

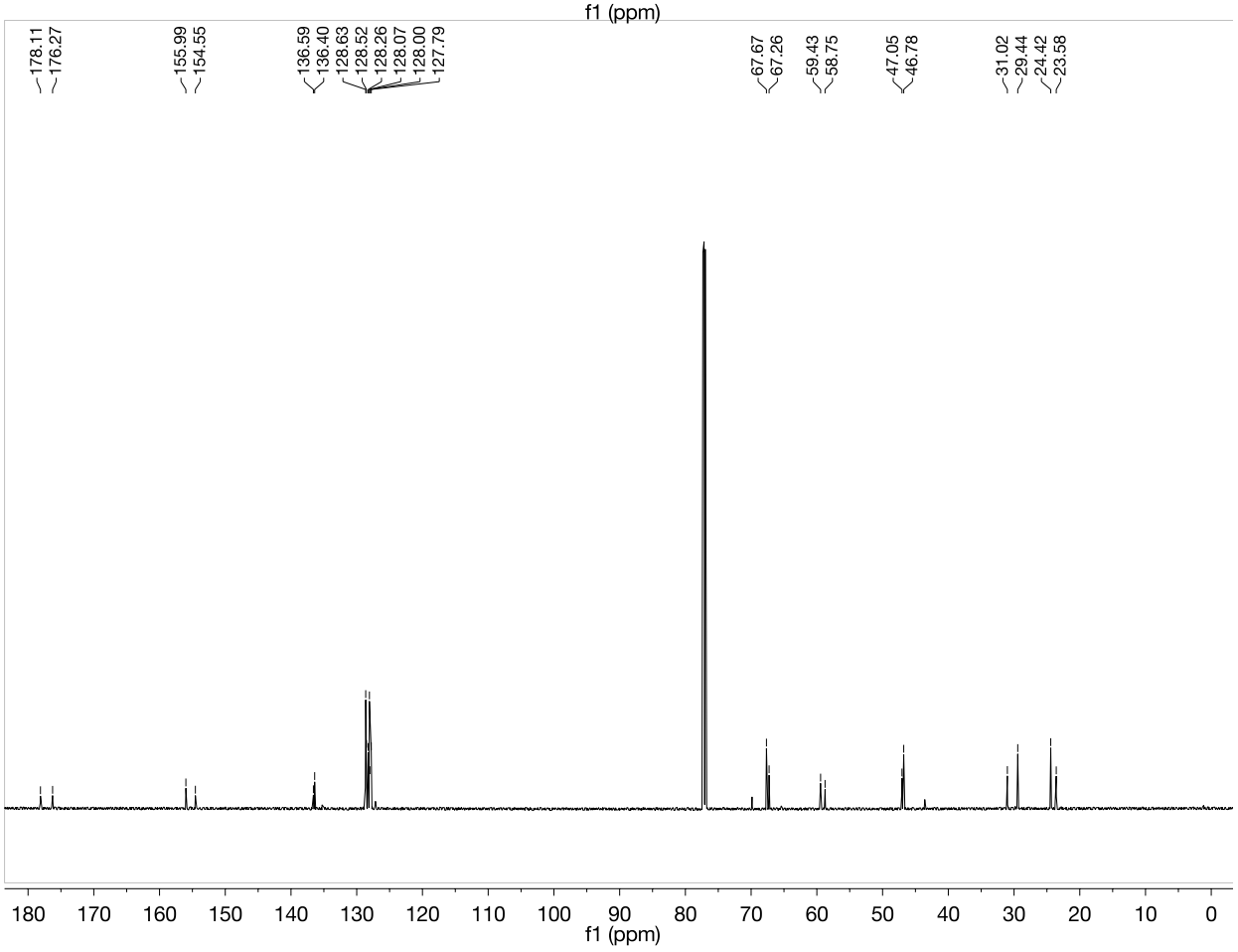
178.11 176.27
155.99 154.55
136.59 136.40 128.63 128.52 128.26 128.07 128.00 127.79
67.67 67.26
59.43 58.75
47.05 46.78
31.02 29.44 24.42 23.58
180 170 160 150 140 130 120 110 100 90 80 70 60 50 40 30 20 10 0
f1 (ppm)

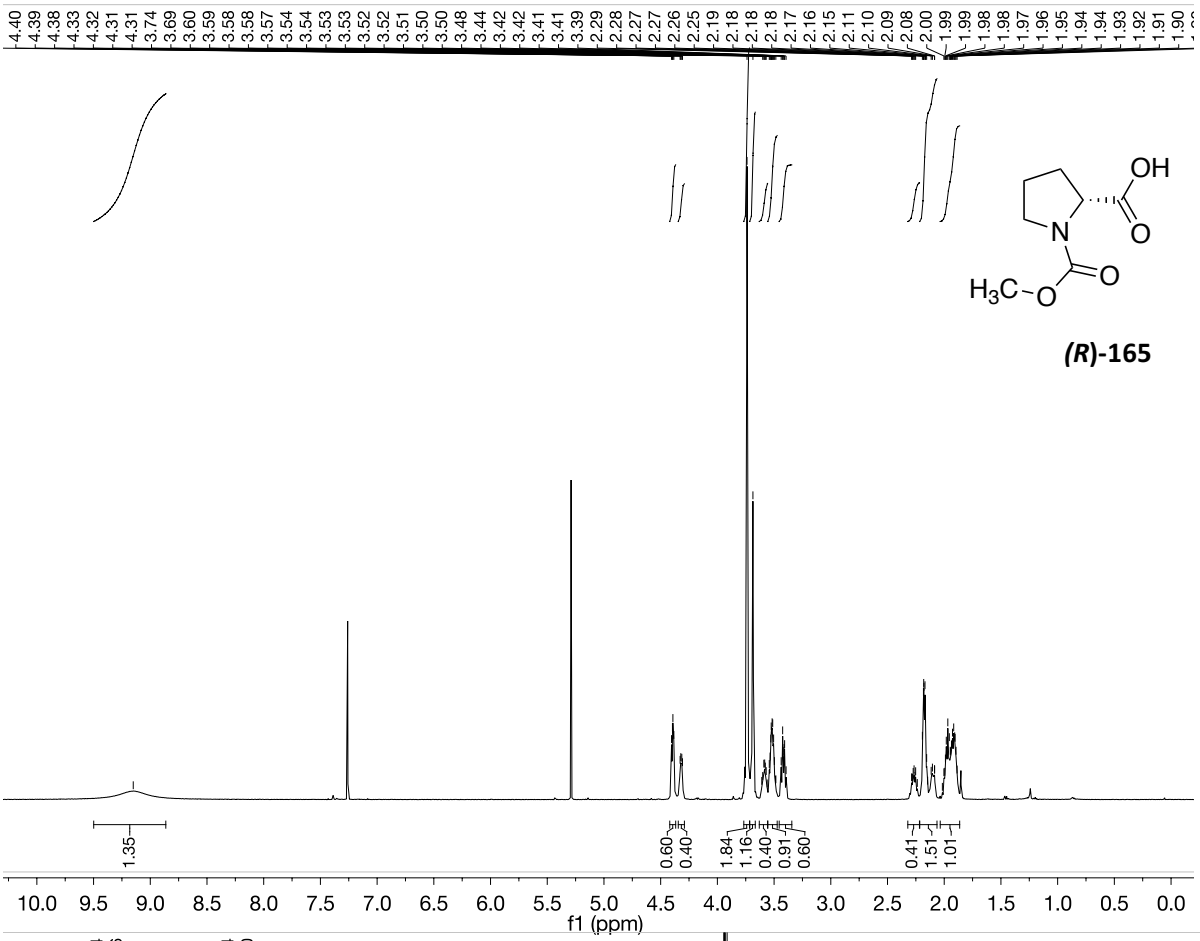

***(R)*-165**

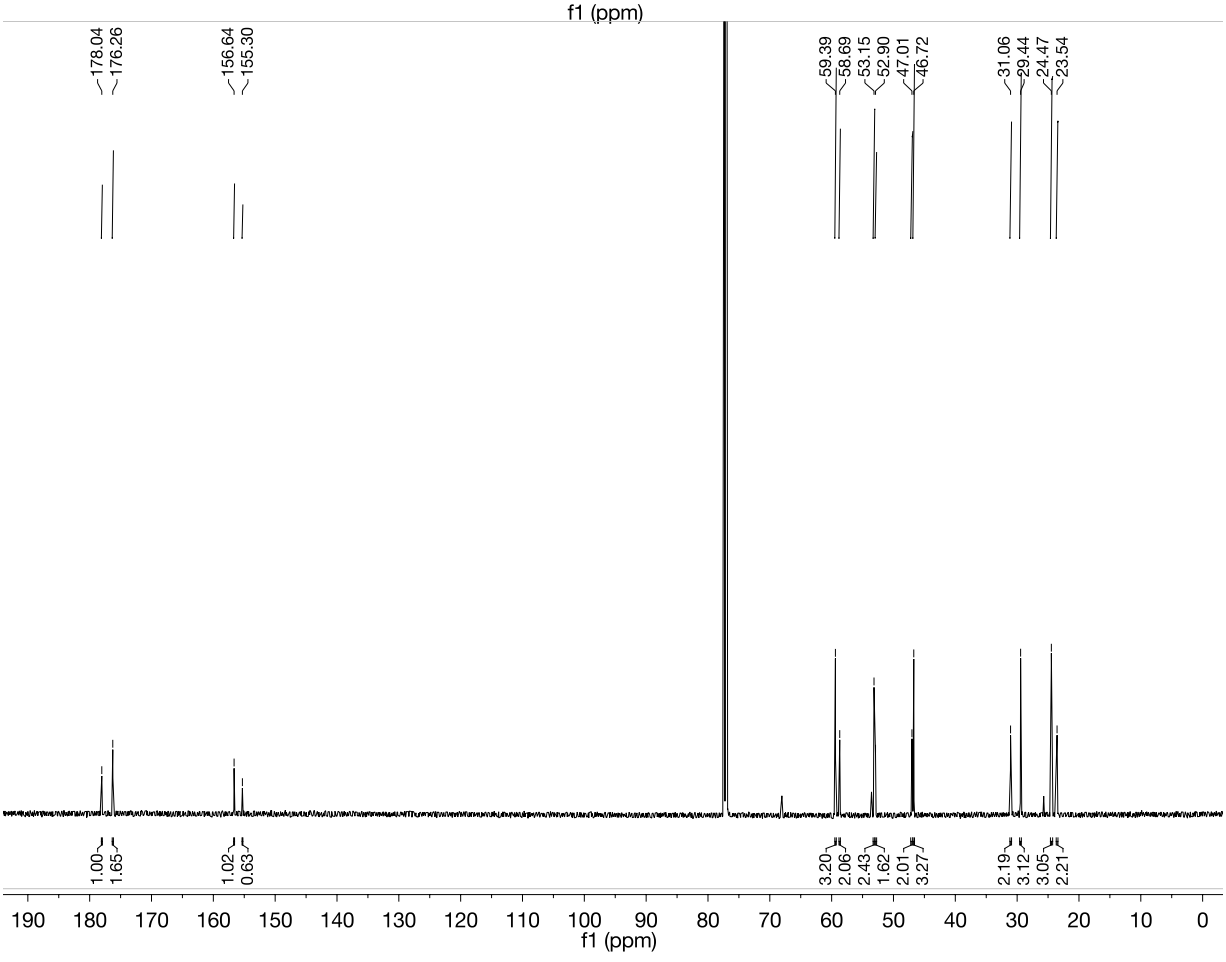

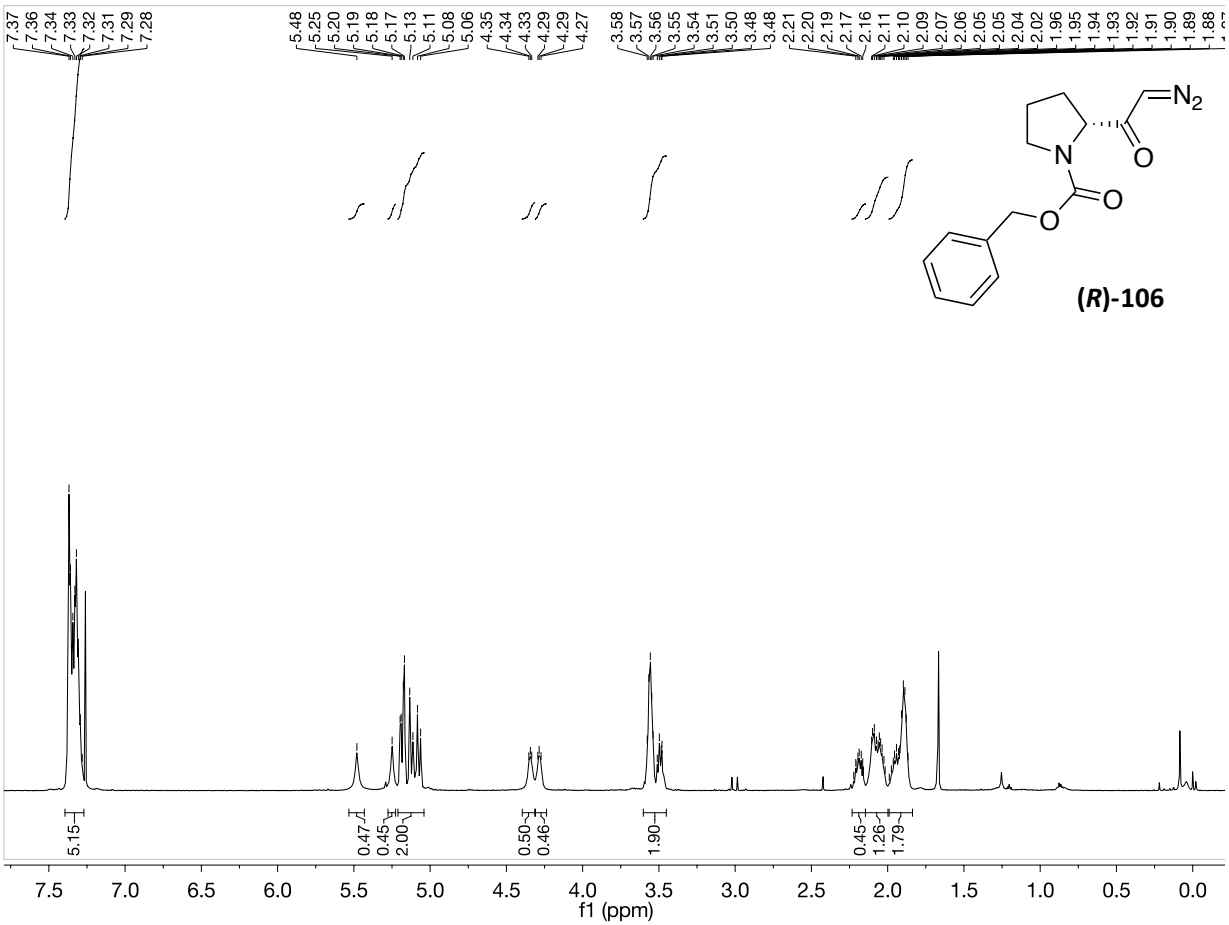
7.37
7.36
7.34
7.33
7.32
7.31
7.29
7.28
5.48
5.25
5.20
5.19
5.18
5.17
5.13
5.11
5.08
5.06
4.35
4.34
4.33
4.29
4.29
4.27
3.58
3.57
3.56
3.55
3.54
3.51
3.50
3.48
3.48
2.21
2.20
2.19
2.17
2.16
2.11
2.10
2.09
2.07
2.06
2.05
2.05
2.04
2.02
1.96
1.95
1.94
1.93
1.92
1.91
1.90
1.89
1.88
N2
O
N
O
O
O
5.15
0.47
0.45
2.00
0.50
0.46
1.90
0.45
1.26
1.79
7.5
7.0
6.5
6.0
5.5
5.0
4.5
4.0
3.5
3.0
2.5
2.0
1.5
1.0
0.5
0.0
f1 (ppm)

(*R*)-106

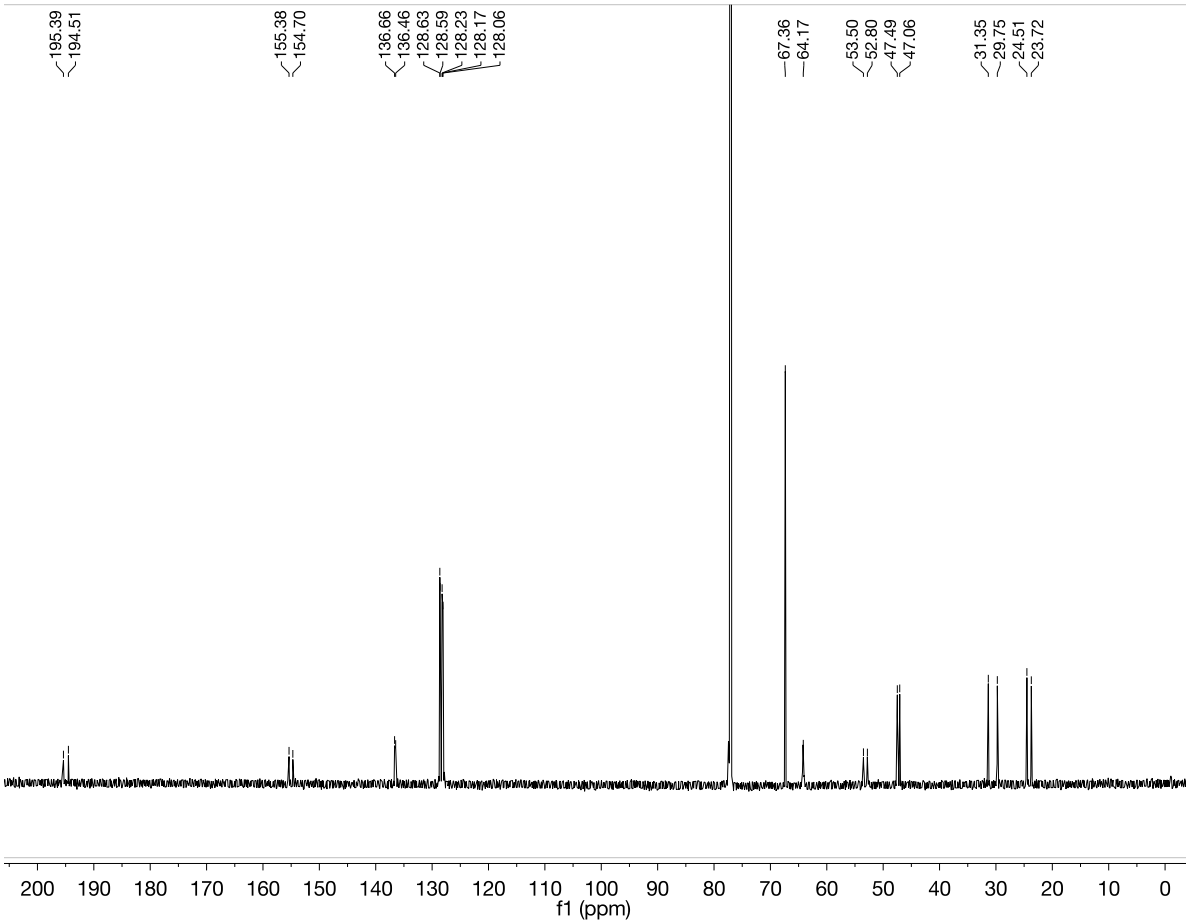
195.39
194.51
155.38
154.70
136.66
136.46
128.63
128.59
128.23
128.17
128.06
67.36
64.17
53.50
52.80
47.49
47.06
31.35
29.75
24.51
23.72
200
190
180
170
160
150
140
130
120
110
100
90
80
70
60
50
40
30
20
10
0
f1 (ppm)

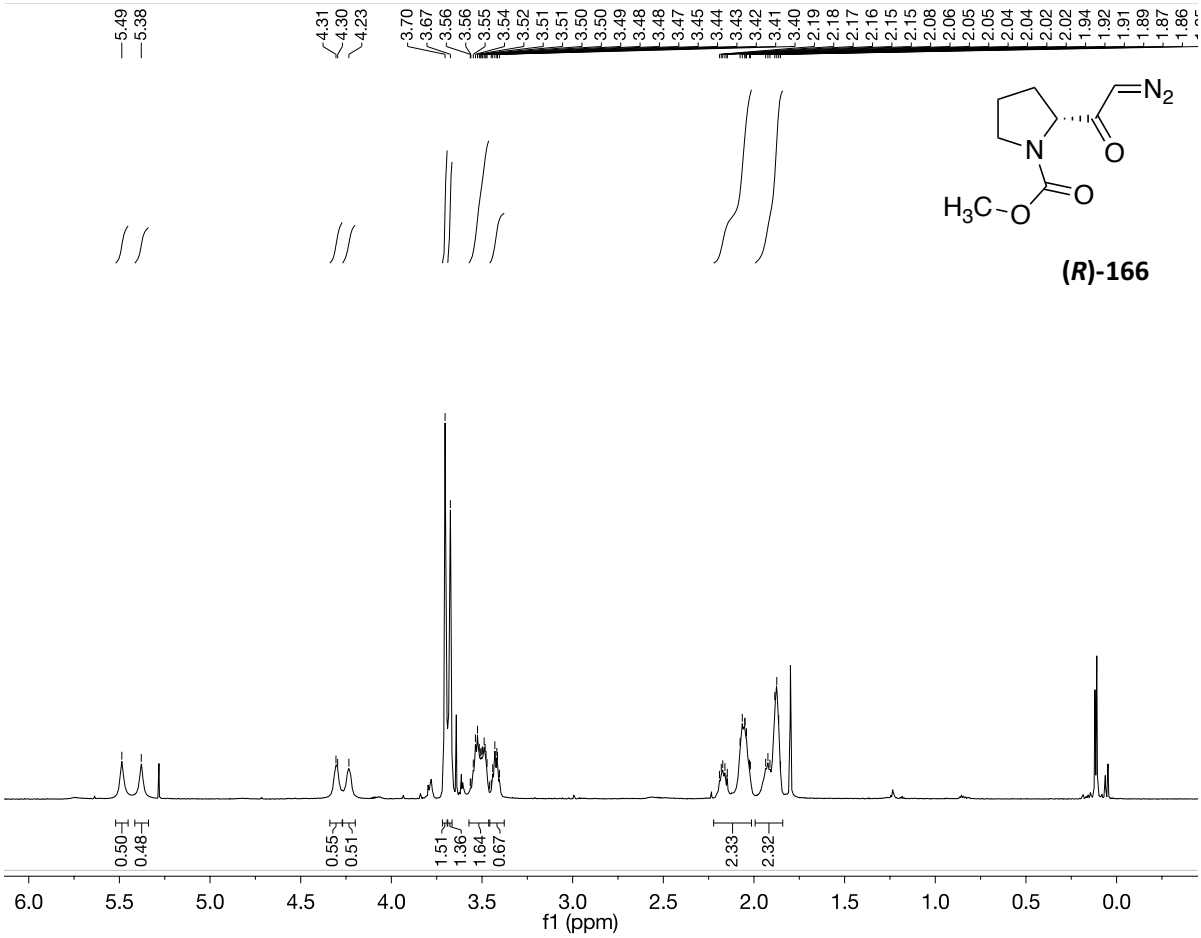
5.49
5.38
4.31
4.30
4.23
3.70
3.67
3.56
3.56
3.55
3.54
3.52
3.51
3.51
3.50
3.50
3.49
3.48
3.48
3.47
3.45
3.44
3.43
3.42
3.41
3.40
2.19
2.18
2.17
2.16
2.15
2.15
2.08
2.06
2.05
2.05
2.04
2.04
2.02
2.02
1.94
1.92
1.91
1.89
1.87
1.86
N2
O
N
O
H3C
O
0.50
0.48
0.55
0.51
1.51
1.36
1.64
0.67
2.33
2.32
6.0
5.5
5.0
4.5
4.0
3.5
3.0
2.5
2.0
1.5
1.0
0.5
0.0
f1 (ppm)

(*R*)-166

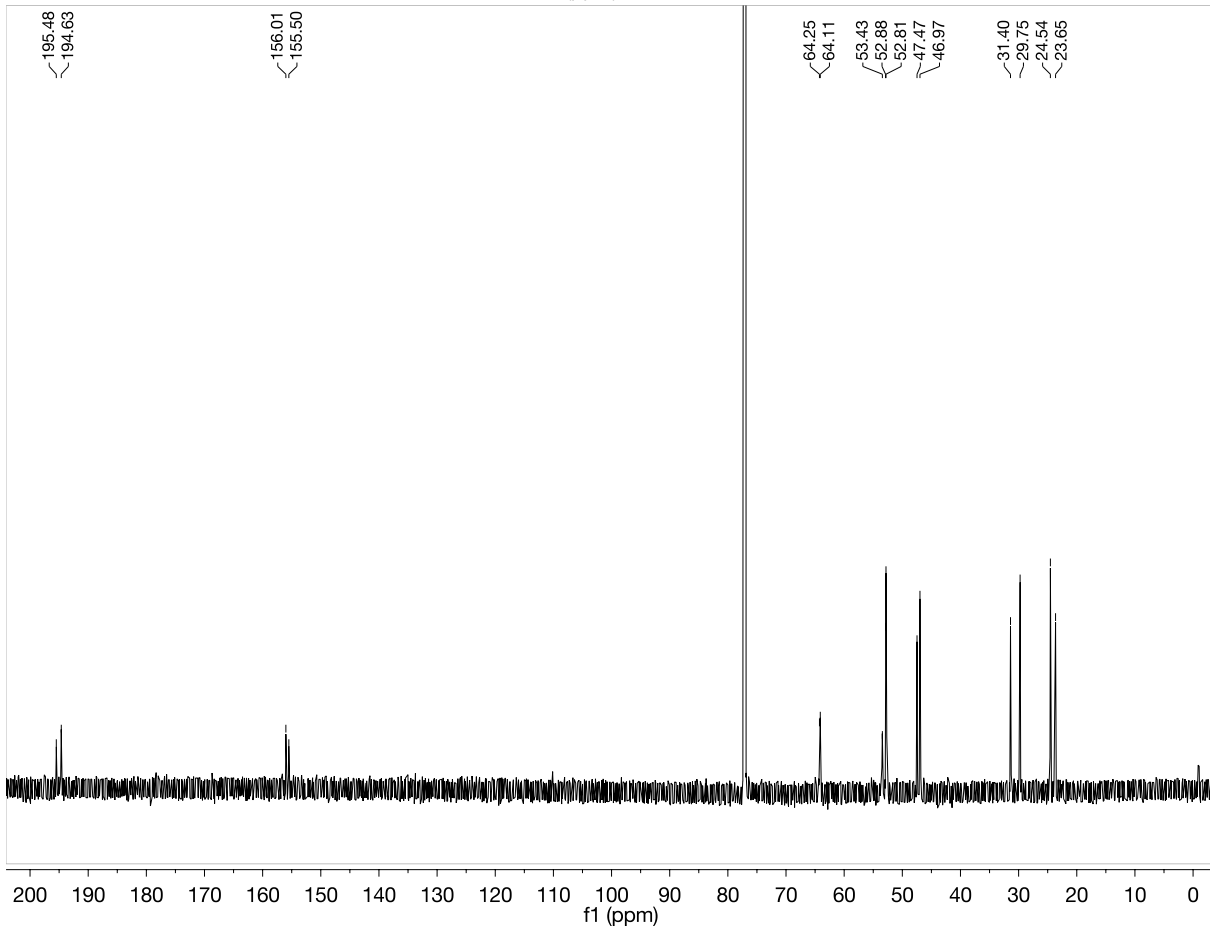
195.48
194.63
156.01
155.50
64.25
64.11
53.43
52.88
52.81
47.47
46.97
31.40
29.75
24.54
23.65
200
190
180
170
160
150
140
130
120
110
100
90
80
70
60
50
40
30
20
10
0
f1 (ppm)

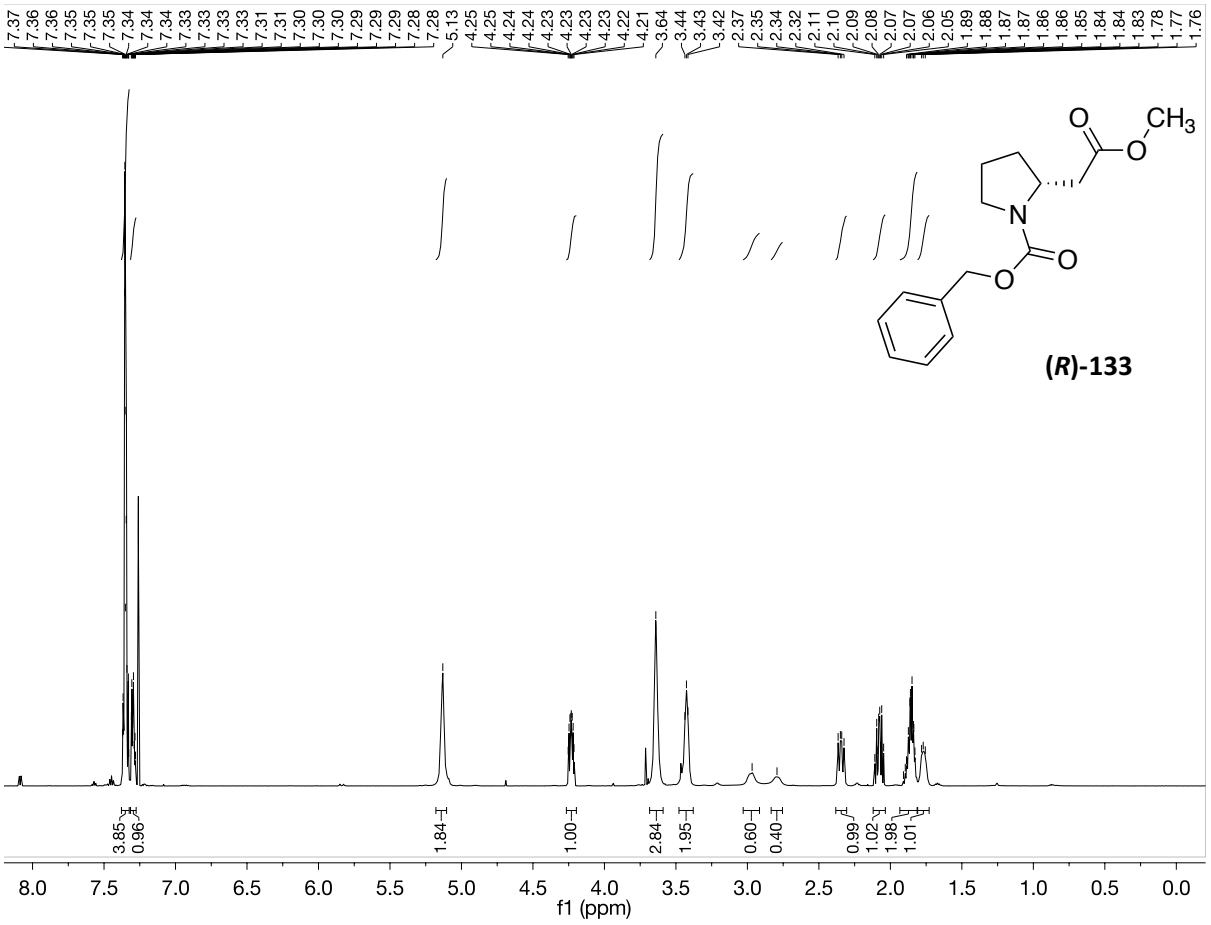
7.37 7.36 7.36 7.35 7.35 7.35 7.34 7.34 7.34 7.33 7.33 7.33 7.33 7.31 7.31 7.30 7.30 7.30 7.29 7.29 7.29 7.28 7.28 5.13 4.25 4.25 4.24 4.24 4.23 4.23 4.23 4.23 4.22 4.21 3.64 3.44 3.43 3.42 2.37 2.35 2.34 2.32 2.11 2.10 2.09 2.08 2.07 2.07 2.06 2.05 1.89 1.88 1.87 1.87 1.86 1.86 1.85 1.84 1.84 1.83 1.78 1.77 1.76
O
CH3
O
N
O
O
O
(R)-133
3.85 0.96 1.84 1.00 2.84 1.95 0.60 0.40 0.99 1.02 1.98 1.01
8.0 7.5 7.0 6.5 6.0 5.5 5.0 4.5 4.0 3.5 3.0 2.5 2.0 1.5 1.0 0.5 0.0
f1 (ppm)

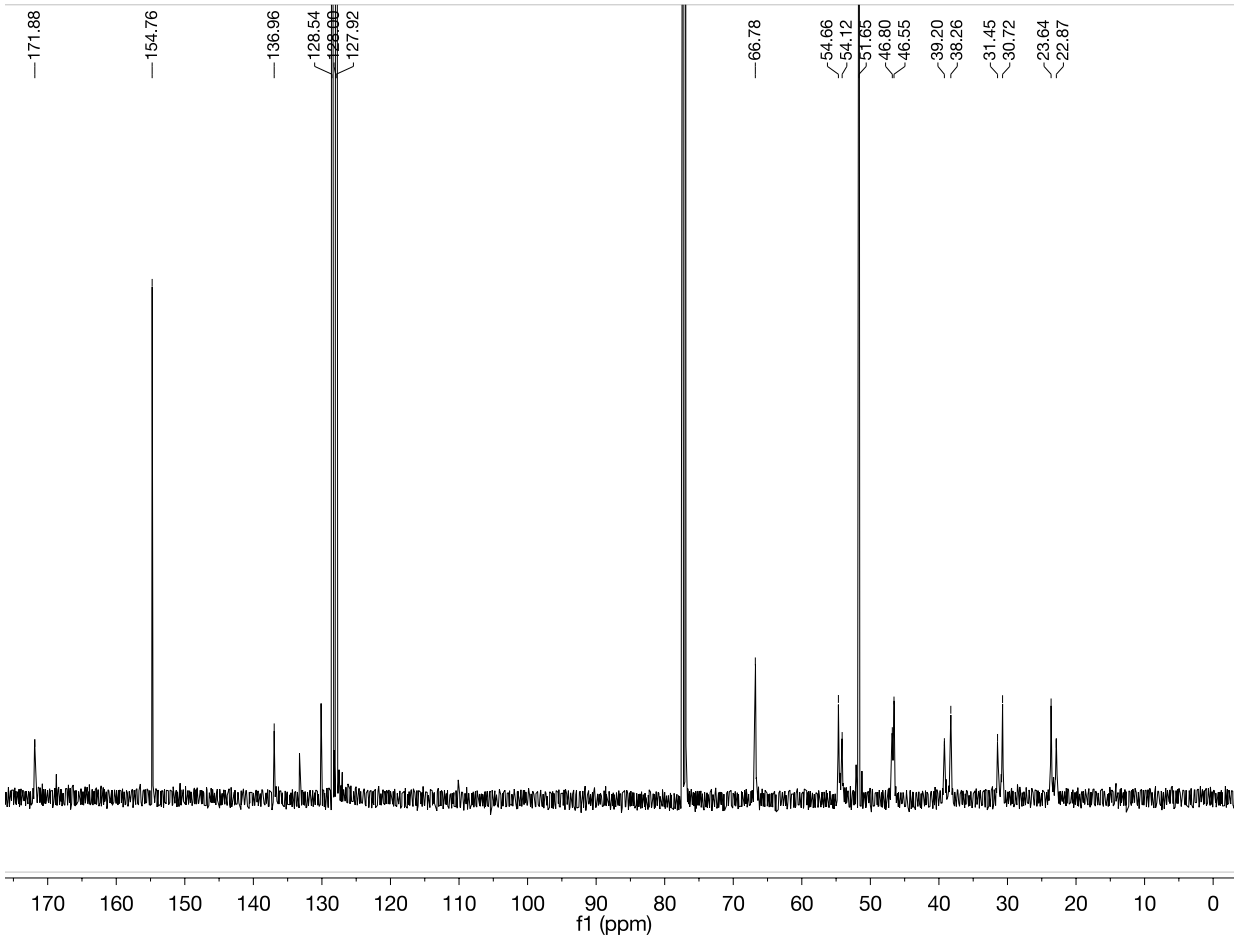
171.88 154.76 136.96 128.54 128.00 127.92 66.78 54.66 54.12 51.65 46.80 46.55 39.20 38.26 31.45 30.72 23.64 22.87
170 160 150 140 130 120 110 100 90 80 70 60 50 40 30 20 10 0
f1 (ppm)

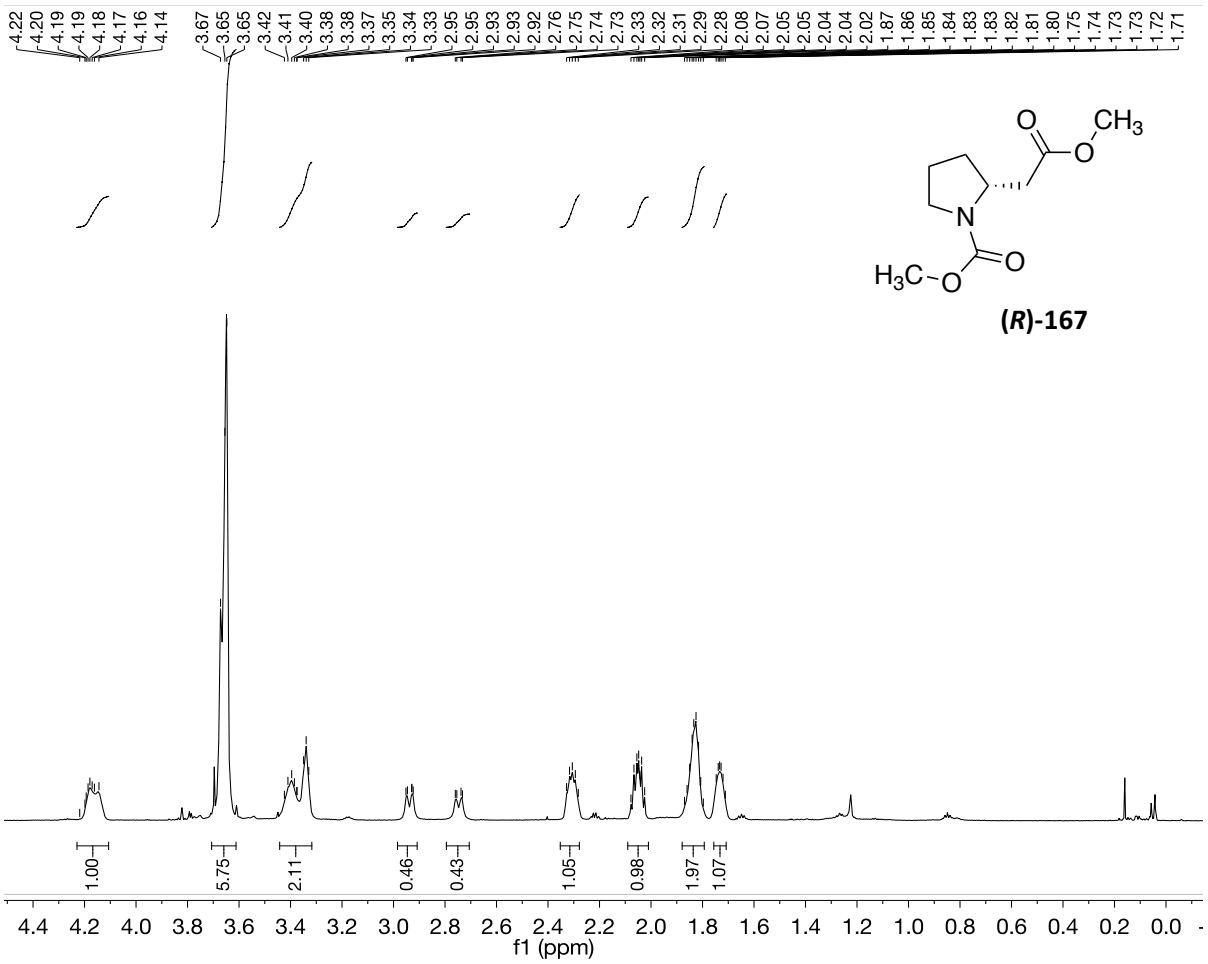
4.22 4.20 4.19 4.19 4.18 4.17 4.16 4.14
3.67 3.65 3.65 3.42 3.41 3.40 3.38 3.38 3.37 3.35 3.34 3.33 2.95 2.95 2.93 2.92 2.76 2.75 2.74 2.73 2.33 2.32 2.31 2.29 2.28 2.08 2.07 2.05 2.05 2.04 2.04 2.02 1.87 1.86 1.85 1.84 1.83 1.82 1.81 1.80 1.75 1.74 1.73 1.73 1.72 1.71
O
O
CH3
N
O
H3C
O
1.00 5.75 2.11 0.46 0.43 1.05 0.98 1.97 1.07
4.4 4.2 4.0 3.8 3.6 3.4 3.2 3.0 2.8 2.6 2.4 2.2 2.0 1.8 1.6 1.4 1.2 1.0 0.8 0.6 0.4 0.2 0.0
f1 (ppm)

(*R*)-167

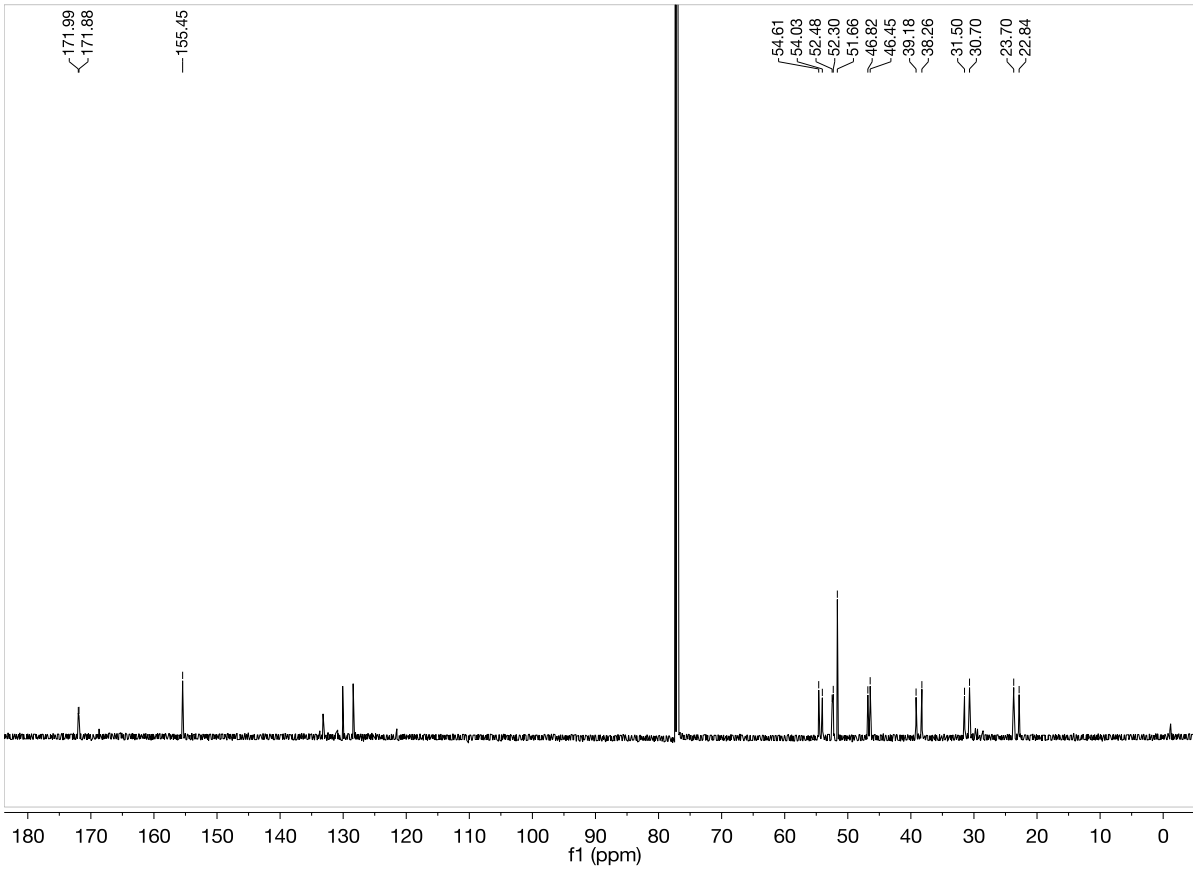
171.99
171.88
155.45
54.61
54.03
52.48
52.30
51.66
46.82
46.45
39.18
38.26
31.50
30.70
23.70
22.84
180 170 160 150 140 130 120 110 100 90 80 70 60 50 40 30 20 10 0
f1 (ppm)

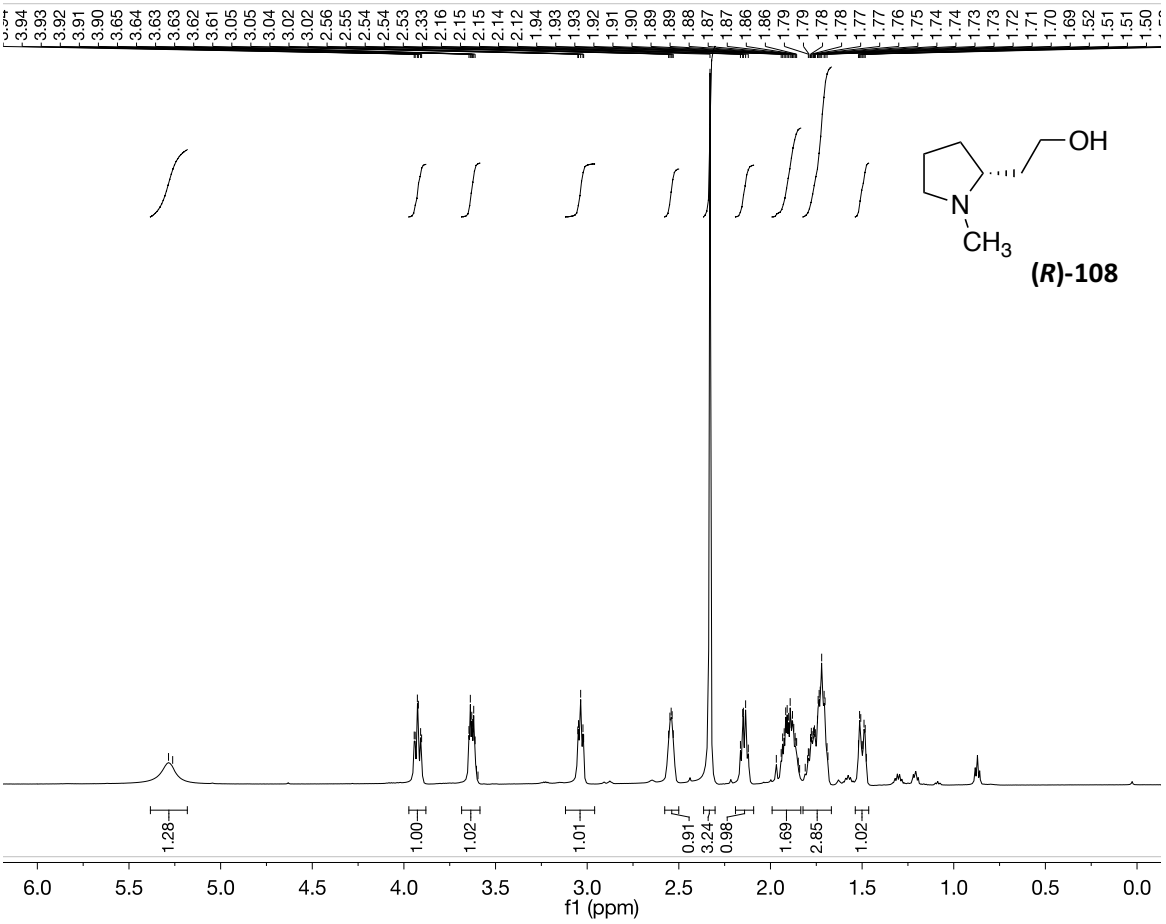
OH
N
CH3
(R)-108
1.28
1.00
1.02
1.01
0.91
3.24
0.98
1.69
2.85
1.02
f1 (ppm)

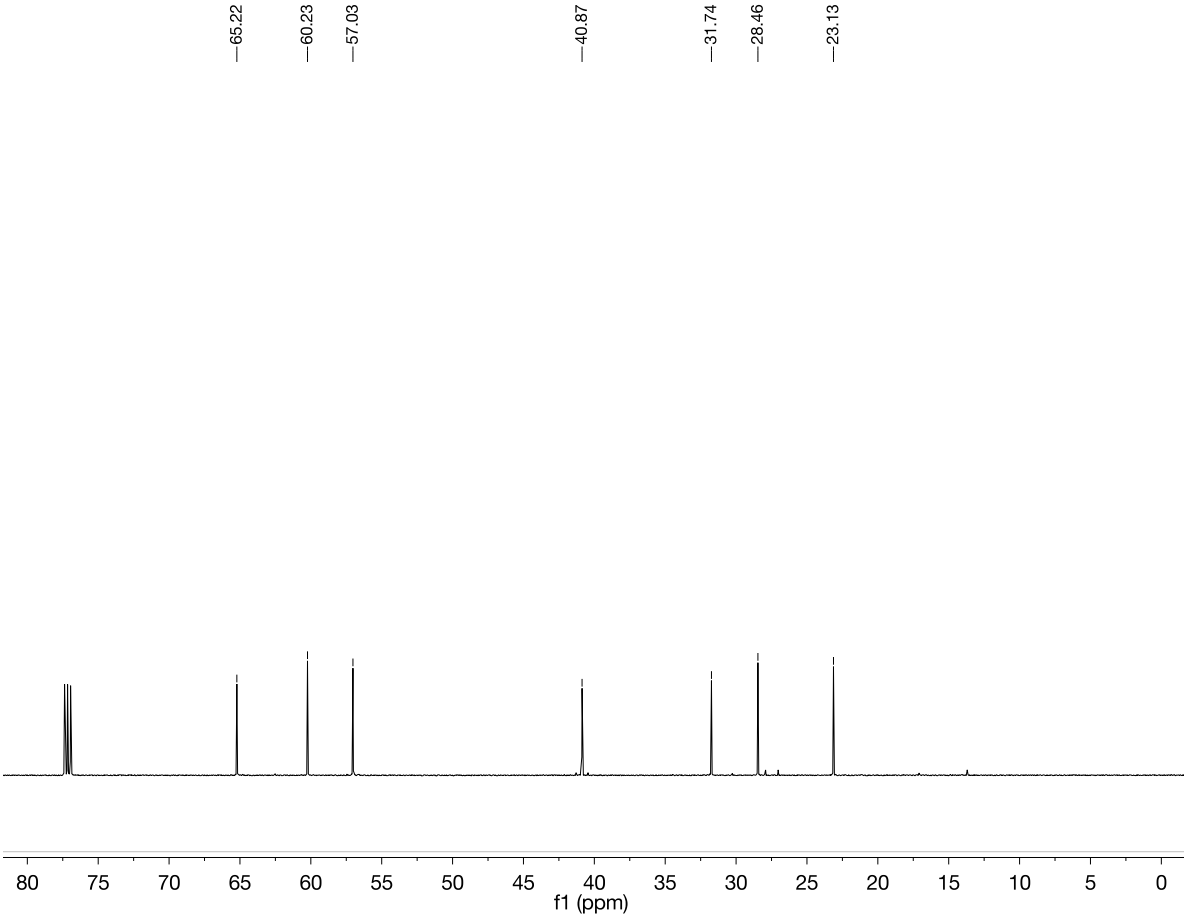
65.22
60.23
57.03
40.87
31.74
28.46
23.13
f1 (ppm)

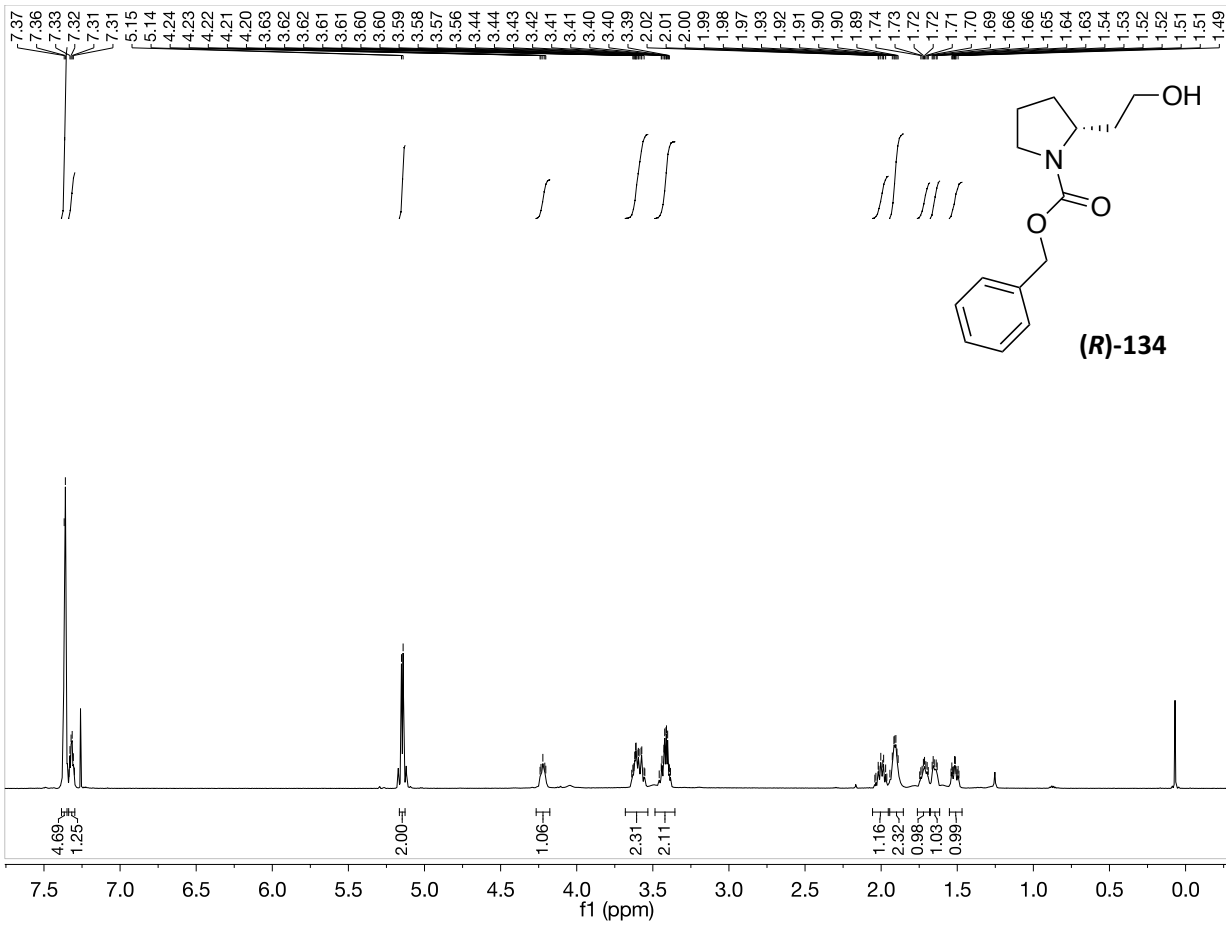
7.37
7.36
7.33
7.32
7.31
5.15
5.14
4.24
4.23
4.22
4.21
4.20
3.63
3.62
3.62
3.61
3.61
3.60
3.60
3.59
3.58
3.57
3.56
3.44
3.44
3.43
3.42
3.41
3.41
3.40
3.40
3.39
2.02
2.01
2.00
1.99
1.98
1.97
1.93
1.92
1.91
1.90
1.90
1.89
1.74
1.73
1.72
1.72
1.71
1.70
1.69
1.66
1.66
1.65
1.64
1.63
1.54
1.53
1.52
1.52
1.51
1.51
1.49
OH
N
O
O
4.69
1.25
2.00
1.06
2.31
2.11
1.16
2.32
0.98
1.03
0.99
7.5
7.0
6.5
6.0
5.5
5.0
4.5
4.0
3.5
3.0
2.5
2.0
1.5
1.0
0.5
0.0
f1 (ppm)

(*R*)-134

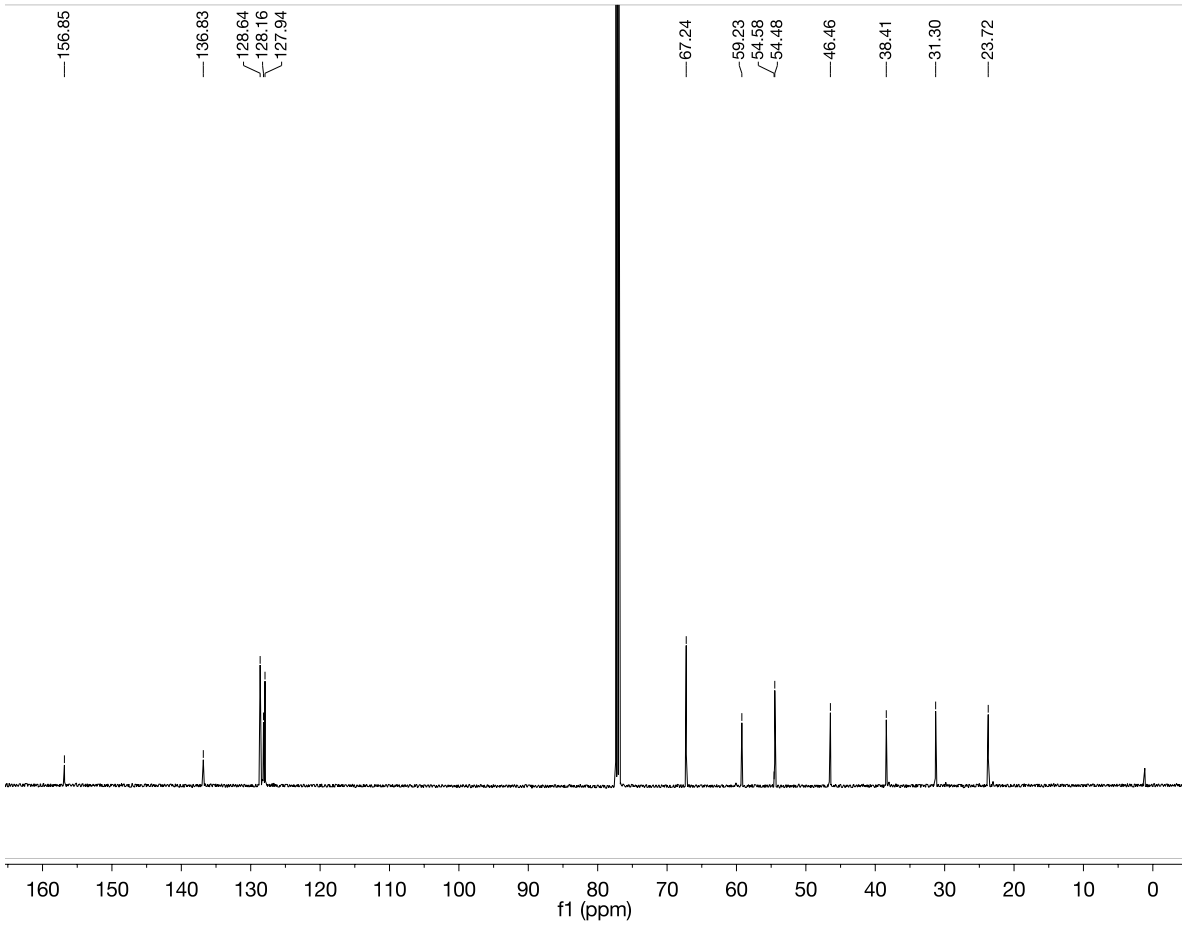
156.85
136.83
128.64
128.16
127.94
67.24
59.23
54.58
54.48
46.46
38.41
31.30
23.72
160
150
140
130
120
110
100
90
80
70
60
50
40
30
20
10
0
f1 (ppm)

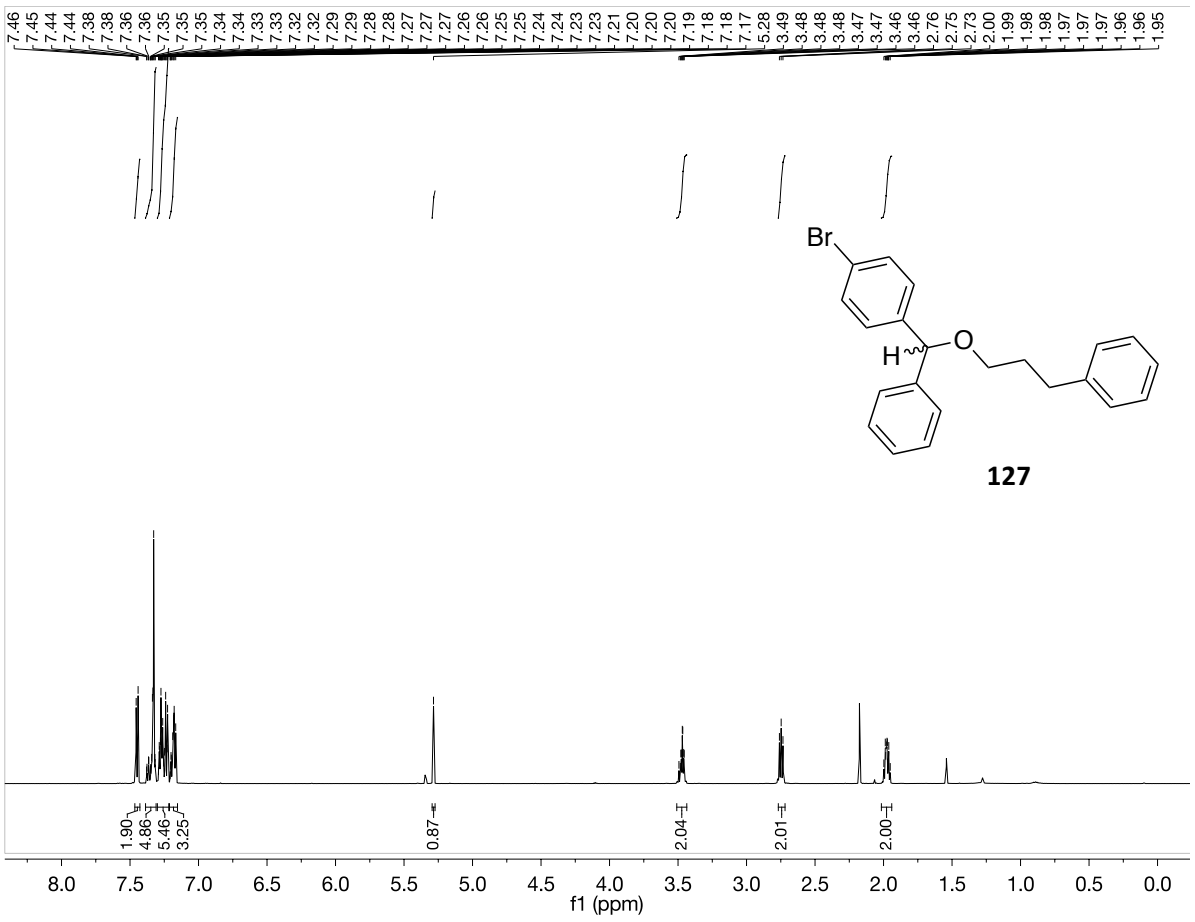
7.46 7.45 7.44 7.44 7.38 7.38 7.36 7.36 7.35 7.35 7.35 7.34 7.34 7.33 7.33 7.32 7.32 7.29 7.29 7.28 7.28 7.27 7.27 7.27 7.26 7.26 7.25 7.25 7.24 7.24 7.23 7.23 7.21 7.20 7.20 7.20 7.19 7.18 7.18 7.17 5.28 3.49 3.48 3.48 3.48 3.47 3.47 3.46 3.46 2.76 2.75 2.73 2.00 1.99 1.98 1.98 1.97 1.97 1.97 1.96 1.96 1.95
Br
H
O
127
1.90 4.86 5.46 3.25 0.87 2.04 2.01 2.00
8.0 7.5 7.0 6.5 6.0 5.5 5.0 4.5 4.0 3.5 3.0 2.5 2.0 1.5 1.0 0.5 0.0
f1 (ppm)

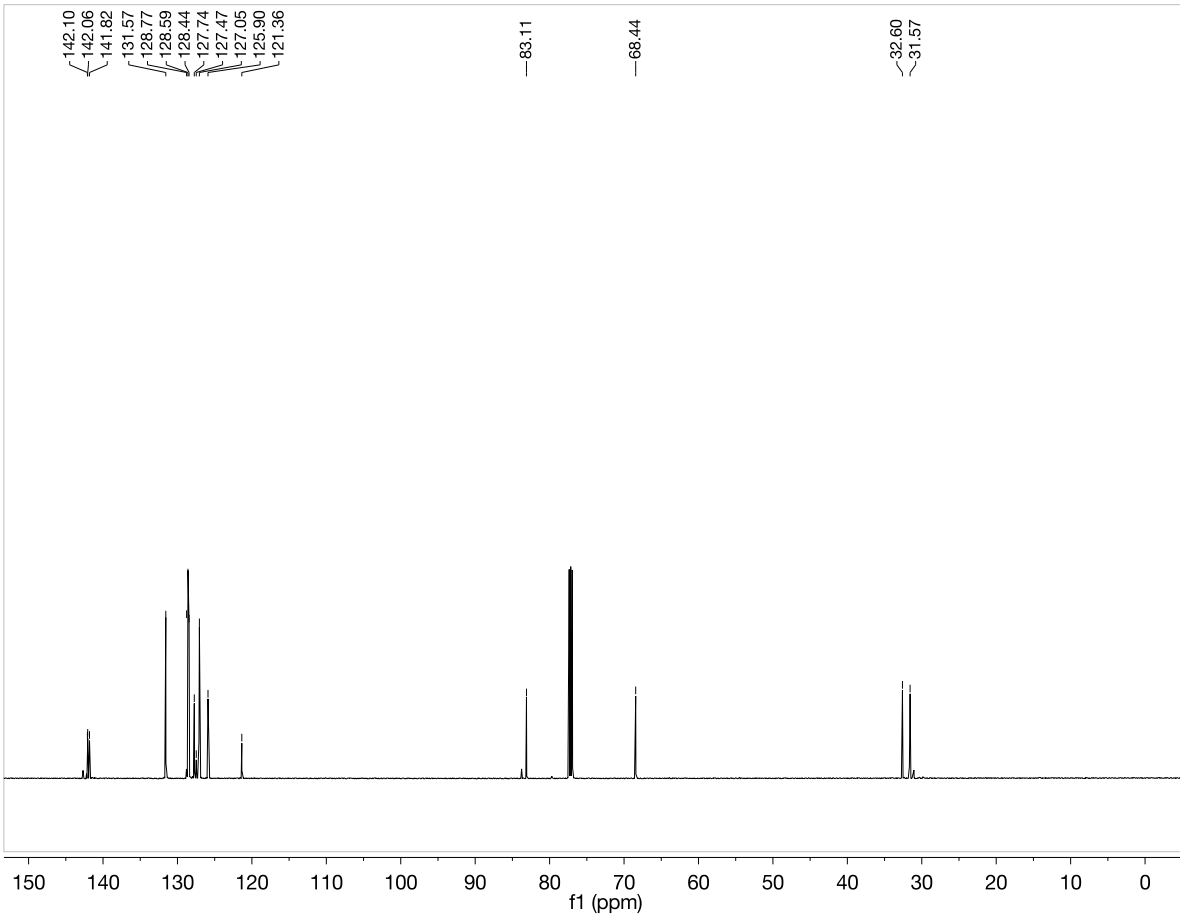
142.10 142.06 141.82 131.57 128.77 128.59 128.44 127.74 127.47 127.05 125.90 121.36
83.11
68.44
32.60 31.57
150 140 130 120 110 100 90 80 70 60 50 40 30 20 10 0
f1 (ppm)

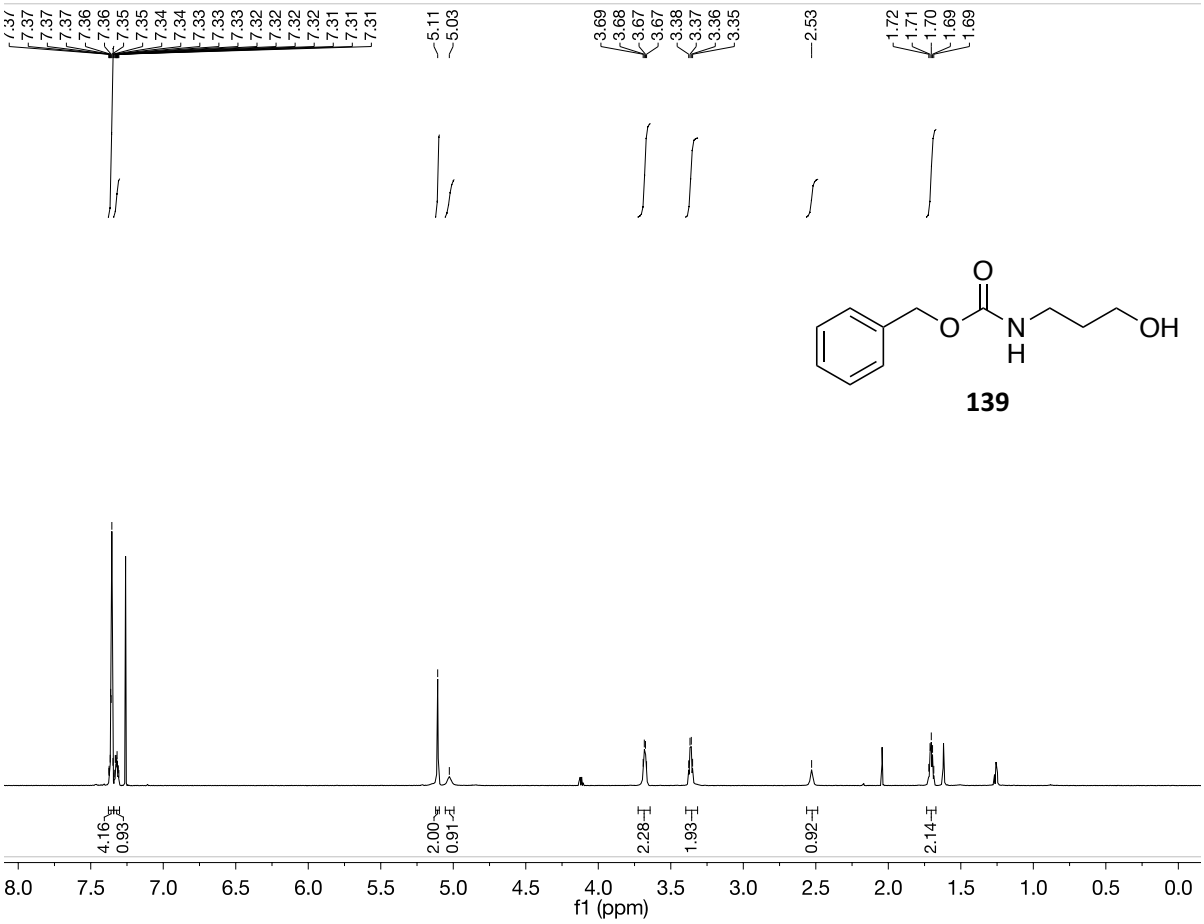
7.37
7.37
7.37
7.36
7.36
7.35
7.35
7.34
7.34
7.33
7.33
7.33
7.32
7.32
7.32
7.32
7.31
7.31
7.31
5.11
5.03
3.69
3.68
3.67
3.67
3.38
3.37
3.36
3.35
2.53
1.72
1.71
1.70
1.69
1.69
O
O
N
H
OH
4.16
0.93
2.00
0.91
2.28
1.93
0.92
2.14
8.0
7.5
7.0
6.5
6.0
5.5
5.0
4.5
4.0
3.5
3.0
2.5
2.0
1.5
1.0
0.5
0.0
f1 (ppm)

139

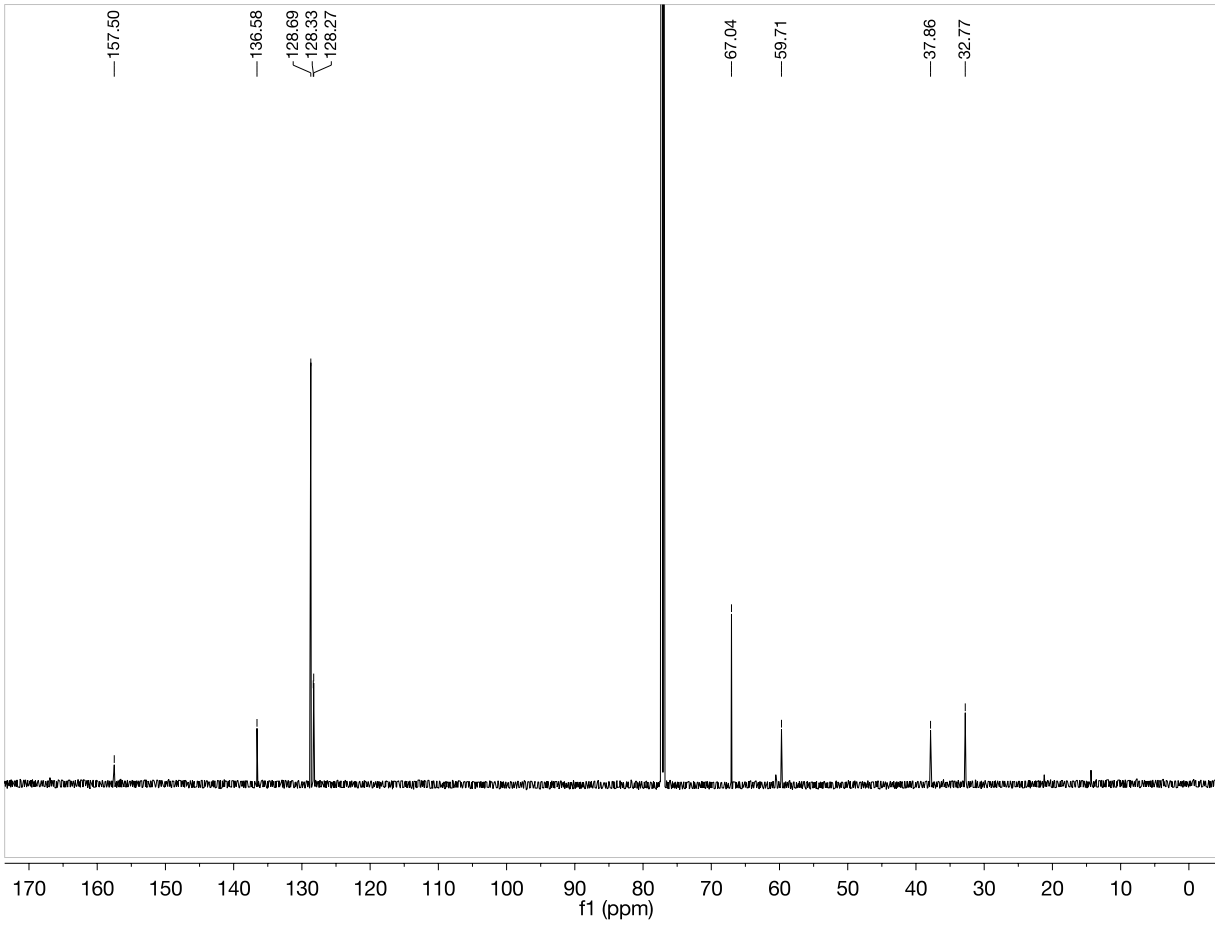
157.50
136.58
128.69
128.33
128.27
67.04
59.71
37.86
32.77
170
160
150
140
130
120
110
100
90
80
70
60
50
40
30
20
10
0
f1 (ppm)

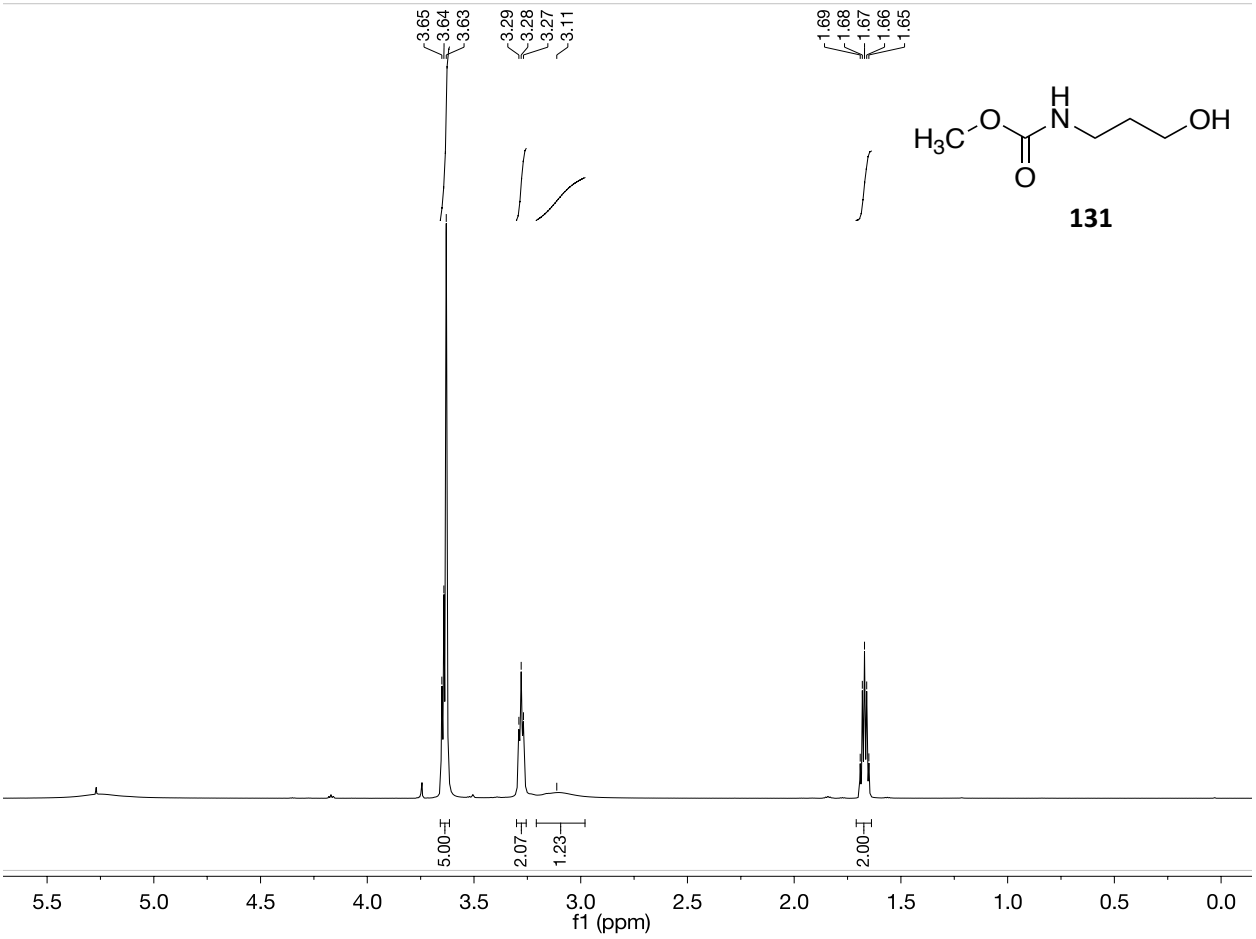
3.65
3.64
3.63
3.29
3.28
3.27
3.11
1.69
1.68
1.67
1.66
1.65
H
N
O
H3C
O
OH
131
5.00
2.07
1.23
2.00
5.5
5.0
4.5
4.0
3.5
3.0
2.5
2.0
1.5
1.0
0.5
0.0
f1 (ppm)

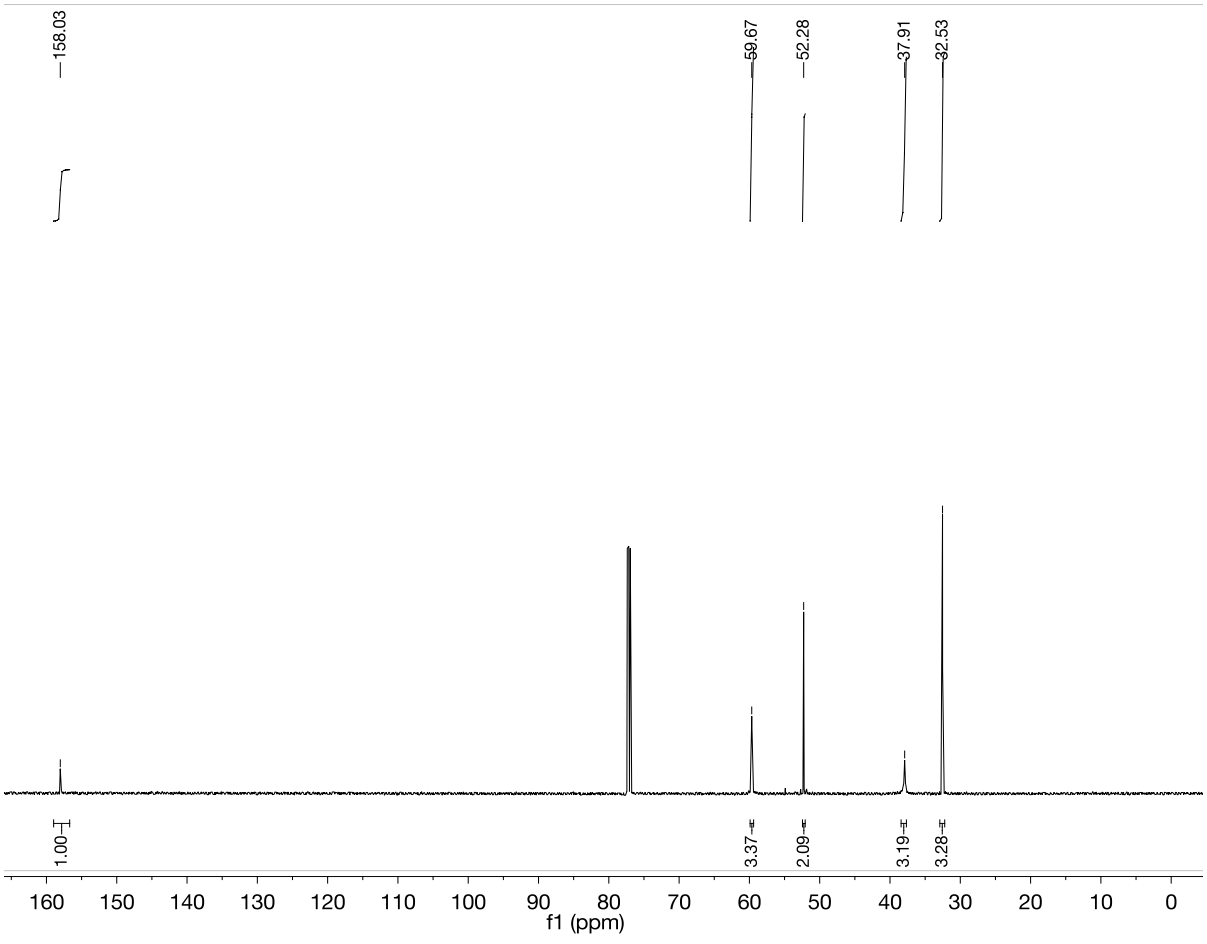
158.03
59.67
52.28
37.91
32.53
1.00
3.37
2.09
3.19
3.28
160
150
140
130
120
110
100
90
80
70
60
50
40
30
20
10
0
f1 (ppm)

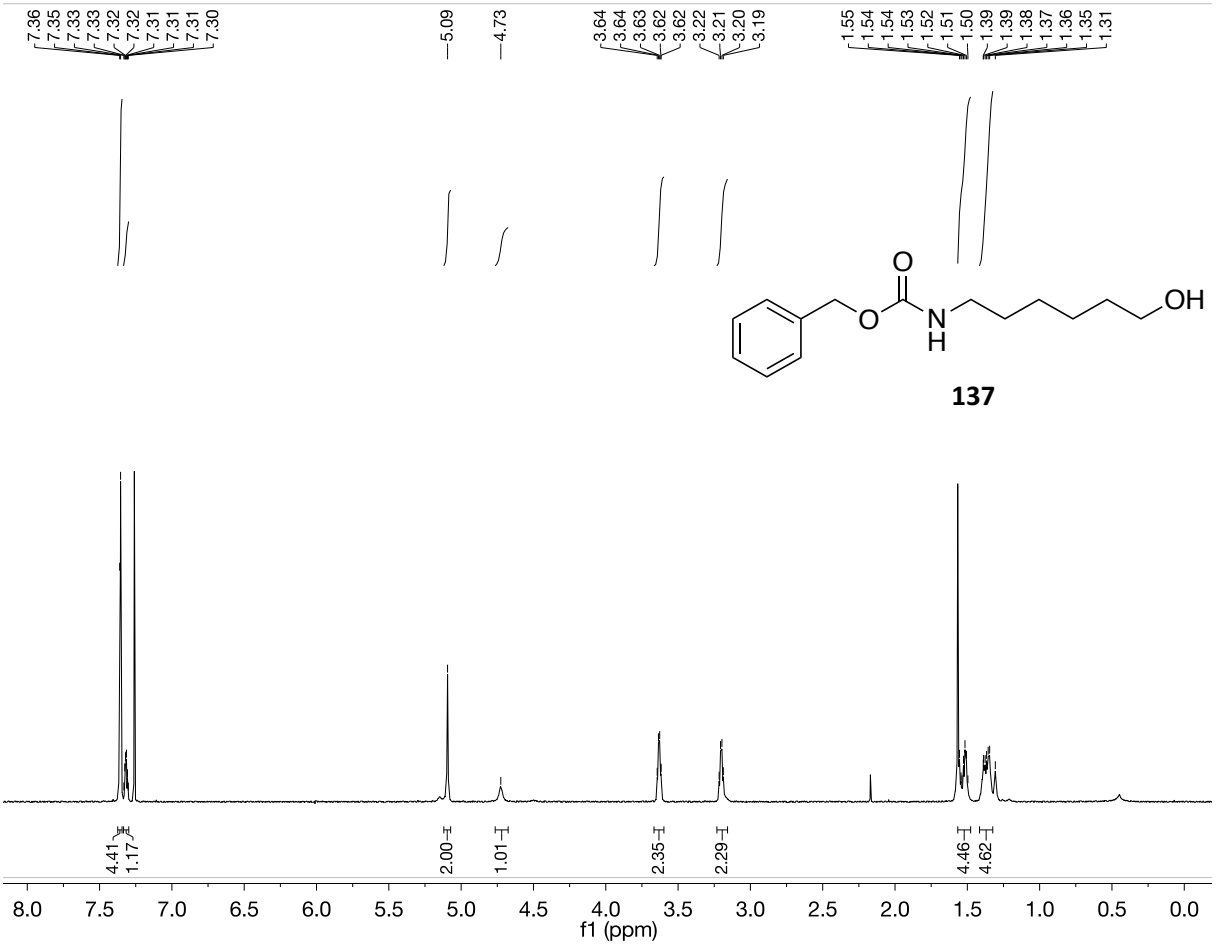
7.36
7.35
7.33
7.33
7.32
7.32
7.31
7.31
7.31
7.30
5.09
4.73
3.64
3.64
3.63
3.62
3.62
3.22
3.21
3.20
3.19
1.55
1.54
1.54
1.53
1.52
1.51
1.50
1.39
1.39
1.38
1.37
1.36
1.35
1.31
O
O
N
H
OH
4.41
1.17
2.00
1.01
2.35
2.29
4.46
4.62
8.0
7.5
7.0
6.5
6.0
5.5
5.0
4.5
4.0
3.5
3.0
2.5
2.0
1.5
1.0
0.5
0.0
f1 (ppm)

137

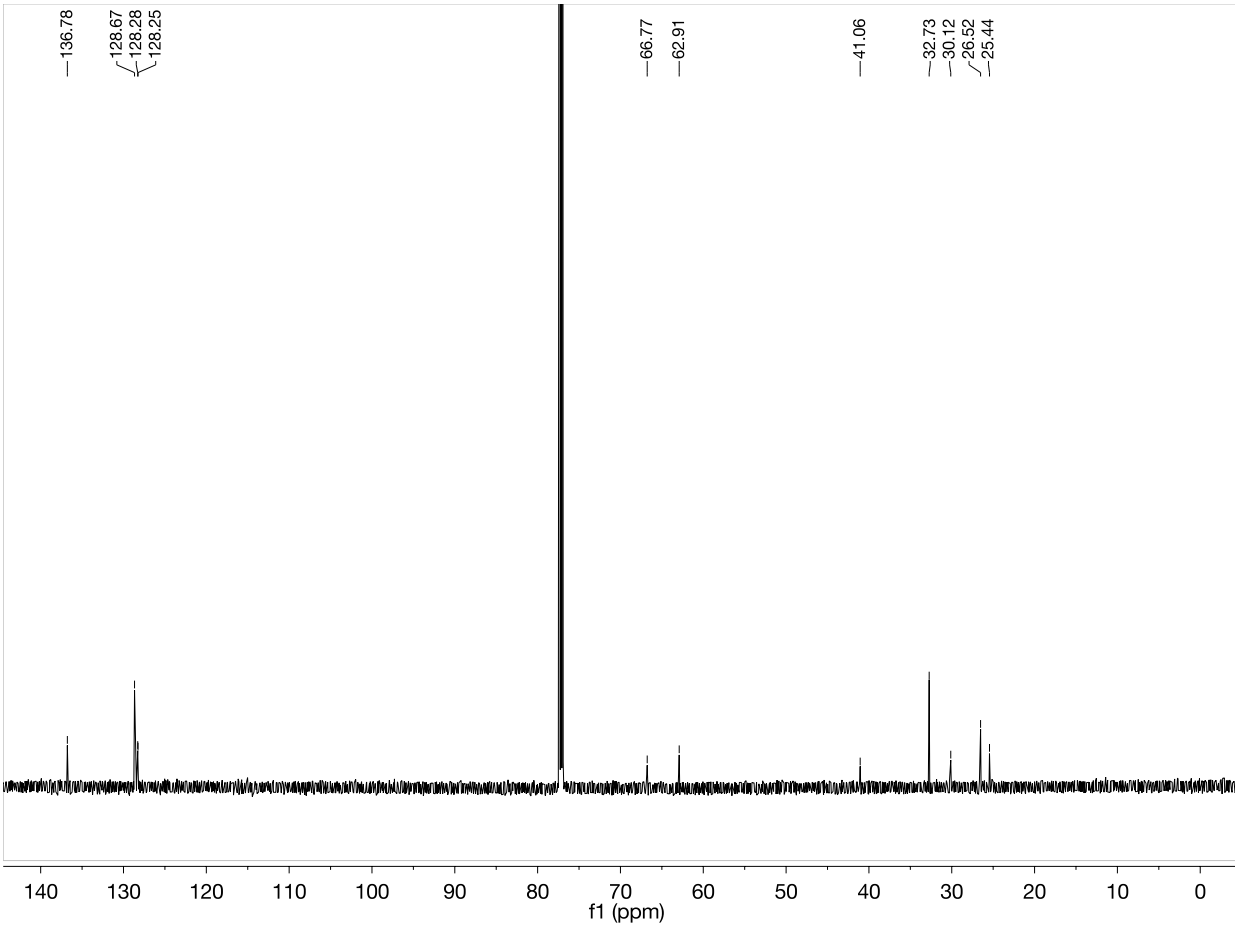
136.78
128.67
128.28
128.25
66.77
62.91
41.06
32.73
30.12
26.52
25.44
140
130
120
110
100
90
80
70
60
50
40
30
20
10
0
f1 (ppm)

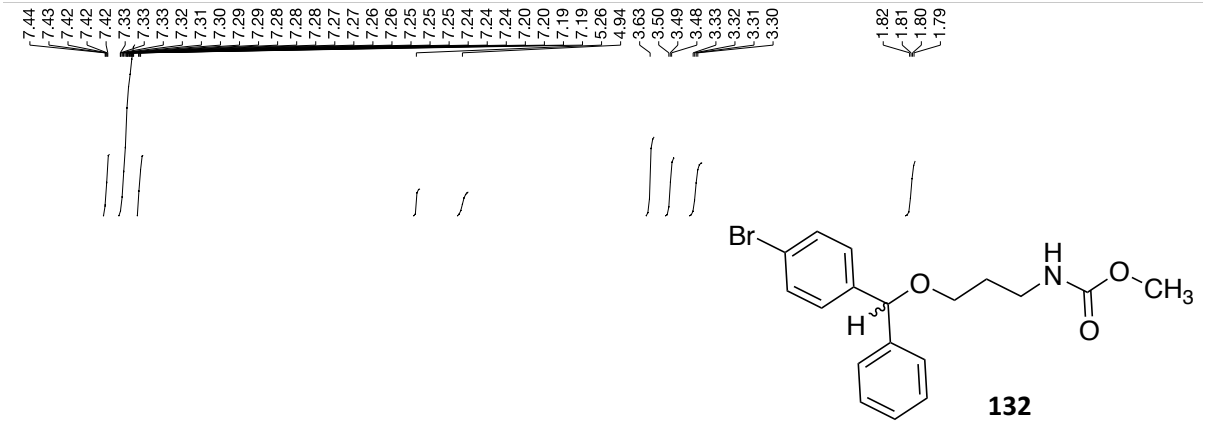
7.44
7.43
7.42
7.42
7.42
7.42
7.33
7.33
7.33
7.32
7.31
7.30
7.29
7.29
7.28
7.28
7.28
7.27
7.27
7.26
7.26
7.25
7.25
7.25
7.24
7.24
7.24
7.20
7.20
7.19
7.19
5.26
4.94
3.63
3.50
3.49
3.48
3.33
3.32
3.31
3.30
1.82
1.81
1.80
1.79
Br
O
H
N
O
O
CH3
H

132

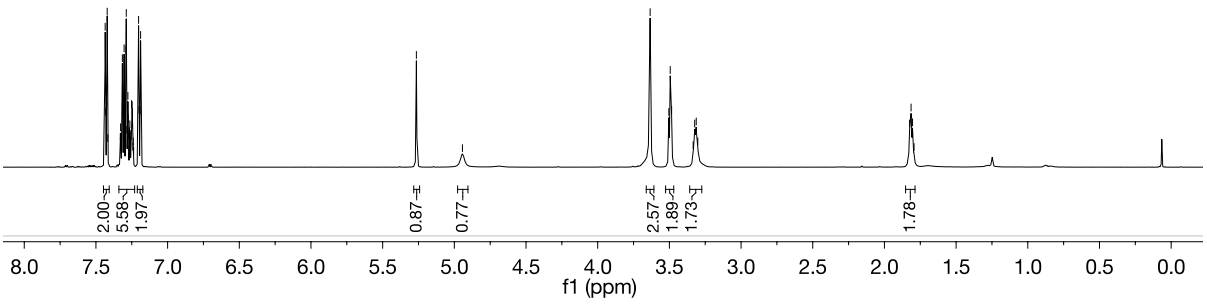
2.00
5.58
1.97
0.87
0.77
2.57
1.89
1.73
1.78
8.0
7.5
7.0
6.5
6.0
5.5
5.0
4.5
4.0
3.5
3.0
2.5
2.0
1.5
1.0
0.5
0.0
f1 (ppm)

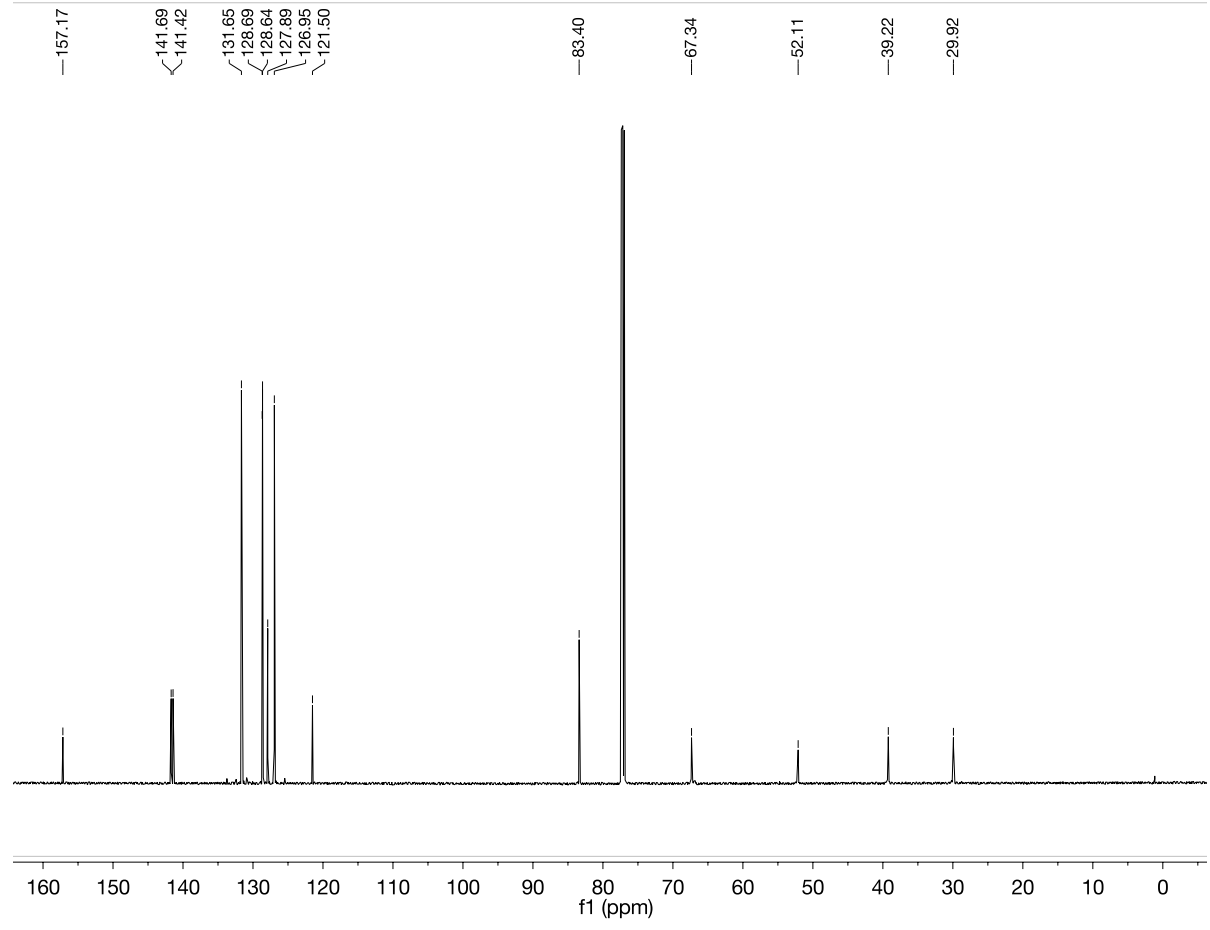
157.17
141.69
141.42
131.65
128.69
128.64
127.89
126.95
121.50
83.40
67.34
52.11
39.22
29.92
160
150
140
130
120
110
100
90
80
70
60
50
40
30
20
10
0
f1 (ppm)

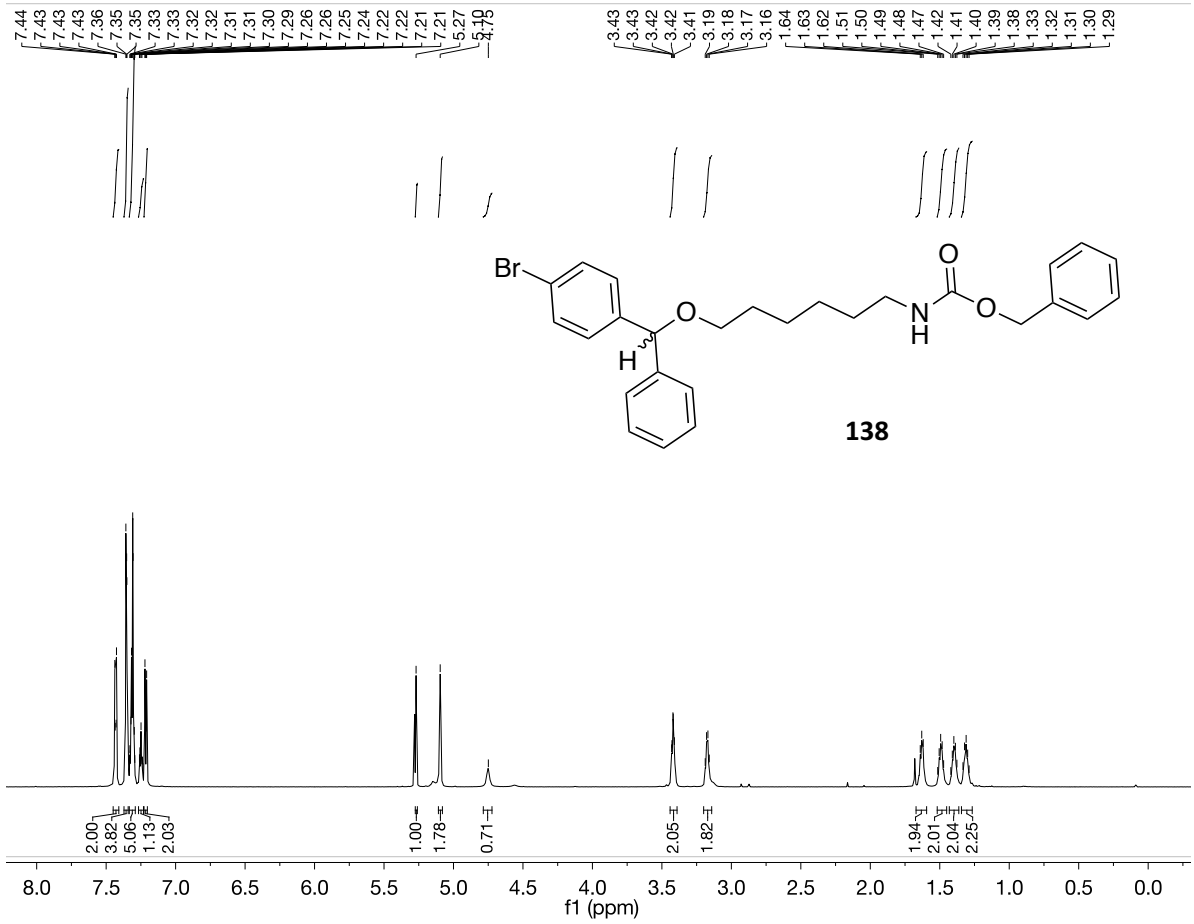
7.44 7.43 7.43 7.43 7.36 7.35 7.35 7.33 7.33 7.32 7.32 7.31 7.31 7.30 7.29 7.26 7.26 7.25 7.24 7.22 7.22 7.21 7.21 5.27 5.10 4.75
3.43 3.43 3.42 3.42 3.41 3.19 3.18 3.17 3.16 1.64 1.63 1.62 1.51 1.50 1.49 1.48 1.47 1.42 1.41 1.40 1.39 1.38 1.33 1.32 1.31 1.30 1.29
Br
O
N
H
O
O
H
138
2.00 3.82 5.06 1.13 2.03 1.00 1.78 0.71 2.05 1.82 1.94 2.01 2.04 2.25
8.0 7.5 7.0 6.5 6.0 5.5 5.0 4.5 4.0 3.5 3.0 2.5 2.0 1.5 1.0 0.5 0.0
f1 (ppm)

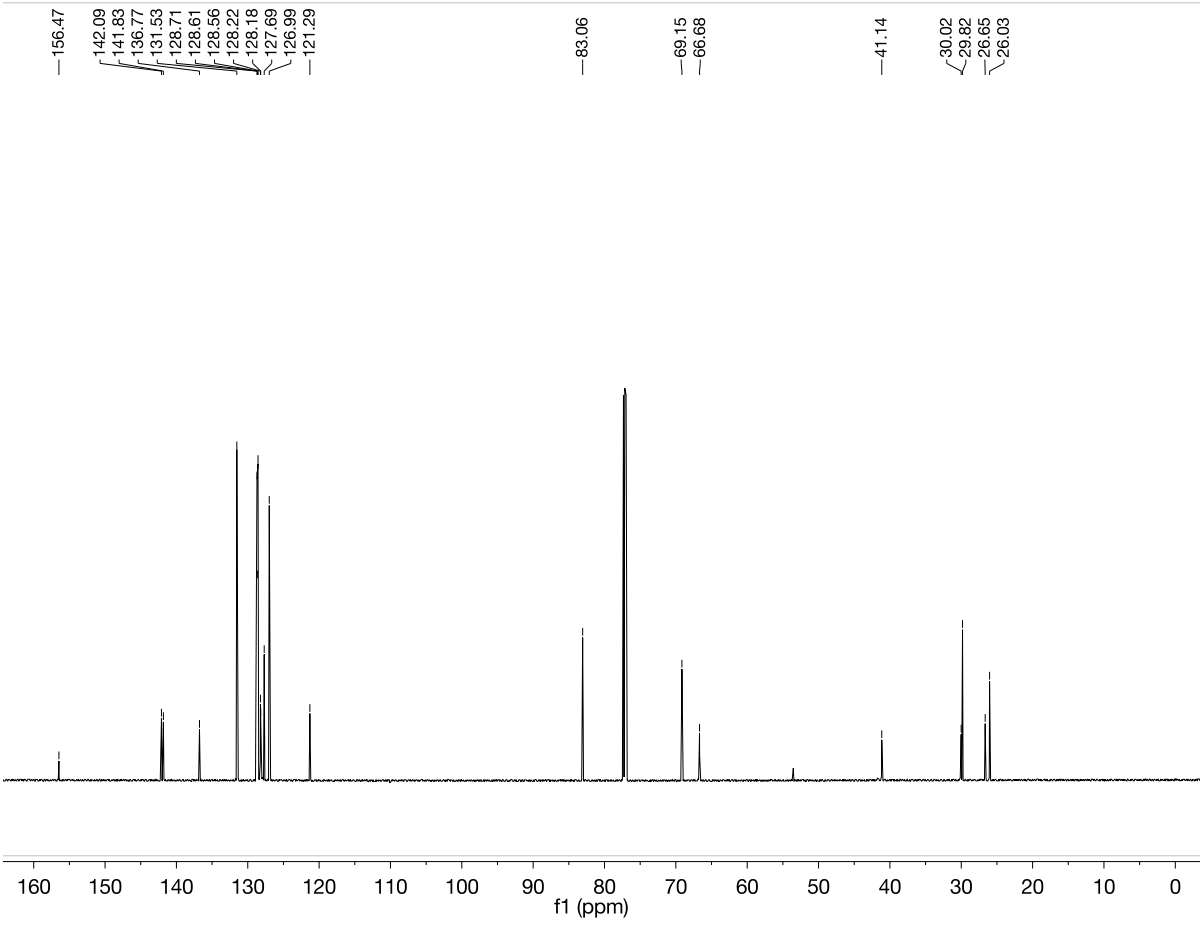
156.47 142.09 141.83 136.77 131.53 128.71 128.61 128.56 128.22 128.18 127.69 126.99 121.29 83.06 69.15 66.68 41.14 30.02 29.82 26.65 26.03
160 150 140 130 120 110 100 90 80 70 60 50 40 30 20 10 0
f1 (ppm)

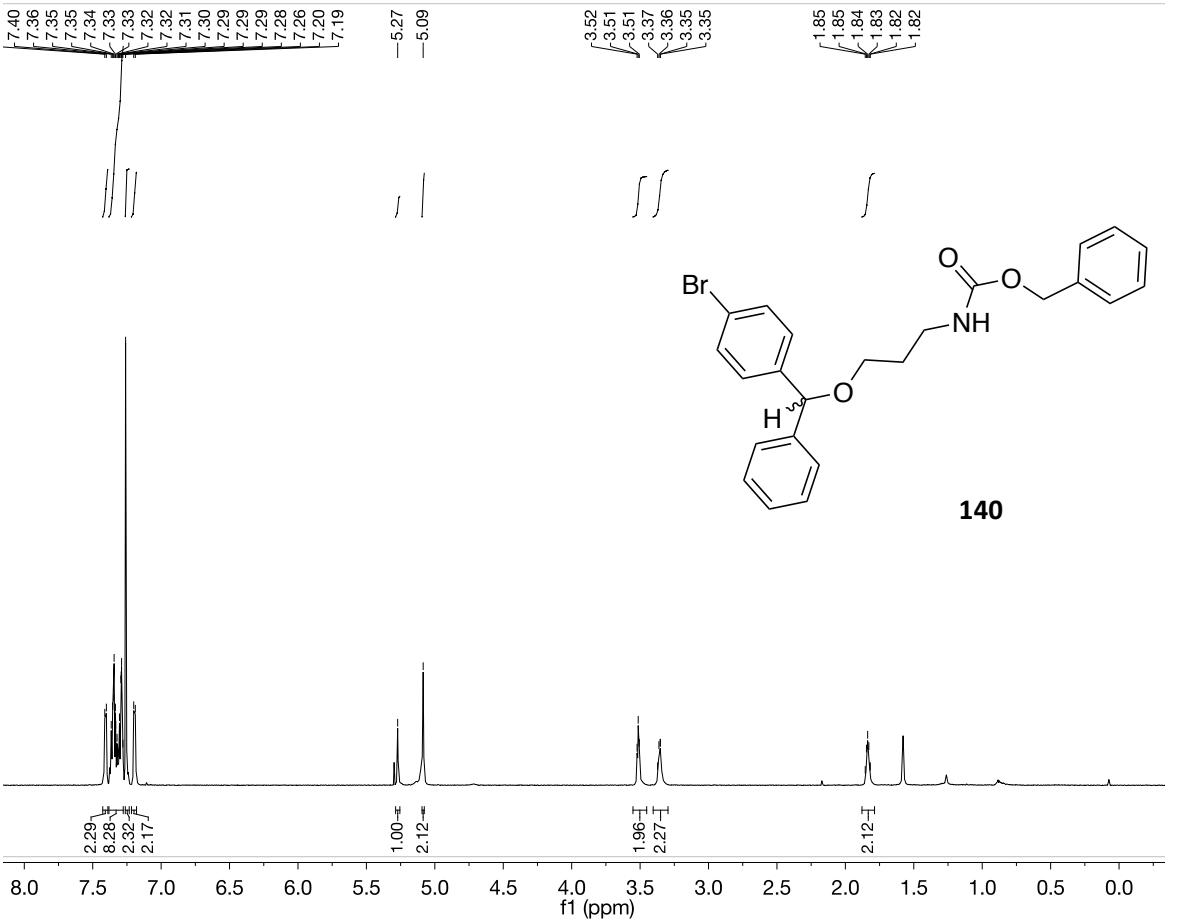
7.40
7.36
7.35
7.35
7.34
7.33
7.33
7.32
7.32
7.31
7.30
7.29
7.29
7.29
7.28
7.26
7.20
7.19
5.27
5.09
3.52
3.51
3.51
3.37
3.36
3.35
3.35
1.85
1.85
1.84
1.83
1.82
1.82
Br
O
O
NH
O
H
2.29
8.28
2.32
2.17
1.00
2.12
1.96
2.27
2.12
8.0
7.5
7.0
6.5
6.0
5.5
5.0
4.5
4.0
3.5
3.0
2.5
2.0
1.5
1.0
0.5
0.0
f1 (ppm)

140

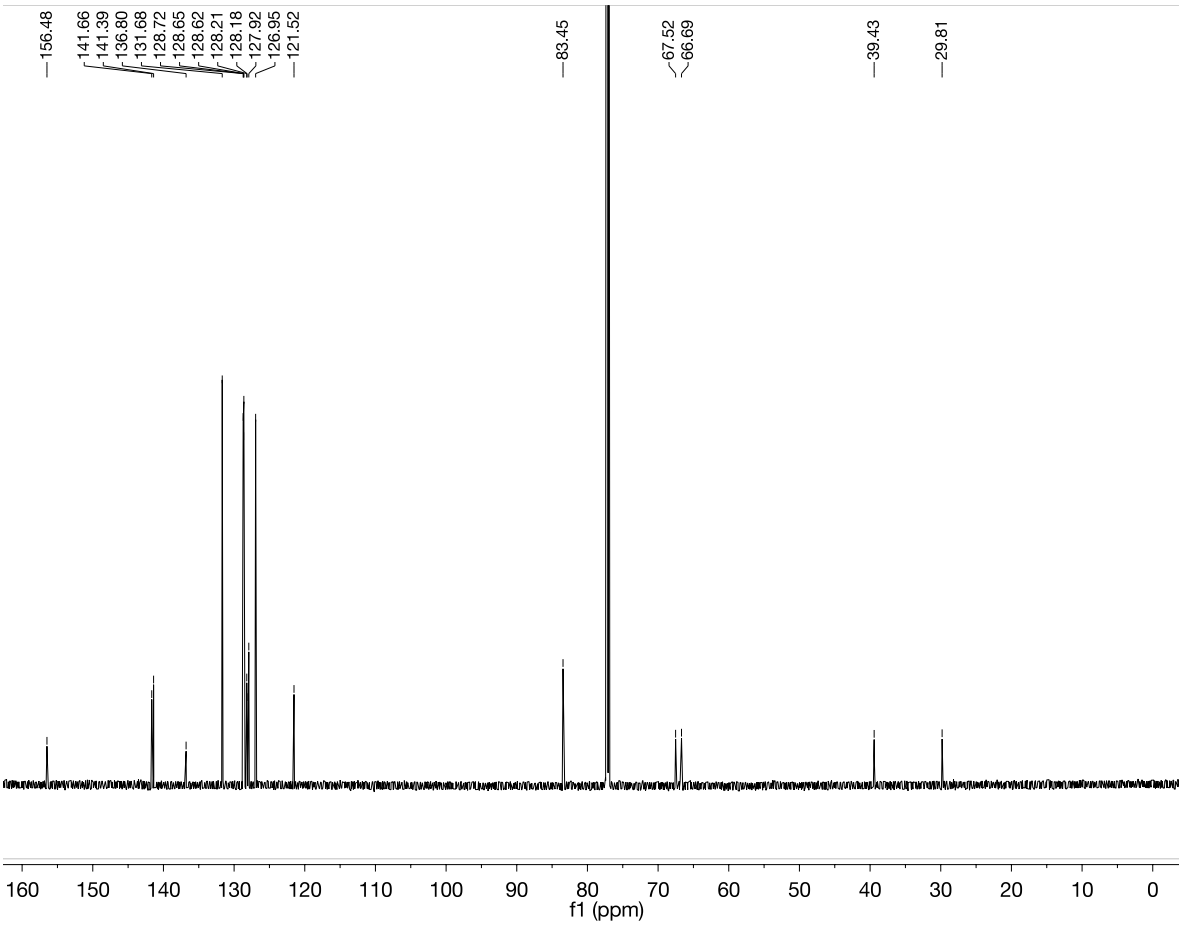
156.48
141.66
141.39
136.80
131.68
128.72
128.65
128.62
128.21
128.18
127.92
126.95
121.52
83.45
67.52
66.69
39.43
29.81
160
150
140
130
120
110
100
90
80
70
60
50
40
30
20
10
0
f1 (ppm)

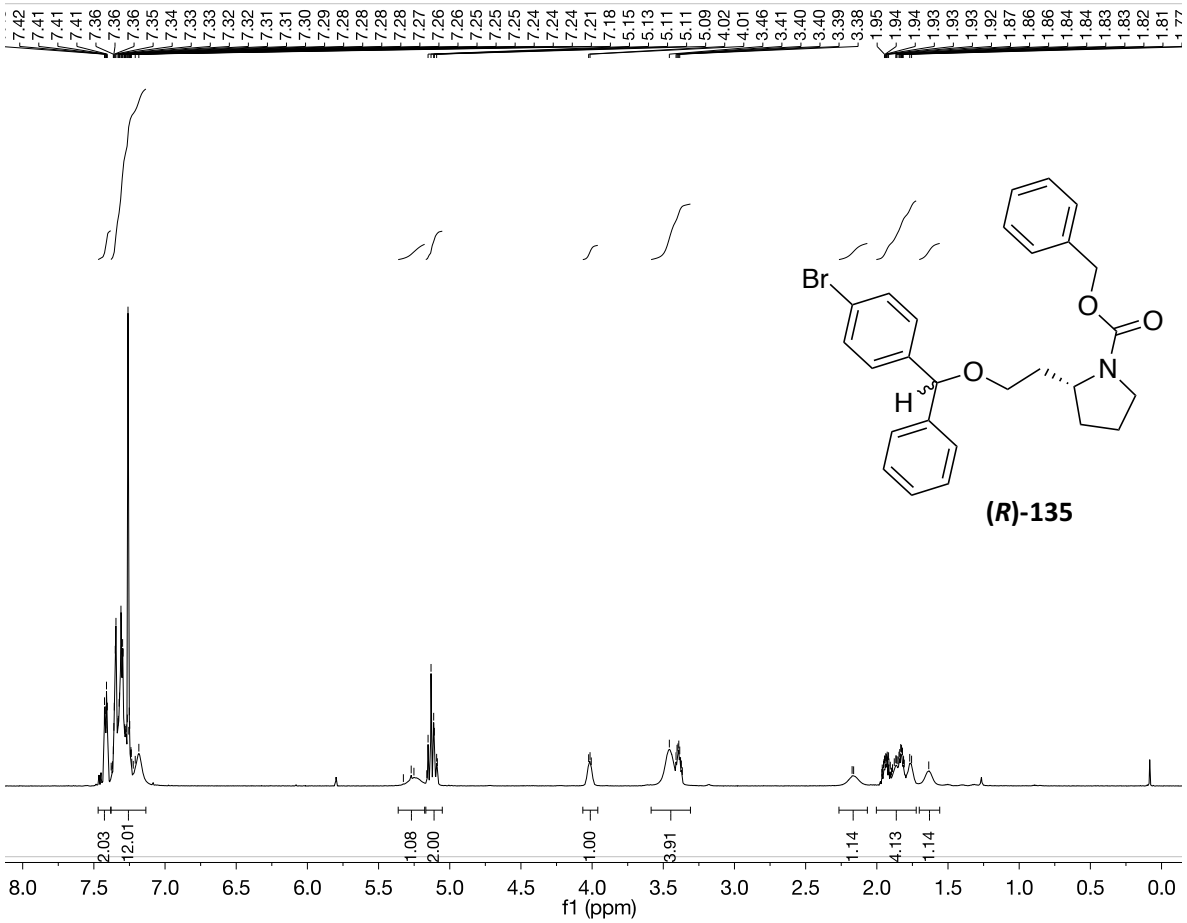

(*R*)-135

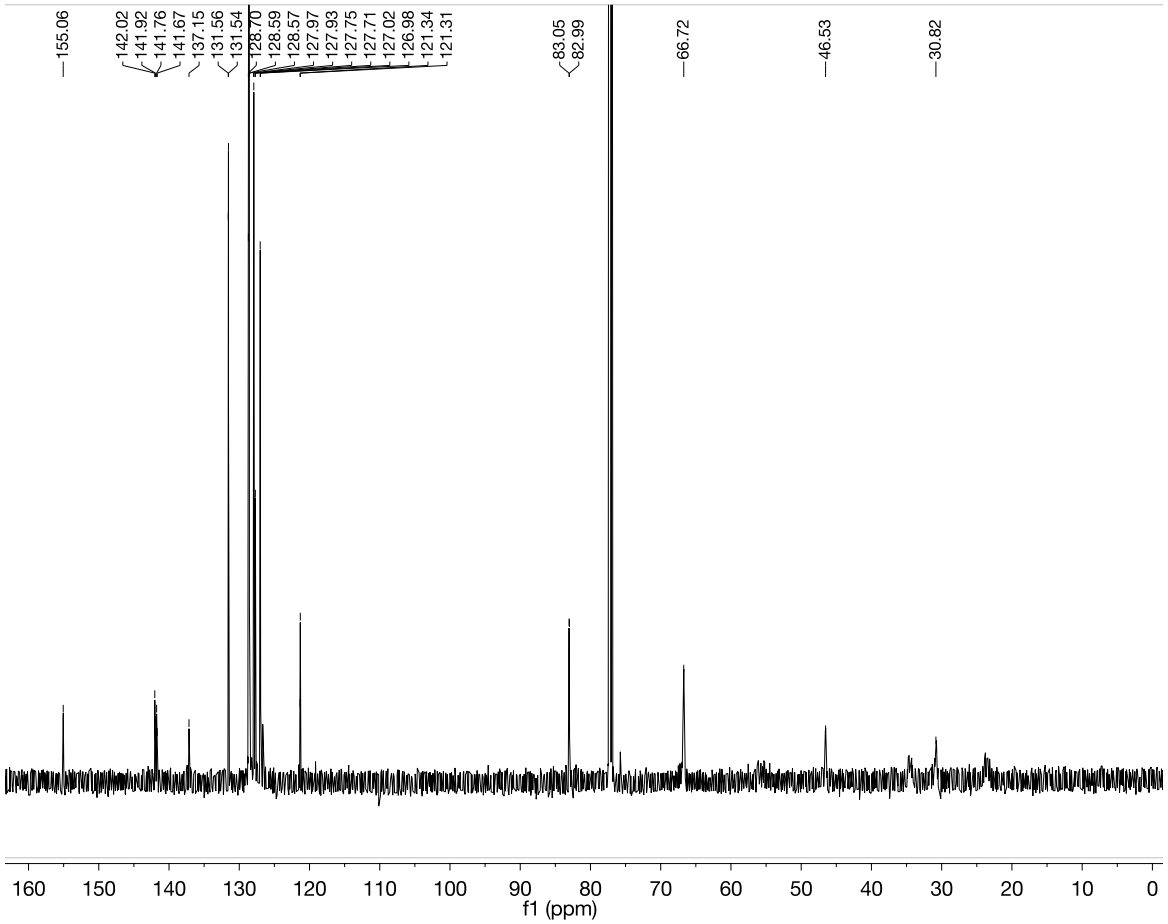

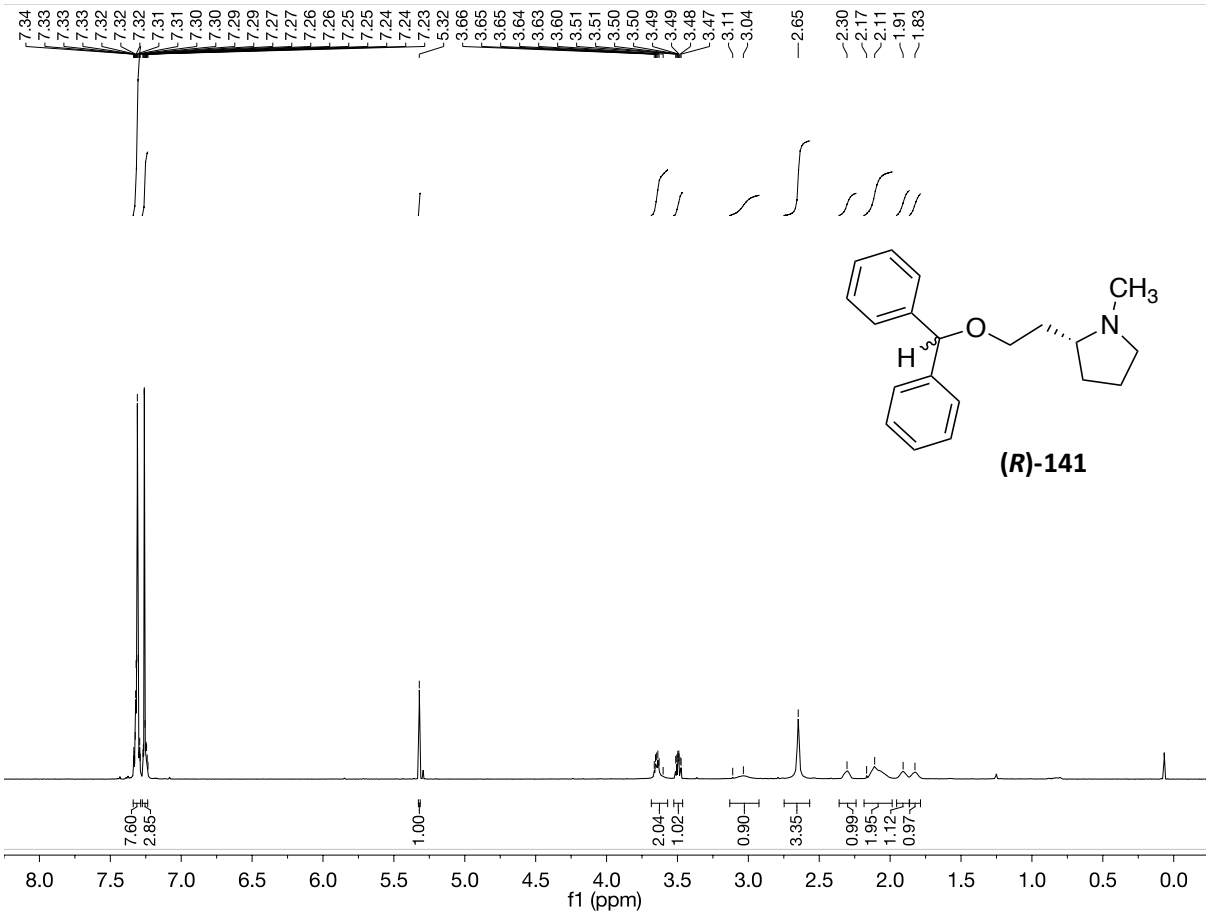
7.34 7.33 7.33 7.33 7.32 7.32 7.32 7.31 7.31 7.30 7.30 7.30 7.29 7.29 7.27 7.27 7.26 7.26 7.25 7.25 7.24 7.24 7.23 5.32 3.66 3.65 3.65 3.64 3.63 3.60 3.51 3.51 3.50 3.50 3.49 3.49 3.48 3.47 3.11 3.04 2.65 2.30 2.17 2.11 1.91 1.83
CH3
N
O
H
(R)-141
7.60 2.85 1.00 2.04 1.02 0.90 3.35 0.99 1.95 1.12 0.97
8.0 7.5 7.0 6.5 6.0 5.5 5.0 4.5 4.0 3.5 3.0 2.5 2.0 1.5 1.0 0.5 0.0
f1 (ppm)

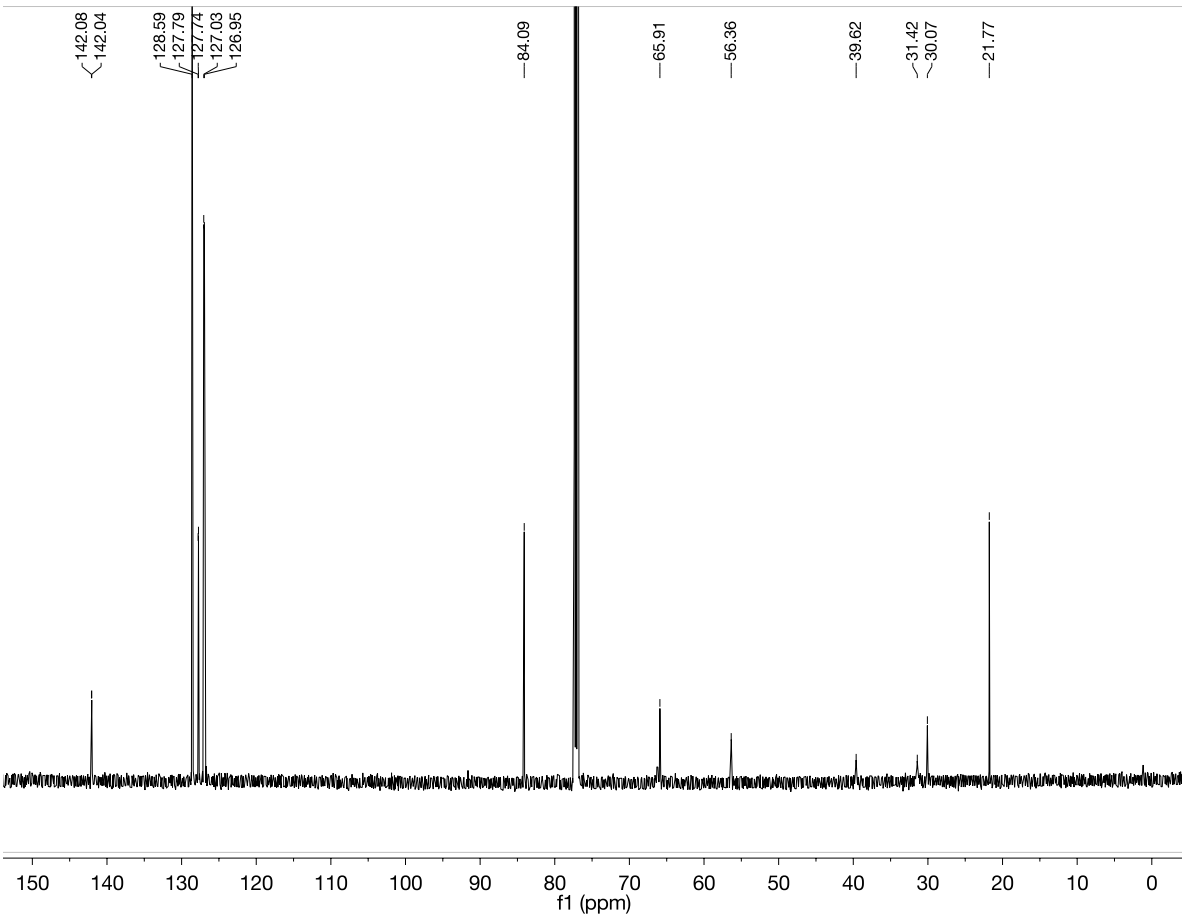
142.08 142.04 128.59 127.79 127.74 127.03 126.95 84.09 65.91 56.36 39.62 31.42 30.07 21.77
150 140 130 120 110 100 90 80 70 60 50 40 30 20 10 0
f1 (ppm)

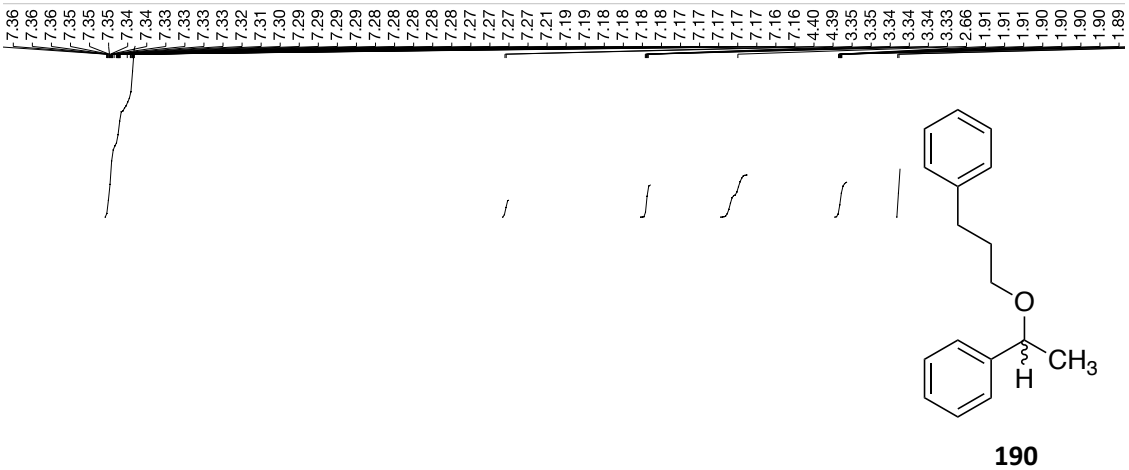
7.36 7.36 7.36 7.35 7.35 7.35 7.34 7.34 7.33 7.33 7.33 7.32 7.31 7.30 7.29 7.29 7.29 7.28 7.28 7.28 7.28 7.27 7.27 7.27 7.21 7.19 7.19 7.18 7.18 7.18 7.17 7.17 7.17 7.17 7.16 7.16 4.40 4.39 3.35 3.34 3.34 3.33 2.66 1.91 1.91 1.90 1.90 1.90 1.89
O
CH3
H

190

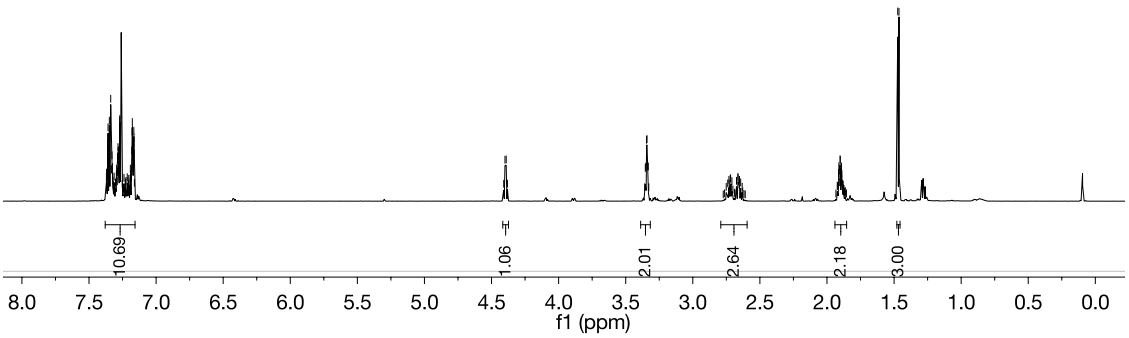
10.69
1.06
2.01
2.64
2.18
3.00
8.0 7.5 7.0 6.5 6.0 5.5 5.0 4.5 4.0 3.5 3.0 2.5 2.0 1.5 1.0 0.5 0.0
f1 (ppm)

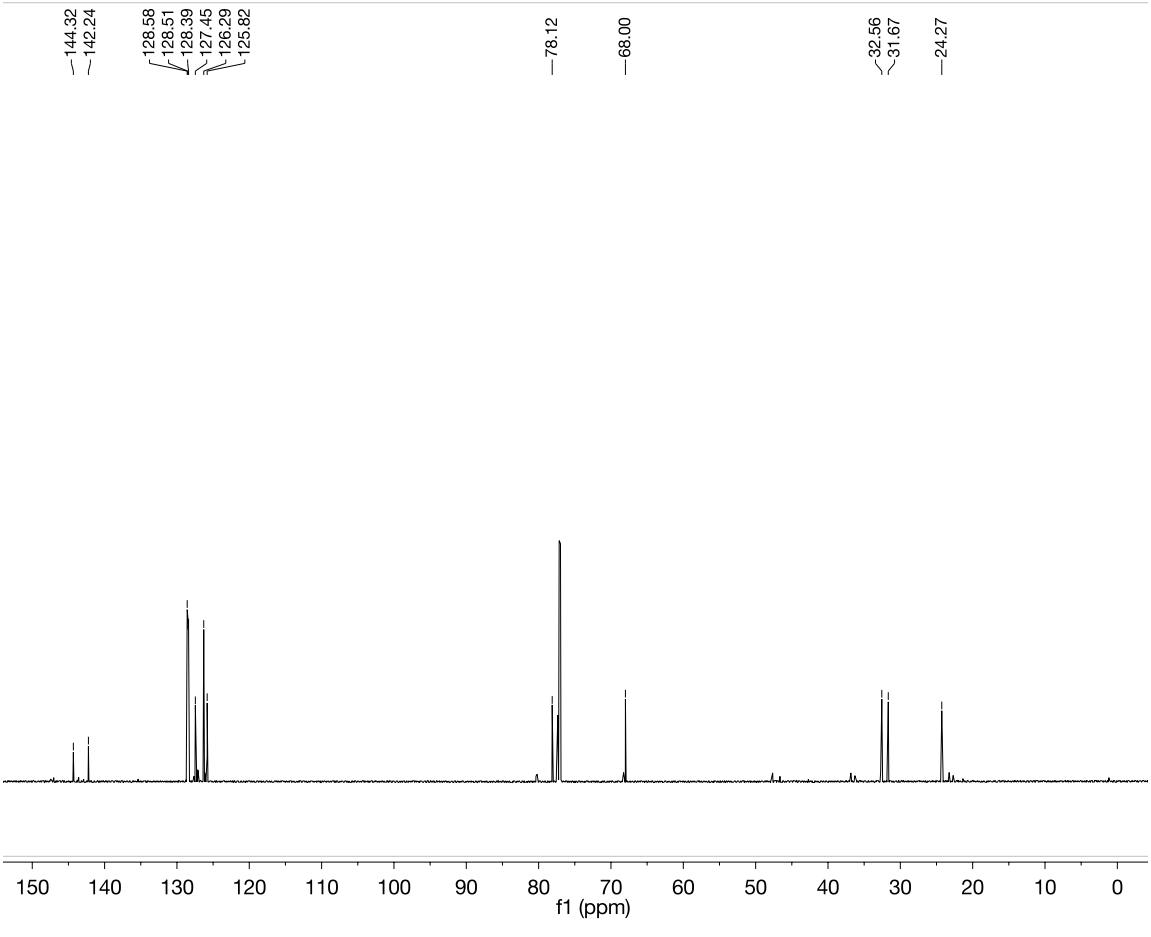
144.32
142.24
128.58
128.51
128.39
127.45
126.29
125.82
78.12
68.00
32.56
31.67
24.27
150 140 130 120 110 100 90 80 70 60 50 40 30 20 10 0
f1 (ppm)

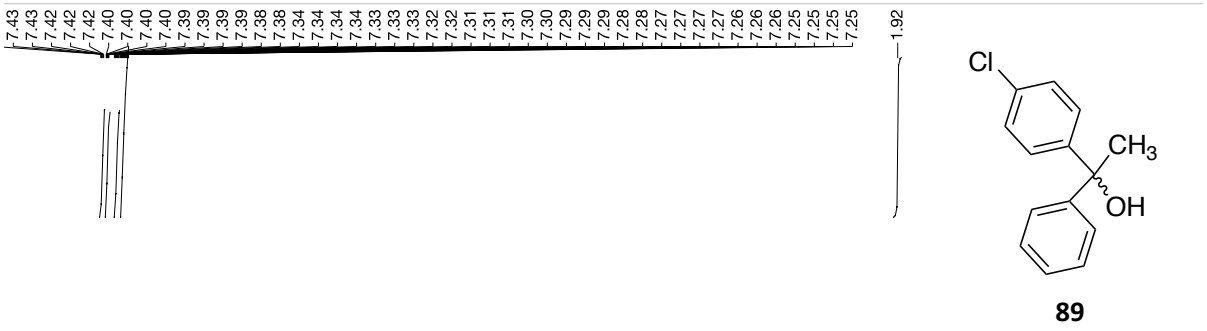
7.43 7.43 7.42 7.42 7.42 7.40 7.40 7.40 7.40 7.39 7.39 7.39 7.39 7.38 7.38 7.34 7.34 7.34 7.34 7.33 7.33 7.33 7.32 7.32 7.31 7.31 7.31 7.30 7.30 7.29 7.29 7.29 7.28 7.28 7.27 7.27 7.27 7.26 7.26 7.26 7.25 7.25 7.25 7.25
1.92
Cl
CH3
OH

89

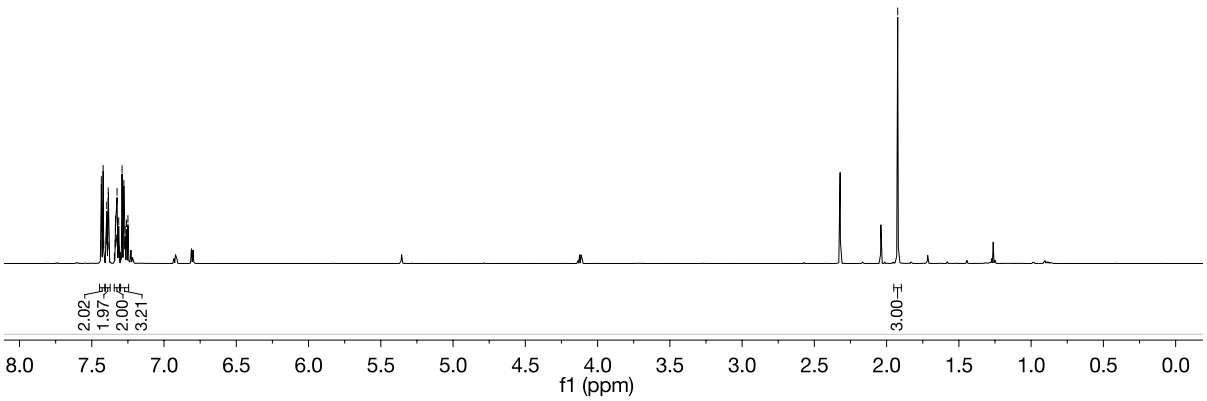
2.02
1.97
2.00
3.21
3.00
8.0 7.5 7.0 6.5 6.0 5.5 5.0 4.5 4.0 3.5 3.0 2.5 2.0 1.5 1.0 0.5 0.0
f1 (ppm)

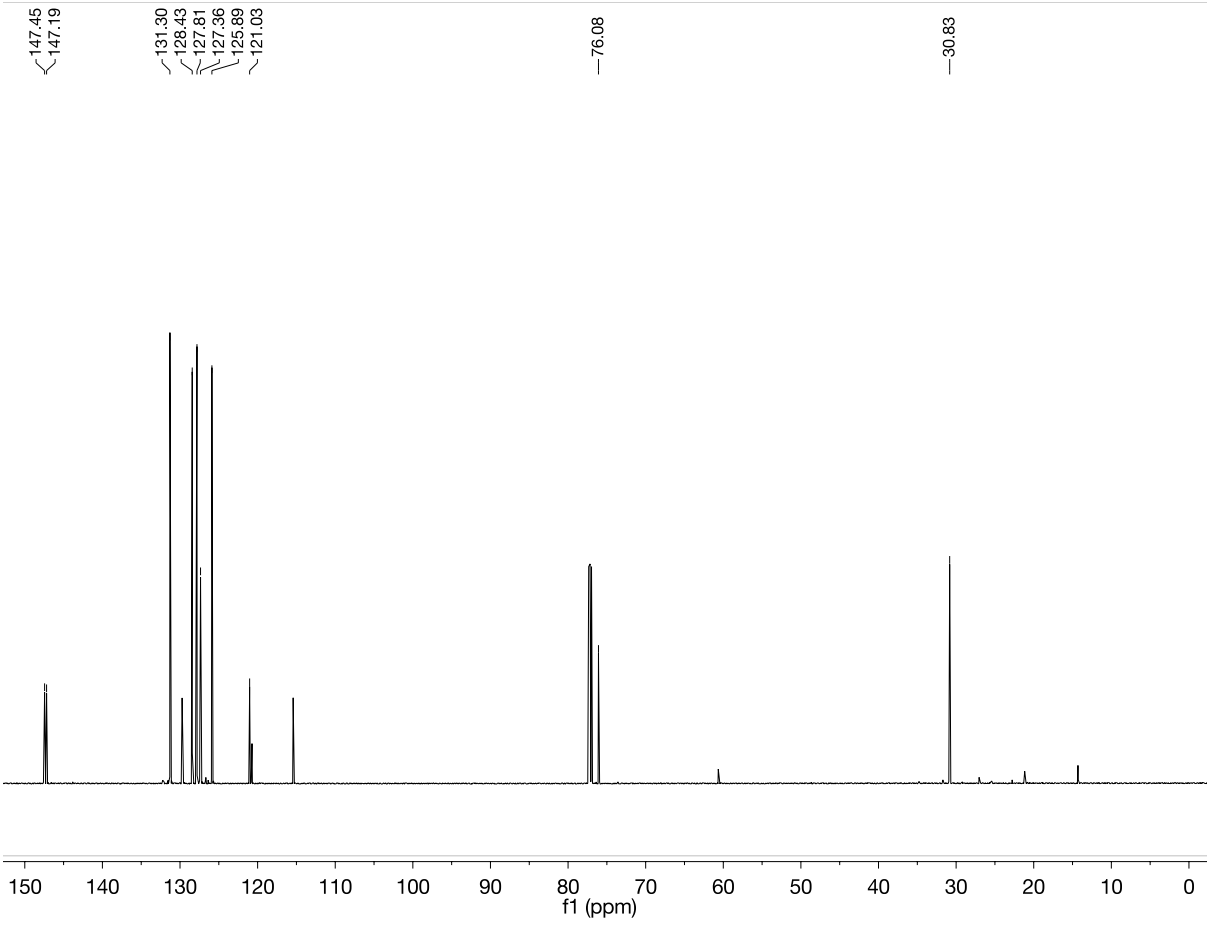
147.45
147.19
131.30
128.43
127.81
127.36
125.89
121.03
76.08
30.83
150 140 130 120 110 100 90 80 70 60 50 40 30 20 10 0
f1 (ppm)

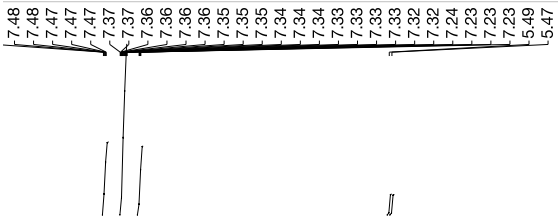
7.48
7.48
7.47
7.47
7.47
7.37
7.37
7.36
7.36
7.36
7.36
7.35
7.35
7.35
7.34
7.34
7.34
7.33
7.33
7.33
7.33
7.32
7.32
7.24
7.23
7.23
7.23
5.49
5.47

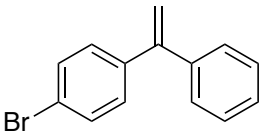
Br

111

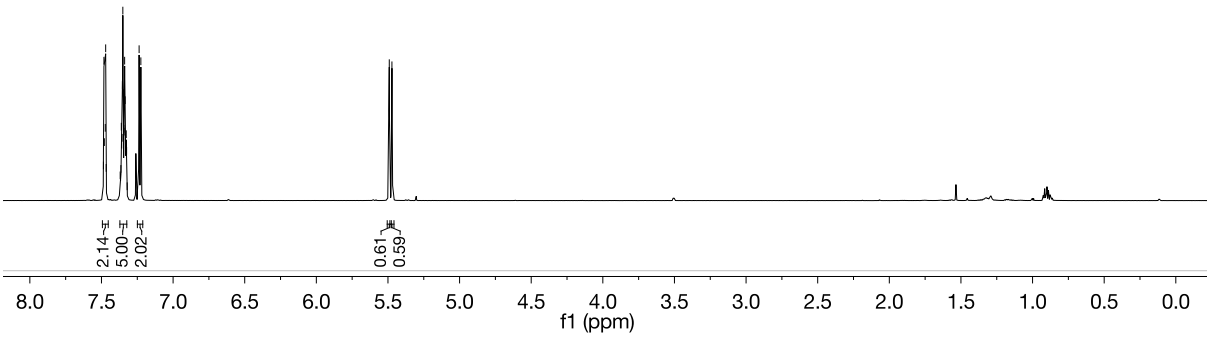
2.14
5.00
2.02
0.61
0.59
8.0
7.5
7.0
6.5
6.0
5.5
5.0
4.5
4.0
3.5
3.0
2.5
2.0
1.5
1.0
0.5
0.0
f1 (ppm)

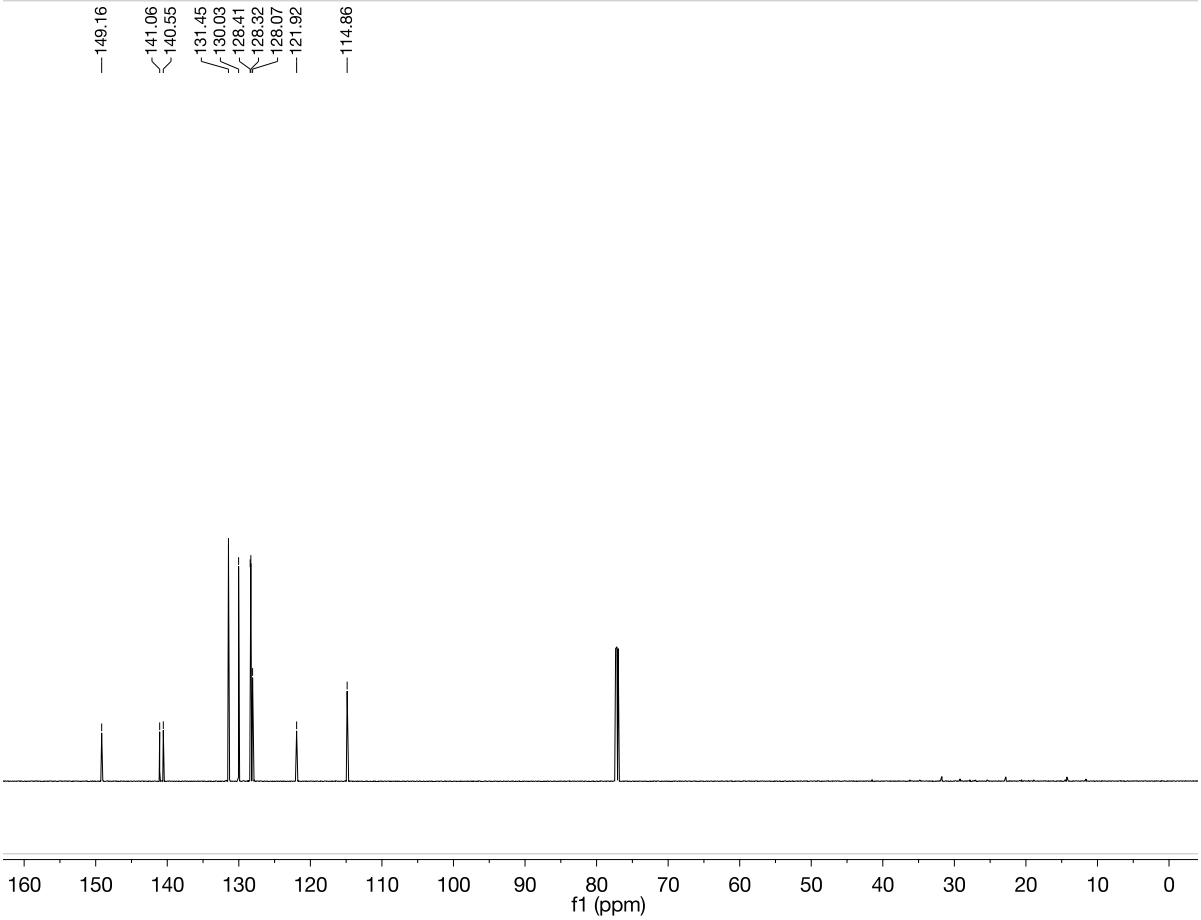
149.16
141.06
140.55
131.45
130.03
128.41
128.32
128.07
121.92
114.86
160
150
140
130
120
110
100
90
80
70
60
50
40
30
20
10
0
f1 (ppm)

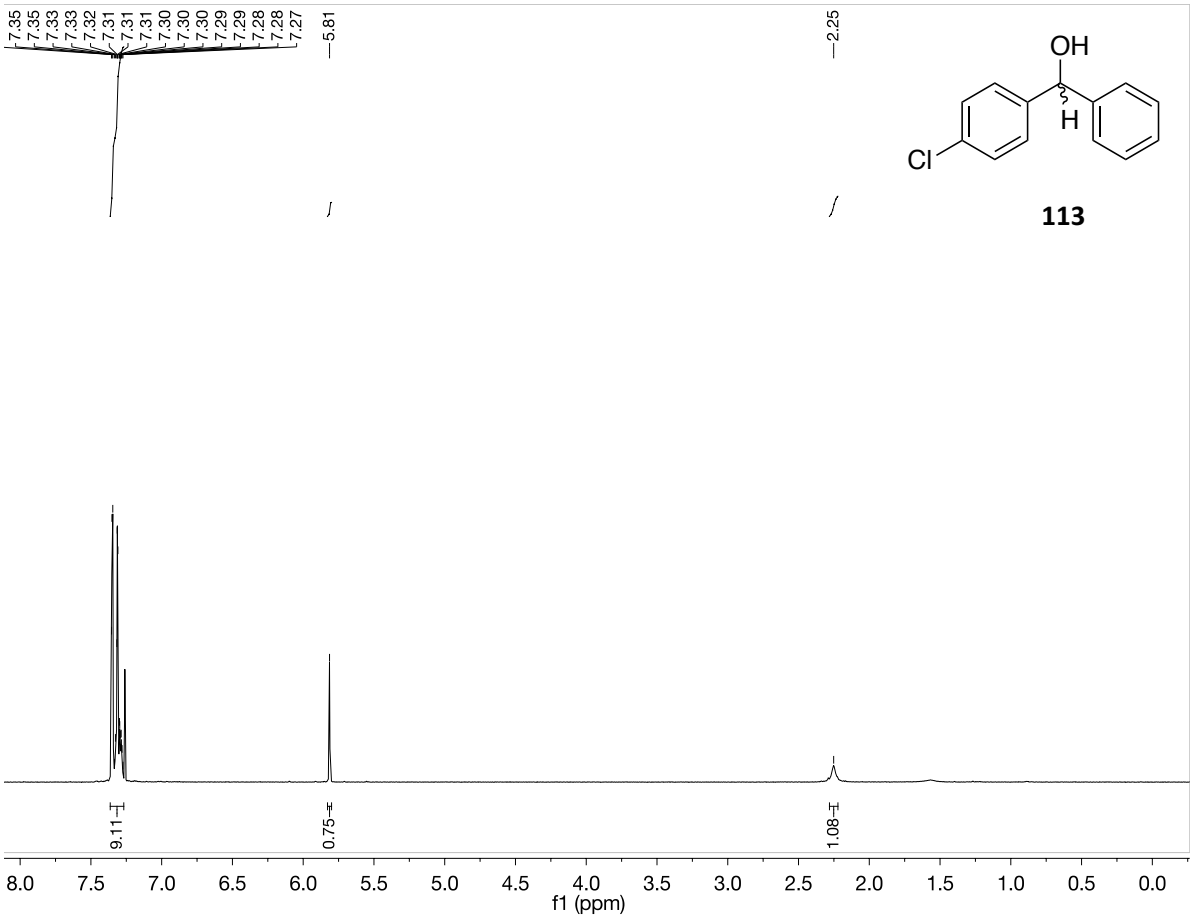
7.35
7.35
7.33
7.33
7.32
7.31
7.31
7.31
7.30
7.30
7.30
7.29
7.29
7.28
7.28
7.27
5.81
2.25
OH
H
Cl
113
9.11
0.75
1.08
8.0
7.5
7.0
6.5
6.0
5.5
5.0
4.5
4.0
3.5
3.0
2.5
2.0
1.5
1.0
0.5
0.0
f1 (ppm)

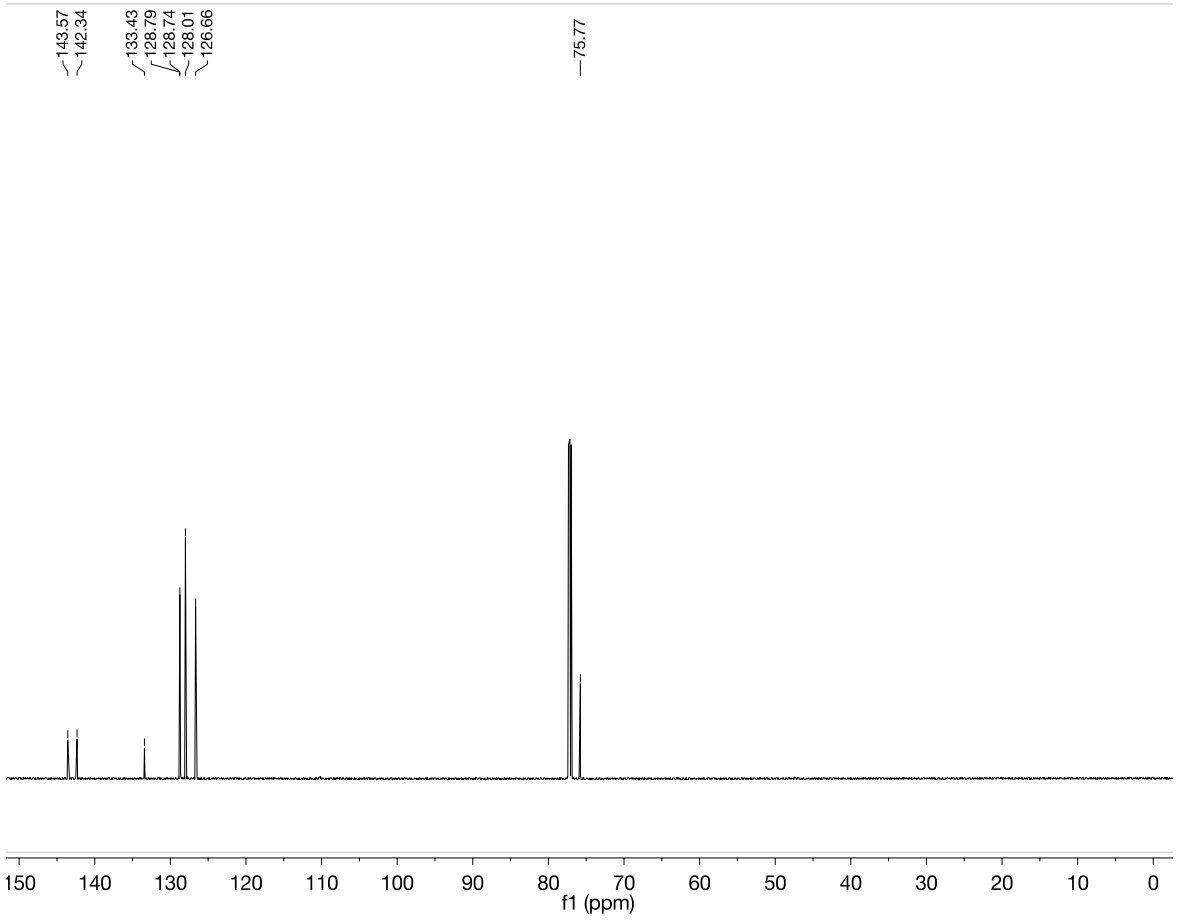
143.57
142.34
133.43
128.79
128.74
128.01
126.66
75.77
150
140
130
120
110
100
90
80
70
60
50
40
30
20
10
0
f1 (ppm)

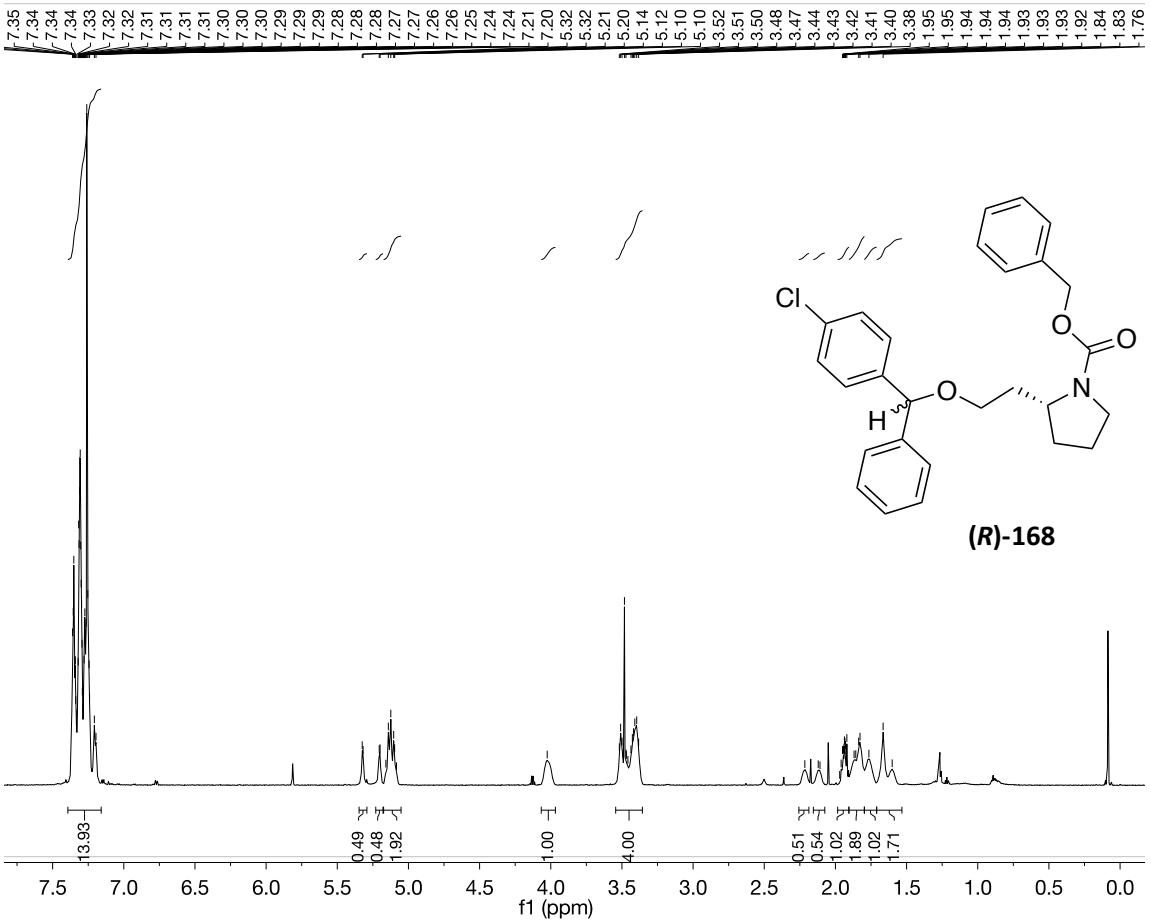
7.35 7.34 7.34 7.34 7.33 7.32 7.31 7.31 7.31 7.30 7.30 7.30 7.29 7.29 7.29 7.28 7.28 7.28 7.27 7.27 7.26 7.26 7.25 7.24 7.24 7.21 7.20 5.32 5.32 5.21 5.20 5.14 5.12 5.10 5.10 3.52 3.51 3.50 3.48 3.47 3.44 3.43 3.42 3.41 3.40 3.38 1.95 1.95 1.94 1.94 1.94 1.93 1.93 1.92 1.84 1.83 1.76
Cl
O
O
O
N
H
(R)-168
13.93 0.49 0.48 1.92 1.00 4.00 0.51 0.54 1.02 1.89 1.02 1.71
7.5 7.0 6.5 6.0 5.5 5.0 4.5 4.0 3.5 3.0 2.5 2.0 1.5 1.0 0.5 0.0
f1 (ppm)

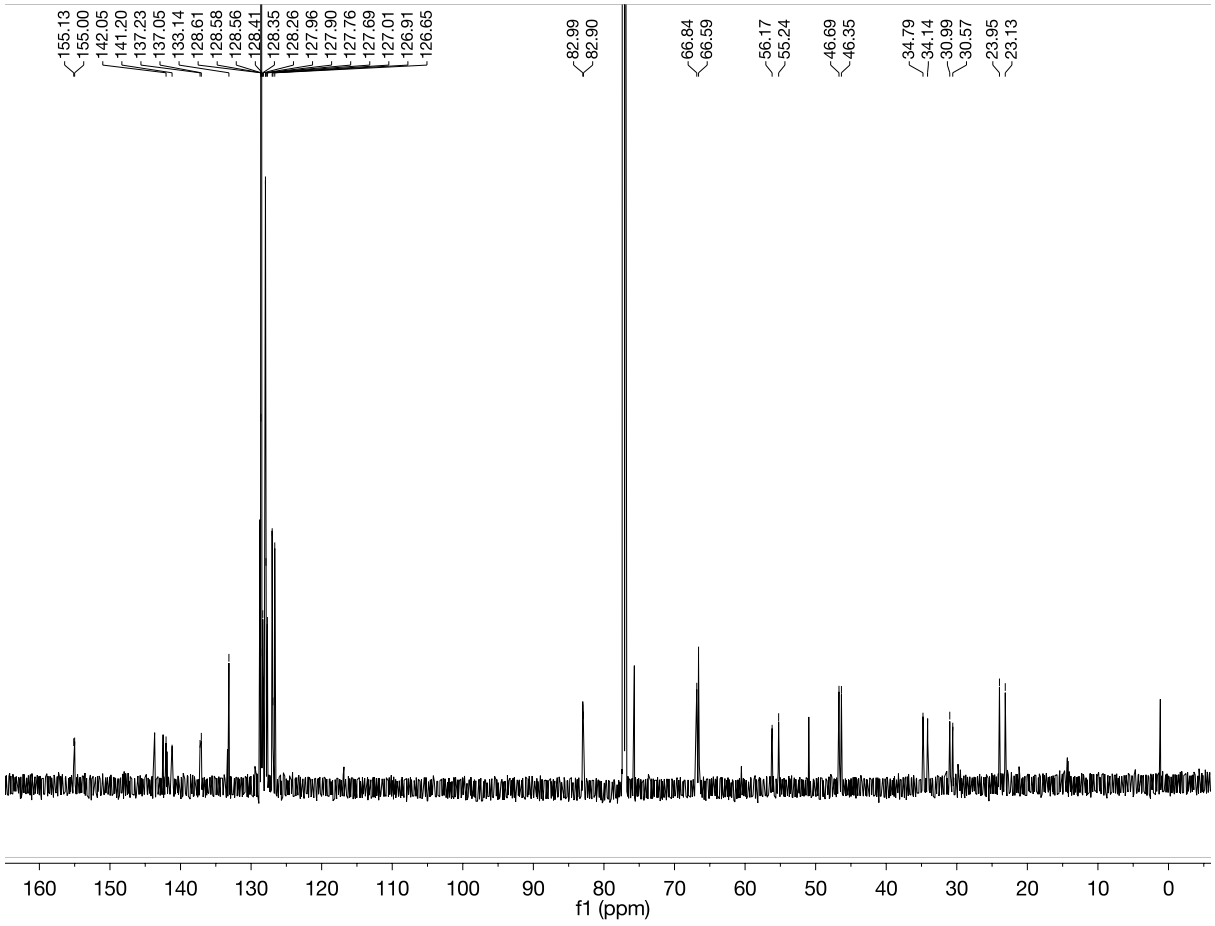
155.13 155.00 142.05 141.20 137.23 137.05 133.14 128.61 128.58 128.56 128.41 128.35 128.26 127.96 127.90 127.76 127.69 127.01 126.91 126.65
82.99 82.90
66.84 66.59
56.17 55.24
46.69 46.35
34.79 34.14 30.99 30.57
23.95 23.13
160 150 140 130 120 110 100 90 80 70 60 50 40 30 20 10 0
f1 (ppm)

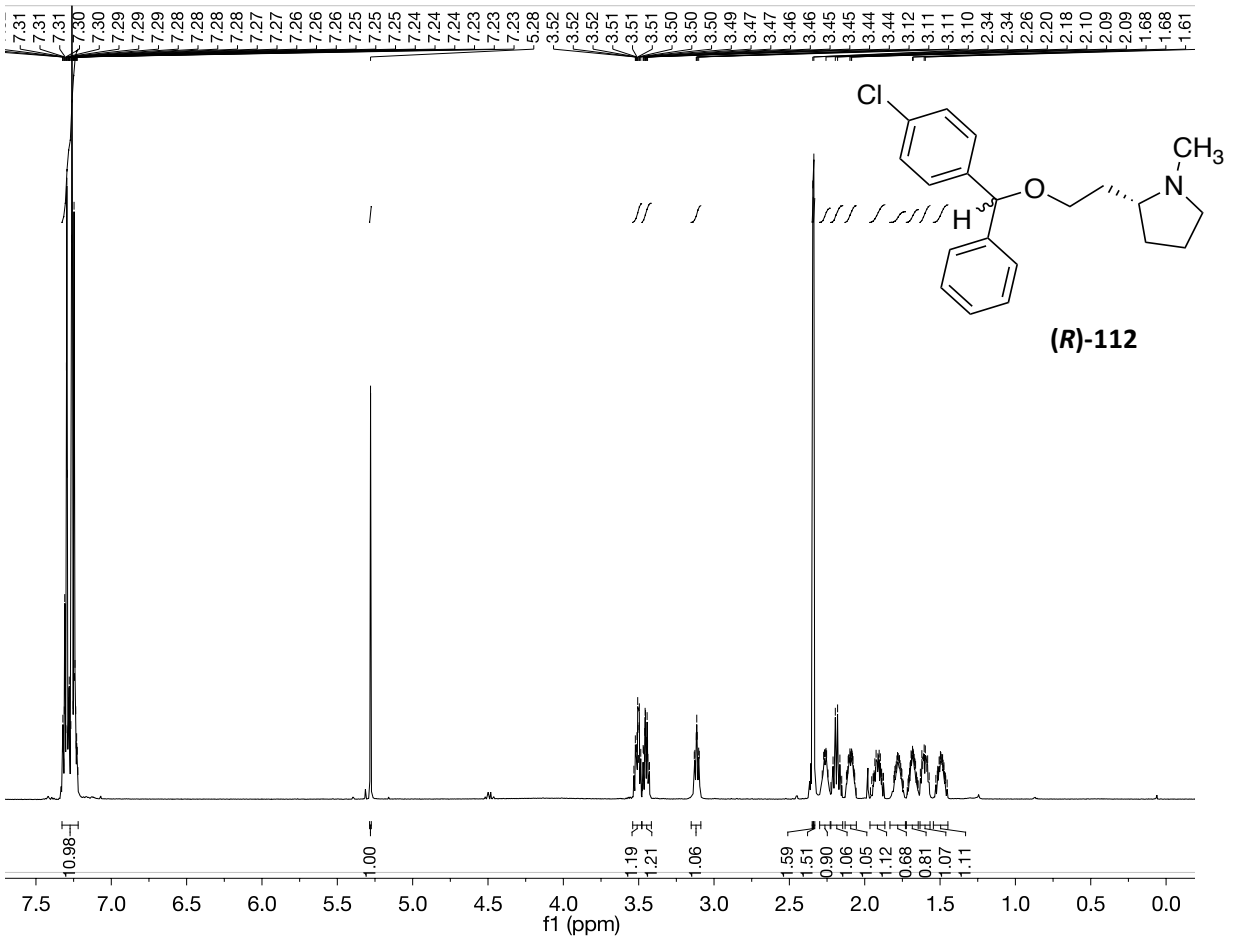
Cl
CH3
O
N
H
(R)-112
f1 (ppm)

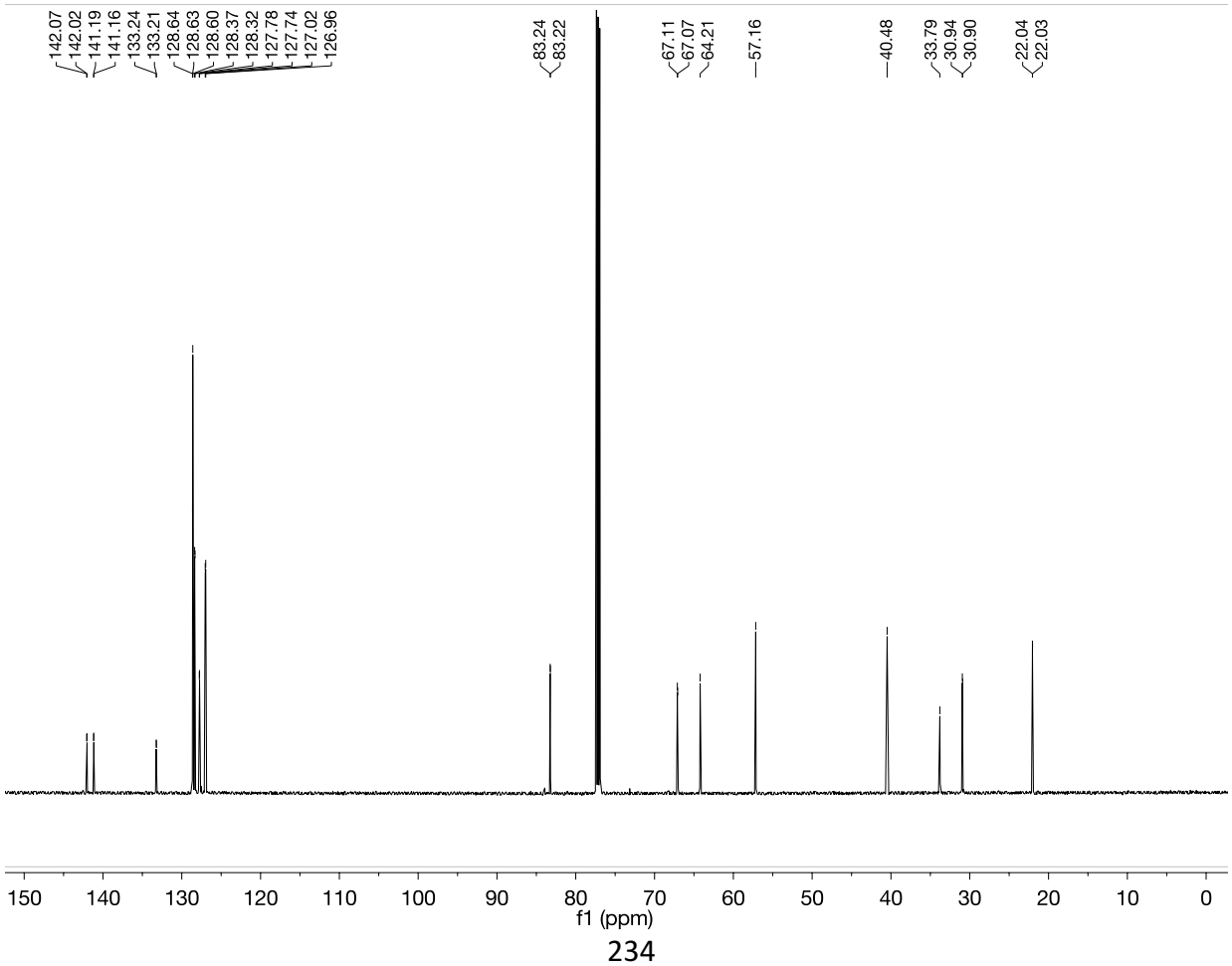
f1 (ppm)

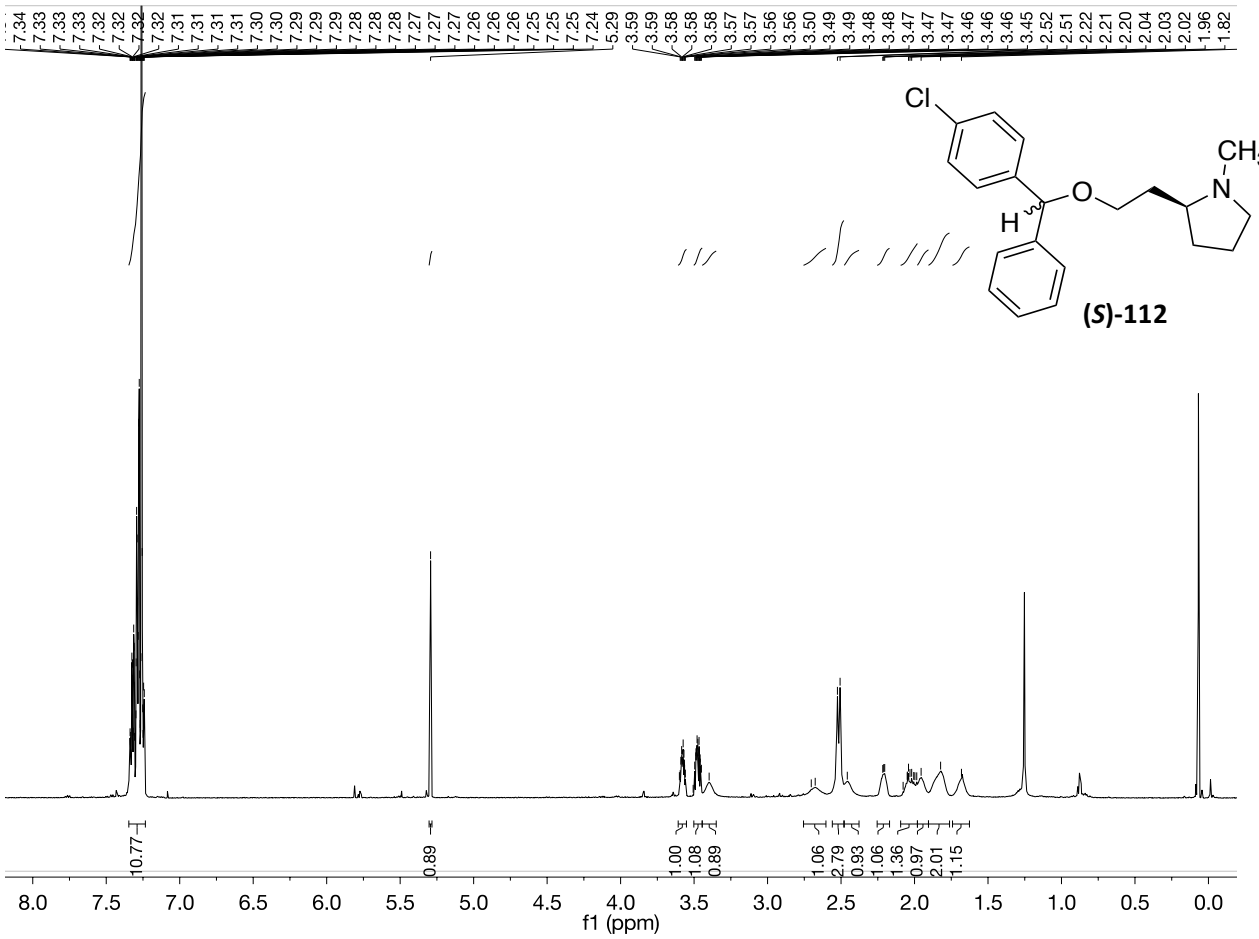
Cl
CH3
O
N
H
(S)-112
f1 (ppm)

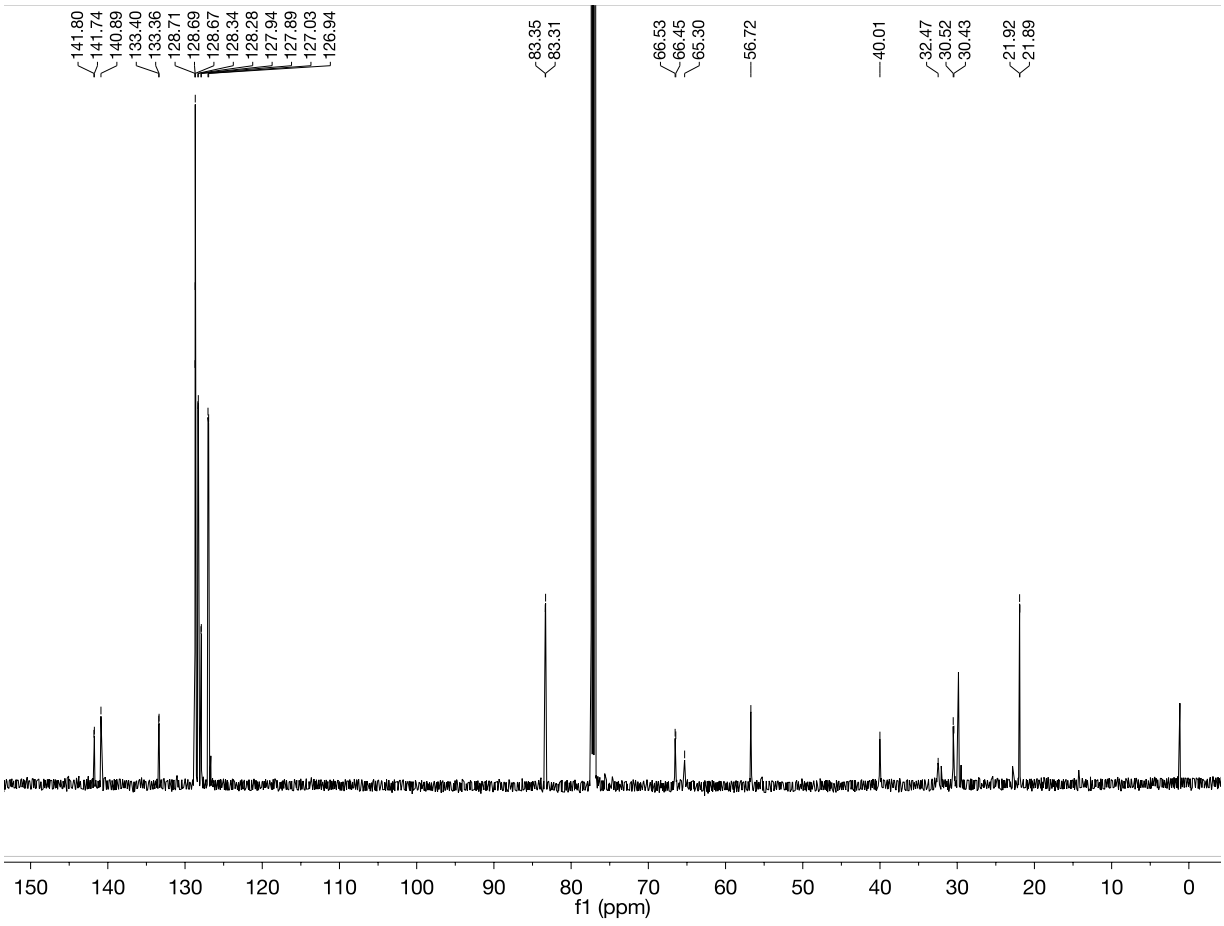
f1 (ppm)

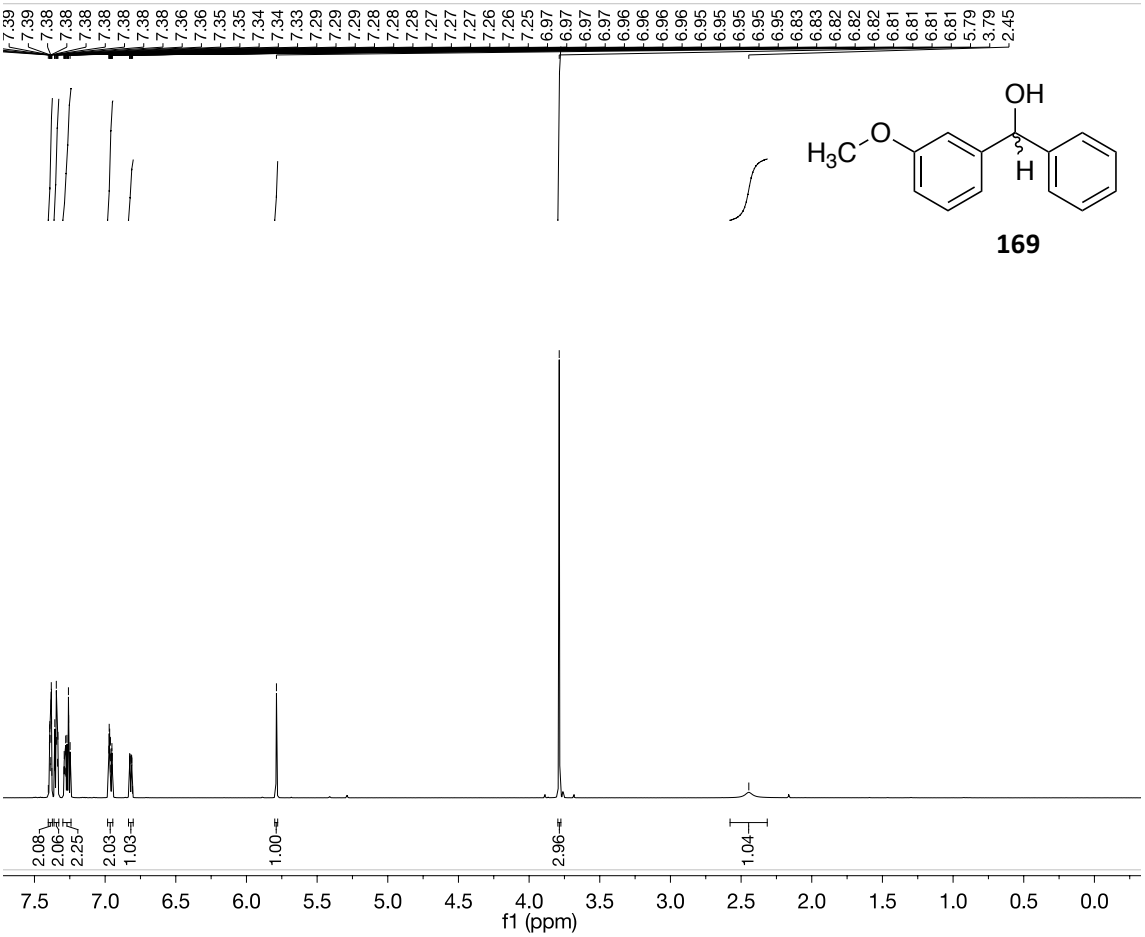
7.39 7.39 7.38 7.38 7.38 7.38 7.38 7.38 7.38 7.36 7.36 7.35 7.35 7.34 7.34 7.33 7.29 7.29 7.29 7.28 7.28 7.28 7.27 7.27 7.27 7.26 7.26 7.25 6.97 6.97 6.97 6.96 6.96 6.96 6.96 6.95 6.95 6.95 6.95 6.83 6.83 6.82 6.82 6.82 6.81 6.81 6.81 6.81 5.79 3.79 2.45
OH
H3C
O
H
169
2.08 2.06 2.25 2.03 1.03 1.00 2.96 1.04
7.5 7.0 6.5 6.0 5.5 5.0 4.5 4.0 3.5 3.0 2.5 2.0 1.5 1.0 0.5 0.0
f1 (ppm)

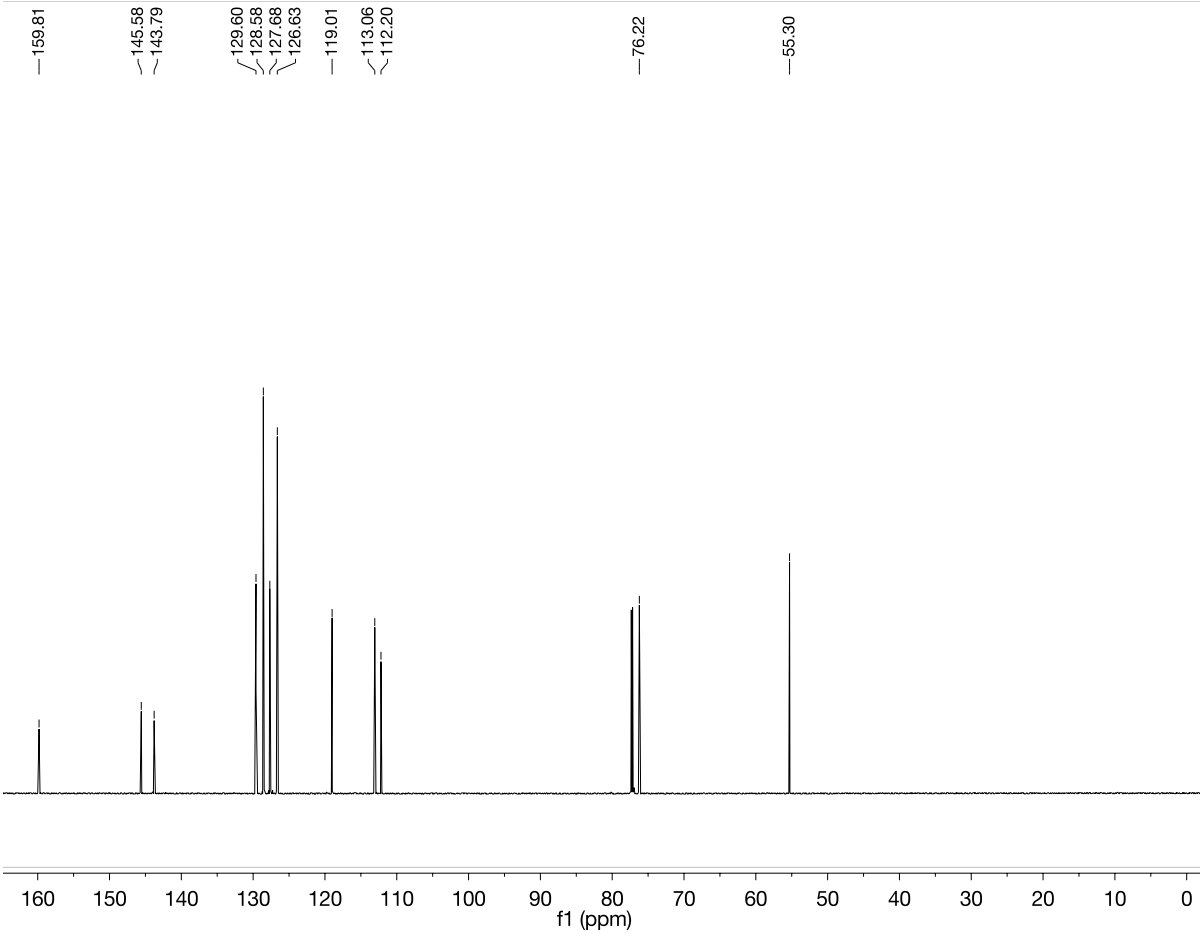
159.81 145.58 143.79 129.60 128.58 127.68 126.63 119.01 113.06 112.20 76.22 55.30
160 150 140 130 120 110 100 90 80 70 60 50 40 30 20 10 0
f1 (ppm)

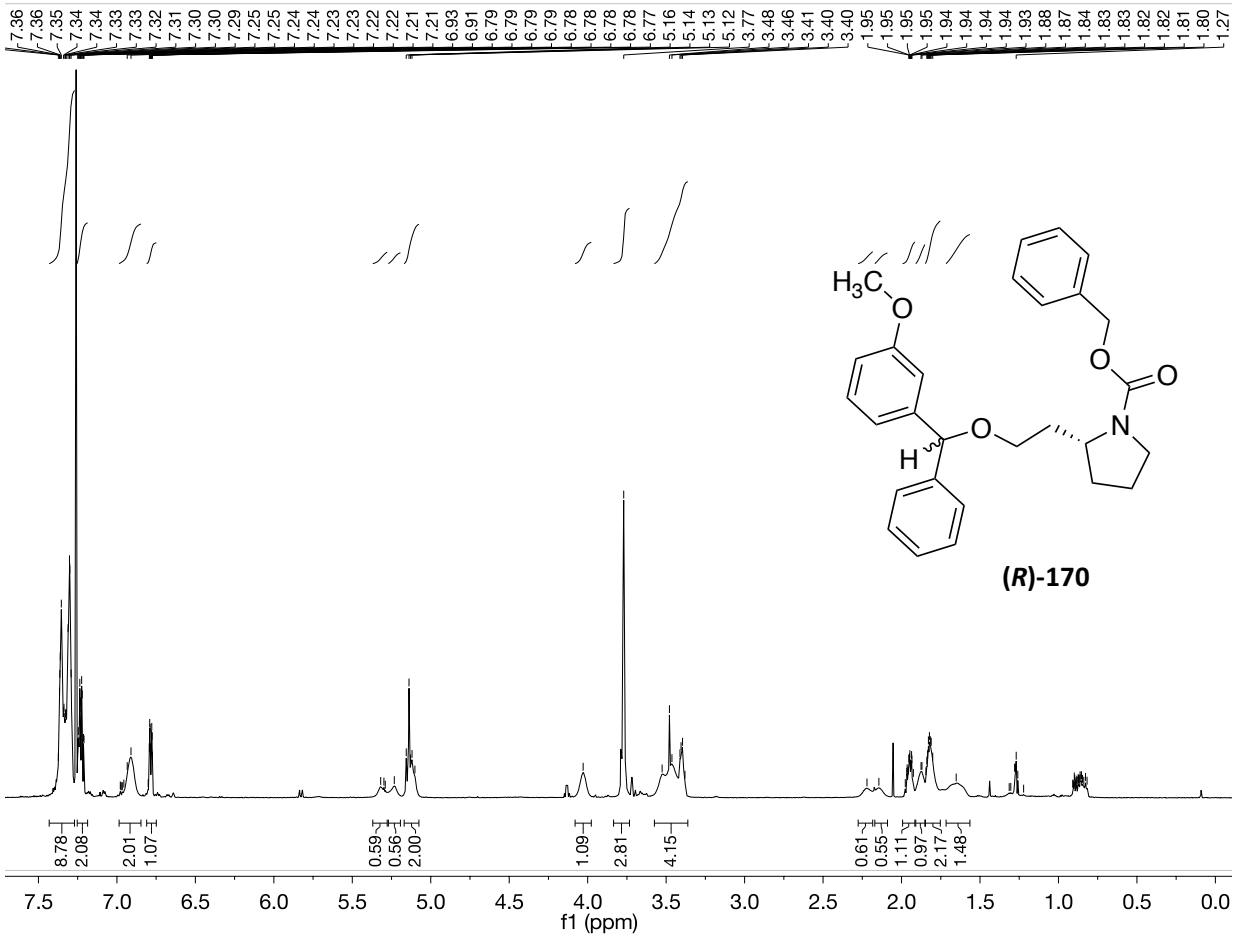
7.36 7.36 7.35 7.34 7.34 7.33 7.33 7.32 7.31 7.30 7.30 7.29 7.25 7.25 7.24 7.24 7.23 7.23 7.22 7.22 7.21 7.21 6.93 6.91 6.79 6.79 6.79 6.79 6.78 6.78 6.78 6.78 6.77 5.16 5.14 5.13 5.12 3.77 3.48 3.46 3.41 3.40 3.40 1.95 1.95 1.95 1.94 1.94 1.94 1.94 1.93 1.88 1.87 1.84 1.83 1.83 1.82 1.82 1.81 1.80 1.27
8.78 2.08 2.01 1.07 0.59 0.56 2.00 1.09 2.81 4.15 0.61 0.55 1.11 0.97 2.17 1.48
7.5 7.0 6.5 6.0 5.5 5.0 4.5 4.0 3.5 3.0 2.5 2.0 1.5 1.0 0.5 0.0
f1 (ppm)

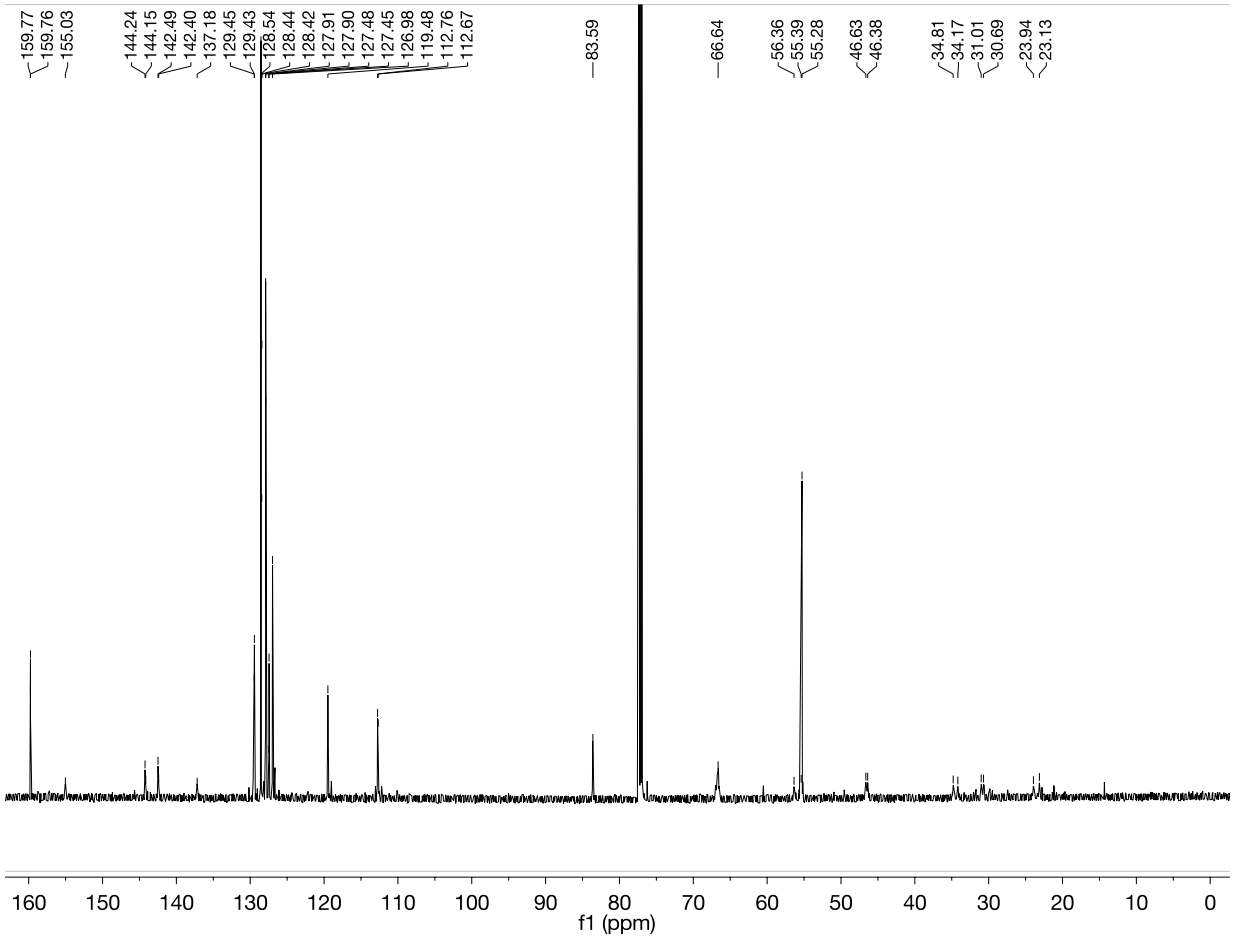
159.77 159.76 155.03 144.24 144.15 142.49 142.40 137.18 129.45 129.43 128.54 128.44 128.42 127.91 127.90 127.48 127.45 126.98 119.48 112.76 112.67 83.59 66.64 56.36 55.39 55.28 46.63 46.38 34.81 34.17 31.01 30.69 23.94 23.13
160 150 140 130 120 110 100 90 80 70 60 50 40 30 20 10 0
f1 (ppm)

H3C
O
O
O
O
N
H

(*R*)-170

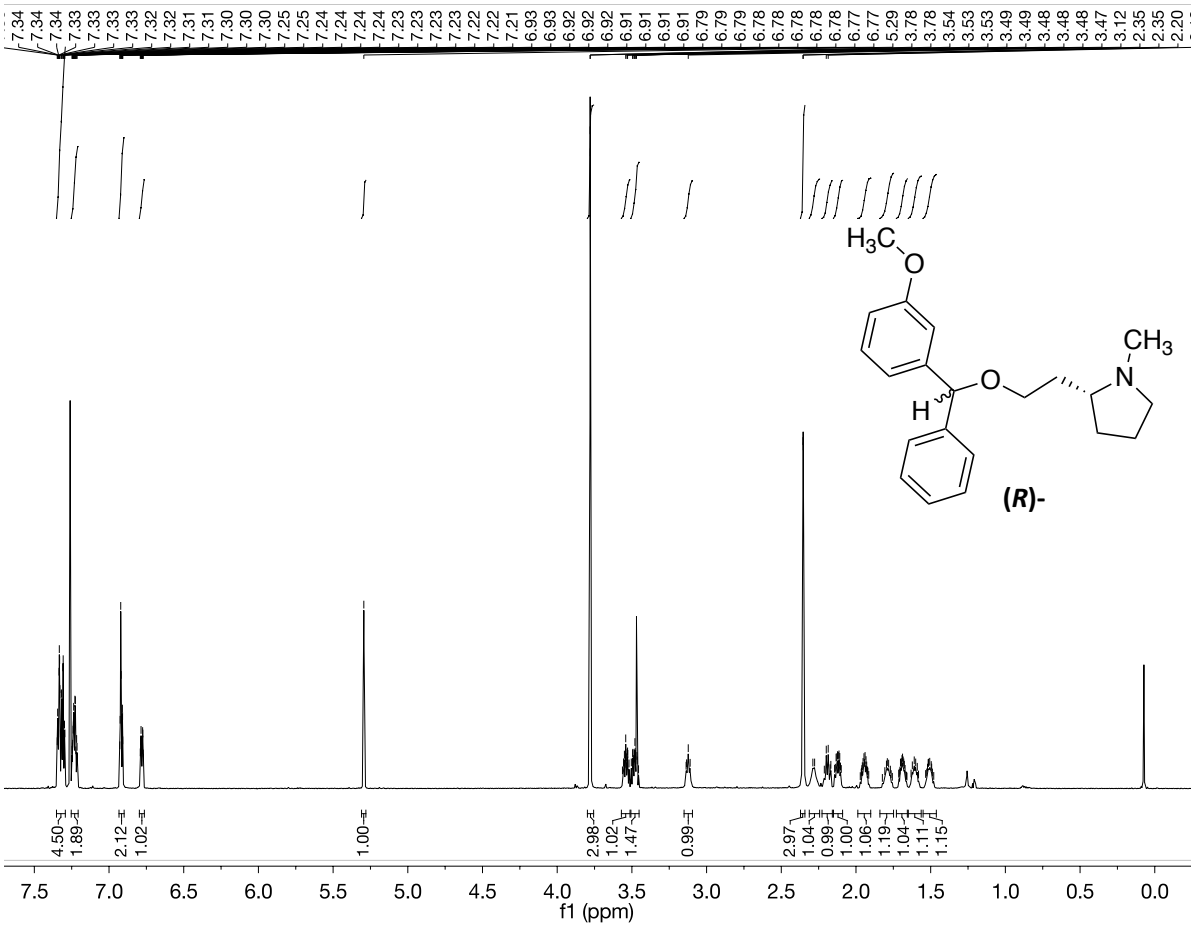
H3C
O
CH3
N
O
H
(R)-
f1 (ppm)

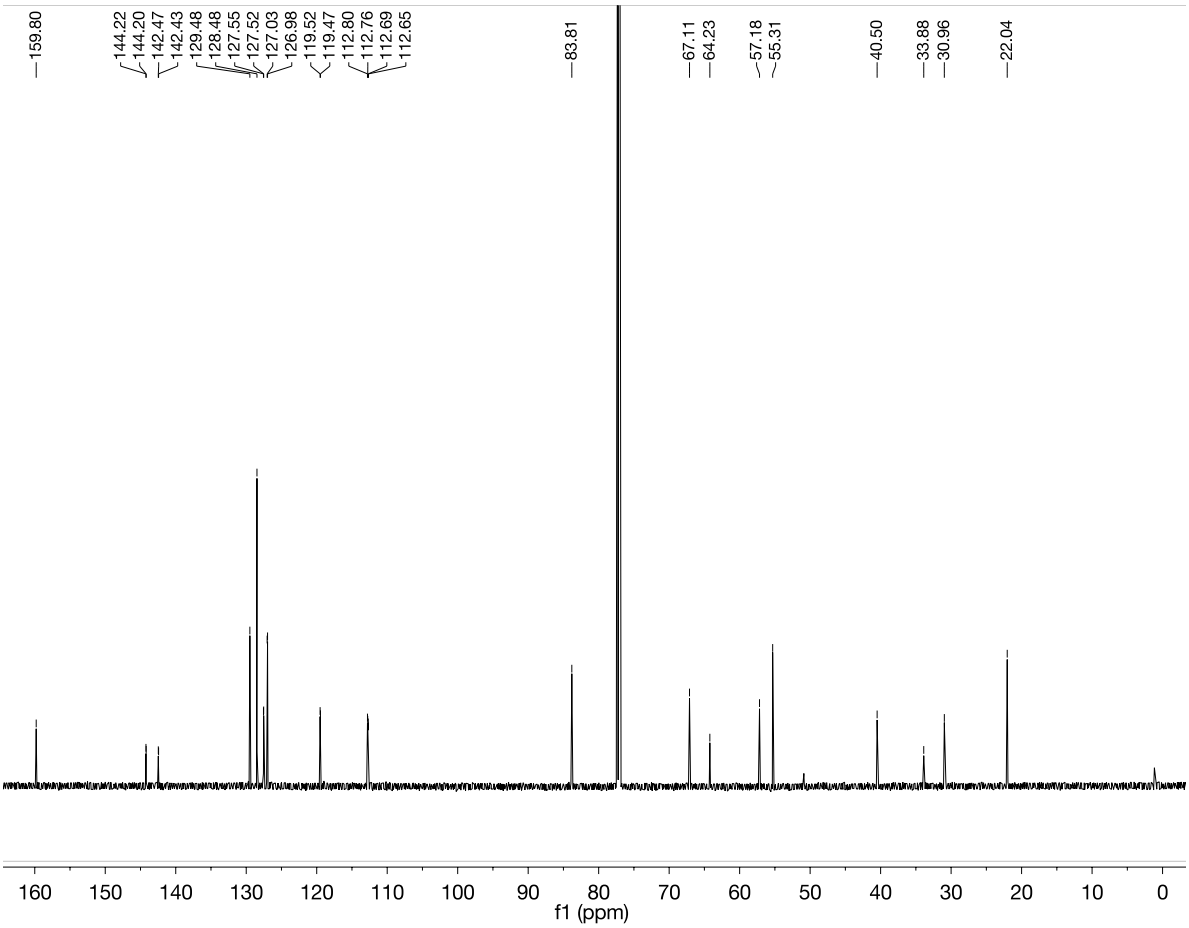
f1 (ppm)

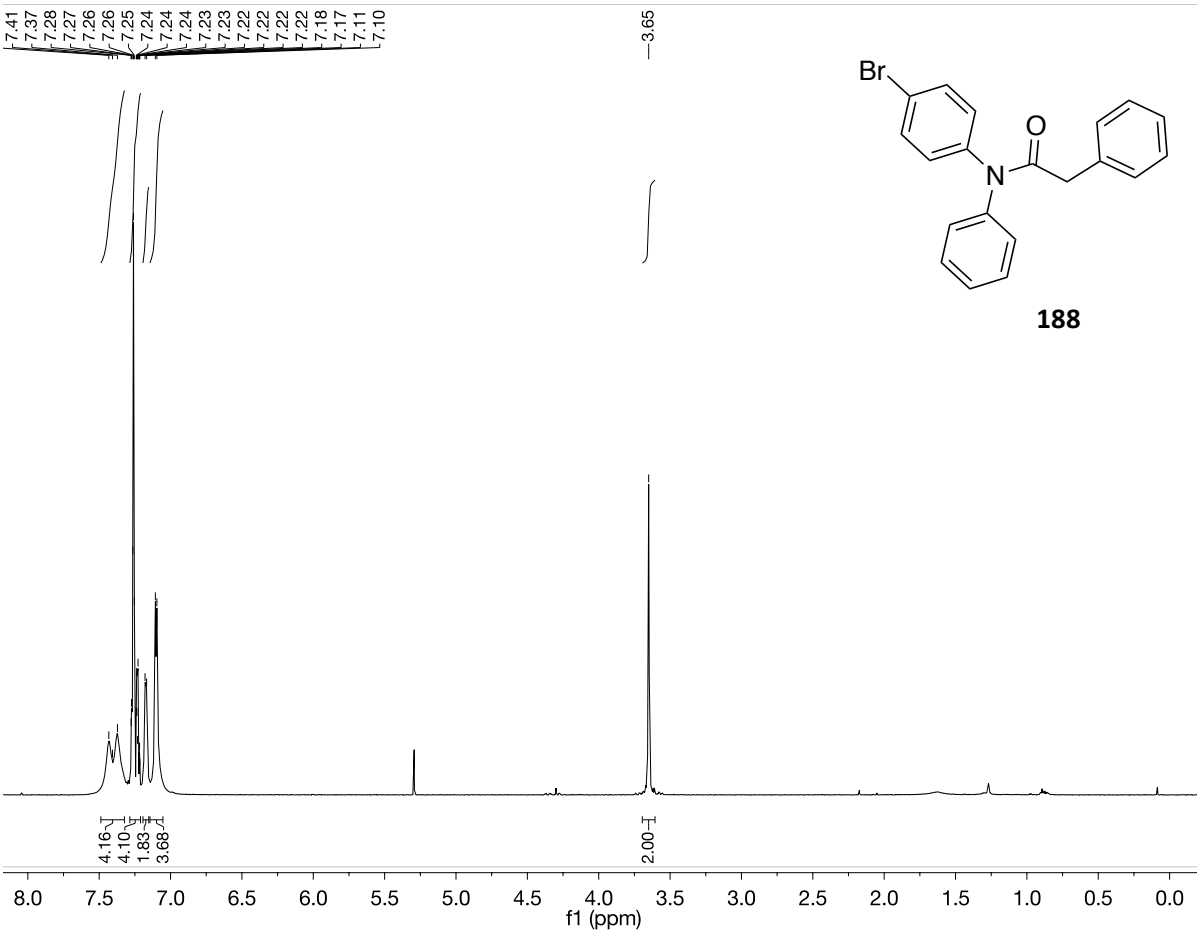
7.41
7.37
7.28
7.27
7.26
7.26
7.25
7.24
7.24
7.24
7.23
7.23
7.22
7.22
7.22
7.22
7.18
7.17
7.11
7.10
3.65
Br
O
N
4.16
4.10
1.83
3.68
2.00
8.0
7.5
7.0
6.5
6.0
5.5
5.0
4.5
4.0
3.5
3.0
2.5
2.0
1.5
1.0
0.5
0.0
f1 (ppm)

188

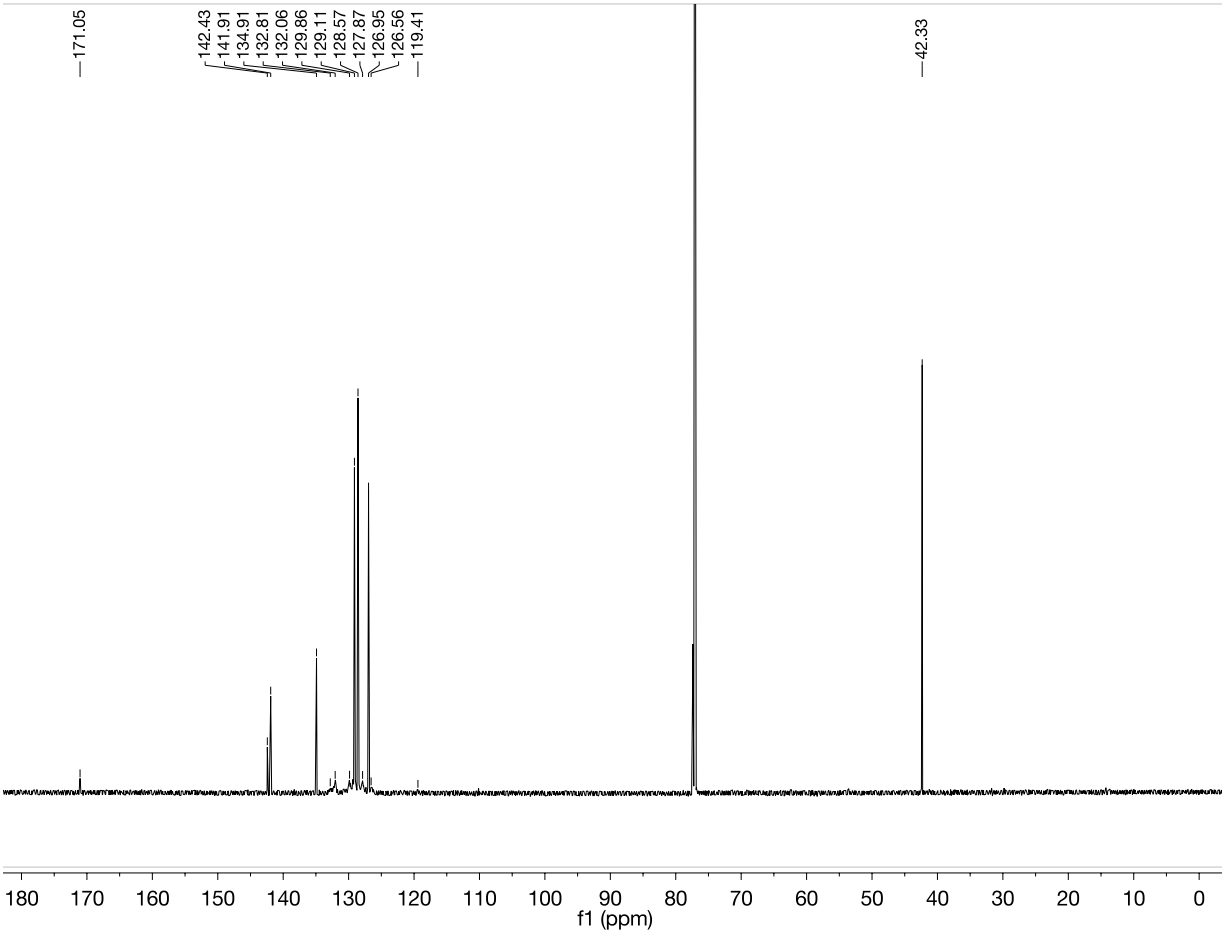
171.05
142.43
141.91
134.91
132.81
132.06
129.86
129.11
128.57
127.87
126.95
126.56
119.41
42.33
180
170
160
150
140
130
120
110
100
90
80
70
60
50
40
30
20
10
0
f1 (ppm)

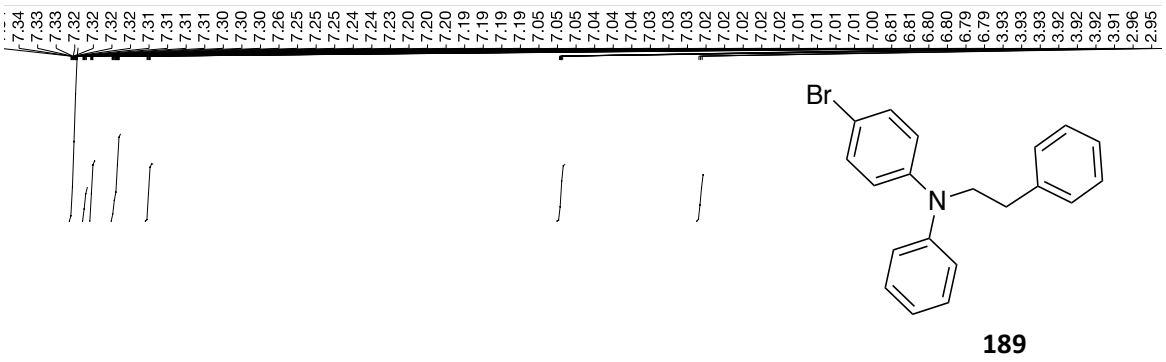
Br
N

189

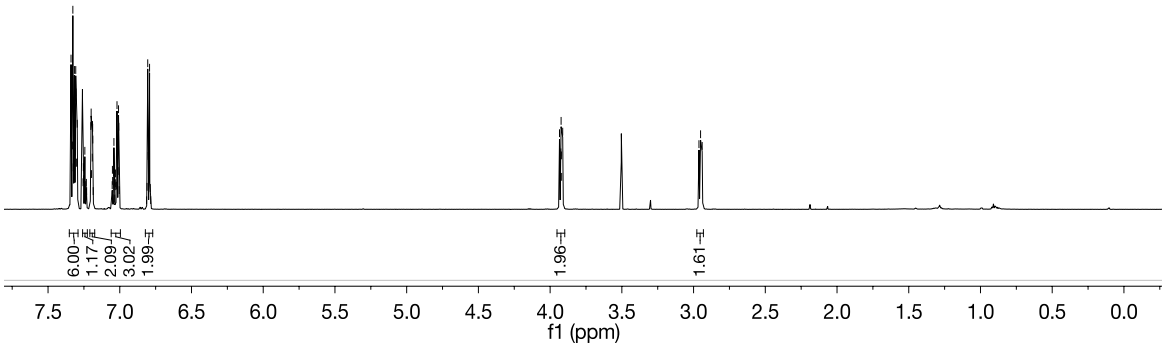
6.00
1.17
2.09
3.02
1.99
1.96
1.61
f1 (ppm)


147.35
147.09
139.34
132.21
129.65
128.92
128.72
126.53
122.70
122.52
121.27
112.81
54.16
33.73

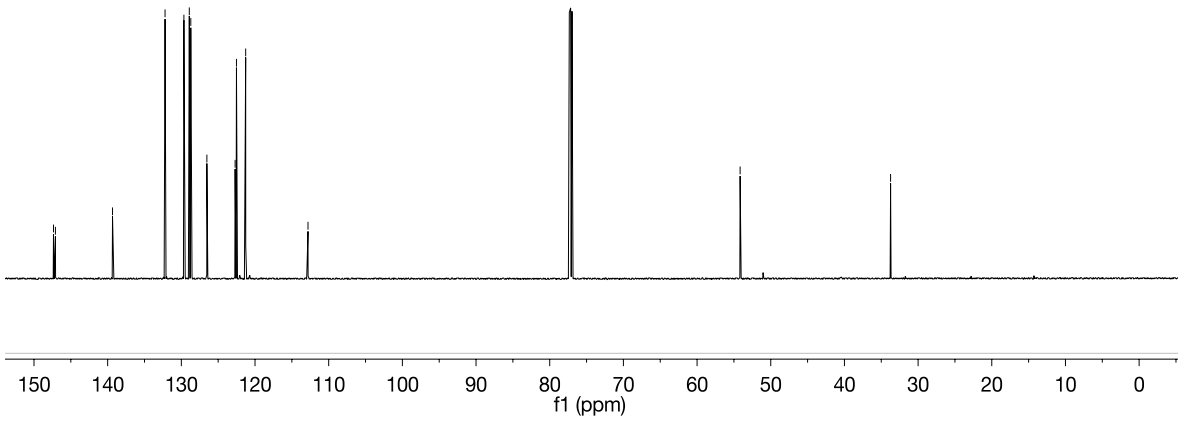
f1 (ppm)

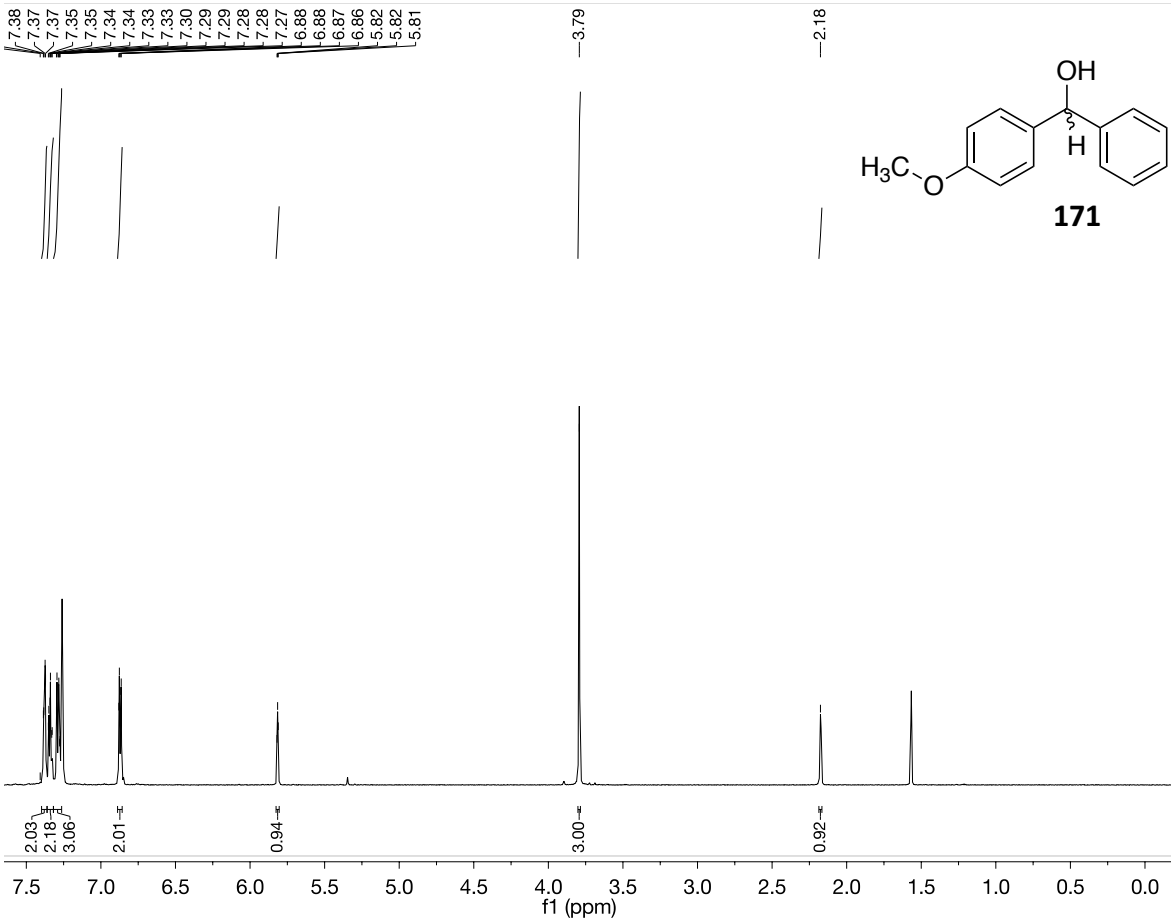
7.38
7.37
7.37
7.35
7.35
7.34
7.34
7.33
7.33
7.30
7.29
7.29
7.28
7.28
7.27
6.88
6.88
6.87
6.86
5.82
5.82
5.81
3.79
2.18
OH
H
H3C
O
171
2.03
2.18
3.06
2.01
0.94
3.00
0.92
7.5
7.0
6.5
6.0
5.5
5.0
4.5
4.0
3.5
3.0
2.5
2.0
1.5
1.0
0.5
0.0
f1 (ppm)

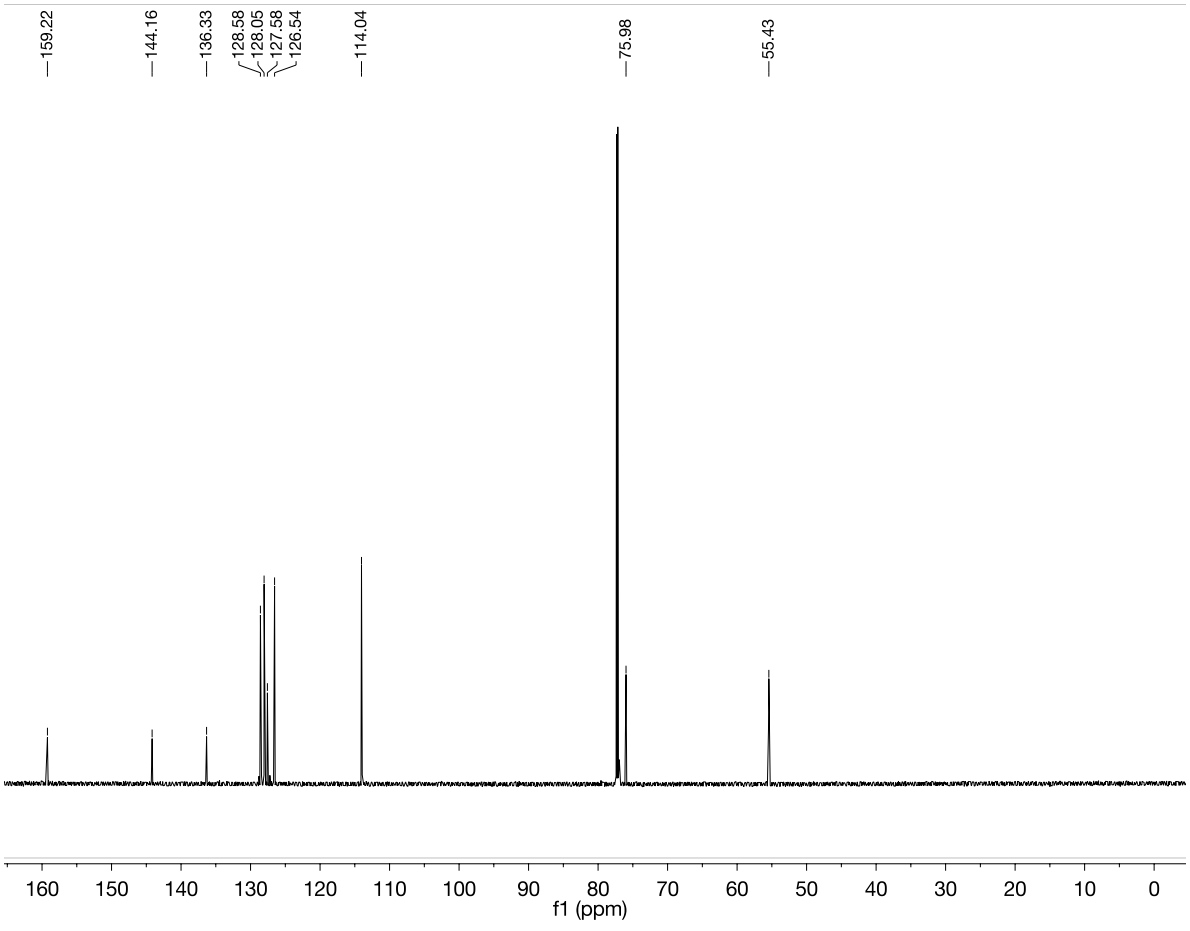
159.22
144.16
136.33
128.58
128.05
127.58
126.54
114.04
75.98
55.43
160
150
140
130
120
110
100
90
80
70
60
50
40
30
20
10
0
f1 (ppm)

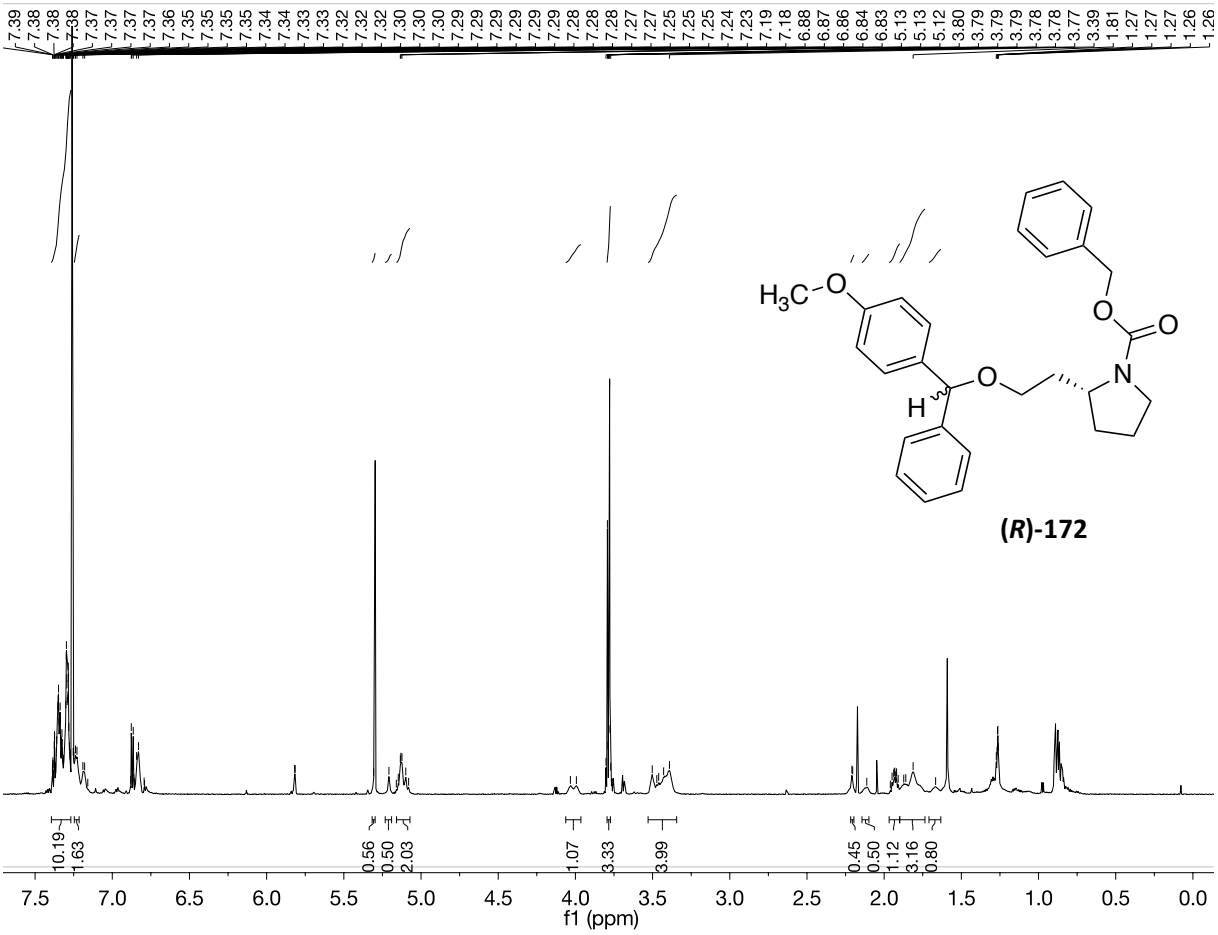
7.39 7.38 7.38 7.38 7.37 7.37 7.37 7.37 7.36 7.35 7.35 7.35 7.35 7.34 7.34 7.33 7.33 7.32 7.32 7.32 7.30 7.30 7.30 7.29 7.29 7.29 7.29 7.29 7.29 7.28 7.28 7.28 7.27 7.27 7.25 7.25 7.24 7.23 7.19 7.18 6.88 6.87 6.86 6.84 6.83 5.13 5.12 3.80 3.79 3.79 3.79 3.78 3.78 3.77 3.39 1.81 1.27 1.27 1.27 1.26 1.26
H3C O
O
O
O
N
H
10.19 1.63 0.56 0.50 2.03 1.07 3.33 3.99 0.45 0.50 1.12 3.16 0.80
7.5 7.0 6.5 6.0 5.5 5.0 4.5 4.0 3.5 3.0 2.5 2.0 1.5 1.0 0.5 0.0
f1 (ppm)

(*R*)-172

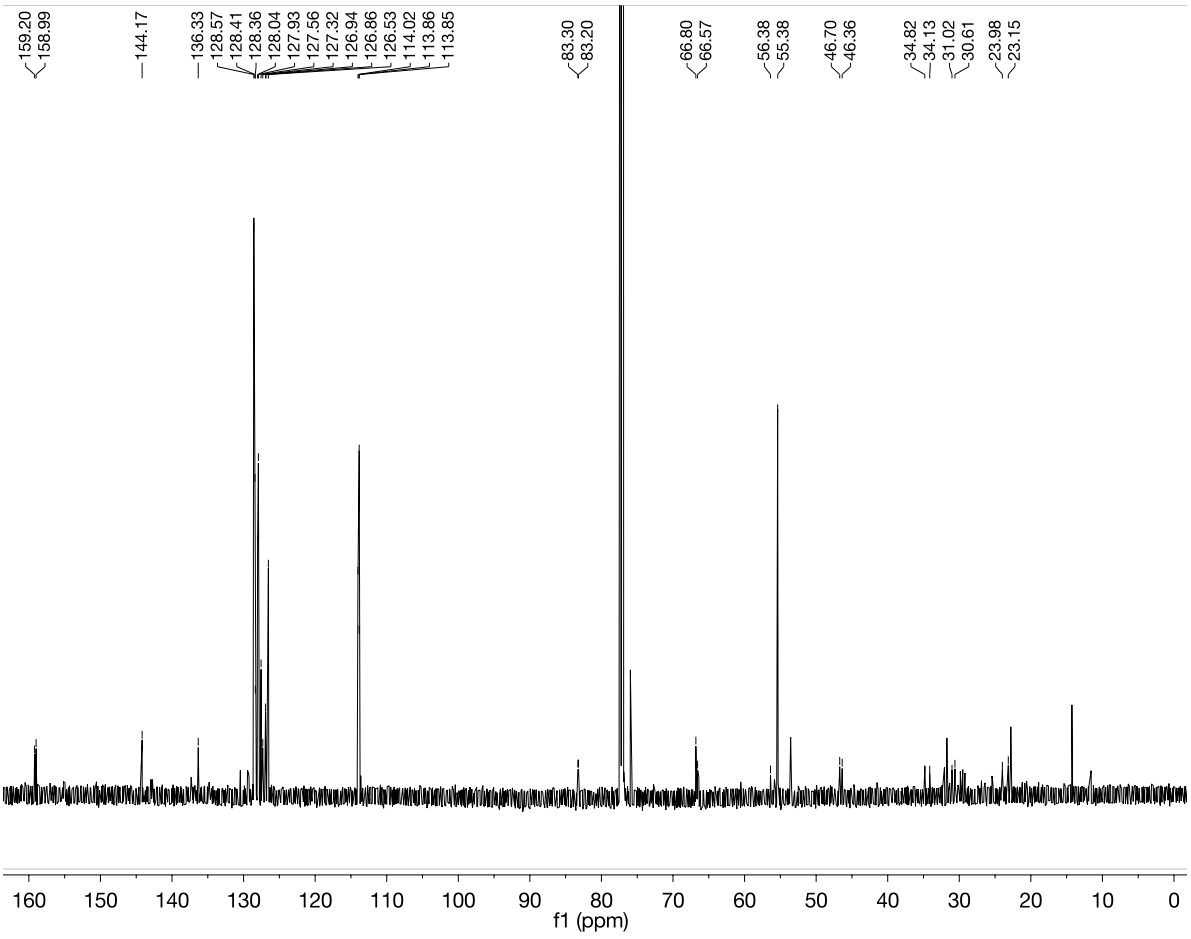
159.20 158.99 144.17 136.33 128.57 128.41 128.36 128.04 127.93 127.56 127.32 126.94 126.86 126.53 114.02 113.86 113.85 83.30 83.20 66.80 66.57 56.38 55.38 46.70 46.36 34.82 34.13 31.02 30.61 23.98 23.15
160 150 140 130 120 110 100 90 80 70 60 50 40 30 20 10 0
f1 (ppm)

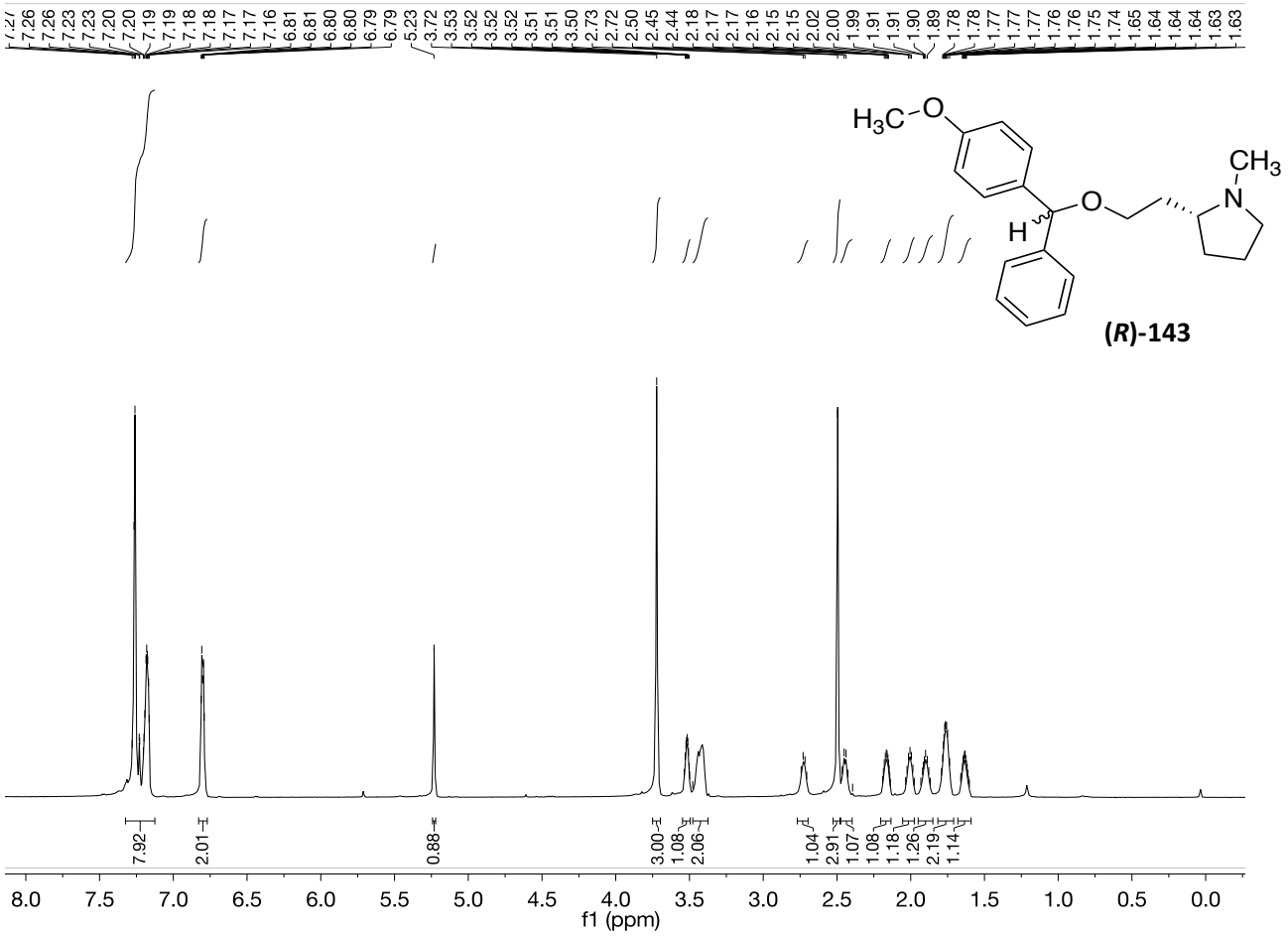
7.26
7.23
7.20
7.19
7.18
7.17
7.16
6.81
6.80
6.79
5.23
3.72
3.53
3.52
3.51
3.50
2.73
2.72
2.50
2.45
2.44
2.18
2.17
2.16
2.15
2.02
2.00
1.99
1.91
1.90
1.89
1.78
1.77
1.76
1.75
1.74
1.65
1.64
1.63
H3C
O
CH3
N
O
H
7.92
2.01
0.88
3.00
1.08
2.06
1.04
2.91
1.07
1.08
1.18
1.26
2.19
1.14
8.0
7.5
7.0
6.5
6.0
5.5
5.0
4.5
4.0
3.5
3.0
2.5
2.0
1.5
1.0
0.5
0.0
f1 (ppm)

(*R*)-143

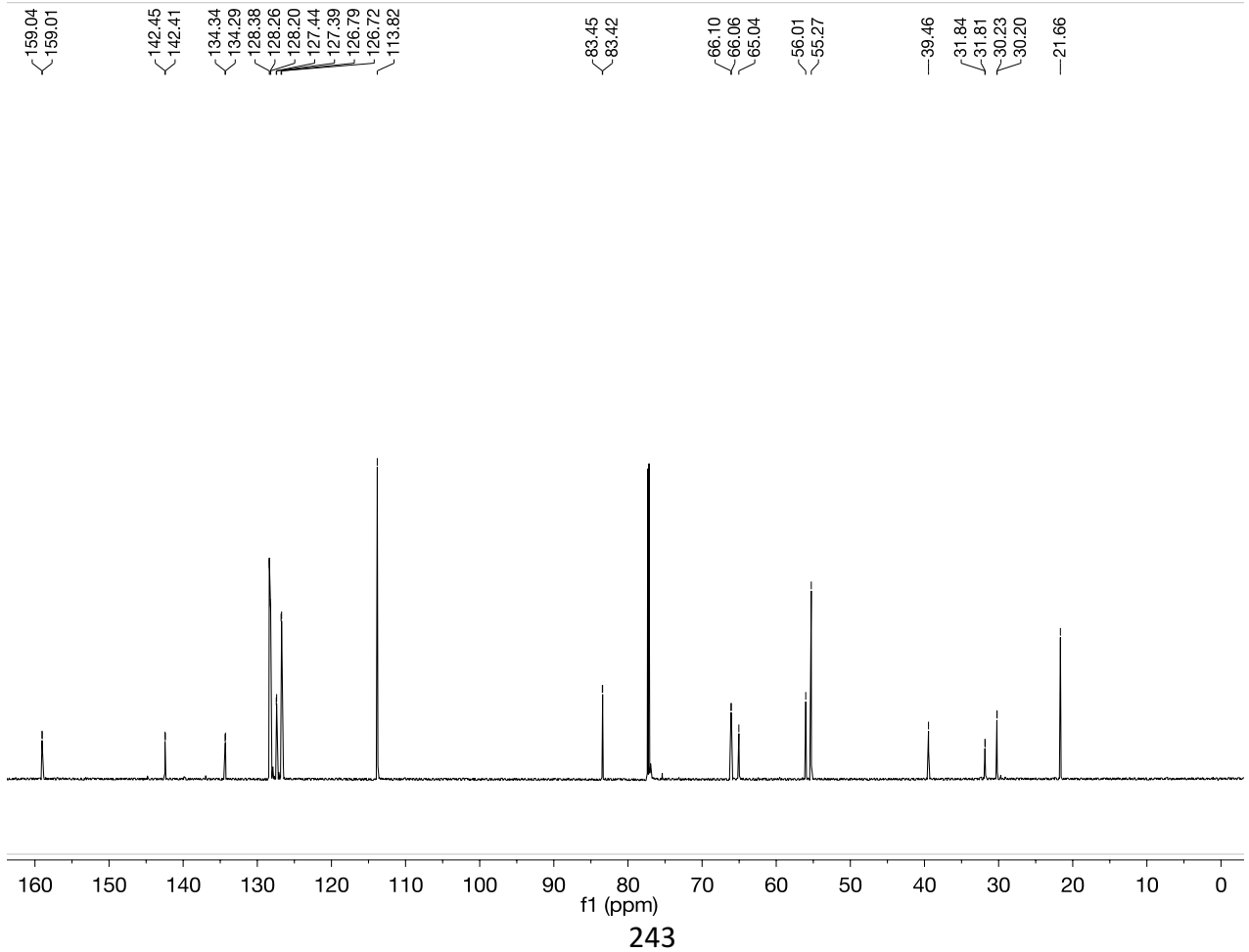
159.04
159.01
142.45
142.41
134.34
134.29
128.38
128.26
128.20
127.44
127.39
126.79
126.72
113.82
83.45
83.42
66.10
66.06
65.04
56.01
55.27
39.46
31.84
31.81
30.23
30.20
21.66
160
150
140
130
120
110
100
90
80
70
60
50
40
30
20
10
0
f1 (ppm)

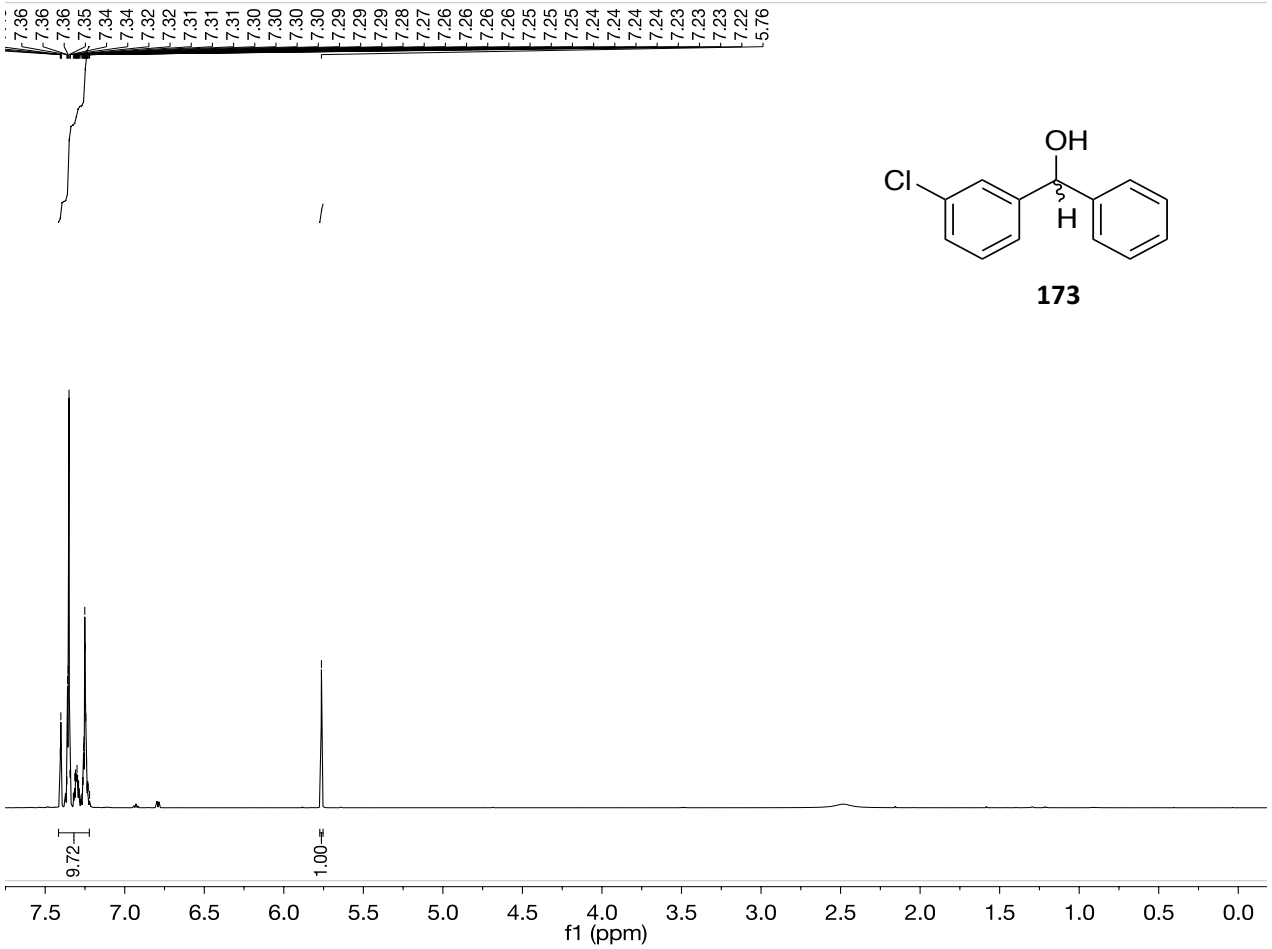
7.36 7.36 7.36 7.35 7.34 7.34 7.32 7.32 7.31 7.31 7.31 7.30 7.30 7.30 7.30 7.29 7.29 7.29 7.28 7.27 7.26 7.26 7.26 7.26 7.25 7.25 7.25 7.24 7.24 7.24 7.24 7.23 7.23 7.23 7.22 5.76
OH
Cl
H
9.72
1.00
7.5 7.0 6.5 6.0 5.5 5.0 4.5 4.0 3.5 3.0 2.5 2.0 1.5 1.0 0.5 0.0
f1 (ppm)

173

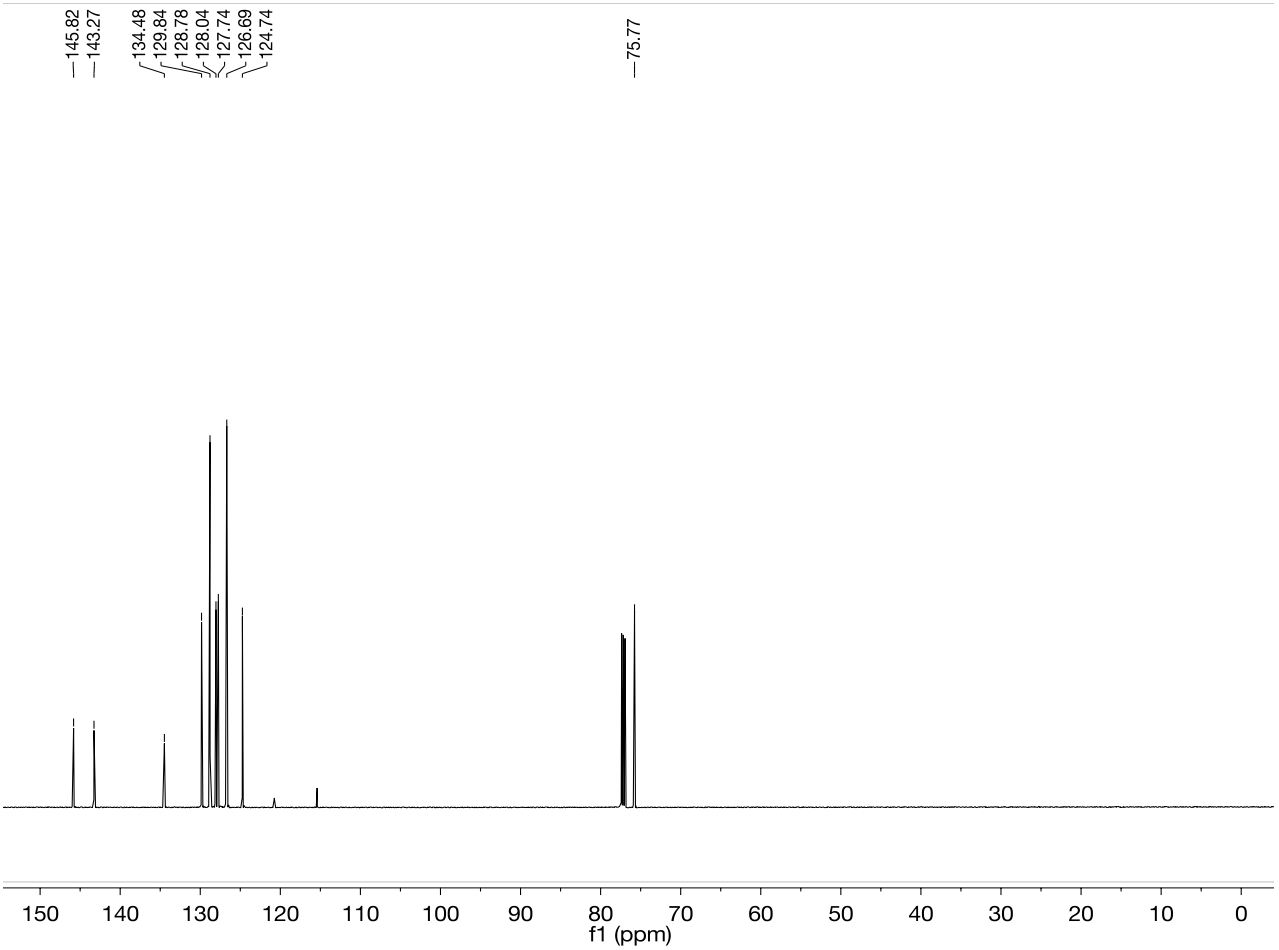
145.82
143.27
134.48
129.84
128.78
128.04
127.74
126.69
124.74
75.77
150 140 130 120 110 100 90 80 70 60 50 40 30 20 10 0
f1 (ppm)

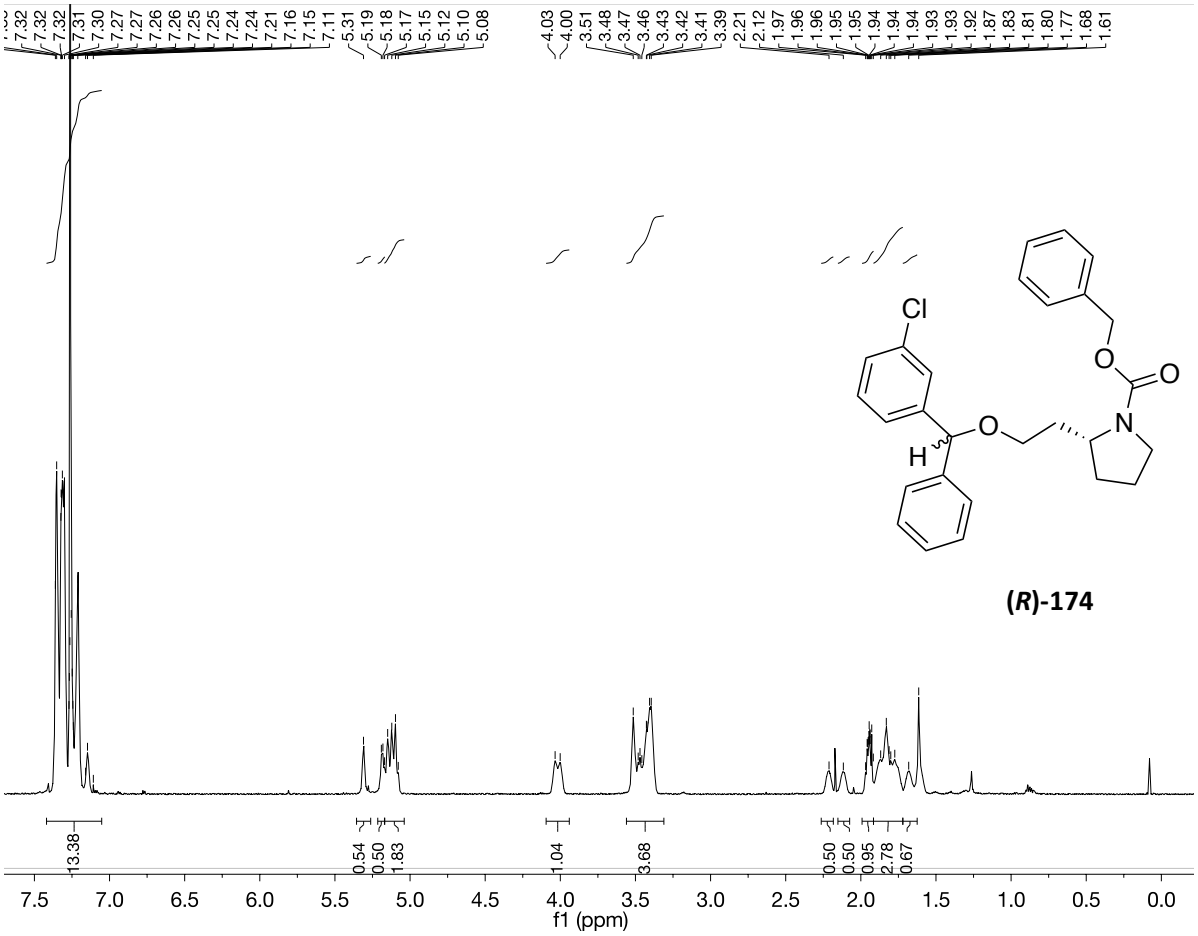
Cl
O
O
N
O
H
(R)-174
f1 (ppm)

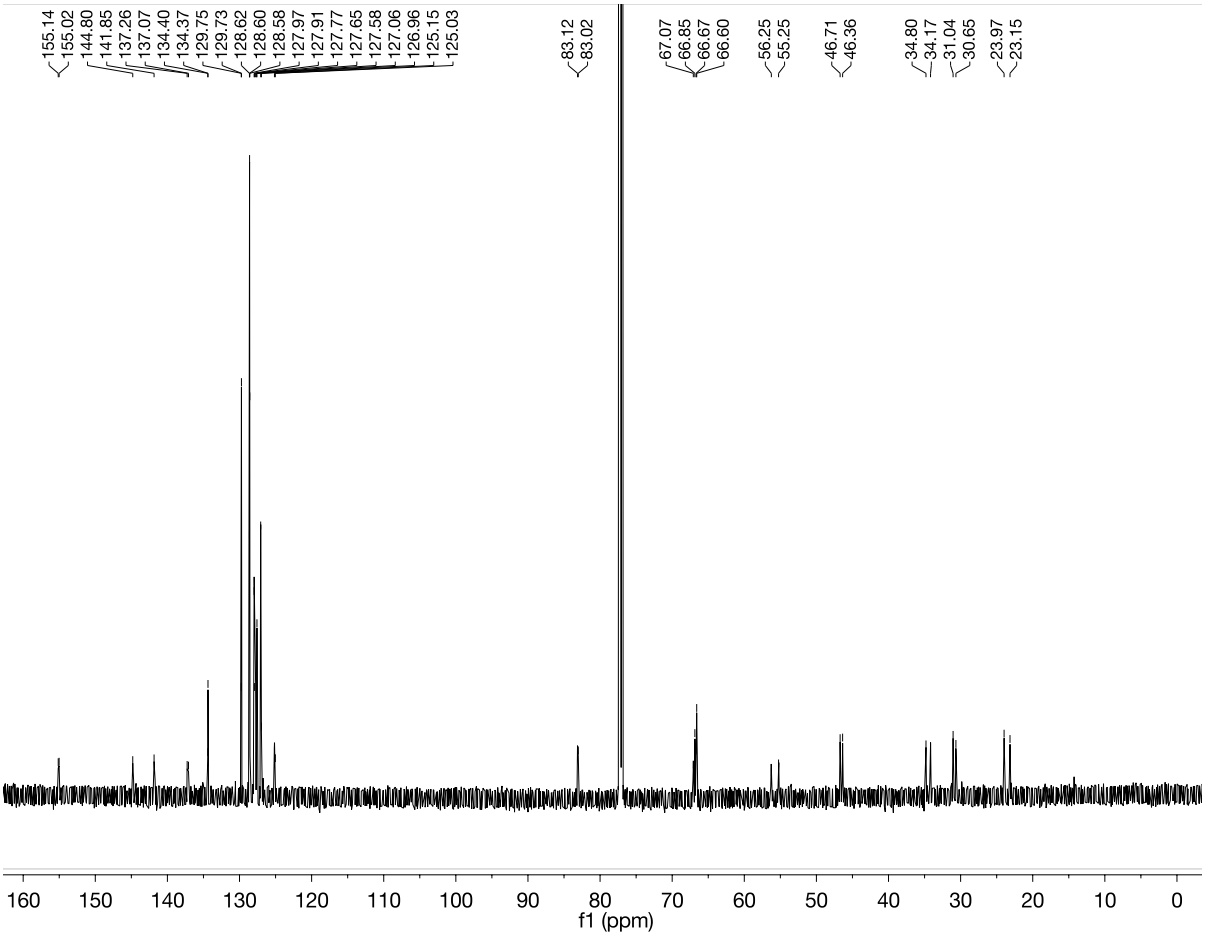
f1 (ppm)

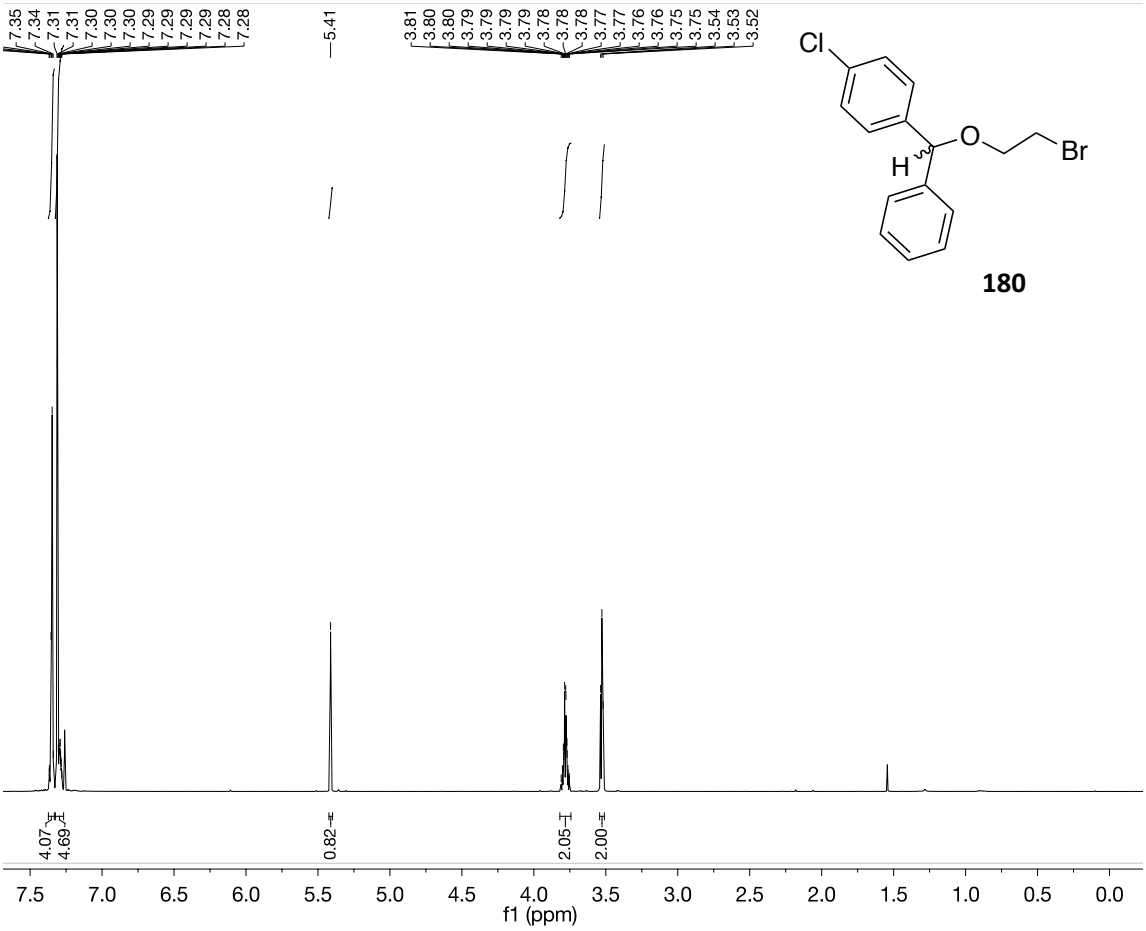
7.35
7.34
7.31
7.31
7.30
7.30
7.30
7.29
7.29
7.29
7.29
7.28
7.28
5.41
3.81
3.80
3.80
3.79
3.79
3.79
3.79
3.78
3.78
3.78
3.77
3.77
3.76
3.76
3.75
3.75
3.54
3.53
3.52
Cl
O
H
Br
180
4.07
4.69
0.82
2.05
2.00
7.5
7.0
6.5
6.0
5.5
5.0
4.5
4.0
3.5
3.0
2.5
2.0
1.5
1.0
0.5
0.0
f1 (ppm)

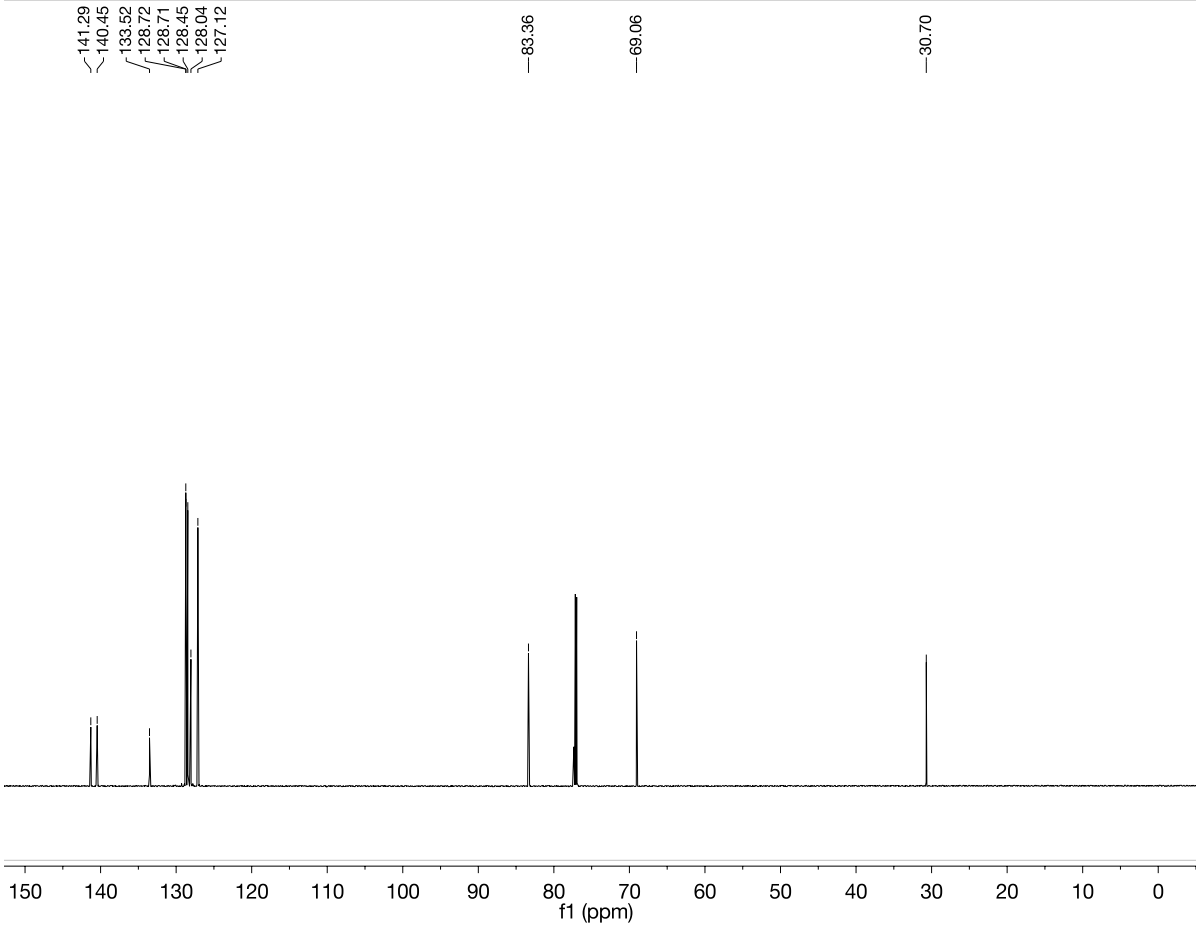
141.29
140.45
133.52
128.72
128.71
128.45
128.04
127.12
83.36
69.06
30.70
150
140
130
120
110
100
90
80
70
60
50
40
30
20
10
0
f1 (ppm)

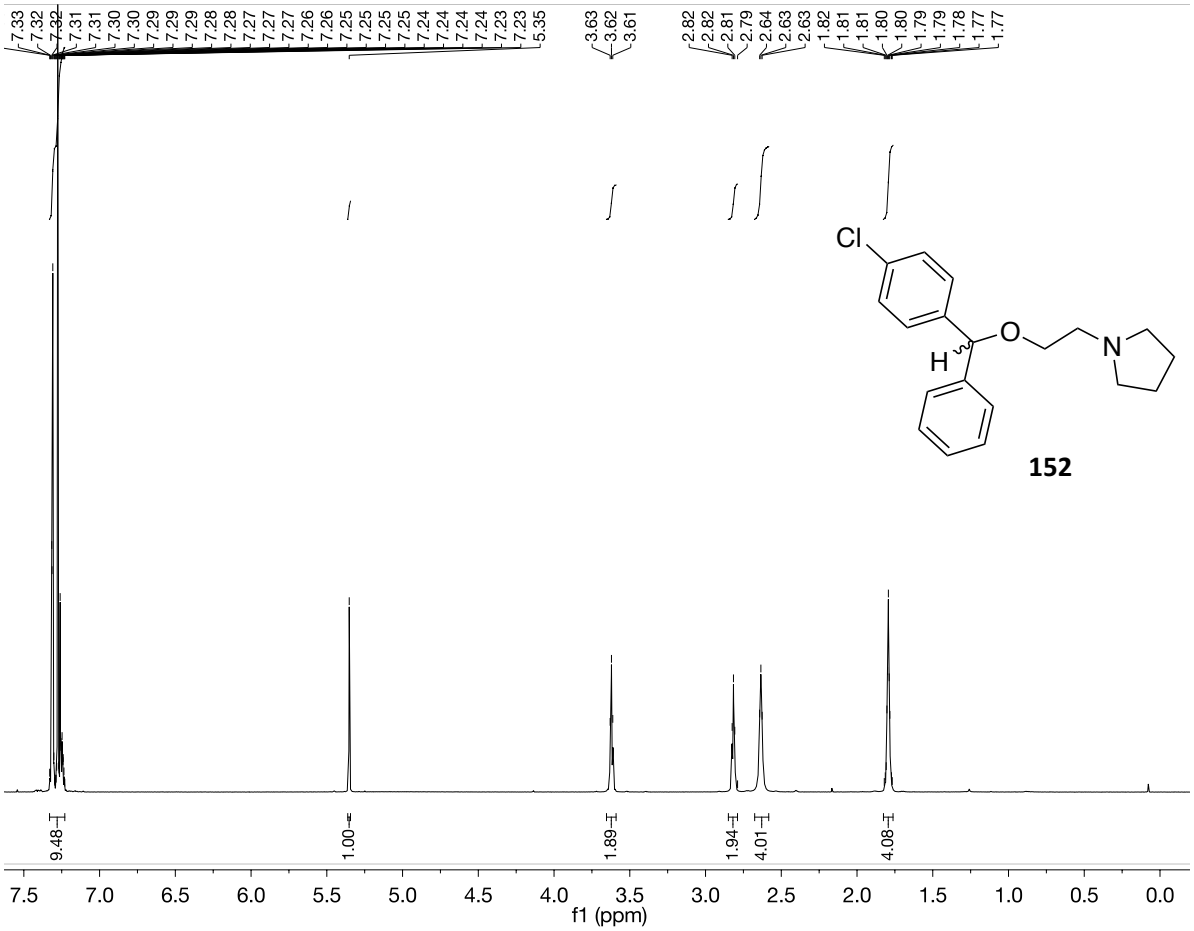
7.33 7.32 7.32 7.31 7.31 7.30 7.30 7.29 7.29 7.29 7.28 7.28 7.27 7.27 7.27 7.26 7.26 7.25 7.25 7.25 7.24 7.24 7.24 7.24 7.23 7.23 5.35
3.63 3.62 3.61
2.82 2.82 2.81 2.79 2.64 2.63 2.63
1.82 1.81 1.81 1.80 1.80 1.79 1.79 1.78 1.77 1.77
Cl
O
N
H
152
9.48
1.00
1.89
1.94
4.01
4.08
7.5 7.0 6.5 6.0 5.5 5.0 4.5 4.0 3.5 3.0 2.5 2.0 1.5 1.0 0.5 0.0
f1 (ppm)

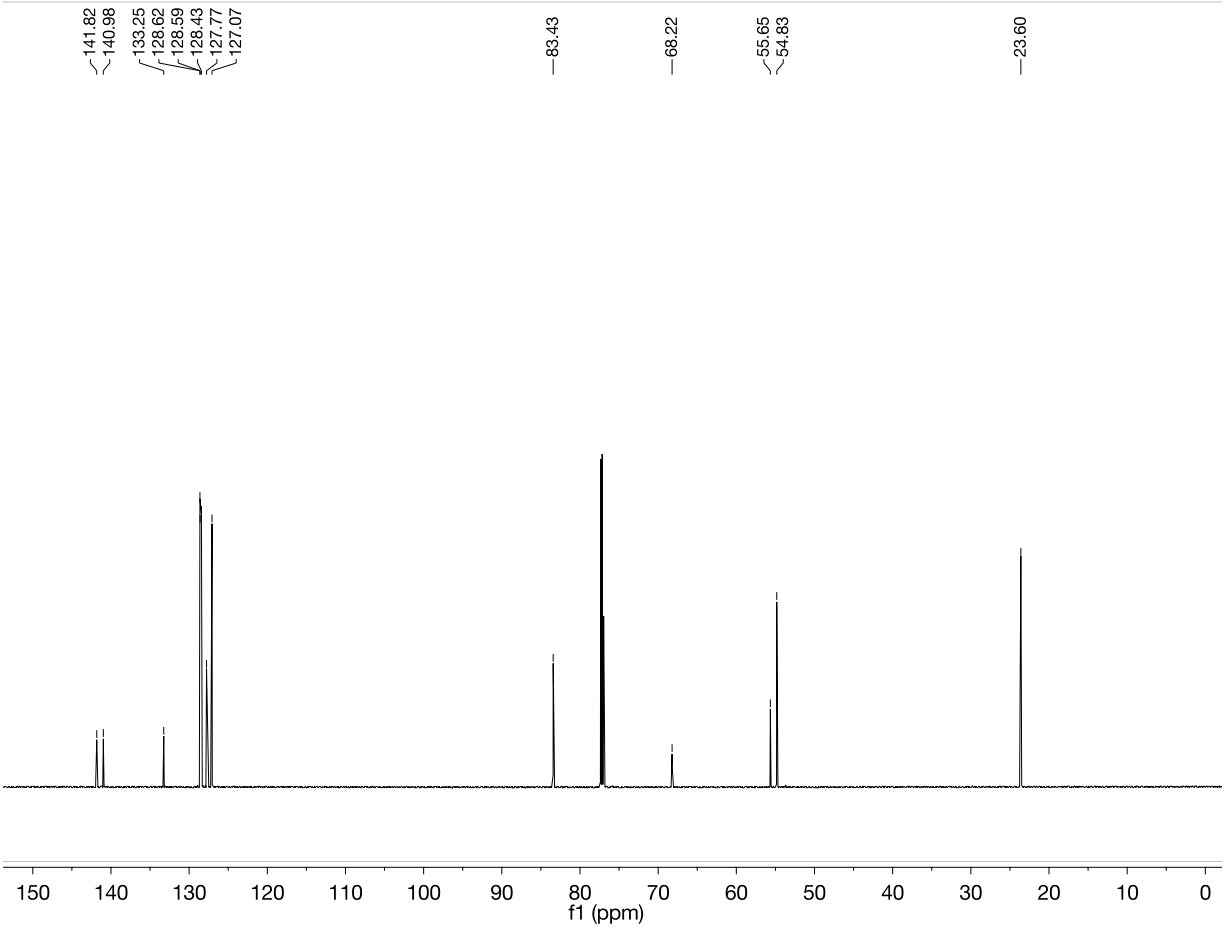
141.82 140.98 133.25 128.62 128.59 128.43 127.77 127.07
83.43
68.22
55.65 54.83
23.60
150 140 130 120 110 100 90 80 70 60 50 40 30 20 10 0
f1 (ppm)

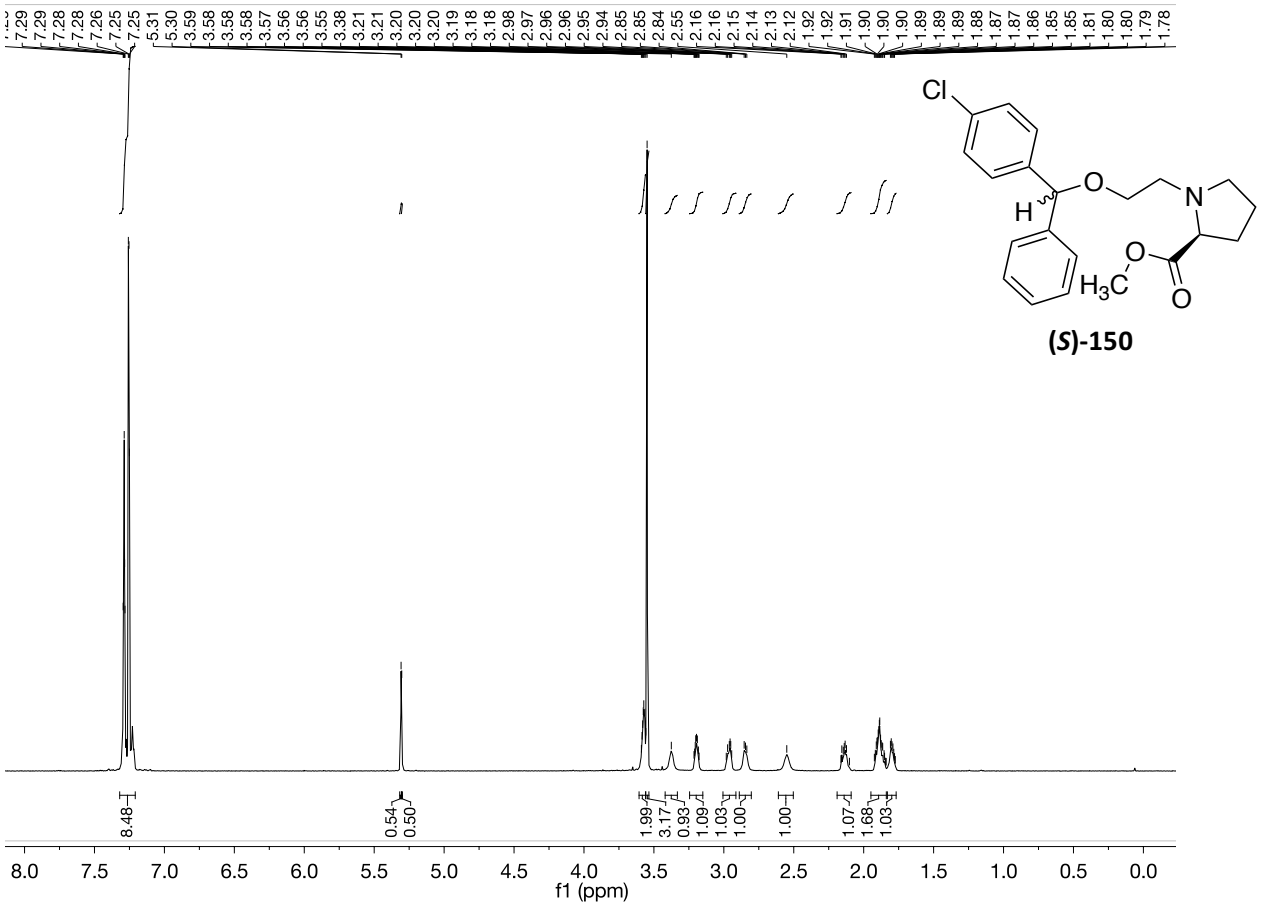
Cl
O
N
H
O
O
H3C
O
(S)-150
f1 (ppm)

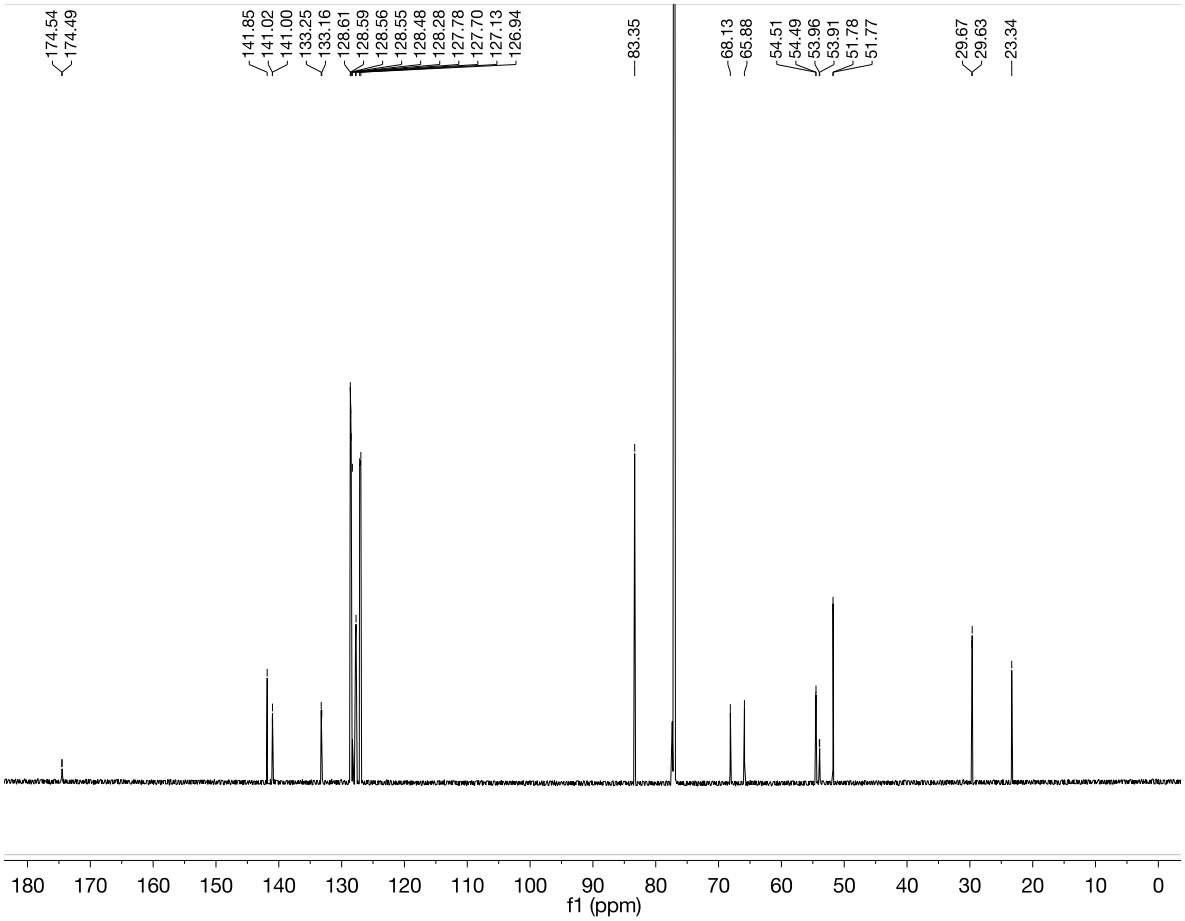
f1 (ppm)

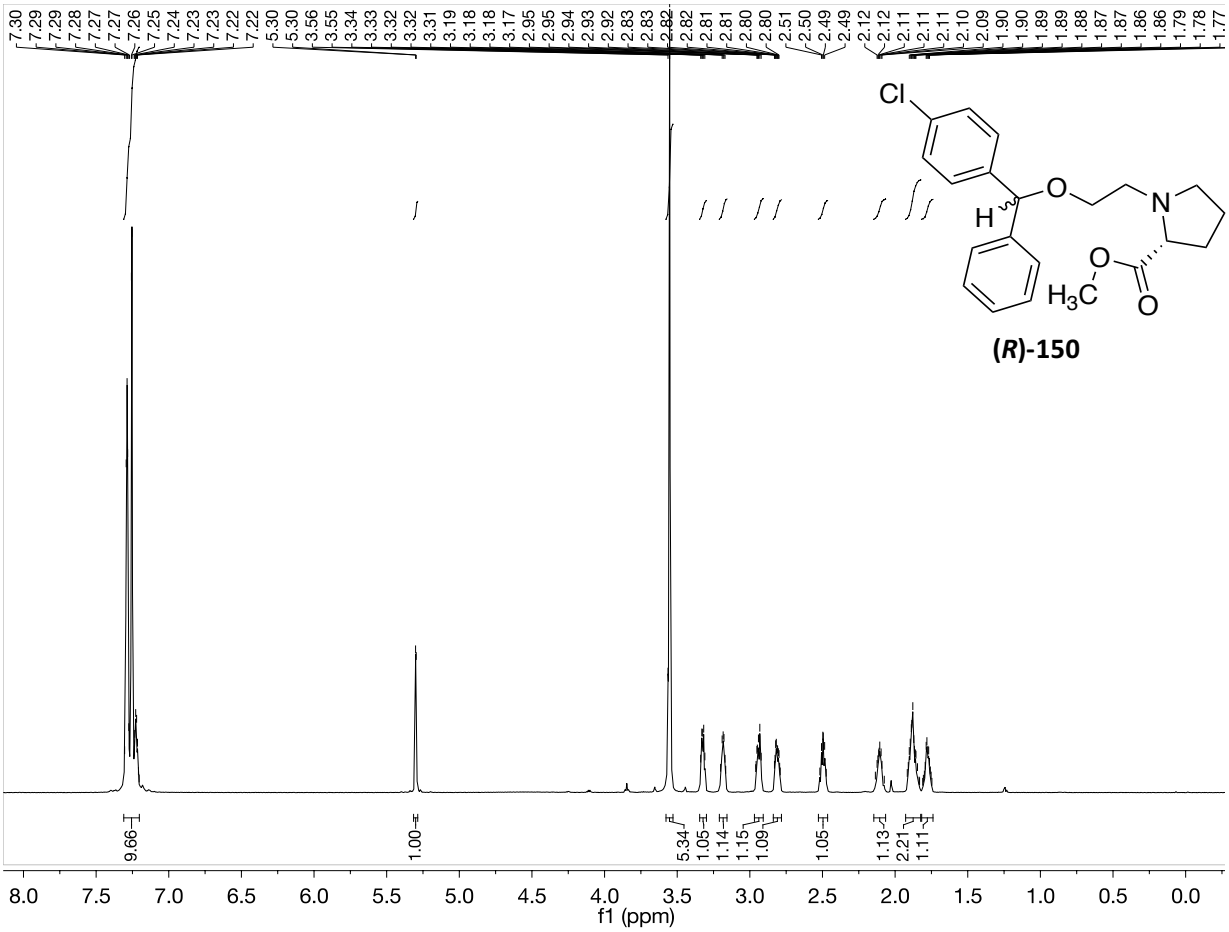
Cl
O
N
H
O
O
H_3C
O
(*R*)-150
f1 (ppm)

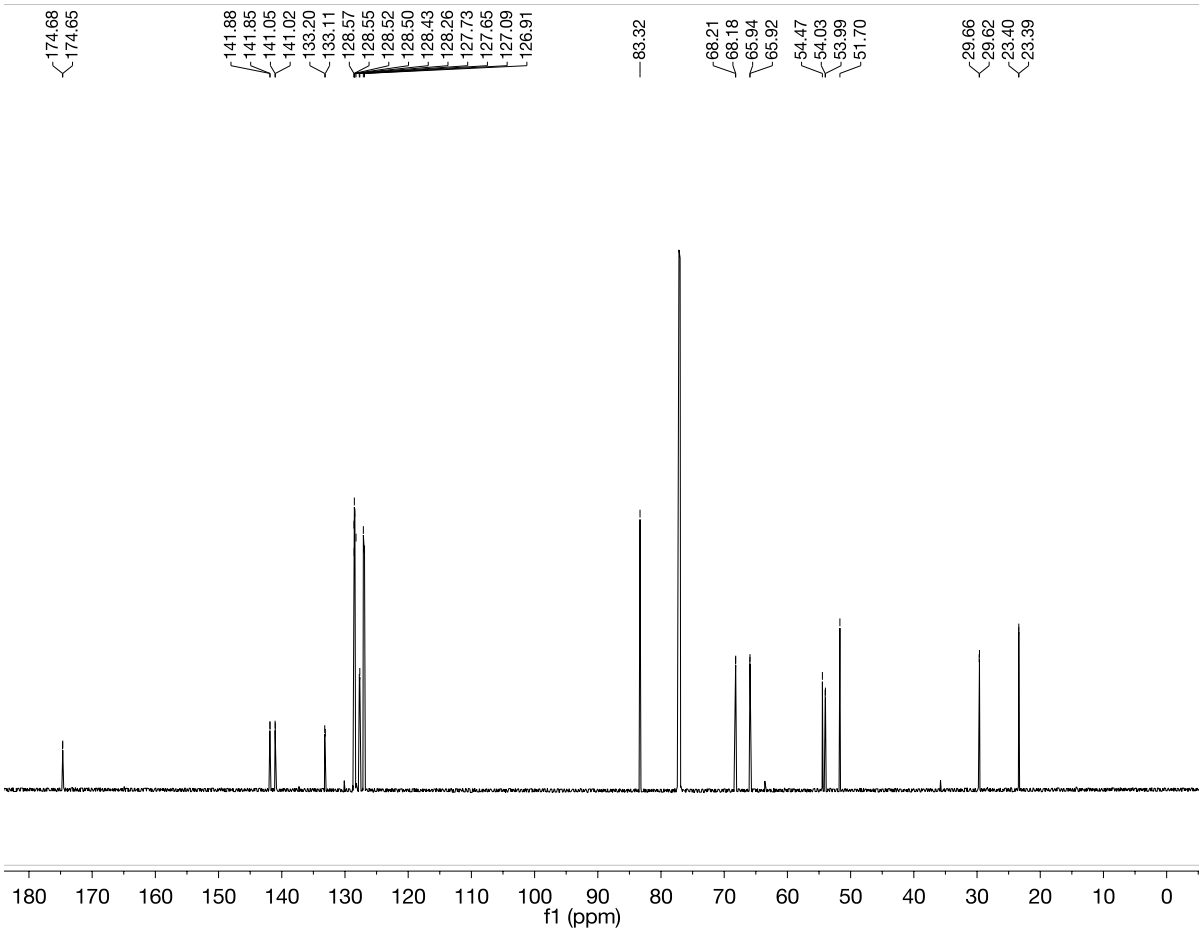
f1 (ppm)

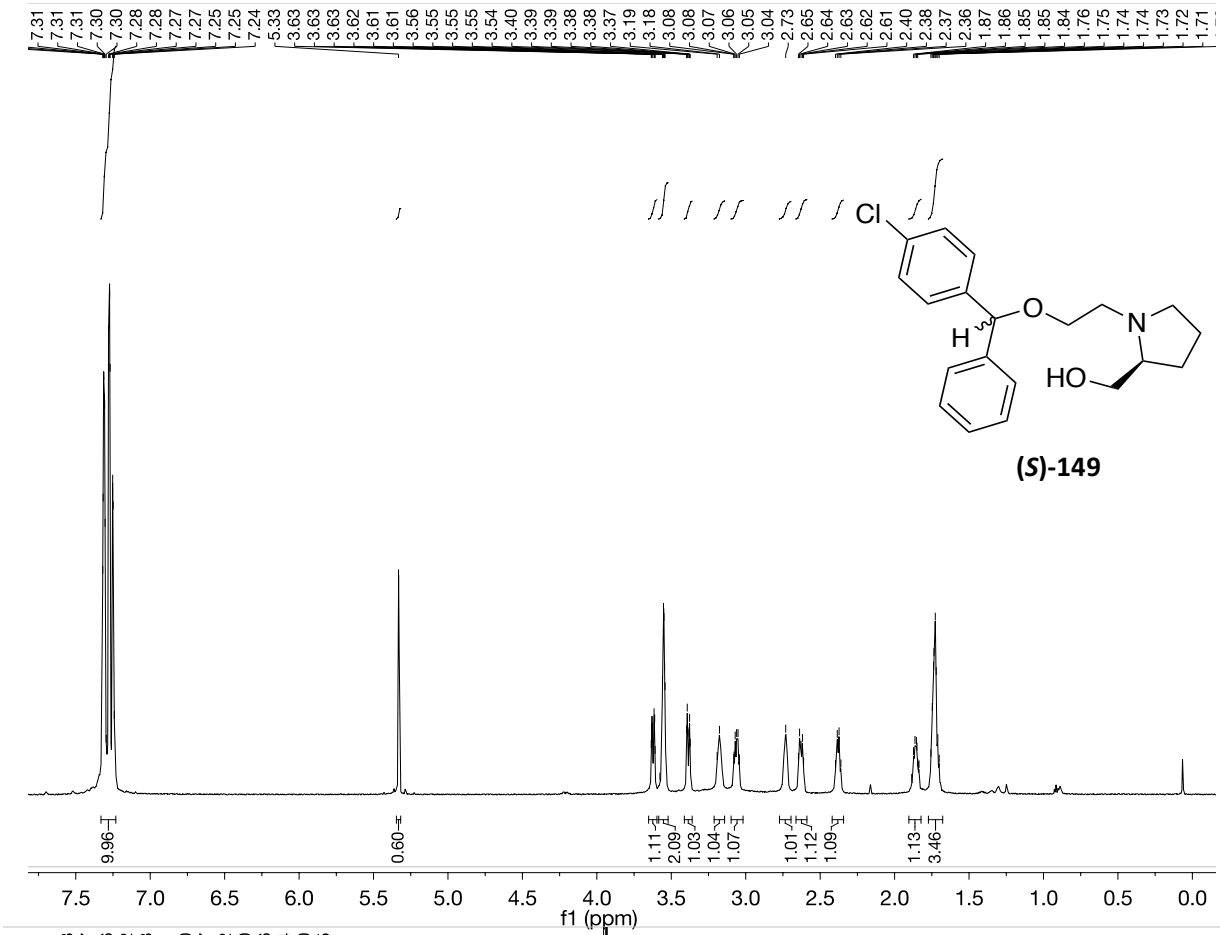
7.31 7.31 7.31 7.30 7.30 7.28 7.28 7.27 7.27 7.25 7.25 7.24 5.33 3.63 3.63 3.63 3.62 3.61 3.61 3.56 3.55 3.55 3.55 3.54 3.40 3.39 3.39 3.38 3.38 3.37 3.19 3.18 3.08 3.08 3.07 3.06 3.05 3.04 2.73 2.65 2.64 2.63 2.62 2.61 2.40 2.38 2.37 2.36 1.87 1.86 1.85 1.85 1.84 1.76 1.75 1.74 1.74 1.73 1.72 1.71
Cl
O
N
H
HO
9.96 0.60 1.11 2.09 1.03 1.04 1.07 1.01 1.12 1.09 1.13 3.46
7.5 7.0 6.5 6.0 5.5 5.0 4.5 4.0 3.5 3.0 2.5 2.0 1.5 1.0 0.5 0.0
f1 (ppm)

(*S*)-149

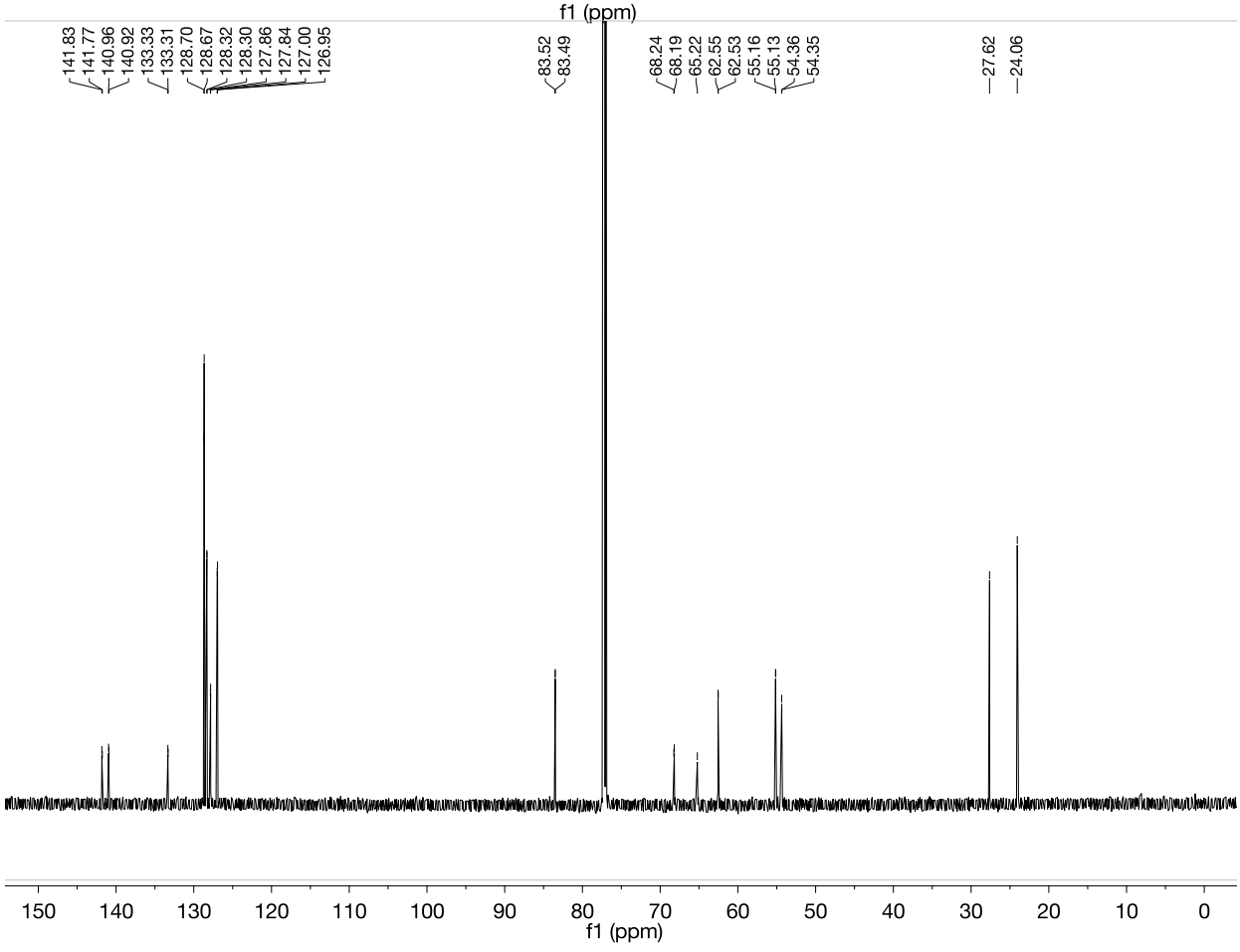
141.83 141.77 140.96 140.92 133.33 133.31 128.70 128.67 128.32 128.30 127.86 127.84 127.00 126.95
83.52 83.49
68.24 68.19 65.22 62.55 62.53 55.16 55.13 54.36 54.35
27.62 24.06
150 140 130 120 110 100 90 80 70 60 50 40 30 20 10 0
f1 (ppm)

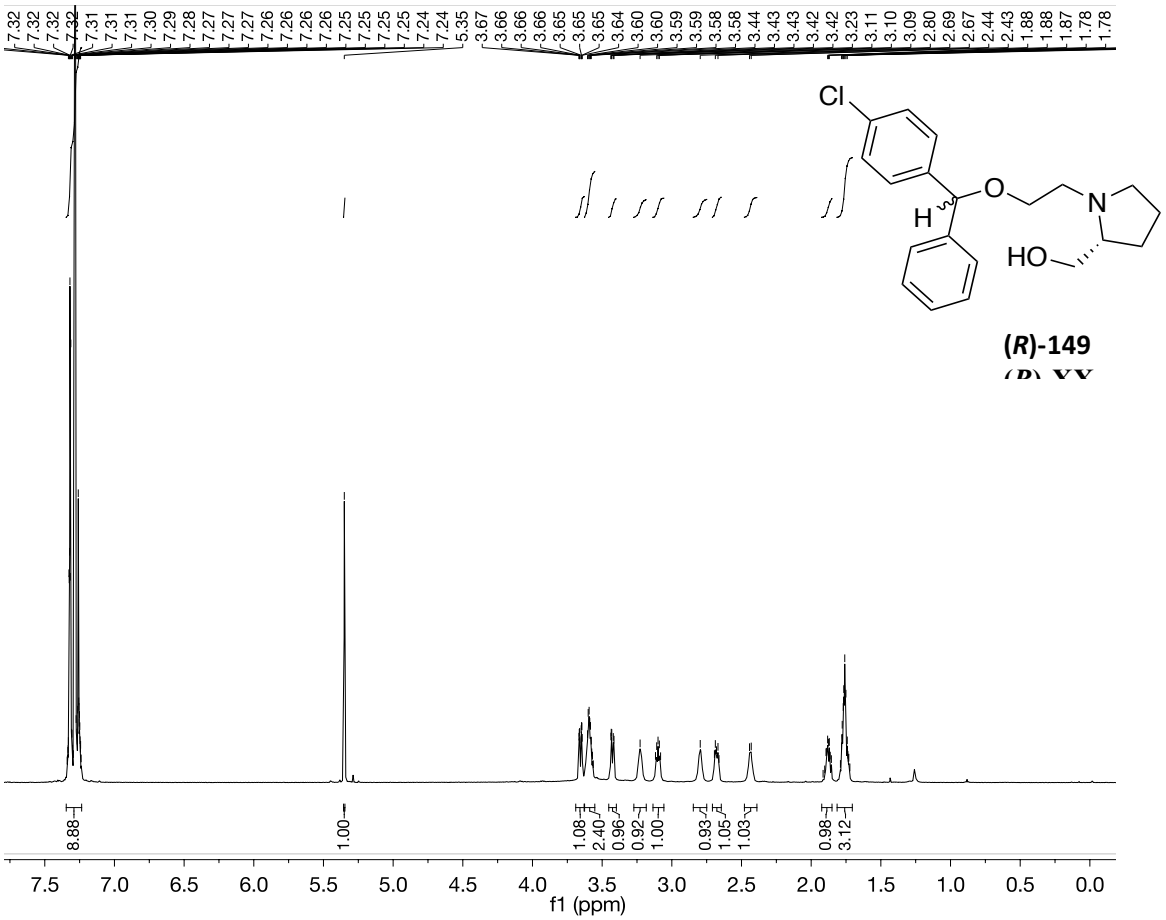

(*R*)-149

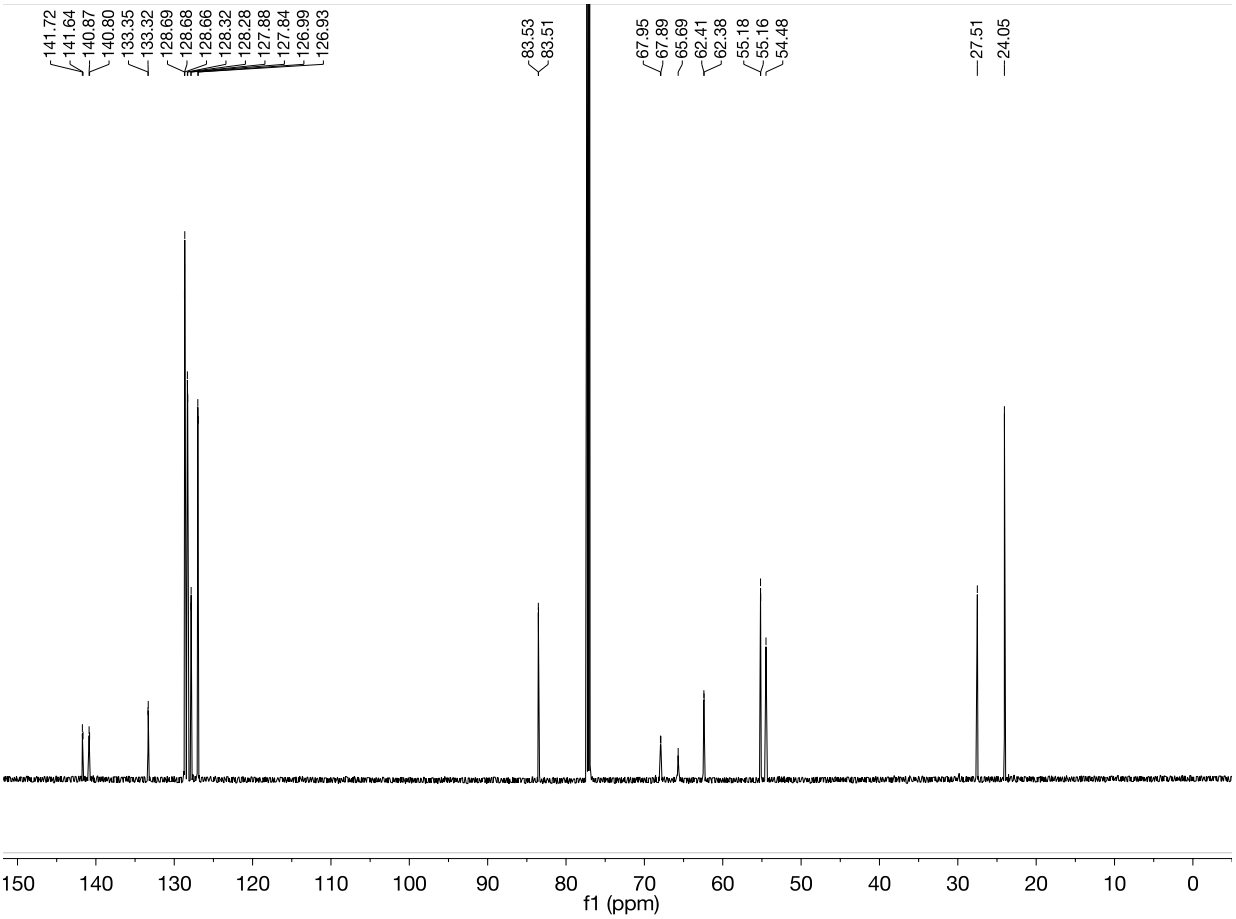

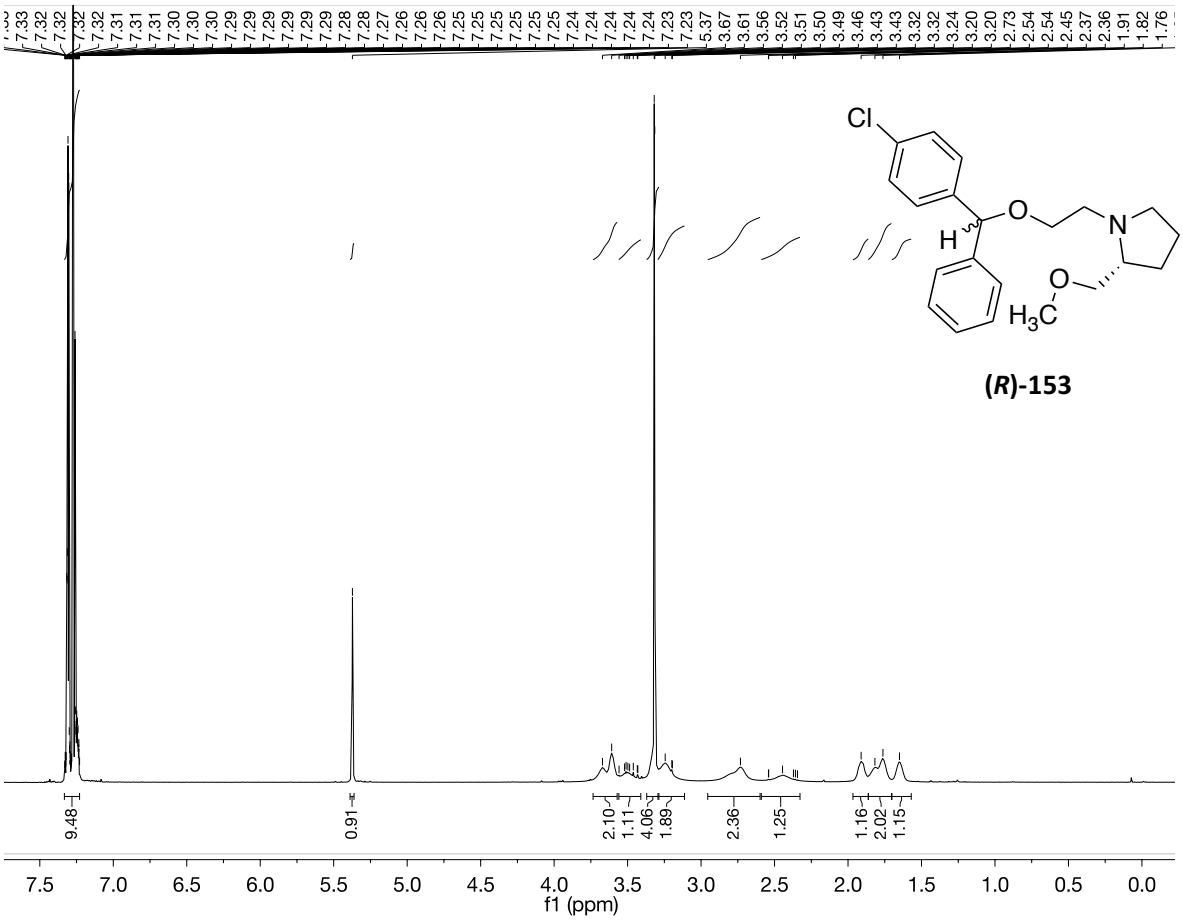
Cl
O
N
H
O
H3C
9.48
0.91
2.10
1.11
4.06
1.89
2.36
1.25
1.16
2.02
1.15
f1 (ppm)

(*R*)-153

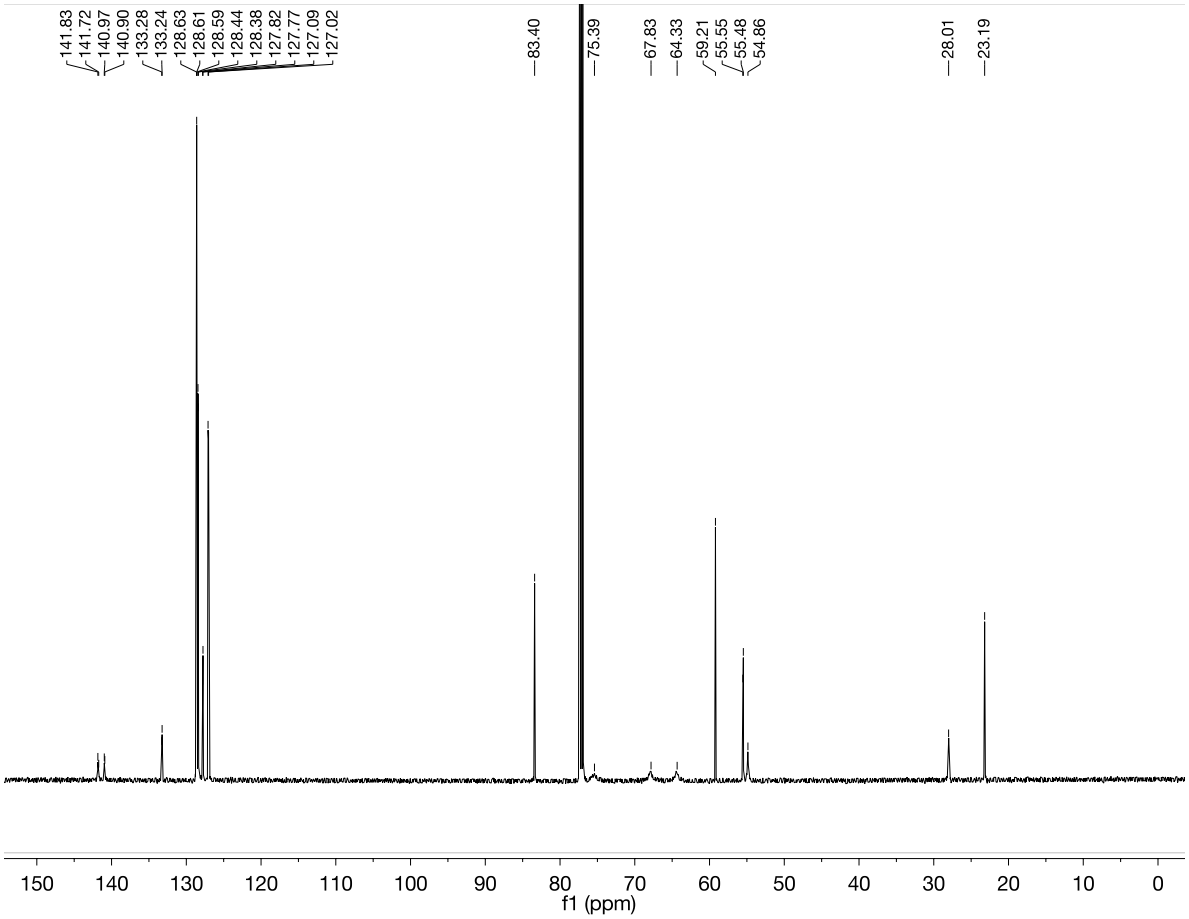
141.83
141.72
140.97
140.90
133.28
133.24
128.63
128.61
128.59
128.44
128.38
127.82
127.77
127.09
127.02
83.40
75.39
67.83
64.33
59.21
55.55
55.48
54.86
28.01
23.19
f1 (ppm)

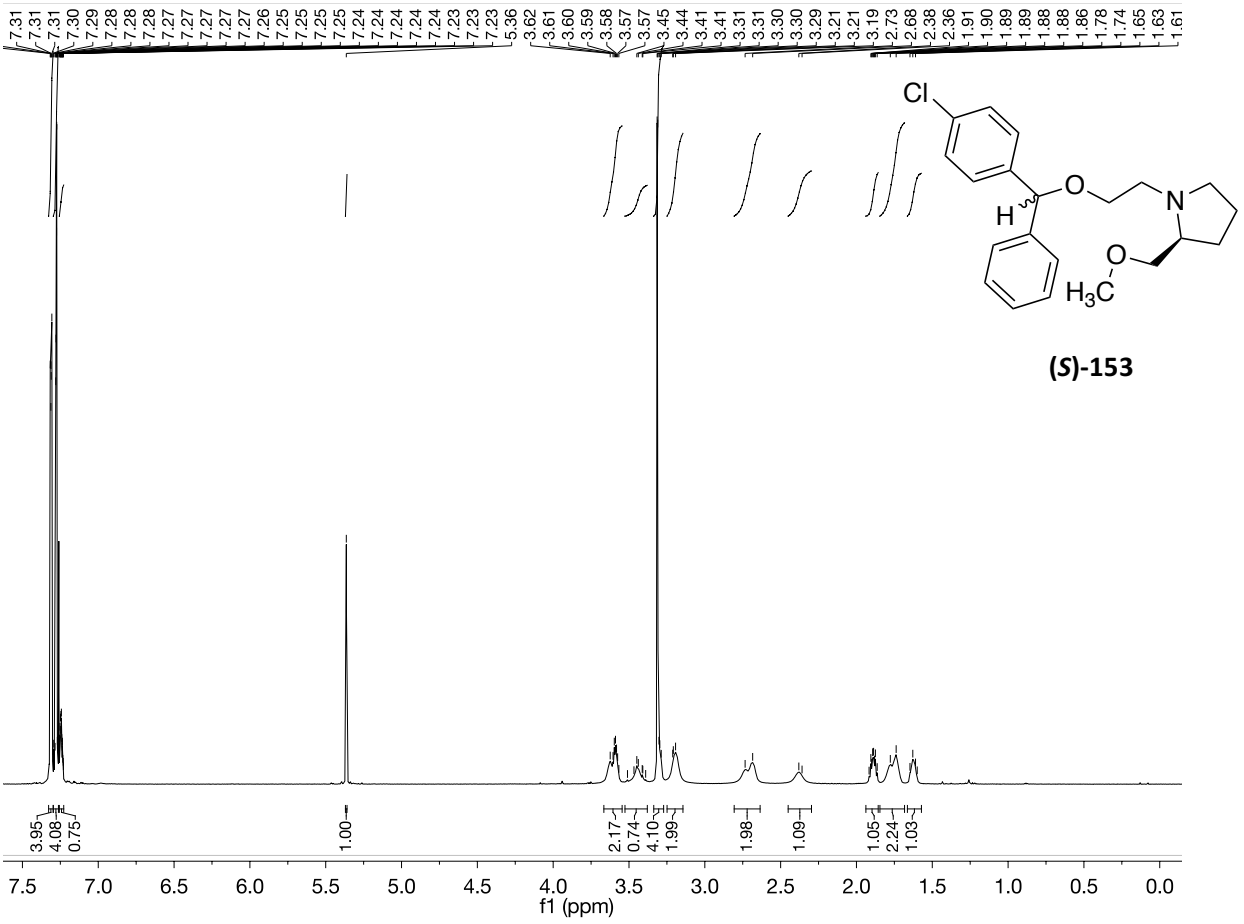

(*S*)-153

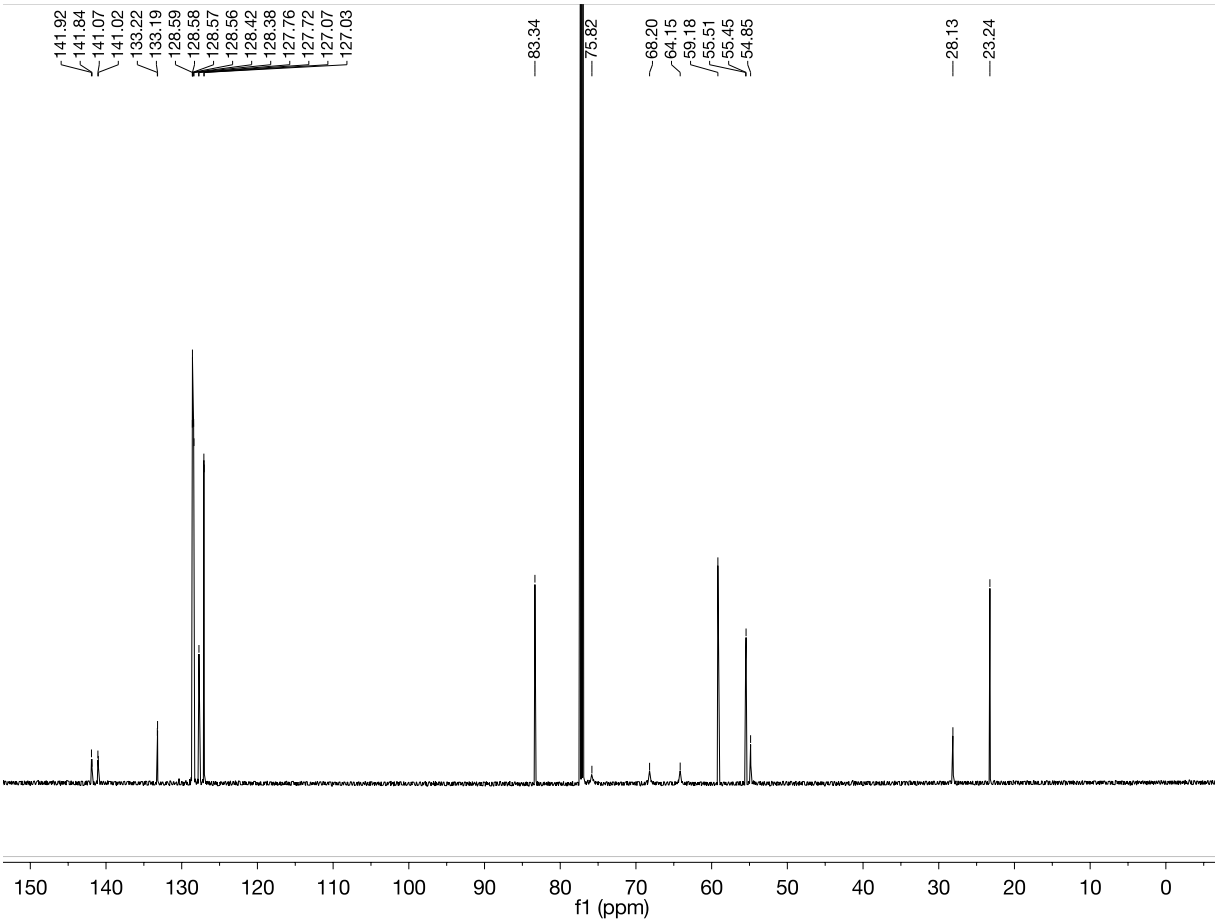

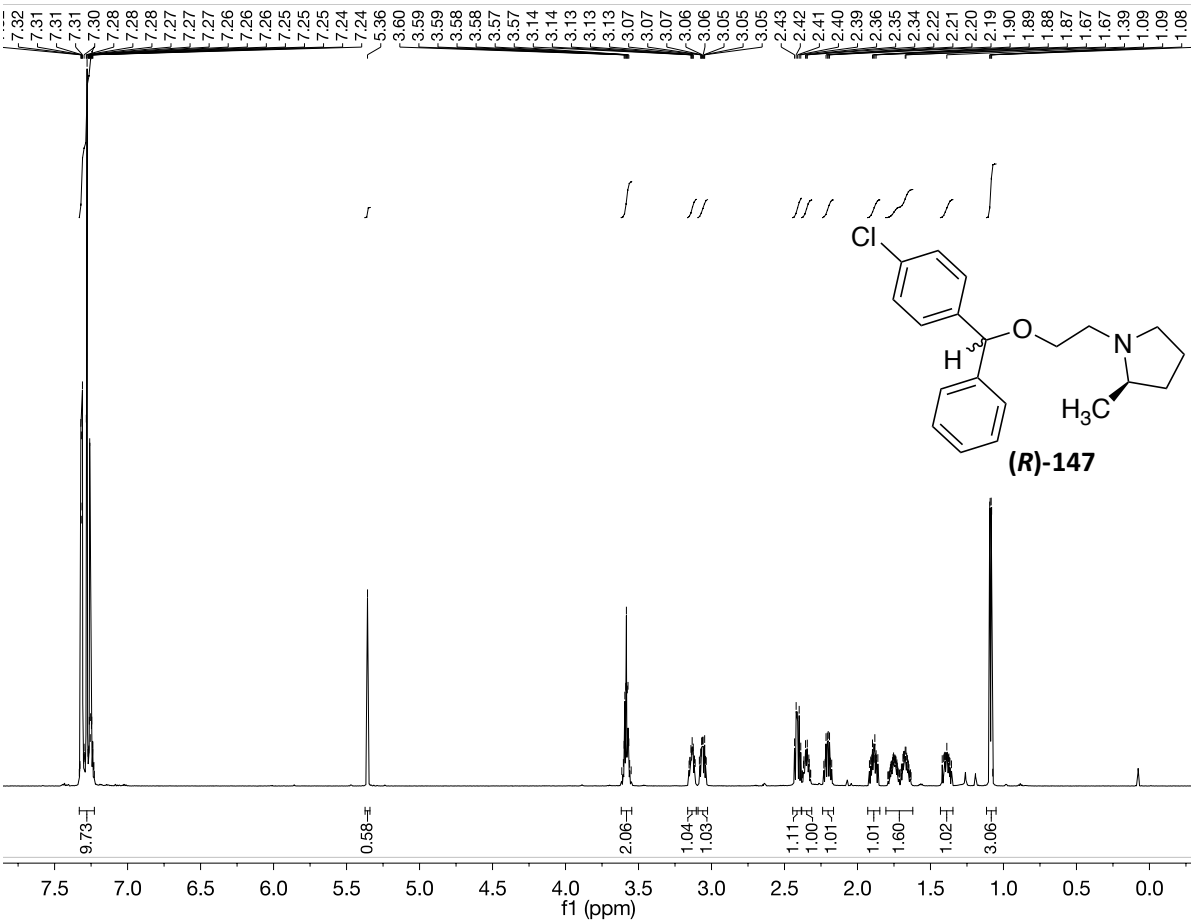

(*R*)-147

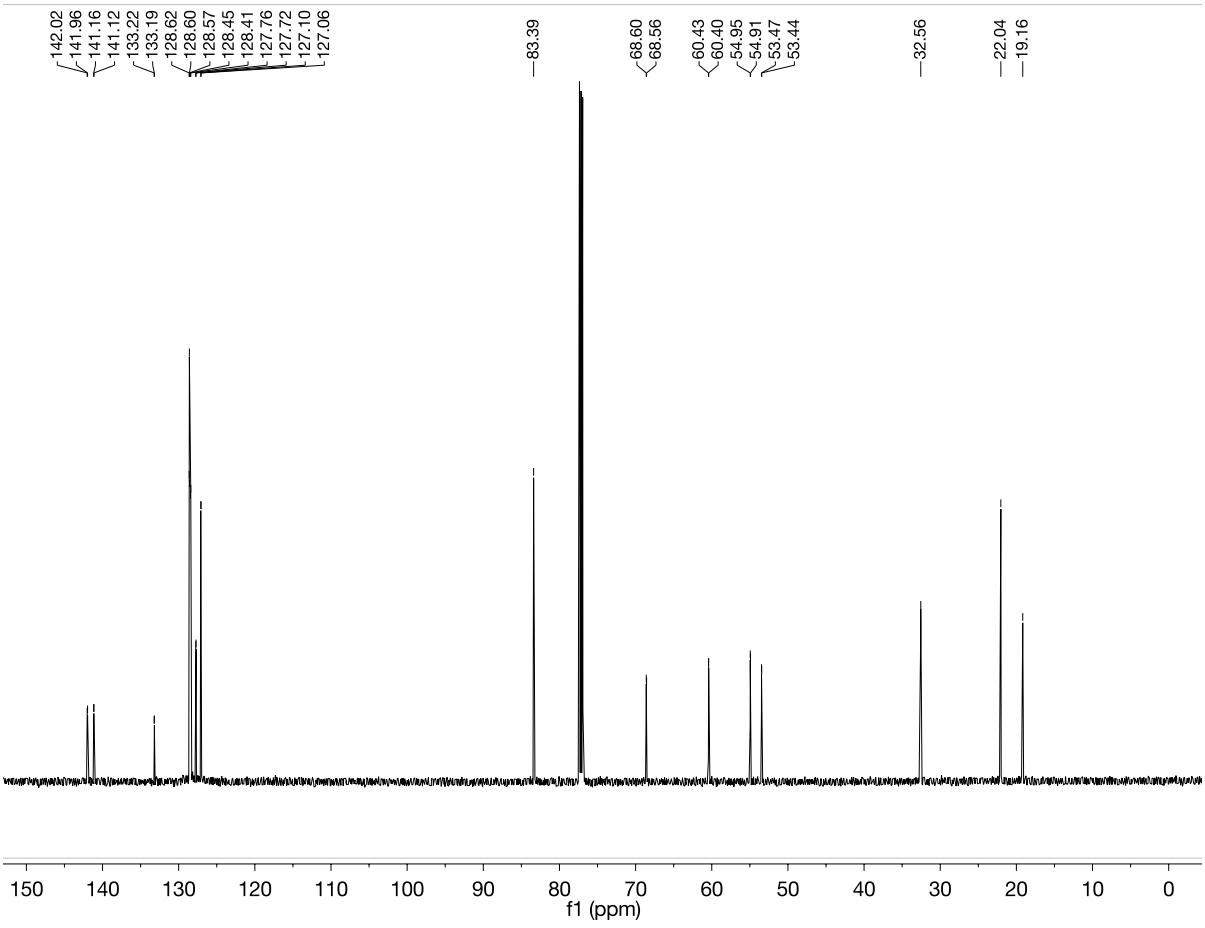

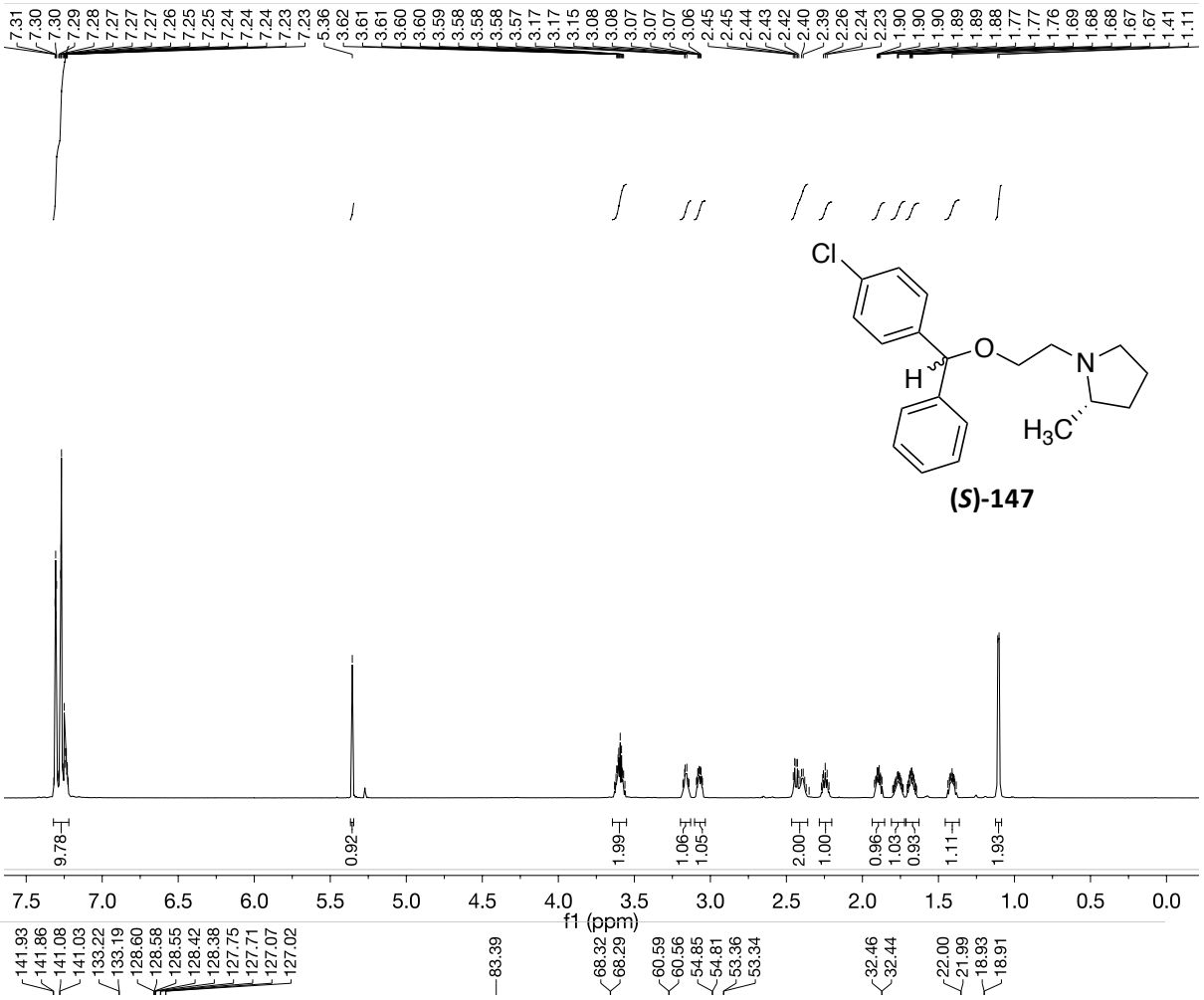
7.31 7.30 7.30 7.29 7.28 7.27 7.27 7.27 7.26 7.25 7.25 7.24 7.24 7.24 7.23 7.23
5.36
3.62 3.61 3.61 3.60 3.60 3.59 3.58 3.58 3.58 3.57 3.17 3.15 3.08 3.08 3.07 3.07 3.07 3.06
2.45 2.45 2.44 2.43 2.42 2.40 2.39 2.26 2.24 2.23
1.90 1.90 1.90 1.89 1.89 1.88 1.77 1.77 1.76 1.69 1.68 1.68 1.67 1.67 1.41 1.11
Cl
O
N
H
H3C
9.78
0.92
1.99
1.06
1.05
2.00
1.00
0.96
1.03
0.93
1.11
1.93
7.5 7.0 6.5 6.0 5.5 5.0 4.5 4.0 3.5 3.0 2.5 2.0 1.5 1.0 0.5 0.0
f1 (ppm)

(*S*)-147

141.93 141.86 141.08 141.03 133.22 133.19 128.60 128.58 128.55 128.42 128.38 127.75 127.71 127.07 127.02
83.39
68.32 68.29 60.59 60.56 54.85 54.81 53.36 53.34
32.46 32.44
22.00 21.99 18.93 18.91

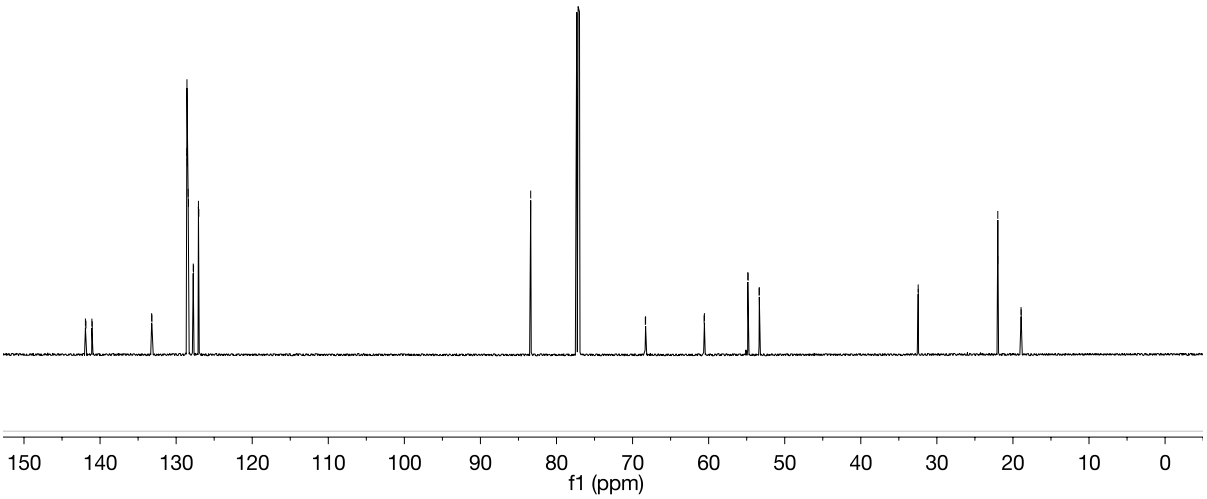
150 140 130 120 110 100 90 80 70 60 50 40 30 20 10 0
f1 (ppm)

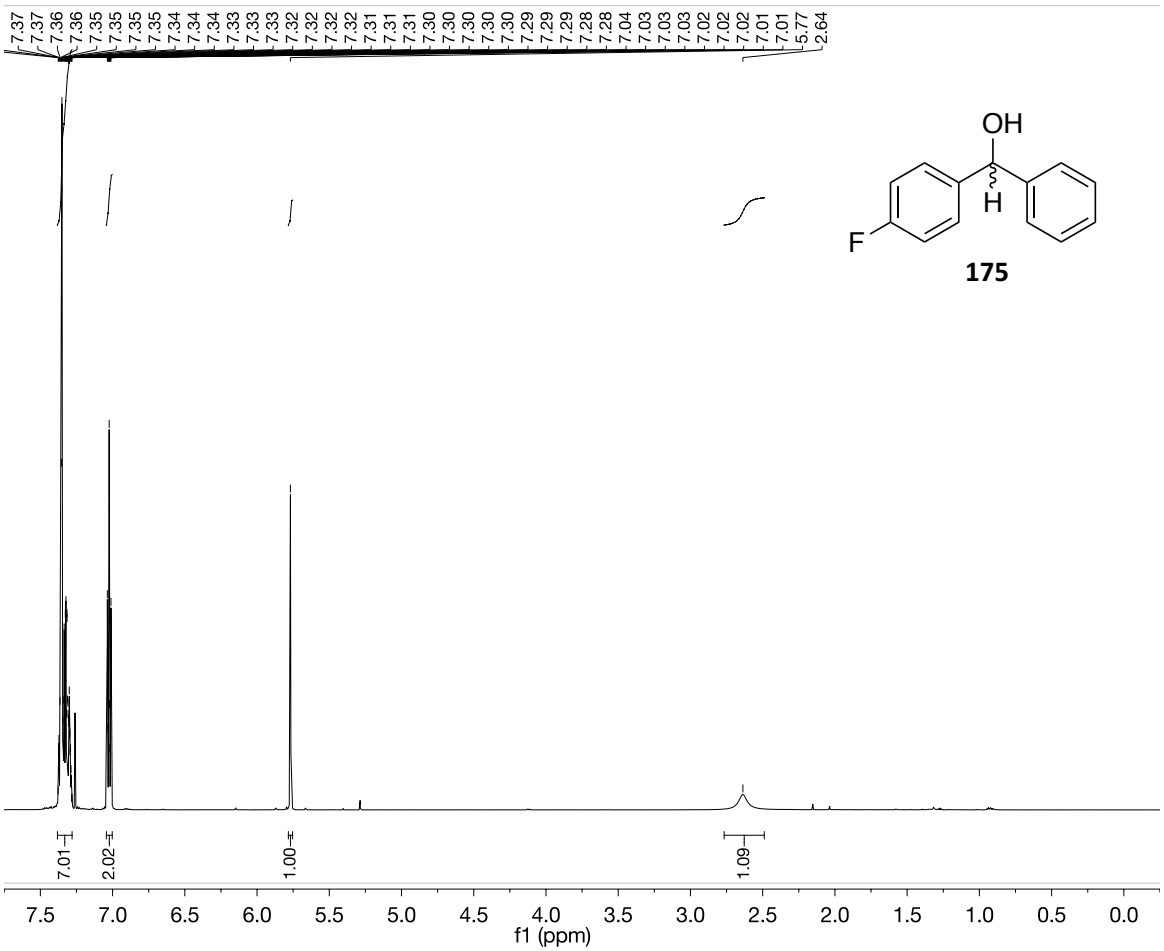
7.37
7.37
7.36
7.36
7.35
7.35
7.35
7.35
7.34
7.34
7.34
7.33
7.33
7.33
7.32
7.32
7.32
7.32
7.31
7.31
7.31
7.30
7.30
7.30
7.30
7.30
7.29
7.29
7.29
7.28
7.28
7.04
7.03
7.03
7.03
7.02
7.02
7.02
7.01
7.01
5.77
2.64
OH
H
F
175
7.01
2.02
1.00
1.09
7.5
7.0
6.5
6.0
5.5
5.0
4.5
4.0
3.5
3.0
2.5
2.0
1.5
1.0
0.5
0.0
f1 (ppm)

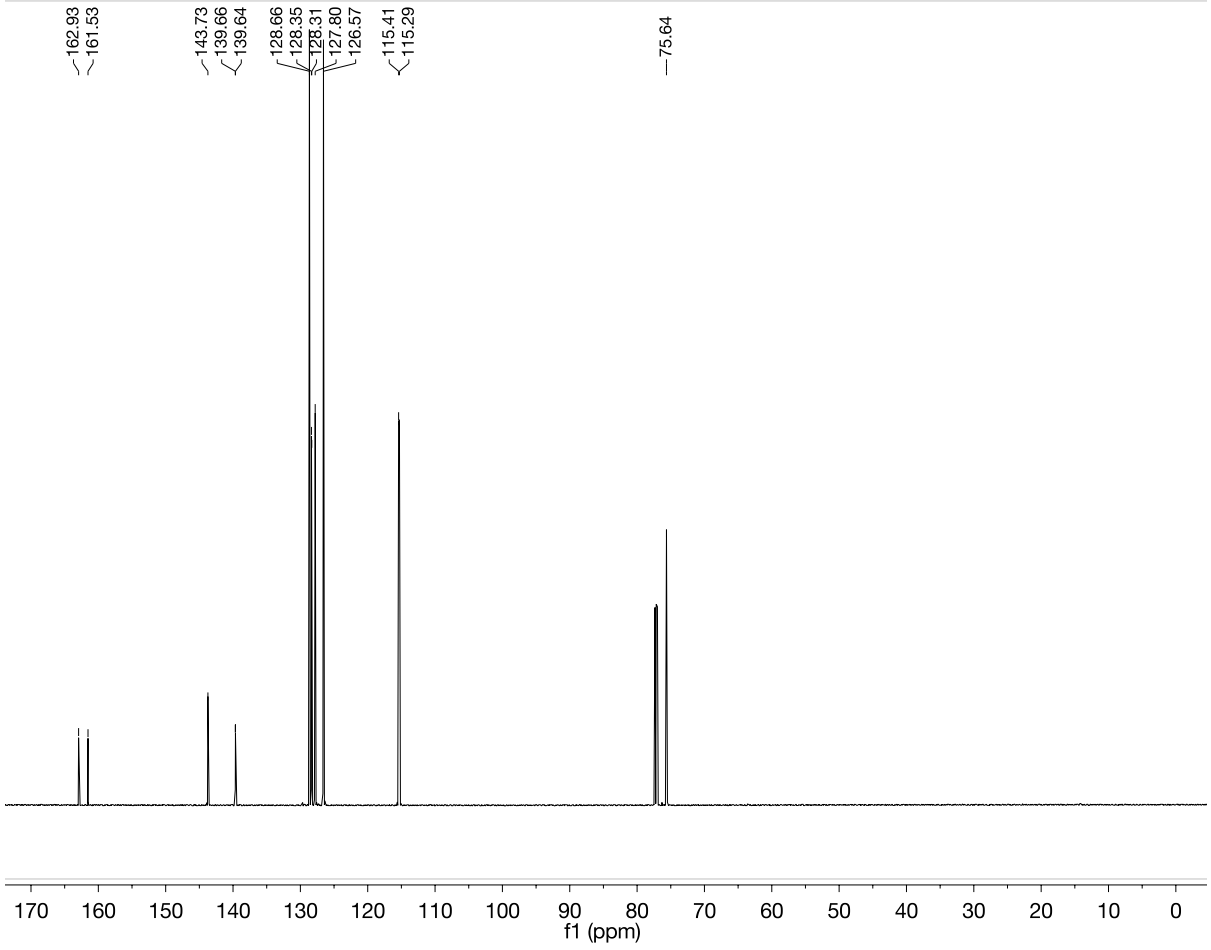
162.93
161.53
143.73
139.66
139.64
128.66
128.35
128.31
127.80
126.57
115.41
115.29
75.64
170
160
150
140
130
120
110
100
90
80
70
60
50
40
30
20
10
0
f1 (ppm)

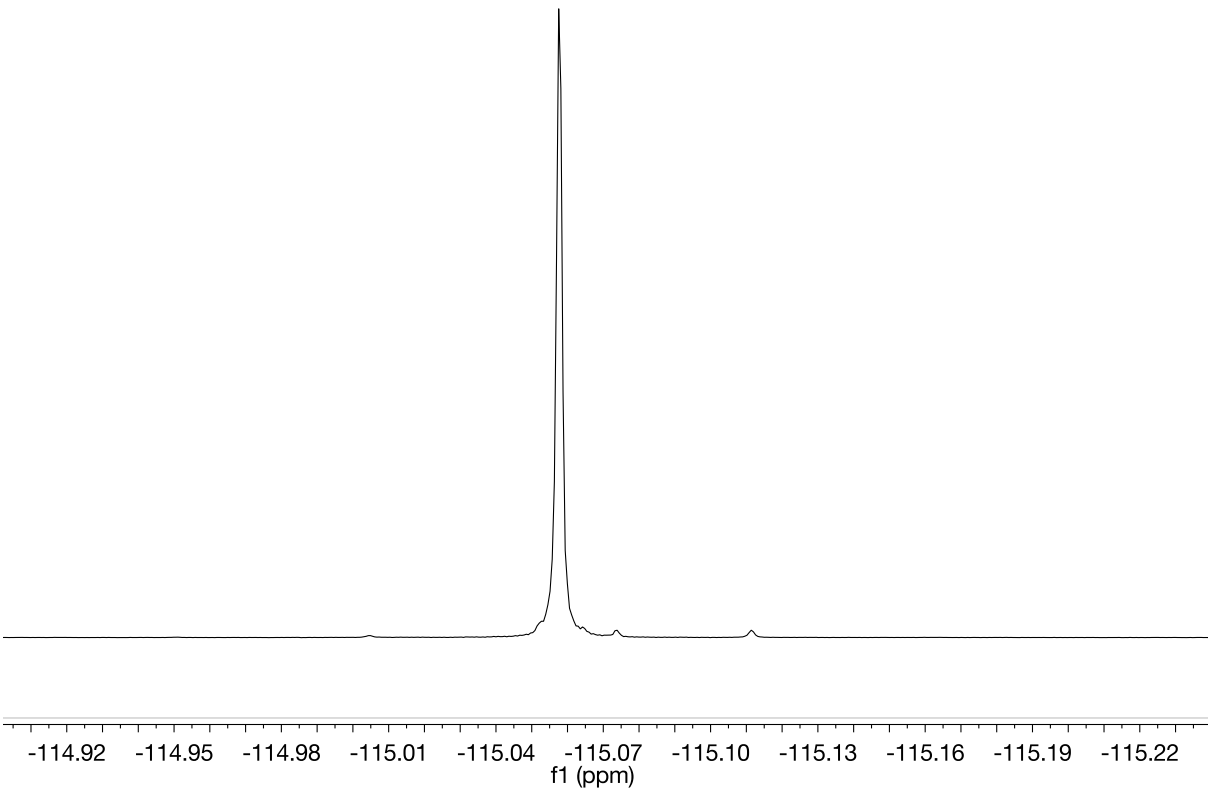
-114.92
-114.95
-114.98
-115.01
-115.04
-115.07
-115.10
-115.13
-115.16
-115.19
-115.22
f1 (ppm)

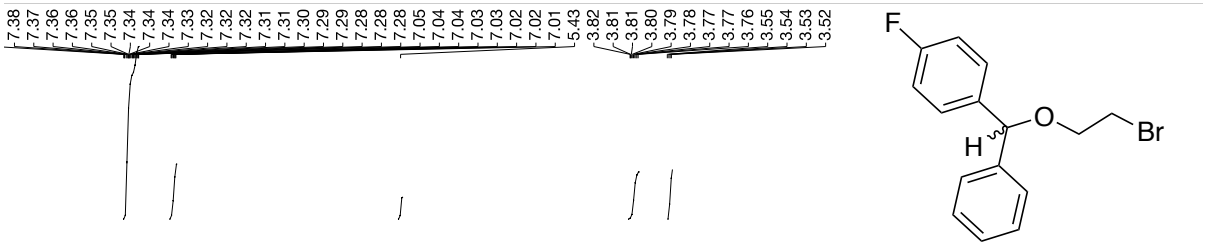
7.38
7.37
7.36
7.36
7.35
7.35
7.34
7.34
7.34
7.33
7.32
7.32
7.32
7.31
7.31
7.30
7.29
7.29
7.28
7.28
7.28
7.05
7.04
7.04
7.03
7.03
7.02
7.02
7.01
5.43
3.82
3.81
3.81
3.80
3.79
3.78
3.77
3.77
3.76
3.55
3.54
3.53
3.52
F
O
H
Br

181

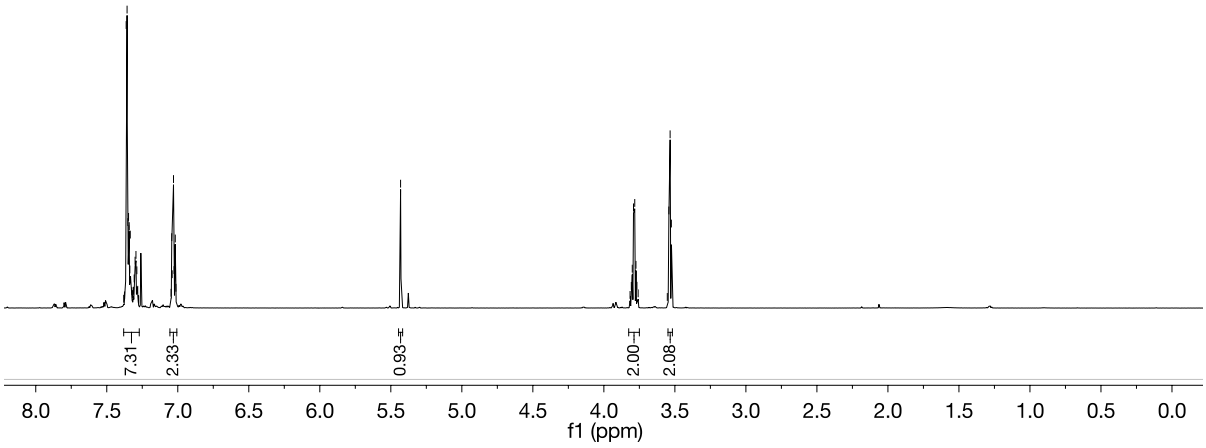
7.31
2.33
0.93
2.00
2.08
8.0
7.5
7.0
6.5
6.0
5.5
5.0
4.5
4.0
3.5
3.0
2.5
2.0
1.5
1.0
0.5
0.0
f1 (ppm)

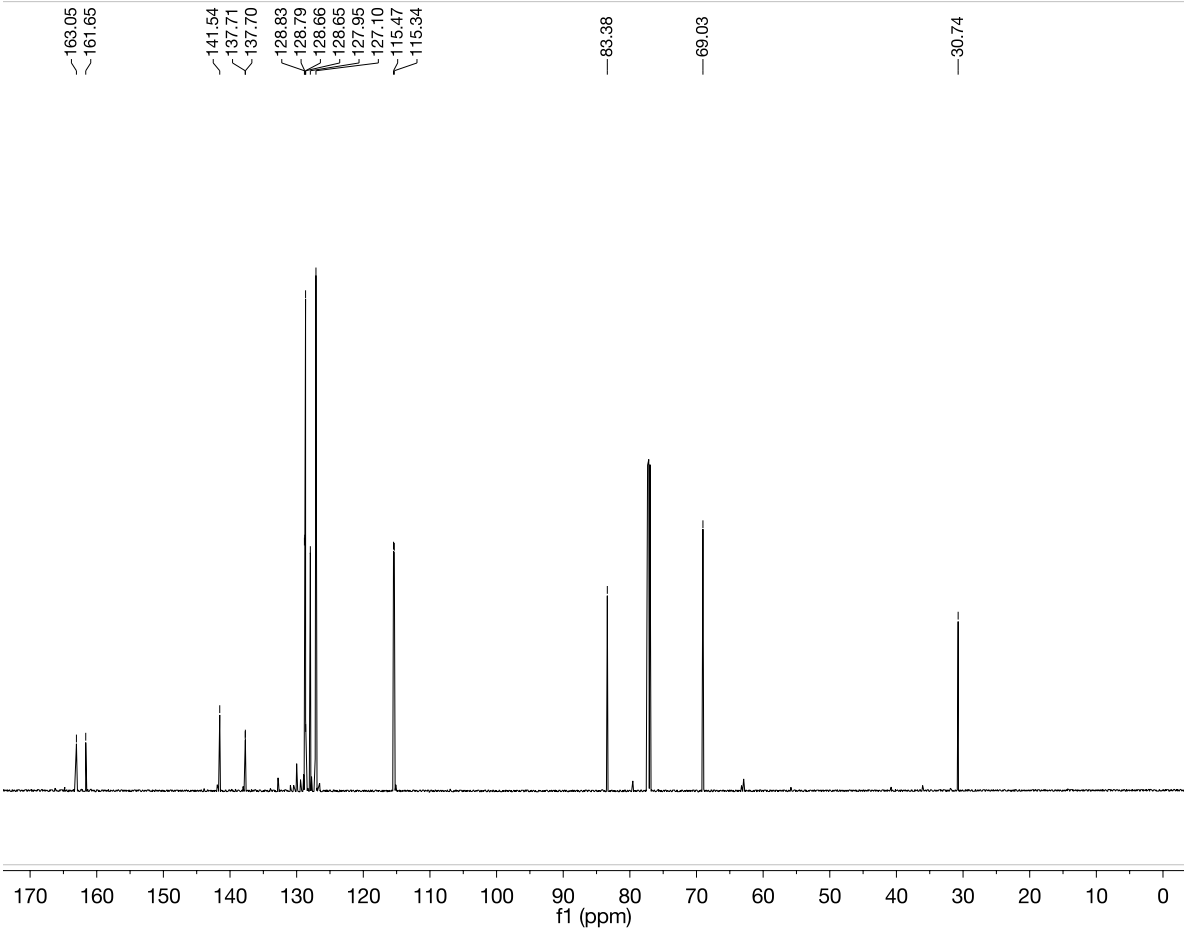
163.05
161.65
141.54
137.71
137.70
128.83
128.79
128.66
128.65
127.95
127.10
115.47
115.34
83.38
69.03
30.74
170
160
150
140
130
120
110
100
90
80
70
60
50
40
30
20
10
0
f1 (ppm)

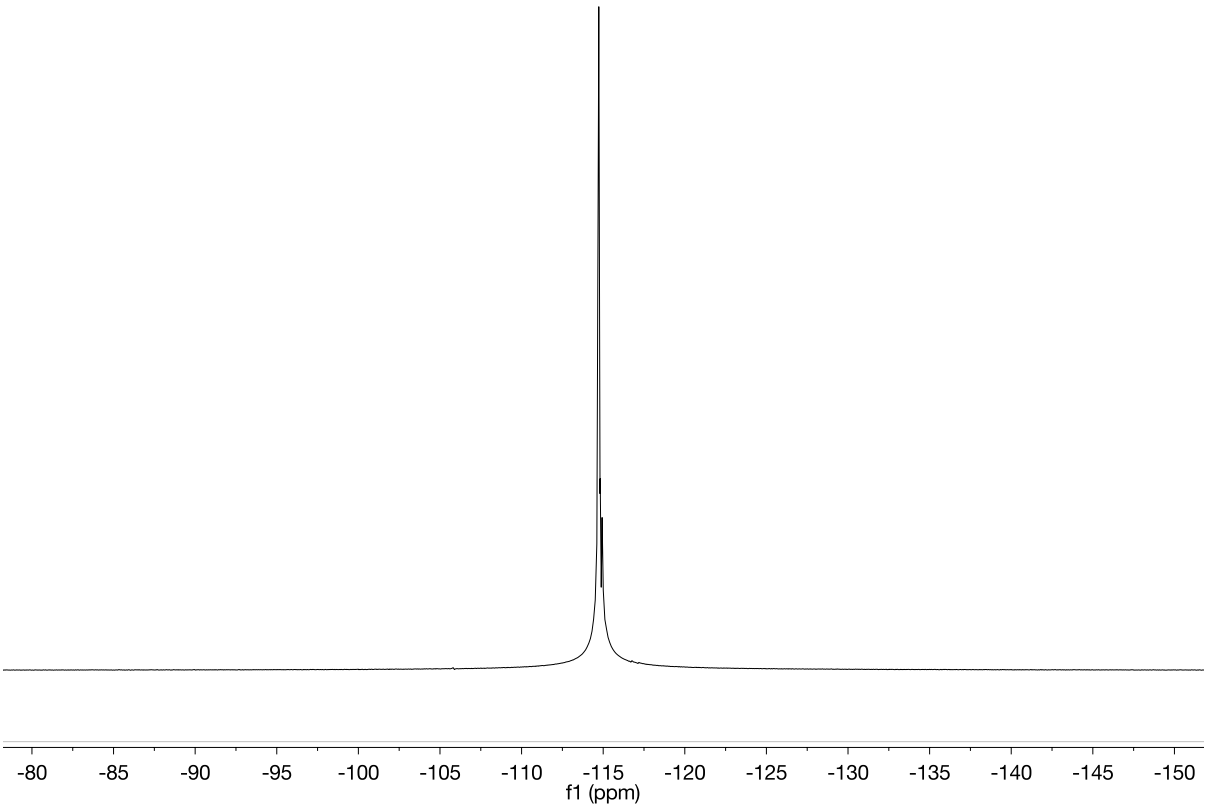
-80
-85
-90
-95
-100
-105
-110
-115
-120
-125
-130
-135
-140
-145
-150
f1 (ppm)

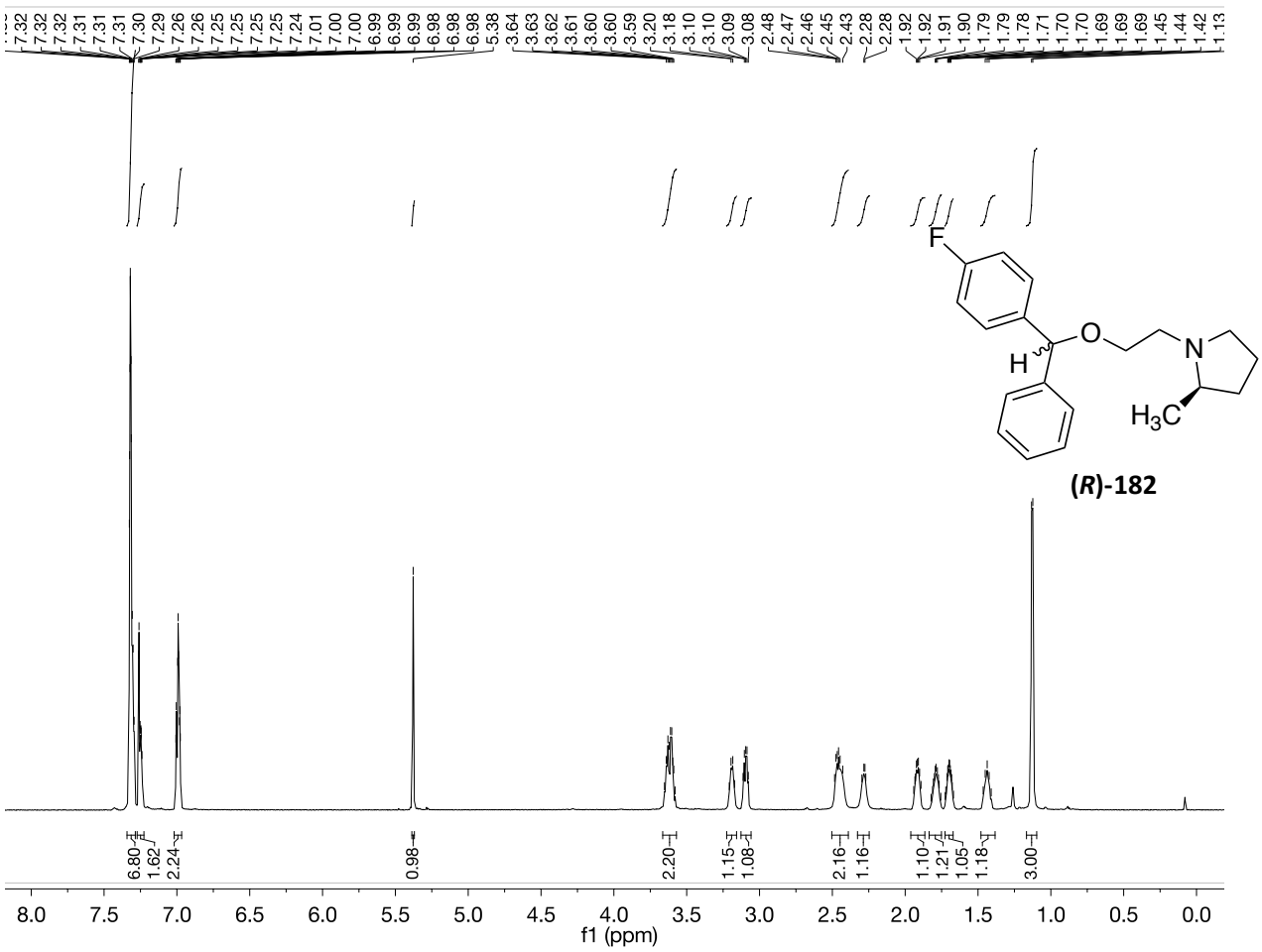

(*R*)-182

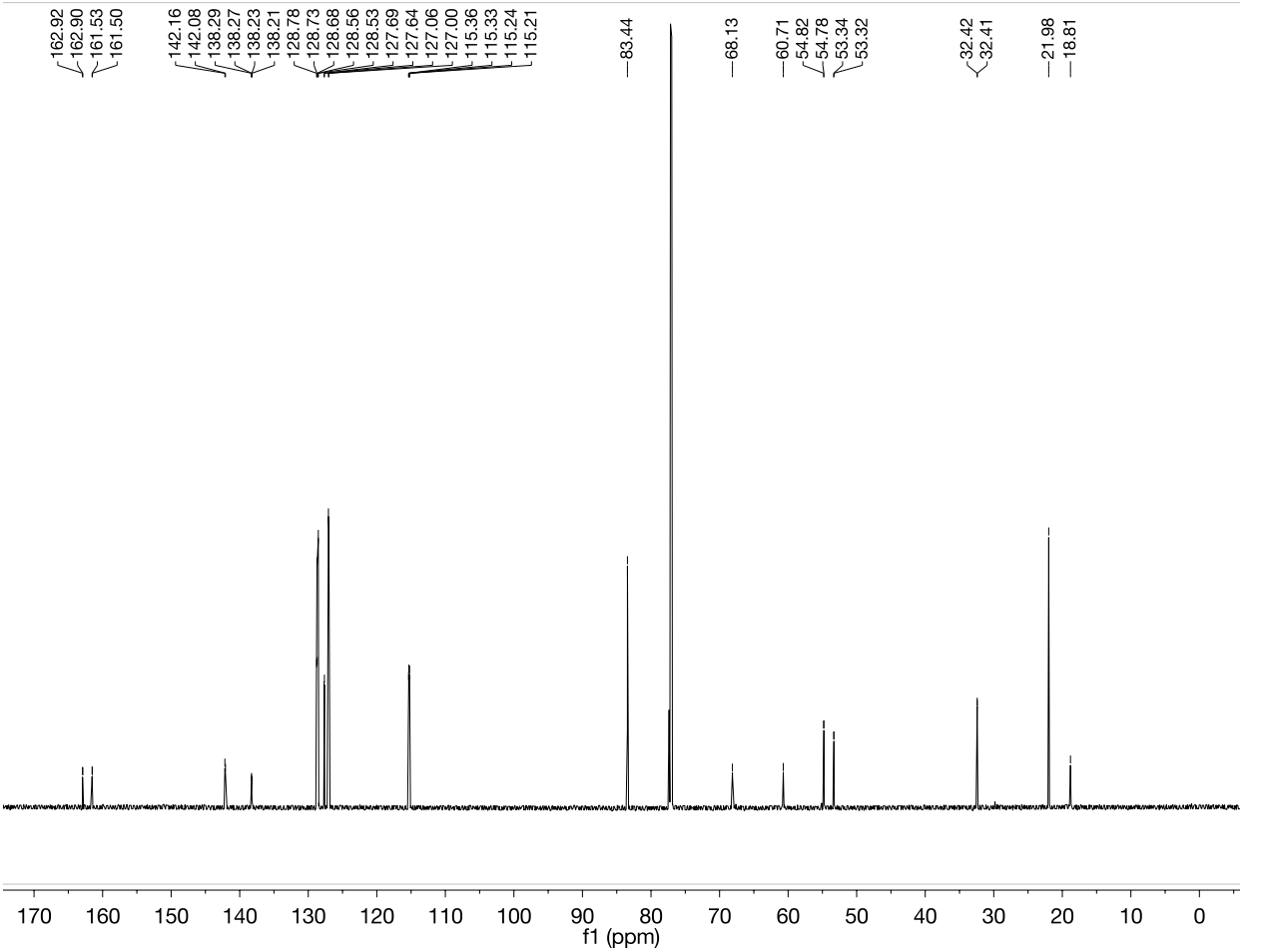

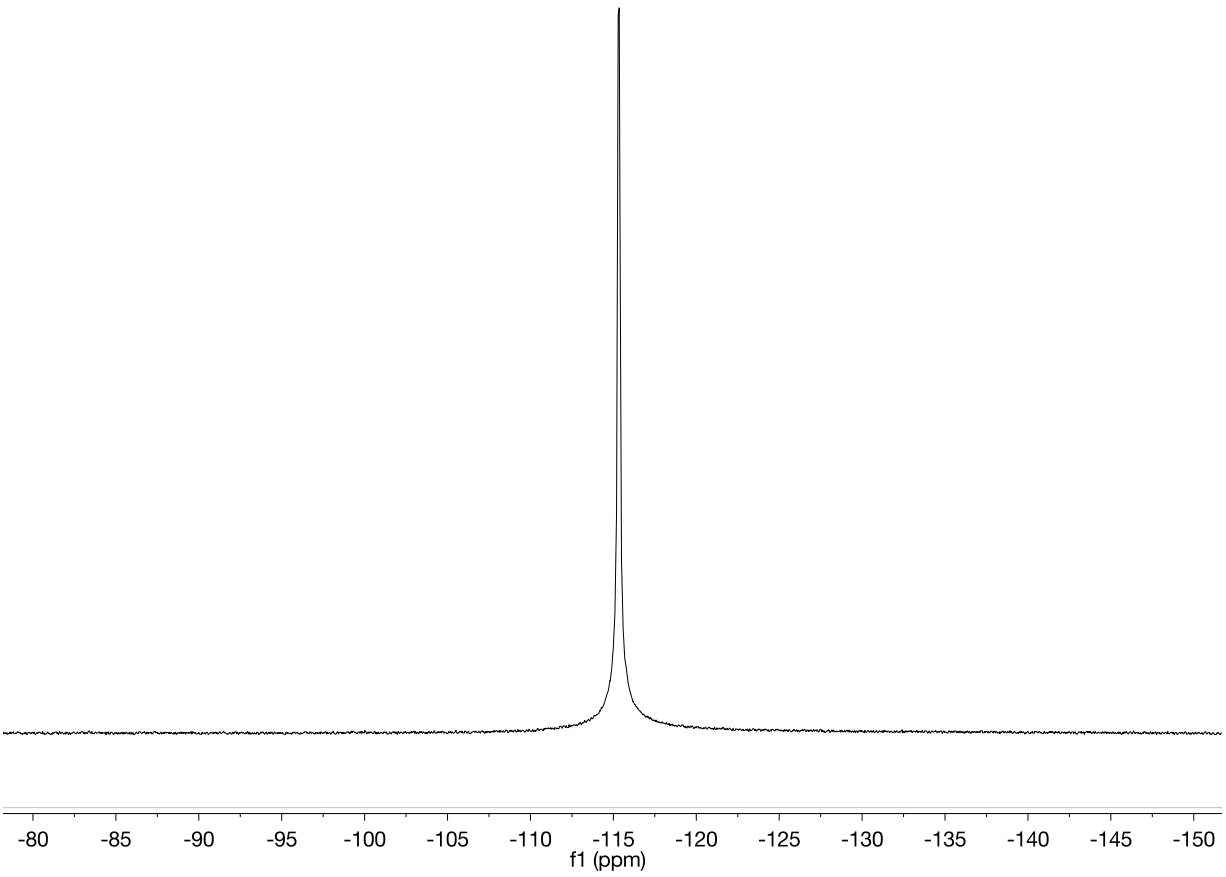
-80
-85
-90
-95
-100
-105
-110
-115
-120
-125
-130
-135
-140
-145
-150
f1 (ppm)

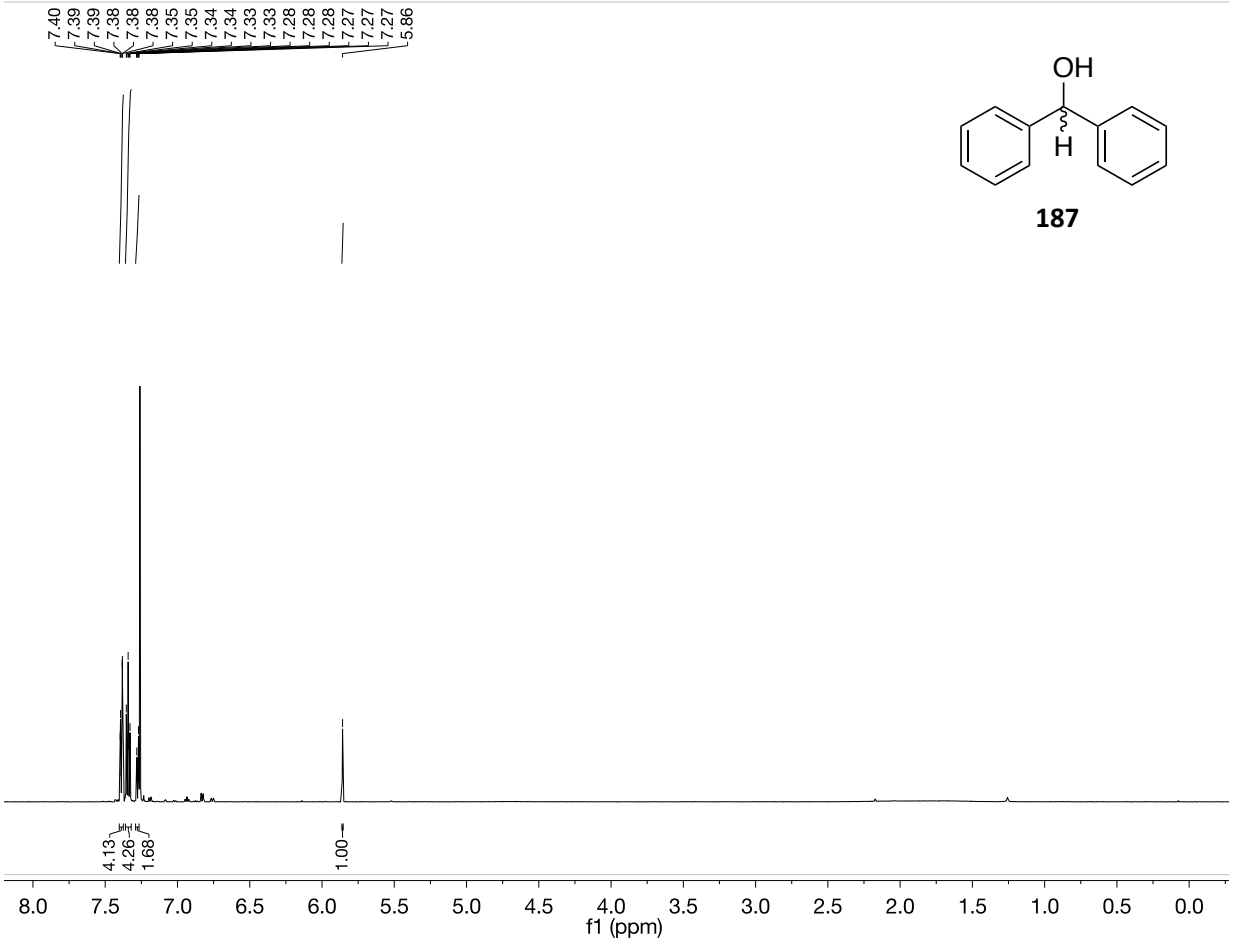
7.40
7.39
7.39
7.38
7.38
7.38
7.35
7.35
7.34
7.34
7.33
7.33
7.28
7.28
7.28
7.27
7.27
7.27
5.86
OH
H
4.13
4.26
1.68
1.00
8.0
7.5
7.0
6.5
6.0
5.5
5.0
4.5
4.0
3.5
3.0
2.5
2.0
1.5
1.0
0.5
0.0
f1 (ppm)

187

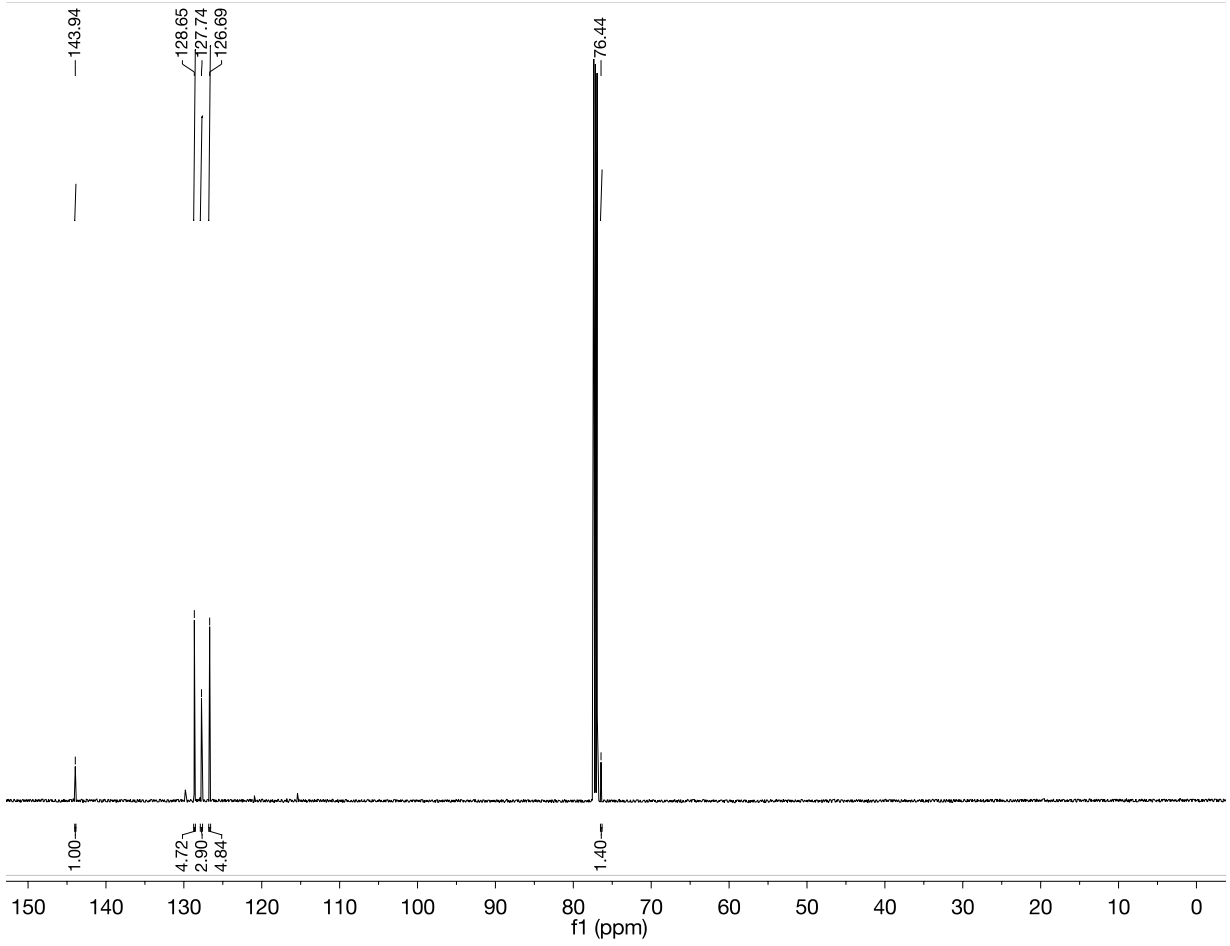
143.94
128.65
127.74
126.69
76.44
1.00
4.72
2.90
4.84
1.40
150
140
130
120
110
100
90
80
70
60
50
40
30
20
10
0
f1 (ppm)

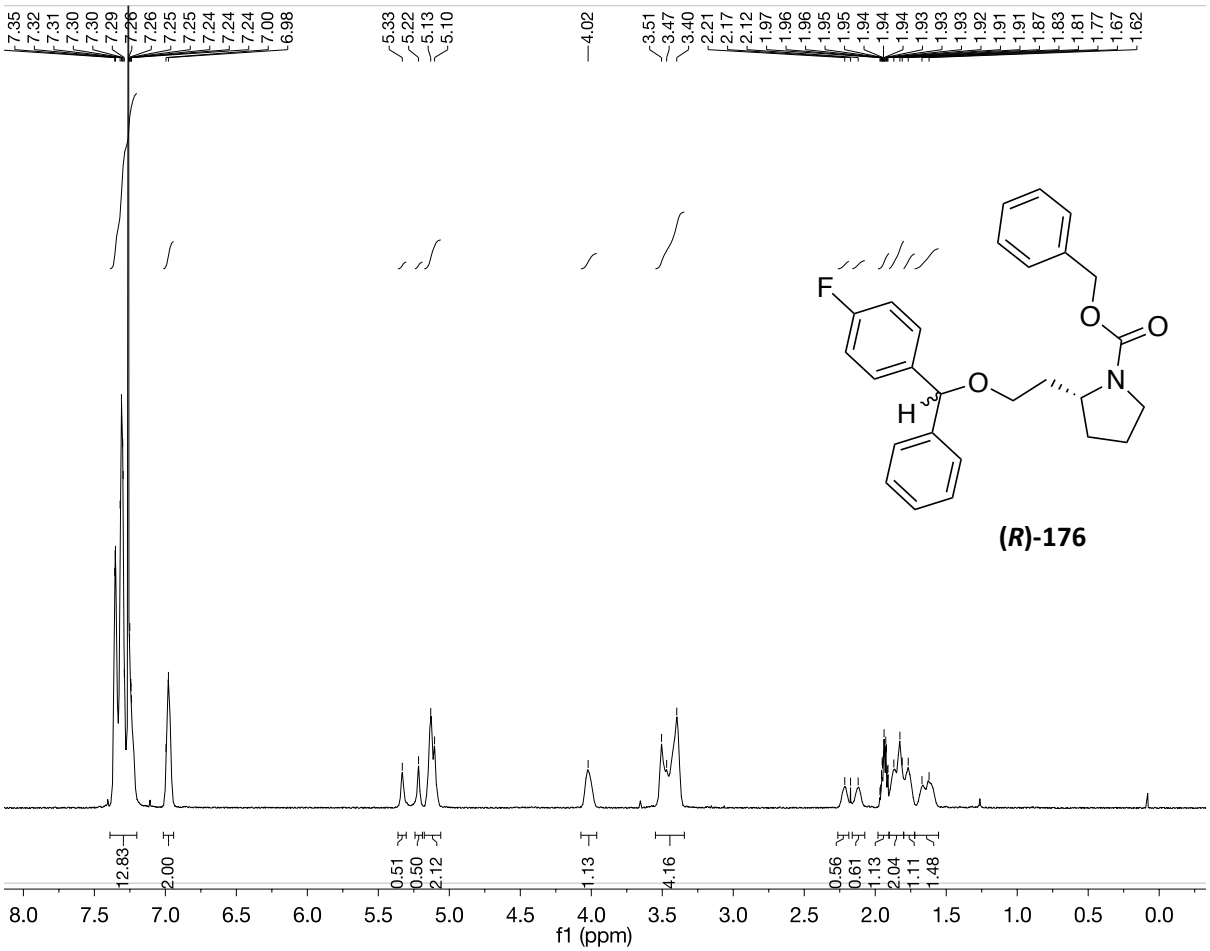
7.35 7.32 7.31 7.30 7.30 7.29 7.26 7.26 7.25 7.25 7.24 7.24 7.24 7.00 6.98
5.33 5.22 5.13 5.10
4.02
3.51 3.47 3.40
2.21 2.17 2.12 1.97 1.96 1.96 1.95 1.95 1.94 1.94 1.94 1.93 1.93 1.92 1.91 1.91 1.87 1.83 1.81 1.77 1.67 1.62
F
O
O
N
O
H
12.83
2.00
0.51
0.50
2.12
1.13
4.16
0.56
0.61
1.13
2.04
1.11
1.48
8.0 7.5 7.0 6.5 6.0 5.5 5.0 4.5 4.0 3.5 3.0 2.5 2.0 1.5 1.0 0.5 0.0
f1 (ppm)

(*R*)-176

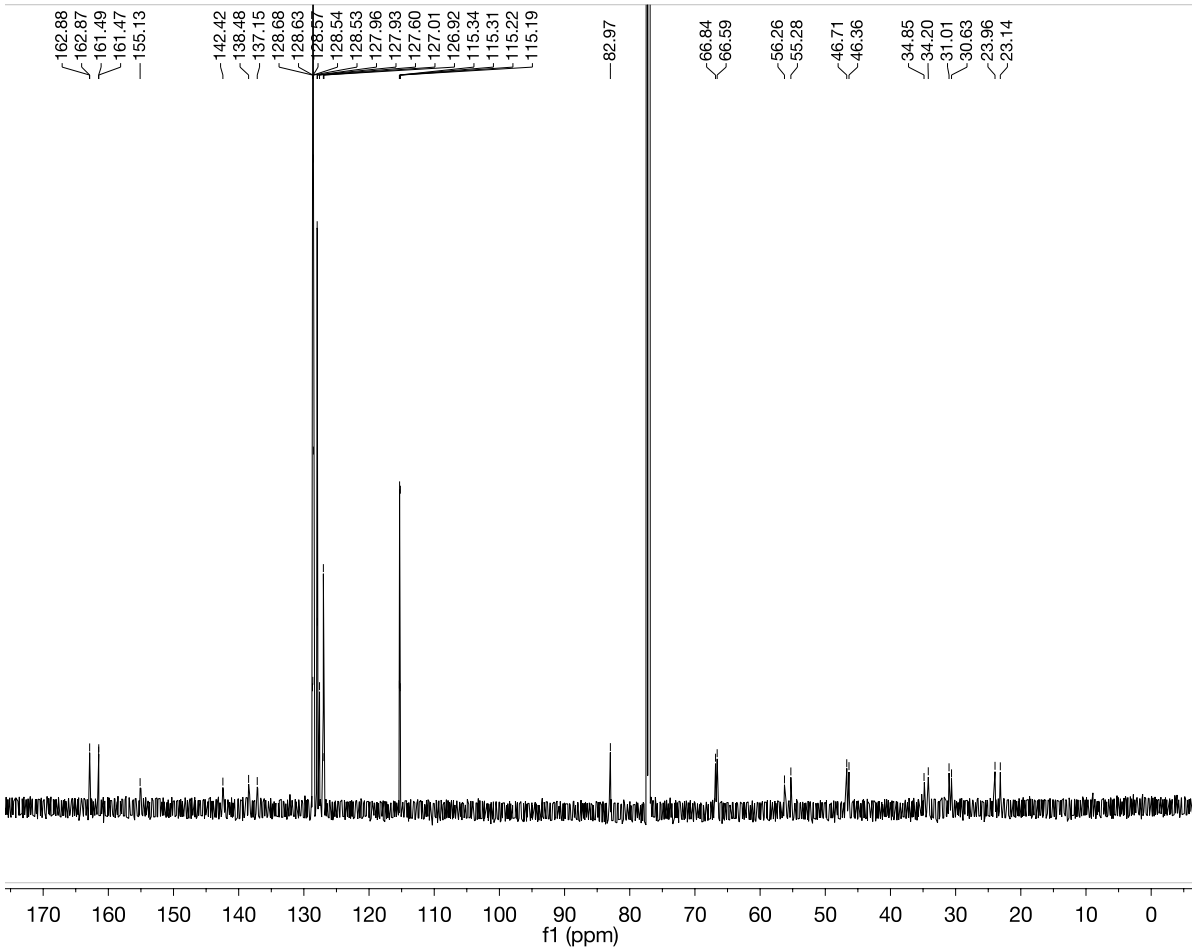
162.88 162.87 161.49 161.47 155.13
142.42 138.48 137.15 128.68 128.63 128.57 128.54 128.53 127.96 127.93 127.60 127.01 126.92 115.34 115.31 115.22 115.19
82.97
66.84 66.59
56.26 55.28
46.71 46.36
34.85 34.20 31.01 30.63
23.96 23.14
170 160 150 140 130 120 110 100 90 80 70 60 50 40 30 20 10 0
f1 (ppm)

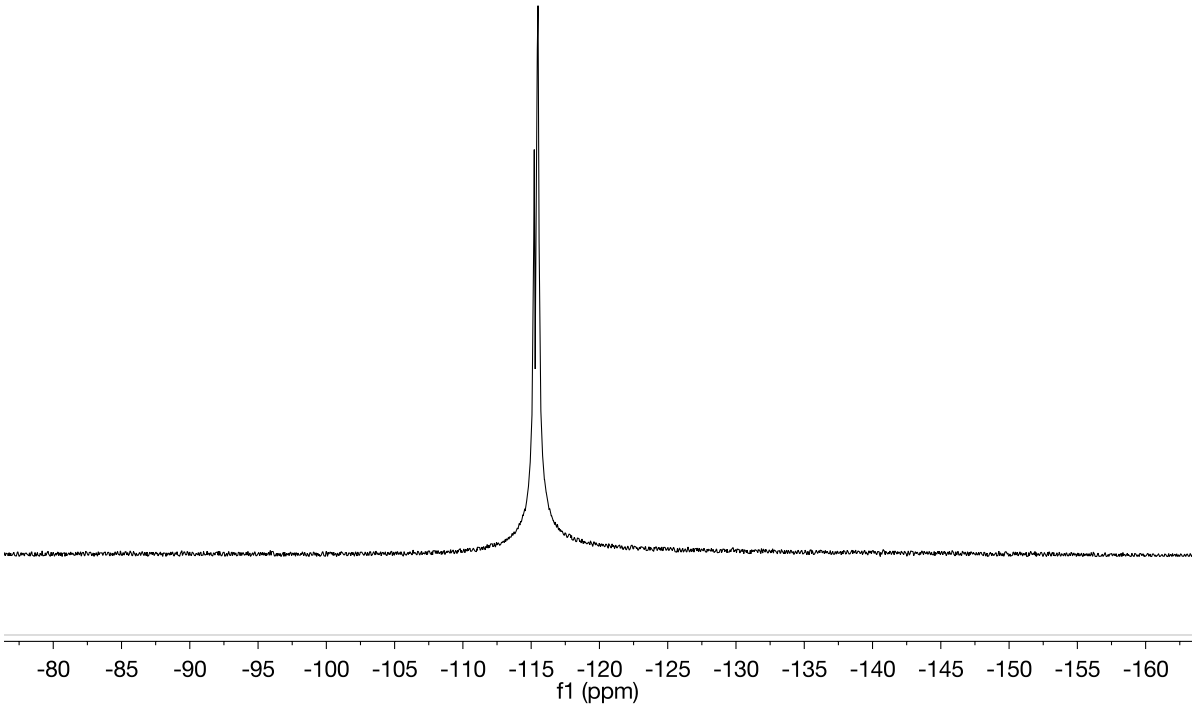
-80 -85 -90 -95 -100 -105 -110 -115 -120 -125 -130 -135 -140 -145 -150 -155 -160
f1 (ppm)

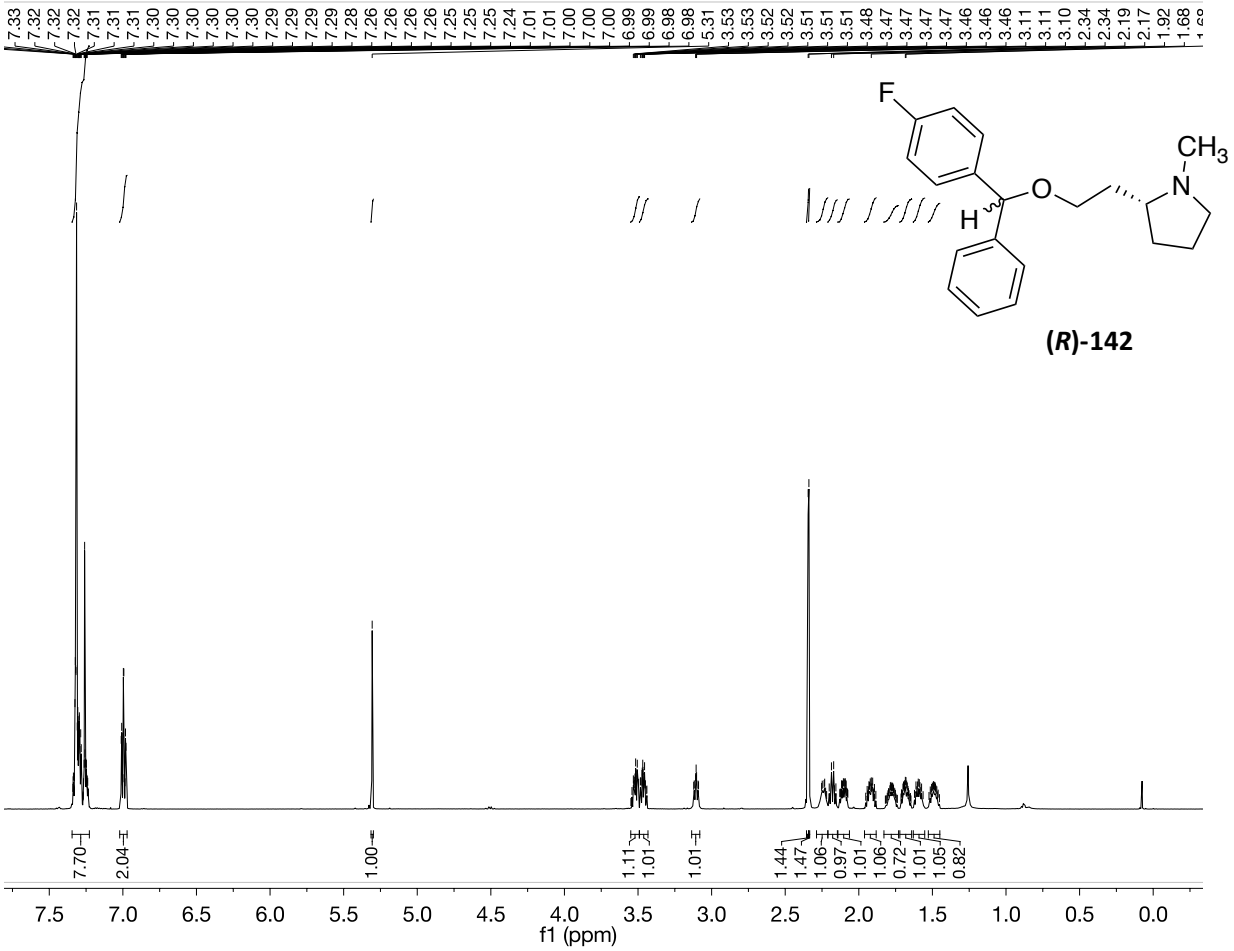
F
CH3
N
O
H
(R)-142
f1 (ppm)

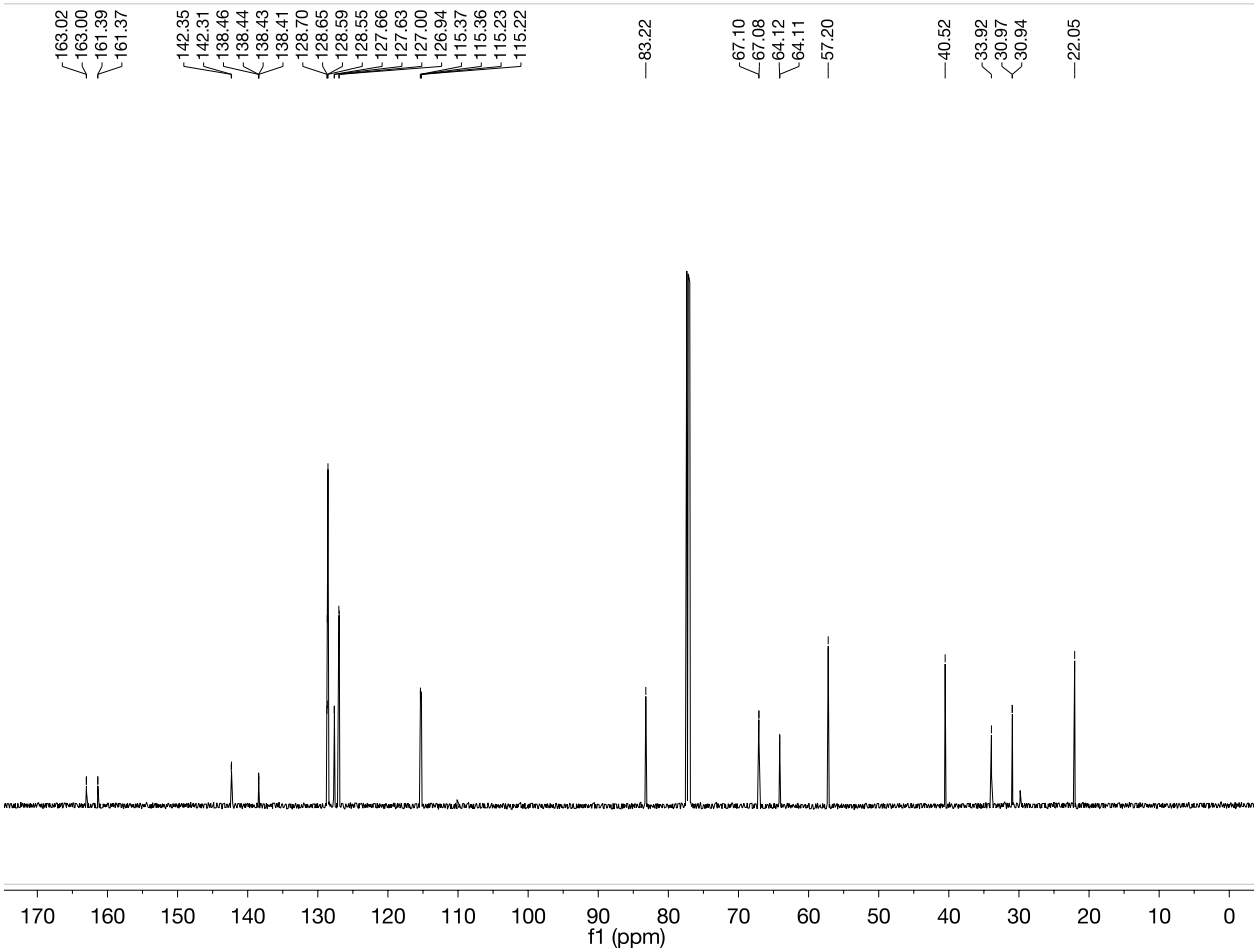
f1 (ppm)

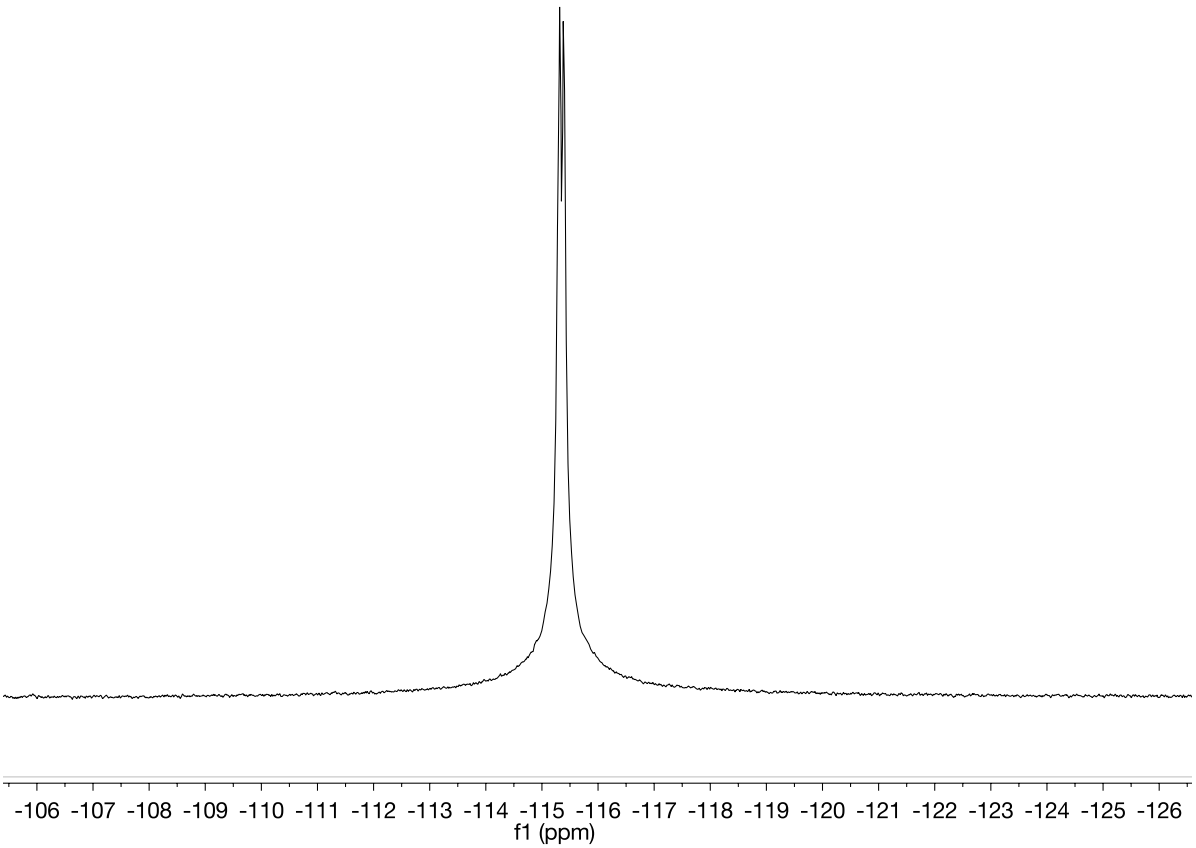
-106 -107 -108 -109 -110 -111 -112 -113 -114 -115 -116 -117 -118 -119 -120 -121 -122 -123 -124 -125 -126
f1 (ppm)

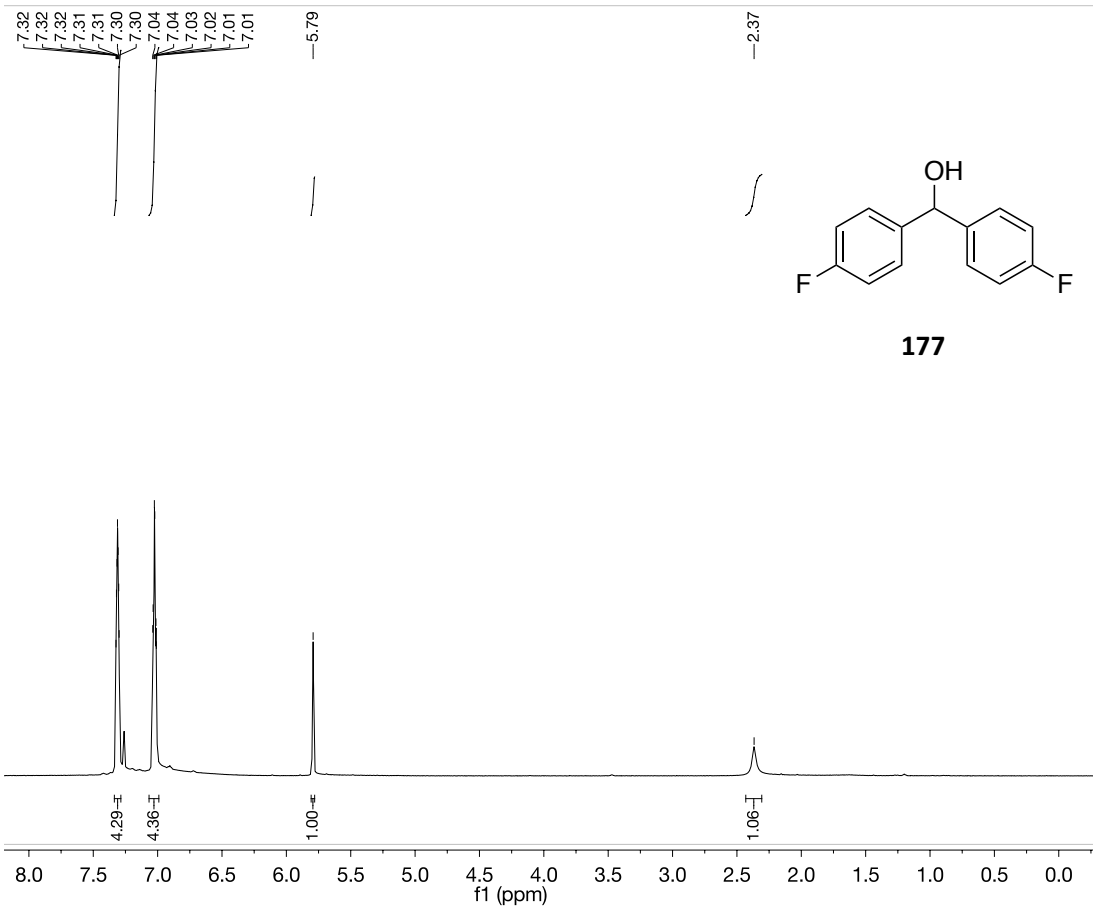
7.32
7.32
7.32
7.31
7.31
7.30
7.30
7.04
7.04
7.03
7.02
7.01
7.01
5.79
2.37
OH
F
F
4.29
4.36
1.00
1.06
8.0
7.5
7.0
6.5
6.0
5.5
5.0
4.5
4.0
3.5
3.0
2.5
2.0
1.5
1.0
0.5
0.0
f1 (ppm)

177

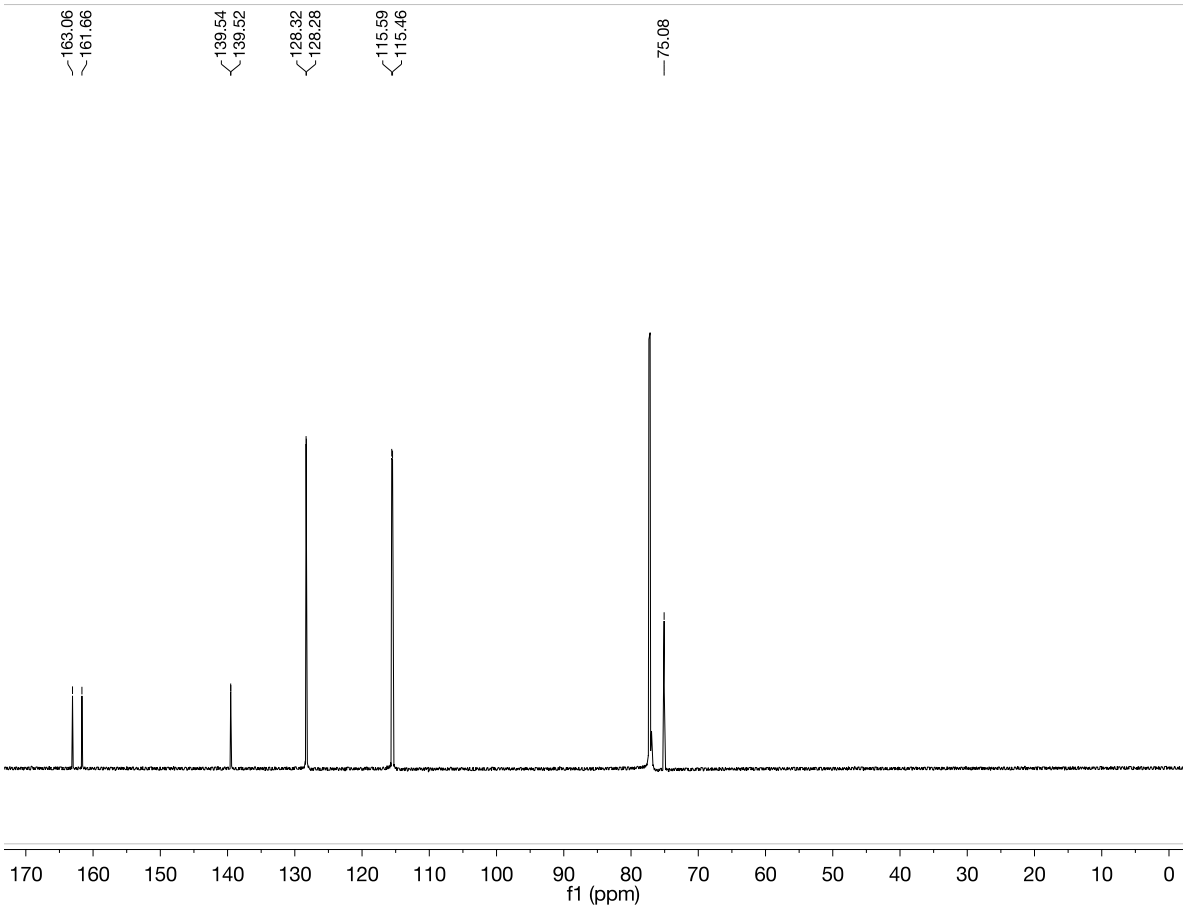
163.06
161.66
139.54
139.52
128.32
128.28
115.59
115.46
75.08
170
160
150
140
130
120
110
100
90
80
70
60
50
40
30
20
10
0
f1 (ppm)

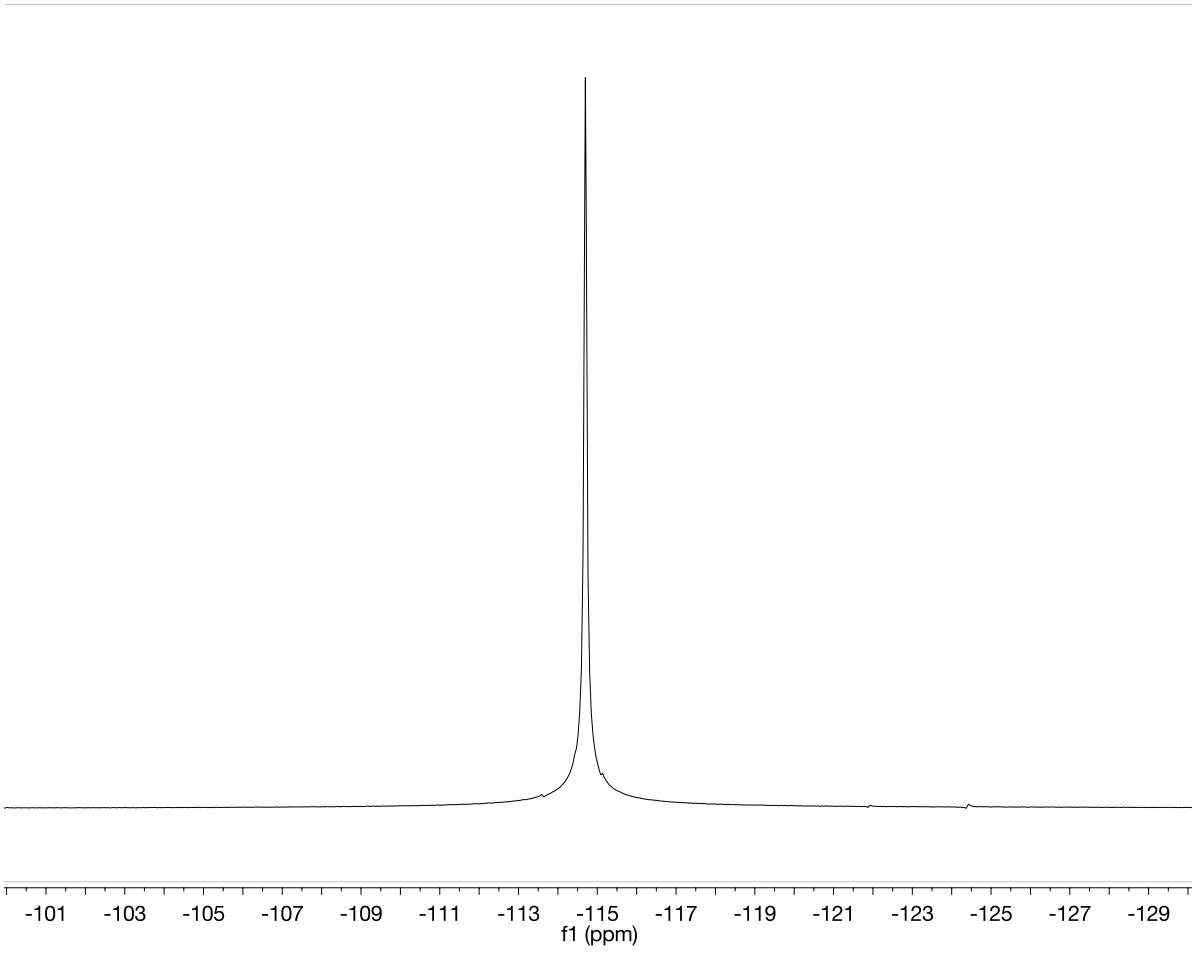
-101
-103
-105
-107
-109
-111
-113
-115
-117
-119
-121
-123
-125
-127
-129
f1 (ppm)

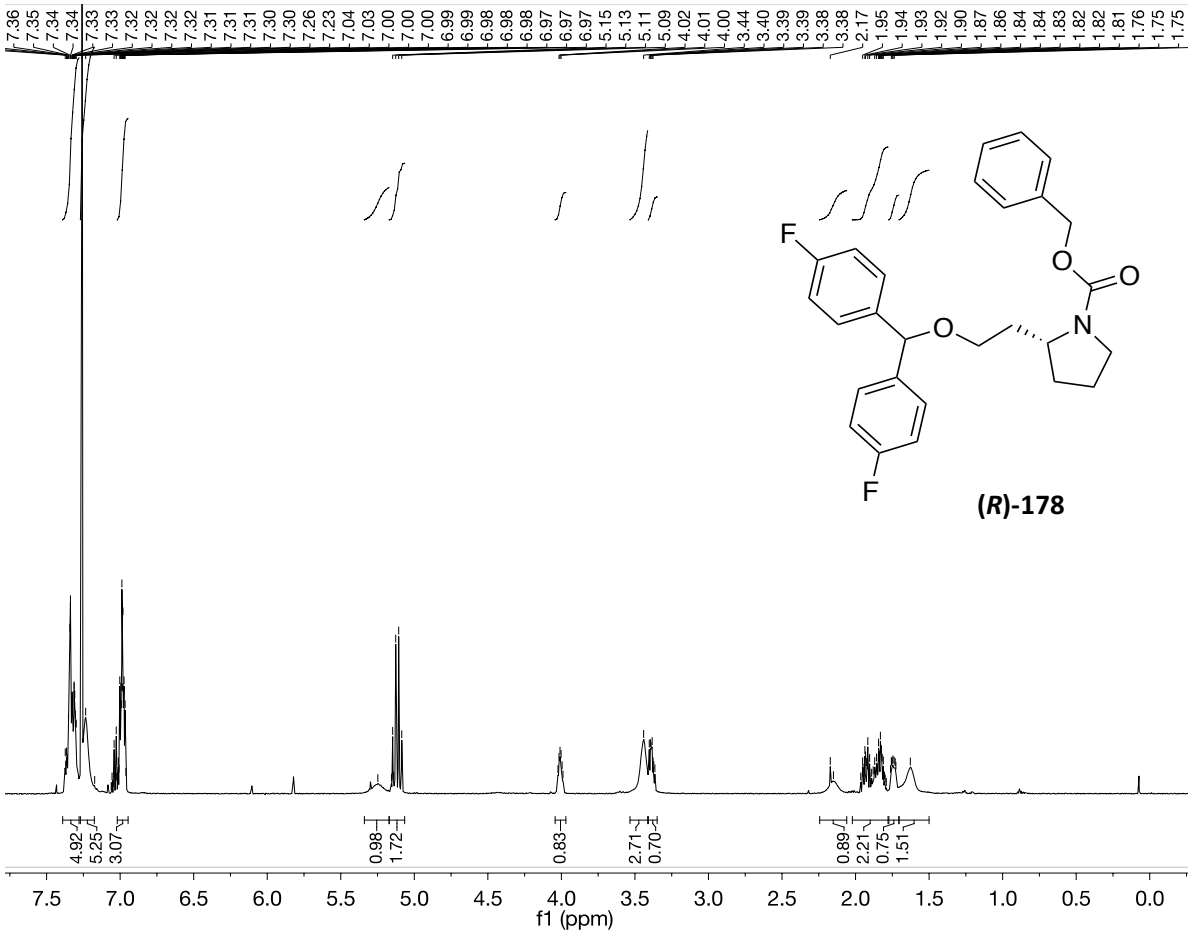
F
O
O
O
N
F
(*R*)-178
f1 (ppm)

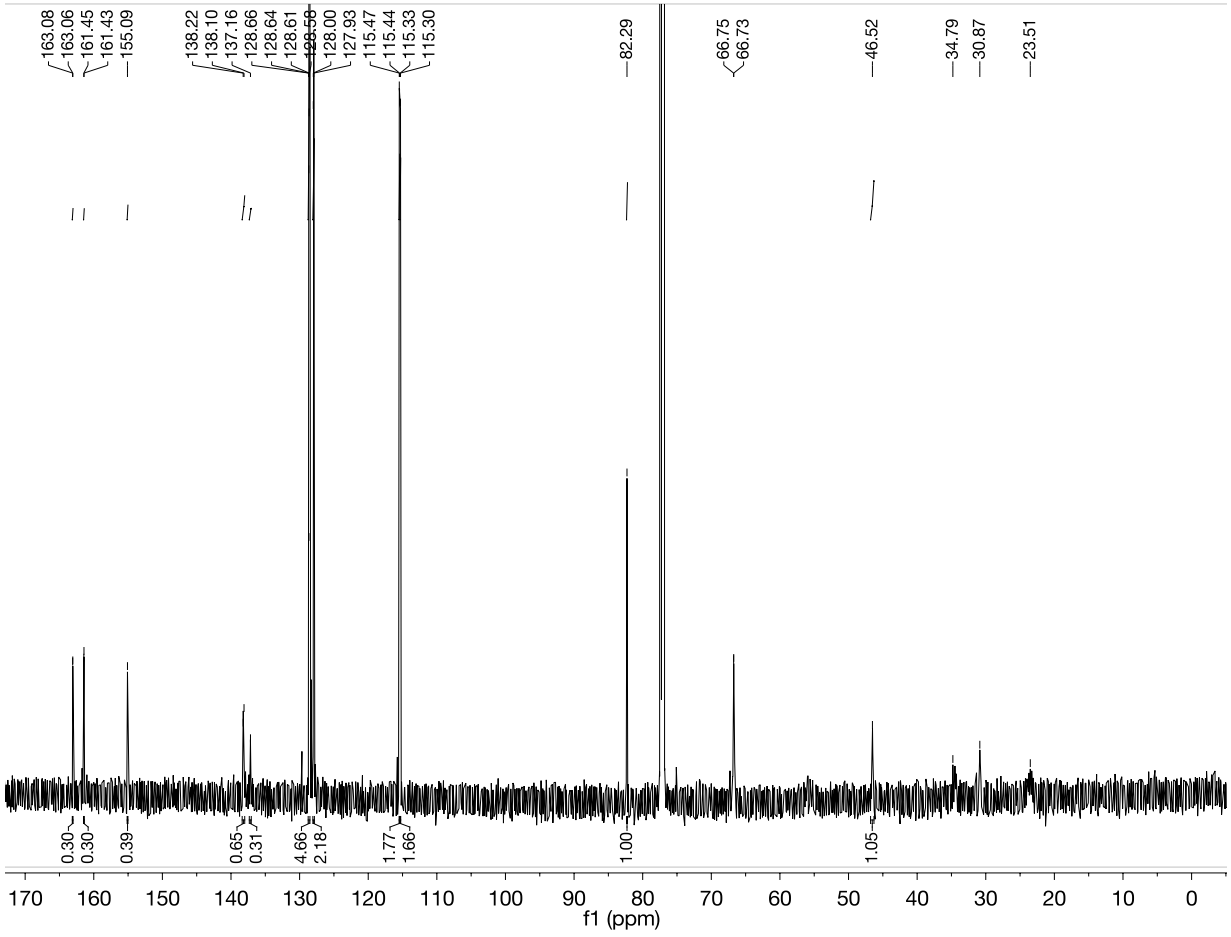
f1 (ppm)

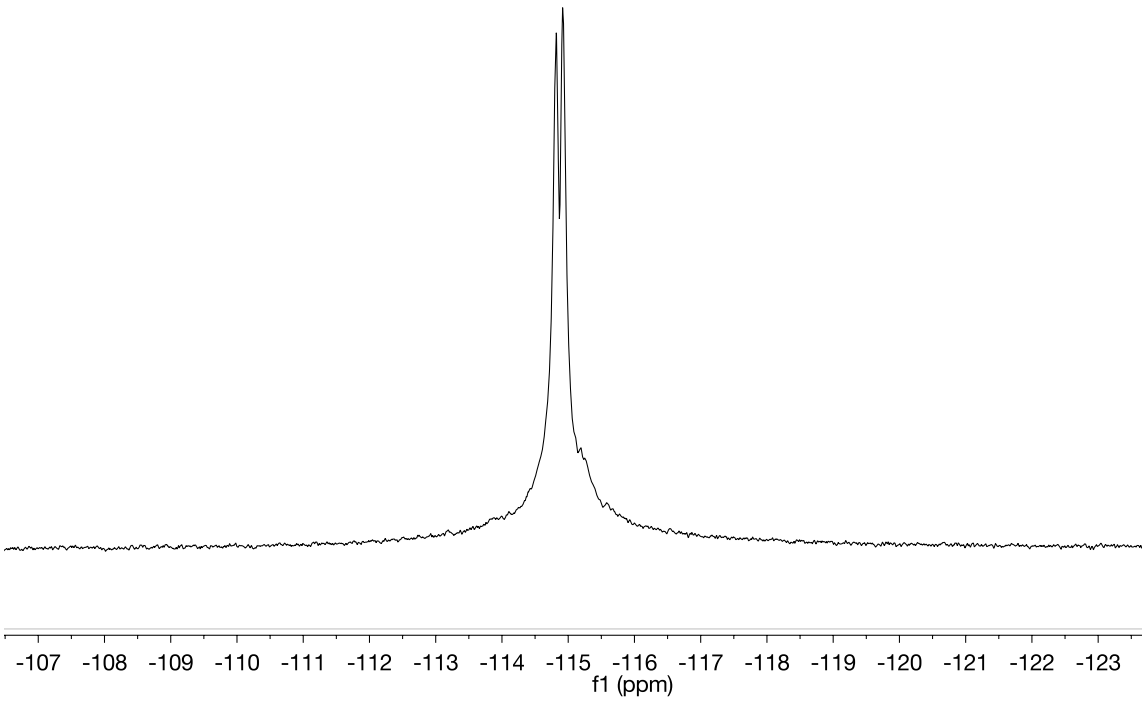
-107 -108 -109 -110 -111 -112 -113 -114 -115 -116 -117 -118 -119 -120 -121 -122 -123
f1 (ppm)

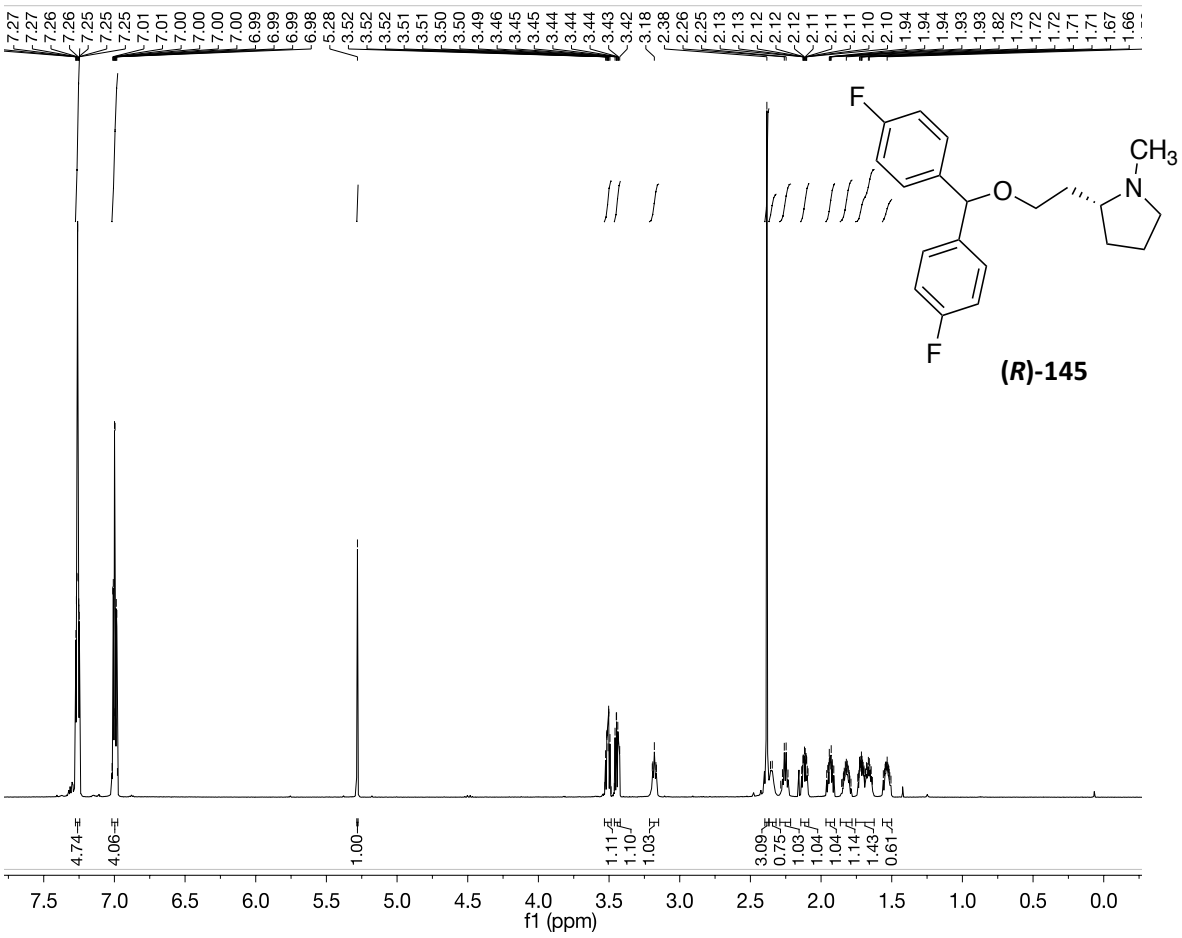
F
CH3
O
N
F
(R)-145
f1 (ppm)

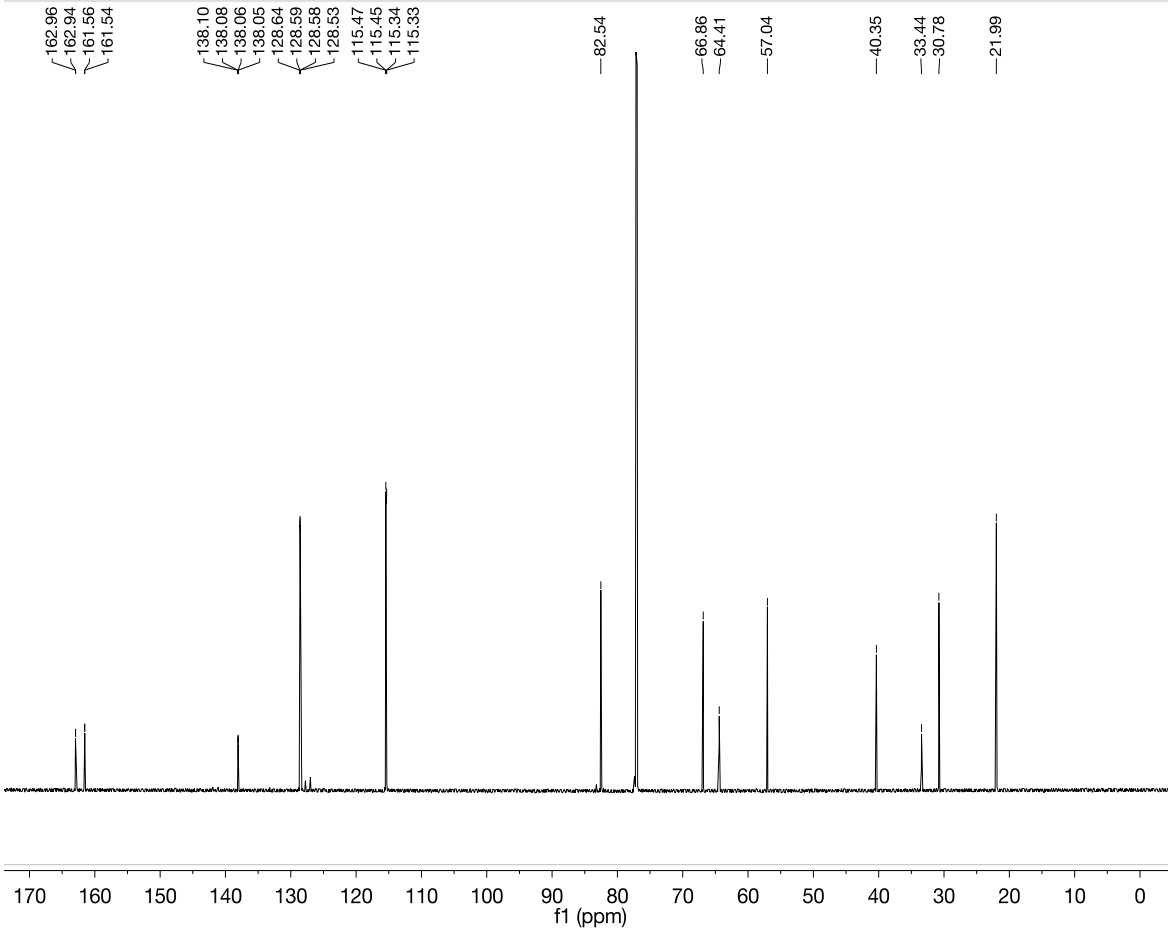
f1 (ppm)

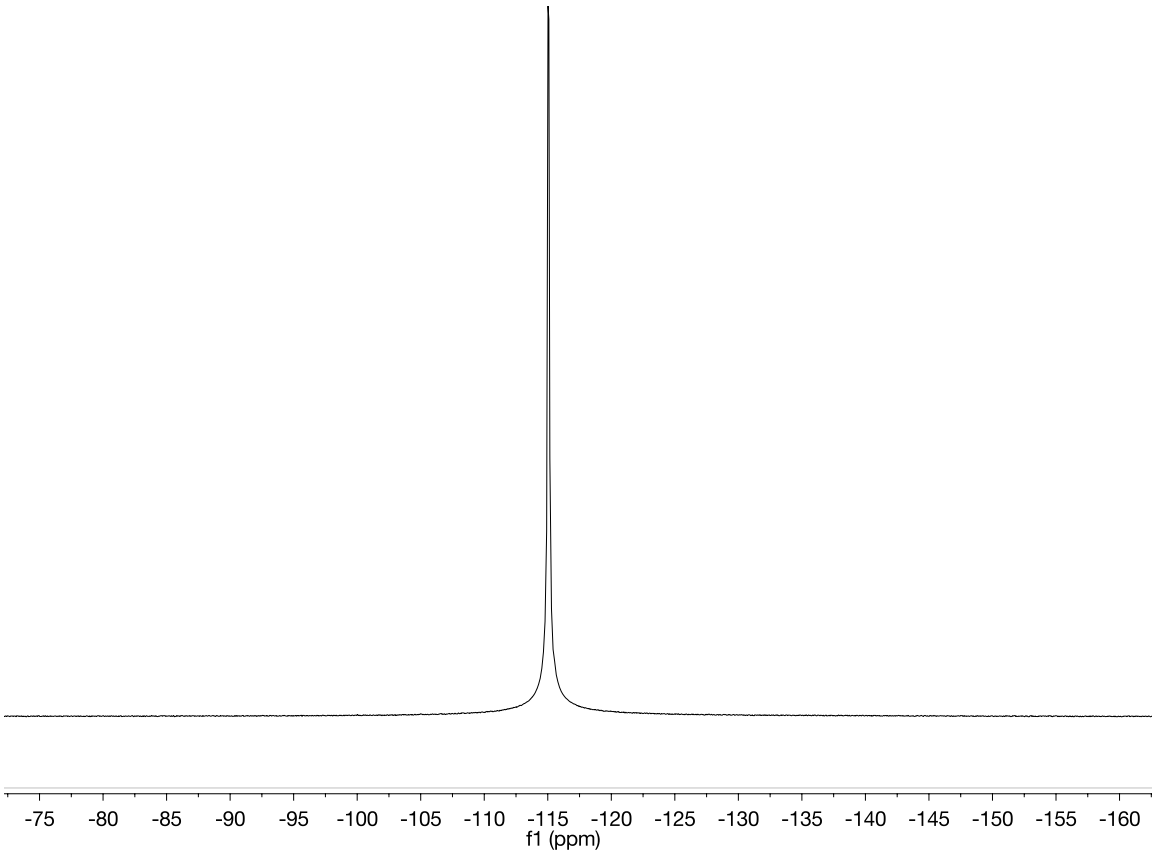
-75
-80
-85
-90
-95
-100
-105
-110
-115
-120
-125
-130
-135
-140
-145
-150
-155
-160
f1 (ppm)

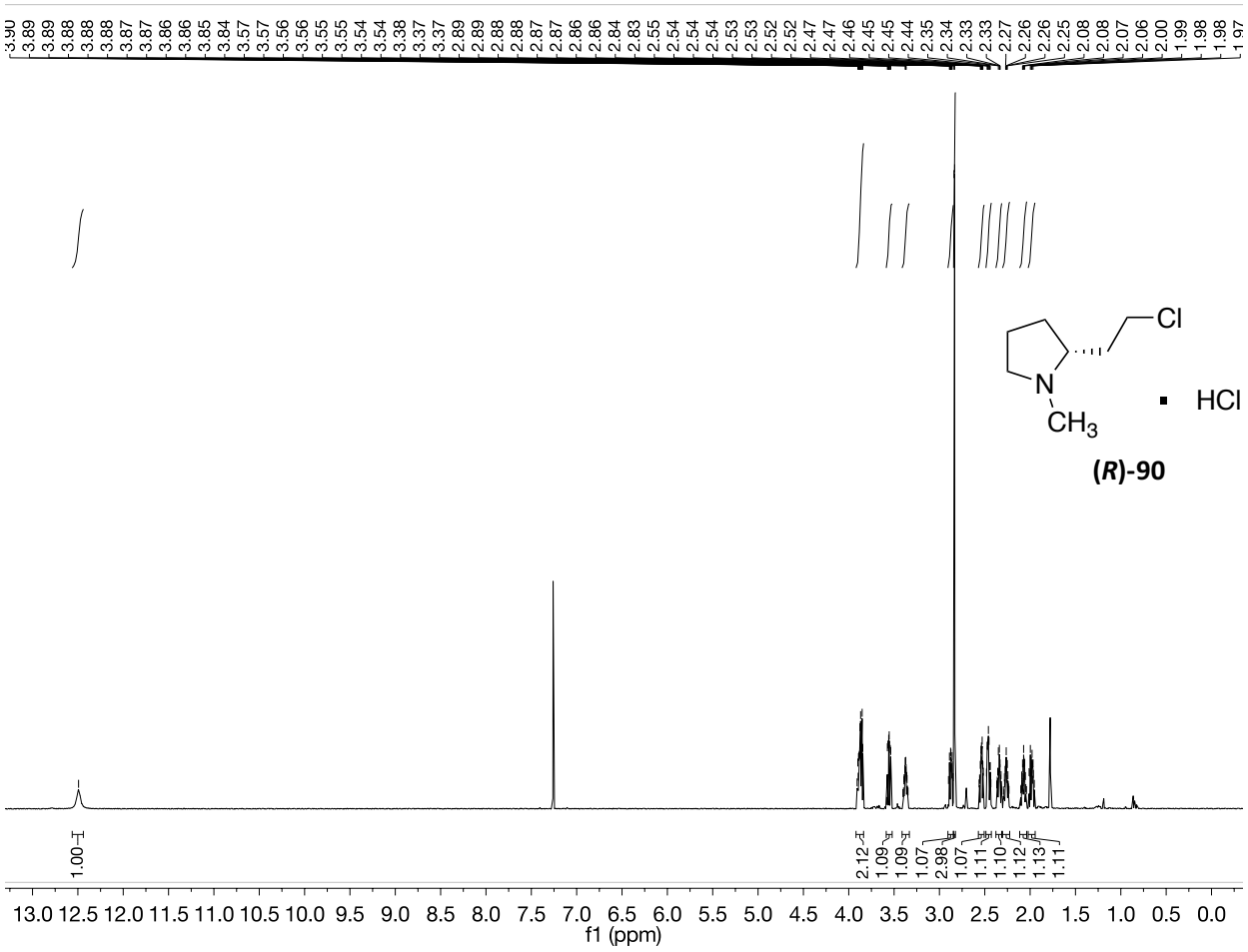
Cl
N
CH3
HCl
(R)-90
1.00
2.12
1.09
1.09
1.07
2.98
1.07
1.11
1.10
1.12
1.13
1.11
13.0 12.5 12.0 11.5 11.0 10.5 10.0 9.5 9.0 8.5 8.0 7.5 7.0 6.5 6.0 5.5 5.0 4.5 4.0 3.5 3.0 2.5 2.0 1.5 1.0 0.5 0.0
f1 (ppm)

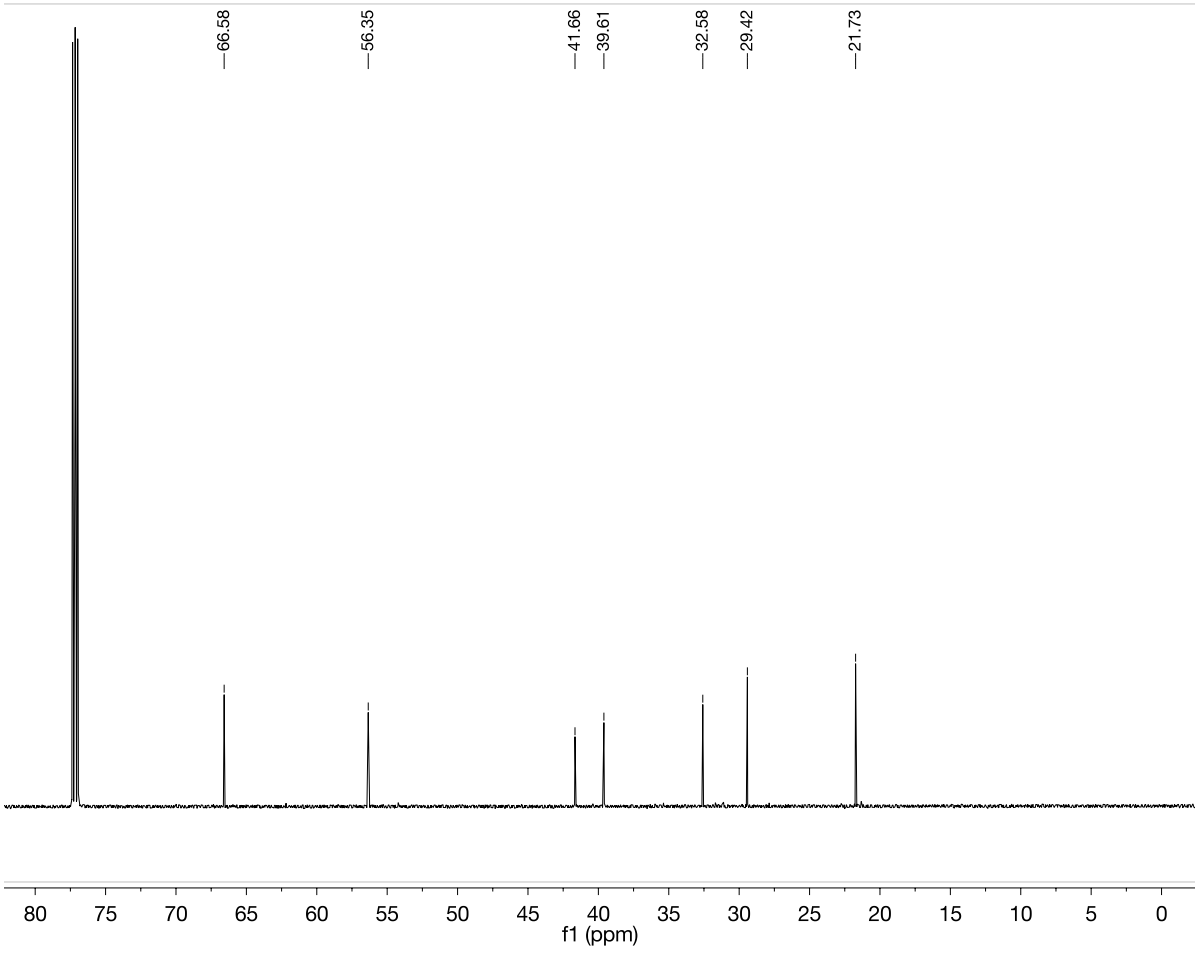
66.58
56.35
41.66
39.61
32.58
29.42
21.73
80 75 70 65 60 55 50 45 40 35 30 25 20 15 10 5 0
f1 (ppm)

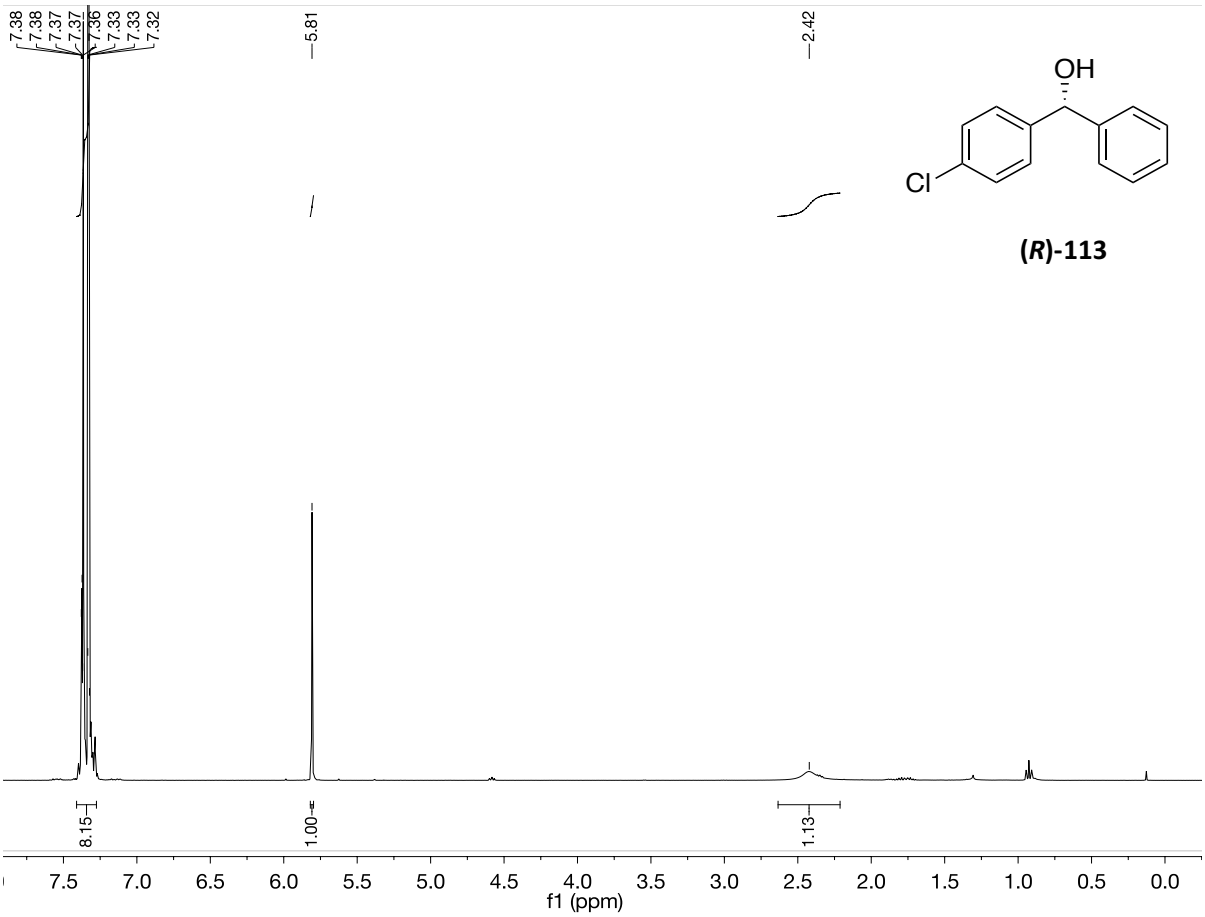
7.38
7.38
7.37
7.37
7.36
7.33
7.33
7.32
5.81
2.42
OH
Cl
8.15
1.00
1.13
7.5
7.0
6.5
6.0
5.5
5.0
4.5
4.0
3.5
3.0
2.5
2.0
1.5
1.0
0.5
0.0
f1 (ppm)

(*R*)-113

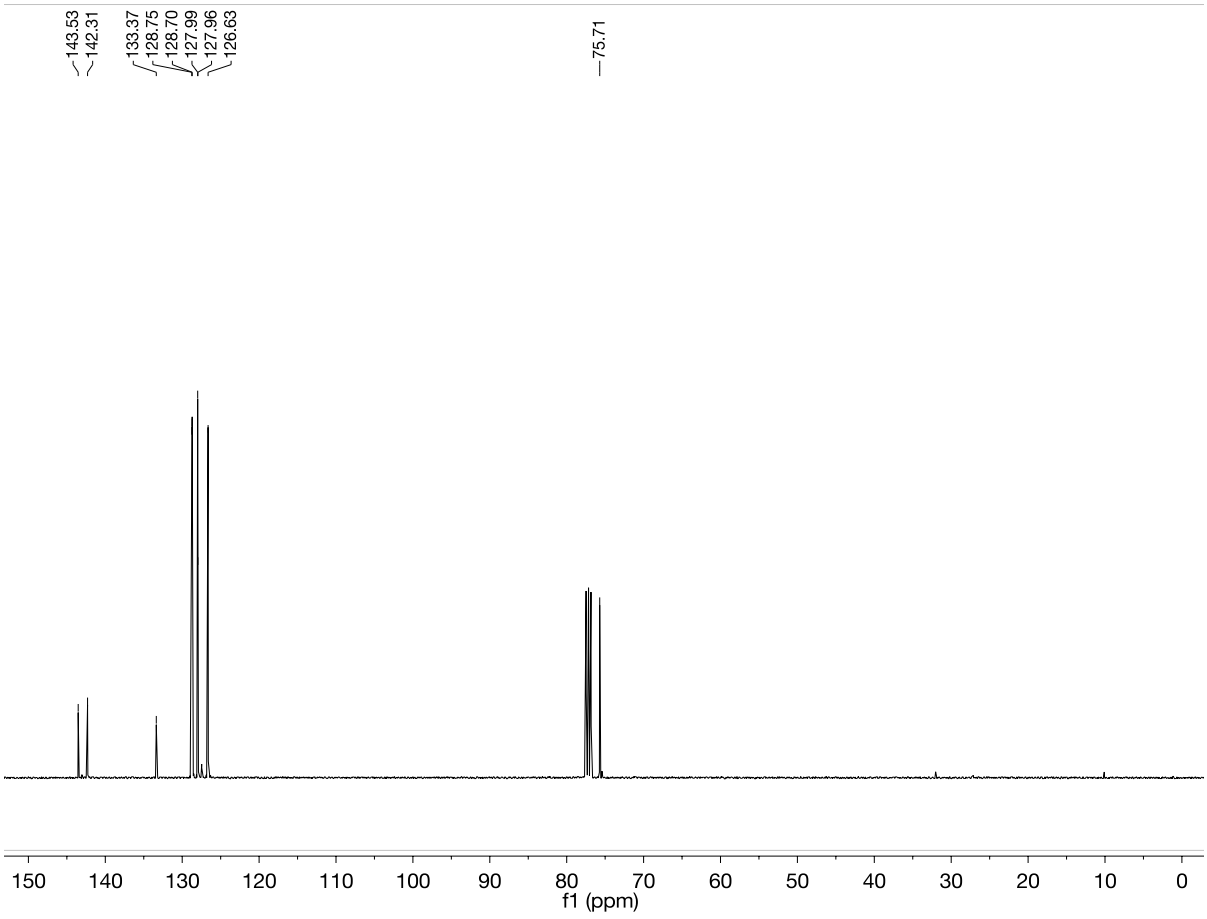
143.53
142.31
133.37
128.75
128.70
127.99
127.96
126.63
75.71
150
140
130
120
110
100
90
80
70
60
50
40
30
20
10
0
f1 (ppm)

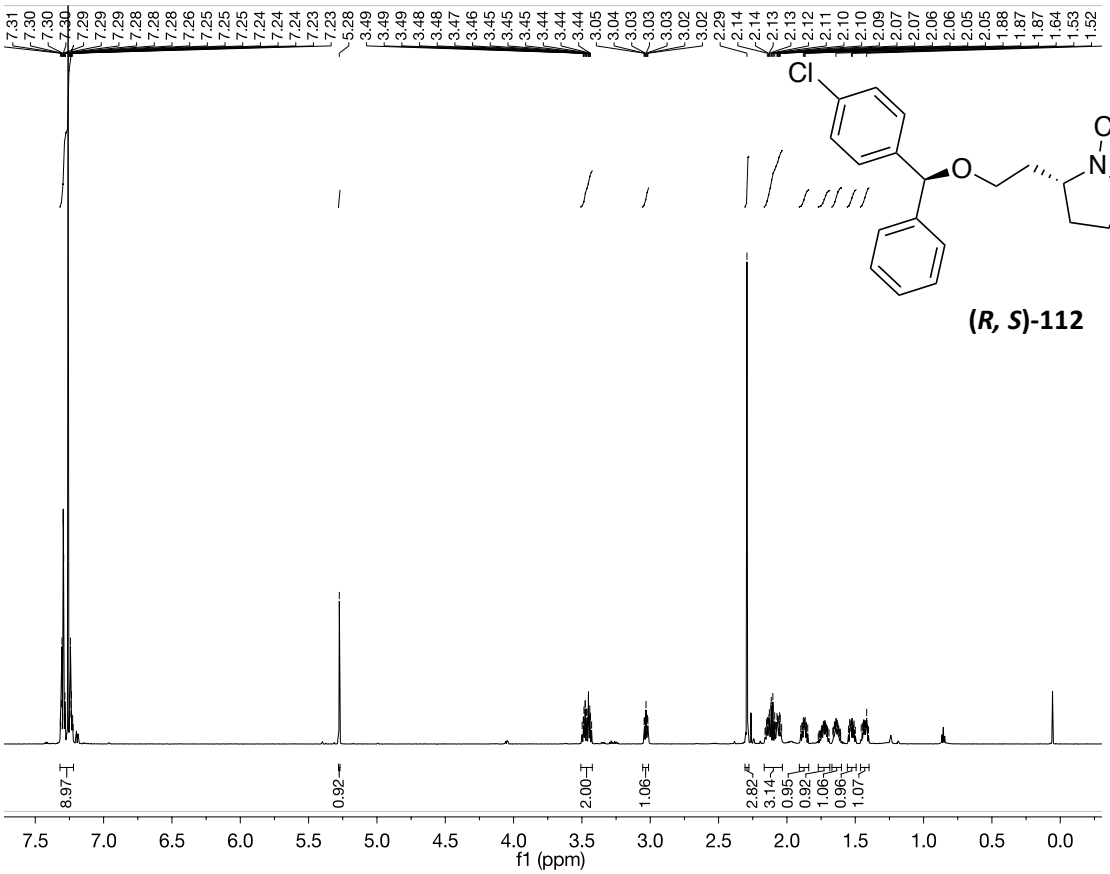
7.31 7.30 7.30 7.30 7.29 7.29 7.29 7.28 7.28 7.28 7.26 7.25 7.25 7.24 7.24 7.24 7.23 7.23 5.28 3.49 3.49 3.49 3.48 3.48 3.47 3.46 3.45 3.45 3.44 3.44 3.44 3.05 3.04 3.03 3.03 3.03 3.02 3.02 2.29 2.14 2.14 2.13 2.13 2.12 2.11 2.10 2.10 2.09 2.07 2.07 2.06 2.06 2.05 2.05 1.88 1.87 1.87 1.64 1.53 1.52
Cl
CH3
N
O
(R, S)-112
8.97 0.92 2.00 1.06 2.82 3.14 0.95 0.92 1.06 0.96 1.07
7.5 7.0 6.5 6.0 5.5 5.0 4.5 4.0 3.5 3.0 2.5 2.0 1.5 1.0 0.5 0.0
f1 (ppm)

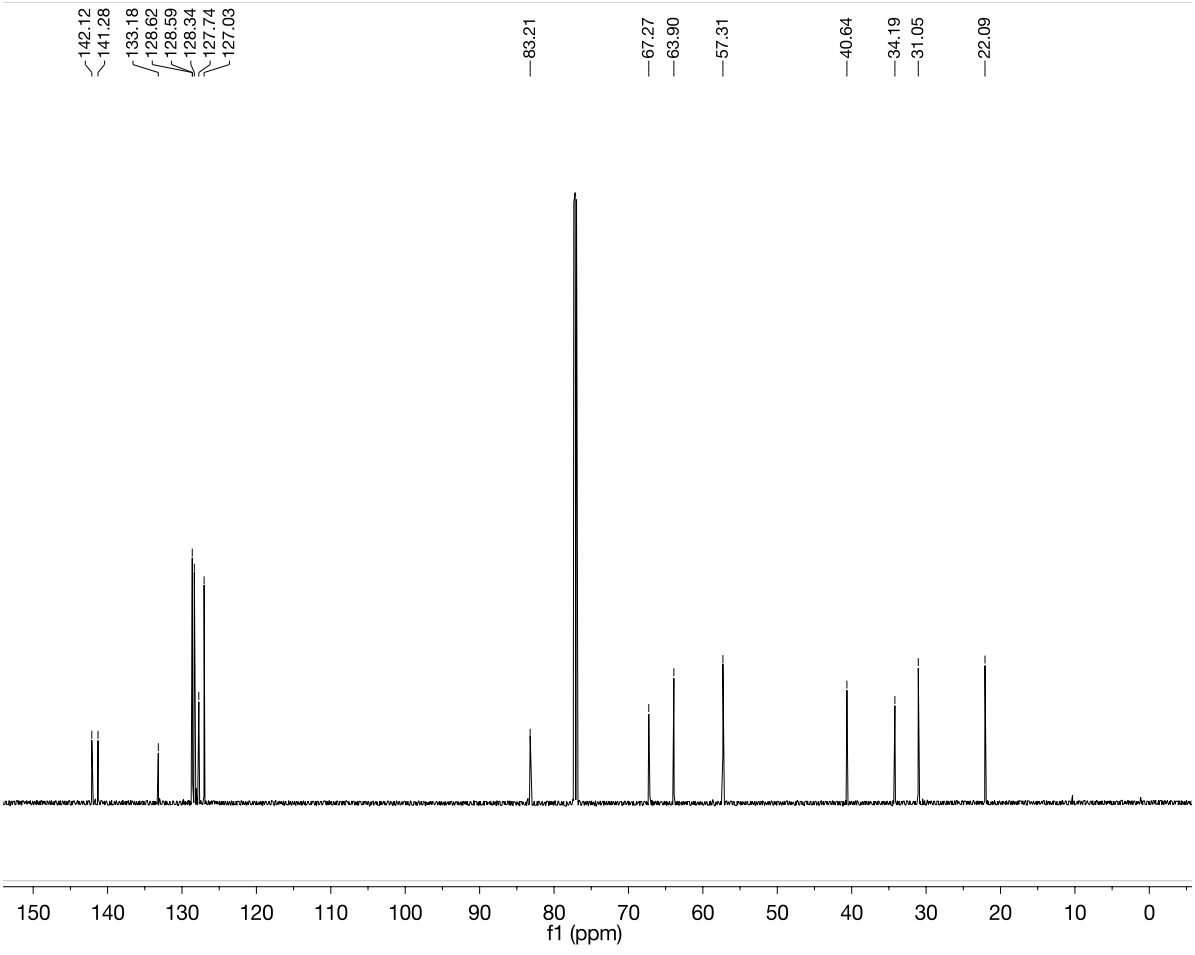
142.12 141.28 133.18 128.62 128.59 128.34 127.74 127.03 83.21 67.27 63.90 57.31 40.64 34.19 31.05 22.09
150 140 130 120 110 100 90 80 70 60 50 40 30 20 10 0
f1 (ppm)

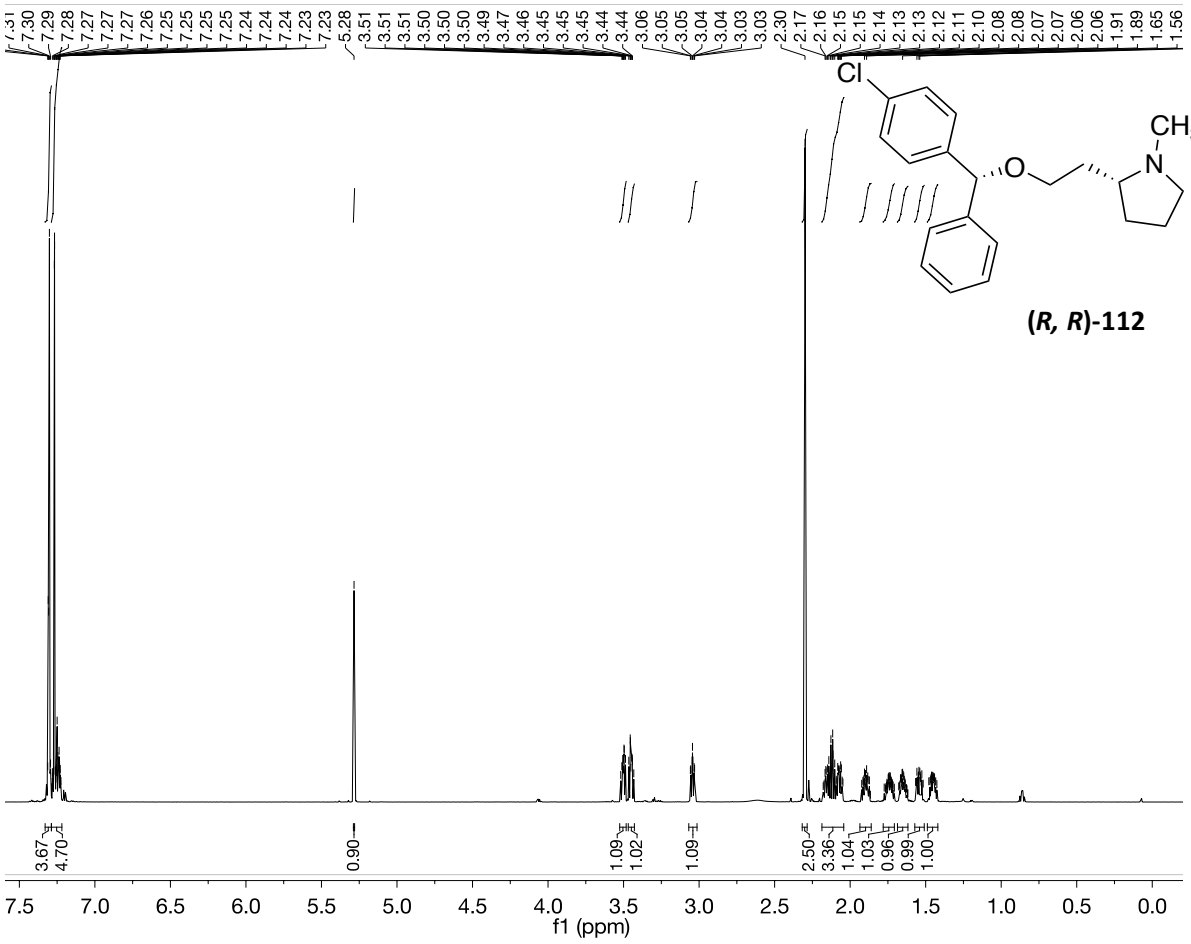
Cl
CH3
O
N
(R, R)-112
f1 (ppm)

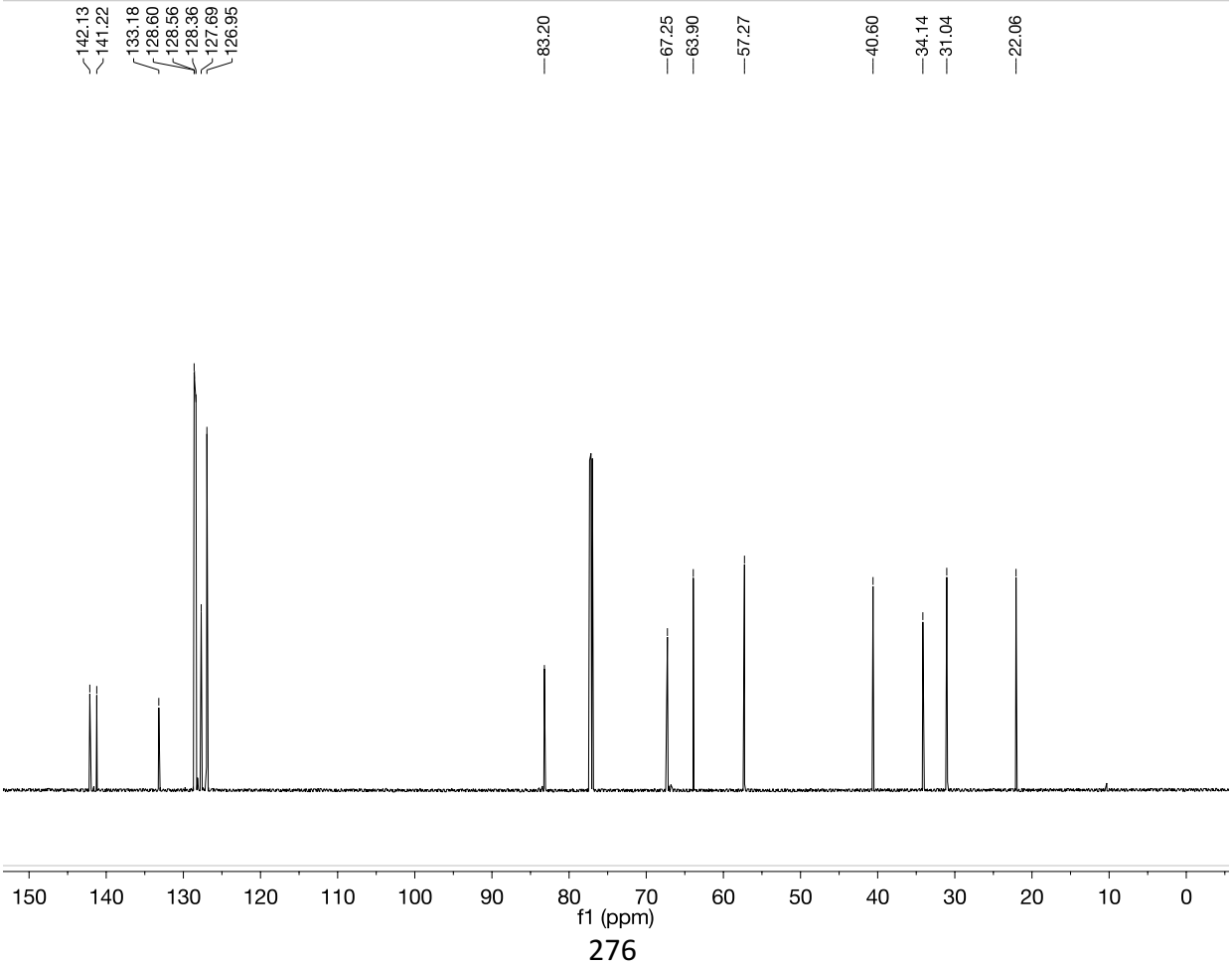
f1 (ppm)

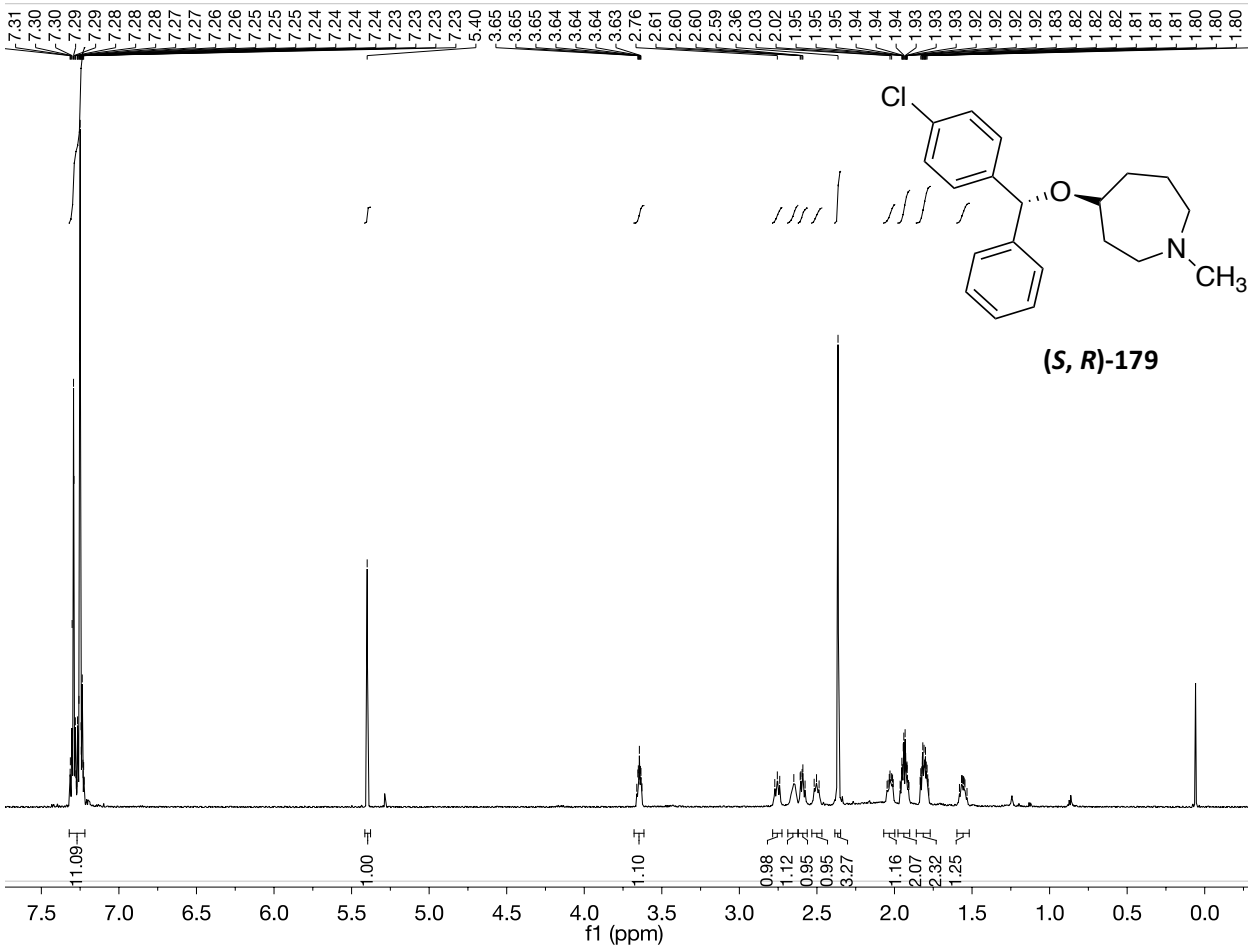

(*S*, *R*)-179

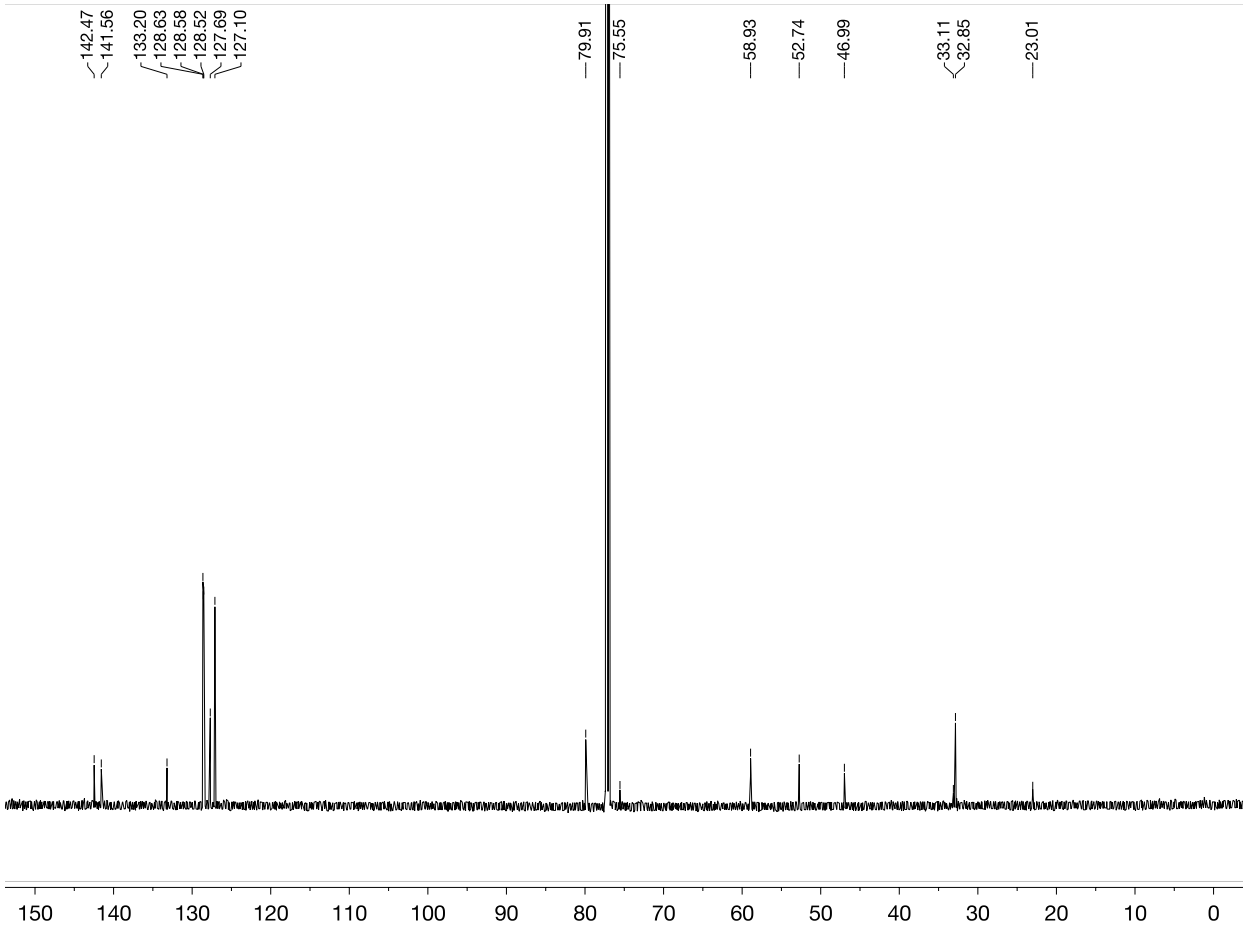

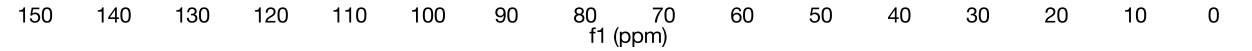

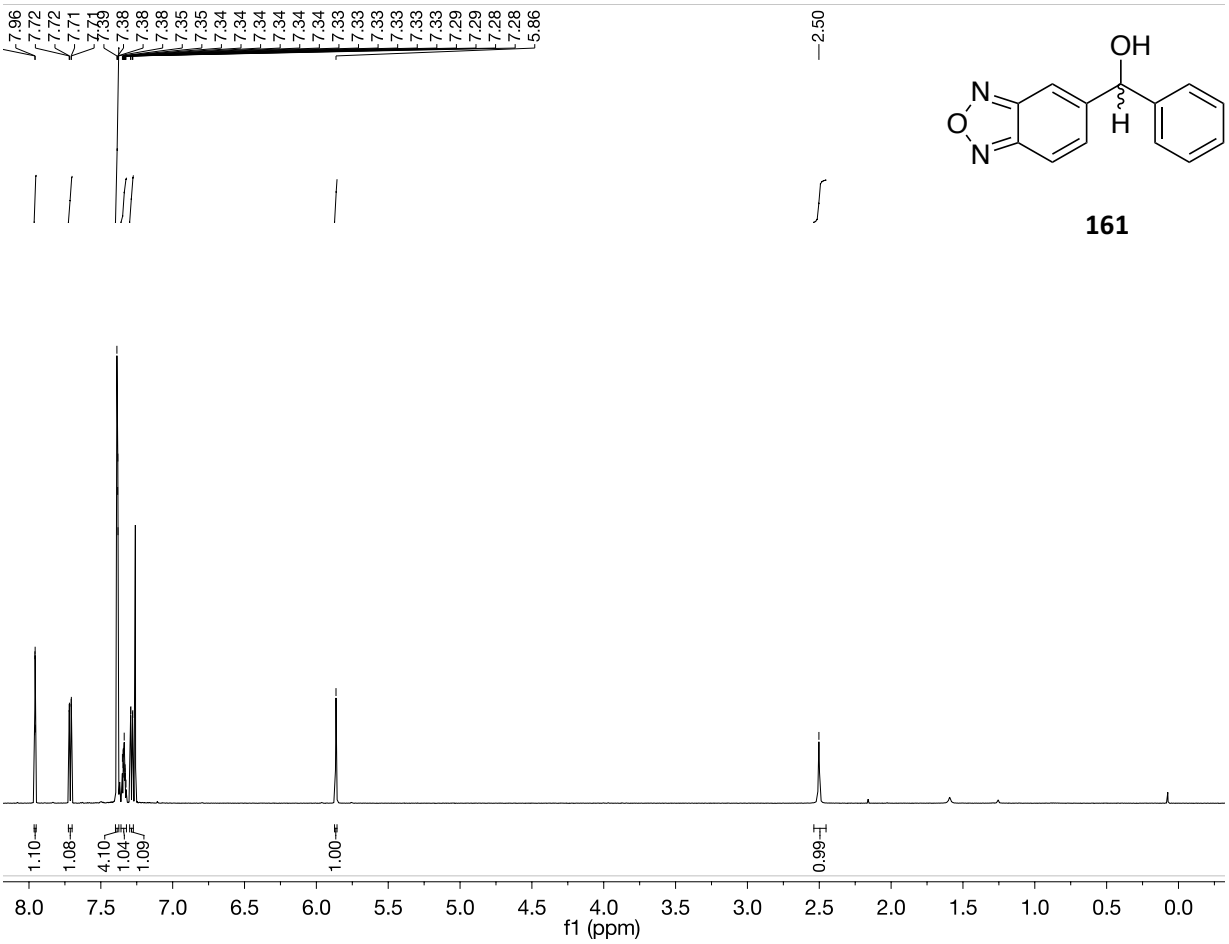
7.96
7.72
7.72
7.71
7.71
7.39
7.38
7.38
7.38
7.35
7.35
7.34
7.34
7.34
7.34
7.34
7.34
7.33
7.33
7.33
7.33
7.33
7.33
7.29
7.29
7.28
5.86
2.50
OH
N
O
N
H
1.10
1.08
4.10
1.04
1.09
1.00
0.99
8.0
7.5
7.0
6.5
6.0
5.5
5.0
4.5
4.0
3.5
3.0
2.5
2.0
1.5
1.0
0.5
0.0
f1 (ppm)

161

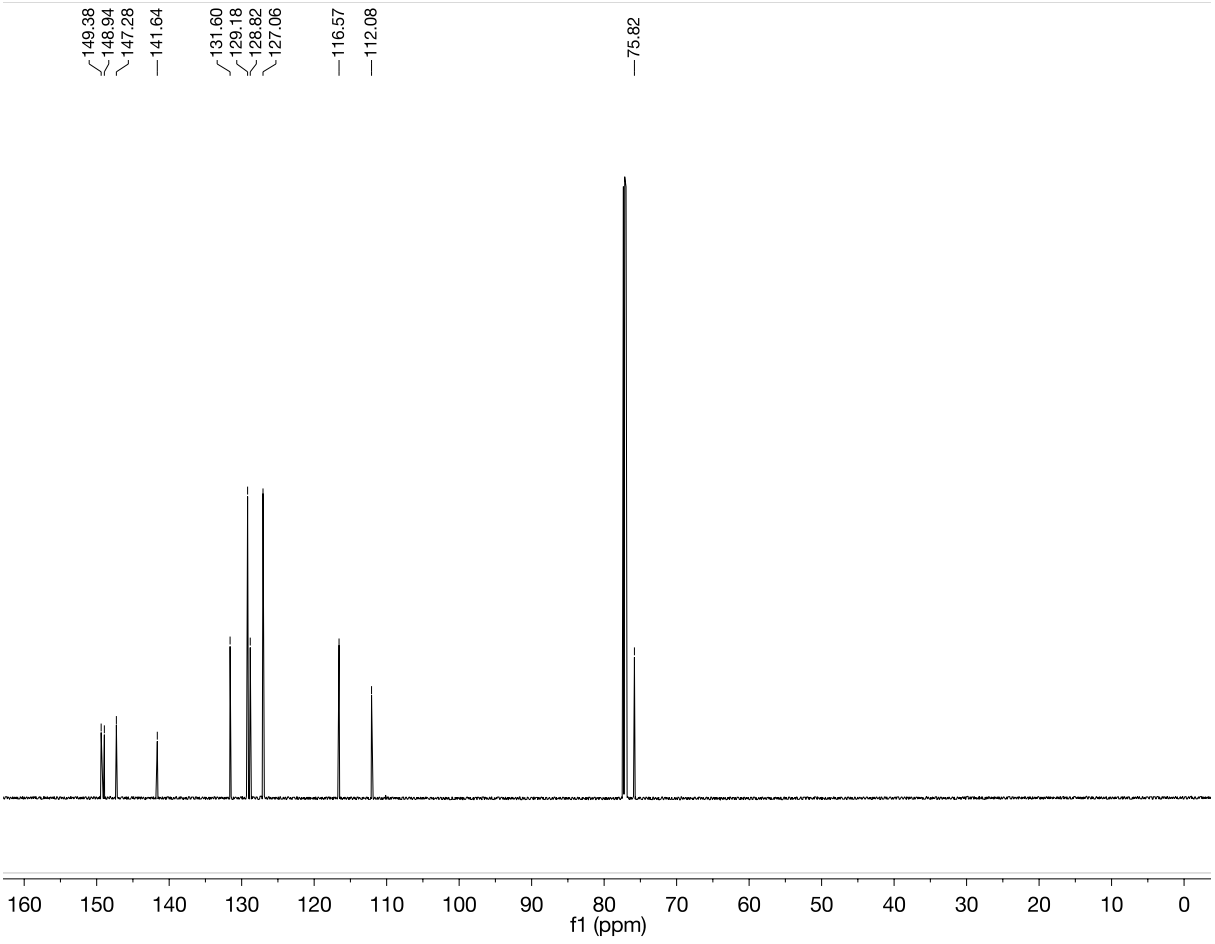
149.38
148.94
147.28
141.64
131.60
129.18
128.82
127.06
116.57
112.08
75.82
160
150
140
130
120
110
100
90
80
70
60
50
40
30
20
10
0
f1 (ppm)

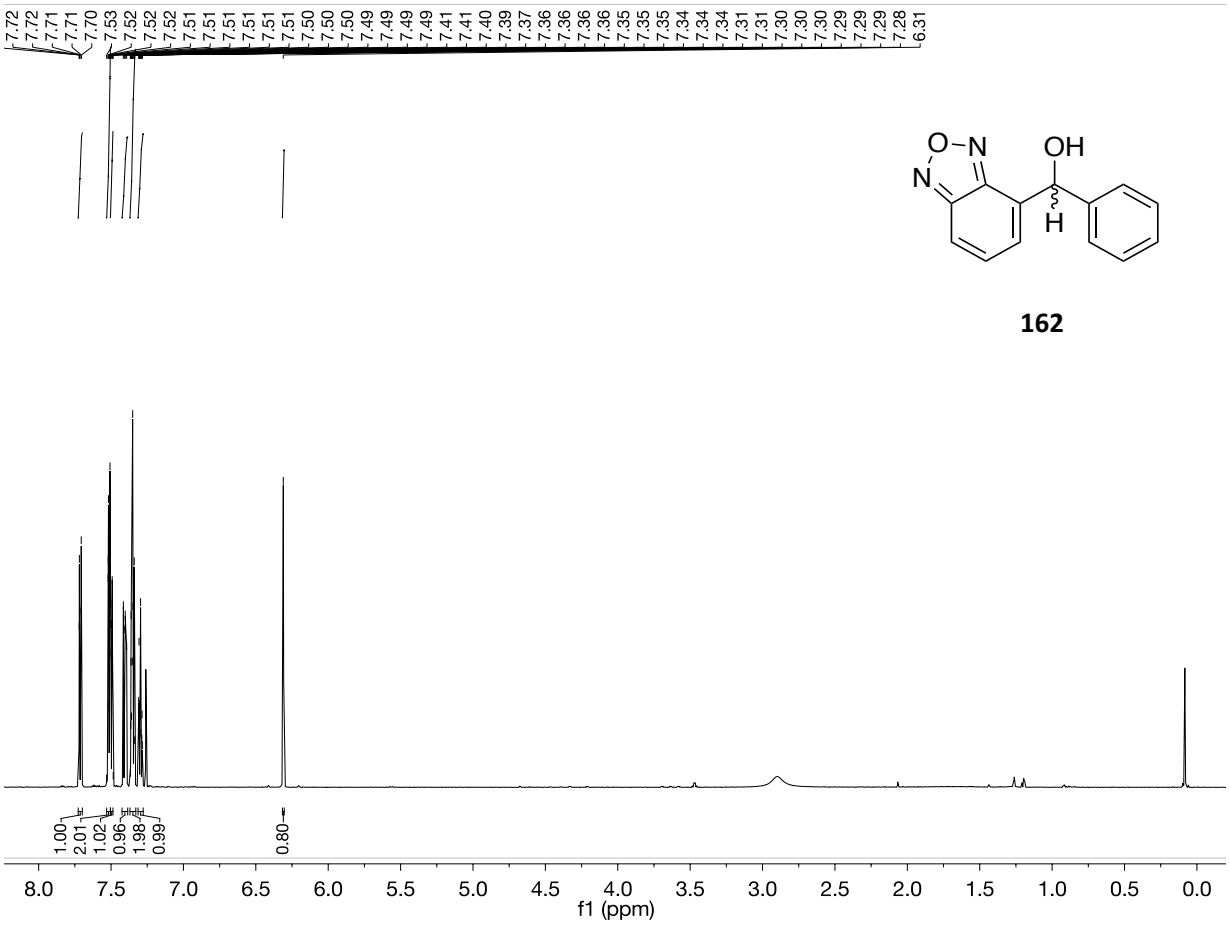
7.72 7.72 7.71 7.71 7.70 7.53 7.52 7.52 7.52 7.51 7.51 7.51 7.51 7.51 7.51 7.50 7.50 7.50 7.49 7.49 7.49 7.49 7.41 7.41 7.40 7.39 7.37 7.36 7.36 7.36 7.35 7.35 7.35 7.34 7.34 7.34 7.31 7.31 7.30 7.30 7.30 7.29 7.29 7.29 7.28 6.31
O N OH N H
1.00 2.01 1.02 0.96 1.98 0.99 0.80
8.0 7.5 7.0 6.5 6.0 5.5 5.0 4.5 4.0 3.5 3.0 2.5 2.0 1.5 1.0 0.5 0.0
f1 (ppm)

162

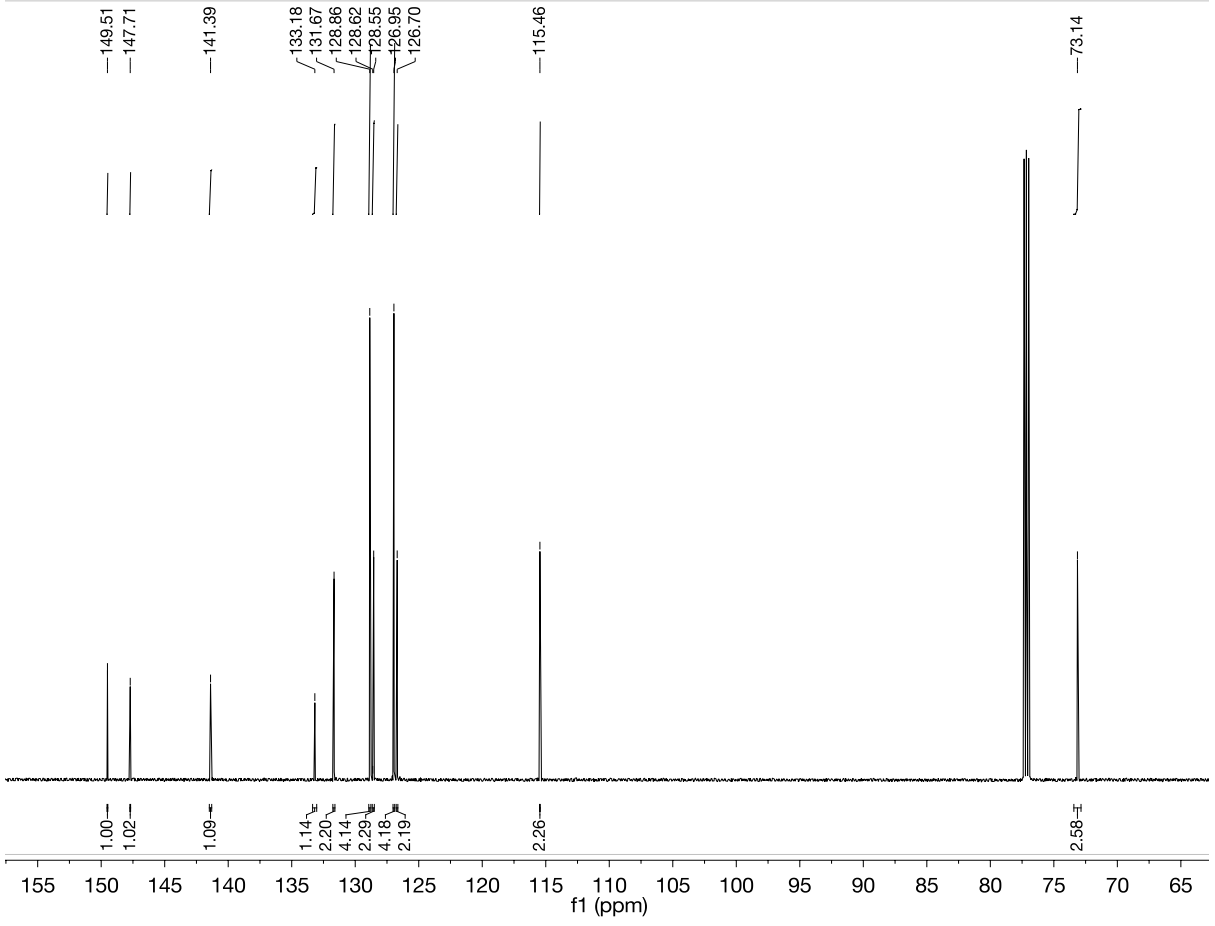
149.51 147.71 141.39 133.18 131.67 128.86 128.62 128.55 126.95 126.70 115.46 73.14
1.00 1.02 1.09 1.14 2.20 4.14 2.29 4.18 2.19 2.26 2.58
155 150 145 140 135 130 125 120 115 110 105 100 95 90 85 80 75 70 65
f1 (ppm)

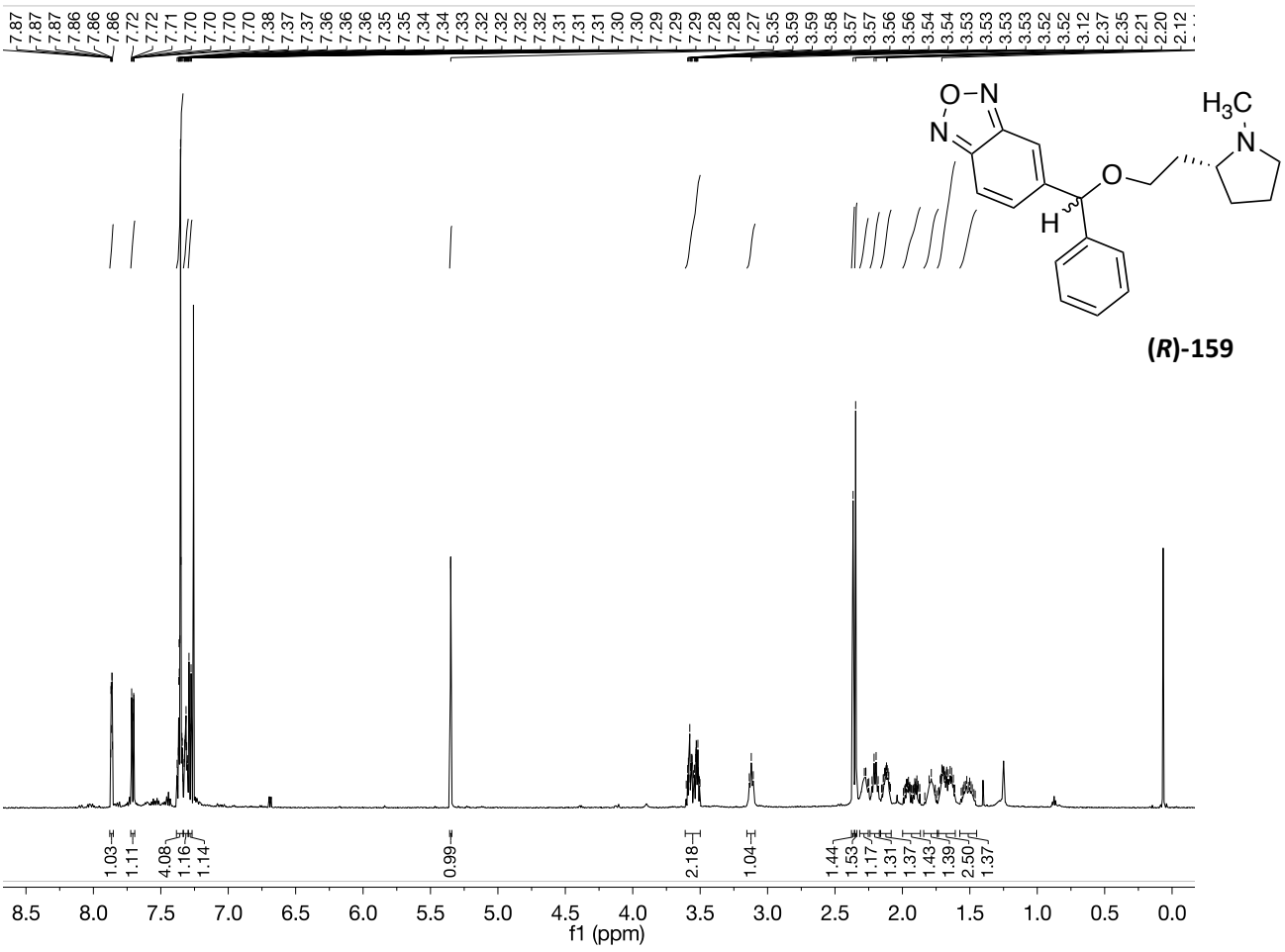
7.87 7.87 7.87 7.86 7.86 7.86 7.72 7.72 7.71 7.70 7.70 7.70 7.70 7.38 7.37 7.37 7.36 7.36 7.36 7.35 7.35 7.34 7.34 7.33 7.32 7.32 7.32 7.32 7.31 7.31 7.31 7.30 7.30 7.29 7.29 7.29 7.28 7.28 7.27 5.35 3.59 3.59 3.58 3.57 3.57 3.56 3.56 3.54 3.53 3.53 3.53 3.53 3.52 3.52 3.12 2.37 2.35 2.21 2.20
O−N
N
H3C
N
O
H
1.03 1.11 4.08 1.16 1.14 0.99 2.18 1.04 1.44 1.53 1.17 1.31 1.37 1.43 1.39 2.50 1.37
8.5 8.0 7.5 7.0 6.5 6.0 5.5 5.0 4.5 4.0 3.5 3.0 2.5 2.0 1.5 1.0 0.5 0.0
f1 (ppm)

(*R*)-159

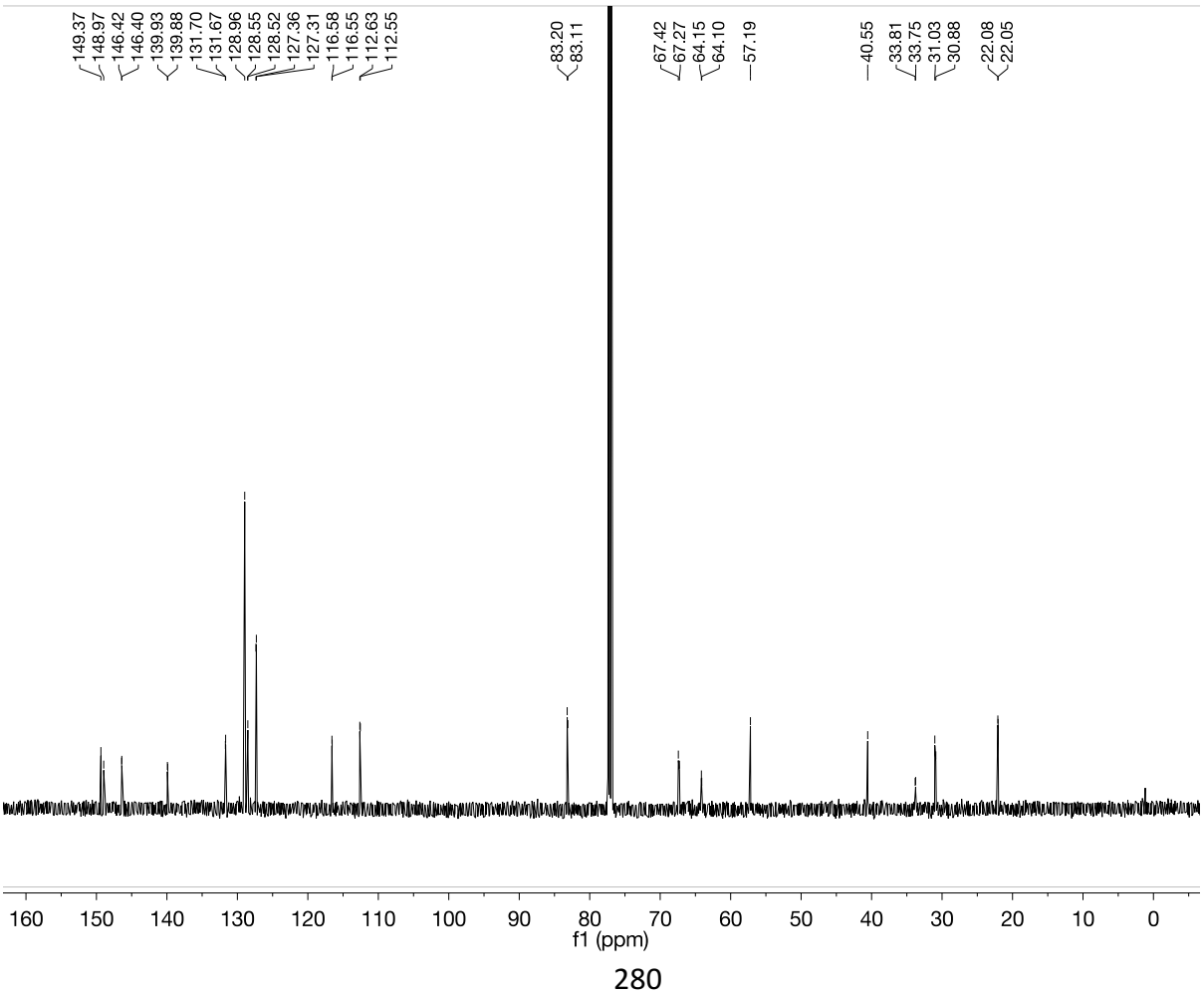
149.37 148.97 146.42 146.40 139.93 139.88 131.70 131.67 128.96 128.55 128.52 127.36 127.31 116.58 116.55 112.63 112.55
83.20 83.11
67.42 67.27 64.15 64.10 57.19
40.55 33.81 33.75 31.03 30.88 22.08 22.05
160 150 140 130 120 110 100 90 80 70 60 50 40 30 20 10 0
f1 (ppm)

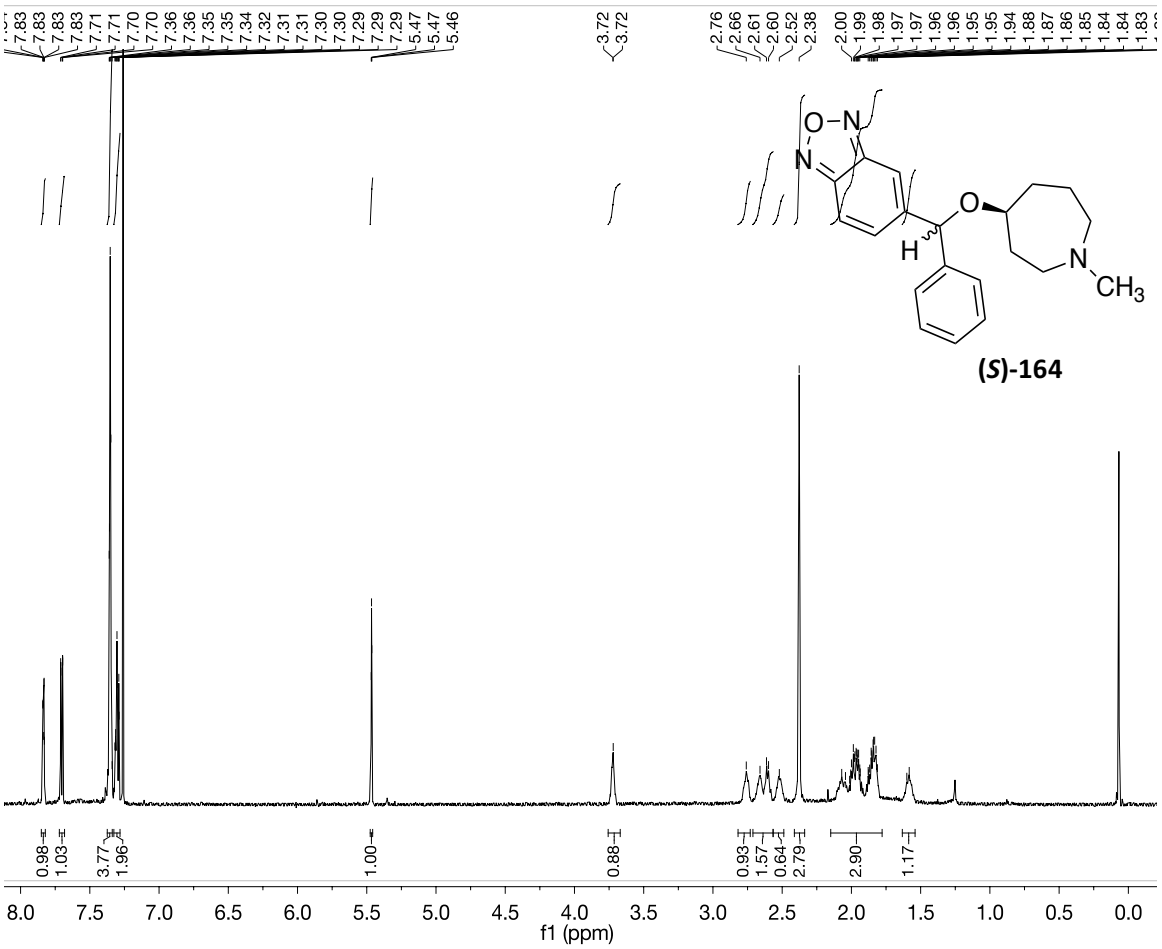
7.83
7.83
7.83
7.83
7.71
7.71
7.70
7.70
7.36
7.36
7.35
7.35
7.34
7.32
7.31
7.31
7.30
7.30
7.29
7.29
7.29
5.47
5.47
5.46
3.72
3.72
2.76
2.66
2.61
2.60
2.52
2.38
2.00
1.99
1.98
1.97
1.97
1.96
1.96
1.95
1.95
1.94
1.88
1.87
1.86
1.85
1.84
1.84
1.83
O
N
O
H
N
CH3
0.98
1.03
3.77
1.96
1.00
0.88
0.93
1.57
0.64
2.79
2.90
1.17
8.0
7.5
7.0
6.5
6.0
5.5
5.0
4.5
4.0
3.5
3.0
2.5
2.0
1.5
1.0
0.5
0.0
f1 (ppm)

(*S*)-164

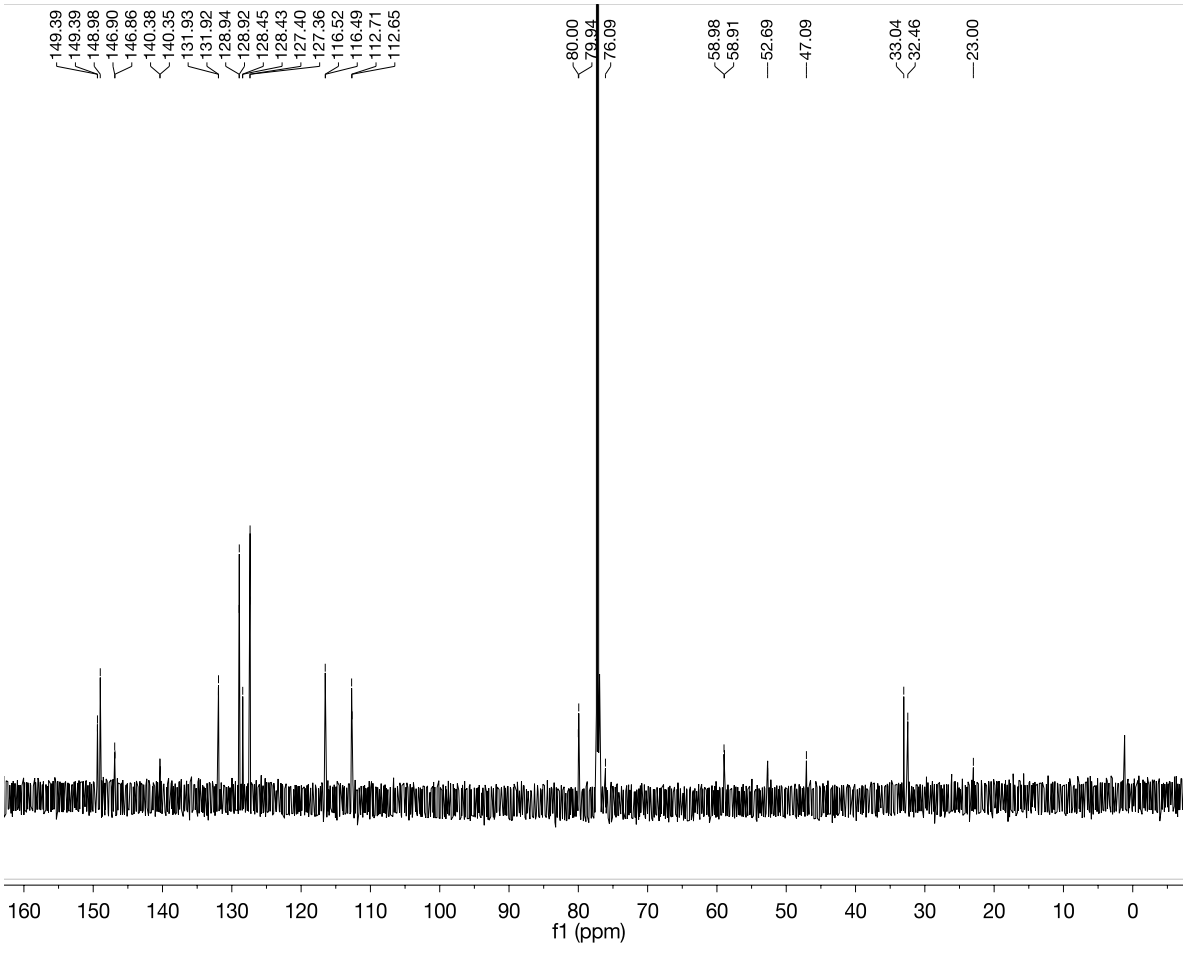
149.39
149.39
148.98
146.90
146.86
140.38
140.35
131.93
131.92
128.94
128.92
128.45
128.43
127.40
127.36
116.52
116.49
112.71
112.65
80.00
79.94
76.09
58.98
58.91
52.69
47.09
33.04
32.46
23.00
160
150
140
130
120
110
100
90
80
70
60
50
40
30
20
10
0
f1 (ppm)

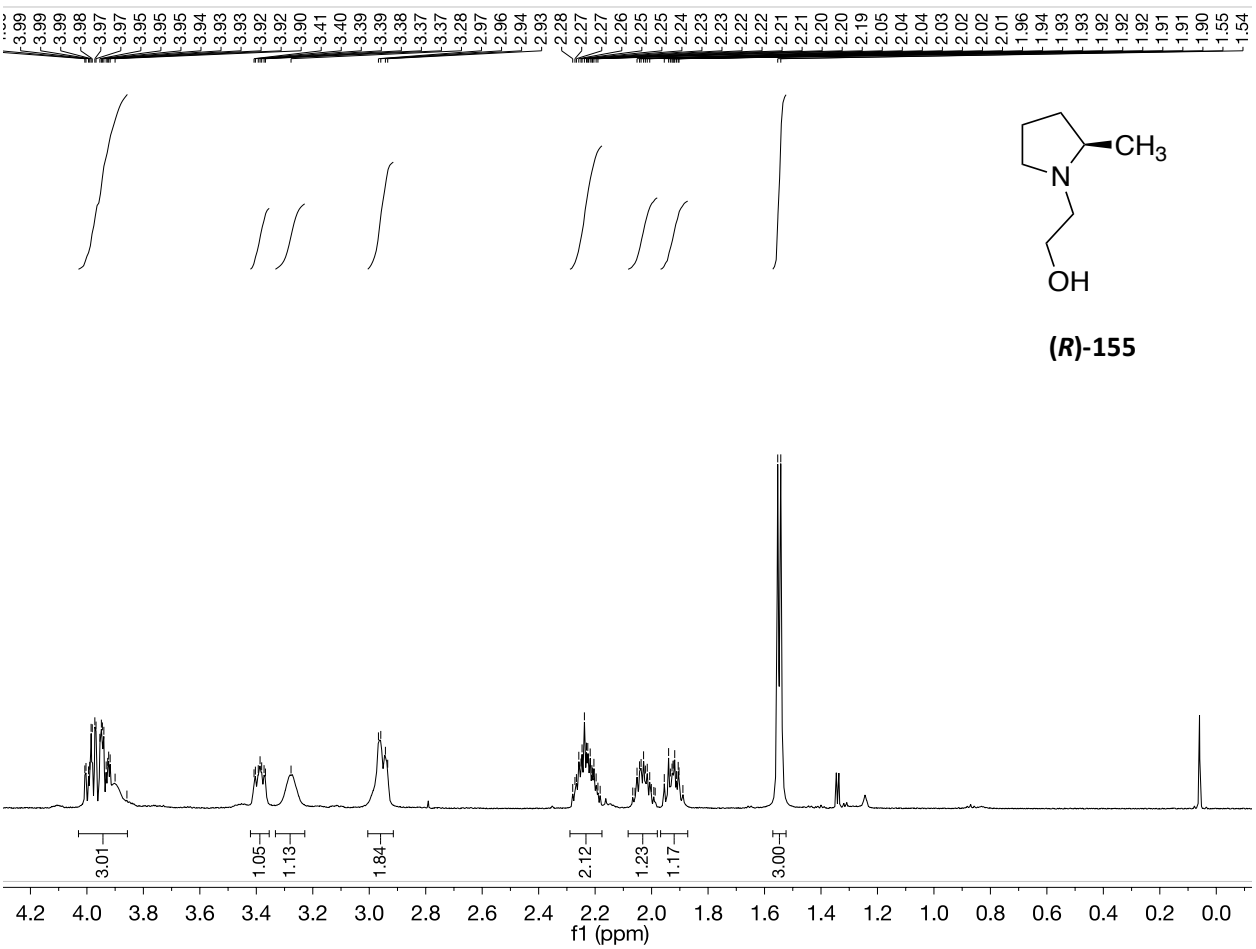
CH3
N
OH
3.01
1.05
1.13
1.84
2.12
1.23
1.17
3.00
f1 (ppm)

(*R*)-155

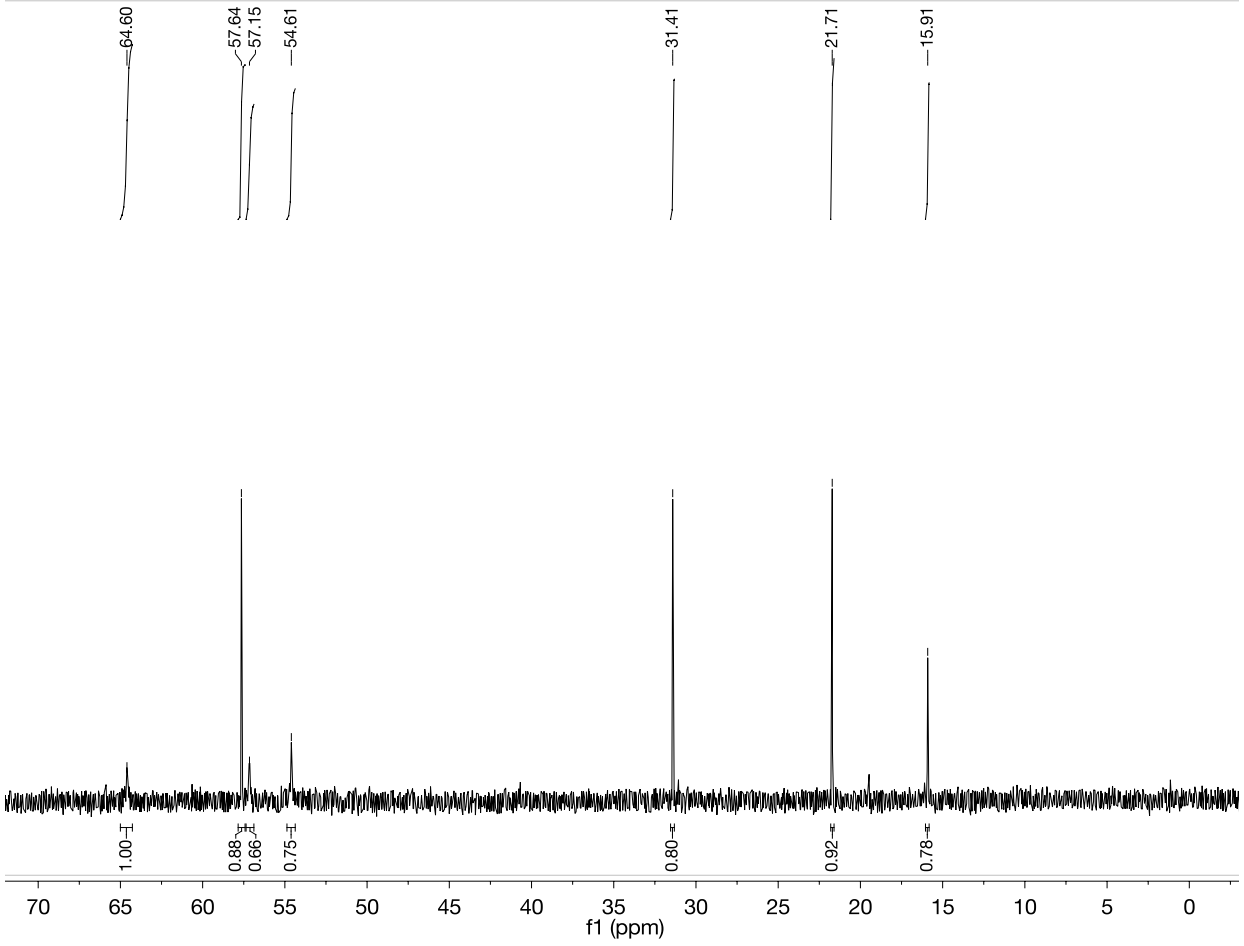
64.60
57.64
57.15
54.61
31.41
21.71
15.91
1.00
0.88
0.66
0.75
0.80
0.92
0.78
f1 (ppm)

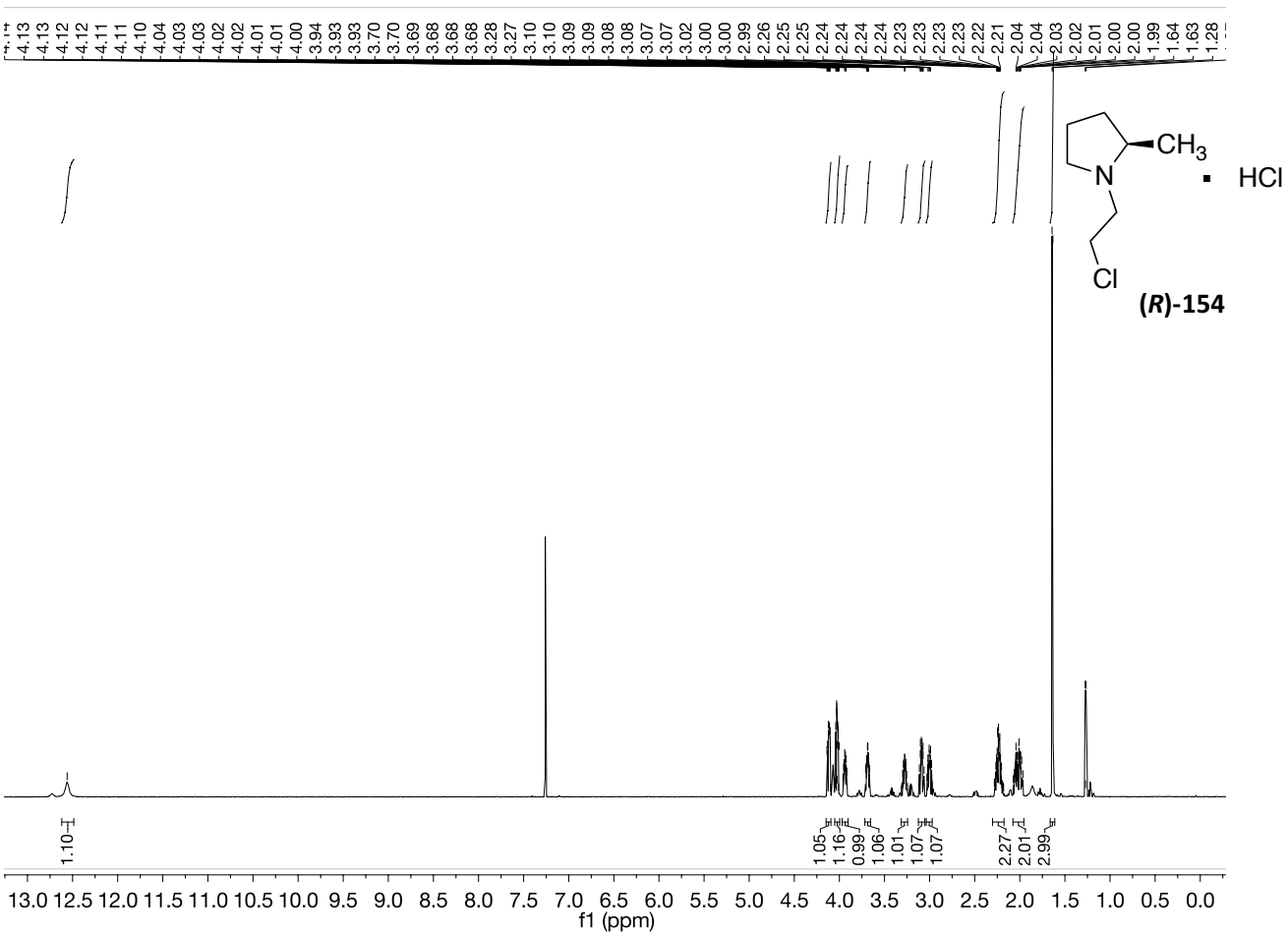
CH3
N
HCl
Cl
(R)-154
1.10
1.05
1.16
0.99
1.06
1.01
1.07
1.07
2.27
2.01
2.99
f1 (ppm)

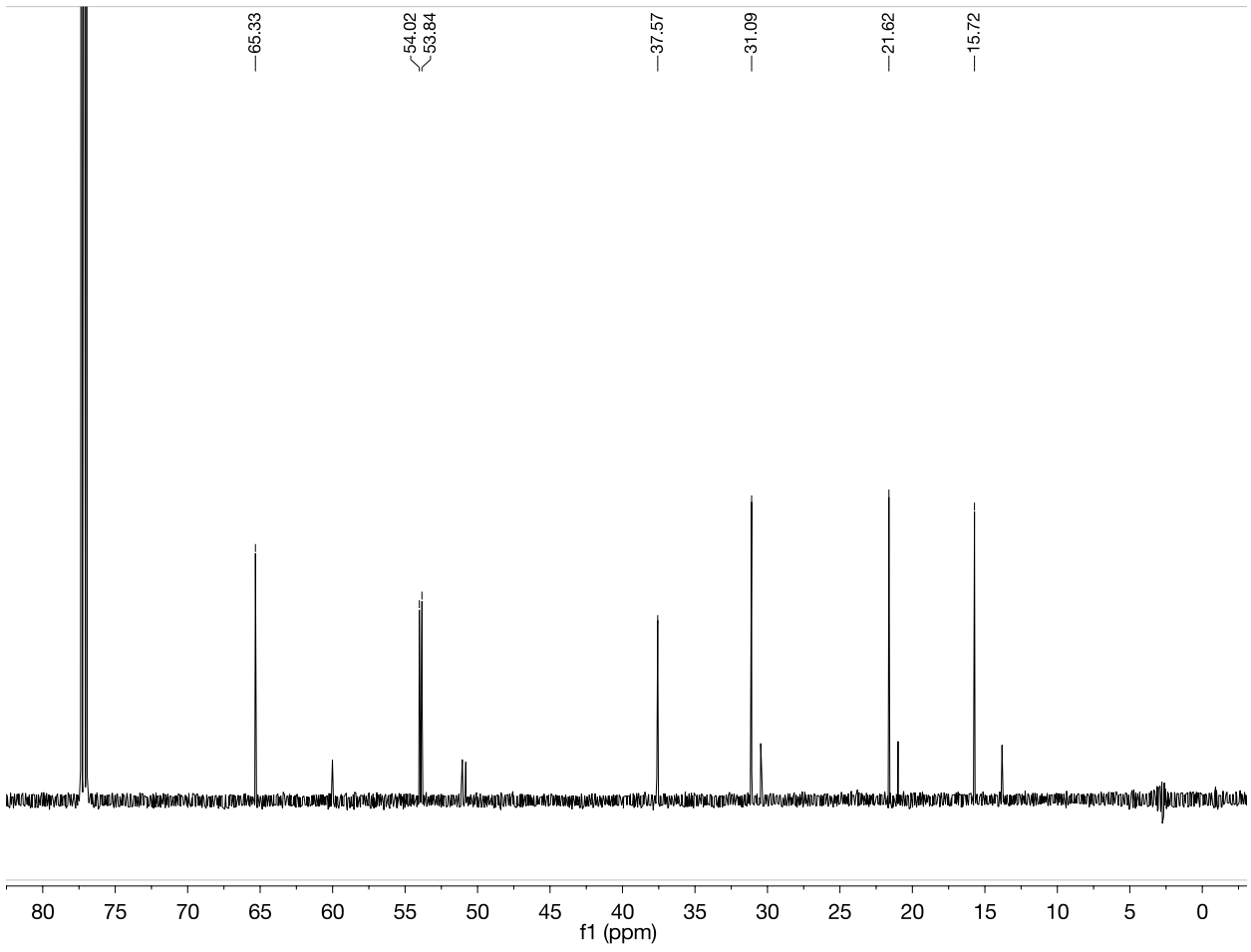
65.33
54.02
53.84
37.57
31.09
21.62
15.72
f1 (ppm)

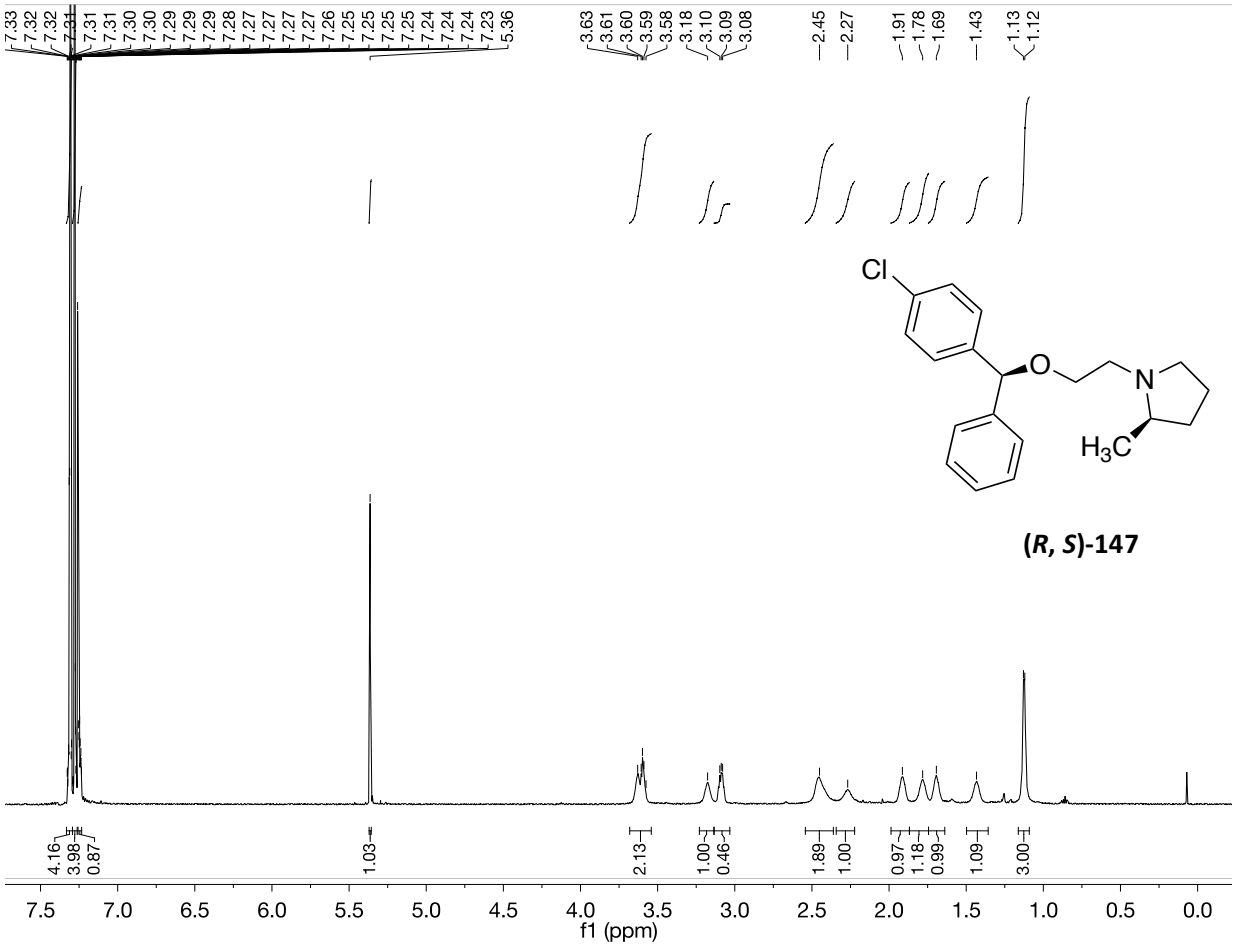
7.33 7.32 7.32 7.31 7.31 7.31 7.30 7.30 7.29 7.29 7.29 7.28 7.27 7.27 7.27 7.27 7.26 7.25 7.25 7.25 7.24 7.24 7.24 7.23 5.36
3.63 3.61 3.60 3.59 3.58 3.18 3.10 3.09 3.08
2.45 2.27
1.91 1.78 1.69 1.43 1.13 1.12
Cl
O
N
H3C
4.16 3.98 0.87 1.03 2.13 1.00 0.46 1.89 1.00 0.97 1.18 0.99 1.09 3.00
7.5 7.0 6.5 6.0 5.5 5.0 4.5 4.0 3.5 3.0 2.5 2.0 1.5 1.0 0.5 0.0
f1 (ppm)

(*R*, *S*)-147

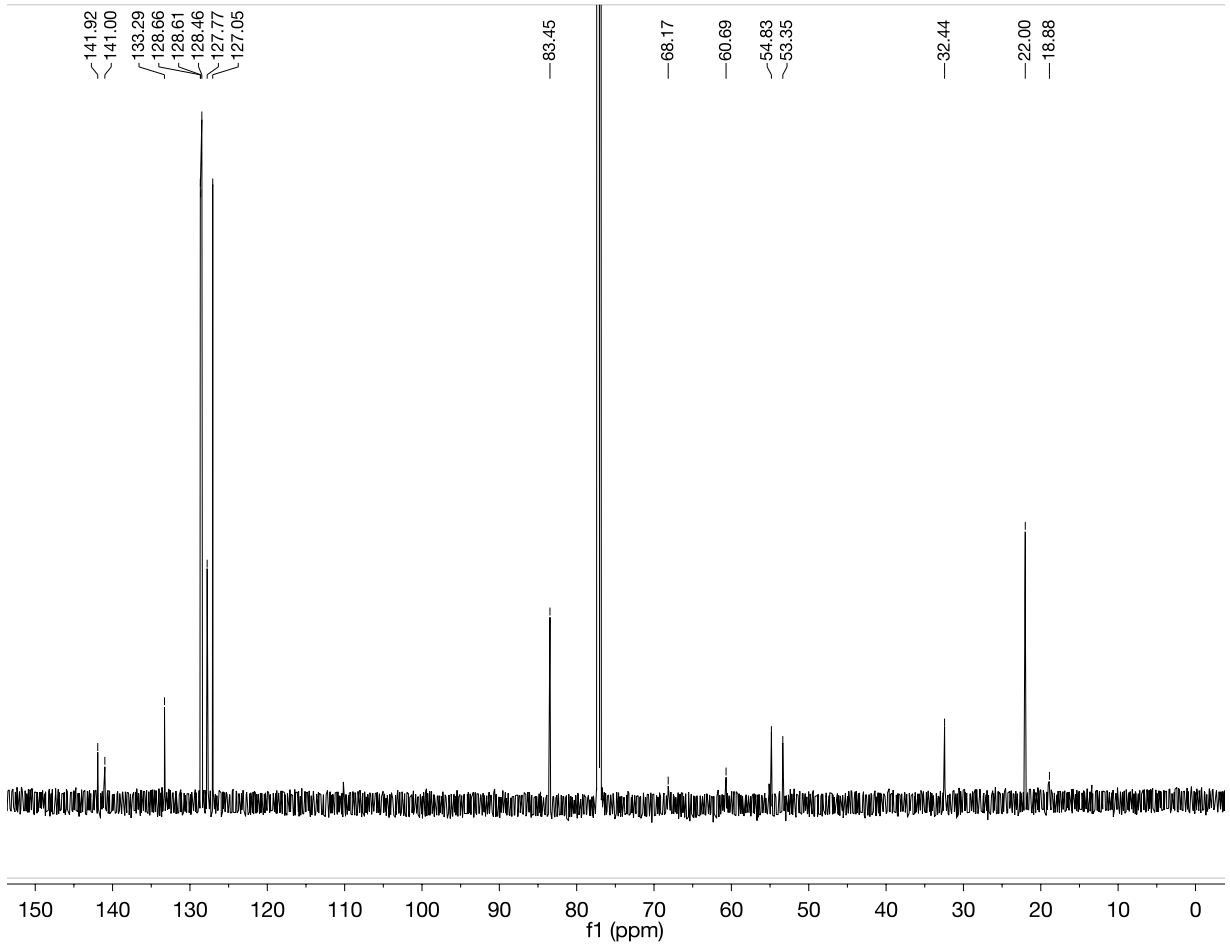
141.92 141.00 133.29 128.66 128.61 128.46 127.77 127.05
83.45 68.17 60.69 54.83 53.35 32.44 22.00 18.88
150 140 130 120 110 100 90 80 70 60 50 40 30 20 10 0
f1 (ppm)

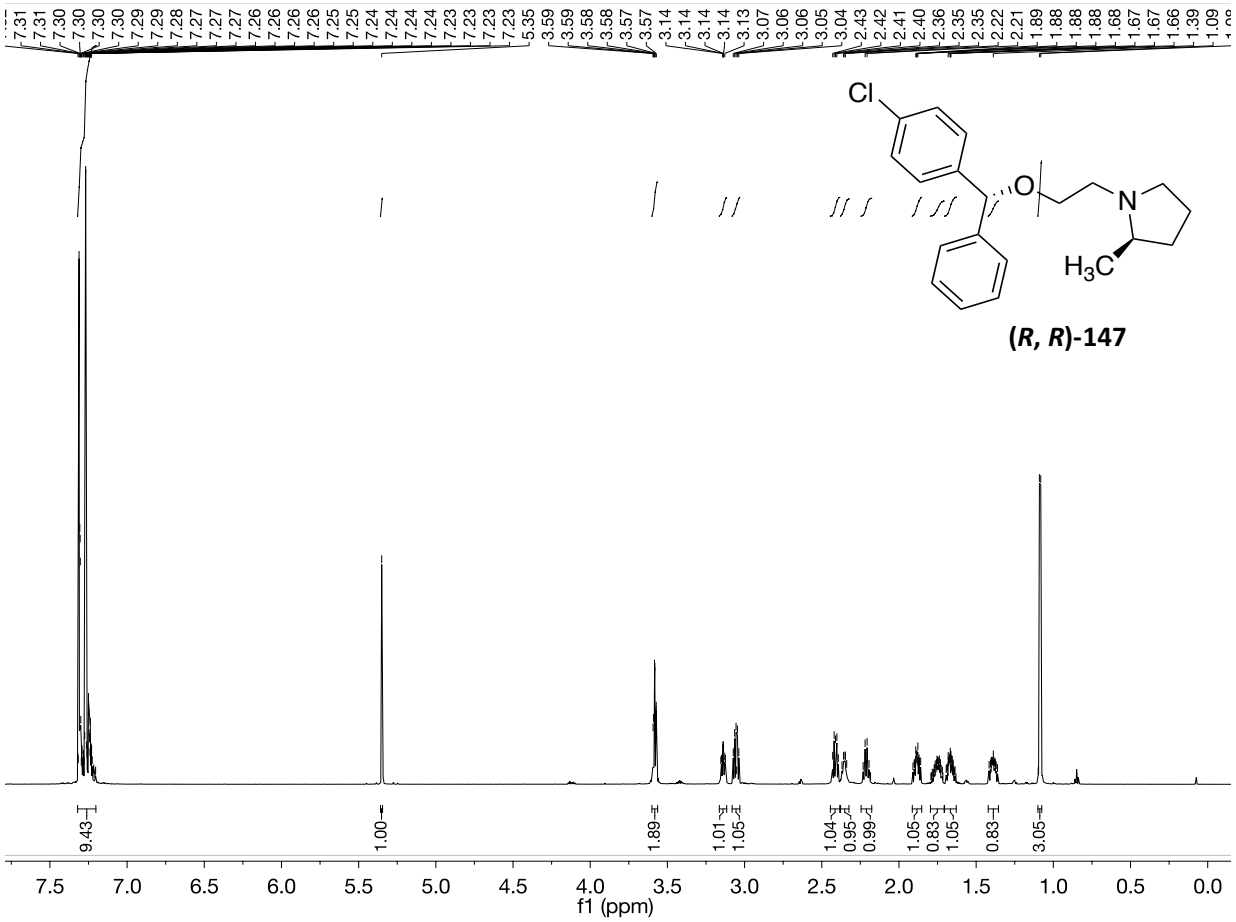
Cl
O
N
H_3C
9.43
1.00
1.89
1.01
1.05
1.04
0.95
0.99
1.05
0.83
1.05
0.83
3.05
f1 (ppm)

(*R*, *R*)-147

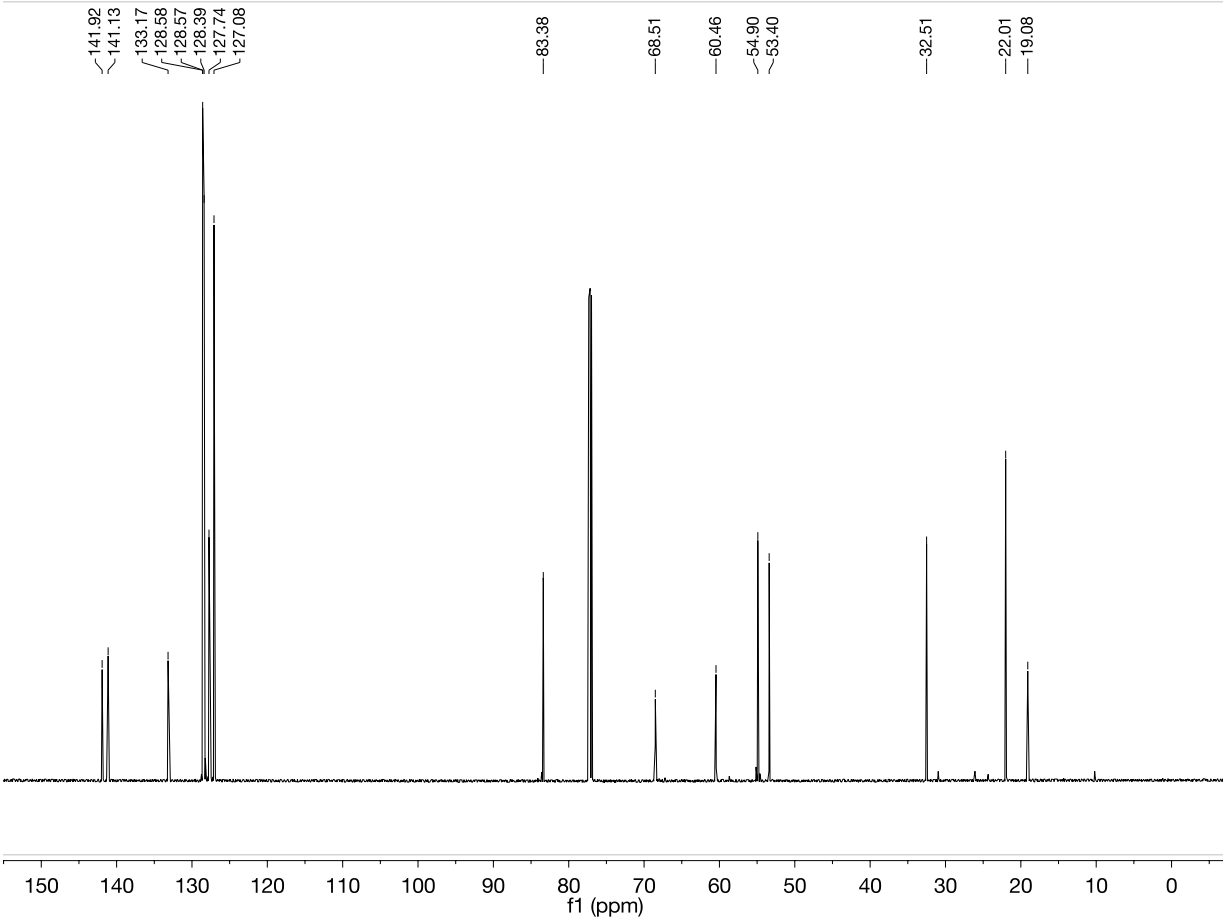
141.92
141.13
133.17
128.58
128.57
128.39
127.74
127.08
83.38
68.51
60.46
54.90
53.40
32.51
22.01
19.08
f1 (ppm)

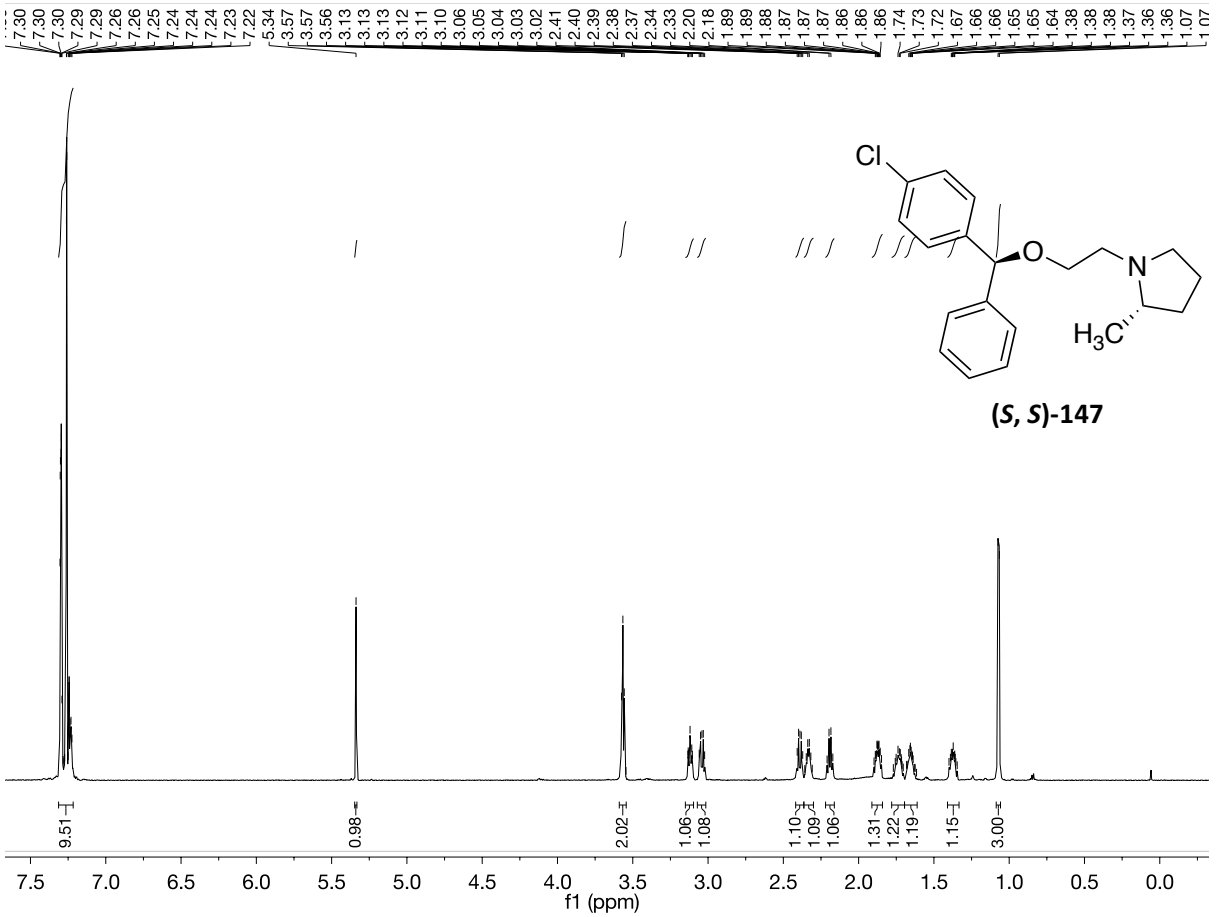
Cl
O
N
H3C
9.51
0.98
2.02
1.06
1.08
1.10
1.09
1.06
1.31
1.22
1.19
1.15
3.00
f1 (ppm)

(*S*, *S*)-147

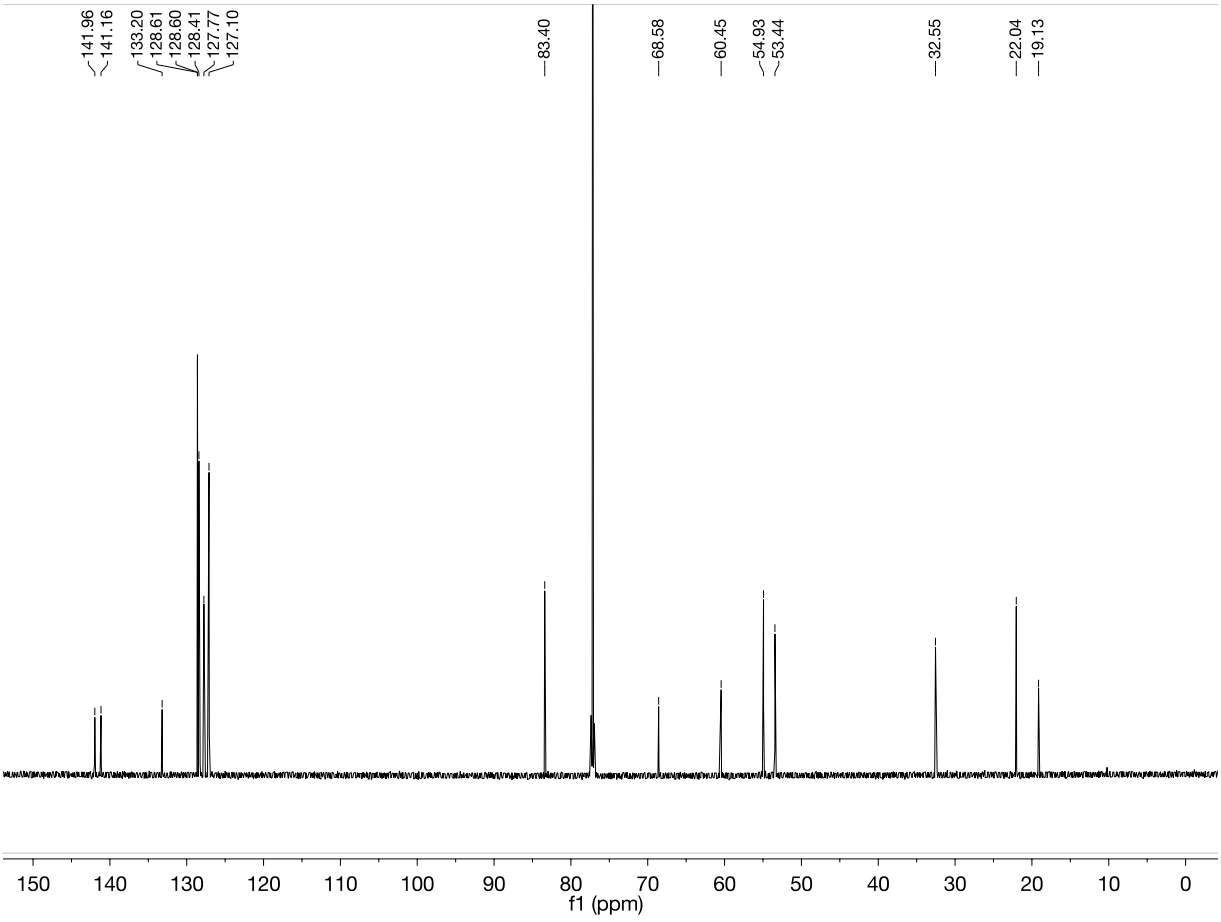
141.96
141.16
133.20
128.61
128.60
128.41
127.77
127.10
83.40
68.58
60.45
54.93
53.44
32.55
22.04
19.13
f1 (ppm)

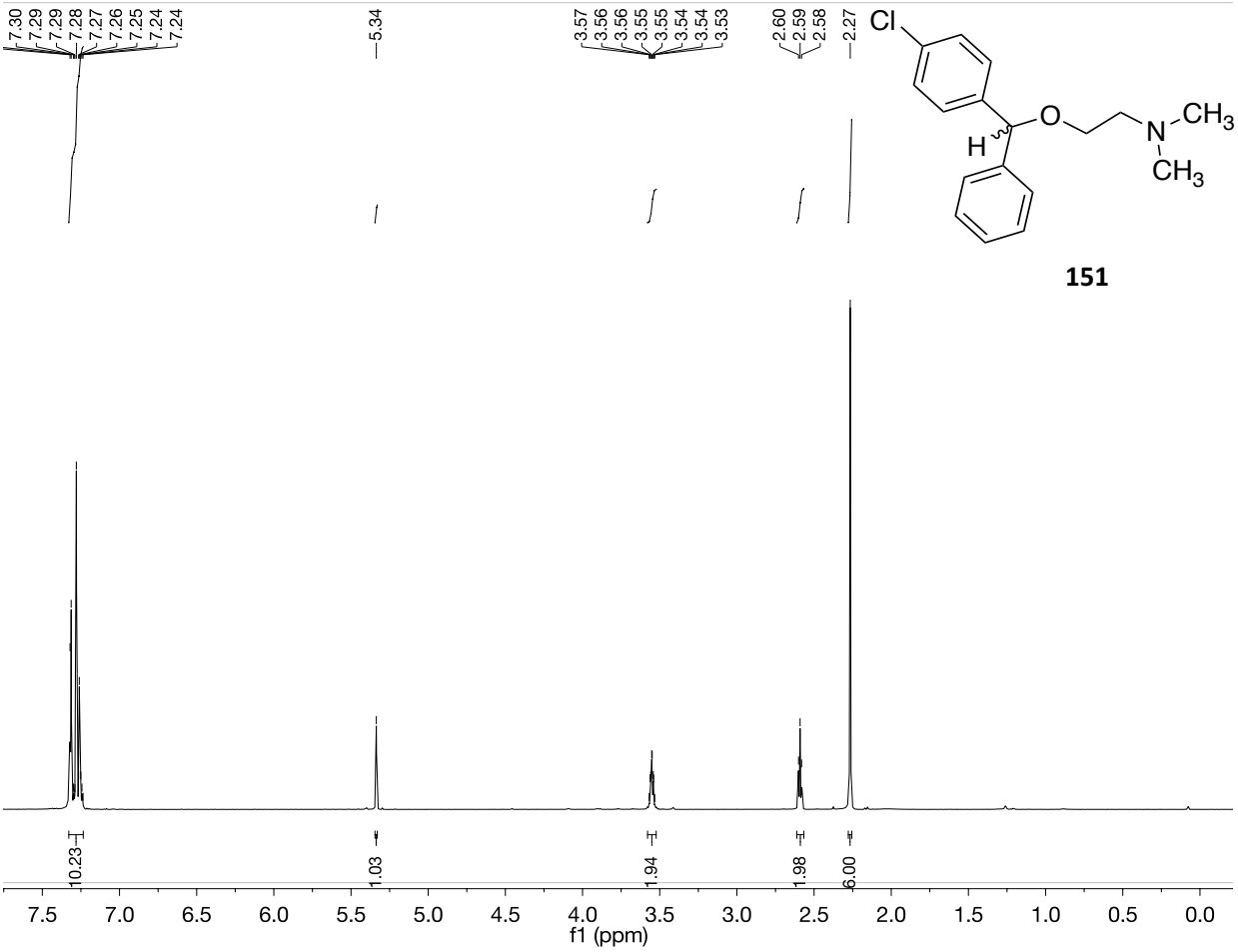
7.30
7.29
7.29
7.28
7.27
7.26
7.25
7.24
7.24
5.34
3.57
3.56
3.56
3.55
3.55
3.54
3.54
3.53
2.60
2.59
2.58
2.27
Cl
O
H
N
CH3
CH3
10.23
1.03
1.94
1.98
6.00
7.5
7.0
6.5
6.0
5.5
5.0
4.5
4.0
3.5
3.0
2.5
2.0
1.5
1.0
0.5
0.0
f1 (ppm)

151

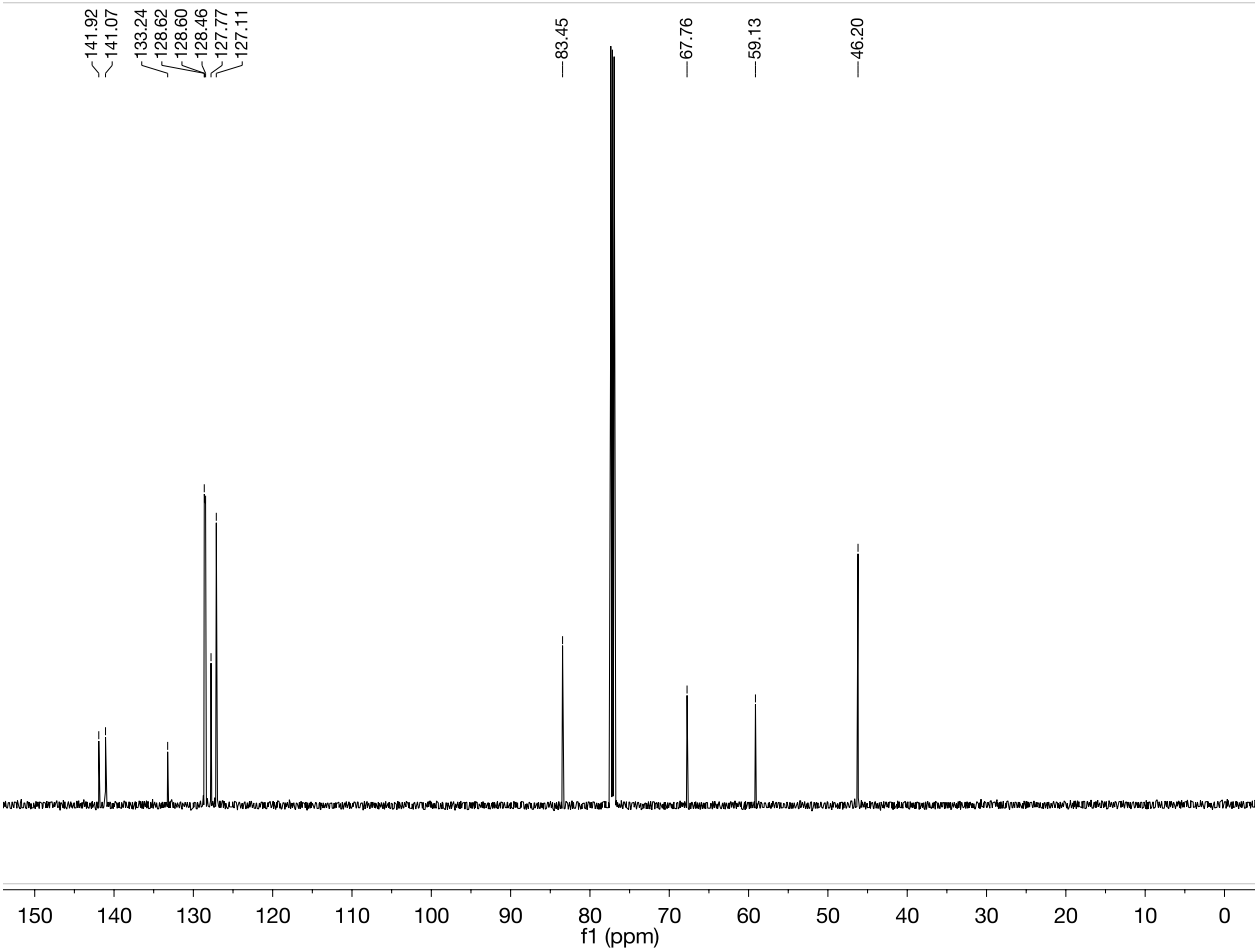
141.92
141.07
133.24
128.62
128.60
128.46
127.77
127.11
83.45
67.76
59.13
46.20
150
140
130
120
110
100
90
80
70
60
50
40
30
20
10
0
f1 (ppm)

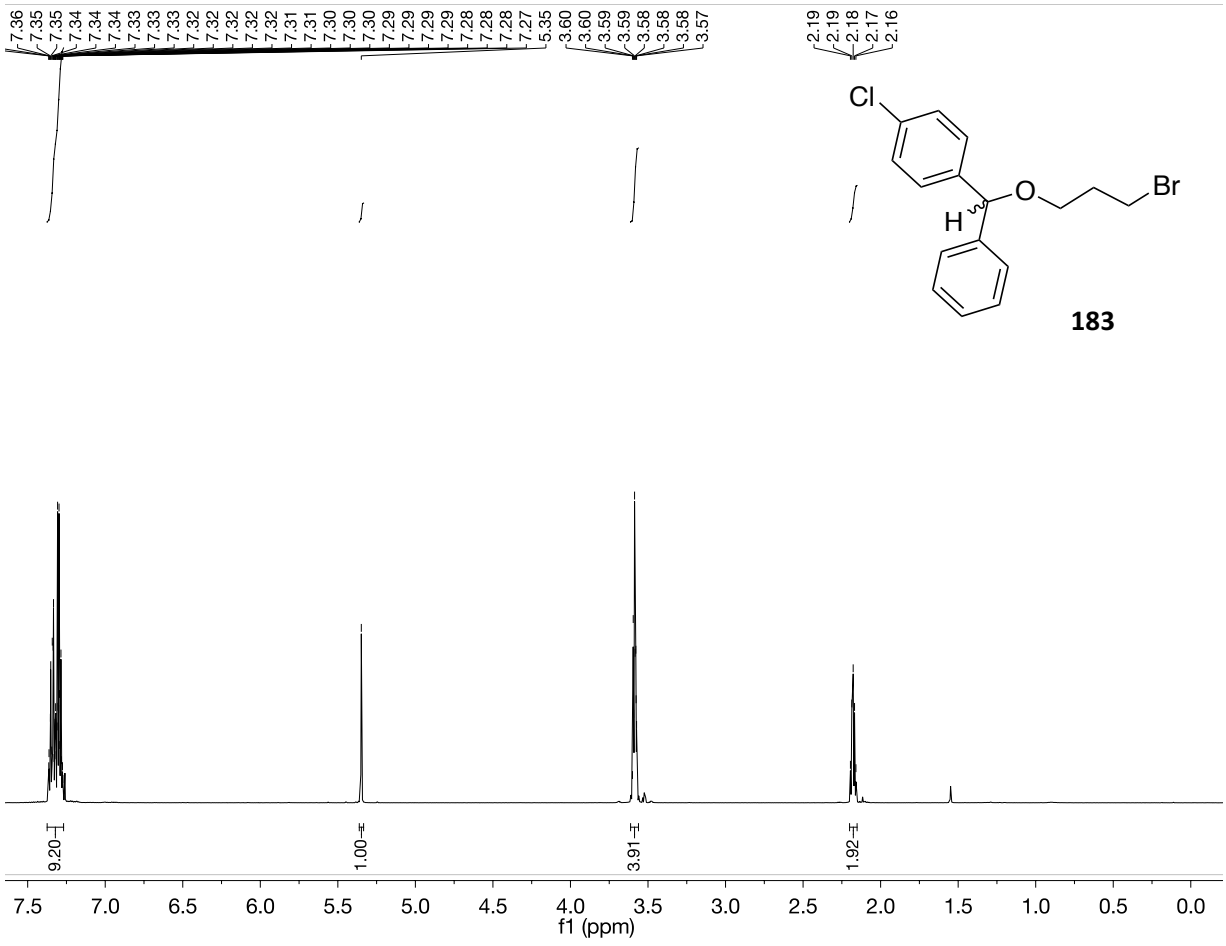
7.36 7.35 7.35 7.34 7.34 7.34 7.33 7.33 7.32 7.32 7.32 7.32 7.31 7.31 7.30 7.30 7.30 7.29 7.29 7.29 7.29 7.28 7.28 7.28 7.27 5.35 3.60 3.60 3.59 3.59 3.58 3.58 3.58 3.57
2.19 2.19 2.18 2.17 2.16
Cl
O
Br
H
183
9.20
1.00
3.91
1.92
7.5 7.0 6.5 6.0 5.5 5.0 4.5 4.0 3.5 3.0 2.5 2.0 1.5 1.0 0.5 0.0
f1 (ppm)

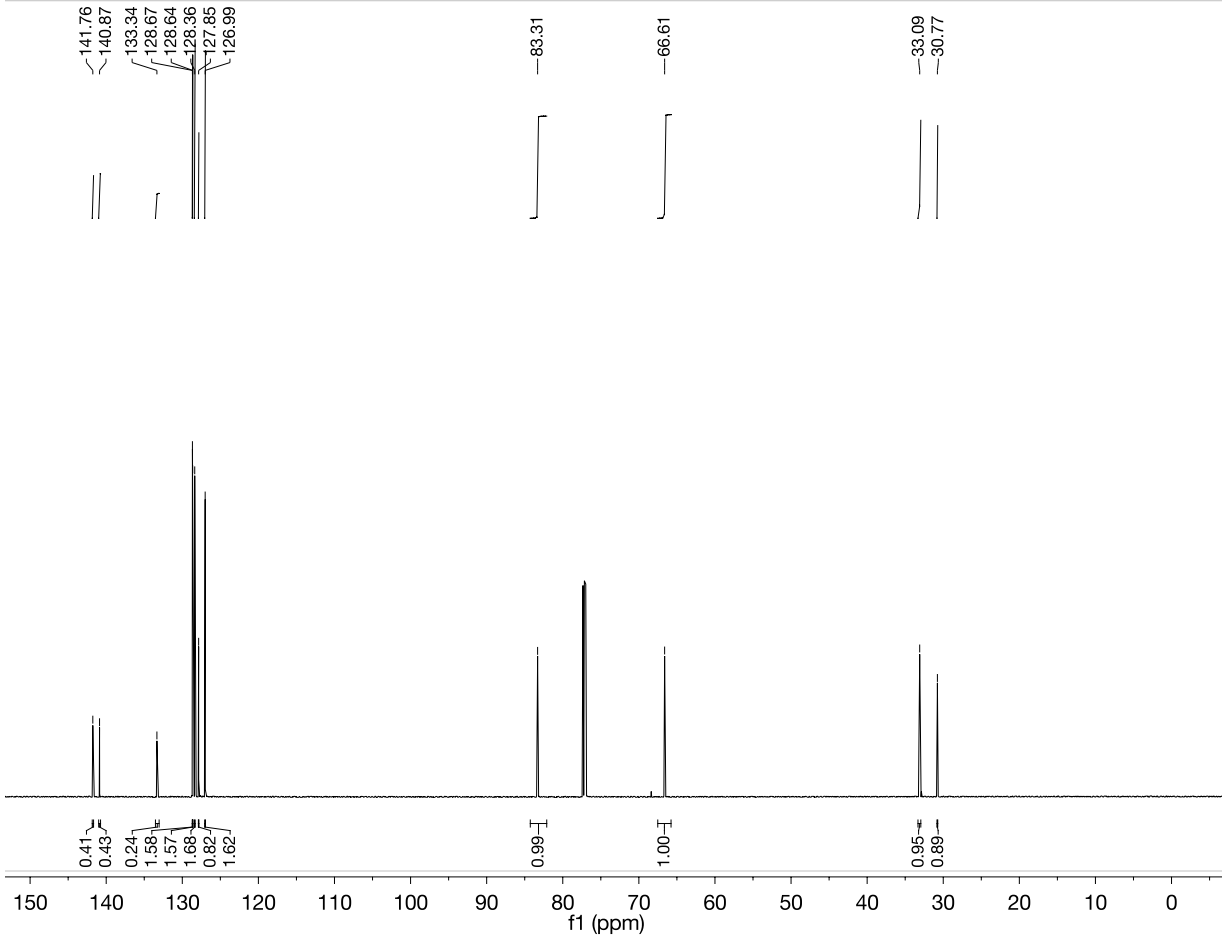
141.76 140.87 133.34 128.67 128.64 128.36 127.85 126.99
83.31
66.61
33.09 30.77
0.41 0.43 0.24 1.58 1.57 1.68 0.82 1.62
0.99
1.00
0.95 0.89
150 140 130 120 110 100 90 80 70 60 50 40 30 20 10 0
f1 (ppm)

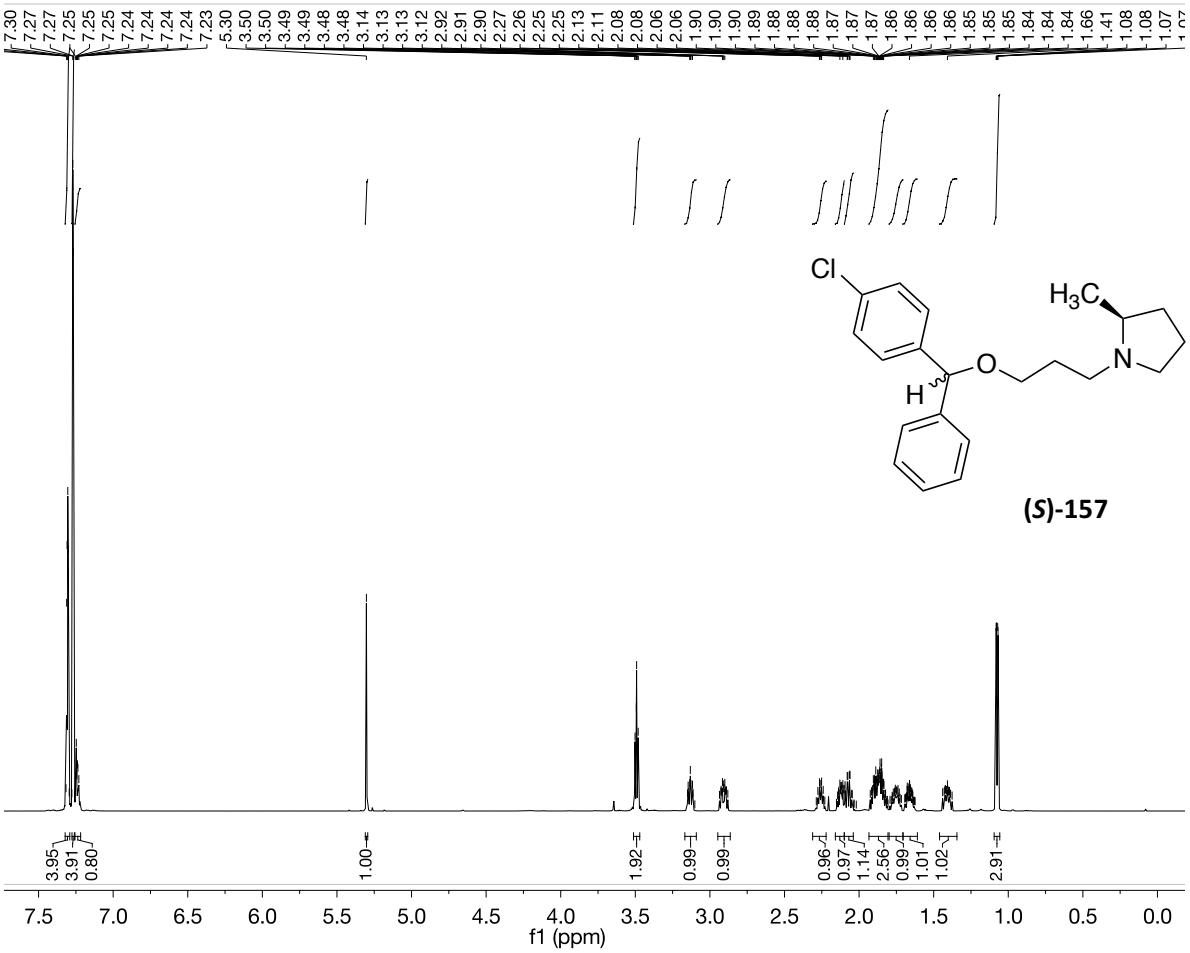
Cl
H3C
O
N
H
(S)-157
f1 (ppm)

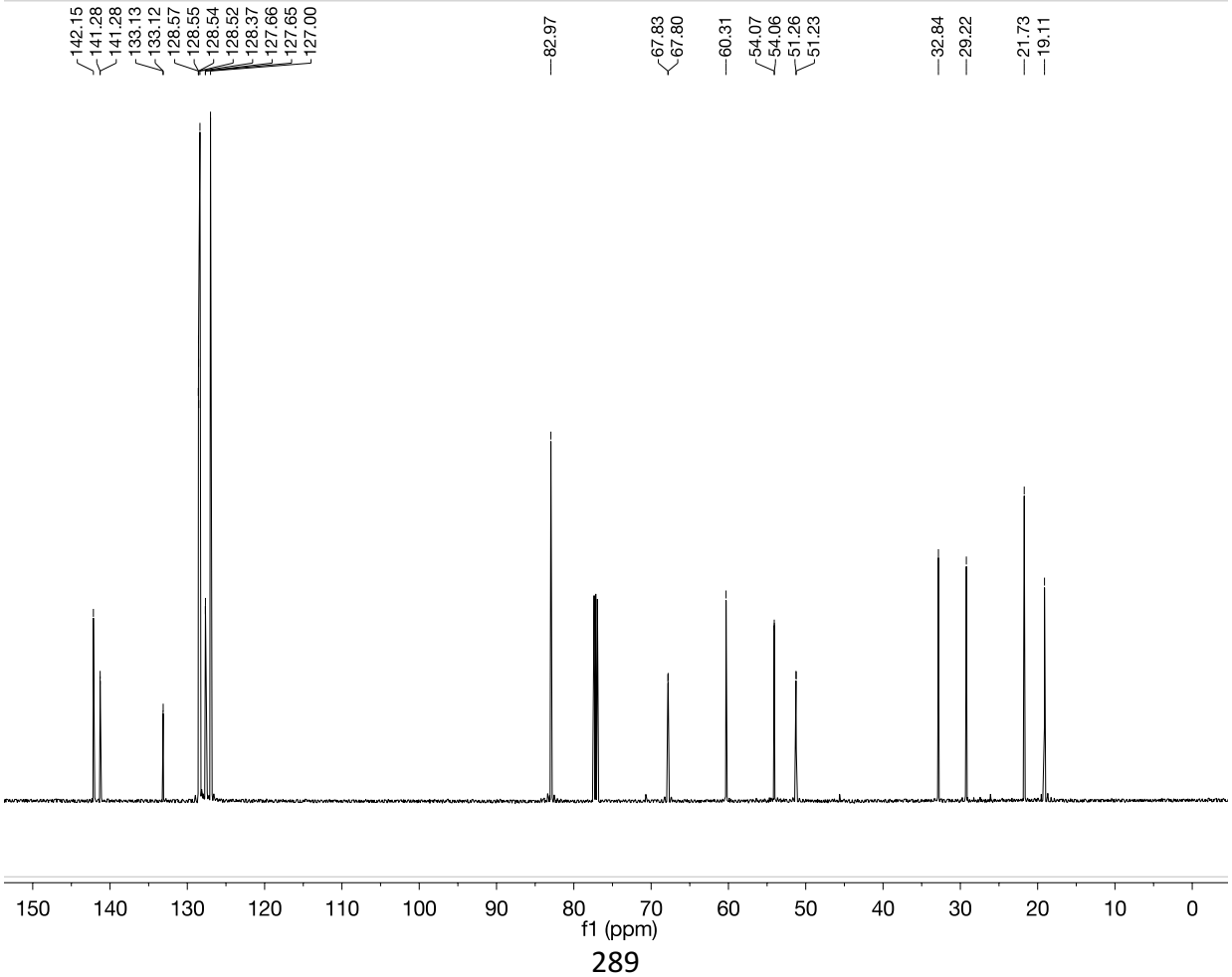
f1 (ppm)

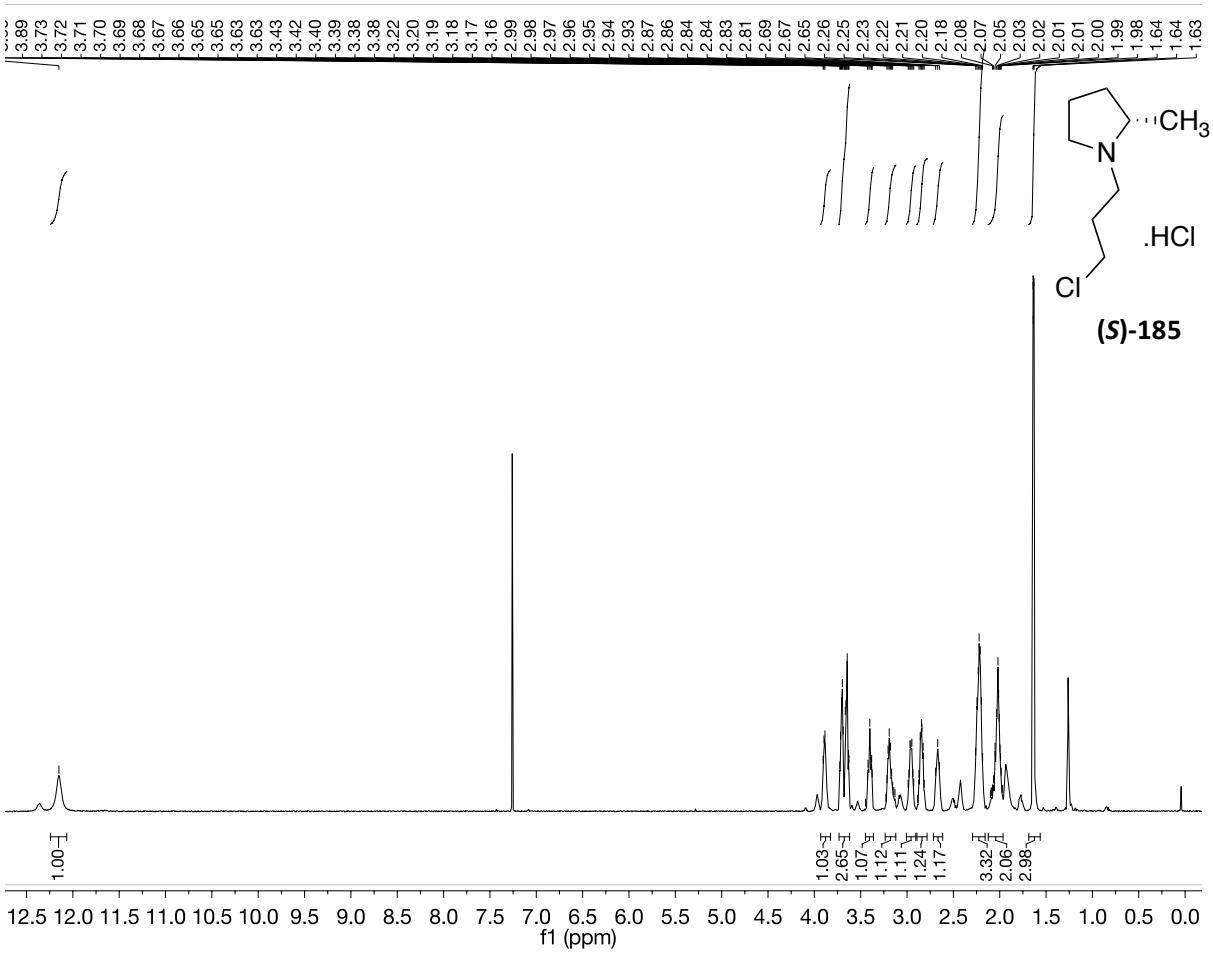
CH3
N
.HCl
Cl
(S)-185
f1 (ppm)

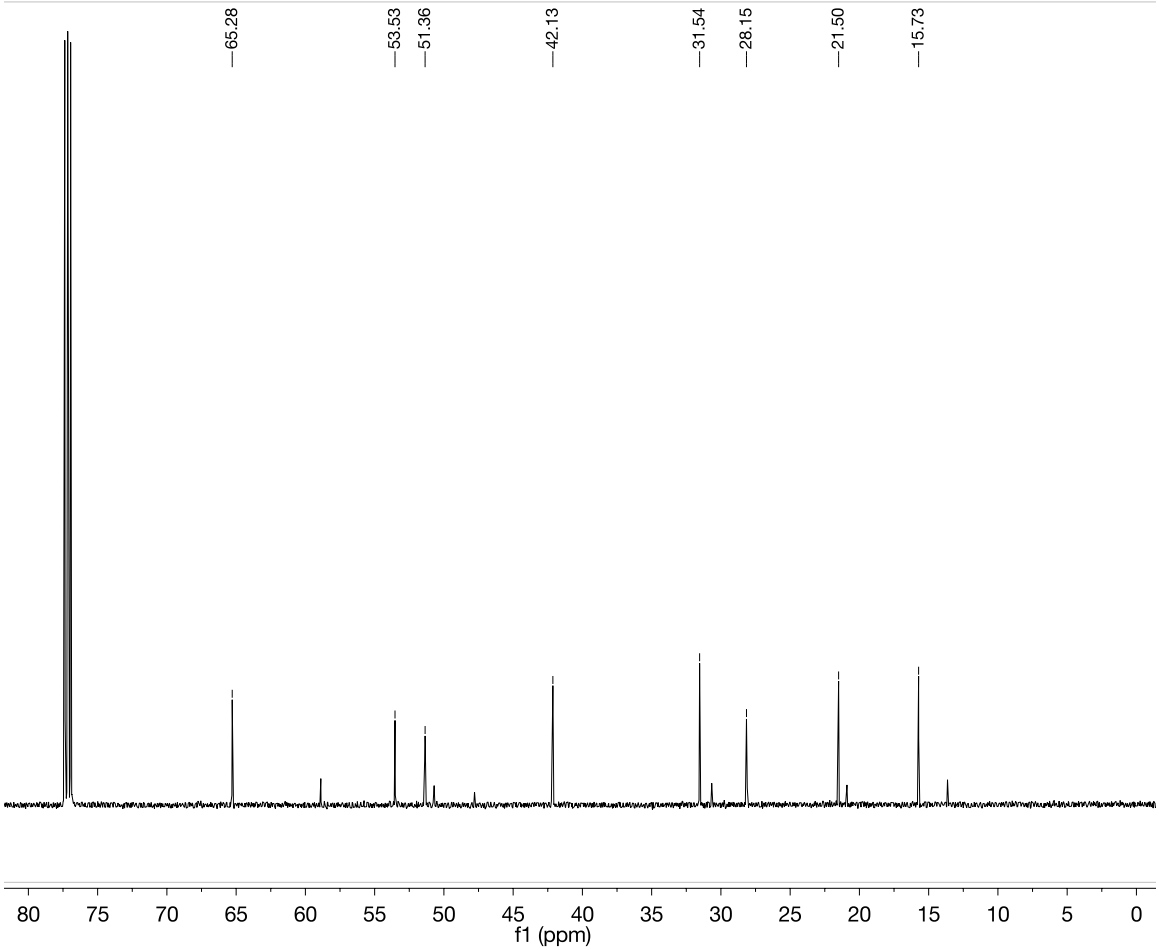
65.28
53.53
51.36
42.13
31.54
28.15
21.50
15.73
f1 (ppm)

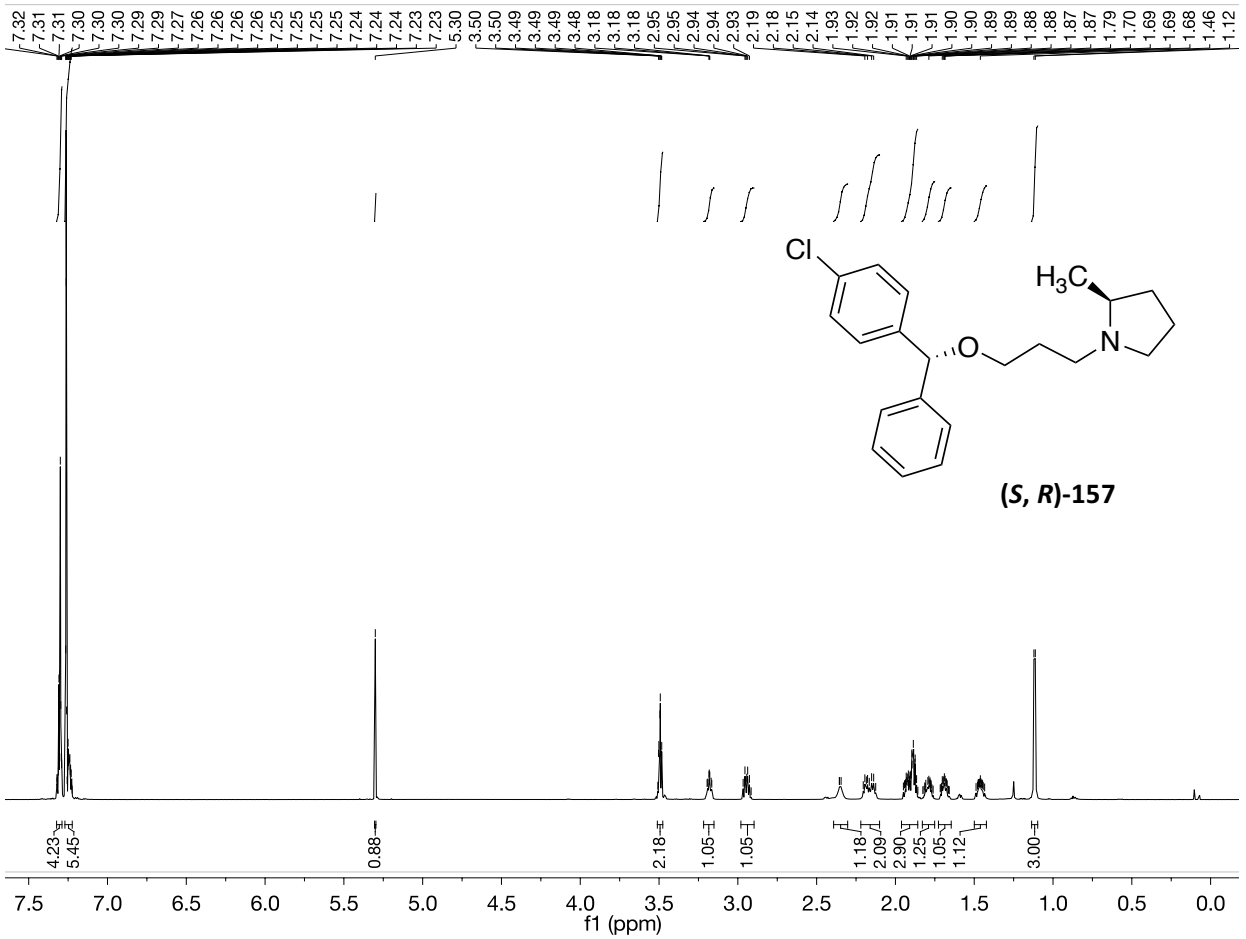
Cl
H3C
O
N
(S, R)-157
f1 (ppm)

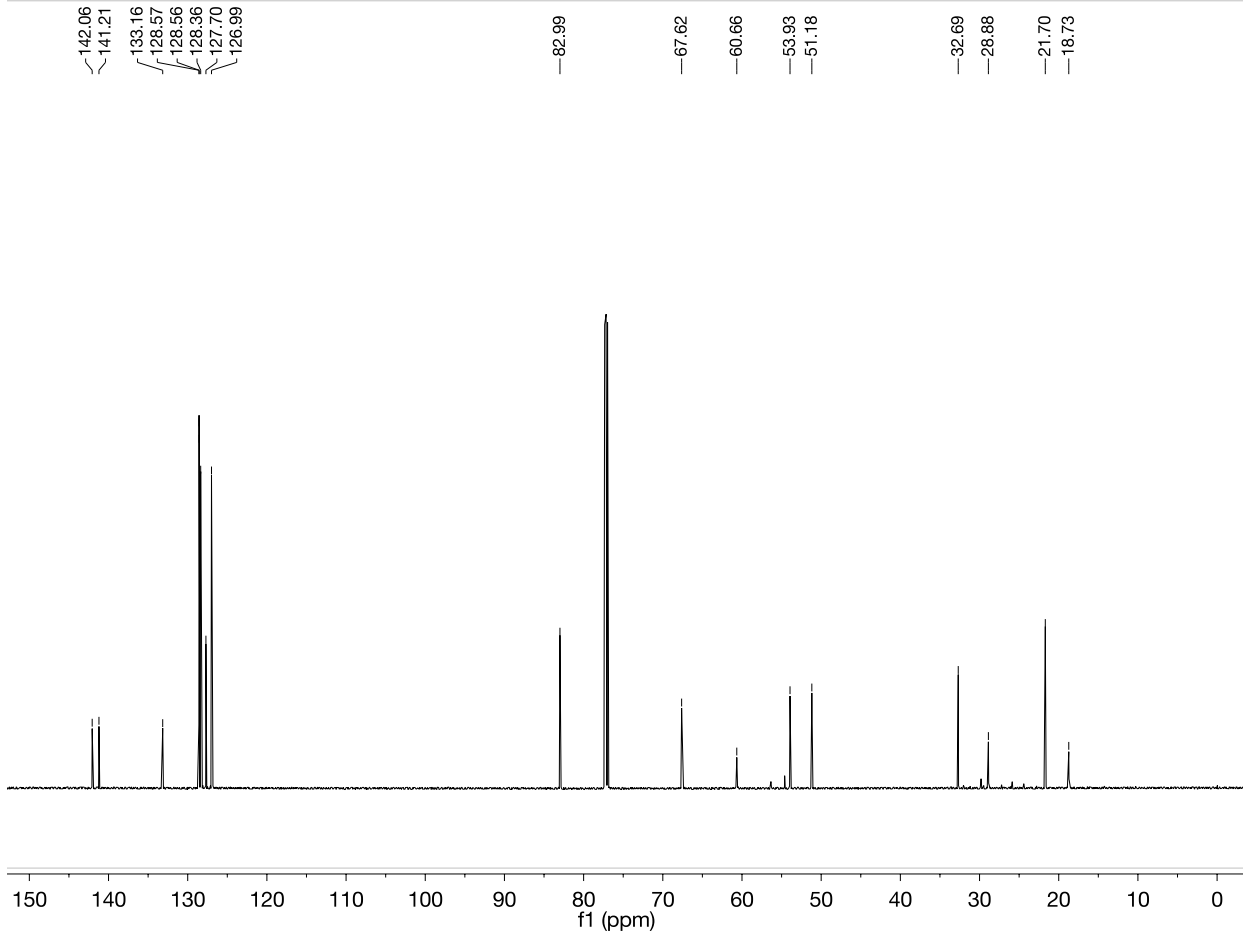
f1 (ppm)

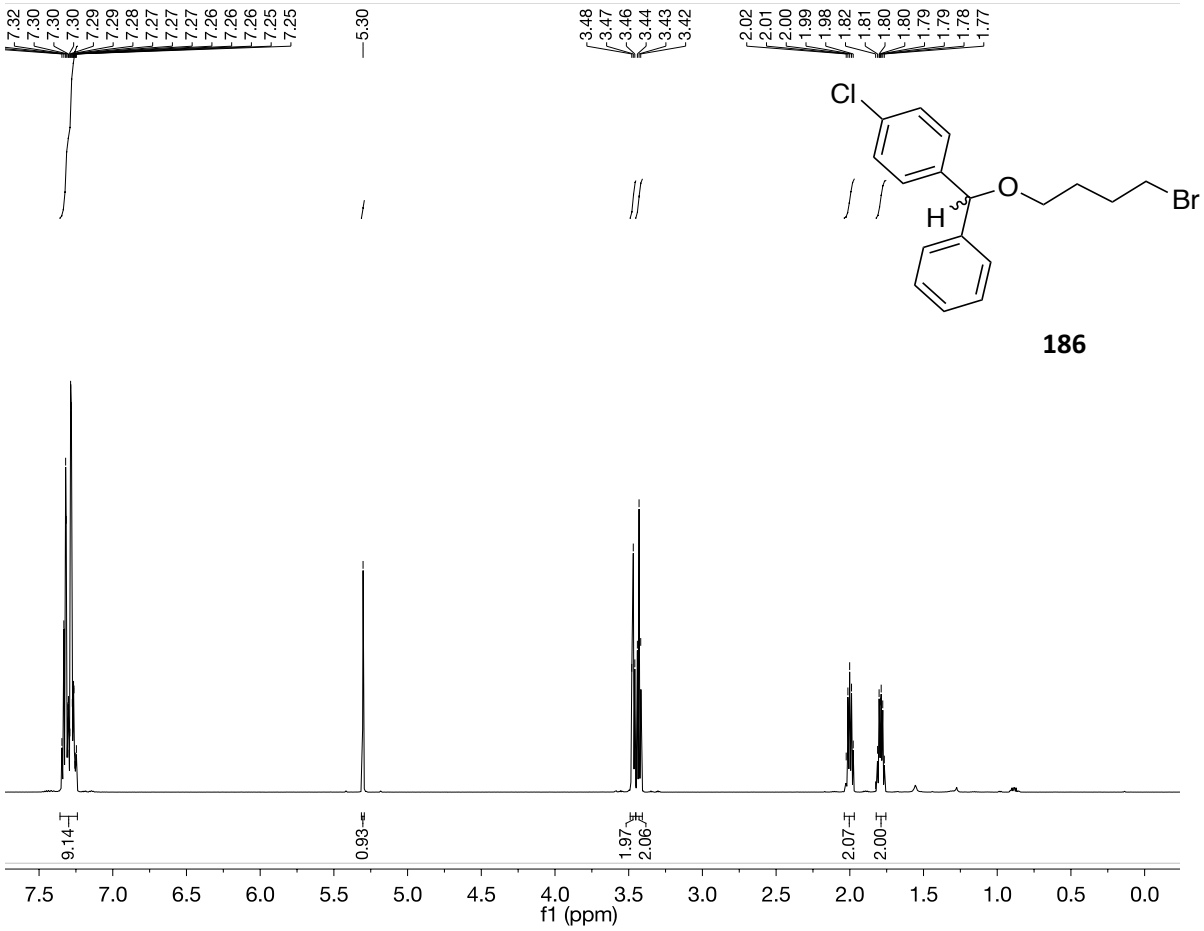
7.32
7.30
7.30
7.30
7.29
7.29
7.28
7.27
7.27
7.27
7.26
7.26
7.26
7.25
7.25
5.30
3.48
3.47
3.46
3.44
3.43
3.42
2.02
2.01
2.00
1.99
1.98
1.82
1.81
1.80
1.80
1.79
1.79
1.78
1.77
Cl
O
H
Br
9.14
0.93
1.97
2.06
2.07
2.00
7.5
7.0
6.5
6.0
5.5
5.0
4.5
4.0
3.5
3.0
2.5
2.0
1.5
1.0
0.5
0.0
f1 (ppm)

186

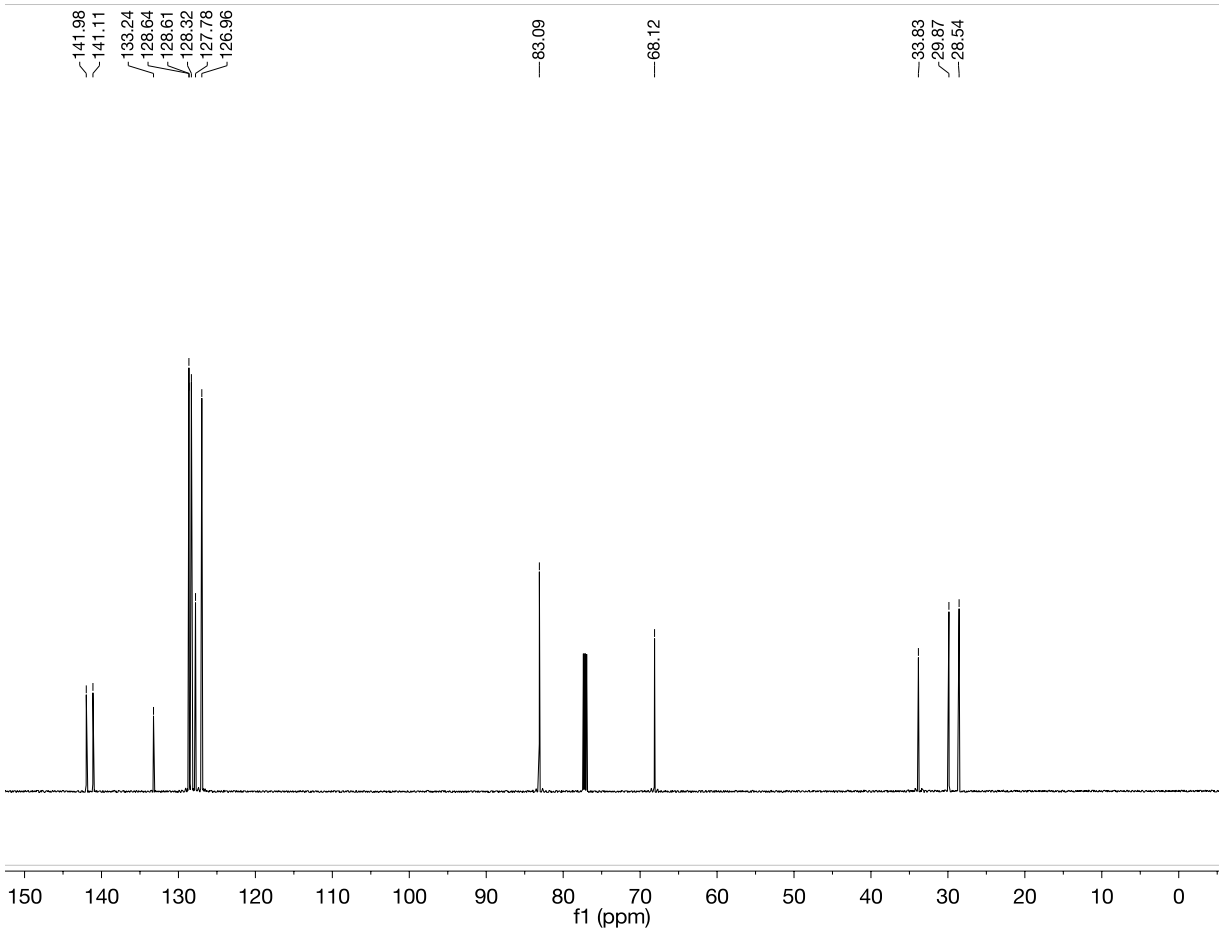
141.98
141.11
133.24
128.64
128.61
128.32
127.78
126.96
83.09
68.12
33.83
29.87
28.54
150
140
130
120
110
100
90
80
70
60
50
40
30
20
10
0
f1 (ppm)

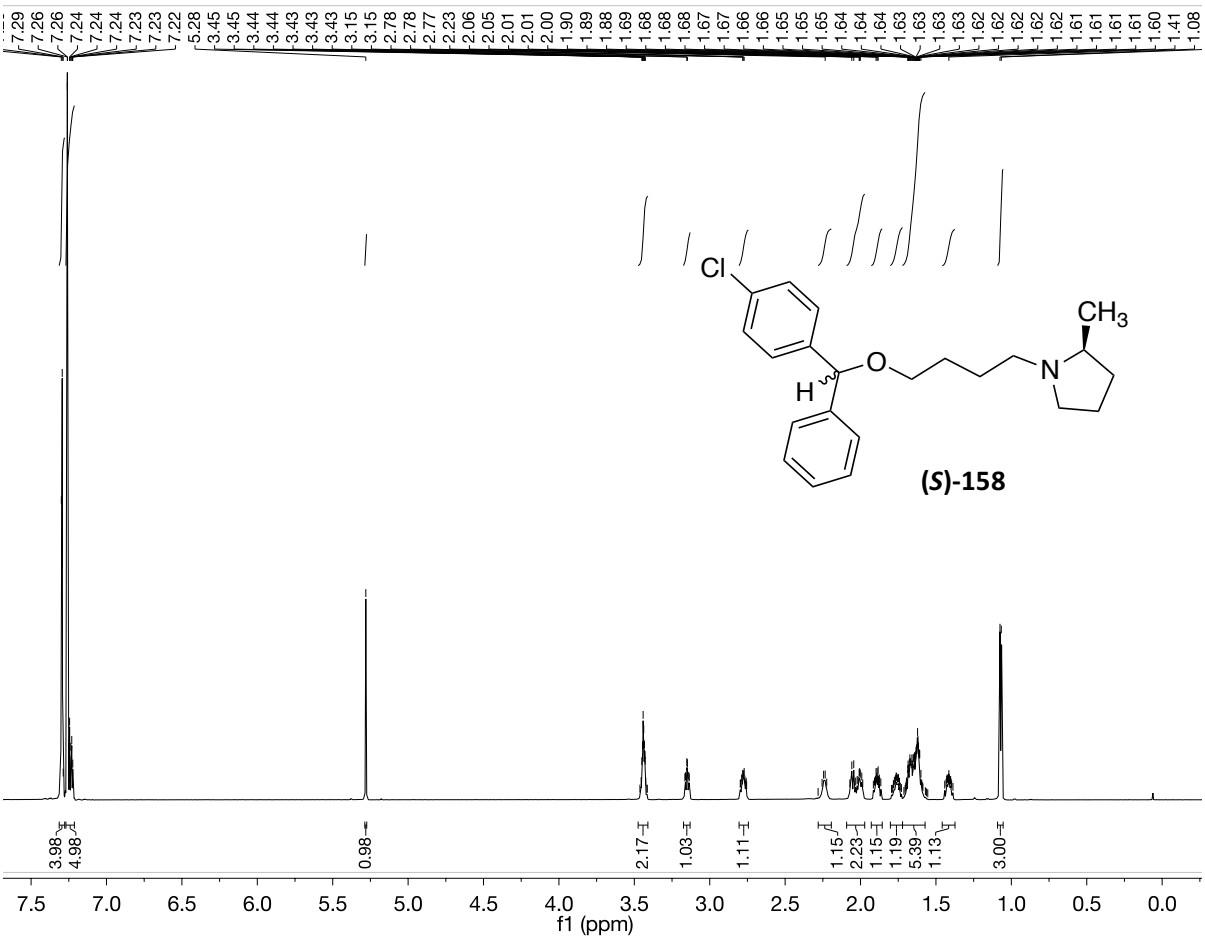
Cl
CH3
O
N
H
(S)-158
f1 (ppm)

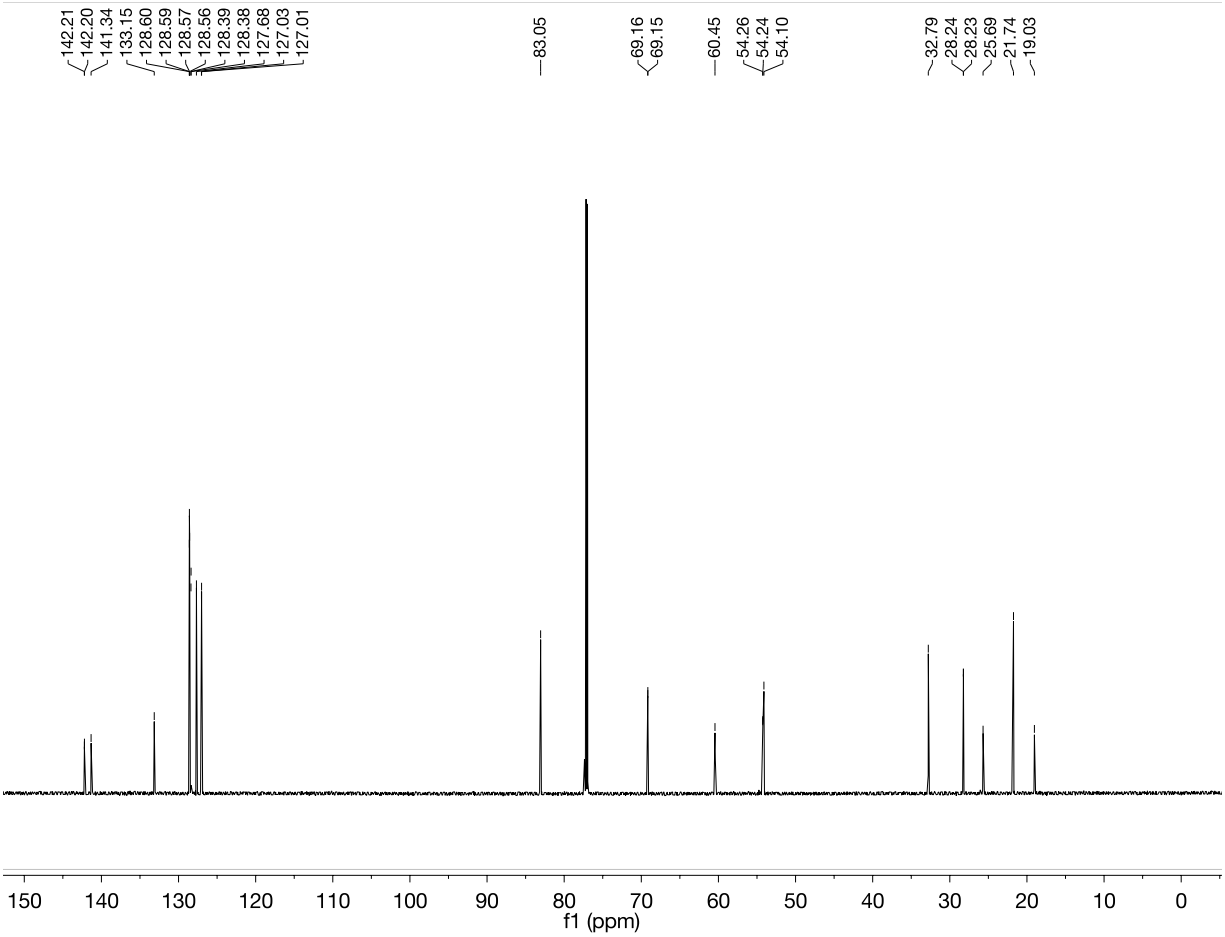
f1 (ppm)